Compréhension et modélisation des processus hydrologique dans un petit bassin versant périurbain à l'aide d'une approche spatialisée orientée objet et modulaire. Application aux sous-basins de la chaudanne et du mercier (bassin de l'Yzeron, France)

Sonja Jankowfsky

UNIVERSITÉ DE GRENOBLE

THÈSE

Pour obtenir le grade de

DOCTEUR DE L'UNIVERSITÉ DE GRENOBLE

Spécialité : **Océan, Atmosphère, Hydrologie**

Arrêté ministérial : 7 août 2006

Présentée par

Sonja Jankowfsky

Thèse dirigée par **Isabelle Braud**
et codirigée par **Flora Branger**

préparée au sein **de l'unité de recherche Hydrologie-Hydraulique, Cemagref/IRSTEA de Lyon**
et de **l'Ecole Doctorale Terre Univers Environnement**

Understanding and modelling of hydrological processes in small peri-urban catchments using an object-oriented and modular distributed approach.

Application to the Chaudanne and Mercier sub-catchments (Yzeron catchment, France).

Thèse soutenue publiquement le **le 15 décembre 2011**,
devant le jury composé de :

M. Jean-Dominique Creutin
Dir. de Recherche CNRS, Grenoble, Président
M. Roger Moussa
Dir. de Recherche INRA, Montpellier, Rapporteur
M. Peter Krause
PD., TLUG, Jena, Allemagne, Rapporteur
M. Fabrice Rodriguez
Dr. Ing.-chercheur IFSTTAR, Nantes, Examinateur
Mme. Isabelle Braud
Dir. de Recherche Cemagref, Lyon, Directrice de thèse
Mme. Flora Branger
Dr. Ing.-chercheur Cemagref, Lyon, Co-Directrice de thèse

Acknowledgements

This PhD thesis was performed at the Cemagref Lyon in the context of the ANR AVuPUR (Assessing the Vulnerability of Peri-Urban Rivers) project. Cemagref and ANR provided the funding for this PhD. Special acknowledgment goes to Michel Lang and André Paquier, as chiefs of the Hydrology-Hydraulics research unit, who agreed to my demands concerning the financial support for conferences, classes, field trips, etc.

First of all, I would like to thank Flora Branger and Isabelle Braud, my supervisors, for their guidance and feedback and their invaluable help, whenever needed.

Special acknowledgment goes to Fabrice Rodriguez, who was always there for questions with URBS, and who participated in my thesis committee as well as jury. Furthermore, he gives me the opportunity to continue working on urban hydrology under his supervision at IFSTTAR.

I would also like to thank Pierre Viallet and Samuel Debionne, who provided the modelling framework LIQUID and who helped me with all questions concerning the development of PUMMA. Furthermore, Samuel Debionne took part in the thesis committee.

I am deeply thankful to my interns Pedro Sanzana, Yvan Paillé and Florent Brossard, who developed the pre-processing of the model. Furthermore, thanks to them I learnt a great bit about supervising.

Additional thanks go to Michel Estèves and Christophe Bouvier for their constructive comments during the thesis committees, as well as Roger Moussa, Peter Krause and Jean-Dominique Creutin for having accepted to be part of the thesis jury and read the 300 pages of my PhD thesis.

I express my gratitude to Kristell Michel and Christine Jacqueminet from the UMR5600 who spent long hours digitalizing the land use of the Chaudanne and Mercier catchments, as well as Kristell's help with ArcInfo and her reception at the ENS.

I take this opportunity to thank the GRASS user community, especially Michael Rabotin, Glynn Cements and Markus Neteler, without their help we would still be stuck in GRASS, Python or generally preprocessing problems.

I would also like to thank Erwan Bocher for his explanations about OrbisGIS. And, if I had the time I would love to work with this promising GIS and contribute to its development.

Special thanks also to all the other participants of the AVuPUR project for the comments and discussions during the project meetings.

I express my gratitude to M. Ruffin, M. Giol, M. Lachise who took the time to enlighten me about the complex drainage system of the Chaudanne catchment, as well as to all the data providers such as IGN, SIAHVY, MeteoFrance, BRGM, SIRA, UMR5600,... and the technicians of the Cemagref who took care about the data quality of the hydro-meteorological data. Furthermore, they explained the BICHE data base to me and took me the first time to the Chaudanne catchment even before the start of the PhD.

I am grateful to Kamal El Kadi for having me encouraged to do the PhD at the Cemagref during my internship.

Many thanks to Hélène Faurant, Anne Eicholz, Adeline Dubost who were the embodiment of efficiency for administrative matters and the "service informatique" with Antoine Gallavardin, Yves Badel and Jean-Pierre Dalleau who were always there for resolving informatics problems.

I would also like to mention Olivier Vannier, as it was good to know that there is at least one person working with the same tool. Furthermore, I would like to thank him for accompanying me to field, as well as Charlotte Michel, and not to forget our skiing together.

Furthermore, I would like to thank all the current users of the coffee room and frequenters of the canteen for their distraction and discussions at lunch time, as well as Etienne Leblois and Bernard Chastan for their support during the final period of the PhD and Etienne's offer of proof-reading of my PhD.

Special thanks to my office room colleagues who were always there for a short distraction from work: Judicael Dehotin, Jean-Marie Lepioufle, Jan, Ignazio Guintoli, Laurent Bonnifait, Carlos Mastachi, Amel Bekreti, Stephanie Moore, Pierre-Henri Bazin, Sabine Radanovics, Florian Linde,...

And it would be difficult not to mention Emilie Andries, Marina Launay, Meriem Labbas, Stephanie Moore, Claire Beraud, Elise Butel, Antoine Bard, Ignazio Guintoli who were there when times were difficult. And all those who went climbing, skiing, running or hiking with me and helped me to get some movement beside all the time sitting in front of the computer.

Furthermore, I want to thank Anna, Vincent, Loes, Meriem, Emilie and Olivier for their help during the thesis defense.

Above all I want to thank Vincent, Ulli and Anna who were always there to cheer me up in the last three years, and who had to listen to quite a bit of hydrological problems.

And I have surely forgotten lots of names, but I would like to express my sincere gratitude to all those who made this PhD possible.

Contents

List of Figures

List of Tables

List of Abbreviations

ANR	Agence Nationale de la Recherche, French national research agency
AVuPUR	Assessing the Vulnerability of Peri-Urban Rivers, French research project funded by ANR (2008-2011)
AET	Actual evapotranspiration
BEST	Beerkan Estimation of Soil Transfer parameters (Lassabatère et al., 2006)
BVFT	Rural model based on LIQUID framework
ChauLech	Discharge measurement station at La Léchère
DEM	Digital Elevation Model
DHI	Danish Hydraulic Institute
DONESOL	French National soil database
FRER1D	LIQUID module, resolving a 1D solution of Richards equation
GIS	Geographical Information System
GRU	Grouped Response Units (Kouwen et al., 1990)
HEDGE	LIQUID module simulating vegetated areas
HRU	Hydrological Response Units (Flügel, 1995)
ICS	Integrated Catchment Simulator (Gustafsson, 2000)
IFSTTAR	Institut Français des Sciences et Technologies des Transports, de l'Aménagement et des Réseaux / French institute of sciences and technology for transport, development and networks
INVASION	French research project funded by ANR (2010-2013)
LIQUID	Modelling framework developped by Hydrowide, Grenoble, France
LTHE	Laboratoire d'étude des Transferts en Hydrologie et Environnement, Research laboratory in Grenoble, France
OLAF	LIQUID module, OverLAnd Flow
OTHU	Observatoire de Terrain en Hydrologie Urbaine, Lyon, France, Field observatory for urban hydrology
PEF	Liquid module, Ponding Extraction Flow
PEP	Potential Evaporation
PET	Potential Evapotranspiration
PdB	Pont de la Barge, discharge measurement station in the Chaudanne catchment
PUMMA	Peri-Urban Model for landscape MAnagement
REW	Representative Elementary Watershed
RIVER1D	LIQUID module, 1D channel flow routing module
RWB	Receiving water body, river or lake
SED	Structures Etudes Diagnostics ingénierie conseil, name of company
SIAHVY	Syndicat Intercommunal d'Assainissement de la Haute Vallée de l'Yzeron
SISTBA	LIQUID module, SImulation of STorage BAsins
SOD	Measurement station in Sewer Overflow Device in the Chaudanne catchment
SS	Measurement station in Sewer system in the Chaudanne catchment
SUDS	Sustainable Urban Drainage Systems

TDSO	LIQUID module, Threshold Dependent Stormwater Overflow device
TIN	Triangular Irregular Network
UHE	Urban Hydrological Element, URBS model units
UMR	Unité mixte de recherche, mixed research unit
UMR 5600	UMR Environnement, ville, société Research, laboratory in Geography in Lyon, France
UpstreamSOD	Measurement station upstream of SOD in the Chaudanne catchment = Pont de la Barge station
URBS	Urban Runoff Branching Structure model (Rodriguez et al., 2008), introduced as a LIQUID module
VPdB	Vieux Pont de la Barge measurement station downstream of SOD
WSUD	Water Sensitive Urban Design
WTI	LIQUID module, Water Table Interface
WTRI	LIQUID module, Water Table River Interface
WWTP	Waste Water Treatment Plant

Abstract

Urban expansion mainly affects peri-urban areas. These areas are subject to rapid modifications such as an increase of impervious areas or concentration of runoff in sewer systems. These changes have an impact on local hydrology and can induce floods, pollution or decrease of groundwater resource. Modelling tools allowing a quantification of the sensitivity of peri-urban catchments to urbanization are therefore useful in this context. The hypothesis underlying this PhD is that a continuous distributed hydrological model, taking explicitly into account the spatial organization of the landscape (urban, agricultural, forest areas, hedges,..) and the water pathways, as determined by topography but also roads and sewer networks, can help to understand and hierarchize the role of various landscape elements on the hydrological response of small hydrosystems. We therefore designed the Peri-Urban Model for landscape MAnagement (PUMMA) simulating the rainfall-runoff processes both in urban and in rural areas. For this, the urban model URBS was integrated into the LIQUID modelling framework already containing modules describing hydrological processes in rural areas. Additionally, three process modules were developed describing sewer overflow devices, overland flow as well as retention basins and lakes. PUMMA follows an object-oriented approach. The landscape is discretized into cadastral parcels in urban areas and irregular hydrological response units in rural areas. In order to apply PUMMA to the catchment scale, automatic methods were developed for the pre-processing of the geographical data. Furthermore, a method for the delineation of suburban catchments including the separation into dry and wet weather contributing areas was developed. The model was then applied to the Chaudanne catchment, a sub-basin of the Yzeron, located in the peri-urban area of Lyon, France. The model was run continuously for two contrasting years (dry and humid) using parameters values taken from observations and the literature. Although summer peak discharge is often overestimated, the results show that, the model is able to simulate realistically the observed discharges and in particular different responses under dry and wet conditions, controlled by the soil saturation. Sensitivity tests to various processes/parameters showed the importance of the urban influenced processes on the hydrological response, in particular surface runoff generation on impervious and natural urban surfaces, infiltration into the sewer system and the connexion of urban areas to the natural hydrographic network. Soil depth and lateral saturated hydraulic conductivity were also found influential on the base flow dynamics. We finally showed the model potential for the evaluation of various rain water management scenarios.

Keywords:

Suburban catchment, peri-urban, Distributed hydrological modelling, Yzeron, LIQUID, Sewer system, Ditches, Pre-processing, object oriented approach

Résumé

La densification actuelle de l'urbanisation conduit à un changement d'occupation du sol et du réseau de drainage en zone péri-urbaine. L'écoulement est concentré dans des fossés ou des réseaux d'assainissement et ainsi accéléré. Ces phénomènes peuvent avoir des conséquences importantes pour les nappes et les cours d'eau, comme par exemple l'aggravation des crues et des sécheresses et l'altération de la qualité chimique et/ou biologique du milieu. Sous la pression réglementaire (Directive Cadre Européenne sur l'Eau) et la demande sociale, les gestionnaires sont donc confrontés à des choix complexes en terme d'aménagement. Ainsi, il est nécessaire de mettre au point des méthodes et des modèles capables de quantifier l'impact de l'augmentation de l'urbanisation sur la vulnérabilité des hydro-systèmes péri-urbains. Dans ce travail, nous formulons l'hypothèse qu'une modélisation hydrologique spatialisée continue, prenant explicitement en compte les objets des paysages périurbains (parcelles urbaines, agricoles, forestières, haies,..) et les éléments déterminant les chemins de l'eau (topographie, mais aussi réseaux d'assainissement ou de routes) peut aider à comprendre et hiérarchiser le rôle des différents objets du paysage sur la réponse hydrologique. Pour ce faire, le modèle distribué PUMMA (Peri-Urban Model for landscape Management) adapté aux bassins versants péri-urbains, a été développé dans le cadre de cette thèse. Il consiste en une intégration du modèle existant URBS, décrivant des processus hydrologiques urbains à l'échelle d'une parcelle cadastrale, dans la plate-forme de modélisation LIQUID, qui contient déjà des modules représentants des processus hydrologiques en zone rurale. PUMMA a également été complété par de nouveaux modules simulant les déversoirs d'orage, les bassins de rétention et le transfert du ruissellement de surface. Le modèle suit une approche orientée objet dans laquelle le paysage est divisé en mailles irrégulières, correspondant aux parcelles cadastrales en zone urbaine et aux unités de réponse hydrologiques (HRUs) en zone rurale. Afin de pouvoir appliquer le modèle à l'échelle d'un bassin versant, des méthodes automatiques pour la préparation des données géographiques ont été mises au point. De plus, une méthode a été développée pour déterminer les contours de bassins versants péri-urbains, en distinguant les surfaces contributives de temps sec et humide. Le modèle a été appliqué au bassin versant de la Chaudanne, un sous-bassin de l'Yzeron, situé en zone péri-urbaine lyonnaise pour deux années en conditions contrastées (sèche et humide). Les paramètres du modèle ont été spécifiés à partir des observations disponibles et des données de la littérature. Les résultats montrent un comportement du modèle réaliste et une aptitude à représenter les comportements différents en période sèche et humide, en lien avec des degrés de saturation des sols différents, même si les pics de débits d'été sont en général surestimés. Différents tests de sensibilité sur certains processus/paramètres montrent l'importance des processus urbains sur la réponse hydrologique du bassin, comme en particulier la génération de ruissellement de surface par les surfaces imperméables et naturelles urbaines, le drainage de l'eau du sol par les réseaux d'assainissement et les connexions entre les îlots urbains et le réseau hydrographique naturel et artificiel. L'épaisseur des sols et la conductivité hydraulique à saturation latérale jouent aussi un rôle important sur la dynamique du débit de base. Nous montrons aussi le potentiel du modèle pour tester différents scenarii

d'aménagement ou de gestion des eaux pluviales.

Mots clés:

Bassin versant péri-urbain, Modélisation hydrologique distribuée, Yzeron, LIQUID, Réseau d'assainissement, Fossés, Pré-processing, approche orientée objet

Résumé étendu

Compréhension et modélisation des processus hydrologiques dans un petit bassin versant péri-urbain à l'aide d'une approche spatialisée orientée objet et modulaire. Application aux sous-bassins de la Chaudanne et du Mercier (bassin de l'Yzeron, France)

Contexte général

Environ 68,7% de la population mondiale et 94,1% de la population française vivra en ville en 2050 selon la perspective d'urbanisation mondiale des Nations unies de 2009[1], ce qui représente une augmentation de 18,4% pour le monde et 8,8% pour la France entre 2010 et 2050. Cette urbanisation croissante conduit à l'expansion des zones péri-urbaines. Ces zones d'interface, qui sont constituées de juxtapositions de surfaces rurales et urbaines, se transformeront donc lentement en zones urbaines avec des impacts probables sur l'hydrologie locale.

Tout d'abord, la construction de bâtiments, de routes et de places de stationnement crée des zones imperméables où l'eau ne peut plus s'infiltrer. Par conséquent, le développement de nouvelles zones urbaines augmente le ruissellement de surface (jusqu'à 45% pour 75% à 100% de zone imperméable (WMO, 2008)) et diminue la recharge des nappes phréatiques (jusqu'à 20%) tout comme l'évapotranspiration (jusqu'à 10%) . L'accroissement du ruissellement de surface augmente l'érosion et peut induire des inondations dans les zones en aval (Aronica and Lanza, 2005; Mignot et al., 2006; Paquier, 2009).

En outre, afin d'adapter le territoire à un usage urbain, l'eau est canalisée et déviée, soit dans des réseaux d'assainissement, des fossés ou des rivières artificielles. Dans les zones périurbaines, selon l'âge de l'aménagement urbain, plusieurs systèmes de gestion des eaux pluviales urbaines peuvent coexister. Les réseaux traditionnels d'assainissement étaient des réseaux unitaires dans lesquels les eaux usées et les eaux de pluie étaient mélangées. Ensuite, la gestion des eaux pluviales a progressivement évolué vers des réseaux séparatifs. Aujourd'hui, la tendance est de promouvoir des techniques dites alternatives de gestion des eaux pluviales comme leur rétention à la source (Roy et al., 2008; Morison and Brown, 2011; Ashley et al., 2010; Kuhn, 2010). Les zones périurbaines peuvent donc être caractérisées par une mosaïque de zones rurales et urbaines et un système de drainage complexe composé de ruisseaux naturels, de fossés et de canalisations, avec la co-existence possible de différents types de réseaux d'assainissement dans le même bassin versant.

Par ailleurs, les réseaux d'assainissement sont conçus pour une certaine capacité en fonction de critères locaux tels que des conditions pédo-climatiques, mais également l'espace

[1] http://esa.un.org/unpd/wup/unup/p2k0data.asp

disponible et les coûts de construction. Avec l'augmentation de l'urbanisation, cette capacité peut être dépassée. Dans ce cas, au lieu d'augmenter la capacité des réseaux, ce qui peut se révéler trop coûteux, la solution est souvent de construire des déversoirs d'orage, qui se déversent vers la rivière naturelle pendant les épisodes pluvieux intenses. Cependant, ces déversements polluent les cours d'eau naturels (Lafont et al., 2006). Des études récentes dans le cadre du projet de recherche ANR INVASION[2] ont montré une dégradation des milieux récepteurs, avec la présence de germes pathogènes en aval de ces déversoirs d'orage. L'urbanisation n'est donc pas seulement un problème pour la quantité d'eau, mais aussi pour sa qualité et la santé humaine.

Afin de diminuer cet impact négatif, la directive Cadre sur l'Eau de 2000[3] impose que les masses d'eau (eaux de surface ou souterraines) reviennent à un bon état écologique d'ici 2015. Les municipalités doivent donc proposer des solutions pour améliorer la situation actuelle et elles doivent aussi surveiller les rejets d'eau polluée vers les cours d'eau naturels. Cependant, nos connaissances actuelles sur l'ensemble des processus impliqués et leurs interactions restent encore insuffisante (p. ex. Walsh et al. (2005)). Afin d'améliorer la situation, des outils numériques de modélisation, permettant de faire progresser la compréhension des processus, peuvent être utiles pour une meilleure gestion de l'eau dans ces zones péri-urbaines. Comme indiqué par O'Loughlin et al. (1996) "les modèles pluie-débit sont le pilier de la quasi-totalité des études de gestion des eaux pluviales urbaines". En particulier, les modèles hydrologiques distribués peuvent contribuer à cette compréhension des processus et améliorer la connaissance de leurs interactions (Jacobson, 2011), car ils peuvent prendre explicitement en compte les zones de production du ruissellement et les chemins de l'eau.

Objectifs et méthodologie

Dans cette thèse, nous formulons l'hypothèse qu'une modélisation hydrologique spatialisée continue, prenant explicitement en compte les objets des paysages périurbains (parcelles urbaines, agricoles, forestières, haies,..) et les éléments déterminant les chemins de l'eau (topographie, mais aussi réseaux d'assainissement ou de routes) peut aider à comprendre et hiérarchiser le rôle des différents objets du paysage sur la réponse hydrologique. L'objectif général de cette thèse est donc d'accroître notre compréhension du fonctionnement hydrologique des bassins versants périurbains, en construisant une approche de modélisation détaillée adaptée aux petits bassins versants (d'environ 1-10 km^2), qui s'appuie sur des observations de terrain et la collecte de données SIG. L'approche choisie pour mener à bien ce travail est de mettre en oeuvre le modèle en utilisant les informations existantes, tirées des observations de terrain ou de la littérature, sans étalonnage. Ceci permet l'utilisation du modèle pour tester des hypothèses de fonctionnement. Dans l'application du modèle, l'objectif n'est donc pas d'obtenir un ajustement optimal entre les débits modélisés et observés, comme c'est souvent le cas pour les modèles utilisés à des fins opérationnelles.

La méthodologie mise en œuvre a été la suivante.

1. Tout d'abord, une revue bibliographique et une analyse des études de terrain précédentes ont permis de déterminer les principaux processus hydrologiques rencontrées

[2]ANR INVASION CESA 2008 022

[3]http://eur-lex.europa.eu/LexUriServ/LexUriServ.do?uri=OJ:L:2000:327:0001:0072:EN:PDF

dans les bassins versants périurbains et leur importance. Les principales approches de modélisation existantes adaptées aux zones rurales et/ou urbaines ont également été examinées, en considérant aussi bien la représentation des processus que la discrétisation spatiale des modèles. Cette étape a permis de définir le cahier des charges du modèle périurbain et a fourni des indications sur les modèles/modules existants, représentant explicitement des processus urbains et ruraux, qui pouvaient être utiles pour la construction de notre modèle périurbain.

2. Le modèle lui-même, appelé PUMMA pour "Peri-Urban Model for landscape Management ", a été développé. PUMMA consiste en une intégration du modèle existant URBS (Rodriguez et al., 2008), qui décrit les processus hydrologiques urbains à l'échelle d'une parcelle cadastrale, dans la plate-forme de modélisation LIQUID (Branger et al., 2010), qui contenait déjà des modules représentants les principaux processus hydrologiques en zone rurale. PUMMA a également été complété par de nouveaux modules simulant les déversoirs d'orage, les bassins de rétention et le transfert du ruissellement de surface. Le modèle suit une approche orientée objet dans laquelle le paysage est divisé en mailles irrégulières, correspondant aux parcelles cadastrales en zone urbaine et aux unités de réponse hydrologiques (HRUs) en zone rurale.

   Par ailleurs, les outils nécessaires pour la préparation des données géographiques (pré-processing géographique), la discrétisation automatique du paysage à l'échelle d'un bassin versant et la génération du maillage ont été développés. Une méthode pour la délimitation des bassins versants et la détermination du réseau de drainage dans les zones périurbaines a d'abord été proposée, car la connaissance exacte du système de drainage et des zones contributives est cruciale pour la modélisation hydrologique. Ensuite, des maillages vectoriels orientés objet avec plus de 2000 mailles ont été créés en s'appuyant sur les nouveaux outils de pré-processing. Ces maillages intègrent des informations importantes sur les processus pertinents, tels que des chemins anthropiques de l'eau, les caractéristiques du sol, l'occupation du sol et le cadastre, la pente, etc. Ils répondent aussi à plusieurs contraintes numériques permettant d'obtenir un maillage adapté à la stabilité des équations résolues. Les fonctions de prétraitement permettent également la détermination de la direction du ruissellement en surface et subsurface ainsi que l'intégration des voies d'écoulement artificielles (telles que les connexions au réseau d'assainissement) nécessaires pour la modélisation hydrologique distribuée dans les zones périurbaines.

3. Enfin, le modèle a été appliqué à un cas test réel dans le bassin versant de l'Yzeron, le sous-bassin de la Chaudanne($2.2 km^2$), situé en périphérie lyonnaise et instrumenté depuis 1997 par le Cemagref dans le cadre de l'Observatoire de Terrain en Hydrologie Urbaine (OTHU). L'occupation du sol en amont du bassin versant est principalement constituée de zones agricoles, tandis que la partie avale subit une forte urbanisation. La partie rurale est drainée par la rivière naturelle et des fossés et la partie urbaine par un mélange de réseaux d'assainissement unitaires et séparatifs.

Principaux résultats

Tout d'abord, l'application de la méthode de délimitation des bassins versants et la détermination du réseau de drainage de la Chaudanne a montré que la superficie du bassin

versant par temps humide est d'environ 30% plus grande que la frontière topographique du bassin versant, qui est souvent utilisée pour la modélisation hydrologique. La carte finale des sous-bassins pour la Chaudanne, dans laquelle les sous-bassins ont été classés en urbains, naturels et drainés par un fossé, est également intéressante pour la qualité de l'eau et les questions de gestion de l'eau.

La Chaudanne est un ruisseau intermittent avec des périodes sèches en été interrompues par des orages et un débit de base continu en hiver. Les crues d'été et d'hiver sont donc nettement différentes, tandis qu'en été, la principale contribution au débit provient d'un ruissellement sur des zones imperméables. En hiver, tout le bassin versant se sature et contribue au débit dans la rivière. Par conséquent, les événements d'hiver ont des pics de crues plus élevés et des volumes écoulés plus importants.

Pour l'application du modèle PUMMA, les années 2008 et 2009, de caractéristiques constrastées (plutôt humide pour 2008 et plutôt sèche pour 2009) ont été choisies pour les simulations. Les paramètres du modèle ont été spécifiés à partir des observations disponibles et des données de la littérature. La comparaison des sorties du modèle avec des points de mesure sur le bassin (débits dans la rivière, dans le réseau d'assainissement et dans un déversoir d'orage), à des échelles temporelles longues et à l'échelle de l'événement, a montré un comportement du modèle réaliste et une aptitude à représenter les comportements différents en période sèche et humide, en lien avec des degrés de saturation des sols différents, même si les pics de débits sont en général surestimés en été. Différents tests de sensibilité sur certains processus/paramètres montrent l'importance des processus urbains sur la réponse hydrologique du bassin, en particulier la génération de ruissellement de surface par les surfaces imperméables et naturelles urbaines, le drainage de l'eau du sol par les réseaux d'assainissement et les connexions entre les îlots urbains et le réseau hydrographique naturel et artificiel. L'épaisseur des sols et la conductivité hydraulique à saturation latérale jouent aussi un rôle important sur la dynamique du débit de base. Le potentiel du modèle pour tester différents scenarii d'aménagement ou de gestion des eaux pluviales a aussi été illustré.

Conclusions et perspectives

Cette thèse a contribué à faire converger des approches utilisées en hydrologie urbaine et rurale par la création d'un outil unique bénéficiant des progrès de la recherche dans les deux domaines. Nous avons ainsi enrichi la modélisation urbaine avec l'ajout de l'écoulement souterrain et de l'écoulement de surface dans le modèle URBS (Rodriguez et al., 2008). Ceci permet l'intégration des zones urbaines et hameaux isolés dans les zones naturelles à la modélisation d'un bassin périurbain. Dans les modèles de bassins ruraux, les zones urbaines étaient décrites auparavant par des pourcentages d'imperméabilisation. Nous avons ajouté une description détaillée des zones urbaines à ces modèles et donc la possibilité de prendre en compte l'effet de l'organisation spatiale des zones urbaines sur la génération du ruissellement. Il est donc désormais possible de modéliser la génération du ruissellement dans les zones périurbaines d'une manière intégrée. D'autre part, plusieurs hypothèses de fonctionnement ont été proposées et évaluées afin de mieux comprendre l'impact des objets urbains sur la réponse hydrologique. Les connaissances acquises par cette approche de modélisation peuvent donner des indications utiles pour la construction d'approches de modélisation simplifiées, utilisables pour répondre à des questions de gestion de l'eau.

1. Introduction

1.1. Motivation

About 68.7% of the world population and 94.1% of the French population will live in cities in 2050 according to the UN world urbanization prospect 2009[1], which represents an increase of 18.4% for the world and 8.8% for France since 2010. This growing urbanization leads to urban expansion in peri-urban areas. These areas, which can be defined as a juxtaposition of rural and urban areas, will thus slowly change into urban areas with probable impacts on the local hydrology.

First, the construction of buildings, roads and parking places creates impervious areas on which water cannot infiltrate any longer. Consequently, the development of new urban areas increases surface runoff (up to 45% for 75%-100% of impervious areas, see Figure 1.1.1 (WMO, 2008)) and decreases groundwater recharge (up to 20%) and evapotranspiration (up to 10%). The increase of surface runoff enhances erosion and it can induce floods in downstream areas (Aronica and Lanza, 2005; Mignot et al., 2006; Paquier, 2009).

In addition, in order to adapt the territory for urban use, water gets channelized and deviated, either in sewer pipes, ditches or artificial river beds. In peri-urban areas, according to the age of the urban development, several urban stormwater management systems can be found. At the start of urbanization, the traditional urban drainage systems were combined sewer systems in which waste and rain water are mixed. Then, the rain water management gradually moved towards separated sewer systems. Nowadays, the trend is to promote rainwater source control and water sensitive urban design (Roy et al., 2008; Morison and Brown, 2011; Ashley et al., 2010; Kuhn, 2010). Peri-urban areas can therefore be characterized by a complex drainage system consisting of a mix of natural streams, ditches and pipes, with the possible co-existence of various types of sewer systems within the same catchment.

Furthermore, sewer pipes are designed for a certain capacity, depending on criteria such as local pedo-climatic conditions, but also available space and construction costs. With the increase of urbanization, this capacity may be exceeded. In this case, instead of increasing the sewer capacity, which is too expensive, the solution is to build sewer overflow devices, which discharge towards the natural river during heavy rain storms. However, the discharge of combined sewer overflow adds pollution to the natural river courses (Lafont et al., 2006). Recent studies in the framework of the ANR research project INVASION[2] showed the presence of pathogenic germs downstream of those combined sewer overflow devices. The urbanization is thus not only a problem for water quantity, but also for water quality and human health.

[1] http://esa.un.org/unpd/wup/unup/p2k0data.asp
[2] ANR INVASION CESA 2008 022

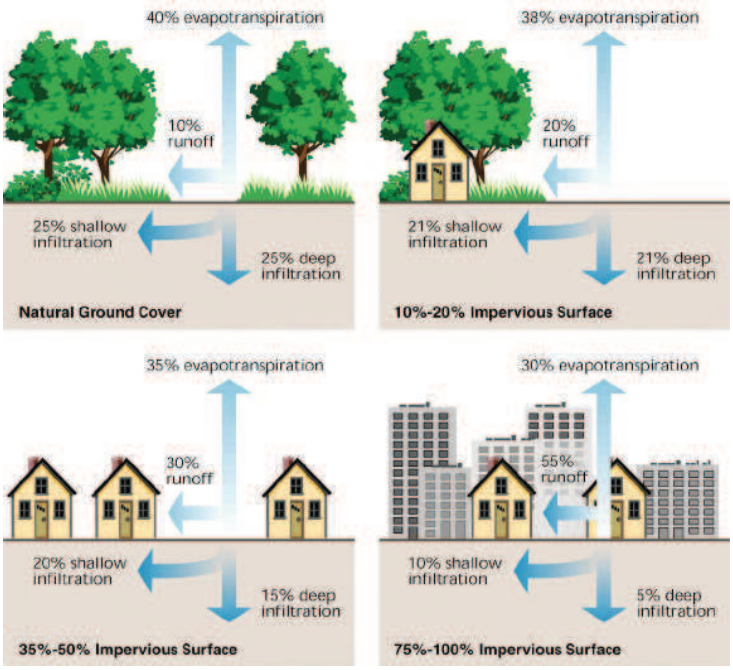

Figure 1.1.1.: The influence of urbanization on different components of the water cycle (WMO, 2008).

In order to decrease this negative impact, the Water Framework Directive[3] of 2000 defines that all water bodies should attain their best possible ecological status by 2015. Municipalities must therefore propose solutions to improve the current situation and they must monitor the discharge of polluted water towards natural river courses.

However, our present knowledge about all the involved processes and their interactions is still deficient (e.g. Walsh et al. (2005)). In order to improve the situation, numerical modelling tools, allowing enhanced process understanding, may be useful for a better water management in these peri-urban areas. As stated by O'Loughlin et al. (1996) "rainfall-runoff models are the backbone of almost all urban stormwater management studies". In particular, distributed hydrological models can contribute to this process understanding and enhance the comprehension of causal relationships (Jacobson, 2011), as they can explicitly take into account runoff generation areas and water pathways.

1.2. Framework of the PhD thesis

The work presented in this PhD thesis was conducted within the framework of the ANR AVuPUR[4] project (Assessing the Vulnerability of Peri-Urban Rivers) (Braud et al., 2010a, 2011a). The project addressed the hydrology of peri-urban catchments. Those catchments are particularly difficult to handle as they are a juxtaposition of natural or cultivated areas, and urban areas, with numerous different networks. For all these reasons, they had been poorly studied before the start of the project. The objectives of the project were thus to enhance the understanding and modelling capacity of water fluxes within peri-urban catchments, focusing on the whole water cycle, i.e. including the hydrological regime, low

[3]http://eur-lex.europa.eu/LexUriServ/LexUriServ.do?uri=OJ:L:2000:327:0001:0072:EN:PDF
[4]http://avupur.hydrowide.com/

and high flows, at both long term and event temporal scales. The project only addressed water quantity problems, which is a pre-requisite for addressing more complex questions such as quality problems. The AVuPUR project followed a multi-disciplinary approach which gathered rural and urban hydrologists, geographers and specialists in remote sensing and GIS and hydro-informatics scientists and engineers.

The project was structured in five work packages shown in Figure 1.2.1. The first work package was dedicated to the hydrological and GIS data collection such as detailed land use maps, field survey of water pathways or infiltration rates, and measurement of rainfall and discharge data. A meta database gathering all necessary GIS layers was created (Dehotin, 2009b).

The second work package, to which this PhD thesis contributes, concerns the detailed hydrological modelling of small catchments (< 10 km^2) with an explicit representation of natural and artificial water pathways. This work package aims for a better understanding of the functioning of peri-urban catchments and at determining hierarchy of the dominant objects/processes (in particular urban hydrological elements) in small hydrosystems. The main challenge is hereby an adequate representation of the heterogeneity of peri-urban areas and its integration into long term hydrological simulation models in order to address the whole hydrological cycle (Braud, 2007).

In order to provide modelling tools usable at intermediate scales (catchments of 10 to 100 km^2), the third work package aims at improving the peri-urban representation of simplified modelling approaches for such catchments. For this purpose, it was chosen to adapt existing models so that they can handle specific characteristics of peri-urban catchments. Three models were considered: an urban model CANOE (Sogreah and Insavalor, 2005) to which the characteristics of rural parts were added and two models initially dedicated to rural catchments: ISBA-Topmodel (Furusho, 2011) and J2000 (Labbas, 2011),where features of urban areas were included.

The objective of the fourth work package is to run long-term simulations based on past and future land use scenarios and to quantify the land use impact on the hydrological regime and the vulnerability of peri-urban rivers to urbanization (Braud et al., 2010a).

Two study catchments were chosen for the project: the Chézine catchment (34 km^2) in the suburbs of Nantes, France and the Yzeron catchment (150 km^2) in the suburbs of Lyon, France. They both belong to long term research observatories: the ONEVU[5] for the Chézine and OTHU[6] for the Yzeron catchment. The detailed hydrological model, which is part of work package 2 and developed during this PhD thesis, is applied to the Chaudanne (4 km^2) and Mercier (6 km^2) sub-basins of the Yzeron catchment. The Mercier catchment is representative of a rural catchment with a land use dominated by forests and agricultural fields. The Chaudanne catchment is representative of more urbanized areas with an upstream cultivated area and a dense downstream urbanization.

This PhD thesis contributes to the research program of OTHU. OTHU gathers several research laboratories and operational partners in Lyon, France. The observatory was

[5]Observatoire Nantais des EnVironnements Urbains, http://irstv.fr/index.php?option=com_content&view=article&id=32%3Asap&catid=5%3Asecteur-atelier-pluridisciplinaire&Itemid=29&lang=fr

[6]Observatoire de Terrain en Hydrologie Urbaine http://www.graie.org/othu/

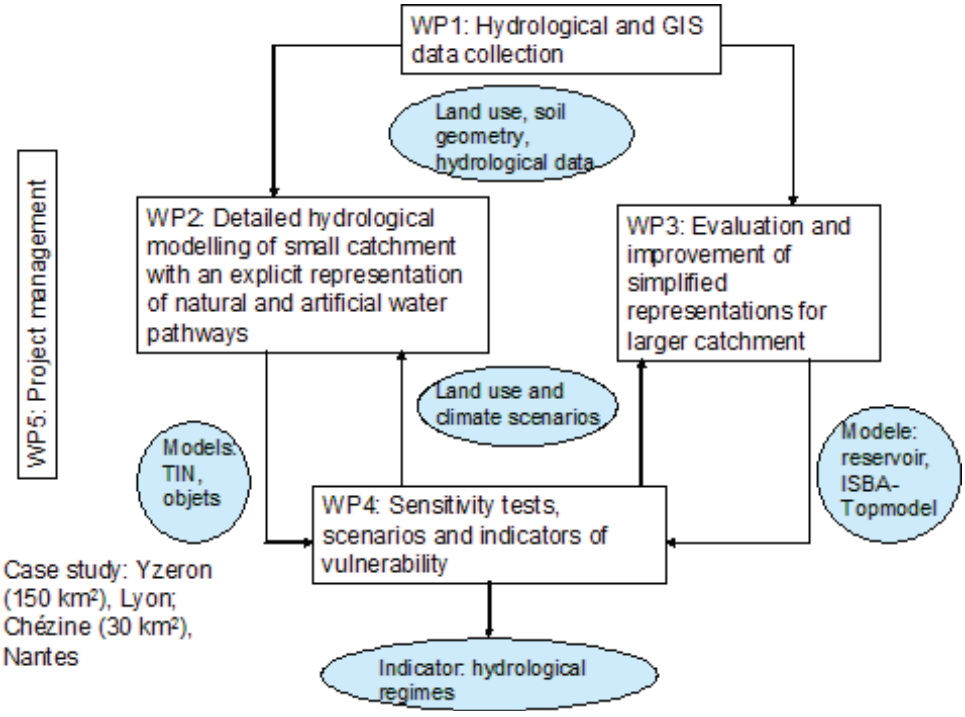

Figure 1.2.1.: Organigram of the ANR AVuPUR project (Braud et al., 2011a).

created in 1999 and it aims at acquiring reliable data on urban wet weather effluents. For this, several representative management structures or catchments, such as the Yzeron catchment, were equipped for long term observation around Lyon. The measurement sites are continuously upgraded and new ones were also installed. The idea is to assess the sustainability of urban water systems and to propose support for operational decision makers.

1.3. Objectives

The general objective of this PhD thesis is to increase our understanding of the hydrological functioning of peri-urban catchments, by constructing a detailed modelling approach adapted to small catchments (of about 1-10 km^2) combined with field observations and collection of GIS data layers . The idea is to build a model which takes explicitly into account the spatial organization of peri-urban areas and a representation of the corresponding hydrological processes. Such a model will also include an explicit representation of water pathways and in particular the disturbance induced by the various networks as compared to a water routing only governed by the topography. A distributed modelling approach is therefore needed. The approach chosen in this work is to setup and run the model using the existing information, taken from field observation or the literature, without calibration. This allows the use of the model as hypotheses tester, in order to understand the roles of the various objects in the catchment and hierarchize their influence on the hydrology of the peri-urban catchments, for the whole range of hydrological responses and temporal scales. In the model application, the objective was thus not to obtain an optimal fit between modelled and observed discharges, as performed with models used for operational purposes. On the other hand, several hypotheses were implemented

and assessed in order to better understand their impact on the hydrological response. The understanding gained by this modelling approach can give valuable feedback for the building of simpler modelling approaches, such as those developed in the AVuPUR third work package (see section 1.2) and usable for answering water management questions. As mentioned previously for the AVuPUR project, this PhD focuses on water quantity and fluxes only and do not address water quality modelling.

In order to reach those objectives and build the peri-urban model presented in this PhD thesis, the methodology was the following. 1) First, hydrological processes encountered in peri-urban catchments and their importance were determined based on a literature review and/or previous field studies. Existing modelling approaches addressing both rural and urban areas were also reviewed. Both the process representation and spatial discretization were considered in this analysis. This step allowed the definition of the peri-urban model requirements and provided guidelines about the existing models or pieces of models, representing explicitly urban and rural processes, which could be useful for the building of our peri-urban catchment model. 2) Second, the model itself, called PUMMA for Peri-Urban Model for landscape Management, as well as the tools required for its automatic landscape discretization were developed. 3) Finally the model was applied to a real test case in the Yzeron catchment and its potential as hypotheses tester and processes understanding tool was demonstrated.

1.4. Thesis outline

This thesis is structured in three parts. The first part describes the scientific context of this work and contains chapter 2 and 3. Chapter 2 reviews the hydrological processes of peri-urban areas and provides a review of the main hydrological modelling approaches applied to peri-urban catchments. As mentioned before, this review provided a first set of guidelines for the design of our modelling approach.

Chapter 3 presents the Chaudanne and Mercier sub-basins and the available data. It also reviews existing field studies as well as model applications to the Yzeron and its sub-basins. The main observed processes are then summarized and discussed from a modelling perspective.

The second part describes the building of the modelling tool kit and contains three chapters. Chapter 4 translates the conclusions drawn from the process and model review into a modelling concept. It presents the principles of the PUMMA model and of the LIQUID modelling framework within which PUMMA was built. Chapter 5 presents the process modules of the LIQUID framework which were used for the development of the PUMMA model and the model technical realization. PUMMA is based on eight process modules. Four of them were developed in the framework of this PhD thesis. For each developed module as well as for the PUMMA model, we present the concepts, their implementation in LIQUID and simple model setups aiming at illustrating the modules/model behavior and their validation.

Chapter 6 presents the methodology developed for the determination of the model mesh, or geographical preprocessing. The first step consists of a method for the determination of the drainage networks and delineation of catchment borders and sub-basins in peri-urban

catchments. A paper describing this work was submitted to Hydrological Processes. The second step is the geographical preprocessing itself, which uses the drainage network and sub-basin map as input along with other geographical data. The complete preprocessing method and its results are described and discussed.

The third part describes the application of the model to the Chaudanne catchment. Chapter 7 presents the model set up and explains how the model parameters were specified from existing data and the literature for the various modules. Furthermore, the strategy for the choice of simulation period and climatic forcings is presented. This model setup provides a first simulation which is compared to existing observations and serves as reference for the subsequent sensitivity tests. Chapter 8 presents the model results for two year continuous simulations with a middle-term analysis and a focus on a selection of events. First, the results of the reference simulation are described in detail. Then, several sensitivity tests are undertaken and the influence of two of the new developments proposed in this PhD thesis are assessed. In the last part, the model capability to simulate different management scenarios is shown.

Finally, Chapter 9 discusses the developed methods and model as well as the model results and summarizes the main conclusions of this work. It also gives some perspectives for future work.

Part I.

General context: hydrological processes and modelling in peri-urban watersheds

2. Hydrological processes and modelling in periurban catchments: a short review

This chapter first gives an overview of the hydrological processes encountered in peri-urban areas. It distinguishes natural processes and anthropogenic influence on those hydrological processes. Then, a review of the spatial discretization of distributed hydrological models, which means different possibilities of model meshes, is given before entering into a detailed review of model concepts and process representations. This review provides elements to answer the question, which models or model pieces are adapted to peri-urban areas? It is found that such a model is more easily built when using integrated modelling and modelling frameworks, which are therefore briefly presented. The final section presents a synthesis in terms of model pieces, concepts and principles which are retained for the building of the periurban model presented in this PhD thesis.

2.1. Hydrological processes in suburban areas

2.1.1. Natural catchments

Flow paths in natural catchments is mainly determined by topography. The catchment and its subcatchments are delineated along ridge lines following the topography. The geology of the underground can further influence the flow paths and deviate water against the topographical design. At the scale of a single hillslope, the soil and land use characteristics gain influence on the runoff generation processes. Depending on the soil permeability, water will infiltrate or create surface runoff. This separation depends also on the slope, which means topography again, and on the climatic conditions. A heavy rainstorm for which the rain intensity exceeds the infiltration capacity will provoke Horton overland flow (Horton, 1939), whereas a long low intensity rainfall will contribute to the soil saturation. If the soil profile is saturated, excess water will create ponding and saturation excess overland flow (Dunne and Black, 1970). The infiltrated water is stored in the soil until the retention capacity is exceeded and it percolates then towards the groundwater table. Macropores can accelerate the infiltration process and tight soil layers retard it. This can cause interflow parallel to the hillslope additionally to the groundwater flow. Additionally, vegetation and evaporation extract water from the soil profile. A warmer region will thus have less water available than a colder region having the same annual rainfall amount. These are the main processes in natural catchments even if this enumeration is not complete.

2.1.2. Anthropogenic influence

Urbanized areas are designed by humans. Buildings, roads and parking places are built, gardens designed and drainage networks are constructed. Water is used for multiple purposes, such as drinking water, for irrigation, for recreation and cleaning. All this has an influence on the local hydrology.

The soil impermeabilization reduces infiltration and creates thus a higher surface runoff (Figure 1.1.1). Only a small percentage of the rainfall is stored on impermeable areas due to initial wetting and surface roughness. The lower infiltration rate reduces the groundwater recharge and can thus cause a decrease of the groundwater table. In urban areas, which are constructed on old wetland sites, this can be useful. Nevertheless, not all urbanized area is impermeabilized. It is a patchwork of buildings, roads, yards, trees, etc and natural processes like interception and evapotranspiration are still present. Berthier et al. (2004) emphasizes the role of soil in the generation of urban runoff. Urban soil corresponds no longer to the antecedent natural soil profile, but is generally replaced by construction material of different composition. Not many information is usually available about its composition and hydraulic properties (Berthier et al., 2004). A groundwater table adjusts itself below the different land use properties, which is often drained by leaking drainage pipes (Gustafsson et al. (1996); Karpf and Krebs (2011)). Depending on the level of the groundwater table, the water can infiltrate or exfiltrate from the pipes. The draining effect of pipes can prevent the flooding of cellars, as it keeps the groundwater table below a certain depth. The construction of cellars influences themselves the hydrology, as the cellars create a barrier for interflow (Klawitter, 2006). Furthermore, leaking sewer pipes can contaminate groundwater.

The drainage network of urban areas is often strongly modified in order to fulfil human needs. The modifications depend on cultural factors such as the age of the urban settlement, its history, the density and pattern of the development, which influences the nature of the constructed stormwater drainage network (O'Loughlin et al., 1996). The complete drainage network in suburban areas can consist of the following network types:

- The natural river and lake network.
- The combined sewer system evacuates waste and rainwater in the same pipe system towards a waste water treatment plant (WWTP). Some parts of the network can be connected to a pumping station in order to direct all water, even against topography, towards the WWTP. In case of surcharge, the network can be connected via storm water overflow devices to the natural river. If no storm water overflow device is installed for extreme rainfall events, the water will flow out of the manholes onto the street. Combined sewer systems are common in old European settlements (Semadeni-Davies et al., 2008).
- The separated sewer system consists of two unconnected rain and waste water networks. The rainwater network is often directly connected to the natural river, whereas the waste water flows to the WWTP. Retention or infiltration basins and oil water solid separators are sometimes located upstream of rain water injection points to the natural river. Nowadays, separated systems are common practice and can thus be found in newer urban districts (Semadeni-Davies et al., 2008).
- Roads in rural areas can function as corridors, barriers, sinks or sources (Jones et al., 2000). They are often sided by ditches which intercept surface runoff. The ditches can be connected to the natural river network or end in a dead end (Duke et al., 2006).
- Road independent artificial ditches in rural areas might be used for irrigation, drainage purpose or even retention if they are not connected. Depending on the

bottom characteristics, concrete or natural, water exchange with the groundwater is possible.

- Retention ponds can serve for flood attenuation and water storage for irrigation purposes.

The effects of the urbanization on the local hydrology are miscellaneous: faster runoff concentration and higher peak discharges due to emphasized surface runoff, the decrease of the groundwater table and a change of the water balance (O'Loughlin et al. (1996); Zoppou (2001); Jacobson (2011)). Ditches and pipes can deviate water and consequently change the catchment borders. Many authors (Zoppou (2001); Niemczynowicz (1999), etc.) mention the impact on the water quality due to combined sewer overflow devices and road runoff. Urbanization induces further increased erosion with undercutting of banks, and consequently also a higher sedimentation (O'Loughlin et al., 1996).

Ostrowski (2000) and Praskievicz and Chang (2009) show that anthropogenic modifications have a greater influence on small catchments than on large catchments. Whereas large catchments usually contain large natural parts, the percentage of impermeabilization can get relatively high in small catchments. Also, the impact of changes in the drainage network, as the deviation of rainwater to a WWTP is important for small catchments, in which the WWTP is outside the catchment boundary. The global water balance of a large catchment stays the same if the WWTP is inside the catchment. For this reason, a detailed consideration of the processes is only reasonable for small catchments (Klawitter, 2006). Praskievicz and Chang (2009) mention the concept of urbanization thresholds, which means that the hydrologic response of the catchment does not change linearly with rising urbanization. After exceeding of a certain urbanization threshold, the impact will be much higher. The location of the urbanization also plays a role; increased impervious surface areas in headwater regions have more influence on the hydrology than developments further downstream.

The impact of impermeabilization is higher for small rainfall events than for high intensity storms (O'Loughlin et al., 1996). This is due to the fact, that rainfall on impervious areas is transformed nearly directly to runoff, whereas rainfall losses on natural areas are high and discharge occurs only if a certain threshold value is exceeded.

The hydrology of a catchment is rarely purely natural or urban. Often it is a patchwork of urban and natural areas where natural and urban hydrological processes interplay (Klawitter, 2006).

The right functioning of the artificial drainage network depends on their design capacities. However, especially suburban areas are subject to continuous modifications (Niemczynowicz, 1999). New buildings and roads are constructed, adding more impervious area, which is generally directly connected to the closest drainage system. If the dimension of the pipes was designed for a specific situation, the new connected area, which was not considered during the conception, can cause a surcharge of the drainage system. Due to the progressive construction of the drainage system, often the knowledge of the exact layout and connections of the drainage system is lost. Wrong connections, such as waste water which is injected to the rainwater system or rainwater pipes connected to combined sewer systems are quite common.

This malfunctioning and generally, the anthropogenic influence on the catchment hydrology can be minimized by means of an optimized water management. The manner of

disposal of roof water has an influence on the catchment hydrology. A direct connection with the help of gutters to the sewer system creates fast runoff, whereas local infiltration in yards or retention in small detention ponds can help to rise the groundwater level. The retention capacity can also be increased by grassed roofs or porous pavements. The right design of sewer dimensions can help to avoid polluted sewer overflow to natural streams. The use of separated sewer systems decreases the amount of water which has to be treated by WWTPs.

Detailed distributed models can help to determine the main hydrological factors. Different management scenarios, such as local retention, introduction of retention basins at different locations or changes in the drainage system can be tested. However, in order to capture all processes and interactions with the model, both, natural and urban processes have to be integrated in a detailed manner into the model. The next sections give thus an overview over urban, rural and mixed modelling approaches.

2.2. Hydrological modelling

Many hundreds of hydrological models exist and each was constructed in a different context and for a specific purpose. In order to get a better overview, they are usually classified according to different criteria (Refsgaard (1996); Zoppou (2001), etc.). The process description determines whether it is a stochastical or a deterministic model. Deterministic models can be further divided in conceptual, empirical or physically based models. Depending on the spatial distribution of the input parameters, models are classified into lumped, if the model area consist of a single model unit having averaged parameters, semi-distributed, if the model area consists of aggregated areas, such as sub-watersheds and distributed (Daniel et al., 2010). A distributed model has the advantage to take into account explicitly spatially distributed information such as soil properties, land use, etc. and they give information about the hydrological state at every place in the catchment (O'Loughlin et al., 1996).

The applied time scale determines whether the model is classified into a continuous model or an event-based model. Models are also designed for different spatial scales, from small local scales to the simulation of large catchments of several thousands of square kilometers. A difference can also be found between models used for research or water management and flood forecasting. Research models are interested in process understanding, whereas only the capacity to simulate hydrographs accurately is important in flood forecasting. Therefore, these models have usually a limited number of parameters and they are calibrated. In contrast, models used for process understanding are often kept uncalibrated, as the parameters are based on measured values or the literature.

Not all models can be clearly classified and the trend is to develop multi-functional models which can be applied at several temporal and spatial scales. Nevertheless, we will base our literature review on existing classifications. We will start with a review of different spatial discretizations (which means model mesh possibilities) used in distributed models. Then, we review several models and try to figure out their applicability to periurban areas. This will lead us naturally to the subject of modelling frameworks. The last section explains then the choice of the modelling approach based on the presented review.

2.2.1. Spatial discretization of distributed hydrological models

In order to simulate hydrological processes with a distributed hydrological model, the model domain, generally corresponding to the catchment area, has to be represented by a model mesh. Different possibilities for such model meshes, and thus the spatial discretization of a catchment, exist. This can be a regular mesh, consisting of square or rectangular grid cells, as for example in the MIKE-SHE model (Abbott et al. (1986b), Abbott et al. (1986a)) or TOPKAPI (Ciarapica and Todini, 2002). Several authors such as Valeo and Moin (2000) showed the effect of grid resolution on the model result. Instead of rectangles, some models use Triangular Irregular Networks (TINs) as discretization (Palacios-Velez and Cuevas-Renaud (1992); Schubert et al. (2008) or Bocher and Martin (2009)). The routing of water from the grid cells or triangles to the river network has to be determined separately based on average altitudes of the model units. The approach of (O'Loughlin, 1986) and (Grayson et al., 1992a) using polygons created by intersection of iso-contours and stream-lines overcomes this problem, as the whole model mesh is derived from the topography and implies thus the routing. The same is valid for the concept of Representative Elementary Watersheds (REWs) proposed by Reggiani et al. (1998), as each subwatershed corresponds to one network reach. None of the above mentioned approaches include catchment characteristics, such as land use, soil or geology in the creation of the model mesh.

However, Flügel (1995) and Bongartz (2003) show the influence of land use on the hydrological processes in a catchment. Therefore, Flügel (1995) proposes the Hydrological Response Units (HRU) concept, which is applied in the SWAT (FitzHugh and Mackay, 2000), PRMS (Flügel, 1995) or J2000 (Krause, 2002) models. An HRU represents an area of similar runoff generation. The hydrological processes, which can be determined by different factors depending on the catchment and scale, should be similar in one HRU. The inner HRU variation of hydrological processes should thus be smaller than the variation between different HRUs (Flügel, 1995). The next section gives a more detailed review about different HRU applications.

2.2.1.1. Hydrological Response Units

Before creating a HRU model mesh, a detailed analysis of the catchment dynamics and the main influencing factors, including field investigations, is necessary. The criteria depend upon the research question, scale, available data and local situation. The HRUs of Flügel (1995) are based on land use, soil, aspect and slope criteria, FitzHugh and Mackay (2000) use soil and land-cover as characteristics for their 48 km^2 catchment, Dehotin and Braud (2008) use land-cover, lithology and terrain slope for a 11 700 km^2 basin, whereas Marce et al. (2008) include additionally meteorological data to form the HRUs in the Ter catchment (1680 km^2). Santra et al. (2011) delineates HRUs based on soil hydraulic properties. Devito et al. (2005) start the discussion which variable to consider first. According to them "a hydrologist must determine which feature, or factor, explains the greatest variation in the dominant hydrologic process without masking the influence of factors lower in the order." In their study case in the boreal plains, the following order of factors was determined: first climate, then bedrock geology, superficial geology, soil type and depth and at last the topography and drainage network. Beighley et al. (2005) add a hydrogeological interpretation approach to the HRU concept. Hereby, the dominant runoff components in each HRU, which are surface runoff from urban and rural surfaces, interflow and ground-

water, are determined. In their approach, each HRU can only have one form of surface and subsurface flow, respectively. Bongartz (2003) differentiate between process oriented HRUs as described above, topographic based HRUs out of flow panels and channels and topological flow routing between process based HRUs. Subsurface flow, possible due to routing from one model unit to the next is only implemented in the topographic and topological approach. The topological approach combines the first two approaches and outperforms them during modelling (Bongartz, 2003). In order to reduce the number of model parameters Kouwen et al. (1990) proposes grouped response units (GRUs), which correspond to sub-basins in which several HRUs are grouped. The response of each HRU is modelled separately and the resulting discharge is then weighted over the GRUs. In general, model parameters are spatially averaged at HRU scale (Beighley et al., 2005), leading to a reduction of parameters to the necessary detail.

HRUs are different from the hydrologic landscape concept presented by Winter (2001), which is applicable at a broader scale. A hydrologic landscape consists of an upland, an intervening steep slope and a lowland part, whereas HRUs represent only one of these parts in order to have similar runoff generation processes.

Spatial and temporal scale are two important points, which have to be considered when choosing the model mesh. Flügel (1995) highlights that time and spatial scale are linked. In that, if only a daily time step is available for measured flow and precipitation data, a detailed mesh is not reasonable. O'Loughlin et al. (1996) insists on the appropriate level of detail, which depends on the research questions. For urban stormwater drainage systems, different spatial discretizations are imaginable, such as property drainage, street drainage, trunk drainage, river basin, urban areas considered as single catchments, trunk systems with broad sub-catchment areas or street drainage systems with detailed property drainage components and sub-catchments (O'Loughlin et al., 1996). Mitchell and Diaper (2006) developed a nested approach consisting of the study area, the neighbourhood and the land block, for their urban UVQ model.

Dehotin and Braud (2008) propose a framework for spatial discretizations of watersheds, which is valid for different scales and research questions. It is a nested discretization, where the first level consists of subcatchments organized by a river network topology, the second level consists of hydro-landscapes or HRUs and the third level consists of an adaptation to numerical constraints. In the second level, depending on the size of the catchment and the desired detail, land use objects can be taken directly as model units, such as in Branger (2007b), or different factors can be combined to create HRUs (Dehotin and Braud, 2008).

Technically, the HRUs are obtained by intersection of different GIS layers, representing the chosen factors. Usually, the GIS layers are transformed into raster maps for the intersection, such as in Schwarze (2008) or Dehotin and Braud (2008) and for the creation of SWAT (FitzHugh and Mackay, 2000), PRMS (Flügel, 1995) and J2000 Schwarze (2008) model meshes. In order to reduce the number of combinations, some simplifications are necessary. Traditional methods are based on area thresholds, where the smallest units are deleted (Dehotin and Braud, 2008). Santra et al. (2011) uses fuzzy classification, whereas Dehotin and Braud (2008) uses a technique proposed by Robbez-Masson (1994), in which the neighborhood composition at each location enters in the classification algorithm. The generalization algorithms can lead to a loss of particular objects, which can have an influence on hydrological processes, such as hedge rows or ditches. Object oriented and vector based approaches, designed for small scales, try to take this aspect into account.

2.2.1.2. Object oriented approaches

Different kinds of object-oriented approaches can be found in the literature. Branger (2007b) uses a vectorized land use map as model mesh, in which each land use unit, such as agricultural fields, hedgerows, ditches or drained areas represents a single model unit. Moussa et al. (2002) showed the influence of the spatial organization of agricultural management on the hydrology of a small catchment using the MHYDAS model, in which the model mesh consists of agricultural fields associated to ditches.

In urban modelling, an object oriented approach was proposed by Rodriguez et al. (2003). They define urban hydrological elements (UHEs) as model units, consisting of one cadastral parcel and half of the adjoining street.

2.2.1.3. Conclusions

We have seen that distributed hydrological models can be applied on different kinds of model meshes such as rectangular grids, TINs, polygons created by intersection of iso-contours of elevation and stream-lines, REWs or subwatersheds, HRUs or vector based, object oriented approaches. The model mesh is one of the criteria used in the model classification presented in the following sections. However, the main focus of this review will be to answer the question, which model is able to represent the hydrological processes of peri-urban areas.

2.2.2. Modelling in peri-urban areas

While looking for modelling of suburban or peri-urban areas in the literature few studies appear. However, when taking a closer look, most of the hydrological models were applied to areas with urban influence. This is due to the fact, that pure natural catchments are nearly non-existent in our civilized world. If we want to distinguish urban and rural models, it is useful to separate the runoff generation part of models from the transfer and routing part. On the one hand, most of the urban models used by engineering companies, concentrate on the routing part, which is necessary for design questions of urban stormwater pipes, and have a simpler description of the runoff generation part (Braud, 2007). These models are usually applied to local communities for event simulations, which means small spatial and temporal scales. On the other hand, most rural models focus on the runoff generation part, as they are used for water balance modelling or flood forecasting. They are thus applied to larger spatial scales. Nowadays the limits are getting more and more fuzzy, as models are improved and missing processes are integrated. Beside water quantity questions, many models provide also water quality functionalities. Here, we focus only on water quantity.

Several state of the art reviews of models exists, each evaluating the models after different criteria and only some of them answer the question, whether the models are rather rural, urban or mixed. The following paragraph describes the classification criteria of these reviews, on which the next sections, separating the models into rural, urban or mixed, are based.

Burton and Pitt (2001) separated the models in watershed and receiving water models, which corresponds to the classification into runoff generation and routing part. They classified 13 watershed models in simple and detailed models and describe different criteria

such as urban or rural land use, time scale, hydrology or pollutants. Zoppou (2001) concentrated on the routing part of 12 urban stormwater models, whereas Singh and Woolisher (2002) evaluated different criteria of 70 watershed models. Borah and Bera (2003) reviewed the mathematical basis of 11 watershed scale hydrological models. Kampf and Burges (2007) classified 19 distributed hillslope and catchment hydrologic models according to the description of hydrological processes such as subsurface, overland and channel flow and space and time scales. Elliot and Trowsdale (2007) concentrated on the capacity of 10 urban stormwater drainage models to simulate sustainable urban drainage systems (SUDS). Mitchell et al. (2007) evaluated 65 integrated urban models from which they chose 7 for a detailed review. Their aim was to find models suitable for integrated urban water management, which means that they should be able to simulate the whole urban water cycle including drinking water supply, stormwater, wastewater as well as groundwater. Borah (2011) reviewed all hydrological processes such as runoff generation, routing and subsurface flow of 14 storm event watershed models. He also classified the models after their complexity and gave information about their applicability to rural or urban areas. Klawitter (2006) and Bach (2010) separated the models in rural and urban models.

The question of whether a model has the capability to simulate urban and rural areas is not always answered similarly in the literature. Often, only the fact that the models can simulate impervious areas is considered. This might be appropriate for large scale hydrological models, but when descending to a smaller scale the capability of the models to simulate sewer systems and anthropogenic flow paths gets important (Bach, 2010). In tables 2.2.1 and 2.2.2 we show a summary of the different reviews concerning the model classification into urban, rural or mixed, their capability to simulate the sewer network, the type of model mesh the models use and the spatial scale to which the models are applied. We also added some more models not mentioned in the reviews, which address hydrological modelling in peri-urban areas. The spatial scale refers to the definition in Borah (2011), who reviewed storm event watershed models, where small catchments have a drainage area of less than 25 km^2, medium between 25 and 200 km^2, and large more than 200 km^2. In contrast, Praskievicz and Chang (2009) who reviewed the modelling of climate change and urban development impacts on water quality, classified small basins as $<$1000 km^2 and medium up to 10 000 km^2. They also highlighted the fact that studies of urban development impacts are highly scale dependent.

Here, we do not detail the different equations used by the models, as this is done by most of the above mentioned reviews. Due to the large amount of available models, only the most currently used models will be addressed as well as models of special interest.

2.2.2.1. Modelling in rural areas

Typical rural models are SWAT, AGNPS, ANSWERS, J2000, LARSIM, TOPOG, MHYDAS and BVFT, see Table 2.2.1 for references. Most of them can simulate land use change and impact of impermeabilization by means of runoff coefficients based on impervious percentages. Franczyk and Chang (2009) used the SWAT model to simulate the effect of urbanization on the runoff on a catchment in the Portland metropolitan area, USA, whereas Jürgens (2001) applied ANSWERS to determine the impact of impermeabilization in two small German catchments. Krause (2002) simulated the impact of land use change in a large German watershed with the model J2000. The distributed character of

Model	Sewer	Mesh	Spat. scale	Temp. scale	Time step	Source
rural						
SWAT	no	HRU	m,l	c	d	Arnold et al. (1998)
AGNPS	no	square grids, ch.	s,m	e	storm event	Young et al. (1989)
ANSWERS	no	square grids, ch.	s	e-c	s,m	Beasley et al. (1980)
J2000	no	HRU	m,l	e-c	d	Krause (2002)
LARSIM	no	HRU	m,l	e-c	h	Bremicker (2000)
TOPOG	no	mesh of stream and contour lines	s	e-c		Vertessy et al. (1993)
MHYDAS	no	HRU	s	e-c		Moussa et al. (2002)
BVFT	no	Land use	s	e-c	s,m,h	Branger (2007b)
mixed						
TopUrban	no	square grid	s	e-c		Valeo and Moin (2000)
MERCEDES	(yes)	square grid	s,m	e	m	Lhomme et al. (2004)
HSPF	yes	pervious/imperv. lands and channels	s,m,l	e-c	h	Bicknell et al. (2005)
PRMS	no	HRU	s,m,l	e-c	s,m,l	Leavesley and Stannard (1995)
GSSHA	no	rect. grids	s	e-c	s,m	Downer et al. (2006)
MIKE-SHE	no	2D rect. grids	s	e-c	s,m	Abbott et al. (1986a)
KINEROS	no	ov + ch	s	e	s,m	Woolisher et al. (1990)
ArcEGMO -URBAN	yes	ELU (HRU)	m,l	c	mon	Biegel et al. (2005)

Table 2.2.1.: Review of rural and mixed models. Spatial scale s=small, m=middle, l=large; Temporal scale e=event, c=continuous; Time step s=seconds, m=minutes, h=hours, d=day, var.=variable; Mesh ov=overland planes, ch=channel, dr. net. = drainage network, UHE = urban hydrological element, HRU = hydrological response units, ELU = elemental units.

the models allows hereby the representation of different land use characteristics spatially distributed over the catchment.

Carluer and Marsily (2004) integrated man-made networks, consisting of ditches, roads, hedges and underground drainage pipes into the TOPOG model. However, the structure of the TOPOG model mesh, consisting of stream tubes delimited by stream and contour lines, makes the integration of the anthropogenic flow paths difficult. This is due to the fact, that the mesh is based on natural topography, whereas the anthropogenic flow paths do not always follow topography.

In order to avoid this problem, Branger (2007b) used an object oriented, vector based approach with her BVFT model (Branger et al., 2010) to simulate the influence of hedgerows and agricultural drainage on the catchment response of a rural catchment. In a similar object oriented approach, Moussa et al. (2002) and Tiemeyer et al. (2007) developed the MHYDAS model, which simulates also the effect of spatial organization of agricultural management, such as field limits, tillage practices, ditch and tile drainage. Even if these models try to simulate part of the anthropogenic influence, none of the rural models is able to model sewer systems or to describe the urban hydrological processes in a detailed manner.

2.2.2.2. Modelling in mixed areas

Most of the models classed as mixed were defined as this by Borah (2011), such as GSSHA, MIKE SHE, HSPF, PRMS and KINEROS (Table 2.2.1). However, the limit between rural and mixed models is in reality not very clear. Most of the mixed models were originately designed for rural zones, so the main focus is on the runoff generation part and not on the routing part (refer to section 2.2.2). Im et al. (2009) simulated the impact of land use change, including increasing impermeabilization caused by growing urbanization in a large watershed in Korea using the physically based MIKE SHE model. The land use change is simulated by means of modifications of land use specific vegetation parameters on the affected grid cells.

Cho et al. (2009) simulated the impacts of land use change on groundwater levels in a Virginia watershed using the HSPF model coupled to MODFLOW. The watershed, having an area of 148 km ^{2}, was divided in 10 subwatersheds. Different land use scenarios with high, medium and low density developments and different locations in the watershed were tested. The development density was represented with different impervious percentages. The average recharge output of HSPF was the input for the MODFLOW simulation.

Lhomme et al. (2004) applied the GIS-based geomorphological routing model MERCEDES on a catchment in the peri-urban area of Quito, Ecuador. The catchment was discretized in grid cells, and the effective rainfall, obtained by application of a constant runoff coefficient, was routed towards the catchment outlet following the topography. The artificial drainage system was integrated into the digital elevation model (DEM) by means of stream burning, which means that the elevation of the DEM grid cells overlapping with the artificial drainage network was reduced.

Valeo and Moin (2000) adapted the rural model Topmodel (Beven and Kirkby, 1979) to urban areas, calling the new model TOPURBAN. In TOPURBAN impervious areas receive no recharge, and the precipitation falling on those areas becomes directly overland flow. The impervious area is thus not considered in the upstream area for the calculation of the topographic index for natural grid cells. The model was applied to the Ancaster

catchment, Ontario, Canada, which has a size of 8 km^2.

Biegel et al. (2005) developed the ArcEGMO-URBAN model based on the rural model ArcEGMO. The model focuses on water quality, combining approaches from urban waste water modelling with catchment wide hydrological modelling. Compared to the other mixed land use models, this is the only model, which simulates explicitly the discharge in the sewer system. The simulated runoff is separated into surface runoff, combined sewer system runoff and stormwater system runoff. The catchment is divided into HRUs with homogenous characteristics and the effective rainfall is calculated under consideration of temperature, interception, depression storage, gradient and degree of sealing. The model was applied to a sub-basin (120 km^2) of the Havel river basin in Germany.

Klawitter (2006) mentions the continuous modelling of subsurface flow under both urban and rural zones and exchanges with the sewer system as a critical point for peri-urban modelling. Models such as TOPURBAN, MIKE SHE or HSPF are capable of simulating the subsurface flow under both urban and rural zones, whereas ArcEGMO-URBAN does not simulate subsurface flow. None of the above mentioned models is capable of simulating the infiltration into the sewer pipes, as either no sewer system or no subsurface flow is modelled.

2.2.2.3. Modelling in urban areas

Urban models such as MOUSE, CANOE, SWMM and MUSIC (Table 2.2.2) are used for operational sewer system modelling. The main focus is therefore more on the hydraulic routing inside the sewer system than on the runoff generation. The choice of the model depends mostly on the region. MUSIC is imposed as reference model for sewer system design for communities in Australia (Fletcher, 2010), whereas CANOE (Sogreah and Insavalor, 2005) is mainly used in France. Among the four cited models, SWMM[1] is the only free and open-source modelling software.

This are semi-distributed models, in which the modelled area is usually divided in subwatersheds connected to a link and node network representing the sewer system. The subwatersheds can be further divided into impervious and pervious areas. In CANOE (Sogreah and Insavalor, 2005) the impervious areas can be separated in areas directly connected to the drainage network and unconnected zones.

Even if CANOE was originally designed for urban watersheds, it is possible to model peri-urban areas using different approaches for rural and urban areas. For the runoff generation either a constant runoff coefficient, a combination of three constant runoff coefficients for different rain intensities or the Horton infiltration function can be applied. As transfer function a linear reservoir or a cascade of linear reservoirs is proposed. The hydrographs produced on the three different surfaces of the subwatershed are then added and routed using the shallow water equations towards the catchment outlet. Lhomme et al. (2004) applied CANOE to a 52 km^2 catchment in the suburbs of Quito, Ecuador. They assigned two different runoff coefficients for the urban and natural part of the catchment. CANOE was also applied to the peri-urban Yzeron catchment (150 km^2) near Lyon, France (Dehchali, 1997; Radojevic, 2002; Braud et al., 2010a).

Hernebring et al. (2002) applied MOUSE to the sewer system of Helsingborg, Sweden. The catchment, having a size of 50 km^2, was divided in 60 subcatchments. Each subcatchment consisted of a pervious and impervious part. The impervious part created direct

[1] http://www.epa.gov/nrmrl/wswrd/wq/models/swmm/

Table 2.2.2.: Review of urban models. Spatial scale s=small, m=middle, l=large; Temporal scale e=event, c=continuous; Time step s=seconds, m=minutes, h=hours, d=day, var.=variable; Mesh ov=overland planes, ch=channel, dr. net. = drainage network, UHE = urban hydrological element, HRU = hydrological response units, subc.=subcatchments.

Model	Sewer	Mesh	Spat. scale	Temp. scale	Time step	Source
urban						
SWMM	yes	subc., perv./imperv. areas, link-node dr. net.	s,m	e-c	s,m,h	Rossman (2010)
MIKE-URBAN/ MOUSE	yes	subc., perv./imperv. areas, link-node dr. net.	s,m	e-c	s,m var.	(DHI)
CANOE	yes	subc., perv./imp. areas, link-node dr. net.	s,m	e-c	m	Sogreah and Insavalor (2005)
MUSIC	yes	subc., perv./imp. areas, link-node dr. net.	s	e-c	m	Wong et al. (2002)
UVQ	yes	land block, neighbourhood, study area	s	c	d	Mitchell and Diaper (2006)
SLAMM	no	lumped	s	c	d	Pitt (1998)
DR3M-QUAL	yes	ov + ch	s	e-c	m	Alley and Smith (1982)
P8 (UCM)	yes	link-node drainage network	s	e-c	h	Palmstrom and Walker (1990)
URBS	yes	UHE	s	e-c	m	Rodriguez et al. (2008)

runoff, whereas the pervious part provided water for infiltration into the sewer system. SWMM (Rossman, 2010) is similar to MOUSE with subcatchments divided in pervious and impervious areas and infiltration into the sewer system from previous surfaces.

Compared to MOUSE, CANOE, SWMM and MUSIC which are for event based and continuous modelling, UVQ (Mitchell and Diaper, 2006) is a water balance and quality model using a daily time step. It is a pure urban model, not suitable for peri-urban areas. However, it has an interesting nested spatial representation consisting of a study area, which contains neighborhoods, which contain on its part single properties (section 2.2.1).

The URBS model (Rodriguez et al., 2008) concentrates on the runoff generation and has a much more detailed spatial description, in which each cadastral unit is represented explicitly including their buildings, yards and adjacent streets (section 2.2.1). URBS was applied to two small catchments, the Gohards (180ha) and Rezé (5ha) catchments, Nantes, France.

2.2.2.4. Conclusions

We have seen that many models exist and that the tendency is going towards multi-functional models. However, when having a closer look, most models are either designed for urban or rural zones and they are missing important points for the other area. Urban zones in rural models are often represented by impervious coefficients, and no sewer system is modelled. Most mixed models are derived from rural models, in which some urban processes were integrated. However, processes such as infiltration into sewer pipes or sewer overflow devices(SOD) are not represented. The runoff generation part in most urban models is simulated in a simplified manner based on sub-basins with permeable and impervious surfaces, as they focus rather on the hydraulic routing in the sewer system. One exception is the URBS model, in which each cadastral parcel is simulated separately.

2.2.3. Integrated modelling

In order to simulate correctly the hydrology of suburban areas, which consist of a patch-work of urbanized, natural and agricultural areas (Andrieu and Chocat, 2004), a mix of urban and rural models is necessary. Hence, the tendency is going towards integrated modelling, where different models are coupled. Often integrated modelling is based on modelling frameworks where different models and process modules can be coupled in order to construct "à la carte"' models. The next section proposes different integrated modelling approaches applied in peri-urban areas.

2.2.3.1. Coupling of models

In urban water management integrated modelling means the simulation of sewer system (SS), waste water treatment plant (WWTP) and receiving water body (RWB) using linked models of the three systems (Lijklema et al. (1993); Rauch et al. (1998); Muschalla et al. (2007); etc.). For this, several linked modelling systems were developed such as WEST (Meirlaen et al., 2002), the MATLAB SIMULINK platform (Erbe et al., 2002) or the Integrated Catchment Simulator (ICS) (Rauch et al., 2002).

The following section describes ICS developed by the DHI[2] in more detail, as also the hydrological model MIKE SHE (see section 2.2.2.2 and table 2.2.1) was added to the modelling system (Gustafsson, 2000). The other components are MOUSE for sewers, MIKE11 (1D flow) for rivers and MIKE21 (2D flow) for estuaries and STOAT for WWTPs (Rauch et al., 2002). Furthermore, the ICS package includes links to SWMM and STORMPAC (Zoppou, 2001) (see table 2.2.2).

Gustafsson (2000) applied ICS to three different catchments in Sweden and showed its capability to simulate the interaction between SS and surrounding groundwater systems. The runoff created on impermeable areas is described with the conceptual surface runoff model in MOUSE, whereas MIKE SHE simulates the infiltration on permeable areas. In addition, the coupling allows a two way interaction between pipes and the aquifer and drainage of groundwater through foundation drains into manholes.

Semadeni-Davies et al. (2008) investigated the impact of urbanization and climate change in Helsingborg, Sweden, using the coupled MIKE SHE - MOUSE model. They tested different urbanization scenarios and found that source control and increased storage capacity can mitigate the influence of urbanization, but not the coupled influence of urbanization and climate change.

Domingo et al. (2010) added a two-way exchange between overland flow and unsealed manholes to the model, which enables the simulation of overland flow caused by surcharge of the sewer system. The modelled 30 km^2 peri-urban catchment in the municipality of Greve in Denmark with the 3D hydrologic - 1D hydraulic model. The whole catchment was divided in 25x25 m^2 grids, and the lower part of the catchment, where flooding occurred was divided in 5x5 m^2 grids.

Besides the "integrated modelling" concept used in urban water management, the concept of "dual drainage" modelling arose from the hydraulic side (Smith, 2006). Dual drainage signifies the coupled hydraulic simulation of the subsurface storm sewer network and the surface system composed of streets, ditches and channels. As the dual drainage modelling comprises a detailed 1D-2D hydraulic modelling, often only parts of urban areas are modelled and no hydrologic components are integrated.

In order to describe not only the sewer system and the receiving water body, but also the rural part of the catchment Klawitter (2006) and Klawitter and Ostrowski (2005) developed a 2-layer approach, coupling the grid-based conceptual hydrological model WB_rM to SMUSI, a pollution load sewer model. The urban areas, simulated with SMUSI, are cut out from the rural grid (Muschalla et al., 2007). Both models calculate independently discharges in their system and exchange water at points of interaction such as stormwater overflows, WWTPs, rainwater from separate systems and infiltration into sewer pipes.

Muschalla et al. (2007) developed a fast integrated simulator including four subsystems: the upstream catchment, the WWTP, the RWB and the urban sewer system. For the urban sewer system, the SMUSI model was also applied, whereas the other systems were simulated with newly developed rainfall-runoff and river water quality models. This was further developed to the BlueM.SIM modelling system by Reussner et al. (2009) and Bach (2010). Reussner et al. (2009) integrated the BlueM.SIM model into the Open Modelling Interface OpenMI (Gregersen et al., 2007). The modelling system contains

[2]http://www.dhigroup.com/

furthermore preprocessing and postprocessing tools as well as optimisation algorithms. In the BlueM.Sim model, the catchment is divided in subbasins with HRUs using the ArcSWAT software, and the urban areas are extracted from this model mesh using the preprocessor. With this model it is possible to simulate peri-urban catchments with multiple urban areas. The model was applied to the Modau catchment in Germany, which has a surface area of 37 km^2 (Bach et al., 2007).

As we can see from the review shown above, the desire to model complex systems such as peri-urban catchments has led naturally to the development of adaptable modelling approaches based on modelling frameworks. In the following section we will describe in more detail modelling frameworks and will then come back to the choice of the model pieces which will be used for the construction of the peri-urban areas specific model.

2.2.3.2. Review of modelling frameworks

Modelling frameworks are based on the concept of reusability and draw on object oriented principles (Argent (2004); Branger (2007b)). They contain a library of components, also called modules, out of which integrated models can be composed. By assembling different components, case specific models can be obtained (Leavesley et al. (2002); Argent (2004); etc.). They aim at reducing software development costs and at increasing the efficiency of cooperative research (Jagers, 2010). The researcher can thus concentrate on his topic of interest (Argent, 2004).

Voinov (2010) differentiates "Integrated models" from "Integrating models". Integrating models signifies the integration of existing models, usually in legacy code, into frameworks designed for the communication and data exchange between models. Hereby, the framework provides wrappers for the legacy code and interfaces for data exchange including pull or push mechanisms at runtime. Examples of "integrating models" are the US Environmental Protection Agency's (EPA) framework FRAMES (Frames, 2011), the Common Component Architecture (CCA) (Bernholdt et al., 2006), OASIS/PALM (Valcke and Morel, 2006) or OpenMI (Gregersen et al., 2007). Integrated models are developed within frameworks, where model components are rewritten or newly developed in the language of the framework. The framework provides tools for easy construction of new components, and offers common library standards as well as input and output support tools. Furthermore, it manages the data exchange and execution sequence of single model components. Examples of integrated models are the German JAMS (Kralisch and Krause, 2006) and the American OMS (David et al., 2004), MMS (Leavesley et al., 2002) and SME (Voinov et al., 2004), the Australian TIME with WaterCAST (Cook et al., 2009) or the French frameworks MIMOSA (Müller, 2009), OpenFluid (Fabre et al., 2010) and LIQUID (Branger et al., 2010).

Even if the concept of reusability and community is good, Voinov (2010) draws attention on problems which may appear concerning the integration of models. When coupling several models, not only the correct programming of the exchange has to be considered, but also the scientific concept behind the software. As such, both models have to speak the same language, and the scales and geometries should correspond. The problem is less distinct for integrated models, as the components are rewritten and thus, they should be designed for the interaction.

Beside the above mentioned frameworks, many more frameworks are emerging, issued

from different research communities and intended for various environmental questions. Argent et al. (2006) and Jagers (2010) give an overview of some of the frameworks. The frameworks can be differentiated by their programming language, their general structure, the allowed model mesh, their user interface and set of facilities, the reusability of existing codes or the capability to simulate feedback between process modules.

Modelling frameworks offer a perfect environment for the construction of hydrological models for peri-urban areas. They are capable of dealing with different time scales such as fast hydrological response in urban zones and slower response in natural zones. Using a modelling framework instead of a single model has the advantage that different processes can easily be coupled under consideration of physical coherence and that new processes/objects can be added without much difficulty if "integrated models" are considered. In the following concluding section, we discuss thus the models presented in section 2.2.2, which are based on modelling frameworks, and choose the model pieces and modelling framework, which we will use for the construction of the peri-urban specific model.

2.3. Choice of modelling approach

Peri-urban catchments consist of a patchwork of urban, rural and natural areas, with different runoff generation processes. Urban areas, which have a higher percentage of impervious areas due to buildings, streets and parking places create more Horton overland flow and lead thus to a faster catchment response. However, urban zones also contain green areas such as gardens and trees, where water can infiltrate or evaporate. The spatial organization of built-up and natural areas and the connection of impervious areas to the drainage system or natural soil can thus be crucial for the generation of hydrographs. Especially in peri-urban areas the classification in urban or natural sub-basins can be difficult, due to the presence of dispersed settlements.

Approaches such as the BlueM.Sim model (Bach (2010) and Reussner et al. (2009)) based on the OpenMI framework try to model both, the rural and urban components and allow to consider several urban settlements. However, urban settlements are considered as entity. Therefore, the effects of dispersed settlements and the spatial organization of land use classes inside the urban, or agricultural areas are lost. Furthermore, interaction of urban and rural areas happens only at predefined places of interaction.

J2000 (Krause, 2002), built inside the JAMS modelling framework, is a rural model, in which urban areas are only represented by imperviousness percentages and artificial drainage networks cannot be simulated.

Combinations like MikeSHE and MOUSE based on the ICS framework (Gustafsson, 2000) also allow to model both components, but the description of the urban objects and land use classes are subject to the raster resolution.

Regarding urban models, only URBS seems to represent in a detailed manner urban objects and its spatial organization. However, subsurface flow is only modelled as infiltration to the sewer pipes, because no exchange to other model units is possible. This limits the application of URBS for natural catchments, as lateral subsurface flow is an important processes there.

Concerning rural areas, only the BVFT (Branger, 2007b) and MHYDAS (Moussa et al., 2002) models, based on the LIQUID and OpenFluid frameworks, respectively, seem to be

capable of simulating the hydrological response caused by the effect of spatial organization of agricultural management, even if they do not model urban areas. Comparing MHYDAS and BVFT, BVFT has the advantage that it proposes process modules for hedgerows and a physically based description of water flow in agricultural fields and forests. Furthermore, it provides interfaces allowing lateral subsurface flow between model units in the saturated zones.

The BVFT model is built inside the LIQUID modelling framework by coupling of different process modules. This modelling framework is built on a fully object-oriented approach. Not only the programming concept is object-oriented, having different processes as separate classes, but also the model mesh can be described as object-oriented due to its vector structure. Depending on the spatial scale of the model application, the land use map can be directly used as model mesh, creating objects such as hedges, agricultural fields, ditches, etc. This object-oriented approach, based on the modelling framework, is interesting for the modelling of peri-urban areas, as different equations and process descriptions can be applied on different model mesh parts. Furthermore, on the one hand each object, if natural or anthropogenic, has its own processes, and on the other hand, the objects can easily interact with other objects. The vector-based approach allows an exact description of the hydrological objects, without the influence of grid size. However, no module describing urban areas is part of the LIQUID modelling framework. The integration of URBS, which is also based on an object oriented model mesh consisting of cadastral parcels, into the LIQUID modelling framework in order to combine it with the BVFT model, seems thus to be an adequate approach to model peri-urban areas for process understanding. We propose thus an approach based on the LIQUID modelling framework, which combines the BVFT and URBS model.

3. Presentation of the study catchments and synthesis of previous studies

This chapter gives an overview of the two catchments under study: the Chaudanne and Mercier sub-basins. They are part of the Yzeron periurban catchment, located in the south west of Lyon city. We present the data available for modeling and a review of field experiments aimed at improving the hydrological process understanding in this catchment. This chapter also presents a synthesis of the modelling studies conducted in the Yzeron catchment and its sub-basins. The conclusions summarize what can be deduced from previous work in terms of hydrological functioning of the study basins and the processes which should be included in the PUMMA model presented in the next chapter.

3.1. Geographical description

3.1.1. General description of the Yzeron catchment

The Yzeron catchment is located in the peri-urban area southwest of Lyon, France. The upper part of the Yzeron catchment is in the "Monts du Lyonnais" and the lower part is in the agglomeration of Lyon (Figure 3.1.1). The altitude varies from 917.5 m to 162.5 m at the confluence with the Rhône river (Gnouma, 2006). The surface area of the Yzeron catchment is about 150 km^2.

The climate of the Yzeron catchment is temperate with continental and mediterranean influences. The average annual precipitation is 843 mm (MétéoFrance (2011), Bron) with peaks in May and in October. The climograph after Walter-Lieth[1] (Walter and Lieth, 1967) shown in Figure 3.1.2 indicates that the climate is humid, which means that on average there is no month with a dry period.

In this PhD we focus on two sub-basins of the Yzeron catchment: the Chaudanne and the Mercier (Figure 3.1.1). Both sub-basins border each other, though the Mercier catchment is located higher up in the Mont du Lyonnais. The land use of the Mercier catchment is mainly rural and forest, whereas the Chaudanne catchment is composed of a large urban area in the lower part, and a rural area in the headwaters. The Mercier catchment has a surface of 6.8 km^2 and the Chaudanne of 4.1 km^2.

3.1.2. Geology

The geology of the Chaudanne and Mercier catchments consists of metamorphic rock of the Monts du Lyonnais series containing gneiss and some granite (BRGM, 2011), see Figure 3.1.3. This geological formation was created during the Palaeozoic and lifted in the Tertiary during the convolution of the Alps. During the Quaternary, alluvium was deposited in the valley floors (Gnouma, 2006). Especially in the Chaudanne catchment a large area of alluvium can be found in the headwaters (BRGM, 2011). Furthermore, the metamorphic rock is covered by colluviums of variable thickness: rather thin on top of

[1]Diagramme ombrothermique d'après H. Gaussen et F. Bagnouls in French

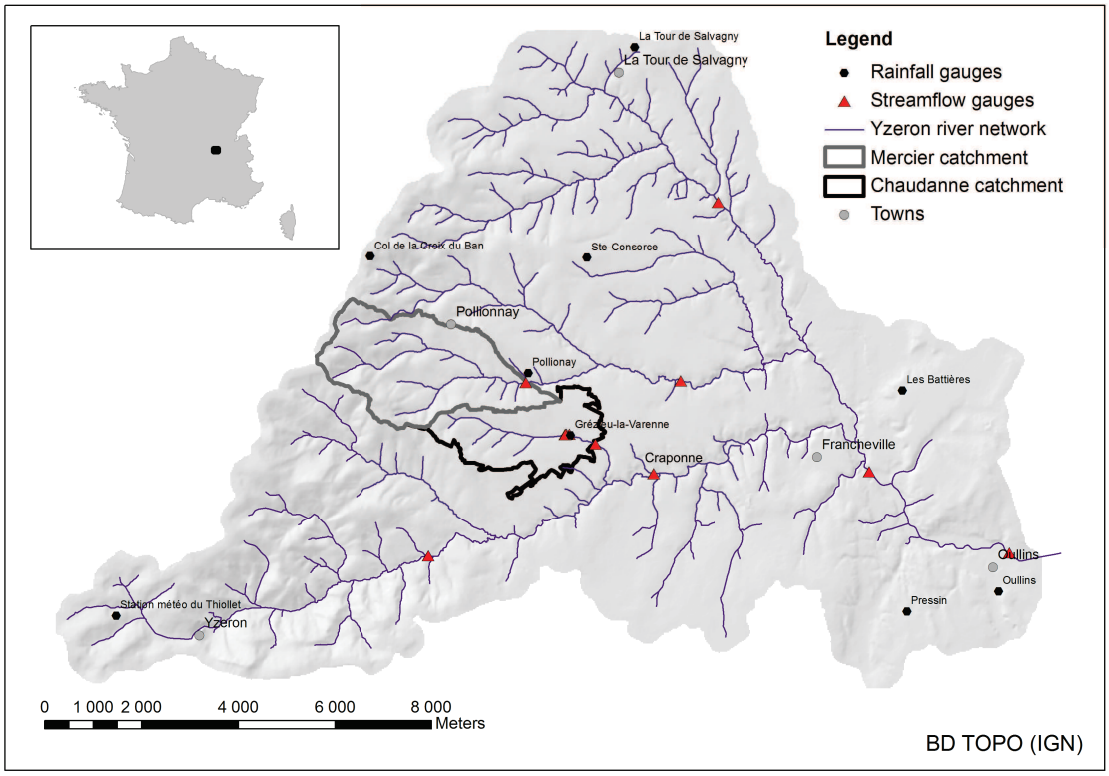

Figure 3.1.1.: Location and topography of the Yzeron catchment with its sub-basins Chaudanne and Mercier. The streamflow and rainfall gauges are indicated.

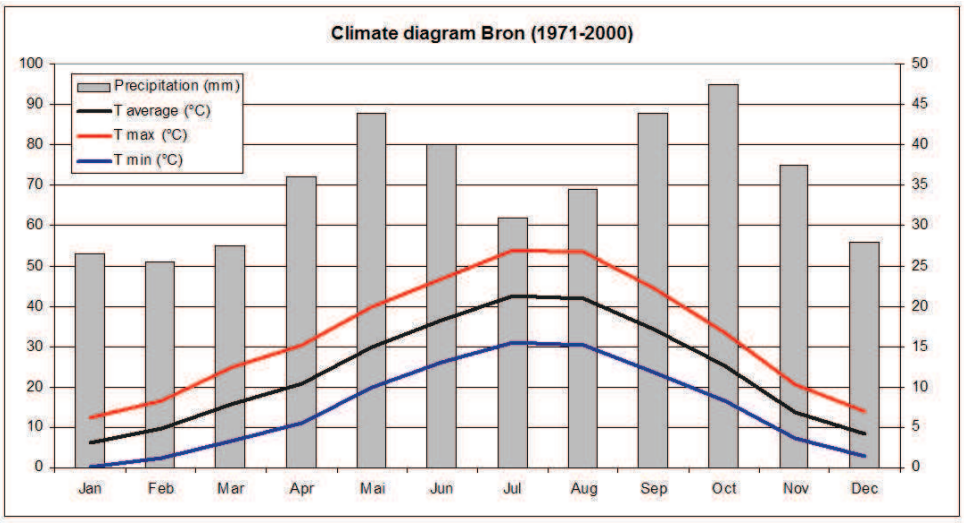

Figure 3.1.2.: The climate diagram for Lyon (Bron) for the 1971-2000 period (MétéoFrance, 2011).

the hillsides and up to several meters on the bottom (Goutaland, 2009). A bore hole at Grézieu-la-Varenne (Grézieu)(see Figure 3.1.1 for its location) showed clay up to a depth of 10 meters, and just then granite. In a bore hole in Craponne (see Figure 3.1.1) the bedrock started only at a depth of 6.3 m and above the rock was weathered. During the alteration of gneiss, the feldspath is transformed to clay, which can explain the thick clay layer in Grézieu (Goutaland, 2009).

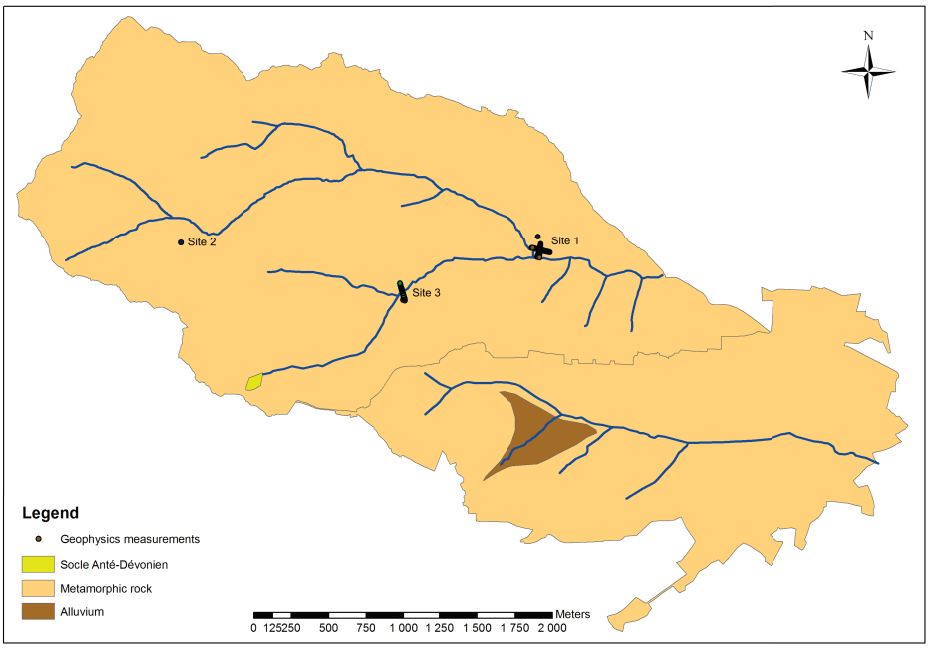

Figure 3.1.3.: Geology map of Mercier and Chaudanne (BRGM, 2011) and location of geophysics measurement (Goutaland, 2009).

In order to get a better idea of the geology and soil depth, Goutaland (2009) made geophysics field investigations on three sites in the Mercier catchment (see Figure 3.1.3 for the locations) using geoelectric methods. Two perpendicular profiles were measured at site 1, which is also the site where Gnouma (2006) installed a couple of piezometers. The interpretation of the profiles can be seen in Figure 3.1.4. In the upper part of the investigated hillside, the bedrock appears at the surface. However, below the Mercier river, the bedrock consisting of fissured gneiss starts at a depth of about 6 m. The alluvium at this site is about 2 to 3 m and between this two layers a layer of sandy-clayey alteration formation was found, which was saturated during the investigation period. This layer covers locally the whole profile (up to 20m). The perpendicular profile allows the interpretation, that the profound alteration follows the structural plan of the Plateau des Monts du Lyonnais. The second site was located in the steep upper part of the Mercier catchment, which is covered by forest. Due to the porous soil at the surface, the contact with the electrodes was bad, which makes the interpretation difficult. Nevertheless, the bottom with less slope could be distinguished from the upper part, as it has a higher conductivity, which can be caused by an elevated clay content or saturation. One profile was measured at the third site, located just below a confluence. This profile is similar to the one at the first site, with a three to four meters layer of alluvium around the Mercier stream and a saturated weathered layer of up to 18 m. On the left bank of the Mercier, the fissured bedrock comes up to 8 m below the surface.

The geophysics investigations showed thus that the bedrock appears between surface level and more than 20 m depths, which is accompanied by a weathered layer varying between 5 and more than 20 m depths. The water storage capacity of the underground in the Mercier and Chaudanne catchments is thus low, due to the high clay content of the weathered gneiss. However, this can induce the creation of local aquifers and soil

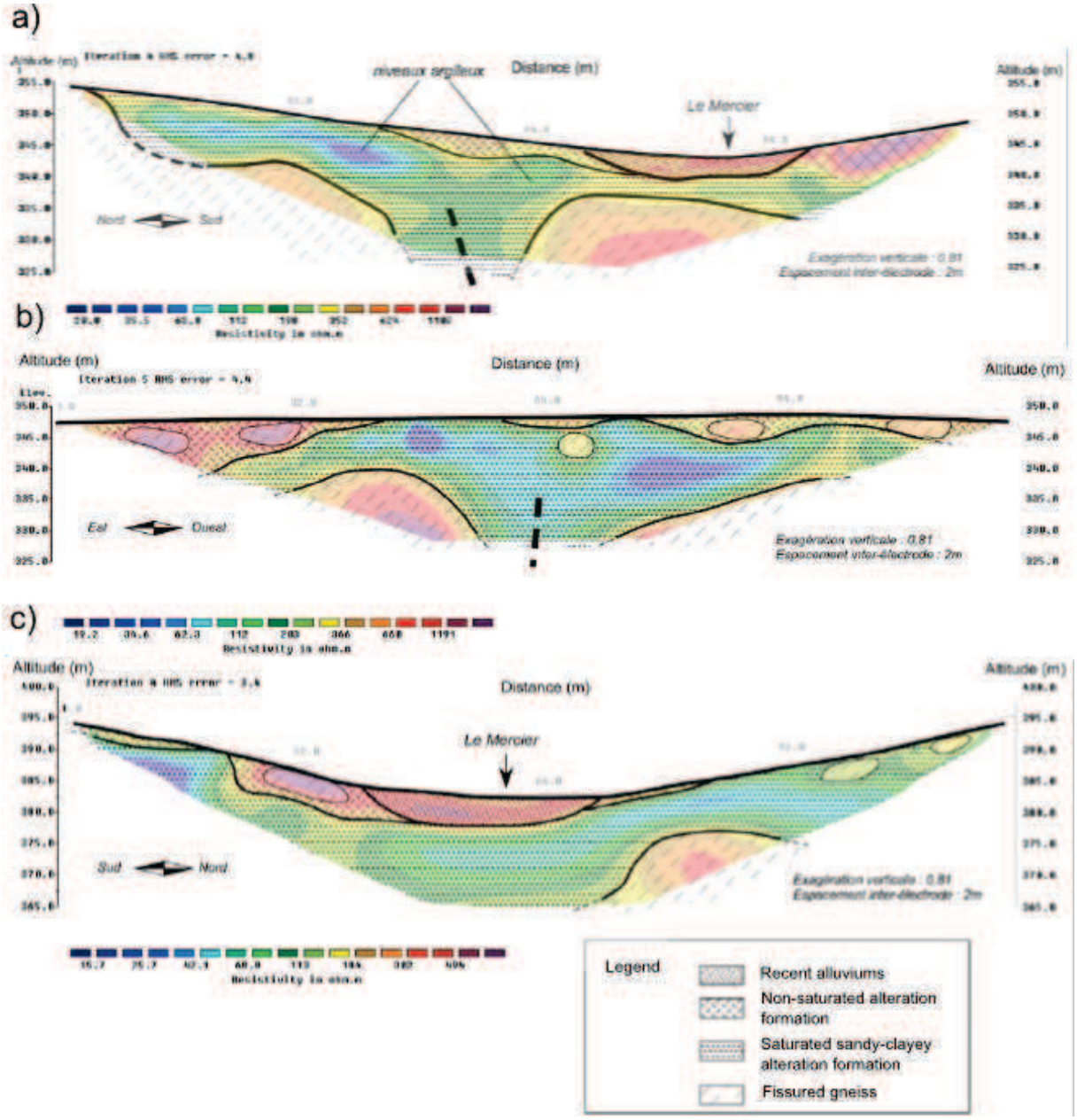

Figure 3.1.4.: Interpretation of profiles obtained by geophysical measurements (electric resistivity). a) site 1 (Gnouma, 2006)(profile crossing the river), b)site 1 (profile perpendicular to profile a)), c) site 3 (profile in the south, crossing the river) (Goutaland, 2009).

saturation, which can be regularly observed on the field. The alluviums and colluviums can represent local aquifers, and some water can be stored in the fissured gneiss which can explain the lean sources found on the field (Gnouma, 2006).

3.1.3. Soil

The soils, shown in Figure 3.1.5 consist mainly of silty or clayey sands developed from gneiss or mica-schists, except a small part on the top of the Mercier catchment, in which the soil developed from tuff. Furthermore, the soils developed from alluviums and colluviums are differentiated, see table 3.1.1. The colluvium soils cover most of the valley floors,

whereas soils developed from alluvium can only be found in the lower Mercier catchment. Some hydromorphic soils can also be found in the Mercier catchment. The soil types are different kinds of brown earth and fluviosols in the valley floors.

The soil data are available within the DONESOL database (SIRA, 2011). The database is linked to the soil map via the cartographic soil units No_uc. One No_uc can have several soil units, see table 3.1.1 for the soil units present in the Chaudanne and Mercier catchments. The soil units can contain several layers (strates) of different thicknesses, which are specific for each soil unit. The structural data and chemical components of the soil are given per soil layer. No information is provided for urban soils.

Table 3.1.1.: Soil data for Chaudanne and Mercier catchment of SIRA (2011) including the cartographic soil type No_uc and the soil type No_us.

NoUc	Soil texture	Soil name	No_us
100	urban soil	urban soil	-
102	Silty sands and clayey sands developed from gneiss and mica-schist	Acid brown earth (typical alocrisol), superficial sandy-silty soil developed from crystalline rock	4(50%)/ 5(50%)
702	Silty sands and clayey sands developed from gneiss	Acid brown earth (typical alocrisol), superficial sandy-silty soil developed from crystalline rock	4
704	Sandy-silty to sandy-clayey colluviums on slope	Colluvial brown earth (typical colluviosol), silty-sandy to sandy-silty, average depth, thalweg, developed from crystalline rock	12
1031	Silty sand developed from tuff, alt. $>$ 70m, pine forest	Ocher brown earth, cryptopodzolic and ocher podzolic characteristics (alocrisols and humus podzosols) rocky, developed from crystalline rock	9(70%)/ 8(30%)
7021	Silty sands and clayey sands developed from gneiss (colluvium)	Acid brown earth (typical alocrisol), silty-sandy, average depth, developed from crystalline rock	5
7041	Sandy-silty to sandy-clayey colluviums of thalwegs	Colluvial soil (typical colluviosol), silty-sandy to sandy-silty, deep, thalweg, developed from crystalline rock	13
7042	Sandy-clayey to clayey-sandy alluviums of thalwegs and narrow valleys	Alluvial soil (typical fluviosol), silty-sandy to sandy-silty, deep, from valleys with crystalline relief	15(70%)/ 16(30%)
7043	Sandy-clayey to clayey-sandy alluviums of thalwegs and large valleys	Hydromorph alluvial soil (reduced fluviosol), sandy-silty, deep, from valleys with crystalline relief	16

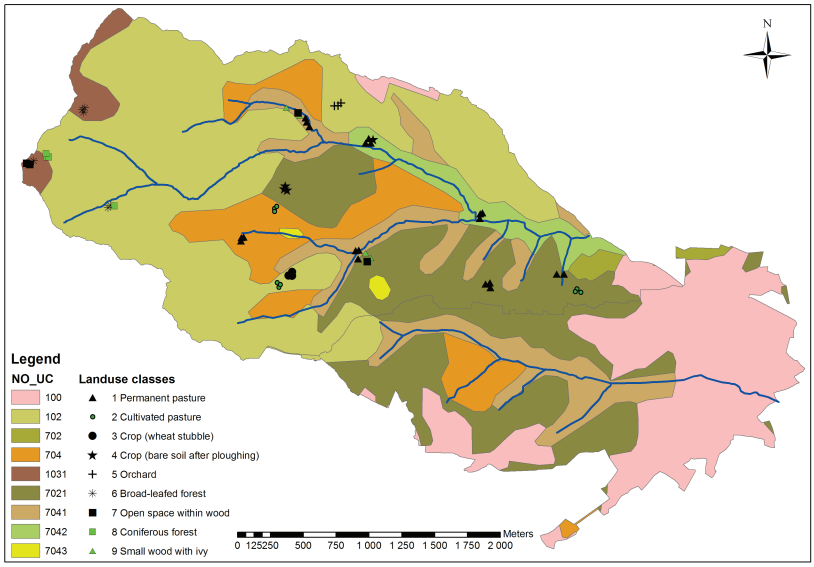

Figure 3.1.5.: Soil map with cartographic soil units (No_uc) for the Chaudanne and Mercier catchment (SIRA, 2011) and the measurement points of the field campaign including the on site land use classification (Gonzalez-Sosa et al., 2010).

Additionally to the information available in the database, Gonzalez-Sosa et al. (2010) conducted a field campaign in order to document the topsoil hydraulic properties. Initially, the sampling sites were chosen based on the overlapping of soil (Figure 3.1.5) and Corine land cover map (EuropeanEnvironmentAgency, 1994), but the data were analyzed according to the actual in situ land use. The objective was to get values for each combination. The measurement sites are shown on map 3.1.5. The infiltration rate was measured with single ring infiltrometers under positive head and mini-disk infiltrometers under -20 mm suction. Each measurement was repeated three times. Furthermore, the particle size and organic matter were analyzed in the laboratory (Gonzalez-Sosa and Braud, 2009a). The BEST (Beerkan Estimation of Soil Transfer parameters, Lassabatère et al. (2006)) method was used to derive soil hydraulic properties. This field campaign showed the strong influence of land use on the topsoil hydraulic properties, which means that soil texture data alone might not be sufficient to characterize the soil hydraulic properties. The results were summarized in the soil hydraulic properties map shown in Figure 3.1.6. Seven dry-bulk and saturated hydraulic conductivity classes were determined and attributed to a certain land use type. The saturated hydraulic conductivities classes ranged from 0.1 mm s^{-1} to 2.87 mm s^{-1} and the dry bulk densities from 695 to 1382 kg m^{-3} on average (Gonzalez-Sosa and Braud, 2009a). During the first field campaign in October 2008 only the topsoil hydraulic characteristics were measured. So, a second field campaign in February 2009 aimed at measuring the soil hydraulic properties at 15 and 30 cm depths. The experiment protocol and data analysis were the same as for the first field campaign (Gonzalez-Sosa and Braud, 2009a).

3.1.4. Land use

The land use of the Mercier and Chaudanne catchment is discernible from the aerial photography of Figure 3.1.7. The zones can be distinguished. The upper part of the

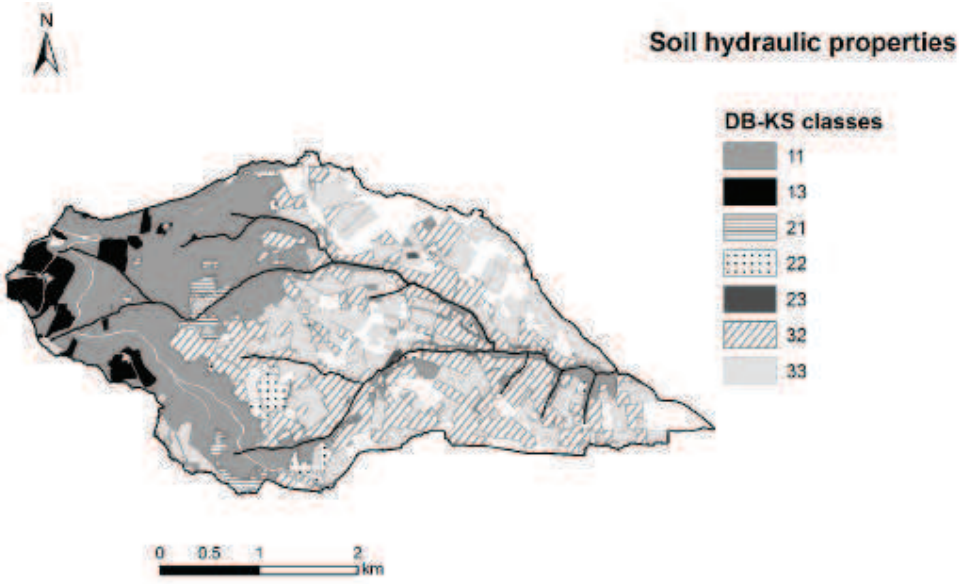

Figure 3.1.6.: Soil hydraulic properties map of the Mercier basin from reclassified dry-bulk (DB) and saturated hydraulic conductivities (KS) (Gonzalez-Sosa et al., 2010). The following land use was attributed to the DB-KS classes: 11 broad-leaved forest; 13 coniferous forest; 21 scattered trees, hedges; 22 moors, heathland, fallow land; 23 pasture; 32 ploughed fields, scattered grass; 33 orchards, berry plantation, wasteland, dump sites, spaces under construction, cemeteries

Mercier catchment is mainly covered with broad-leaved forest and a little bit of pine trees. The lower part of the Mercier and upper part of the Chaudanne catchment are covered by rural zones with agricultural activity, some settlements and trees along the river network and field borders. The lower part of the Chaudanne catchment consists of urban areas with residential zones, business parks and a big supermarket adding the largest impervious surface in the catchment.

The 2008 aerial photography (Figure 3.1.7) was the basis for the detailed land use map shown in Figure 3.1.8. The land use map was digitized manually by remote sensing specialists of the UMR 5600 in the framework of the AVuPUR project (Béal et al., 2009; Jacqueminet et al., 2011). 22 land use classes were determined which describe forest (values starting from 100), agricultural objects (values starting from 200), water bodies (403), roads (502, 513) and urban objects (starting from 600). The zoom in Figure 3.1.8 shows the same extract as shown in the aerial photography (Figure 3.1.7) and thus, it illustrates the interpretation of the aerial photography. The agricultural field borders and urban parcels of the land use map are aligned with the cadastral limits.

3.1.5. Topography

A digital elevation model (DEM) of 5m grid size was created with the point elevation data of the BD Topo (IGN) with a precision of 25m by Dehotin (2009b) and a DEM with 25m grid size by Gnouma (2006). The slope derived from the DEM is shown in Figure 3.1.9. We can see that the upper part of the Mercier catchment is steep with slopes up to 45 degrees. The topography of the lower Chaudanne catchment is less pronounced, except along the stream valleys.

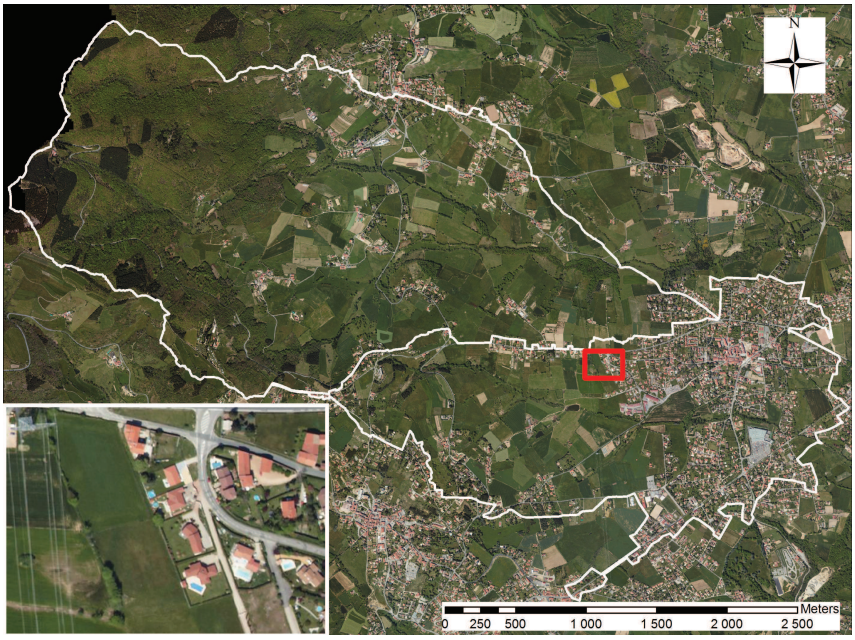

Figure 3.1.7.: 2008 aerial photography of the Chaudanne and Mercier catchments (IGN BDOrtho) including the zoom of a rural/urban limit with hedgerows.

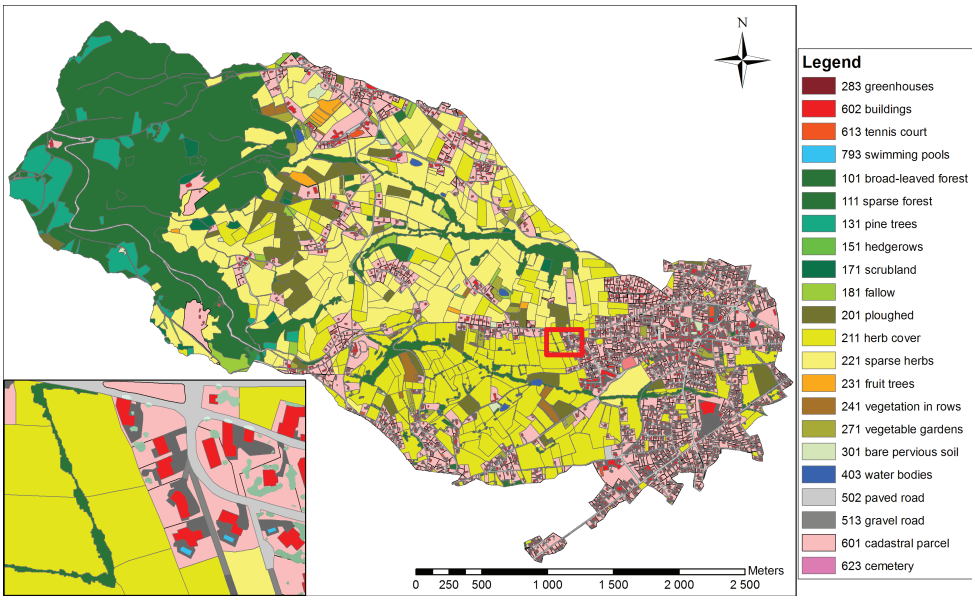

Figure 3.1.8.: Detailed land use map of Mercier and Chaudanne catchment based on the 2008 aerial photography (IGN BDOrtho). The land use map was digitized by the UMR 5600 in the framework of the AVuPUR project (Béal et al., 2009; Jacqueminet et al., 2011). The same zoom is shown as for the aerial photography.

For the Mercier catchment and the upper part of the Chaudanne catchment Lidar data were obtained in the framework of the AVuPUR project, see Figure 3.1.10. A DEM of 2m resolution was created in the context of the PhD thesis of Sarrazin (2012). The high precision of the Lidar data allows the distinction of anthropogenic objects such as roads. The altitude of the Chaudanne catchment goes from 300 m up to 520 m a.s.l., and the altitude of the Mercier catchment from 325 m to 750 m a.s.l.

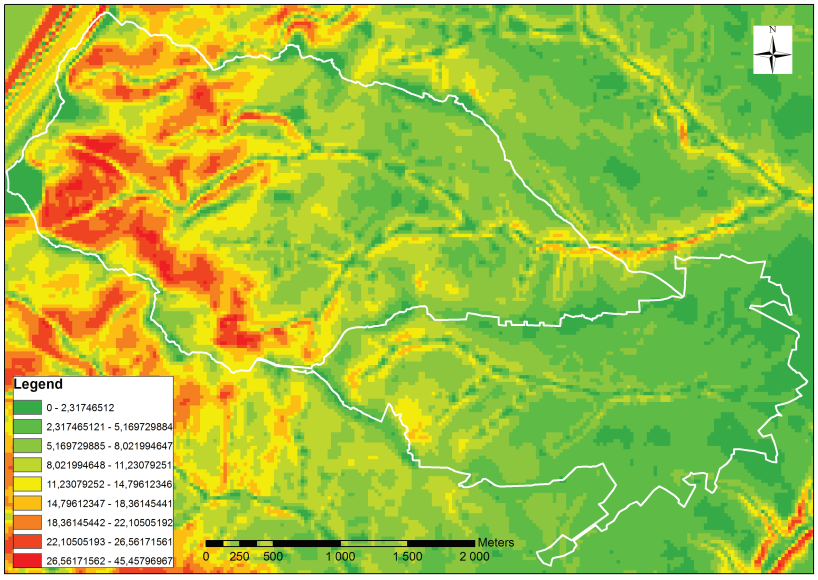

Figure 3.1.9.: Slope map (in degrees) of Mercier and Chaudanne catchment calculated from the 25m resolution DEM (BD Topo IGN).

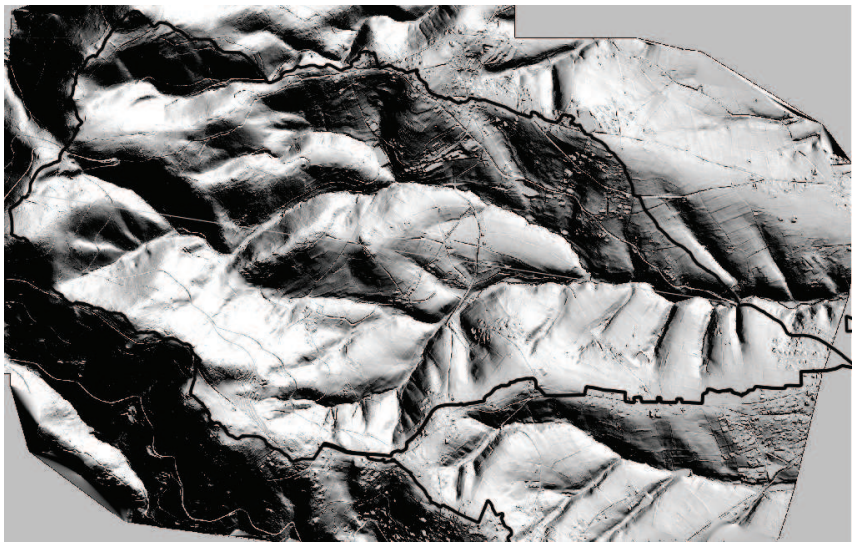

Figure 3.1.10.: Lidar DEM and extent including the catchment borders of Mercier and Chaudanne.

3.1.6. Drainage network

The natural drainage network of the Chaudanne and Mercier catchments is given by the BD Topo (IGN), see Figure 3.1.11. The catchment outlets to which we refer to in this PhD thesis are defined by the Cemagref gauging stations. The Chaudanne stream has four intermittent tributaries, whereas the Mercier stream arises from the confluence with the Bouillon and Presles streams. It drains eight thalwegs with temporary tributaries. The Chaudanne is a direct tributary of the Yzeron river, whereas the Mercier flows into the Ratier stream. Parts of the Chaudanne and the Mercier are retained in artificial lakes for irrigation purpose. No sewer system is connected to the Mercier stream, although, a waste water pipe is installed below the stream bed, which can induce a draining effect. The sewer data of the Mercier catchment were digitized manually at the community of

Pollionnay (see Figure 3.1.1 for location). The sewer pipe location is approximative. A sewer network, consisting of combined and separated sewer pipes, covers the lower urban part of the Chaudanne catchment. The combined sewer system leads to a WWTP outside the catchment area. The sewer data were provided by the SIAHVY, which is responsible for the waste water of Grézieu. The sewer data indicate four storm water overflow devices connected to the Chaudanne stream and eight pumping stations. The parts close to the river are equipped with separate rain water pipes directly connected towards the river. The data of the rainwater pipes were gathered separately by means of a visit to the SIAHVY and the town hall of Grézieu, as no rainwater data were originally available.

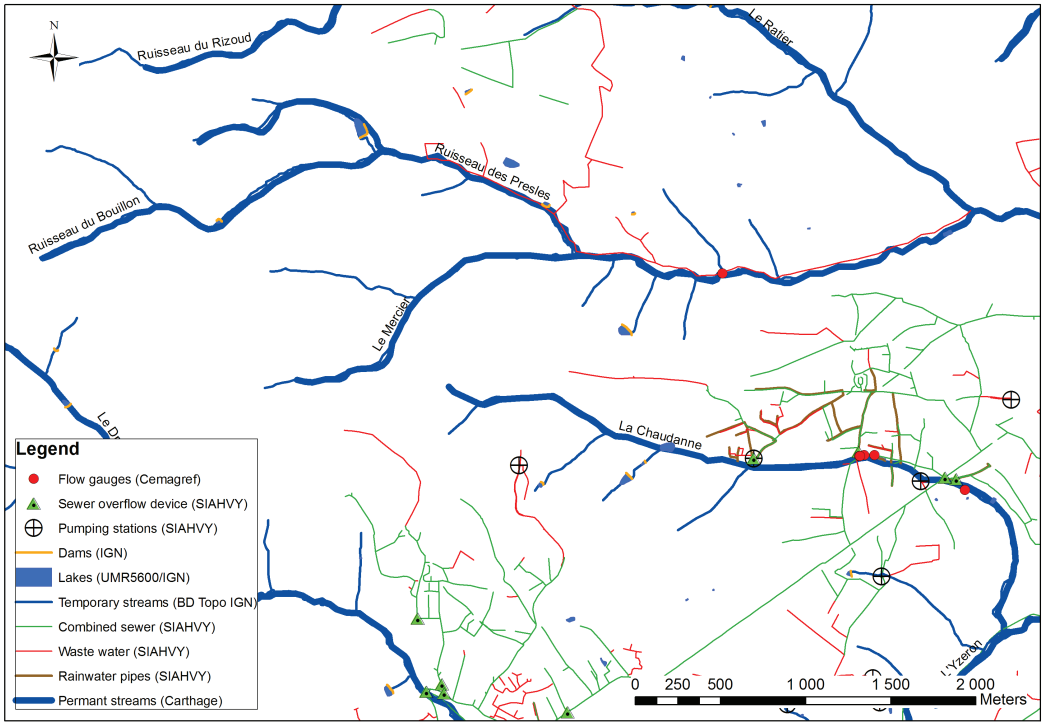

Figure 3.1.11.: The drainage network of the Mercier and Chaudanne catchment consisting of the natural river, lakes, the combined sewer system and waste water pipes.

3.2. Description of hydro-climatic data

The following chapter describes the available hydro-climatic data time series, such as evapotranspiration, precipitation, discharge or water levels. The measurement stations and their data availability are summarized in table 3.2.1. Furthermore, a review of the data analysis and statistics is given.

3.2.1. Evapotranspiration

Direct measurements of meteorological parameters are scarce on the Yzeron catchment. The weather station "Le Thiollet" in the Yzeron catchment, located at Montromant, was only installed in 2008 by the Cemagref (table 3.2.1, see Figure 3.1.1 for its location). The closest weather station with a longer time series is in Bron, which is about 19 km away

Table 3.2.1.: Hydro-climatic data of the Mercier and Chaudanne catchments (Thollet and Branger (2008), Lagouy (2009) and Braud (2008a)). The catchment area is shown for the discharge data and the altitude for the rest of the data. SOD means sewer overflow device, PdB is the Pont de la Barge in Grézieu-la-Varenne, DO8 is the sewer overflow device 8 (SIAHVY) and PET is the potential evapotranspiration. The abbreviations for the stations used in the text are given in brackets.

Type	Catchment	Location (Name)	Altitude/ Area	Data availability since
Rain	Mercier	Pollionnay	320m	21/12/1996
	Mercier	Col de la Luère		03/04/2009
	Mercier	Sarrazin 1		09/2008-03/2011
	Mercier	Sarrazin 2		04/2009
	Mercier	Pluvio Dehotin 1		05/2010-05/2011
	Mercier	Pluvio Dehotin 2		05/2010-05/2011
	Mercier	Pluvio Dehotin 3		05/2010-05/2011
	Chaudanne	Grézieu PdB 0.1mm Grézieu PdB 0.2mm new location at retention basins	320m 320m 313m	21/12/1996-2001 2001-2005 2005
	Yzeron	Croix du Ban	602m	10/02/2005
Rain & PET	Yzeron	Le Thiollet, complete climate station		04/2008
PET	Yzeron	SAFRAN data		1970-2010
Discharge	Mercier	D610 (MerD610)	6.7km^2	1988
	Chaudanne	PdB before SOD (UpstreamSOD)	2.18km^2	16/06/1997 gap 07/2001-12/2004
	Chaudanne	PdB after SOD (VPdB)	2.38km^2	1988
	Chaudanne	PdB in SOD (SOD)	0.16km^2	06/2001
	Chaudanne	PdB sewer system (SS)	0.16km^2	13/8/1997
	Chaudanne	La Léchère (ChauLech)	4.1km^2	01/01/1999 reliable since 2005
	Chaudanne	DO8 Léchère (LechSOD)	1.06km^2	07/2010
	Chaudanne	Inflow/outflow 1. basin	0.24km^2	09/2011
Water level	Chaudanne	PdB retention basin 1	0.24km^2	2003-2010
	Chaudanne	PdB retention basin 2	0.24km^2	2003-2010
	Chaudanne	PdB retention basin 3	0.24km^2	2003-2010
	Mercier	18 limnimeters (Sarrazin, 2012)		2007-2009
Piezometers	Mercier	Site Gnouma (2006)		2005-2006
	Chaudanne	PdB Ruysschaert	320m	2004-2005
	Chaudanne	PdB Invasion downstream SOD		11/2010
	Chaudanne	PdB Invasion upstream SOD		01/2011
Soil moisture	Mercier	8 sites (DeLavenne, 2010)		05/2010-05/2011
	Mercier	15 sites (Braud, 2009)		2009-03-12/13
	Chaudanne	PdB Ruysschaert	320m	2004-2005

from Grézieu. However, it is located at a lower altitude in the Rhône plain, compared to the mountainous topography of the Yzeron catchment (Vannier and Braud, 2010). However, the climatic data of the meteorological reanalysis SAFRAN (Quintana-Seguàŋ et al. (2008), Vidal et al. (2010)), having a time step of one hour and a resolution of 8x8 km^2, are available for whole France from 1958 on. The SAFRAN data are derived from observations leading to 6h vertical profiles of temperature, humidity, wind speed and cloudiness. These data are further temporally and spatially interpolated to obtain the final gridded hourly output since 1958 (Vidal et al., 2010). The hourly SAFRAN data were available on the Yzeron catchment on the period 1970-2010. Based on the SAFRAN data, the potential evapotranspiration (PET) can be calculated using different equations. Vannier and Braud (2010) compared the calculation of PET based on the FAO method (Allen et al., 1998) and a method proposed by Etchevers (2000) based on the Penman equation. They also compared those results with data from the Météo France Climathèque which uses a formula derived from the Penman-Monteith equation with different surface resistance. Common international practice is the use of the Penman-Monteith equation for the calculation of the PET, which is recommended by the FAO (Vannier and Braud, 2010). Vannier and Braud (2010) compared the results of both equations using the SAFRAN climatic data with the PET from the Bron weather station for the 1997-2004 period. Even if the PET obtained with the Penman-Monteith equation was inferior to the Bron PET and the Penman PET, Vannier and Braud (2010) suggest to use the Penman-Monteith equation. This is justified by the fact, that all three PETs are estimations, and we do not have knowledge about the right PET. Furthermore, the Penman-Monteith equation corresponds to the international standard. For this reason, Vannier and Braud (2010) prepared the PET from 1970 to June 2010 for use as input variable for the hydrological modelling in this PhD. Only the time series of one grid cell was used as input, because of the coarse resolution of 8x8 km^2 and the small differences amongst grid points.

Figure 3.2.1 shows the monthly values of the potential PET and its interannual variability. The PET follows a seasonal trend, reaching its maximum in July with values around 120 mm and its minimum in December with values around 20 mm.

3.2.2. Precipitation

3.2.2.1. Measurement stations

The locations of the rain gauges are visible in Figure 3.2.2 and the data availability is shown in table 3.2.1. At the end of 1996 the Cemagref installed a tipping bucket rain gauge in the Chaudanne and Mercier catchments, respectively. These rain gauges have been recording continuously using a variable time step since then. Only in 2001 the bucket capacity of the Chaudanne rain gauge was changed from 0.1 to 0.2 mm and in 2005 it was moved to the retention basins at the Pont de la Barge (PdB), see zoom in Figure 3.2.2. In 2005 the rain gauge at Croix du Ban, which is at an altitude of 602 m, compared to the altitudes of 320 and 313 m of the Chaudanne and Mercier rain gauges, was added (Braud, 2008a). This station gives more representative values for the upper part of the Mercier catchment, as it is located higher up in the Mont du Lyonnais. During the PhD thesis of Sarrazin (2012) two rain gauges (named Sarrazin-1 and 2) were installed in the Mercier catchment. The first one was installed in September 2008 close to Pollionnay (see Figure 3.2.2) and it was removed in March 2011. The other one was installed in April 2009 in

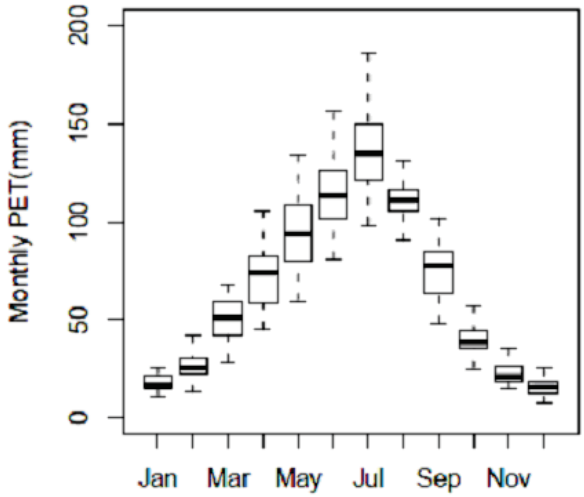

Figure 3.2.1.: Monthly PET values (mm) values and its interannual variability for the period 1970-2010 calculated from SAFRAN data for the Mercier catchment. The graphic was provided by I.Braud.

the south of the catchment (Lagouy, 2009). A complete climate station, "Le Thiollet", was set up on the top of the Yzeron catchment at Montromant (see Figure 3.1.1). It has a balance rain gauge to measure liquid and solid precipitation continuously (Thollet and Branger, 2008). The long-term Cemagref measurement stations are part of the OTHU program.

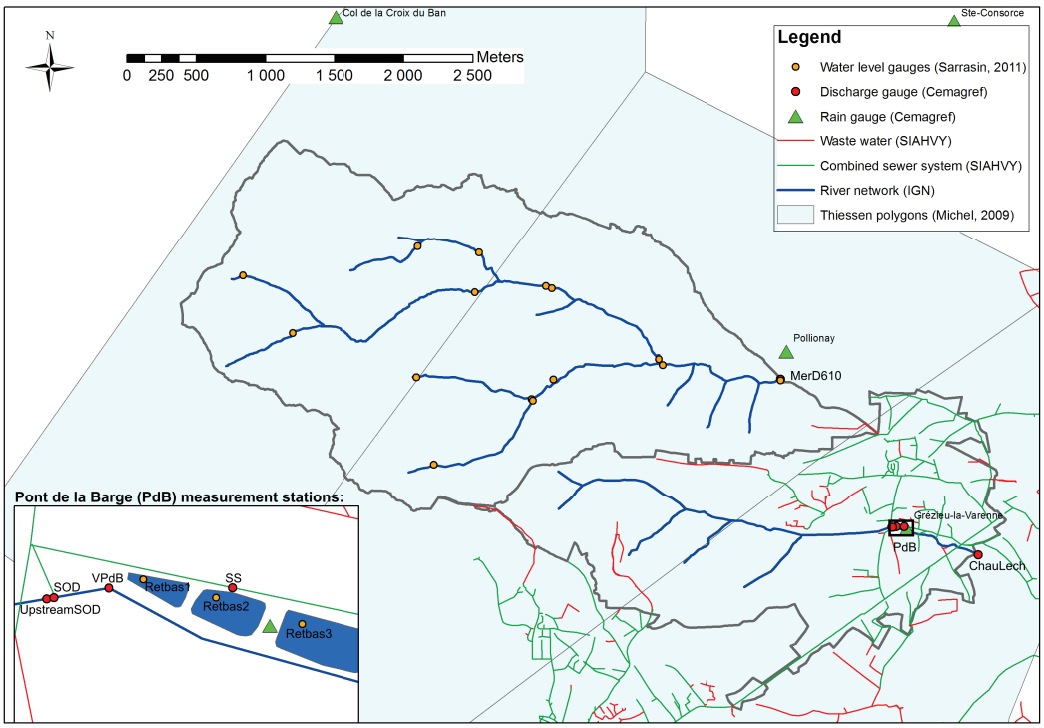

Figure 3.2.2.: The drainage network and rain, discharge and water level measurement stations in the Chaudanne and Mercier catchment. The Thiessen polygons (Michel, 2009) are also shown.

3.2.2.2. Main characteristics of rainfall series

Braud (2008a) analyzed and corrected the rain data of the Mercier and Chaudanne rain gauges for the period 1997 to 2007. The data were validated by comparison of the daily rainfalls of the Chaudanne and Mercier rain gauges. Periods with missing data were then replaced with the data of the other station (Chaudanne or Mercier), respectively. If no data were available for both stations, the average of four nearby stations from the Grand Lyon was taken (see Figure 3.1.1 for the location of the other stations). A time series with a time step of 6 min (time step of Grand Lyon data) was then generated. This lead to a complete rain data time series from 1997 to 2007 for both stations with variable, or 6 min time step, which is available as model input. Michel (2009) continued the analysis and correction of the data including the data of 2008. She used the same correction method as Braud (2008a), in which missing values were replaced by close-by rain gauge data. The Sarrazin-1 rain gauge was used additionally to fill the gaps. However, it had too many gaps to create an independent time series itself. Michel (2009) also processed the data of the Croix du Ban rain gauge by replacing the missing data with the average of the Mercier and St Consorce rain gauge. Chapuis (2010) corrected the 2009 data of the Mercier, Chaudanne, Croix du Ban and Le Thiollet rain gauges. He replaced the missing data with the data of the station with the best correlation, which could be the four mentioned stations or the stations of the Grand Lyon, when no records of the Cemagref gauges were available. Finally, the 2010 rain data were corrected by Braud et al. (2011b).

Michel (2009) calculated Thiessen polygons for the Yzeron catchment out of the Grand Lyon gauges and Mercier, Chaudanne, Croix du Ban and Le Thiollet. The Mercier and Chaudanne catchments can thus be covered with the values of Mercier, Chaudanne and Croix du Ban rain gauges, see Figure 3.2.2. This segmentation corresponds also relatively well to the altitude distribution of both catchments. For these reasons, the Thiessen polygons were considered sufficient as model input.

The precipitation has a strong inter annual variability with yearly rainfalls from 450 mm (1998) to 950 mm (2002) (Braud, 2008a). This means that there are relatively dry and in contrast wet years. The yearly rainfall data for the three stations Mercier, Chaudanne and Croix du Ban from 1997 to 2010 are shown in table 3.2.2 (Chapuis, 2010). The catchment average rainfall was calculated using weighted average of the gauging stations, based on Thiessen polygons. The average annual precipitation between 1997 and 2010 was thus 741 mm for the Mercier catchment and 744 mm for the Chaudanne Léchère catchment with standard deviations of 156 mm and 165 mm, respectively.

Daily maximal rainfall values can reach up to 130-140 mm, and each year from 2002 to 2009 there was at least one day with a total rainfall of 44.60 to 76.0 mm (see "annuaires hydrologiques du bassin versant de l'Yzeron" from 2001 on, Cemagref). The study of the rainfall regimes (Figure 3.2.3) shows that the rainfall is usually higher in October and November, which leads to a recharge of the groundwater table (Gnouma, 2006). The winter months from December to March are marked by relatively low rainfall rates. The extreme events can happen all over the year.

Braud (2008b) extracted rain events from the 1997-2007 data series using the software developed by Berthier (1999) and calculated frequency statistics for the Mercier and Chaudanne catchment (see also Morena (2004)). More than 275 events in both catchments were induced by a total rainfall of less than 10 mm and about 100 events had a

Table 3.2.2.: Yearly rainfall (mm) and averages at Mercier, Chaudanne and Croix du Ban rain gauges (Braud (2008a), Michel (2009), Chapuis (2010), Braud et al. (2011b)).

Rain gauge	Mercier	Chaudanne	Croix du Ban	Average
1997	576.7	521.3	-	549
1998	446.7	472.1	-	459.4
1999	737.1	737.2	-	737.1
2000	663.5	676.3	-	669.9
2001	816.2	825.6	-	820.9
2002	955.8	973	-	964.4
2003	653	655.3	-	654.2
2004	915.2	892.8	-	904
2005	656.2	650.3	617.2	653.3
2006	745	677.8	751.4	711.4
2007	920	938.2	863.8	929.1
2008	826.4	965.4	965.4	919.1
2009	558.6	578.3	678.9	605.3
2010	909.3	855.1	847.9	870.8
Average	741.4	744.2	793.1	
Std	156.3	165.7	127.8	

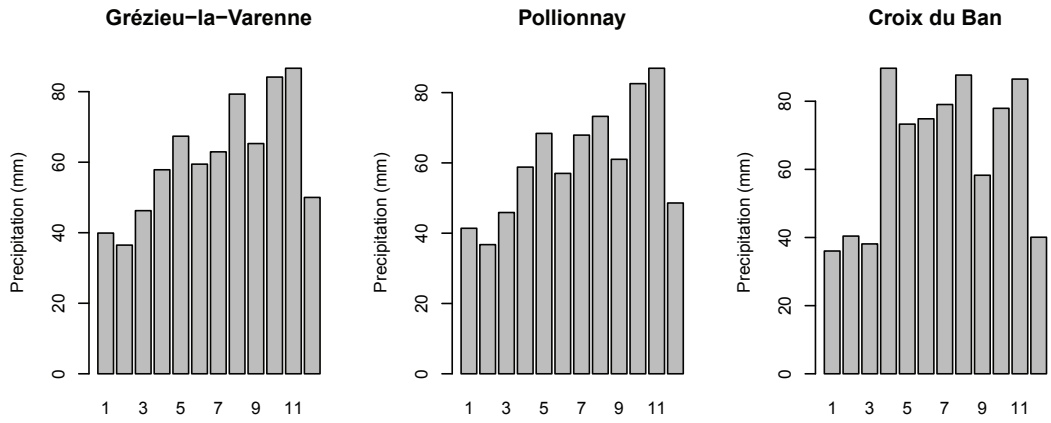

Figure 3.2.3.: Average monthly rainfall from 1997 to 2009 at Grézieu-la-Varenne and Pollionnay and from 2005 to 2009 at Croix du Ban. Data from Cemagref, R scripts provided by I.Braud.

total rainfall between 10 and 20 mm. Some extreme events reached a total rainfall of up to 140 mm. The maximal rain intensity is between 0 to 10 mm/hr for most events (around 300). Around 100 events per catchment reached a maximal rain intensity of 10 to 20 mm/hr. The highest measured rain intensity in the period 1997-2007 was around 130 mm/hr. The dry weather rainfall (sum of rainfall between events) is mostly between 0 and 5 mm, but can reach up to 50 mm in the Mercier catchment, and up to 40 in the Chaudanne catchment. Michel (2009) calculated the statistics for the period 2005-2008 with similar results.

3.2.3. Discharge

3.2.3.1. Description of measurement stations

The locations of the discharge measurement stations are shown in Figure 3.2.2 and the data availability is listed in table 3.2.1. The informations given below are taken out of the yearbooks (from 2000 to 2009) of the Cemagref HHLY metrological team, especially Thollet and Branger (2008), Lagouy (2009) and the hydrological data analysis of Braud (2008a). In 1988 the Cemagref installed the measurement stations under the bridge of the D610 over the Mercier stream (MerD610) and under the old bridge at Pont de la Barge over the Chaudanne (VPdB). The Mercier stream at the measurement station drains an area of 6.77 km^2 and the Chaudanne a surface of 2.18 km^2. The water level is measured continuously with a variable time step and the data are transmitted daily to the Cemagref via automatic telephonic calls. The water level can be transformed to discharge data using rating curves. In 1997 two stations were added to the site at the Pont de la Barge: in the river just upstream of a sewer overflow device (UpstreamSOD) and in the sewer system downstream of the sewer overflow device (SS). The distance between the two stations in the Chaudanne river is just about 10 meters. In 1999 a measurement station was added further downstream to the Chaudanne river at "La Léchère" (ChauLech), draining an area of 4.1 km^2. However, the data are only reliable since 2005. In 2001 a flowmeter was installed in the sewer overflow device (SOD). All the measurement stations are part of the OTHU program.

Michel (2009) compared the discharge of the different measurement stations of the Chaudanne river for several events. For some events, the discharge of a downstream station was superior to the discharge of an upstream station. Especially for VPdB this indicates errors in the discharge measurements, as the discharge should correspond to the sum of the SOD discharge and the discharge of the upstream station. Losses due to infiltration between the stations are quite unlikely, as the stations are close to each other. In particular for the VPdB station no discharge gauging for the rating curve was made at higher flows due to a bad site configuration. The rating curve is thus highly extrapolated for higher flows, which leads to strong uncertainties of high discharge values. Furthermore, the low discharge values are also subject to uncertainties as the measurement is difficult due to the large cross-sections of some stations (in particular the VPdB and the MerD610 stations) (Branger, 2008a): The same error of water level measurement will have a higher impact on low flows than on high flows. Of all six measurement stations, only the ChauLech station and the SOD station are equipped with a venturi canal, which allows an accurate measurement at low flows.

3.2.3.2. Main characteristics of river discharge series

Thollet and Branger (2008) describe the hydrology of the Chaudanne and Mercier as marked by flash floods and droughts. The hydrological regimes, calculated with the data period 1997-2010, are shown in Figure 3.2.4. We can see a seasonal effect with lower values from May to October and a maximum in November. The dynamics of the discharge regime do not correspond to the precipitation regime, but to the evapotranspiration regime. Consequently, the seasonal effect is mainly caused by evapotranspiration, as also concluded by Gnouma (2006). The rainfall in October serves thus mainly the recharge and has relatively low flows. The runoff coefficients are important in January and February. The

discharge regimes of the Mercier and Chaudanne show a similar behavior, when comparing to the UpstreamSOD measurement station, for which the same data period is available. We can see that the discharge in the sewer system follows also the seasonal trend, however due to the SOD the differences between minimums and maximums are smaller.

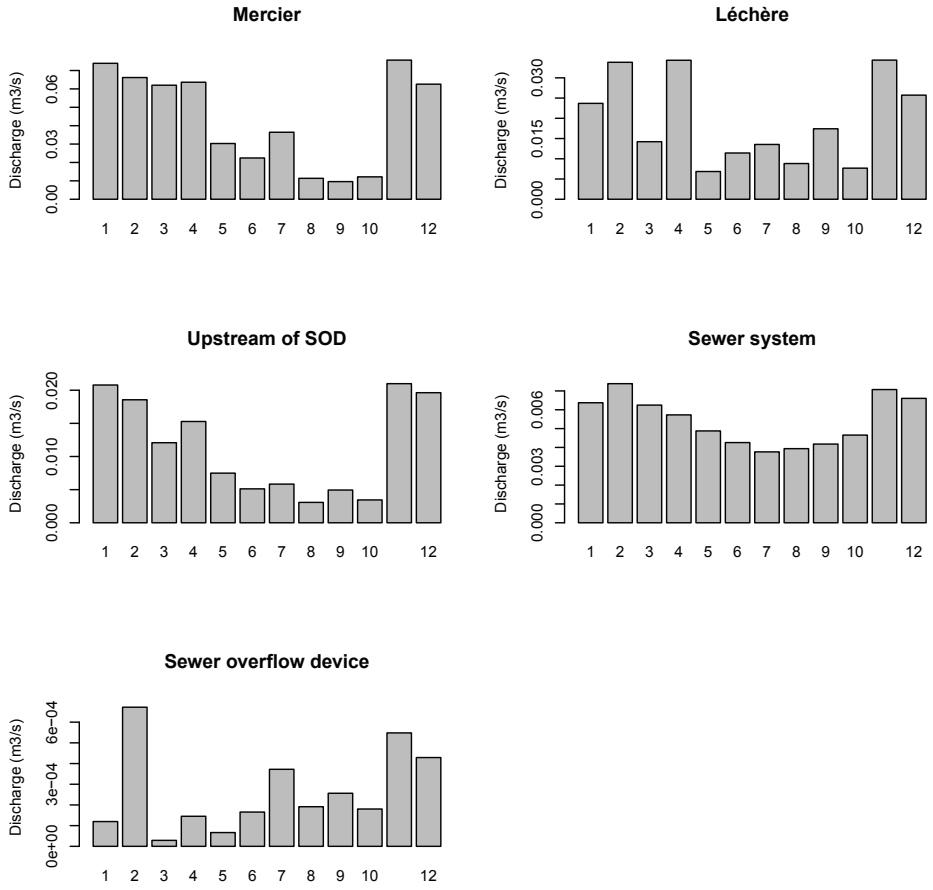

Figure 3.2.4.: Monthly averages of discharge data for the period 1997-2010 of the gauging stations Mercier and upstream of SOD, the period 2000-2010 for the sewer system data,the period 2001-2010 for the SOD data and 2005-2010 for the Léchère. Data from Cemagref, R scripts provided by I. Braud.

The events extracted by Braud (2008a) and Michel (2009) were also analyzed for their discharge data. The average event duration in the Mercier catchment is longer than in the Chaudanne catchment and takes on average about 15 hours. The event duration of the Léchère station is shorter than at UpstreamSOD, which can be explained by the greater urban impact in the lower part of the catchment. When comparing the statistics for the period 1997-2007 and the period 2005-2008 we can remark that the modus for the Mercier event duration changes from 16 to 25 hours in the earlier period to 8 to 16 hours in the later period. Braud (2008a) calculated the response time of the catchments with the 2007 data. The average response time of the Mercier catchment varies between 1 and 3-4 hours, whereas the response time for the Chaudanne catchment is shorter, having values from 30 min to several hours. From his analysis of the 1997-2004 period Gnouma (2006) concluded also that for small events the Chaudanne has shorter response

times caused by the urban zones than the Mercier. However, for intense rainstorms both catchments have similar hydrological comportment despite the difference in land use (Gnouma, 2006). For one event in the Mercier, Gnouma (2006) identifies a first peak with a nearly immediate response as water coming from an artificial ditch. This ditch arrives just before the measurement station and drains an urban area of Grézieu-la-Varenne. The dry weather rainfall duration for the period 2005-2008 is about 4 to 5 days for both catchments (Braud, 2008a). The maximal discharge of the Mercier can reach up to 12 m^3s^{-1} for extreme events, but the average is 0.34 m^3s^{-1} for the 2005-2008 period. In the Chaudanne catchment the extreme discharge values are 3 m^3s^{-1} and the average is 0.47 m^3s^{-1} at the Léchère and 0.13 m^3s^{-1} before the SOD. The exceedance probabilities are shown in Figure 3.2.5. The total event volume is around 9285 m^3 for the Mercier, around 2932 m^3 for the Chaudanne before the SOD and 5982 m^3 at the Léchère. The maximum measured total volume at the Mercier was about 600 000 m^3, and 120 000 m^3 at the Chaudanne before SOD and 180 000 m^3 at the Léchère. Michel (2009) calculated the total annual flow volume, which is very variable from year to year caused by the high variability of the rainfall. The volume for the Mercier is greater than for the Chaudanne at the Léchère station, which corresponds to the larger catchment area of the Mercier catchment. The total annual volume at Léchère is also greater than at PdB.

3.2.3.3. Main flow characteristics in sewer network

Chapuis (2010) analyzed the data of the sewer system and the sewer overflow device for the period 2001 to 2009, and Braud et al. (2011b) added the analysis of the 2010 data. They selected the discharge values in the sewer system at the moments when the sewer overflow device was activated. The activation discharge is variable with minimal values of 0.002 m^3s^{-1}, maximal values of 0.204 m^3s^{-1} and an average of 0.0315 m^3s^{-1}. Chapuis (2010) also applied the combined sewer runoff component separation method developed by Breil (2010) and published in Braud et al. (2011b). The water in the combined sewer system is composed of waste water, which depends on domestic activity, groundwater seepage and rain water. The method consists of four steps. If the sewer system is sufficiently small, the night domestic discharge should be zero. So, during dry periods the remaining discharge corresponds to the groundwater seepage which can be calculated with a minimum moving average. After subtraction of the groundwater seepage from the combined sewer water, a weekly discharge pattern for waste water can be defined. This weekly discharge pattern is considered constant over the year and used to create a yearly waste water time series. The rain water fraction results then from the addition of the SOD discharge to the combined sewer system discharge and subtraction of the waste water and groundwater seepage. For the combined sewer system at PdB the waste water fraction was on average 33.8 %, the groundwater seepage had 30.5 % and the rain water 39.0% for the period 2001-2010. If we compare the total mean annual flow volumes on the 2001-2010 period, the groundwater seepage is 46 184 m^3, whereas the natural Chaudanne stream before the SOD has only 572 265 m^3 (Michel, 2009). This means that the sewer pipe drains about 8 % of the catchment total volume. The average annual amount of waste water is 51 131 m^3 and of rain water 59 011 m^3 (Braud et al., 2011b). Figure 3.2.6 shows the rainwater and groundwater seepage in the combined sewer system from 2001 to 2010 as well as the monthly precipation data. The waste water fraction is not shown, as it is relatively constant over the time (Braud et al., 2011b).

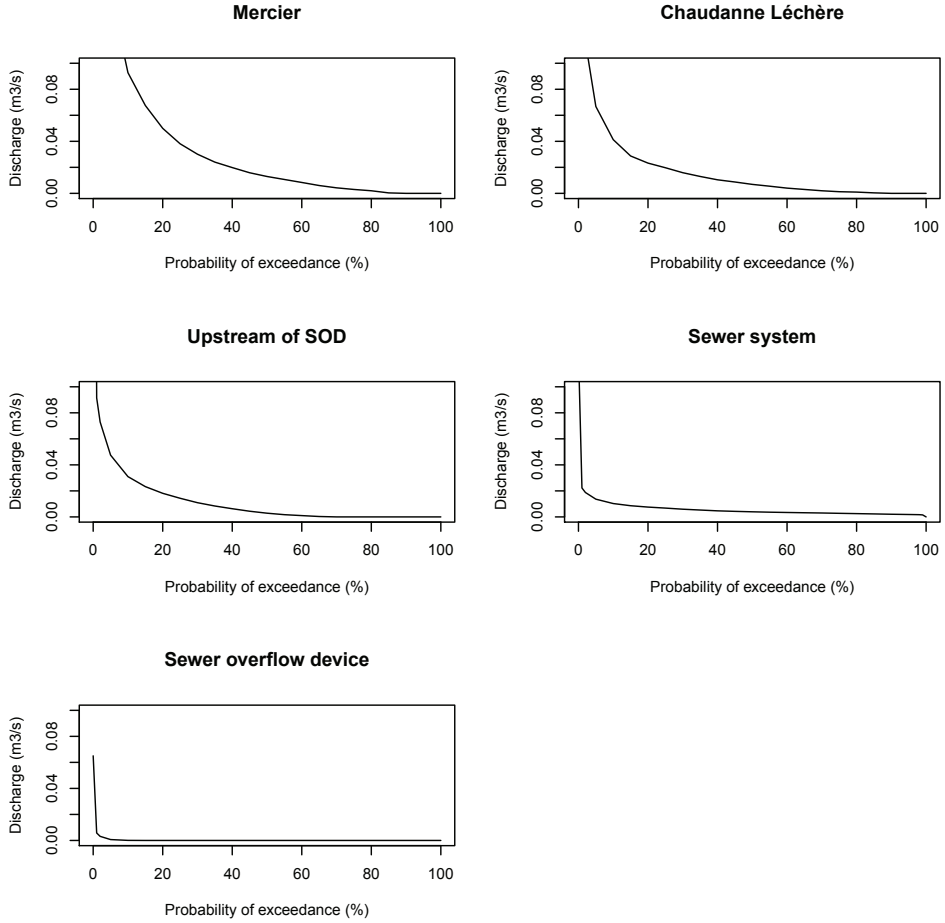

Figure 3.2.5.: Flow duration curves of daily discharges for the period 1997-2010 of the gauging stations Léchère, Mercier and upstream of SOD, the period 2000-2010 for the sewer system data and the period 2001-2010 for the SOD data. Data from Cemagref, R scripts provided by I. Braud.

3.2.4. Additional measured data

In addition to the discharge data mentioned earlier, the water level in each of the three retention basins at PdB is measured since their creation in 2003. However, these piezometric data were never analyzed nor validated. The limnimeters were never calibrated and the evolution of the basin bottom was never recorded. This makes the use of the data rather complicated. In the framework of the FAST project, the inflow and outflow of the first retention basin are measured since September 2011.

The SIAHVY, which is responsible for the sewer system in Grézieu installed in July 2010 a discharge measurement in the SOD upstream of the measurement station La Léchère. This SOD drains a great part of the urban zone of Grézieu.

3.3. Investigations of hydrological processes

In addition to longterm monitoring, temporary experiments on both catchments were carried out in the framework of different research projects, in order to investigate the hy-

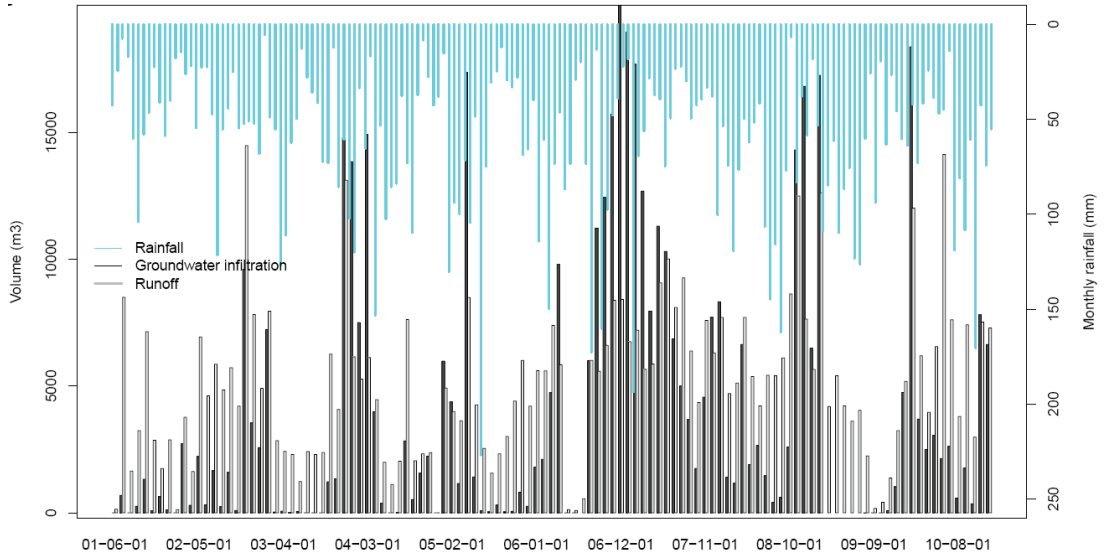

Figure 3.2.6.: Monthly values of rainwater and groundwater seepage in the combined sewer system at Pont de la Barge, as well as precipitation data (Braud et al., 2011b).

drological processes of the catchments. The results of these experiments provide elements for process understanding, which are important for the model construction. Furthermore, some of the data can be used for the validation of the model results. The research areas covered overland and subsurface flow processes, the water exchange between the river and the hyporheic zone, distributed soil moisture measurements, hydrograph separation based on geochemical tracers and the response of intermittent drainage reaches. The results are summarized in the following sections and their use for modelling is explained in section 3.5.3.

3.3.1. Overland flow

In the framework of the IRIP project (Dehotin and Breil, 2011), Dehotin et al. (2010), DeLavenne (2010) and Dehotin et al. (2011a) investigated the risk induced by overland flow in the Mercier catchment. Dehotin et al. (2010) proposed a classification into flow production zones, flow transfer and flow accumulation zones. Maps were produced for the production and accumulation by means of overlapping of five different factors in form of maps (see Figures 3.3.1 and 3.3.2). The topography, land use, infiltration capacity, topographic index and soil thickness were considered for the production map. The classes vary between 1 and 5 depending on how many of the factors enhance flow production see Figure 3.3.1. For example, strong slopes, agricultural, urbanized or bare soils, low infiltration capacities, low topographic indexes and thin soils resulted in the soil production class 5, which signifies the highest overland flow probability. For the accumulation map the geomorphology and upstream production were also considered. High slopes, high topographic indexes, large upstream production areas, round form factors with high convexity and sudden changes in slope produced the flow accumulation class 5, with the highest flow accumulation probability (Figure 3.3.2).

A 1-year field survey (May 2010 - May 2011) was undertaken to validate the methodology and enhance the hydrological process understanding. Eight sites (two accumulation sites, one transfer site and five production sites) in the Mercier catchment were equipped

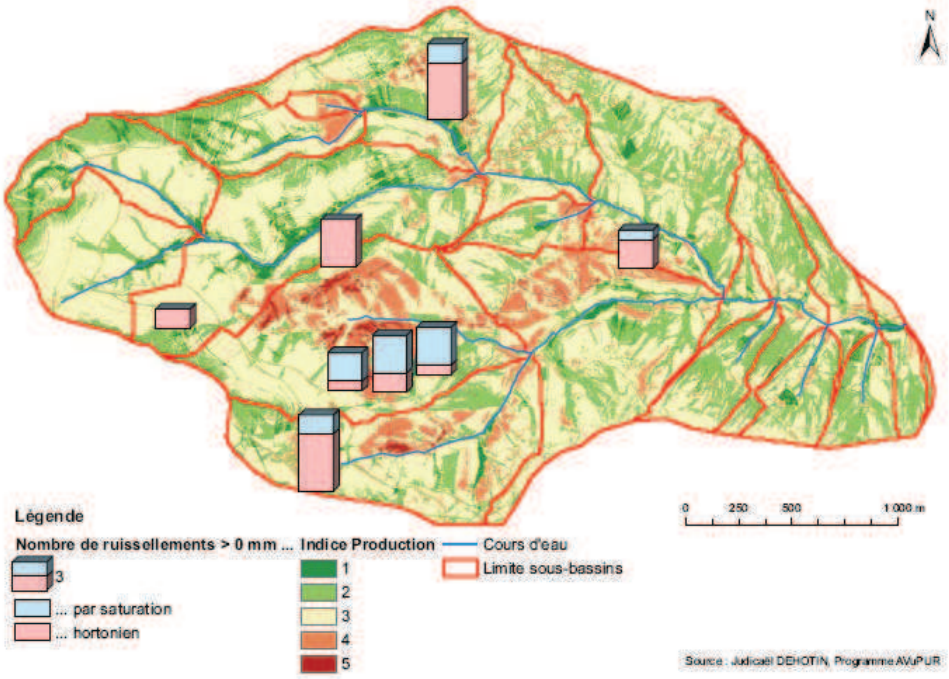

Figure 3.3.1.: Flow production map of Mercier catchment and the number of observed Horton overland flow (red) and saturation excess overland flow (blue). The production index 5 indicates a high probability of flow production and 1 a low probability (DeLavenne (2010) and Dehotin et al. (2010).)

with soil moisture sensors for continuous soil moisture measurement at the surface and water traps, which are perforated plastic tubes that intercept surface runoff and subsurface flow. The water traps were controlled after most of the rain events to verify whether they contained water or not. Three rain gauges were installed additionally to the rain gauges Sarrazin-1 and 2 (DeLavenne, 2010). Horton overland flow and saturation excess overland flow could be differentiated: It was considered, that saturation excess overland flow happens when the measured volumetric water content reaches its maximum at soil saturation. The Horton overland flow was calculated using the Smith and Parlange (1978) equation for the infiltration capacity. Horton overland flow was determined as difference of the rain intensity and the infiltration capacity.

The production sites had low initial soil moistures, high draining velocities and thus high soil moisture variations during the events, sometimes leading to saturation at soil surface level. In transfer zones, even low rain intensities could cause overland flow. The transfer zones had intermediate drainage velocities. The accumulation sites had the highest initial soil moistures and had slow draining velocities. At the accumulation sites, the water traps were mostly filled, which indicates also subsurface flow. On all sites, high initial soil moistures lead to overland flow, whereas no real tendency was determined for low initial soil moistures. The field investigations showed that the type of overland flow (Horton, saturation) does not depend on the type of site (production, transfer, accumulation), but on soil permeabilities and rain characteristics (DeLavenne, 2010). Higher soil permeabilities (0.038 mm s^{-1}) induced rather saturation excess overland flow, whereas lower permeabilities (0.004 mm s^{-1}) lead to Horton overland flow even for small rain intensities. Against expectation, it was shown that long rainfall durations, even with low intensities, induced rather Horton overland flow than saturation excess overland flow due

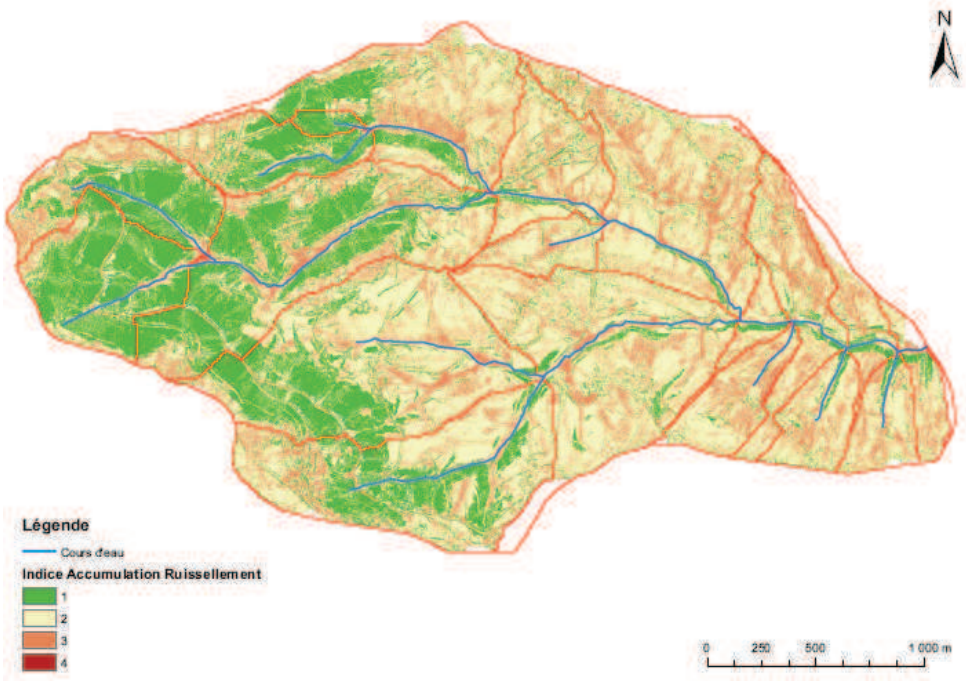

Figure 3.3.2.: Flow accumulation map of Mercier catchment. The accumulation index 4 indicates a high probability of flow accumulation and 1 a low probability (DeLavenne (2010) and Dehotin et al. (2010).)

to decreasing infiltration capacity. In contrast, high rain intensities resulted in short time saturation excess overland flow, caused by saturation of the first soil centimeters. The soil saturation happens thus not from the bottom, but from the top. Only the accumulation sites were completely saturated. Consequently, the soil depth has less influence than the permeability of the first soil layer on the runoff generation. High rain intensities caused overland flow (Horton and saturation excess) nearly all over the catchment, which transforms most of the catchment into runoff production sites. Consequently, the differentiation of runoff production zones may be less important than the definition of the transfer flow paths and accumulation sites for the risk evaluation (DeLavenne, 2010). From the factors used for the determination of the production and accumulation maps, only the influence of slope, morphology and permeability could be confirmed. The slope and morphology influence mainly the drainage capacity of the site and the permeability the differentiation between Horton and saturation excess overland flow. The soil depth is only important for accumulation sites.

3.3.2. Subsurface flow

In order to investigate subsurface flow processes, Gnouma (2006) installed a set of three piezometers equipped with pressure sensors (divers) along a hillslope in the lower part of the Mercier catchment. The divers recorded every ten minutes during the period from the 22^{nd} of November 2005 to the 13^{th} of July 2006. The piezometers had a depth of 130 cm to 190 cm and were at 10, 40 and 60 m distance from the Mercier stream. The first month of the observation period, the water levels did not react to minor rain events. However, starting from February a reaction of the piezometers could be observed for a couple of

rainfall events.

Depending on the event and the piezometers, the response of the water levels was different. The maximum water level variation was about 127.5 cm for a rainfall event of 36.2 mm. But it never reached the soil surface, although the production of saturated zones could be observed. A 66 mm rainfall event in summer caused only 17.2 mm increase in the same piezometer. Gnouma (2006) concludes from the results, that there are different kind of events: (1) intense rainfall events happening on dry soils induce mainly overland flow and only a minor response of the local groundwater, (2) small rainfall events arriving on dry soils create mainly Horton overland flow and no response of the local groundwater, (3) intense rainfall events on humid soils result in a rise of the groundwater table and thus a large flood event with a long decline. Gnouma (2006) also concludes that there are probably two periods: a recharge period from October to November with a moderate catchment response and a larger catchment response during the remaining of the year.

3.3.3. Hyporheic zone

Ruysschaert (2004) analyzed in- and exfiltration processes in the hyporheic zone of the Chaudanne stream close to the PdB. For this, two river reaches of about 10m length were equipped with piezometers organized along three transects and two tensiometers, respectively. The first site was around 70m upstream of the SOD and the second around 100m downstream of the SOD. The transects were located in pool and riffle positions in order to investigate the influence of riffles on the in-or exfiltration of water. The layout of the upper site is shown in Figure 3.3.3. The bank was equipped with ten piezometers and the river bed with three sets of three mini-piezometers with different depth (15, 30 or 50 cm). Some of the bank piezometers reached the bedrock or an impermeable clay layer, and most of them had a depth between 1 and 2m. The bedrock was estimated around 1 to 1.20m below the river bed. It reached the surface level at the right bank and went up to 2m on the left bank. The Chaudanne stream had a width of about 1m at the measurement sites. At each transect the water level in the river was measured continuously and in the middle of the reach two tensiometers on each bank were installed. The lower site had a similar configuration. However, the construction of the retention basins at the period of the measurement influenced the lower site.

The particle size distribution was analysed, showing a relatively homogenous soil consisting of middle sized sand and 30-40% silt or clay. The hydraulic conductivity was measured in situ with slug tests inside the different piezometers. The conductivities of the bank were in average about 1 e-05 m s^{-1} and thus rather homogenous. Two sites had lower conductivities of 5 e-08 m s^{-1} probably due to finer sediments. The conductivities in the river bed decreased with the depth. It was about 1 e-04 m s^{-1} at a depth of 20cm, 1 e-05 m s^{-1} at 50cm depth and 1 e-06 m s^{-1} at 70cm depth. Repeated conductivity measurements during the experiment period showed a decrease in conductivity in the river bed over the time, which was probably caused by clogging. The clogging was also a problem for the piezometric measurements.

In order to test the hypothesis that water infiltrates before riffles and exfiltrates after riffles tracer tests were undertaken. Two piezometers perforated at 10, 30 and 50 cm were installed before and after a riffle at 77cm distance. The electric conductivity was measured at three dates at every depth in both piezometers and in the surface water. Depending on the season the results indicated rather exfiltration (February 2003) or infil-

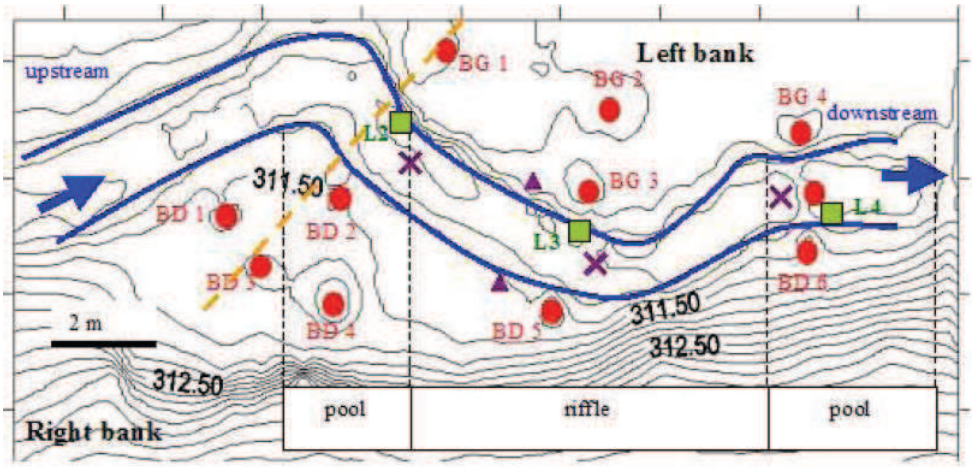

Figure 3.3.3.: Measurement site of hyporheic zone at the Chaudanne river upstream of the SOD at PdB. Three principal transects were equipped with piezometric measurements at the bank (red points), in the stream bed (violet crosses) and of the stream water level (green rectangles). The soil moisture was measured at the bank with two tensiometers (triangles) (Ruysschaert, 2004).

tration (September 2002). Artificial tracers (rhodamine and salt) were injected instantly in the surface water about 100m upstream the measurement site. No rhodamine could be detected in the soil water, and only slight increases of conductivity could be seen in the soil water at 10 cm depth, which makes the interpretation difficult. In a second tracer experiment, uranine and salt were injected at 30cm depth in the upstream piezometer. Three days later an increase in conductivity and the presence of uranine could be observed at 50cm depth in the downstream piezometer, thus proving the lateral subsurface transfer of water through the riffle.

The continuous water level measurements in the piezometers are available from April 2004 to November 2005. (Breil et al., 2007) validated these data and calculated the water surface gradient change with flow rate upstream and downstream of the riffle. Results clearly showed the riffle controlling effect on the water surface gradients that should probably influence downwelling and upwelling distances to the riffle as well the depth of downwelling.

In the framework of the INVASION project (ANR 08-CESA-022), the hydraulic pressure, temperature, electric conductivity, pH, redox potential, dissolved oxygen, nitrate and ammonium were measured in several piezometers in the Chaudanne stream and at the river bank in order to investigate the impact of the SOD on the hyporheic zone. The measurements started in November 2010 downstream of the SOD at PdB and in January 2011 upstream of the SOD.

3.3.4. Soil moisture

Detailed soil moisture measurements were made using capacitive sensors in the Mercier catchment and Ratier catchment on 15 agricultural fields with bare soil (Gonzalez-Sosa and Braud (2009b); Braud (2009) and Braud et al. (2009)). The measurements were made on the 12th of March and repeated on the 13th of March to get an idea of the soil moisture evolution. The objective was to obtain soil moisture data to validate high resolution radar images obtained from the TerraSAR-X satellite with 1m resolution. The

measurement strategy was to obtain data at different scales. The basin scale was assured by the measurements on different agricultural fields all over the basin. In order to take into account the intra-field scale, different transects with 20m spacing were measured and for the local scale crosses with 1 meter spacing of capacitive measurements were made on 5 different agricultural fields. Braud (2009) interpolated the data for both dates by kriging. Figure 3.3.4 shows the maps for both dates. We can see that the initially humid soil drys quickly due to the sunny day. Braud (2009) remarks that a dependence on the exposition is shown by the data.

Figure 3.3.4.: By kriging interpolated soil moisture maps of bare soil parcels in the Mercier and Ratier catchments. The data were obtained by TDR measurements along several transects. The upper map is on the 12th of March 2009 and the lower map on the 13th of March 2009 (Braud, 2009).

3.3.5. Hydrograph separation based on environmental tracers

Gnouma (2006) applied a hydrograph separation using δO18 and electric conductivity to two flood events in the Chaudanne and Mercier catchment in order to determine the provenance of the water. However, the results and interpretations have to be considered carefully. The δO18 values of the rain were very variable, but close to the local meteoric line (LML). The influence of evaporation was thus minor. An altitude gradient of 4.2 % could be determined between δO18 values in the Mercier, Chaudanne and a higher located, wooded catchment. A significant difference in the δO18 values of the stream water could be determined between the three sub-basins. The Chaudanne stream had enriched δO18 values, which were closer to the rain average. This can be caused by overland flow from urban zones. The values of the Mercier were between those of the Chaudanne and the wooded catchment. This difference is probably related to the different land uses of the catchments: mainly forest in the Verdy, forest and agriculture in the Mercier and agriculture and urban zones in the Chaudanne catchment. The investigated flood events were minor floods triggered by thunderstorms arriving on dry soils. Both events showed a high contribution of rain water (more than 50 %). Concerning the groundwater, only the first event seemed to have a significant contribution according to the hydrograph separation. Especially the second event showed a strong contribution of soil water during the decline of the flood peak. Consequently, the analysis of the tracer investigations also leads to the interpretation that overland and subsurface flow are the main hydrological processes in the catchments.

3.3.6. Response of intermittent drainage reaches

During the PhD thesis of Sarrazin (2012) 18 limnimeters were installed in the Mercier drainage and ditch network in order to analyse the dynamics of the hydrographic network and to capture the response of the intermittent tributaries. The location of the limnimeters is shown in Figure 3.3.5. 11 limnimeters were installed in 2007 and the rest gradually until mid-2009. All limnimeters were removed at the end of 2010. Due to the irregular and unstable cross-sections of the measurement sites, no rating curves could be determined. Thus, only the measured water levels were analyzed.

The response rate of the different measurement stations to the rain events varied between 50% and 100%. At some stations the stream bed remained dry (or the water level was below the detection limit) after some of the rain events. Sarrazin (2012) classified the stations in five different classes. The upstream stations under anthropogenic influence, such as ditches or urban zones, react to nearly every rainfall event due to Horton overland flow. Also some of the stations draining agricultural areas tend to follow these dynamics. The upstream stations in forest zones far from roads or ditches react at least and dry out rapidly. They need a more important rain volume of about 25 to 30 mm to be activated. The upstream stations under direct influence of saturated zones are rarely intermittent. Their discharge is controlled by the antecedent cumulative monthly rainfall and they act as buffer zones. The stations in submontane plains, located in the center of the catchment, have a rather persistent baseflow caused by saturated zones. Their activation depends more on the average hourly rain intensity than on the maximal rain intensity. The downstream stations are controlled by the antecendent rainfall, such as the rainfall volume and the length of the rainy period. Sarrazin (2012) further identified four hydrological phenomenas from the data analysis. He attributed three of them to parts

of the Mercier drainage network, which can be seen in Figure 3.3.5. The thalwegs in the forest part depend thus on a threshold of rain volume to be activated. Some reaches are influenced by urban zones where artificial flood waves are perceptible. The agricultural areas can create flood waves due to rapid transfer and overland flow. The thalwegs in the agricultural areas depend on the extension of saturated zones. If an excess of saturation happens in these areas this phenomenon seems to equilibrate the other phenomena and the catchment dynamic converges then to a linear reservoir.

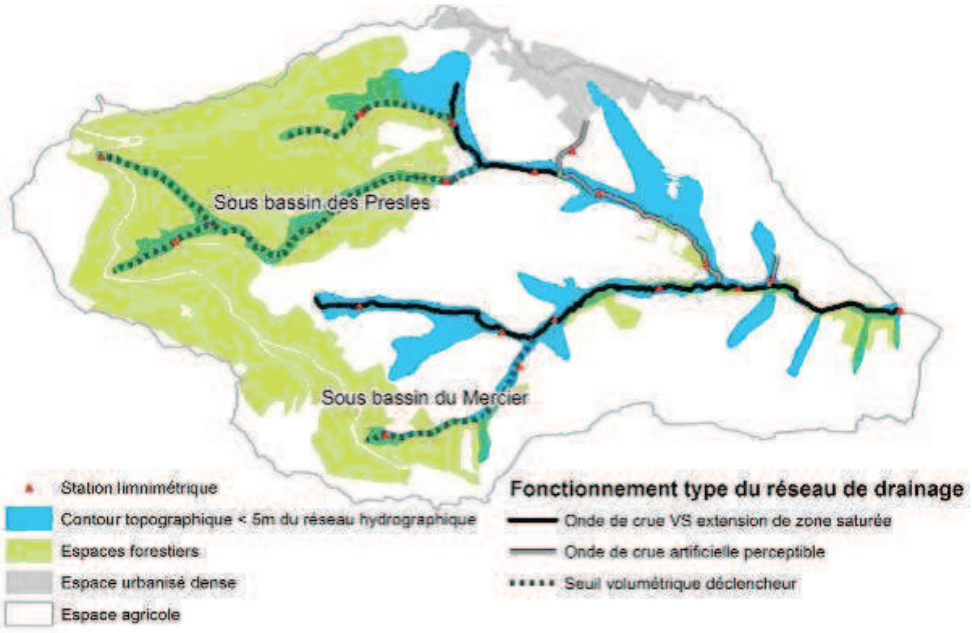

Figure 3.3.5.: Hydrological functioning of the Mercier drainage network derived from the analyses of water levels from 18 gauges (Sarrazin, 2012). Three type of functioning were determined: the upper reaches depending on a threshold of rain volume to be activated, reaches influenced by urban zones where artificial flood waves are perceptible and reaches depending on the extension of saturated zones.

3.4. Modelling of the peri-urban Yzeron catchment and its sub-basins Chaudanne and Mercier

The Yzeron catchment and its sub-basins Chaudanne and Mercier are research catchments of the Cemagref Lyon since 1988. Therefore, several research projects with different objectives used the Yzeron catchment as study site. In this context, different models were applied at different spatial scales (site, sub-basin, catchment) and for different purposes.

The first model applied to the Chaudanne (4 km^2) and the lower part of the Yzeron (130 km^2) catchment was TOPSIMPL by Hulin (1995) during his master thesis. The model worked well for winter rain events. Due to its structure based on the topographic index, the simulation results for summer storm events were unsatisfying. This can be explained by a higher percentage of surface runoff on impervious areas in summer which is not simulated by the model. Even an adaptation of the distribution of the topographic index did not improve the simulation of the peri-urban response. Charef (1996) modelled the rural Mercier sub-basin (6 km^2) with the model GR4h during his master thesis. However, not

satisfied with the results, he concluded that GR4h is more adapted to larger catchments. He determined then the topographic characteristics and sub-basins for the Chaudanne catchment with Demiurge (Charef, 1996) based on a DEM, and simulated the discharge of the Chaudanne catchment up to the measurement station at Pont de la Barge (PdB) with the model TOPASE (Charef, 1996). TOPASE gives as result triangular event hydrographs by indicating the maximum discharge, the peak time and the time of the base flow.

Dehchali (1997) developed a rainfall-runoff model for peri-urban areas during his PhD thesis and applied it to the Chaudanne PdB catchment. Figure 3.4.1 shows a scheme of the model. The catchment is subdivided in three different types of surfaces: urban surfaces connected to the sewer system, urban surfaces connected to the river and rural surfaces connected to the river. The model calculates separately the runoff generation and the transfer function parts of urban and rural areas. The water is routed in the sewer system or natural river. Sewer overflow devices (SODs) connect the sewer system to the natural river. The model has two outlets, the sewer system and the natural river and was later on implemented into the CANOE software.

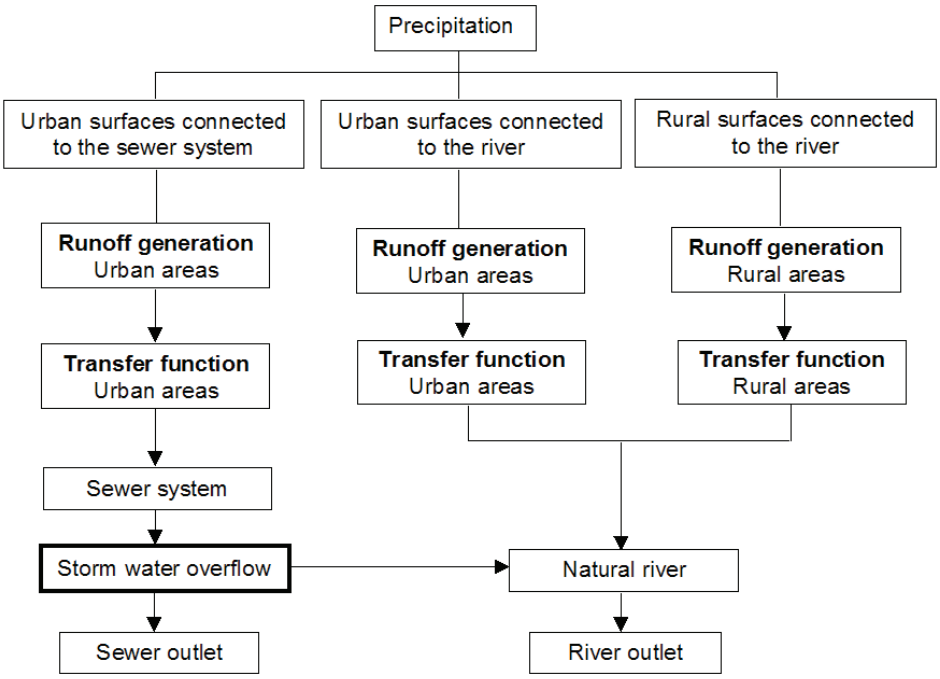

Figure 3.4.1.: Scheme of peri-urban model developed by Dehchali (1997).

In the framework of OTHU, which was created in 1999, several master theses and one PhD thesis including different modelling approaches were initiated. The objective of the thesis were to determine the impact of a combined storm water overflow device at the PdB measurement station in the Chaudanne catchment. Bernoud (1998) simulated the combined sewer system of the Chaudanne PdB catchment with CANOE. This work was continued by the master theses Belhaouane (1999), Gourdol (2000) and Jouan (2001). The chosen model mesh varied each time a little bit, but consisted mainly out of the urban sub-basins and combined sewer pipes shown in Figure 3.4.2. Breil and Jouan (2001) used the calibrated model to simulate a separated rainwater pipe system (grey zone in Figure 3.4.2), which should be connected to a set of retention basins in order to discharge the combined sewer system and reduce the overflow frequency. This study was

done for the municipality of Grézieu-la-Varenne(Grézieu). Jouan (2001) modelled also the Craponne sub-basin of the Yzeron catchment. Belhaouane (1999) and Gourdol (2000) used furthermore the statistical method QDF (Galéa and Prudhomme, 1997).

Figure 3.4.2.: Sub-basins and network reaches of combined sewer system at Grézieu-la-Varenne in the Chaudanne catchment for CANOE modelling (Breil and Jouan, 2001).

During her PhD thesis Radojevic (2002) applied CANOE to the whole Yzeron catchment. She divided the catchment in 23 sub-basins, see Figure 3.4.3, which were classified in urban, peri-urban and rural according to the imperviousness rate and presence of artificial drainage network Radojevic et al. (2010). A sub-basin was classified as rural, when the percentage of imperviousness was smaller than 25 %, and as urban when the percentage was more than 50 %. Radojevic (2002) used land use maps from 1970 and 1990 in order to investigate the impact of land use change on the hydrology. In 1970 only two sub-basins were classified as urban, whereas in 1990 there were ten urban sub-basins. Compared to the modelling of the Grézieu sewer system with CANOE, the sub-basins are much larger here, as the model is applied to a larger domain.The Chaudanne sub-basin is summarized with part of another sub-basin and represents thus the largest sub-basin. It is classified as rural in 1970 and 1990. As can be seen in Figure 3.4.3 the sub-basin delineation was made rather roughly and it feature gaps between the single sub-basins. This can lead to errors in the water balance.

Another CANOE application to the combined sewer system of Grézieu was made by the engineering consultants SOGREAH (2006) by order of the municipality of Grézieu. The neighbouring communities of Vaugneray and Brindas were also modelled. Figure 3.4.4 shows the modelled combined sewer network for Grézieu. The calibrated model was used to demonstrate the disfunctionning of certain drainage parts (Figure 3.4.4) and to simulate the storm water overflow. Hence, best management practices (BMPs), including retention basins and different pipe connections could be proposed.

From 2010 to 2011 another engineering office, the SED, investigated the rainwater network of Grézieu for the municipality. They determined in detail each sub-basin for

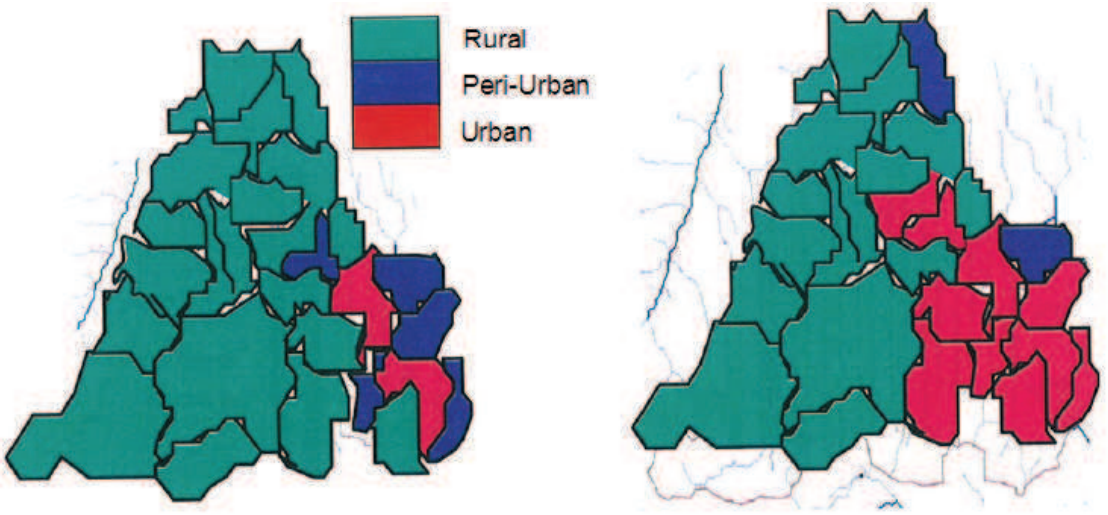

Figure 3.4.3.: Rural, peri-urban and urban sub-basins for CANOE modelling of the Yzeron catchment for 1970 (left) and 1990 (right) (Radojevic, 2002).

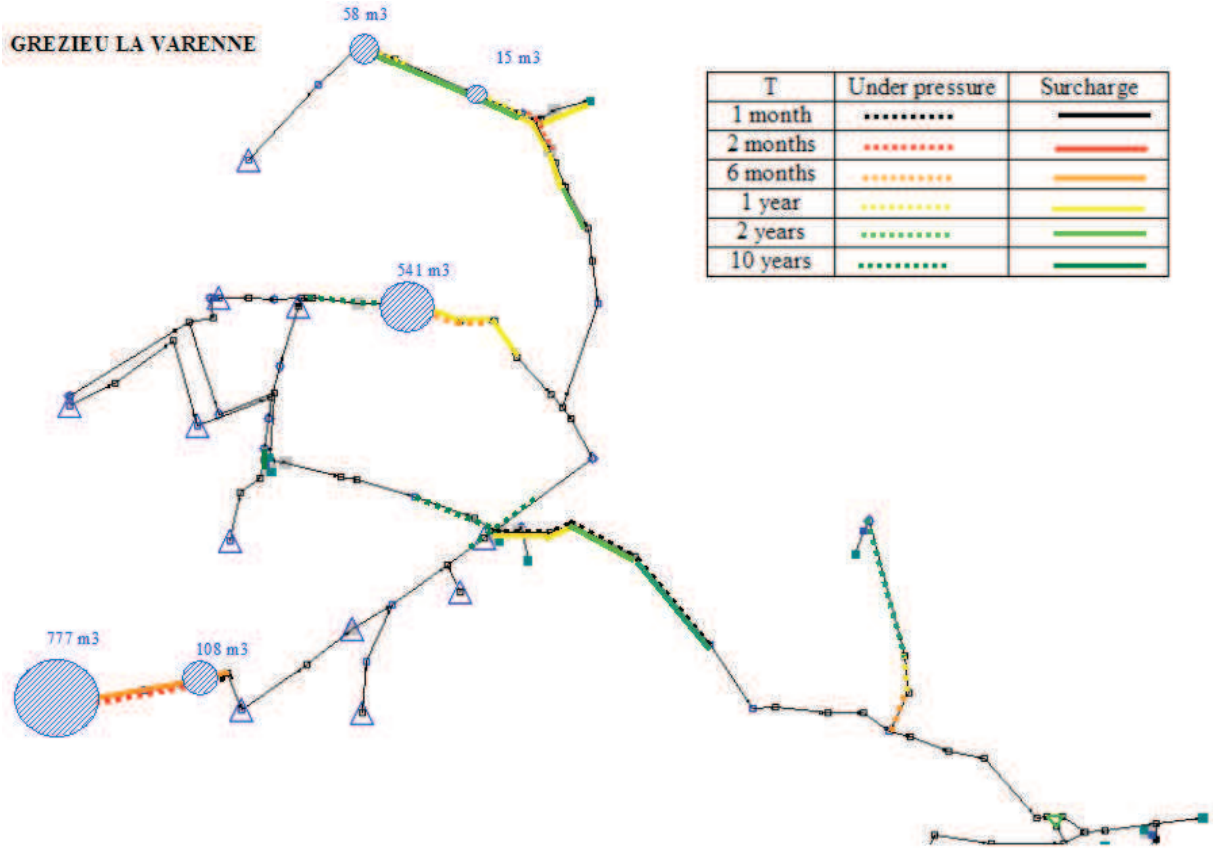

Figure 3.4.4.: CANOE network of combined sewer system at Grézieu-la-Varenne by (SOGREAH, 2006). The circles indicate the quantities of the 10 year overflow of the sewer system.

the rainwater system, see Appendix B. The modeled pipe and ditch network is shown in Figure 3.4.5.

During his PhD Gnouma (2006) applied the distributed hydrological model WISTOO on the Yzeron catchment. WISTOO is based on raster maps, containing grid cells with

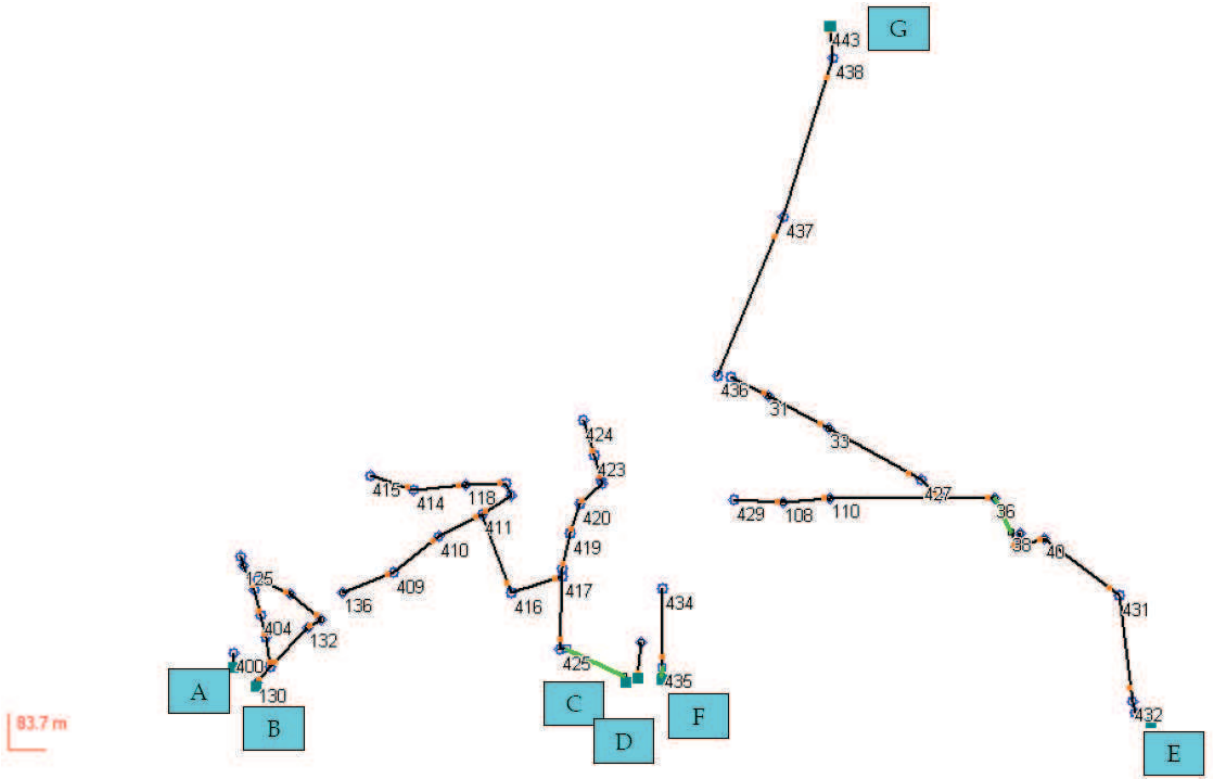

Figure 3.4.5.: CANOE network of rainwater system at Grézieu-la-Varenne (SED, 2011). A to G are the outlets of the rainwater pipe system towards the natural river.

different soil hydraulic properties. The routing is based on the DEM. Consequently, no urban characteristics such as the sewer system are represented by the model. The model reproduced only for the calibration period the measured hydrograph correctly, not for the validation period. The attempt was undertaken to simulate two different kind of storm events with the same simplified soil parameter set. The model was thus successfully calibrated to an event dominated by subsurface flow having a slow decline, which happened due to a large rainfall event on humid soils. However, the model did not simulate correctly an event caused by a summer thunderstorm on dry soils. Gnouma (2006) concluded that this is due to the problem of equifinality.

Another PhD thesis aimed at analyzing the influence of dry dams on the hydrology of the Yzeron catchment and the impact of discharge-frequency regimes (Chennu, 2008) for flood prevention. For this, the TBM rainfall generator (Lepioufle, 2009; Renard et al., 2011) was coupled with the grid-based rainfall-runoff model MARINE (Castaings et al., 2009; Braud et al., 2010b). MARINE provided then the discharge in the river, which was routed with the hydraulic model MAGE. The DEM based model mesh of MARINE on which the flow accumulation is calculated is shown in Figure 3.4.6 as well as the network links of the Yzeron river used by MAGE. Same as for Gnouma (2006) only the natural river network is modelled here, and no sewer network.

In the framework of his master thesis de la Varde (2010) simulated the rainwater network connected to a set of three retention basins at the PdB with CANOE. He also simulated the combined sewer system upstream of the SOD at PdB. For this, he delineated the sub-basins shown in Figure 3.4.7.

The simulation of the rainwater network and the retention basin was improved by

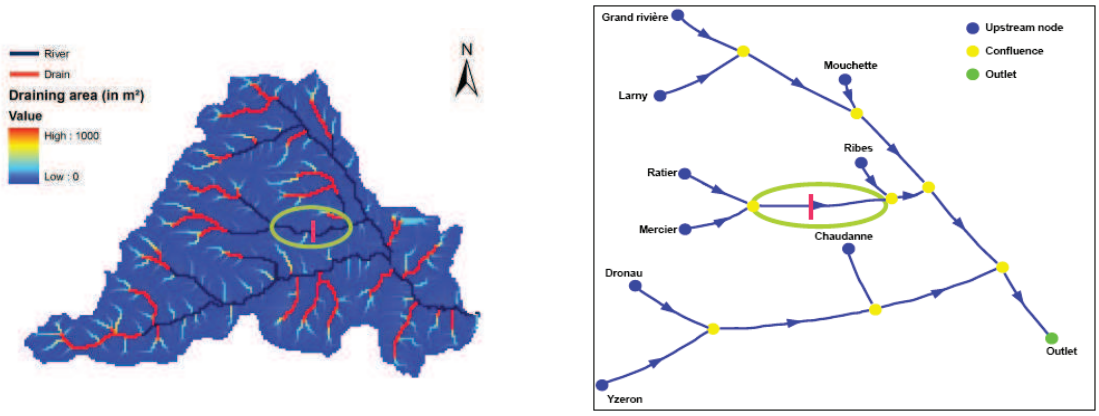

Figure 3.4.6.: DEM based MARINE model mesh with flow accumulation and MAGE network reaches of Yzeron catchment (Chennu, 2008).

Figure 3.4.7.: CANOE sub-basins and rainwater (up) and combined sewer network (down) for Grezieu-la-Varenne by de la Varde (2010). The rainwater network is connected to the three retention basins at Pont de la Barge.

Coulais (2011) during his master thesis. His delineation in sub-basins is shown in Figure 3.4.8.

Figure 3.4.8.: CANOE sub-basins and network of separated sewer system at Grézieu-la-Varenne by (Coulais, 2011).

An application of the Australian urban model MUSIC was done for the Chaudanne

PdB catchment by Dols (2010). The combined sewer system and the rainwater network connected to the retention basins were modelled. No detailed sub-basin delineation happened. The contributing area for the combined sewer system was set to 30 ha and for the rainwater system to 25 ha, see Figure 3.4.9.

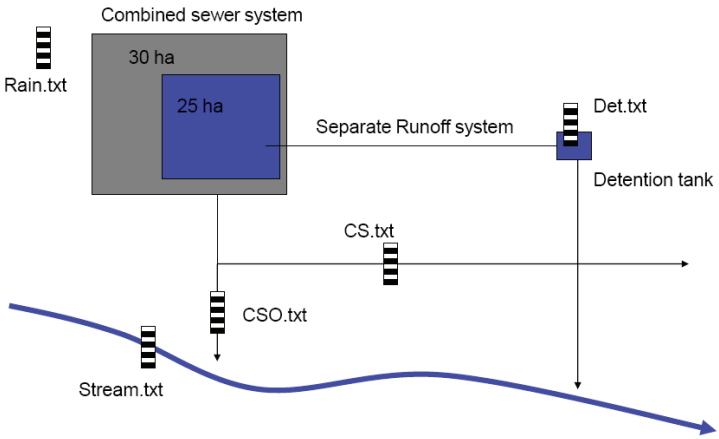

Figure 3.4.9.: MUSIC application to Chaudanne catchment (Dols, 2010).

The operational model implementation of CANOE for the Yzeron catchment used by the Grand Lyon was derived from the model developed during the PhD of Radojevic (2002). It is used for planning and urban water management. The current model mesh, shown in Figure 3.4.10 was improved by Chocat et al. (2010) in the framework of the AVuPUR project. The natural sub-basins were subdivided and the sewer network of the Grand Lyon and the municipalities of Grézieu, Brindas, Yzeron and St Laurent de Vaux were added. A comparison of the CANOE model mesh and the delineation into sub-basins was made by Dehotin (2009a) in order to adapt the model meshes. The sub-basins obtained by Dehotin (2009a) are used for the simulation with the J2000 model, which is based on the JAMS modelling framework. The J2000 model was first implemented during the master thesis of Jandot (2010) also in the framework of the AVuPUR project, and it was improved by Labbas (2011). Different land use maps from 1945 on, and projections to the future were available. Furthermore, different sources of the 2008 land use map were compared (SPOT, aerial photography and Quickbird) (Labbas, 2011). The 2008 sub-basin map resulting from the synthesis of the three maps is shown in Figure 3.4.10. Here, the sub-basins were classified into 5 classes by F. Branger: urban for sub-basins with more than 50 % urban land use, mixed-rural for sub-basins with urban land use between 10 % and 50 % and mainly agricultural land, mixed-forest with the same urban percentage but mainly forest, rural-agricultural for sub-basins with mainly agricultural land use and less than 10 % urban land use and rural-forest for sub-basins with mainly forest and equally less than 10 % urban land use.

Furusho (2011) adapted ISBA-Topmodel to peri-urban areas and applied it to the Yzeron catchment during her PhD thesis. Furthermore, in the framework of the AVuPUR project, a new multi-outlet model was developed, having the natural river, the sewer system and the atmosphere as outlet (Dorval et al., 2010).

The master student Le-Barbu (2007) worked on the two-dimensional hydraulic simulation of a 350m stretch of the Chaudanne river at the measurement station PdB. A field campaign delivered detailed topographic data of the stretch (Thollet, 2007), which served

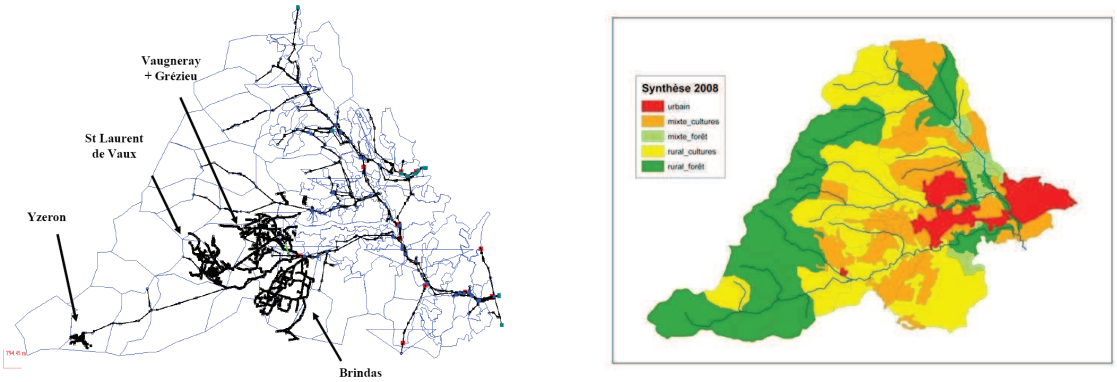

Figure 3.4.10.: For operational purposes used CANOE delineation in sub-basins and network reaches of the Yzeron catchment by (Chocat et al., 2010) on the left side. J2000 urban, rural and peri-urban sub-basins of Yzeron catchment based on the summarized land use classification of 2008 from SPOT, Quickbird and BD Ortho on the right side (Labbas, 2011).

for the construction of the model mesh. The objective was to simulate the exact water level using the software Rubar20. As the discharge measurement at one of the gauging stations is not really exact due to the geometry of the cross section, the influence of a change of the cross section (raising of the drop) was also investigated with the calibrated model. Speisser (2008) continued this work in order to investigate the water exchange with the hyporheic zone before a natural drop on the river bottom. The water exchange depends on the difference in hydraulic charge, which means the water level, before and after the drop. For this, two stretches of about 10m were simulated using an even more detailed topography of the river bottom. The simulated river levels give then the boundary condition for the exchange with the hyporheic zone. However, no further simulation of the exchange was undertaken.

Frequent flooding occurs at Oullins, which is the outlet of the Yzeron catchment, and thus the confluence of the Yzeron river with the Rhône river. The flooding is caused by surcharge of the sewer system and flooding of the Yzeron river. During the RIVES project (Risques d'inondation en ville et Etude de Scénarios) (Paquier, 2009) a coupling of the one-dimensional CANOE model to the two-dimensional Rubar20 (Houdré (2002), Renouf (2004), Kaniewski (2005), Mercado (2006), Jankowfsky (2007)) and TELEMAC models (Rebai, 2007) based on the OpenMI framework was attempted in order to simulate the flooding. Both models worked well independently, but the coupling introduced numerical problems in the CANOE model, so that no results could be obtained. As this was a hydraulical model application, the scale was much smaller than for the above presented hydrological models. The surface model mesh describes the river and the street network concerned by the flooding and consists of triangles, see Figure 3.4.11.

3.5. Discussion and conclusions from a modelling point of view

3.5.1. Summary of main characteristics and processes

The Mercier and Chaudanne catchments are located in the peri-urban area of Lyon. The Mercier catchment has steep slopes in the upper part covered by forest and the lower part consists mainly of agricultural area. The Chaudanne catchment with less slopes has

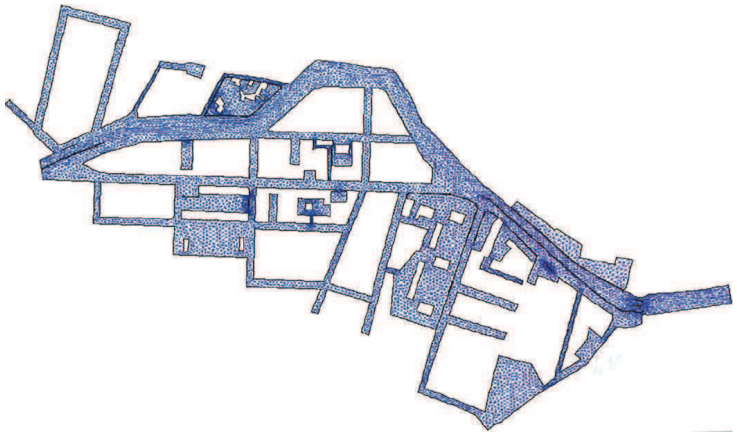

Figure 3.4.11.: Rubar20 and TELEMAC model mesh of Oullins (Paquier, 2009).

a large urban area close to the outlet and agricultural land use in the headwaters. The basin geology consists of metamorphic rock of the Monts du Lyonnais series except one alluvial fan in the headwaters of the Chaudanne catchment producing soils of silty and clayey sand. The Chaudanne catchment has a combined and separated sewer system, additionally to the natural drainage network, leading to a multi-outlet catchment with three outlets: the natural river, the pipe towards the WWTP and an overflow to another sewer system. The Mercier catchment has just a waste water system, and thus only indirectly a second outlet due to possible infiltration of clean water into the sewer system.

The rainfall is very variable and it can reach up to 90 mm per day with maximum intensities of 130 mm hr^{-1}. Especially in summer, the evapotranspiration takes an important role in the water balance. According to Gnouma (2006) the events can be classified in intense rainfall on dry soils causing overland flow and a minor increase in the groundwater table, low rainfall on dry soils only producing overland flow and long rainfall periods on wet soils causing a rise of the groundwater table and large floods with a long decline. The maximal groundwater variation during one event measured by Gnouma (2006) was around 130 cm. The investigation of the drainage system activation effected by Sarrazin (2012) resulted in a classification of different drainage reaches depending on the land use. Hence, the thalwegs in the forest zone are activated with a threshold of 15 to 25 mm of rainfall. The reaches below urban zones react to every rainfall event due to Horton overland flow created on impermeable areas. The thalwegs in agricultural areas depend on the extension of saturated zones, whereas the agricultural hill slopes produce principally overland flow or near surface subsurface flow. According to DeLavenne (2010) the type of overland flow, Horton or saturation excess, depends mainly on the soil permeabilities and rain characteristics. Saturation of the whole soil profile was only found in accumulation sites at the valley bottom. Saturation excess or Horton overland flow, which can happen all over the catchment during intense rain events, depends thus principally on the decreasing infiltration capacity. The hydrograph separation of Gnouma (2006) also showed a high contribution of overland flow and subsurface flow to the stream discharge.

The average event discharge for the Mercier is about 0.35 m^3s^{-1} and for the Chaudanne at La Léchère about 0.5 m^3s^{-1}. Extreme events can reach up to 12 m^3s^{-1} in the Mercier and up to 3 m^3s^{-1} in the Chaudanne. The analysis of the sewer data in the Chaudanne catchment showed that groundwater seepage into the sewer pipes is an important factor, which increases the discharge in the combined sewer pipes about 8% and decreases at

the same time discharge in the natural river. This process is probably also important in the Mercier catchment, as the waste water pipe is just below the river bed. However, no measured data are available. The Chaudanne and Mercier can thus be described as intermittent streams with dry periods in summer interrupted by severe thunderstorms and continuous discharge in winter.

3.5.2. Conclusions concerning modelling studies of Yzeron catchment

The model applications to the Yzeron catchment and its sub-basins Chaudanne and Mercier were driven by different objectives, such as the modelling of the sewer network and the sewer overflow device for design and water quality questions, the influence of dams, local inundation due to sewer surcharge or the influence of land use. The peri-urban character of the Yzeron catchment could only be modeled with CANOE, J2000 and ISBA-Topmodel as the other models did not have an urban model component, or they were purely hydraulic models as MAGE and Rubar20. However J2000 does not simulate the sewer system. A difference can be seen in the sub-basin delineation for the modelling of the whole Yzeron catchment or only the Chaudanne sub-basin. Due to the larger scale, the Chaudanne sub-basin represents only one model unit when the whole Yzeron catchment is modeled. The CANOE applications of the Chaudanne sub-basin focused more on the urban part and the sewer system and disregarded the rural part. We can also see, that the model setup and sub-basin delineation depends mainly on the modeler. No detailed physically based model was applied to the Chaudanne sub-basin. Furthermore, no model investigated the effect of the spatial organization of built-up or rural areas on the hydrology.

3.5.3. Use of the gathered knowledge for modelling

A hydrological model designed for the Mercier and Chaudanne catchments, should be able to simulate Horton overland flow, as well as saturation overland flow caused by saturation of the first soil horizon, and not only by saturation of the whole soil profile. The process module describing the natural zones should thus offer the possibility to represent several soil layers with different properties.

The evapotranspiration is a major process for the long term water balance, and its influence on wet soils was shown during the field campaign on the 12th and 13th of March 2009.

The river process module needs to handle great variations in discharge as well as dry river beds. The model should be able to simulate the infiltration into the sewer pipes, as it was shown that the discharge volume over the year is even more than the natural river discharge. The effect of sewer overflow devices should also be integrated into the model.

The topsoil hydraulic properties, mainly depending on the land use type, seem to play an important role and should be integrated in the model.

Therefore, the object oriented model mesh should integrate the detailed land use information. In order to take into account the difference between production, transfer and accumulation sites the slope or the topographic index should also be integrated into the model mesh. For the Mercier catchment, the 2m resolution DEM and for the Chaudanne catchment, the 25m resolution DEM can be used for the determination of sub-basins and the flow routing. An integration of the aspect would allow to take into account the difference of evapotranspiration caused by different aspects. However, this implies that

the PET is calculated inside the model according to the aspect, which is not done actually.

As model input, continuous time series of precipitation and PET are available for several years. The DONESOL data base (SIRA, 2011) and the field campaign of Gonzalez-Sosa et al. (2010) provide information about soil properties. However, no information is available for urban soil. The location and dimension of the combined sewer system is given, although important information about the rain water part of the separated sewer system is missing.

Distributed hydrological modelling serves the process understanding. However, to verify that the model simulates the correct processes, or as Grayson et al. (1992b) say that the model does not simulate the "right results for the wrong reasons", distributed data are necessary for the model validation. The available data are summarized in table 3.2.1 under discharge, water level, piezometers and soil moisture. Reliable discharge data are available at one station at the Mercier stream from 1997 on, and for two stations at the Chaudanne stream from 1997 and 2005 on, respectively. Additionally, the discharge in the sewer system and in the sewer overflow device at PdB is measured in the Chaudanne catchment since 1999 and 2001, respectively. Since 2010 the discharge in the SOD at the Léchère is also measured. The entering and leaving discharge of the first retention basin at PdB was measured during a short period in 2010 and 2011.

The discharge data can be used for the validation of the model output. However, they only give aggregated information as different hydrological processes can produce the same discharge at the catchment outlet. Consequently, more process oriented data are necessary in order to verify the right functioning of the model. In the Mercier catchment several data are available for the validation of the right process simulation. First of all, the catchment response and activation of intermittent tributaries can be verified with the water levels measured by the 18 limnimeters during the PhD thesis of Sarrazin (2012), but only the right dynamic can be verified not the water quantity. Furthermore, continuous soil moisture measurements are available at 8 sites from May 2010 to May 2011 (DeLavenne, 2010). The soil moisture data from the 12th and 13th of March 2009 can also be used for the model validation. The right simulation of the groundwater table of the Gnouma (2006) site could be verified with the piezometric data for the period 2005-2006. Furthermore, at the scale of the river reach close to the PdB the piezometric and tensiometric data from the study of the hyporheic zone (Breil et al., 2007) can be used for the model validation. However, as we have seen the groundwater table is very variable, and only local piezometric information is available.

In summary, there are more distributed data available for the Mercier catchment than for the Chaudanne catchment. This is due to the fact, that the Mercier catchment has less urbanization, and it is thus easier to gather field data. However, as these are small neighboring catchments, which have the same geology, soil types and climatic setting, an extrapolation of e.g. the distributed soil data of the Mercier catchment to the Chaudanne catchment seems appropriate. Even if it is not possible to close the water balance concerning the Chaudanne PdB and Léchère catchment (one and two sewer system outlets are not measured, respectively), the discharge measurements in the natural stream, the SOD and the sewer system can give valuable information about the different contributions from urban and rural areas. Furthermore, the distributed water level (Sarrazin, 2012) and soil moisture measurements (DeLavenne, 2010) in the Mercier catchment are very valuable

validation data.

The next chapters aim at using these data and acknowledged process understanding to construct a detailed model of the Chaudanne and Mercier catchment, which is able to simulate the observed processes.

Part II.

Construction of modelling tool kit

4. From process understanding to a modelling concept

The following chapter presents the guidelines for the peri-urban areas specific hydrological model based on the analysis of hydrological processes and requirements defined in section 3.5 and existing approaches of software components in LIQUID. As we have seen in section 2.3 the main components will be BVFT and URBS. The first part of the chapter presents thus shortly the LIQUID modelling framework with its available process modules and models. Then the model concept and the choice of its spatial discretization (based on the review in section 2.2.1) is outlined.

4.1. Principles of the LIQUID modelling framework

The LIQUID modelling framework[1] arises from the model POWER (Planner Oriented evaluative Watershed model for Environmental and socio-economic Response) which was developed at the LTHE laboratory during the European project AgriBMPWater (Turpin et al., 2005). In continuity of this project the computer science engineering company HYDROWIDE was created in 2005. They further develop and maintain the LIQUID framework (Branger, 2007b). A detailed overview of the LIQUID framework is given in Branger et al. (2010). Here, we summarize only the main characteristics. The purpose of LIQUID is to provide a framework for easy development of case specific hydrological models. LIQUID follows an object oriented approach. A model is composed of several interacting modules, which represent different hydrological processes (Figure 4.1.1). The

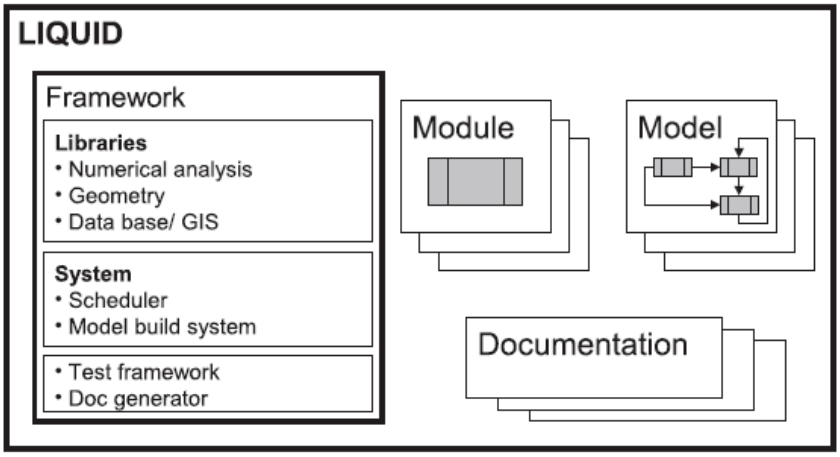

Figure 4.1.1.: Main components of the LIQUID modelling framework (Branger et al., 2010).

framework acts hereby as common-shared calendar (Viallet et al., 2006). At every execution, each module estimates its own time step depending on the current state variables and calendars it to the time scheduler. The scheduler will then trigger an execution at the next time step. Hence, each module has its own variable time step corresponding to

[1] http://hydrowide.com/liquid

the characteristic time scale of the simulated hydrological process. This facilitates water balance and event based simulations within the same simulation run. The exchange of information between modules is possible by means of signals (outputs) and slots (inputs). At each execution, a module signals its variables. This can cause the interruption of the receiving module. This module will then take into account the new values and estimate a new time step. The time step changes thus during the simulation and is smaller the more information has to be passed. This is usually the case when it rains heavily (Branger et al., 2010).

The framework is written in C++ and provides a set of libraries useful for the development of hydrological models such as numerical algorithms, geometrical and mathematical libraries or pre-implemented hydrological objects such as reservoirs.

The next two sections describe the functioning of process modules and the concept of models in more detail.

4.1.1. Concept of modules

Each module is applied to a certain number of model units (polygons or lines), which can be of irregular shape. Figure 4.1.2 shows the structure of a module, which is composed of a pre-processor, a spatial data scheme, a solver, test cases and documentation. Each module inherits from the CModule class and contains at least the CPreproc and CSolver class. The development of new modules is quite easy thanks to template files. For the implementation of a new module, the developer only needs to fill the codes of the solver and pre-processor corresponding to the retained numerical and data schemes.

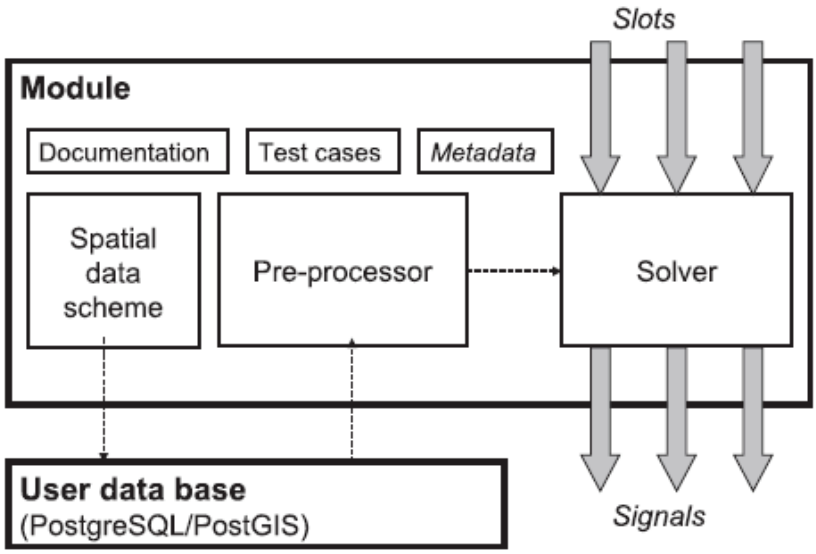

Figure 4.1.2.: Design of a module (Branger et al., 2010).

The solver gets its input data and parameters from the spatial data scheme and the pre-processor. These time-independent input data (parameters, initial and boundary conditions and the spatial extensions of the model units) are specific for each module, which assures the independence of the modules. Instead of reading the input data from a text file, LIQUID has a connection to a PostgreSQL/PostGIS[2] database. The data

[2]http://www.postgresql.org/,http://www.postgis.fr/

scheme of the database is defined during the development of the module pre-processor by means of SQL queries which are integrated into the C++ code. When running the model, empty tables corresponding to the modules data scheme are created in the first step. These tables have to be completed by the modeler and then, the preprocessor has to be run before the execution can be started.

The main function, called "operator()" is part of the solver. It obtains the current time as input variable from the scheduler and estimates the new time step, which will be calendared to the scheduler. Inside this function the course of actions has to be defined. If the module is simple, the governing equations are specified in the solver.h file. In more complicated modules, the hydrological processes are represented by several classes, in which the governing equations can be found. The equations and modelling concepts can be chosen by the developer and can thus follow physically based or rather conceptual approaches. All model parameters and state variables follow the SI base units (meter and seconds), which circumvents conversion errors.

The signals and slots are used by the module to communicate with other modules. They can send or receive values of different types such as scalars, vectors, matrixes, functions, objects or structures. It is the challenge of the module developer to imagine all possible connections and integrate the corresponding signals and slots to the module. The signals are also used for the connection to output modules, which write the values to text files. In order to optimize the calculation time, signals and slots can be surrounded by conditions. The state variables can so be updated only in case that the value, for example the water level, has changed significantly.

Good programming practice implies to write sufficient documentation about the input parameters, the state variables, the algorithms and slots and signals. It also signifies to define test cases in order to check the good functioning of the module. The LIQUID framework offers a test framework, where the test cases are part of the module code. Hereby, all basic algorithms and signals and slots can be tested. However, to check the preprocessing a full model has to be developed and the data have to be entered to the PostgreSQL database (Branger (2007b);Branger et al. (2010); Dehotin (2007)).

4.1.2. Concept of models

A model can be easily developed by defining the connections of slots and signals in a XML file, called *.model* file, as shown in Figure 4.1.3. The xml file contains two different kind of tags: <module> for the declaration of all used modules and <connection> for the connections between modules. During the compilation of the model, the XML file is translated into C++ code and an executable is created (Branger et al., 2010). The executable file can be run independently from the LIQUID framework given that the Microsoft Visual Runtime environment is installed.

The input and output of the model are managed by separate INPUT and OUTPUT modules. The INPUT module can be used to provide one time series per model unit. In order not to store time series such as rainfall or evapotranspiration for each model unit, a spatial weighting module, the FCA module, is available (Branger, 2007b). The OUTPUT module allows to write the signaled values to ASCII files. The output can be written as instantaneous value, with a fix time step, as cumulative values or just the minimal values. The output of different model units can be written to the same or to different files. Time

series can be plotted with statistical software, as for example R[3] and maps containing spatial output can be drawn using GIS.

```
<module>
   <type>river1d</type>
   <instance>river</instance>
   <params>natural river</params>
</module>
<module>
   <type>plus</type>
   <instance>PlusSistba</instance>
   <params>Total inflow</params>
</module>

<connection>
   <name>River2PlusSistbA</name>
   <from>
     <instance>river</instance>
     <signal>m_sigOutletDischarge</signal>
   </from>
   <to>
     <instance>PlusSistba</instance>
     <slot>m_slotA</slot>
   </to>
</connection>
```

Figure 4.1.3.: Extract of .model file with a module declaration at the top and the definition of a connection at the bottom.

In the new version of the LIQUID framework (0.4) module connections are always 1:1. This means, that e.g. a river reach can only receive water from one model unit. As this is not sufficient, the module PLUS was developed by Hydrowide. It enables the coupling of up to ten different signals to the slot of one module, e.g. the surface runoff slot of the river module. The river reach can thus receive surface runoff from different modules. The sum of the incoming signals is calculated by PLUS and sent to the slot of the river reach. The corresponding PostgreSQL table of PLUS has three fields: id for the identifier of the receiving slot based on the 1:1 connection (in our example this would be the river reach id), slot_name for the type of connection (A to J) and slot_id for the id of the incoming signal (id of an urban model unit). Depending on the model size a large number of PLUS connections may be necessary. It is therefore essential for the model developer to document which signal is connected to which PLUS slot (A to J), so that the model user know how to fill the model tables without having to analyze the XML file.

4.2. Review of process modules and models available in the LIQUID framework

Different hydrological processes such as flow generation on natural or urban areas, flow routing in the river network or groundwater flow are simulated by process modules in

[3]http://www.r-project.org/

the LIQUID framework. The following list gives an overview of the modules, which are currently available in the LIQUID framework version 0.3. They were developed by different researchers of the Cemagref, LTHE laboratory and Hydrowide.

- BOUSS2D, a 2-dimensional groundwater model solving the 2D-Boussinesq equation developed by Dehotin (2007) and Dehotin et al. (2011b)
- SIDRA, SIRUP and SILASOL simulating drainage flow, surface runoff and solute transport in sub-surface tile-drained fields, respectively (Branger et al., 2009)
- D2D and ELIXIR simulating a two-dimensional discharge of a drained groundwater table and runoff in pipes and ditches (with and without hydraulic pressure) (Henine, 2010)
- TSEB, calculating an energy balance and ROSISPAT simulating the extraction by roots inspired by the model SiSPAT (Braud et al., 1995)
- GR4 a parsimonious model for rainfall-runoff simulation with four parameters (Nascimento, 1995)
- PEF (Ponding Extraction Flow) simulating overland flow in a simplified manner (Manus (2008); Manus et al. (2009) and Branger et al. (2010))
- FRER1D representing vertical infiltration over natural surfaces and water redistribution using a 1D resolution of the Richards equation (Ross, 2003)
- CRLINPG, ROLI, ETPART and VEGINT simulating the effects of crop rotation, root extraction, evapotranspiration and interception on a FRER1D model unit (Varado et al., 2006b)
- HEDGE (Branger, 2007b) simulating the effect of vegetated field borders (hedgerows) and riparian zones on the surface and subsurface flow using a conceptual approach. HEDGE is a capacity based 1D-infiltration module enabling saturated surface runoff and lateral subsurface flow exchange.
- RIVER1D simulation the routing in a drainage network with open cross sections. It calculates a solution of the one-dimensional kinematic wave approximation of the Saint-Venant equation (Branger et al., 2010)
- WTI simulating lateral sub-surface flow between fields using the Darcy equation and WTRI, which calculates the lateral subsurface flow between fields and the river using the Miles approach (Branger (2007b); Branger et al. (2010))

Several models were constructed with the LIQUID modelling framework based on the above mentioned process modules and applied to different spatial and temporal scales (Branger et al., 2010).

The PESTDRAIN model, which simulates the pesticide transport at the local scale of a tile-drained agricultural field, consists of the coupled SIRUP, SIDRA and SILASOL modules (Branger et al., 2009).

A one-dimensional water balance model for the multi local scale (WBMLS) was constructed by Braud (2008b) coupling the modules FRER1D, ROLI, ETPART, VEGINT and CRLINPG.

The modules ELIXIR and D2D were combined in order to simulate the impact of temporary drainage pipe pressurization on agricultural drainage discharge during heavy rainfall events (Henine et al., 2010). Like the PESTDRAIN model, the model was only applied to a small scale (1.7 ha field).

In the framework of the HYDRATE[4] project a combination of FRER1D and the modules PEF and RIVER1D was used to simulate major flash flood events in the Cevennes, France (Manus (2008); Manus et al. (2009); Braud et al. (2010b); Anquetin et al. (2010)). Hereby, the FRER1D module represents the flow generation part, PEF the transfer and RIVER1D the routing. The model called CVN, uses a HRU based model mesh, where each model unit consists of an intersection of sub-basin and soil property maps. It was applied to several catchments in the Cevennes region, having a maximal size of 2050 km^2, and a maximum of about 7400 model units.

Dehotin et al. (2011b) developed the model BALANCE, which simulates the long-term water balance of large catchments. It consists of a combination of the modules BOUSS2D, FRER1D and RIVER1D and the interface WTRI. It was designed to be applied to the upper Saône catchment which has a size of 11700 km^2. However, only part of the model (without use of WTRI and RIVER1D) was finally applied to a sub-basin of 160 km^2.

The BVFT model (Branger et al., 2008), which we have seen in section 2.2.2.1, is the first model using a fully object-oriented approach where the choice of the module depends on the land use characteristics. The model WBMLS is therefore coupled to the modules SIDRA, SIRUP, HEDGE and RIVER1D using also the interfaces WTI and WTRI. It describes the influence of landscape management practices on the hydrology of small agricultural catchments and was applied to the "Fontaine du Theil" catchment in the north-west of France, which has a size of 1.28 km^2.

4.3. Peri-Urban Model for Landscape MAnagement (PUMMA)

The objective of this PhD thesis is to build the Peri-Urban Model for Landscape MAnagement (PUMMA), which simulates the hydrological processes of peri-urban catchments. The Chaudanne and Mercier catchments (having a size of about 5 km^2), which were presented in chapter 3, serve as example application cases. The review of modelling in peri-urban areas (chapter 2.2.2) showed the potential of a combination of the object oriented BVFT and URBS models for the construction of the PUMMA model. In both models, the choice of the runoff generation modules depends on the land use characteristics. The combination of BVFT and URBS allows thus to model urban objects, represented by built-up cadastral parcels and streets with URBS and rural objects such as agricultural fields and forest areas with the FRER1D module or hedge rows and riparian zones with the HEDGE module (see Figure 4.3.1). Roads can be simulated using the FRER1D module by setting the soil hydraulic conductivity of the first soil layer to that of tarmac. The field studies realized in the Mercier catchment (chapter 3.3) showed the importance of Horton overland flow and saturation excess overland due to saturation of the first soil horizon on the runoff generation. FRER1D offers the possibility to create ponding induced by both processes, as the soil is divided in several horizons with different soil hydraulic properties. No agricultural drainage is present in the Mercier and Chaudanne catchments, so the SIDRA and SIRUP modules will not be integrated into the PUMMA model. The

[4]http://www.hydrate.tesaf.unipd.it/

infiltration into leaky sewer pipes can be simulated with the URBS module. A look at the land use map tells us, that there is still a need for a module simulating lakes or retention basins. Hence, we developed this module, called SISTBA (SImulation of STorage BAsins) during this PhD thesis.

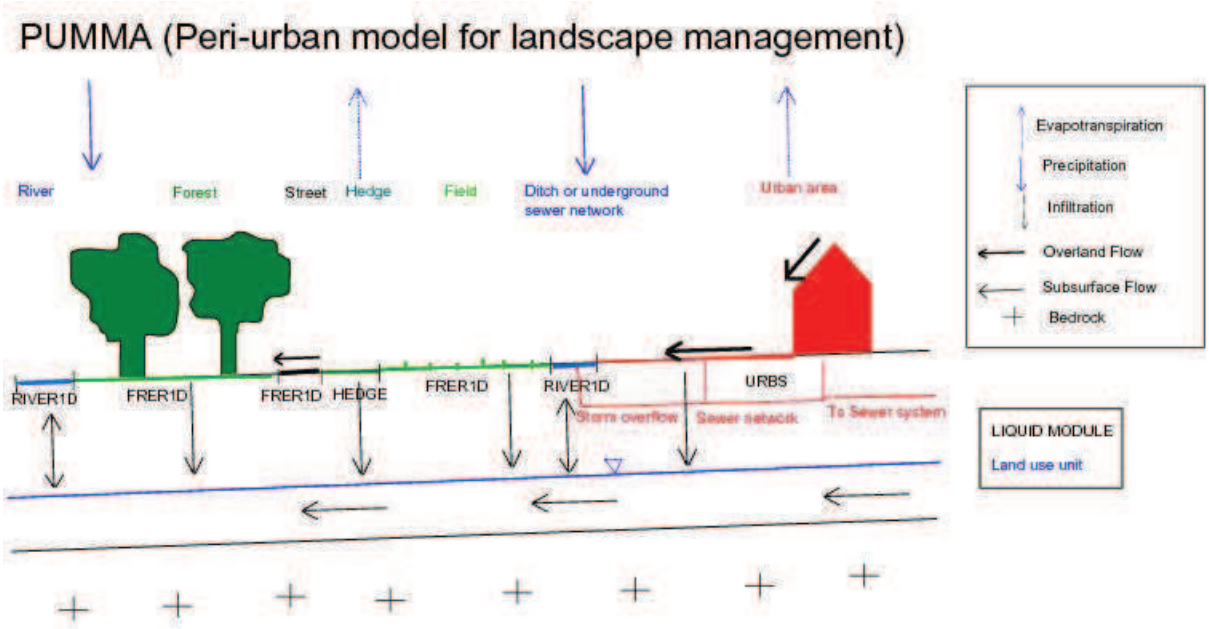

Figure 4.3.1.: Schematic representation of modelled processes and choice of modules in PUMMA. Arrows indicate water fluxes.

For the transfer processes, BVFT provides the WTI and WTRI modules simulating subsurface flow. WTI calculates the lateral subsurface flow between two model units (HEDGE, URBS or FRER1D) and WTRI simulates the subsurface flow exchange between a model unit and the drainage network. The PEF module transfers instantaneously the ponding into the closest river reach of the corresponding sub-basin. This overland flow routing representation was not adapted to the small scale of the PUMMA model. Therefore, we developed a new module, called OLAF. It improves the PEF module by allowing a flow routing from one model unit to another model unit and is based on the Manning equation. The flow routing in PUMMA is simulated with the RIVER1D module. Due to the kinematic wave approach this module is relatively robust and it can thus handle dry river beds and a fast increase of the discharge. Furthermore, this permits to reduce the programming effort, as only the runoff generation part of URBS had to be integrated into the LIQUID framework. However, RIVER1D does not simulate closed pipe systems under hydraulic pressure. As the focus of this PhD is on the runoff generation in peri-urban areas, it was decided to simulate also the sewer system with RIVER1D under the assumption that the sewer systems have open rectangular cross sections instead of circular cross sections. In a further version of PUMMA the ELIXIR module could be taken to simulate the sewer system, which would allow to simulate pipe systems under hydraulic pressure. The development of one more module was necessary for the simulation of the Chaudanne and Mercier catchments: a module simulating storm water overflow devices. Hence, the TDSO module (Threshold Dependent Stormwater Overflow) was developed, which simulates artificial storm water overflow devices such as present in the Chaudanne catchment, or natural divergences like in the Mercier catchment.

During the course of this PhD, a new version of the LIQUID modelling framework was released in order to enhance the number and types of module connexions supported by the framework. The drawback is that the previous modules had to be updated and modified to be compliant with this new version. This required code modifications and further testing of the new modules. The time required to perform this task for all the modules used in PUMMA was such that all the modules were not ready in time to be included in this PhD thesis. In particular, it was not possible to use the FRER1D module in the first version of the PUMMA model. That is why the current version of PUMMA, called PUMMA_SFRER1D, simulates agricultural fields and forests with the HEDGE module and roads with URBS instead of using FRER1D as initially scheduled. This means that overland flow on natural surfaces happens only when the whole soil profile is saturated, which does not correspond to the observations made on the field (compare to chapter 3.3). The FRER1D module is now available in the version 0.4 and will replace the HEDGE module on agricultural areas, forest and roads in the next version of the PUMMA module.

Up to now, we have presented the principles of the process modules used in the PUMMA model. We have also shown that the landscape discretization is another important point in the design of the periurban hydrological model. The following section describes the options retained in terms of spatial discretization for the PUMMA model.

4.4. Choice of spatial discretization for PUMMA model

We have seen that the PUMMA model is an extended mix of the BVFT and URBS model. Both models use an object oriented and vector based model mesh. In BVFT the land use map is directly taken as model mesh, whereas the model units in URBS, called Urban Hydrological Elements (UHEs) consist of one built-up cadastral parcel plus half of the adjoining street, see Figure 4.4.1. One UHE contains thus three compartments: the built-up area, the garden and the road area. The question is now, whether we want to keep the same model mesh for PUMMA, which will be applied at a larger spatial scale as the former BVFT and URBS applications.

For this, we have first to look at the different factors which influence the runoff generation. As we have seen in section 3 the main factor in the Mercier and Chaudanne catchments is the land use, as it also influences the topsoil hydraulic properties (Gonzalez-Sosa et al., 2010) and thus the runoff generation (DeLavenne, 2010). Furthermore, it is the criteria for the choice of the LIQUID module.

The soil and geology are important for the deeper subsurface flow. The difference in production, transfer and accumulation sites depends mainly on the slope and the topographic index (DeLavenne, 2010). The exposition plays a role for the evapotranspiration, although, this is not explicitly simulated in the model. The integration of a sub-basin map and the river and ditch network allows a topographical based flow routing as the model mesh will be intersected along ridge lines and valley bottoms.

Due to the small size of the catchments the climate can be regarded as homogeneous. A special weighting module, FCA, is available in the LIQUID framework, which allows the spatial distribution of rainfall and ETP over the model mesh. Therefore, no integration of these factors into the model mesh is necessary.

Regarding all these factors, an HRU based approach seems to be more suitable as model mesh for the rural part than just the use of the land use map. This would allow to have

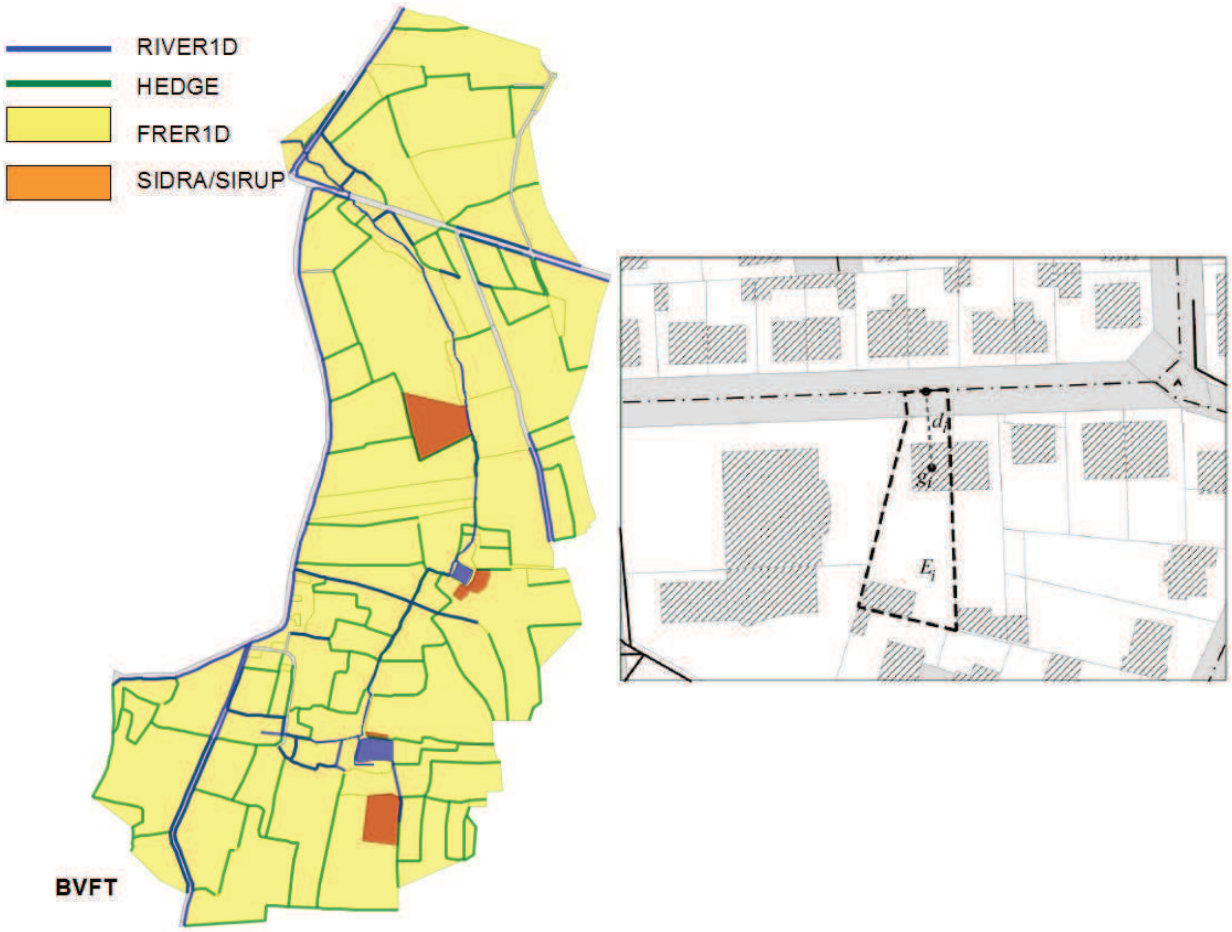

Figure 4.4.1.: Left: Object oriented model mesh of BVFT for the Fontaine du Theil catchment in north France consisting of FRER1D, HEDGE, SIDRA/SIRUP and RIVER1D model units (Branger, 2007b). Right: Concept of an UHE consisting of one cadastral parcel plus half of the adjacent street (Rodriguez et al., 2003).

model units with similar runoff generation processes, which would fit to the chosen object oriented approach.

Nevertheless, let us have a short look at some of the other model mesh opportunities seen in section 2.2.1. We could also apply the PUMMA model on a mesh consisting of TINs, as for example developed by Bocher and Martin (2009). This would allow the integration of man-made features such as ditches. However, in order to represent all of the peri-urban features, the average triangle size would have to be relatively small, which would increase the number of model units and thus the computation time. The object oriented character, in which buildings, streets, etc. are represented explicitly, would also be lost. A model mesh out of contours and stream lines is completely based on topography, and as Carluer and Marsily (2004) show, the integration of man made objects is difficult. The use of REWS, such as a sub-basin map alone, does not allow to represent the influence of the land use on the runoff generation. Finally, using raster maps means that all objects are influenced by the grid size resolution. For all these reasons we chose the HRU approach for the rural part.

Not all of the GIS layers are available at the same scale. The resolution of the land use map is better than that of the soil and geology maps. Two different DEMs are available for the Mercier and Chaudanne catchment with 2m and 25m resolution, respectively. Usually it would be appropriate to take all data at the same resolution, which would mean the coarsest resolution such as available for the soil and geology map. The Corine land cover map would provide land use data in a similar scale. However, using large HRUs for the rural part and small UHEs for the urban part is not consistent either. Also the modelling of the processes found in small peri-urban areas seems to be difficult based on a coarse model mesh. Furthermore, the land use is the most important factor, which justifies the use of the detailed land use map, compared to coarse informations about the soil. Consequently, we decided following the suggestion of Voinov (2010) to take as many input data as available.

4.5. Conclusions

The LIQUID modelling framework allows the construction of "à la carte models", that are composed of different interacting process modules. The review of the already available process modules in LIQUID identified the HEDGE, FRER1D, RIVER1D, WTI and WTRI modules as interesting for the construction of the Peri-Urban Model for landscape MAnagement. Furthermore, for the simulation of the urban zones, it was decided to integrate the URBS model into the framework. The combination of these process modules allows to simulate runoff generation on urban zones, agricultural areas, forest and hedge rows, to simulate subsurface flow as a transfer process between modelling units and to simulate flow routing in artificial and natural channels through the use of the 1D kinematic wave approach. However, it does neither include overland flow routing, nor the effect of retention basins and lakes or sewer overflow devices often present in peri-urban areas. Therefore, three new process modules called OLAF, SISTBA and TDSO, respectively, were added to the LIQUID framework. Due to the change of version of the LIQUID framework the FRER1D module was not available on time and was replaced by the HEDGE module for natural areas and by the URBS module for roads.

For the model mesh of the PUMMA model a mix of vector based HRUs and UHEs was chosen. HRUs are used in the rural part, whereas UHEs (each UHE consisting of one cadastral parcel with half of the adjacent street) are used in the urban part. The HRUs are created by intersection of the detailed land use map, the soil, geology and sub-basin maps, with the integration of slope information. The model mesh needs to be further processed in order to fulfill numerical constraints.

The BVFT and the URBS model were only applied to relatively small scales (1.28 km^2 (Branger et al., 2008) and 180 ha (Rodriguez et al., 2008)) up to now. The challenge for the PUMMA model is thus not only the integration of new peri-urban area specific processes, but also the application of the model to scales involving a larger number of modelling units. This implies the automation of the preprocessing of geographical data, as the manual data processing that was used for BVFT(Branger et al., 2008) is no longer possible. The modelling toolkit presented in the next two chapters is thus composed of two parts: the PUMMA model with its components and the complete methodology developed

for the construction of the model mesh and the extraction of hydrological routing called “automatic preprocessing”.

5. Model development

This chapter describes first the four existing modules (HEDGE, RIVER1D, WTI and WTRI) of the LIQUID framework, which are used for the development of PUMMA and then in more detail the four new developed modules. For each module the main processes, input parameters, signals and slots are presented as well as test applications for the new developments. The last section describes the assembling of the different process modules for the development of PUMMA.

5.1. Description of existing modules

5.1.1. HEDGE

The HEDGE module developed by Branger (2007b) builds on the concepts of the TNT2 model (Viaud et al., 2005). It simulates the blocking of surface runoff and higher evapotranspiration caused by hedge rows. In order to simulate the effect of vertical water fluxes such as transpiration and infiltration and lateral groundwater flow the module is divided in two compartments: retention porosity and drainage porosity. The soil is thus represented by its porosity. Untypical for LIQUID modules, these two compartments have their own time steps and can be considered as two modules merged to one. A scheme of the module is shown in Figure 5.1.1. The retention compartment contains immobile

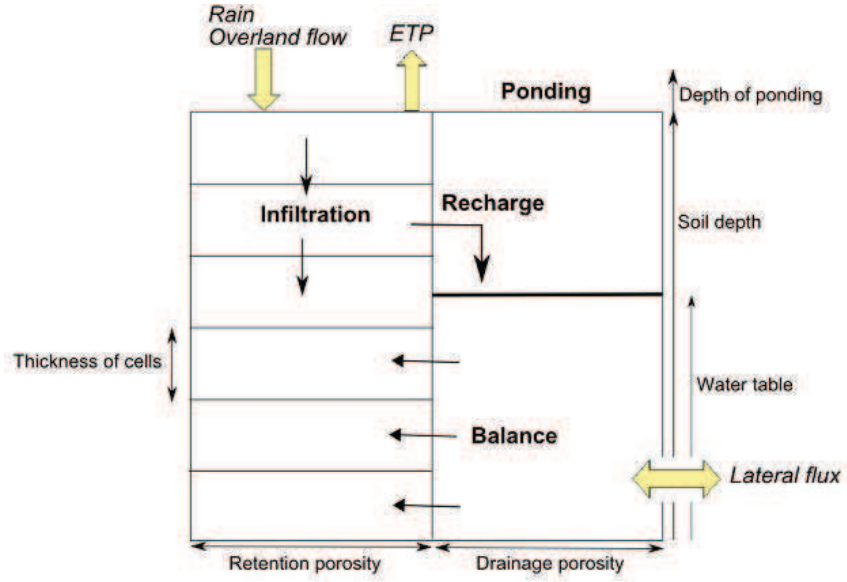

Figure 5.1.1.: Schema of the HEDGE module (Branger, 2007b).

water, which can only be extracted by root extraction and transpiration. The compartment, which is divided into several cells with uniform thickness, but different retention porosities, is filled with rain and overland flow. The main process in this compartment is vertical water flux. Its state variable, which can be different in each cell, is the volumetric

water content. The drainage porosity compartment contains mobile water and serves for the lateral groundwater flow. Its state variable is the water level. The compartment is only characterized by the soil depth and a uniform drainage porosity. It receives water from the retention compartment due to recharge and exchanges groundwater flow with other modules. Transpiration can cause the emptying of retention compartment cells below the current ground water table. HEDGE contains a mechanism that refills the cells by taking water the drainage compartment, thus lowering the water level. The rise of the water level over the soil surface creates ponding.

The input parameters of the HEDGE module are divided into two tables, the hedge_main 5.1.1 and hedge_profile table 5.1.2. The hedge_main table contains the geometry and identifier of the model unit, as well as the parameters relevant for the drainage compartment such as the average drainage porosity, the total depth of the soil profile, the surface level from model reference, the initial water table level from model reference and the number of cells. The geometry is a polygon, representing the real perimeter of the vegetated zone.

Table 5.1.1.: Input parameters of HEDGE module: table hedge_main

Field	Type	Description	Unit
id	integer	Identifier of the hedge model unit	-
ngf_surface_level	double	Average altitude of the model unit from model reference	m
soil_depth	double	Depth of the soil	m
drainable_porosity	double	Drainage porosity averaged over the whole profile	-
nb_cells	integer	Number of cells building the retention porosity	-
init_watertable_ngf	double	Initial water table from model reference	m
the_geom	Geometry	Geometric coordinates of the model unit	polygon

The hedge_profile table 5.1.2 contains the parameters characterizing the retention compartment. The retention compartment is composed of several soil layers with their positions in the soil profile, their retention porosities, their bottom depths and their initial water contents. The soil layers can thus have different realistic thicknesses. Each of these layers can contain several cells which have a uniform thickness. The bottom depth of the layers should therefore be a multiple of the cell thickness. The id represents a foreign key linking to the id of the hedge_main table. If the initial water content is equal to the retention porosity, the retention compartment is saturated.

In order to receive information from other modules, the HEDGE module has five slots shown in Table 5.1.3. The water input slot allows to receive rainfall from an input module, whereas the PETChange slot is designed to receive evapotranspiration. The lateral flow slot allows the exchange of lateral subsurface flow (positive and negative) and the overland flow slot is designed to receive overland flow. The overland flow slot was added during this PhD thesis. Contrarily to the water inputs slot, the water received by the overland flow slot is directly added to the drainage compartment instead of the retention compartment. This provokes a direct impact on the water level in the hedge and thus a direct

Table 5.1.2.: Input parameters of HEDGE module: table hedge_profile

Field	Type	Description	Unit
id	integer	Identifier of the hedge model unit	-
position	integer	Position of the soil layers	-
bottom_depth	double	Bottom depth of each soil layer	m
retention_porosity	double	Retention porosity of each soil layer	-
init_water_content	double	Initial volumetric water content per layer	-

interaction with the ponding created inside the drainage compartment. Consequently, the retention porosity is only indirectly filled with this water due to the balancing between both compartments. The vegetation has thus less influence on the surface runoff than on the rainfall. The growth of vegetation is represented by the crop coefficient which can change over the time. The CropCoeff slot allows to couple an input module with a crop coefficient time series.

Table 5.1.3.: Slots and signals of the HEDGE module

Name	Description	Unit
m_slotWaterInputs	Intensity of precipitation	ms^{-1}
m_slotPETChange	Potential evaporation	m s^{-1}
m_slotLateralFlow	Lateral subsurface flow	m^3s^{-1}
m_slotCropCoeff	Crop coefficient	-
m_slotOverlandFlow	Overland flow	m^3s^{-1}
m_sigWaterTableLevel	Actual water table level from model reference	m
m_sigPonding	Ponding height from the soil level	m
m_sigActualEvapoTranspiration	Actual evapotranspiration depending on the water availability	m s^{-1}
m_sigInfiltrationWaterMass	Total water mass in the Infiltration compartment	m^3

As output variables the HEDGE module calculates and signals the actual water table level from model reference, the height of the ponding above the surface level, the actual evapotranspiration and the total water mass in the retention compartment, see Table 5.1.3. The infiltrating water mass signal is only to observe the internal processes of the HEDGE module and should not be coupled to other modules except the output module.

As the HEDGE module was designed to simulate water fluxes in hedge rows, part of the parameters concerning the vegetation are fixed in the C++ code. The root depth is thus fixed to the soil depth and the water content of the wilting point is fixed to 25 % of the retention porosity. The only way to adapt the model for use with other vegetation types is the change of the crop coefficient.

5.1.2. RIVER1D

The RIVER1D module (Branger (2007a) and Branger et al. (2008)) assures the routing part necessary for the construction of hydrological models. It simulates the flow propagation inside an open dendritic river network (Figure 5.1.2) using the one-dimensional kinematic wave approximation of the Barré de Saint Venant equations.

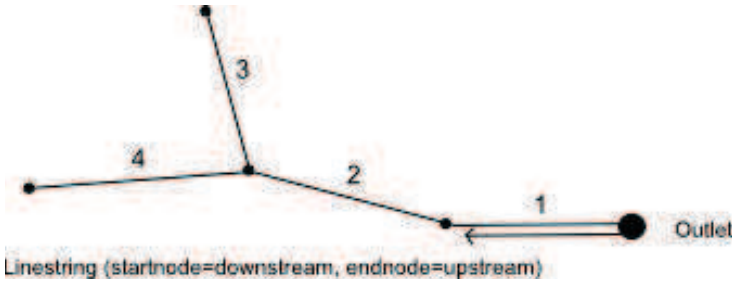

Figure 5.1.2.: Example of dendritic river network. The numbering has to rise from the outlet in upstream direction and the river reach vector lines have to show in upstream direction.

The river is divided in several reaches and for each river reach the one-dimensional shallow water equations (continuity equation 5.1.1 and dynamic equation 5.1.2, Moussa and Bocquillon (1996)) are solved numerically.

$$\frac{\partial S}{\partial t} + \frac{\partial (VS)}{\partial x} = q_{source} \tag{5.1.1}$$

$$\frac{\partial V}{\partial t} + V\frac{\partial V}{\partial x} + g\frac{\partial h}{\partial x} + g(j - i) = 0 \tag{5.1.2}$$

where S is the wetted section in m^2, V the velocity in m s^{-1}, h the water level in m, t the time in s, x the abscissa in m, i the slope j the friction loss, g the gravitational acceleration and q_{source} are the lateral inflows per meter in $m^2 s^{-1}$. The model of the kinematic wave equation supposes a permanent uniform flow in all river reaches, which leads to the disregard of all terms of the dynamic equation except the friction loss. The velocity can then be calculated with the Manning equation:

$$V = \frac{1}{n}\sqrt{i}R_H^{2/3} \tag{5.1.3}$$

where n is the Manning coefficient and R_H the hydraulic radius in m. The continuity equation 5.1.4 is then solved numerically and explicitly using the Runge-Kutta algorithm of the forth order (Press et al., 2002).

$$\frac{\Delta S}{\Delta t} = \frac{Q_{in} - Q_{out} + q_{source}}{l} \tag{5.1.4}$$

where l is the length of the river reach. The calculation variable is the water level. The outflow Q_{out} is the product of the wetted section and the velocity calculated with the Manning equation. The five slots rain, PET, source, lateral subsurface and surface flow (see Table 5.1.4) contribute to the source term q_{source} of equation 5.1.4. No difference is thus made for the five slots. The slots enable the lateral (sub-) surface flow exchange with other modules.

Table 5.1.4.: Slots and Signals the RIVER1D module

Name	Description	Unit
m_slotRain	Precipitation intensity	m s^{-1}
m_slotPET	Potential evaporation	m s^{-1}
m_slotSource	Connection to source	$m^3 s^{-1}$
m_slotLateralSubsurface	Lateral subsurface flow exchange	$m^3 s^{-1}$
m_slotLateralSurface	Lateral surface flow	$m^3 s^{-1}$
m_sigOutletDischarge	Discharge at the river outlet	m^3 s^{-1}
m_sigWaterBalance	The total mass balance of the river	m^3
m_sigReachWaterLevel	Water level of a river reach from river bottom	m
m_sigReachWaterElevation	Water level of a river reach from model reference	m
m_sigReachDischarge	Discharge of a river reach	m^3 s^{-1}

The model calculates the water level and discharge in each river reach as well as the discharge at the outlet and the total mass balance (Table 5.1.4). The signals m_sigOutletDischarge and m_sigWaterBalance refer to the complete river, which means that for the connection to other modules the river id has to be used. On the contrary, the other three signals refer to the reach id. The water level from model reference (altitude + water level) is necessary for the coupling with the WTRI module.

The module has seven PostgreSQL input tables. One table for the section including the section id, the name of the section and the type, which can be trapezoidal, rectangular or triangular. Each section is further described by a table containing the section id, the bottom width and batter. One model can have several rivers, which are indicated in a corresponding table with their id, their name and the id of the outlet reach. The manning values are in a different table containing their id, the name or description and the roughness value. The geometries are stored in the reach table 5.1.5, together with the slope, the mean altitude of the river bottom, the initial water level of each river reach and the references to the manning, river and section tables.

Table 5.1.5.: Input parameters of RIVER1D module: table river1d_reach

Field	Type	Description	Unit
id	integer	Identifier of the river reach	-
river_id	integer	Identifier of the corresponding river	-
manning_id	integer	Identifier of the corresponding manning value	-
section_id	integer	Identifier of corresponding section	-
slope	double	Average slope of the river reach	–
elevation	double	Average altitude of the river reach bottom from model reference	m
water_level	double	Initial water level from river bottom	m
the_geom	Geometry	Geometric coordinates of the model unit	line

For the original version of RIVER1D (Branger, 2007a) a minimum discharge had to

be injected as source term into the river network, as the module ended up in an endless loop at lower water levels. In order to be able to simulate ditch networks which are most of the time dry, the module was adapted. When the water level is below 10^{-3} m and the level variation is below 10^{-6} m s^{-1}, the state variable is not updated. Furthermore, the module was optimized to improve the calculation time. The module cannot simulate pressurized pipe flow, back flow caused by dams nor the extension of real flood plains. For this, more complex hydraulic modules could be used as for example the ELIXIR module for the simulation of pressurized pipe flow.

5.1.3. WTI

The lateral subsurface flow is simulated by means of the Water Table Interface, WTI module (Branger, 2007b). This module calculates the lateral subsurface flow between two flow generation modules such as HEDGE, URBS or FRER1D. The geometry of the module consists of the intersection between the polygons, which is a line (see Figure 5.1.3).

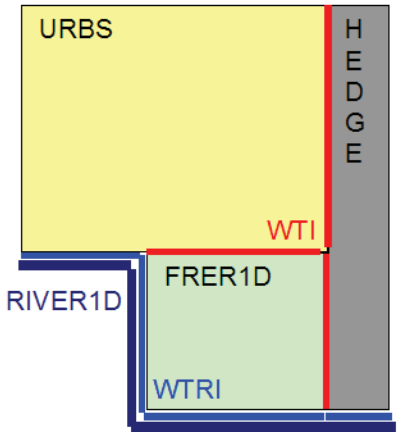

Figure 5.1.3.: Simulation domain of WTI and WTRI (Branger, 2007b).

WTI receives the water level of the adjacent model units A and B by means of the slots m_slotLevelA and m_slotLevelB (5.1.6). It calculates then the discharge $Q_{A\rightarrow B}$ between the model units with the Darcy law:

$$Q_{A\rightarrow B} = k_f S \times \frac{\Delta h}{l} \tag{5.1.5}$$

where k_f is the mean hydraulic conductivity, S the wetted section, l the distance between the centers of the model units and Δh the difference in hydraulic pressure. The wetted section is calculated as product of the water level and length of the interface. The difference in hydraulic pressure equals here the difference in the water table levels. The particularity of a LIQUID interface compared to modules representing objects is, that an interface does not have its own time step. In WTI, the execution is forced as soon as a significant change in one of the water tables is signaled. For its calculation WTI needs the input parameters presented in table 5.1.7. Most input parameters can be derived from the neighboring model units (HEDGE, FRER1D or URBS).

Finally, the module signals the calculated discharge to the adjacent model units. Depending on the flow direction this discharge is positive or negative ($Lateral flux A =$

Table 5.1.6.: Slots and signals of the WTI module

Name	Description	Unit
m_slotLevelA	Water level of model unit A	m
m_slotLevelB	Water level of model unit B	m
m_sigWaterTableLevel	Water table level in the interface	m
m_sigLateralFluxA	Lateral discharge from B to A	$m^3\ s^{-1}$
m_sigLateralFluxB	Lateral discharge from A to B	$m^3\ s^{-1}$

$-1 \times (Lateral flux B)$). The actual water level inside the interface is calculated with the distance weighted average between the model units.

Table 5.1.7.: Input parameters of WTI module

Field	Type	Description	Unit
id	integer	Identifier of the interface	-
id_a	integer	Identifier of model unit A from model reference	-
id_b	integer	Identifier of model unit B from model reference	-
bedrock_a	double	Bedrock altitude of model unit A from model reference	m
bedrock_b	double	Bedrock altitude of model unit B from model reference	m
surface_level	double	Average altitude of the interface from model reference	m
depth	double	Bedrock depth of the interface	m
permeability	double	Mean permeability	$m\ s^{-1}$
the_geom	Geometry	Geometric coordinates of interface	line
center_a	Geometry	Geometric coordinates of the center of model unit A	point
center_b	Geometry	Geometric coordinates of the center of model unit B	point

Each WTI solver has always two neighbors. If one model unit (polygon) is neighbor with several other model units several instances of WTI have to be used. The discharge received by one model unit is then added with the PLUS module. Depending on the amount of model units a high number of interfaces may be necessary. This can induce an increase of the computational time. In order to reduce the computational time, a threshold of 2 cm was introduced concerning the water level. Consequently, the module will only calculate a discharge if the water level difference is higher than the threshold and if the water levels varied by more than the threshold. For the moment this threshold is still defined directly in the source code, but in a further version of the module it should be added to the input parameter table.

5.1.4. WTRI

WTRI (Water Table River Interface) (Branger (2008b); Dehotin (2007)) is similar to the WTI interface. However, it calculates the groundwater exchange between a model unit, which means a polygon, and a river reach, which is represented by a line, see Figure 5.1.3. Instead of the Darcy equation, it uses the Miles approach (Miles, 1985), which considers the water table deformation close to the river based on the Dupuit-Forschheimer hypothesis. This hypothesis assumes that the vertical flow component in the Boussinesq equation is negligible compared to the horizontal flow component. The difference ΔH in water level between the river and the groundwater at the interface between zone I and II (see Figure 5.1.4) can be estimated using the following equation (Branger, 2008b):

$$\Delta H^2 + 2(l_2 C_m + H_{riv} + D_i)\Delta H - D_w(2H_{riv} + 2D_i + D_w) = 0 \tag{5.1.6}$$

where the Miles coefficient C_m can be calculated with

$$C_m = \frac{B[0.25(W_s + W_b) + H_{riv} + s]}{D_i + H_w + s} \tag{5.1.7}$$

where B is a coefficient, s is the seeping depth. Figure 5.1.4 shows the significance of the geometric parameters: W_b is the river bottom width, W_s is the river surface width, D_i is the bedrock depth below the river, D_w is the water level difference between river and groundwater, l_2 the length and H_{riv} is the water level in the river. The discharge is then

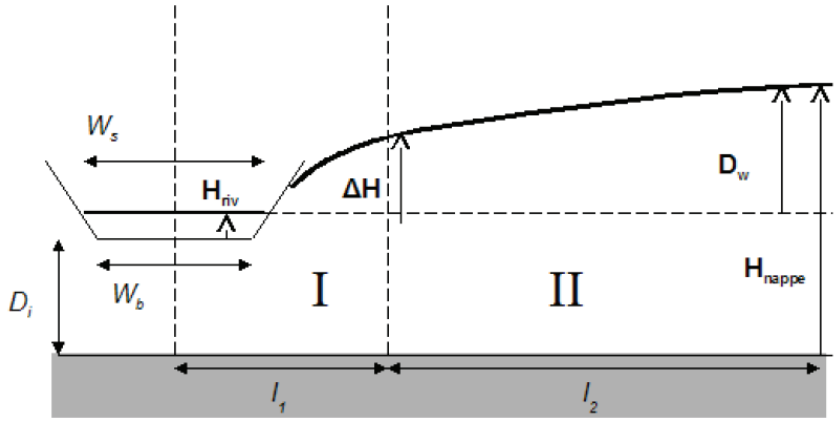

Figure 5.1.4.: Schema indicating the parameters for the Miles method (Branger (2008b); Miles (1985)).

calculated with the following equation:

$$Q_{gw \to river} = L \times K \Delta H C_m \tag{5.1.8}$$

where L is the length of the interface(line) and K is the hydraulic conductivity in m s^{-1}.

As input parameters WTRI needs information from the neighboring plot and river reach, as the ids, the centre of the plot, the bedrock depths and river bottom width and level as well as the average permeability.

WTRI has only two slots and two signals. The slots allow to receive the water levels of the river and the plot and the signals send the calculated discharge. The sign is positive

Table 5.1.8.: Slots and signals of the WTRI module

Name	Description	Unit
m_slotWaterTableLevel	Ground water level in plot from model reference	m
m_slotRiverLevel	Water level in corresponding river reach from model reference	m
m_sigWTRiverLateralFlow	Lateral flux from plot to river	$m^3\ s^{-1}$
m_sigRiverWTLateralFlow	Lateral flux from river to plot	$m^3\ s^{-1}$

Table 5.1.9.: Input parameters of WTRI module

Field	Type	Description	Unit
id	integer	Identifier of the river reach	-
id_plot	integer	Identifier of model unit (plot)	-
id_riv	integer	Identifier of river reach	-
riv_bottomwidth	double	Bottom width of river reach	m
riv_bottomlevel	double	Bottom level of river reach from model reference	m
riv_bedrock	double	Bedrock level below river from model reference	m
plot_bedrock	double	Bedrock level below plot from model reference	m
permeability	double	Mean permeability	$m\ s^{-1}$
the_geom	Geometry	Geometric coordinates of the interface	line
center_plot	Geometry	Geometric coordinates of the centre of the plot	point

or negative depending on the flow direction. In the original version of WTRI the case that the river can be higher than the plot was not considered. Nevertheless, this configuration is possible, for example when roadside ditches cut across a hillside. Therefore this special case was integrated into the WTRI module in the framework of this PhD thesis.

5.2. Development of new modules

To correctly represent the hydrological processes found in suburban areas the URBS model was integrated into the LIQUID framework and three new modules were developed: TDSO simulating storm water overflow devices, SISTBA simulating retention basins and lakes and OLAF, which simulates overland flow based on pre-determined flow directions and connections. They are presented in the following including a description of the module principles, its implementation within LIQUID and simple test cases aiming at verifying and illustrating the module behaviour.

5.2.1. URBS: Urban Runoff Branching Structure

5.2.1.1. Concepts and used equations

URBS for Urban Runoff Branching Structure is originally an independent hydrological model for urbanized areas. It was developed during the PhD theses of Rodriguez (1999) and Morena (2004) and further published by Rodriguez et al. (2008). The model is divided into a production and a routing part, which uses the Muskingum-Cunge Scheme. P. Viallet of Hydrowide rewrote the production part in C++ as LIQUID module for use in this PhD thesis. The RIVER1D module replaces the routing part of the model. Extensive testing and error analysis of the new URBS module was an important part of this PhD thesis. As verification its results were compared with the results of the original URBS code. Once the results agreed, some new functionalities necessary for the coupling to other LIQUID modules were integrated. The model with all its equations is described in detail in Morena (2004) and Rodriguez et al. (2008). This section gives a summary of the main principles and equations and describes the object oriented implementation of the model in the LIQUID code as well as the new functionalities.

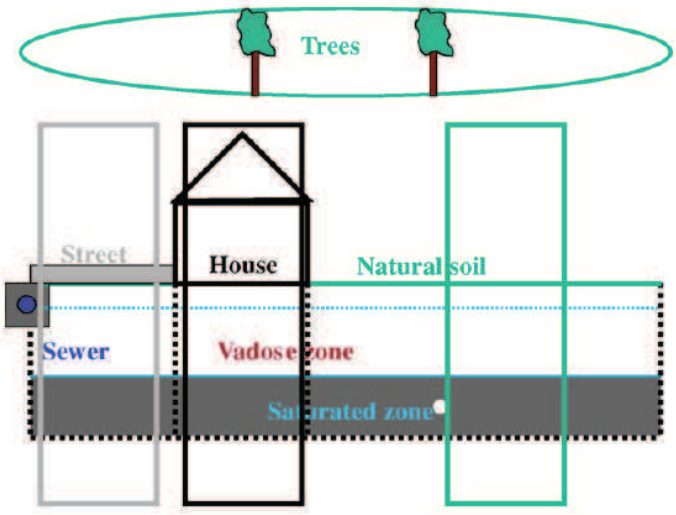

Figure 5.2.1.: Vertical profile of the urban hydrological element including street, house and natural soil (Rodriguez et al., 2008).

The URBS module has as model units so called "Urban Hydrological Elements (UHEs)" (Rodriguez et al., 2003). A UHE consists of a cadastral unit plus half of the adjoining street. It is divided in three parts: the natural soil, the street and the house, see Figure 5.2.1. Each of the three land use classes is further divided in three reservoirs organized vertically: the surface, the vadose zone and the saturated zone. A fourth reservoir which is common to all of the three land use classes represents the interception by trees, see Figure 5.2.2. The principal functions of the model are based on the water balance between the different reservoirs and thus continuity equations. The in- and outcoming fluxes are shown in Figure 5.2.2. The interception is calculated with a simple reservoir model proposed by (Calder, 1977). The size of the reservoir is determined by the wooded percentage covering the UHE. The reservoir is characterized by its minimal level and a discharge coefficient. Both of them are different depending on the season. The water balance of the reservoir is

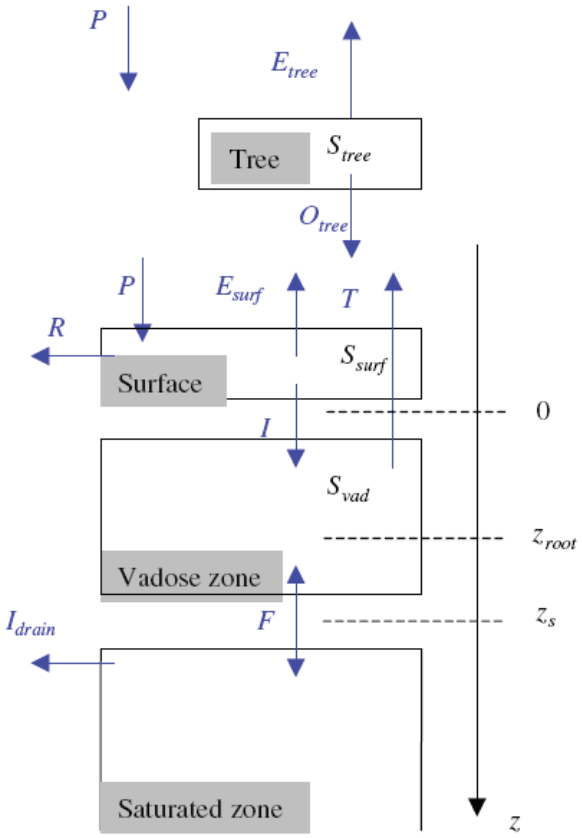

Figure 5.2.2.: Vertical fluxes and reservoirs of one UHE land use type. 0 is the soil surface, z_{root} the root depth, z_s the saturated zone depth, R the surface runoff, I_{drain} the network infiltration, O_{tree} the throughfall, I the infiltration, F the capillary fringe flux, P the precipitation and E the evapotranspiration (Rodriguez et al., 2008).

governed by its inputs (precipitation) and outputs consisting of evapotranspiration and a drainage function in which the discharge coefficient enters as a factor.

The surface reservoirs of each land use type are supplied with water by direct rainfall and throughfall and drained by both infiltration and surface runoff. The surface runoff is calculated for each land use type separately. The infiltration flux depends on the saturated hydraulic conductivity of the land use types, whereas the surface runoff occurs when the maximal level of the reservoir is exceeded (Rodriguez et al., 2008). The link coefficients in table 5.2.1 account for the fact that not all water generated on the cadastral unit is directly connected to the drainage pipe. If the link coefficient of the built and road area is smaller than 1 the rest of the water is transferred to the natural surface reservoir. If the natural link coefficient is smaller than 1, the water will be injected into the natural surface reservoir at the next time step. This allows to consider stagnating water, which evaporates or infiltrates slowly.

In order to take into account the influence of soil structure, which is usually more compact with increasing depth, the saturated hydraulic conductivity is calculated with an exponential function depending on the depth and a scaling parameter (Beven and Kirkby, 1979). The suction and the hydraulic conductivity are calculated with the Brooks and Corey (1964) law and depend thus on water content and the retention curve exponent. The wilting point water content is then calculated by setting the suction head to 150m.

The vadose or non saturated zone is represented by a reservoir with variable thickness and a mean moisture content theta. It receives infiltrated water from the surface reservoir, provides the water transpired by trees and exchanges water with the saturated zone. The exchange flux is calculated with the Darcy law applied between the saturation level and a representative depth which depends on the parameter alpha. The flux can be positive, meaning seepage to the groundwater table or negative caused by capillary rise.

The saturated zone receives water due to seepage from the non saturated zone and drains towards the sewer pipe. It is characterized by the groundwater level, or seen the other way around its deficit. Water can infiltrate into the sewer pipes when the groundwater table is above the pipe. The infiltrating flux I_{drain} depends on the groundwater table $z_s(t)$, which is the average of the three land use classes. It is calculated with the ideal drain approach (Cassan (1986); Gustafsson et al. (1996)):

$$I_{drain}(t) = K_s^{nat} e^{-\overline{z_s(t)/M}} \frac{\lambda}{L} (z_{soil} - z_{net} - \overline{z_s(t)})^{\mu} \tag{5.2.1}$$

where K_s^{nat} is the saturated hydraulic conductivity of the natural part, L is the length of the cadastral unit, z_{soil} is the altitude of the UHE, z_{net} is the depth of the drainage network and μ, M and λ are groundwater drainage parameters.

5.2.1.2. Implementation in LIQUID

In the LIQUID code each of the four reservoirs (interception, surface, non-saturated zone and saturated zone) heritates from the LIQUID class CTank, which is a template for the development of reservoir-based modules. The classes CInterceptionTank, CSurfaceTank, CNSZTank and CSZTank and their relations are shown in the UML diagram (Figure 5.2.3). An extra class describes the soil, which is associated to the non saturated zone. The surface and interception reservoir are also associated to the non saturated zone class. All of the four reservoir are implemented in the CColumn class, which stands for the soil column. The solver has three instances of the CColumn class, one for each land use type. Like for the other modules the CSolver class contains the main function *operator()*. For a better visibility only the main methods are shown in the UML diagram and not the signals, slots, setters and getters.

The input parameters and their significations are shown in table 5.2.1. They can be classified in geomorphological parameters, parameters concerning the tree coverage, the surface, the soil, the sewer system and the connection to the sewer system.

The original version of URBS had only two time dependent input variables, precipitation and evapotranspiration. In order to couple the module URBS with the WTI and WTRI interfaces a new slot (m_slotSZSinkSource) was added to the saturated zone tank, see table 5.2.3. This changes from the original version of URBS, where the saturated zone reservoir was only governed by the drainage to the pipe and the vertical water flux. Another slot was added to URBS creating the possibility to receive overland flow coming from other model units. This slot is directly connected to the surface tank. The current version of URBS provides still a large number of signals which are useful for module testing. Only the signals necessary for connections with other modules and interesting as model output are shown here. The groundwater level is signaled by m_sigZSLevelFromReference to the WTI and WTRI interfaces. The discharge to the drainage network is signaled with m_sigNetworkFlow. A signal ending with "Flow" signifies $m^3\ s^{-1}$, whereas "Flux" means $m\ s^{-1}$. The URBS module used for the construction of

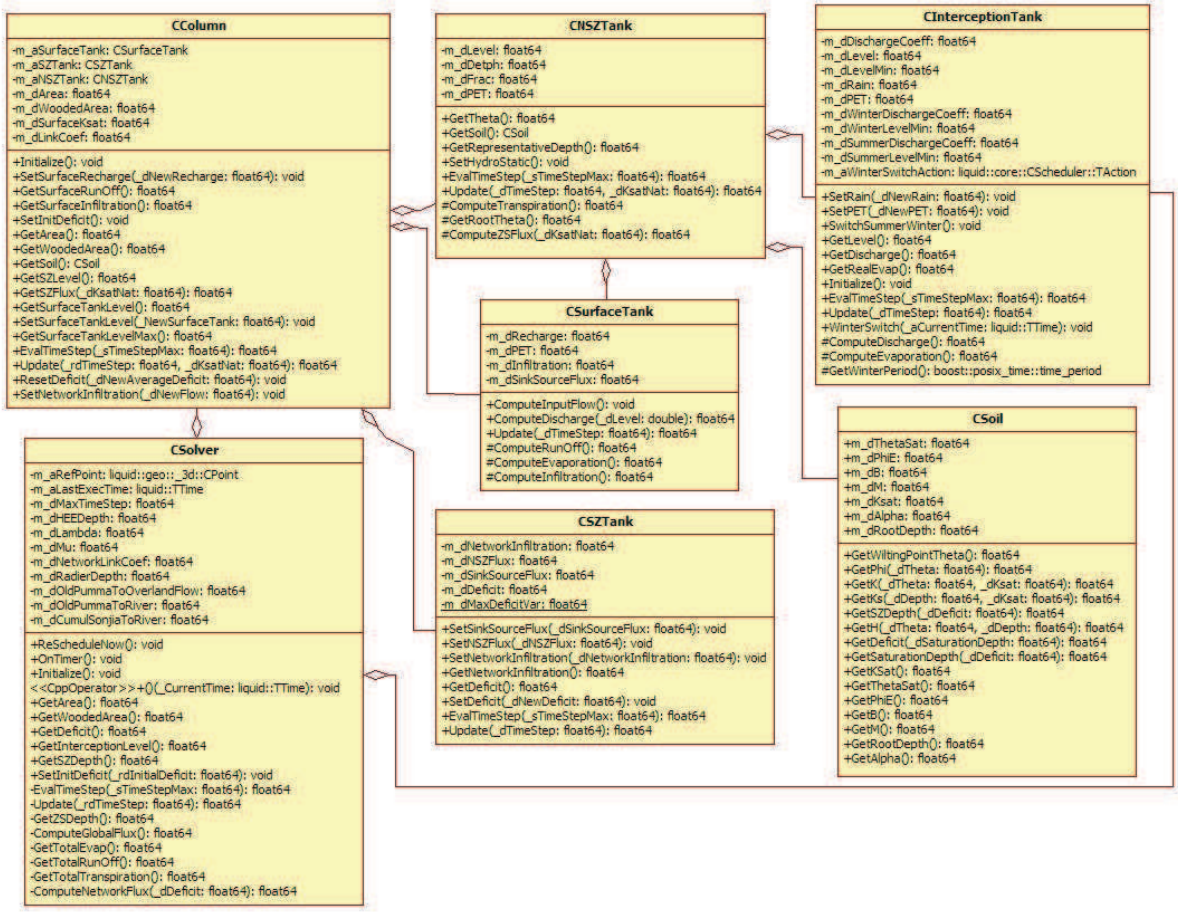

Figure 5.2.3.: The class diagram of the URBS module including the main functions. Each class is divided in three parts: the name, the attributes or members and the operations. Only the main operations are shown due to visibility. Most of the setters, getters, signals and slots are left out. - signifies private, + public and # protected. The connections are aggregations.

PUMMA contains the signals m_sigPummaToRiver and m_sigPummaToOverlandFlow. m_sigPummaToRiver contains the sum of network flow, built and surface runoff, whereas m_sigPummaToOverlandFlow consists only of the natural surface runoff. In order to reduce the calculation time, both signals are activated only if the discharge exceeds the threshold of 0.1 l s^{-1}.

5.2.1.3. Module verification

The test case for the URBS model was borrowed from Morena (2004). The case study was the average UHE of the Rezé catchment (4.7 ha) which is one of the pilot sites of the research laboratory IFSTTAR in the suburbs of Nantes, France. Figure 5.2.4 shows the network flux and the total surface runoff of 1991 in the Rezé catchment, obtained by simulation with the original URBS model and the new LIQUID module. The same parameters as Morena (2004) (p. 33) were used for both simulations. The output of the LIQUID module is here plotted with a variable time step, whereas the URBS model uses a time step of 5 minutes. This explains the difference in the peak values of the total

Table 5.2.1.: Input parameters of URBS module

Field	Type	Description	Unit
GEOMORPHOLOGICAL PARAMETERS			
id	integer	Identifier of the URBS model unit	-
built_area	double	Built surface of the UHE	m^2
road_area	double	Road surface of the UHE	m^2
natural_area	double	Natural surface of the UHE	m^2
hee_depth	double	Surface field depth of UHE	-
the_geom	Geom.	Geometric coordinates of the UHE	line
ref_point	Geom.	3d point of the plot centre with altitude	point
TREES			
built_wooded_percent	double	Wooded percent of the built part	-
road_wooded_percent	double	Wooded percent of the road part	-
natural_wooded_percent	double	Wooded percent of the natural part	-
interception_level_initial	double	Initial level of the interception reservoir	m
interception_level_min	double	Minimal level of the interception reservoir	m
interception_level_ winter_min	double	Minimal level in winter of the interception reservoir	m
interception_level_ discharge_coef	double	Percentage of intercepted water draining to the surface reservoir	-
SURFACE			
built_surface_ level_initial	double	Initial level in the built surface reservoir	m
road_surface_ level_initial	double	Initial level in the road surface reservoir	m
natural_surface_ level_initial	double	Initial level in the natural surface reservoir	m
built_surface_ level_max	double	Maximal level of the built surface reservoir	m
road_surface_ level_max	double	Maximal level of the road surface reservoir	m
natural_surface_ level_max	double	Maximal level of the natural surface reservoir	m
built_surface_k_sat	double	Saturated hydraulic conductivity of roof	m s^{-1}
road_surface_k_sat	double	Saturated hydraulic conductivity of road	m s^{-1}
natural_surface_k_sat	double	Natural saturated hydraulic conductivity	m s^{-1}

surface outflow. Overall, the new URBS module gave the same results as the original URBS model and could thus be validated.

Table 5.2.2.: Input parameters of URBS module. Continuation

Field	Type	Description	Unit
SOIL			
radier_depth	double	Depth of the drainage pipe	m
saturated_zone_depth	double	Depth of saturated zone	m
tetha_sat	double	Water content at natural saturation	-
psi_e	double	Suction head at air entry	-
b	double	Retention curve exponent	-
m	double	Scaling parameter of the hydraulic conductivity	-
alpha	double	Representative position of the vadose zone	-
root_depth	double	Root depth	m
SEWER SYSTEM			
λ	double	Groundwater drainage coefficient	-
μ	double	Groundwater drainage exponent	-
CONNECTION			
built_link_coef	double	Percentage of surface runoff from roof directly connected to the drainage network	-
road_link_coef	double	Percentage of surface runoff from road directly connected to the drainage network	-
natural_link_coef	double	Percentage of surface runoff from natural area directly connected to the drainage network	-
network_link_coef	double	Percentage of water from saturated zone draining to the network	-

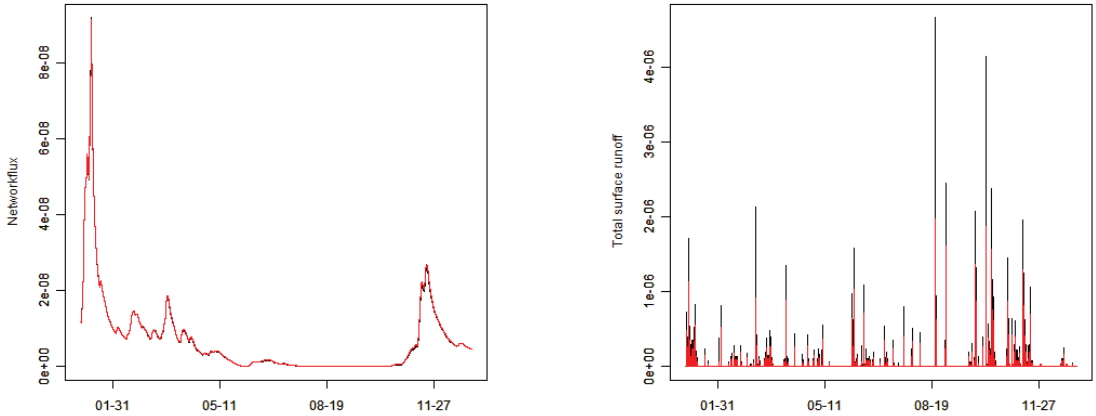

Figure 5.2.4.: Comparison of network flux in m s^{-1} and total surface runoff in m s^{-1} of the original URBS model (red) and the LIQUID module (black).

Table 5.2.3.: Slots and signals of the URBS module

Name	Description	Unit
m_slotRain	Precipitation	m s^{-1}
m_slotPET	Evapotranspiration	m s^{-1}
m_slotSZSinkSource	Groundwater exchange	m^3 s^{-1}
m_slotOverlandFlow	Overland flow	m^3 s^{-1}
m_sigPummaToRiver	Sum of network flow, built and road surface runoff	m^3 s^{-1}
m_sigPummaToOverlandFlow	Natural surface runoff	m^3 s^{-1}
m_sigTotalSurfaceRunOff	Total surface runoff of cadastral unit	m^3 s^{-1}
m_sigZSLevelFromReference	The water table level from model reference	m
m_sigNetworkFlow	Infiltrating flux into the network	m^3 s^{-1}
m_sigRoadSurfaceTankLevel	Water level in the road surface tank	m
m_sigNaturalSurfaceTankLevel	Water level in the natural surface tank	m
m_sigBuiltSurfaceTankLevel	Water level in the built surface tank	m
m_sigInterceptionTankLevel	Water level in the interception tank	m
m_sigTotalEvap	Total evaporation flux from interception tank and surface tank	m s^{-1}
m_sigTotalTranspiration	Total transpiration flux	m s^{-1}
m_sigZSDepth	Depth of the saturated zone	m
m_sigRoadNSZThetha	Road vadose zone water content	%
m_sigNaturalNSZThetha	Natural vadose zone water content	%
m_sigBuiltNSZThetha	Built vadose zone water content	%

5.2.2. TDSO: Threshold Dependent Stormwater Overflow device

5.2.2.1. Concepts and used equations

Sewer overflow devices are installed to discharge overstrained sewer systems. The overflow can lead to the next natural stream, but also towards other sewer systems. The picture in Figure 5.2.5 shows a typical sewer overflow chamber where a lateral sewer overflow is activated when the water level rises over the pipe crest. In this specific case the overflow is further regulated by a sewer port.

Sewer overflow devices can have a large variety of designs, but the basic principle is that of a divergence (Figure 5.2.5). Depending on a certain threshold value water flows over a weir crest into another pipe system. Divergences can also be found in natural river systems, especially during floods when the water level rises above the main river bed.

The objective for the development of the module TDSO was to create a simple module connecting the artificial sewer system and the natural river, which can be used to simulate both, artificial and natural divergences. In the current version of TDSO the equations are only valid for free surface flow without downstream influence. Same as in the hydraulic software CANOE (Sogreah and Insavalor, 2005) no difference is made for lateral and frontal storm water overflow devices. This could be improved in a further version. As the overflow of SODs is usually limited by a pipe diameter, a combination of weir (Poleni)

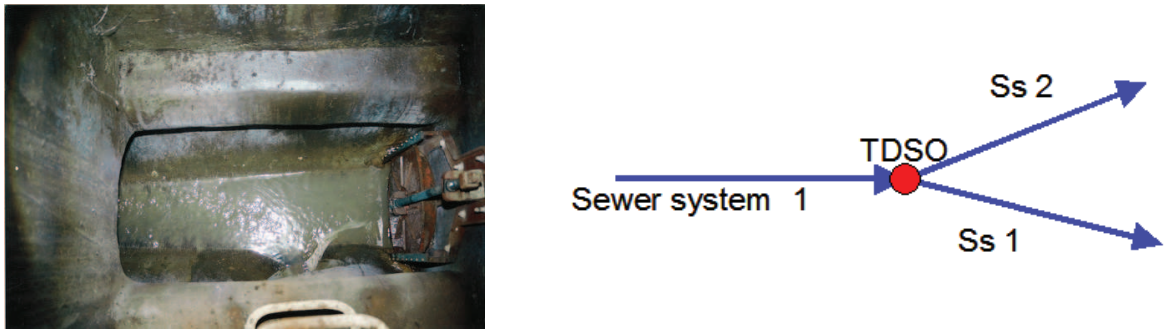

Figure 5.2.5.: Left: Picture of stormwater overflow device in the Chaudanne catchment (Pascal Breil). The overflow is regulated by a sewer port. Right: Spatial configuration for use of TDSO module. Ss means sewer system.

and orifice equations was chosen (Carlier (1972); Sogreah and Insavalor (2005)). Like in the hydraulic software MAGE (Faure, 2007), we consider the discharge coefficient μ [] as constant and equal for both equations.

$$Q = \mu L h \sqrt{2gh} \qquad \text{for } 0 < h \leq T \tag{5.2.2}$$

$$Q = \mu L (T - c) \sqrt{2gh} \qquad \text{for } h > T \tag{5.2.3}$$

where Q is the calculated discharge in $m^3\ s^{-1}$, μ is the discharge coefficient [-], c is the height of the weir crest $[m]$, L the width of the weir crest $[m]$, g the gravitational constant equal to 9.80665 m s^{-2} and h the water level above the weir crest $[m]$(Figure 5.2.6). The

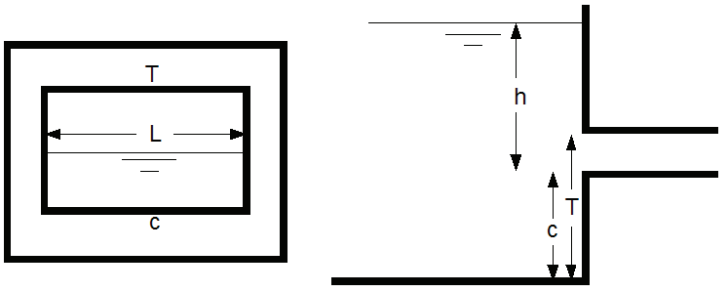

Figure 5.2.6.: Schema of a stormwater overflow. Frontal view on the left and side view on the right side. L is the width of the overflow, c the height of the weir crest, T the top of the weir crest and h the water level from the weir crest.

orifice equation is similar to the weir equation, but the variable cross section, calculated by $L * h$ in equation 5.2.2 is replaced by the constant cross section of the orifice. Even for pipes, the cross section is considered as rectangular and the width is calculated by the square root of the cross section. A default value of 0.82, which corresponds to the value for orifices leading to a pipe (Carlier (1972); p.182) is proposed for μ. After Carlier (1972) the water level of the orifice equation should be calculated from the center of the orifice. However, in order to assure the continuity between the two equations the water level for both equations is calculated from the top of the weir crest, which represents the bottom of the overflowing pipe. This implies an error of half an orifice, which we neglect.

5.2.2.2. Implementation in LIQUID

The TDSO module can be considered as interface in LIQUID, as it does not have an own time step. It is similar to the WTRI module. TDSO has a point geometry and connects two different rivers, the main river or pipe and the diverting river or pipe (Figure 5.2.5). It has a single slot for the upstream water level and signals the with equation 5.2.4.1 calculated discharge as positive to the diverting river reach and negative to the upstream river reach, see Table 5.2.4.

Table 5.2.4.: Slots and Signals of the TDSO module

Name	Description	Unit
m_slotWaterLevel	Water level of connected river reach	m
m_sigInDischarge	Overflowing discharge (negative)	$m^3\ s^{-1}$
m_sigOutDischarge	Overflowing discharge (positive)	$m^3\ s^{-1}$

TDSO has only the CSolver class (Figure 5.2.7) with the CurrentRiverLevel as state variable and the parameters needed for equation 5.2.4.1 as member variables. The weir and orifice equations (5.2.4.1) are implemented in the ComputeOverflow() function. The execution is triggered when the module receives a new water level which differs in more than 1 cm from the old water level.

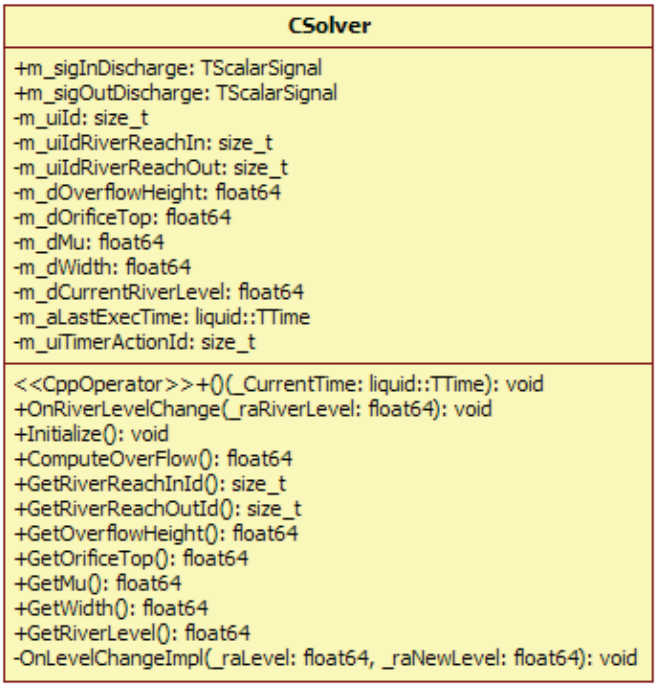

Figure 5.2.7.: The UML diagram of the module TDSO.

Beside the input parameters necessary for the weir and orifice equations TDSO needs as input the id of the upstream and the diverting river reaches and the point geometry, see Table 5.2.5.

Table 5.2.5.: Input parameters of TDSO module

Field	Type	Description	Unit
id	integer	Identifier of stormwater overflow device	-
id_riverreach_in	integer	Identifier of upstream river reach	-
id_riverreach_out	integer	Identifier of diverting river reach	-
overflow_height	double	Weir crest from river bottom	m
orifice_top	double	Height of orifice top from river bottom	m
mu	double	Discharge coefficient	–
width	double	Width of weir crest	m
the_geom	Geometry	Geometric coordinates of overflow device	point

5.2.2.3. Module verification

A simple test case was constructed consisting of a main river with 5 reaches and a diverting river which had just one reach, see Figure 5.2.8. The overflow height of the stormwater overflow was 0.2m, the top of the orifice 0.5m and the width 0.2m. The default value of 0.82 was taken for μ. Both rivers had a rectangular cross section with 0.5m bottom width, a slope of 0.001 and a Manning value of 0.011.

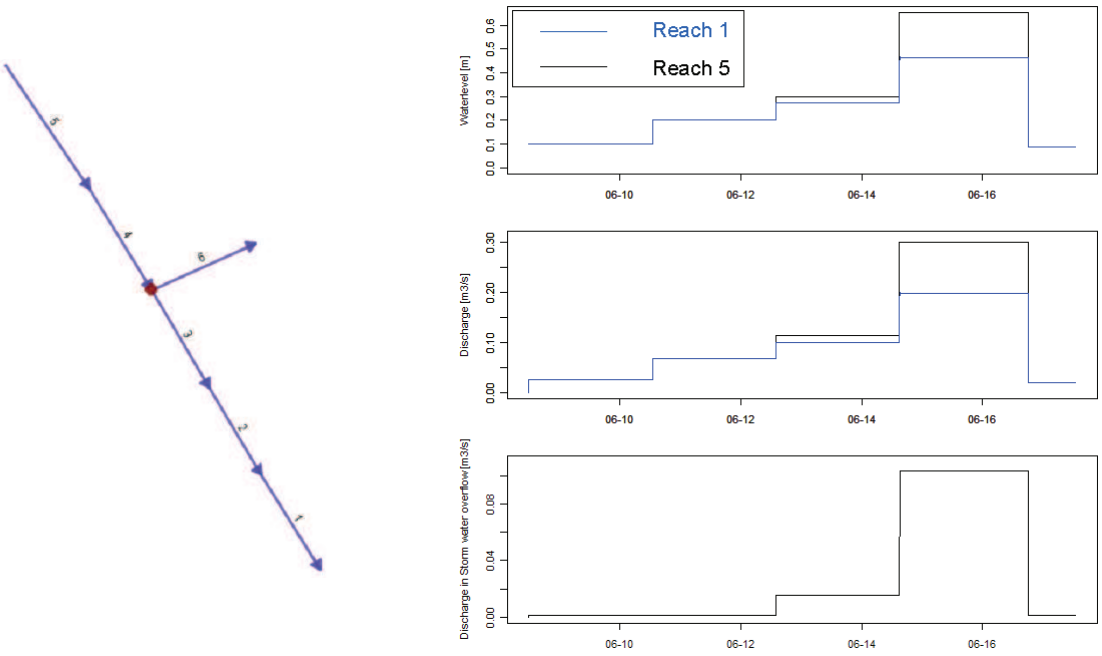

Figure 5.2.8.: Left: The test case for the TDSO module consisting of two rivers with five and one reaches respectively. The reach ids are indicated. The TDSO is coupled to reach 3. Right: The results of the TDSO test case. The upper two panels show the water level and discharge in the main river. Reach 1 (blue) is downstream of TDSO and reach 5 (black) is upstream. The lower panel shows the overflowing discharge. The limits of the y-axis are not the same for the discharge in the main river and the overflowing discharge.

An input module connected to river reach 5, provided the inflow. The water level in all reaches of the main river was initialized with 0.1m and in reach 6 with 0.015m.

Figure 5.2.8 shows the results of the simulation over eight days. We can see that the overflow device is activated when the water level rises over the weir crest of 0.2m, which corresponds to an input discharge of 0.0664 $m^3\ s^{-1}$. When the water level exceeds the top of the orifice, as is the case at 14 o'clock on the 12th of June, the orifice equation is taken for the calculation. As soon as the water level drops below the weir crest the overflow stops.

5.2.3. OLAF: OverLAnd Flow routing

5.2.3.1. Concepts and used equations

Two different hydrological processes concerning overland flow can be observed: Horton overland flow caused by rain intensity which exceeds the infiltration rate and saturation excess overland flow due to saturation of the soil profile. Both processes, simulated by the HEDGE, FRER1D and partly URBS modules create ponding on the model units. In order to simulate overland flow the ponding has to be extracted from the model units and routed downstream. For this, a first version of an overland flow routing module (PEF - Ponding Extraction Flux) was developed by Manus et al. (2009). In PEF the extracted ponding is directly injected into the river reach of the corresponding sub-basin without following a real flow routing from model unit to model unit. This simplification was justified as they simulated flash floods caused by intense rainfall events. In contrast, the new module OLAF takes into account the routing between model units as unidirectional flow path. The overland flow from one model unit flows then only to the lowest neighbouring model unit oder river reach. The flow routing paths can be determined by the automatic pre-processing described in chapter 6.3.

Concerning the calculation of the surface runoff, Manus (2008) tested three different methods: (1) the ponding is extracted instantaneously with a constant flux, (2) the extraction flux is the flux necessary to evacuate the water accumulated during the last time step, (3) the extraction flux [m s^{-1}] is calculated with the Manning equation and it takes thus into account a real flow routing depending on the surface roughness:

$$q = \frac{1}{n} S_e^{1/2} h^{5/3} \tag{5.2.4}$$

where q is the discharge per unit width (m s^{-1}), n the Manning coefficient, S_e the slope of energy line and h the depth of the ponding. Assuming that the water surface is parallel to the ground surface, the slope of the ground surface can be taken instead of the slope of the energy line. According to Turner and Chanmeesri (1984) and Maheshwari (1992) we decided to implement a more general version of the Manning equation, called discharge-depth equation (Turner and Chanmeesri (1984), in which the coefficients of S_e (α) and h (β) can be set as model parameters. β is an exponent which reflects the degree of mixing in the flow (varying between turbulent in channels and laminar on flat surfaces) and α is the exponent of the energy line slope.

$$q = \frac{1}{n} S_e^{\alpha} h^{\beta} \qquad [ms^{-1}] \tag{5.2.5}$$

$$Q = qh\sqrt{A} \qquad [m^3 s^{-1}] \tag{5.2.6}$$

The coefficients of the Manning equation, where α is equal to 1/2, β to 5/3, where set as default values in the input parameter table. The overland flux in m s^{-1} is then transferred

in overland flow in $m^3\ s^{-1}$ by multiplication with the wetted section. The wetted section is calculated out of the product of the ponding depth and the characteristic length of the model unit, which is calculated as square root of the model unit area under ponding. The square root was chosen as it was considered as more representative as the intersection between the two exchanging model units (which can be zero in case of an intersection at just one point).

5.2.3.2. Implementation in LIQUID

The OLAF module is an interface in LIQUID, similar to the WTI and WTRI modules. It has thus no own time step but executes only when receiving a new ponding height. OLAF has one upstream ("in" in Table 5.2.6) and one downstream ("out" in Table 5.2.6) neighbor. The upstream neighbor has to be a polygon (FRER1D or HEDGE), whereas the downstream neighbor can be a polygon (FRER1D, HEDGE or URBS) or a line (RIVER1D). The corresponding ids and geometries have to be filled in table 5.2.6.

Table 5.2.6.: Input parameters of OLAF module

Field	Type	Description	Unit
id	integer	Identifier of the OLAF connection	-
id_in	integer	The id of the overflowing polygon	-
id_out	integer	The id of the receiving polygon	-
n	double	The roughness parameter	-
α	double	Exponent of the height, representing the mixing	-
β	double	Exponent of the slope.	–
ngf_in	double	Altitude of overflowing polygon from model reference	m
ngf_out	double	Altitude of receiving polygon from model reference	m
the_geom	Geometry	Geometric coordinates of the flow direction	line
geom_in	Geometry	Geometric coordinates of the overflowing model unit	polygon/line
geom_out	Geometry	Geometric coordinates of the receiving model unit	polygon/line

OLAF uses no geometry for its calculation. The field the_geom should contain a line leading from the upstream centre to the downstream centre for visualisation of the flow paths. It takes as further input the parameters necessary for the discharge-depth equation and the altitudes of the upstream and downstream model units. By means of the altitudes and the distance between the centres, obtained from the upstream and downstream geometries, the slope is calculated (equation 5.2.7). In the current version of the code, the slope is forced to be greater than 0.00001, which is necessary for the discharge-depth equation. The square root of the upstream model unit area is also obtained from the geometries.

$$slope = \frac{ngf\_in - ngf\_out}{\text{distance}(\text{centre}(geom\_in), \text{centre}(geom\_out))} \tag{5.2.7}$$

OLAF contains only the CSolver class, whose UML diagram is shown in Figure 5.2.9. OLAF has the two state variables current ponding height and current overland flow. The discharge-depth equation 5.2.6 is implemented in the ComputeOverlandFlow() function.

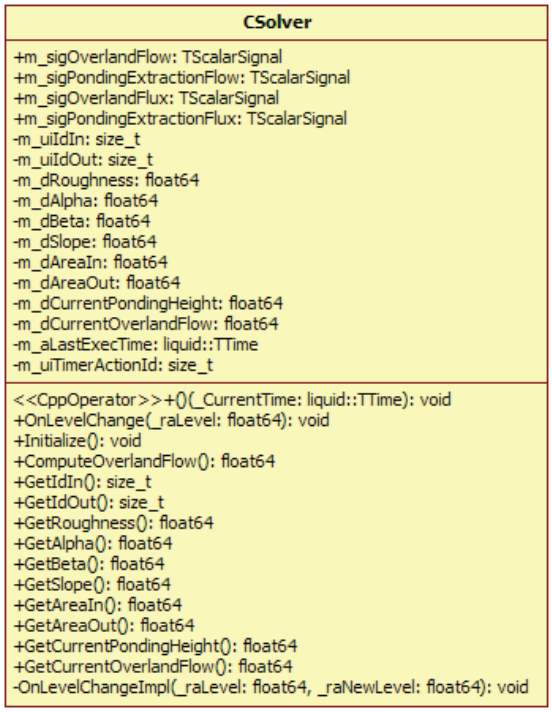

Figure 5.2.9.: The UML diagram of the OLAF module with the name, the attributes and the operations. + means plublic, + private.

When the slot m_slotPondingHeight (see table 5.2.7) receives a new value, which is superior to 1 mm and which differs of more than 1 mm from the old ponding height, the execution is triggered.

Table 5.2.7.: Signals and slots of the OLAF module

Name	Description	Unit
m_slotPondingHeight	The height of the ponding	m
m_sigPondingExtractionFlux	Overland flux leaving the upstream model unit (negative)	m s^{-1}
m_sigOverlandFlux	Overland flux entering the downstream model unit (positive)	m s^{-1}
m_sigPondingExtractionFlow	Overland flow leaving the upstream model unit (negative)	m^3 s^{-1}
m_sigOverlandFlow	Overland flow entering the downstream model unit (positive)	m^3 s^{-1}

In the test cases below this threshold value was set to 2 cm. OLAF calculates then the new overland flow, updates its state variables and signals the overland flow and flux as positive towards the downstream model unit and as negative towards the upstream model unit. The threshold inside the slot represents the initial loss caused inter alias by

the micro-topography. Furthermore, it prevents the signalling of unrealistic small flow quantities and it is thus useful to reduce the computation time.

5.2.3.3. Module verification

All functions of OLAF were tested with the LIQUID test framework. A simple test parameterization is saved in the ModulesOlafTest.cpp file. The test can so be repeated in case changes are made to the LIQUID framework. Furthermore, a simple model consisting of the HEDGE, RIVER1D and OLAF module was constructed. The test case, which is shown in Figure 5.2.10, contains two "hedges", a river consisting of three river reaches and the two OLAF instances olaf_hedge2hedge and olaf_hedge2river. Both OLAF instances

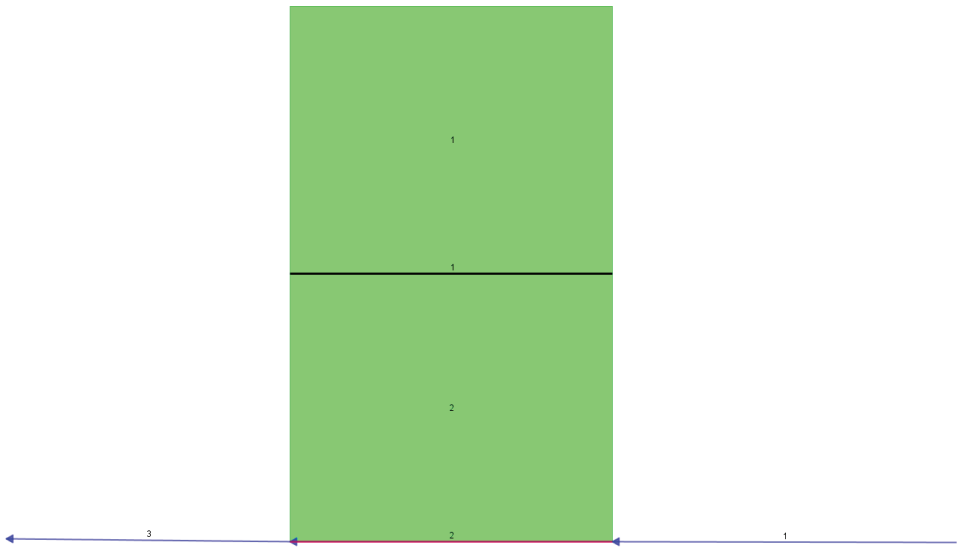

Figure 5.2.10.: The test case for the OLAF module with two HEDGE model units, a river consisting of three reaches and two OLAF instances: olaf_hedge2hedge and olaf_hedge2river.

had a Manning coefficient of 0.08 and the default values for α and β. The soil profile of both hedges was initially saturated and there was no evapotranspiration. The river was completely dry and had no inflow. The only input was precipitation, for which we took the same rainfall time series of the Rezé catchment (Morena, 2004) as used for the URBS test case. We simulated a relatively rainy period of 15 days start of January 1991, see Figure 5.2.11.

With this configuration it is possible to see the direct influence of the precipitation on the ponding and thus the overland flow. Different tests were conducted. First, the ponding was generated without the influence of the OLAF modules, then only the OLAF instance between both hedges was connected and finally both the OLAF instances were connected. The results in form of the ponding on both hedges are shown in Figure 5.2.11.

Without any OLAF instance connected, both hedges accumulate an equal amount of ponding. The introduction of the overland flow between the hedges leads to the decrease of ponding on the upper hedge (hedge 1) and an increase on the lower hedge. Only when the overland flow towards the river is activated, the ponding is extracted towards the river, which leads to an increase of discharge in the second and third river reach, see Figure 5.2.11.

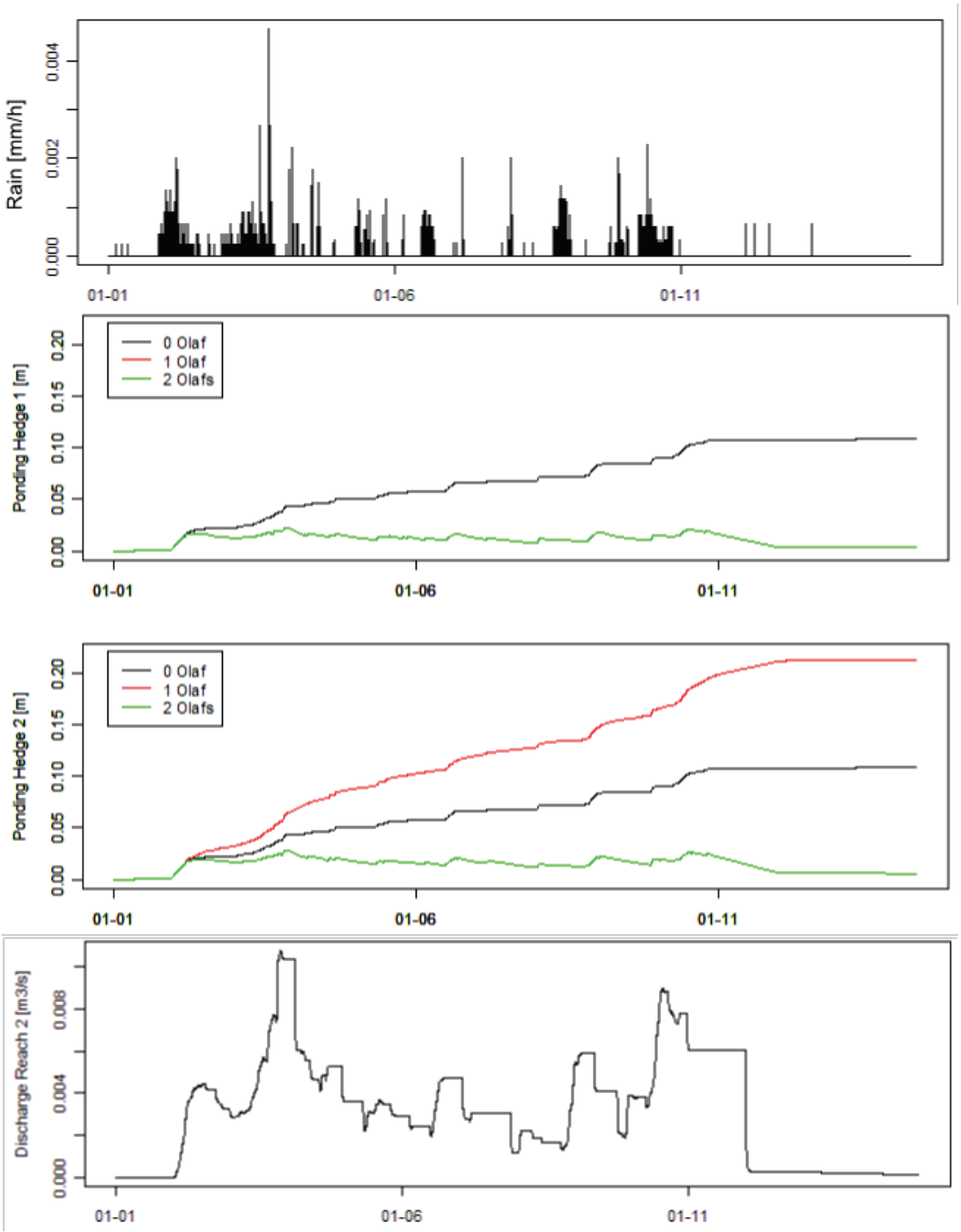

Figure 5.2.11.: Reaction of both hedges and the river to a 15 days rainy period in the Rezé catchment start of 1991. The upper panel shows the rainfall, the middle panels the ponding on the hedges (hedge 1 is upstream, hedge 2 downstream) and the lower panel the discharge of the 2nd river reach. The discharge for the river reach corresponds to the simulation with both OLAF instances activated. The discharge of reach 1 was 0 and of reach 3 similar to the discharge of reach 2. For the hedge ponding three different simulations are shown: without any OlAF instance connected (0), with olaf_hedge2hedge connected (1) and additionally with olaf_hedge2river connected (2). The ponding on the upstream hedge is equal for the cases that one or two OLAF instances are connected.

The introduction of a threshold condition of 2cm in the ponding height slot leads to a different ponding accumulation and thus overland flow dynamic (Figure 5.2.12). The ponding is accumulated until the threshold of 2cm, and then suddenly released provoking a higher rate of instantaneous overland flow and a temporary decrease of the hedge water level of up to 1cm from a constant level at saturation. This change in the dynamics may be important while simulating events over a short period, but can be neglected during long term simulations. The threshold which decreases the computation time, should therefore be chosen carefully depending on the kind of simulation and the desired precision.

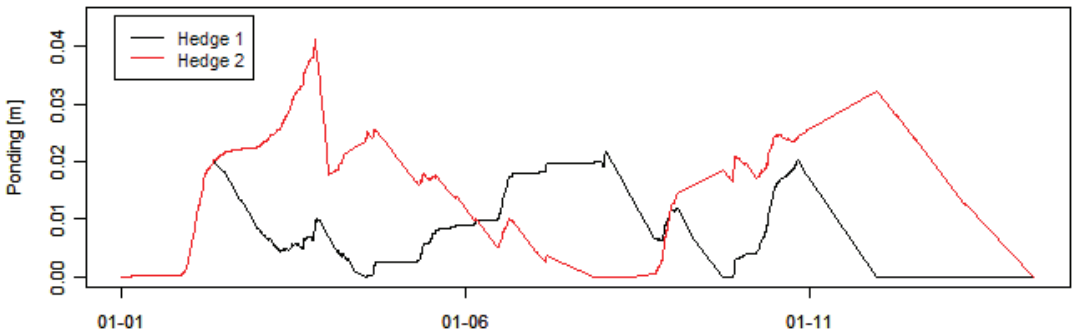

Figure 5.2.12.: Ponding of both hedges for the OLAF test case with a threshold in the ponding height slot of 2cm.

5.2.4. SISTBA: SImulation of STorage BAsins

5.2.4.1. Concepts and used equations

Lakes, anthropogenic dams or retention basins represent storages, which influence the water cycle in a catchment. In the case of flooding, a reservoir in the hydrological network can decrease the flood wave and can act as a retention basin. Contrarily, during dry periods the retentive influence of a reservoir may prevent severe droughts. Water stored in depressions can be used for irrigation or drinking water purposes. The objective for the SISTBA module was thus to add a module to the LIQUID framework, which allows to take into account these processes. However, as we were mainly interested in processes at the catchment scale and not by the exact representation of the hydraulics of retention basins, a simple and robust description was chosen. This could be improved in a further version of the module, and perspectives are given at the end of the section. The next paragraph explains the applied concepts and equations.

The water balance of storage basins is defined by the inflow, rain input, outflow, evaporation, groundwater exchange and water use for irrigation, (see Figure 5.2.13) and can be written as follows:

$$\frac{\delta h}{\delta t} = Inflow + Rain + AEP \pm GW - Discharge - Irrigation \tag{5.2.8}$$

The outflow of natural lakes, except in karstic regions, consists usually of an overflow when the water level exceeds the maximal lake level ($Maxlevel$). In contrast, artificial retention basins such as dams can additionally have a bottom outflow at the level $S3$, see Figure 5.2.13. If $S3$ is equal to $Maxlevel$, there is only one outlet, which is the overflow. There are four different filling states of the reservoir:

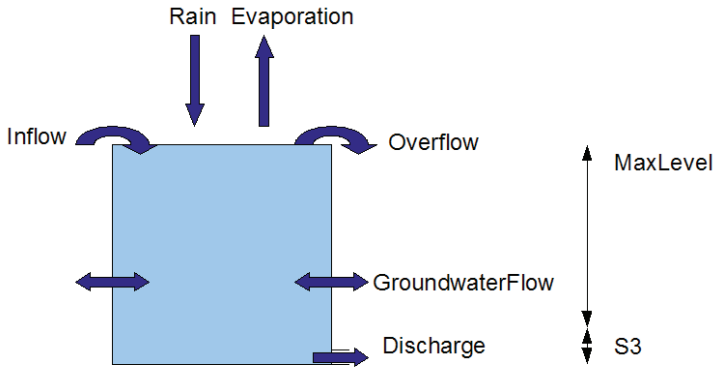

Figure 5.2.13.: Principal functioning of the module SISTBA.

1. If the reservoir is empty, all the outputs are zero, and the reservoir starts to fill with incoming water. If the groundwater table is higher than the lake bottom, water will infiltrate into the reservoir.

2. If the level is below $S3$, no water will exit towards the outlet, but there will still be evaporation and groundwater exchange.

3. If the level is between $S3$ and $Maxlevel$ there will be an outflow additionally to evaporation and groundwater exchange.

4. If the level is higher than $Maxlevel$ all water above the $Maxlevel$ which does not evaporate, infiltrate or discharge will overflow. The overflow is thus calculated via the mass balance:

$$Overflow = Inflow + Rain - AEP \pm GW - Discharge - Irrigation \quad (5.2.9)$$

where AEP is the actual evaporation and GW is the groundwater exchange. The total outflow is thus the sum of the discharge and the overflow.

The bottom outflow of SISTBA can be calculated in two different manners possible due to the new version of LIQUID which allows to have different module variants. These have to be activated in the code itself. In both equations the calculated discharge $Q[m^3s^{-1}]$ depends on the hydraulic charge $(Level - S3)$. The first approach uses a linear reservoir equation (Dingman, 2002):

$$Q = \frac{1}{\mu}(Level - S3) \quad (5.2.10)$$

where $\mu[s]$ is the retention parameter, which can be interpreted as the average residence time.

The second approach, more adapted for artificial retention basins with outlet pipes, calculates the discharge with a weir (Poleni) or orifice equation same as equations used in the TDSO module. The water level h is calculated from the bottom of the outlet pipe, thus the $S3$ level.

5.2.4.2. Implementation in LIQUID

The structure of the SISTBA module is shown in the UML diagramm (Figure 5.2.14). SISTBA is a real LIQUID module and has thus its own time step. The main class is

the CLakeTank, which inherits from the generic LIQUID class CTank, which describes all major processes and variables typical for a reservoir. In this class, the flow specific variables (m_dLevelFlow, m_DischargeFlow and m_dOverflow) are summarized inside the CFlows structure, see Figure 5.2.14. The linear reservoir and weir/orifice equations are implemented in the ComputeDischarge() function belonging to the CLakeTank, which is called by ComputeFlows(). The main calculations (EvalTimeStep()) are part of the CTank class. The calculation variable is the water level. The mass balance equation (5.2.8) is solved numerically. The numerical solution is explicit and uses the Runge-Kutta algorithm of the fourth order (Press et al., 2002). The main time loop, the geometric properties of the reservoir as well as the slots and signals are defined in the Solver. The main time loop consists of the following steps: calculation of the last time step, calculation and export of the water level, taking new input variables into account, calculation of discharge under consideration of new input, estimation of future time step (maximal one week), estimation of future level, export of all state variables and programming of next execution time in the scheduler. 5.2.14.

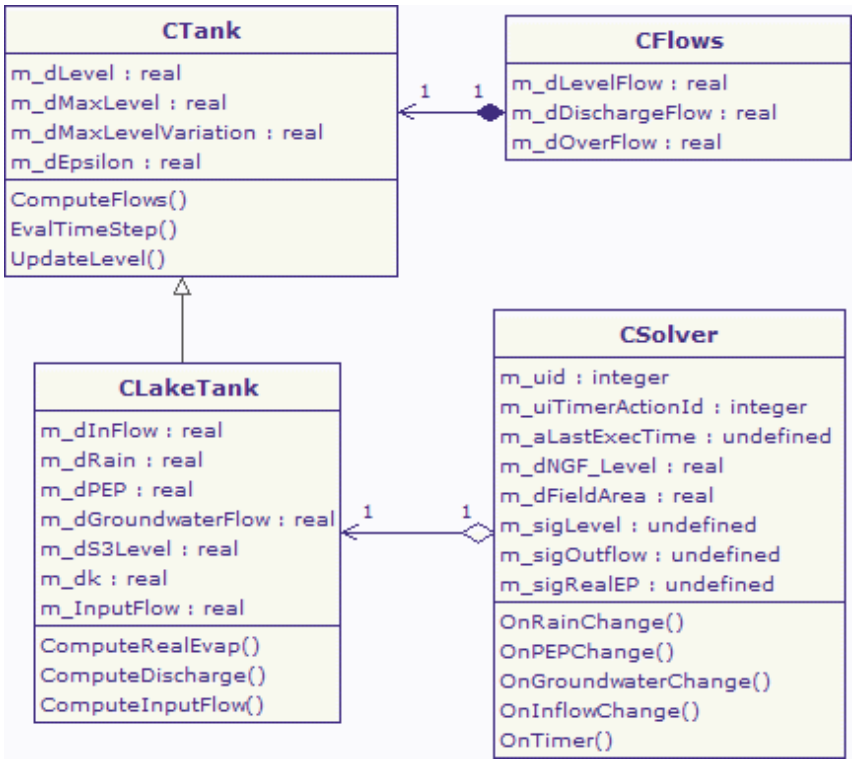

Figure 5.2.14.: UML diagram of the SISTBA module.

The time series input data enter the model via the slots shown in table 5.2.8. Rain, inflow, irrigation and potential evaporation are positive time series, whereas the groundwater exchange can be positive, meaning a flux towards the reservoir or negative. The groundwater exchange will usually be signaled by a WTI module and the inflow by a RIVER1D module. A variation in the value of any of these input variables entail an immediate interruption and re-execution of the module solver under consideration of the new values.

The signals of the module SISTBA allow to export the values of the water level in the

Table 5.2.8.: List of the slots of the module SISTBA

Name	Description	Unit
OnRainChange()	Intensity of precipitation	ms^{-1}
OnPEPChange()	Potential evaporation	m s^{-1}
OnGroundwaterChange()	In-/Exfiltration	m^3s^{-1}
OnInflowChange()	Inflow into the reservoir	m^3s^{-1}
OnIrrigationChange()	Irrigation from the reservoir	m^3s^{-1}

reservoir, the actual evaporation depending on the water level and the reservoir outflow. The outflow is composed of the bottom discharge, depending on the height of the outlet (parameter S3) and the overflow. The outflow can be connected to a RIVER1D module, but also another SISTBA module if there are several retention basins in a row. Due to the Runge-Kutta algorithm the time step can get very small. Therefore, in order to reduce the execution time, a minimal water level and level variation were introduced before the output is signaled.

Table 5.2.9.: List of the signals of the module SISTBA

Name	Description	Unit
m_sigLevel	Water level in the reservoir from the bottom	m
m_sigLevelFromRef	Waterlevel in the reservoir from model reference	m
m_sigRealEP	Actual evaporation	m s^{-1}
m_sigOutflow	Total reservoir outflow consisting of the sum of discharge and overflow	m^3s^{-1}
m_sigDischarge	Bottom outflow	m^3s^{-1}
m_sigOverflow	Overflow of the reservoir	m^3s^{-1}
m_sigError	Error of the mass balance	m^3s^{-1}

The data structure consists of a single table SISTBA_main. The signification of the table headers is explained in Table 5.2.10. In order to reduce the number of columns, the parameter μ signify the retention parameter, in case the reservoir equation is chosen, or the discharge parameter if the weir and orifice equation are chosen. The outlet_surface and orifice_top are only used for the weir and orifice equations.

5.2.4.3. Module verification

For the following tests the linear reservoir equation (5.2.10) was used. A simple model was designed consisting of the SISTBA module coupled to an inflow (input module) and outflow (output module). A real lake geometry of the Mercier land use map (Figure 3.1.8 in Chapter 3.1.4) was chosen as geometry. The test lake had a surface A of 3146 m^2. The maximal level of the storage basin was set to 10 m and the S3 level corresponded to the storage bottom with a value of 0 m. k was set to 4719 s (1 hour and 19 min) and the

Table 5.2.10.: Input parameters of SISTBA module

Field	Type	Description	Unit
id	integer	Identifier of the model unit	-
id_river_in	integer	Identifier of the incoming river	-
id_river_out	integer	Identifier of the outcoming river reach	-
NGF_surface_level	double	Average altitude of the model unit	m
Maxlevel	double	Maximal reservoir level from bottom	m
S3	double	Height of outlet from reservoir bottom	m
init_stock	double	Initial level of the reservoir	m
μ	double	Retention parameter k, or discharge coefficient	$s/-$
outlet_surface	double	Outlet cross section area	m^2
orifice_top	double	Top of the outlet pipe from reservoir bottom	m
the_geom	Geometry	Geometric coordinates of the model unit	polygon

initial level to 6 m, which gives a total volume of about 18876 m^3. The starting outflow Q_{out} was thus about 4 m^3 s^{-1}. The rain, evaporation and groundwater exchange were set to 0 and the time step Δt of the analytical solution was one hour. The analytical solution for the discharge Q_{out} is given by Maniak (1997):

$$Q_{out}(t) = Q_{out}(t-1)\exp(\frac{-\Delta t}{\mu}) + Q_{in}(t)(1-\exp(\frac{-\Delta t}{\mu})) \tag{5.2.11}$$

whereas the equation changes for the calculation of the water level W to the following equation:

$$W(t) = (W(t-1)\exp(\frac{-\Delta t}{\mu})A + Q_{in}(t)\mu(1-\exp(\frac{-\Delta t}{\mu})))/A \tag{5.2.12}$$

The analytical and numerical solutions of the linear reservoir equations were compared for two cases, a draining storage without inflow and a storage with steady state conditions (inflow=outflow). In both examples the analytical and numerical solutions corresponded to each other and showed an exponential decrease, only the results for the draining storage are shown in Figure 5.2.15.

Furthermore, we tested the SISTBA module during overflowing conditions. The results were not compared with an analytical solution, but only the physical coherence was verified. The lake had the same parameters as described for the first test case. However, the discharge varied with the time. The resulting discharge, waterlevel and overflow is shown in Figure 5.2.16. In the beginning of the simulation a constant inflow rate of 2 m^3 s^{-1} assured steady state conditions. Then, the inflow rose to a value of 5 m^3 s^{-1}, stabilizing again at a steady state flow. The inflow increased at 11 p.m. abruptly to 10 m^3 s^{-1} and

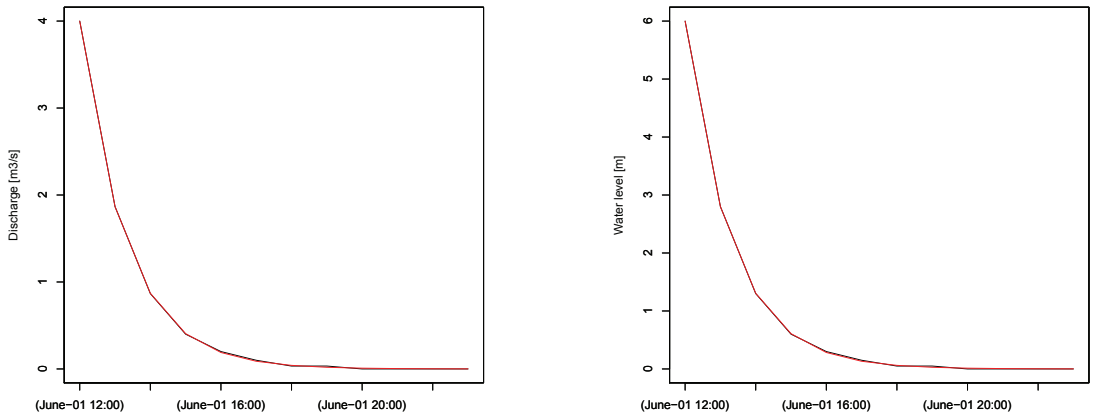

Figure 5.2.15.: Discharge and water level of a draining storage basin. The numerical solution is in black, whereas the analytical solution is in red.

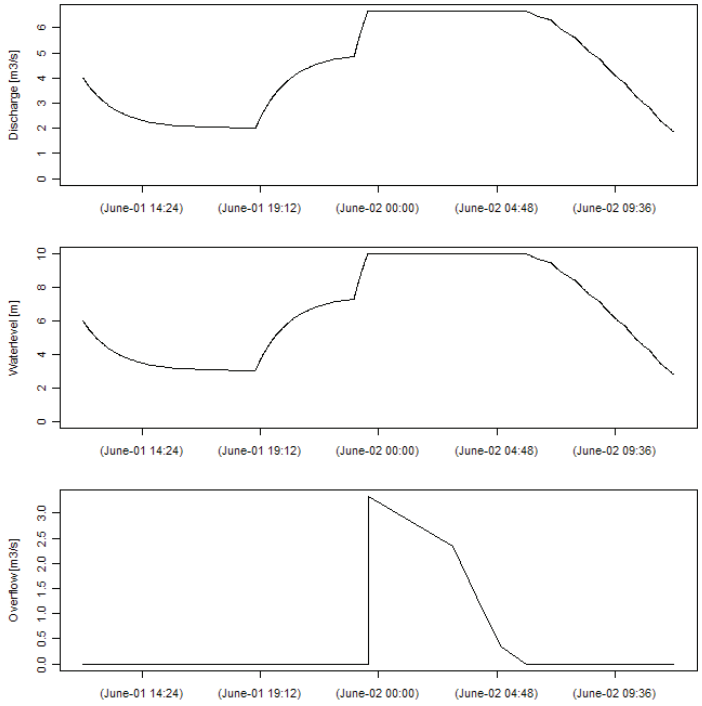

Figure 5.2.16.: Discharge, water level and overflow of a lake in overflowing conditions.

caused the basin to overflow, which can be seen in the third graphic of Figure 5.2.16. Starting at 3 a.m. the inflow decreases continuously to a constant rate of 1 m^3 s^{-1}. Fig. 5.2.16 shows that the water level rises maximal to a level of 10 m, which corresponds to the maximal level indicated in the parameters of the storage basin, and the discharge maximal to 6.7 m^3 s^{-1}, depending on the maximal hydraulic charge. However, the basin overflow increases to assure the water balance of the retention basin.

5.3. Model construction

The PUMMA model was developed based on the LIQUID framework by connecting the process modules described above. In LIQUID the exchanges or water fluxes are determined by module connections. Due to the object oriented approach, the model developer has free choice for the determination of the module connections and can thus represent purposeful all hydrological processes and water fluxes observed on the field. It is possible to propose different kind of connections with the same module by creating several *instances* of the module. Furthermore, during the parameterization and pre-processing of the model the model builder can freely decide which model units or areas he wants to implement or connect by filling the input tables, which is called module *implementation*.

5.3.1. General concept of PUMMA

Figure 5.3.1 shows all modules applied in PUMMA with their main connections, which are further described in the next paragraph. The input to the model are time series of precipitation and evapotranspiration, which are weighted over the model mesh using the FCA module. This allows to use time series of different measurement stations, which were spatialized e.g. with Thiessen polygons directly as model input. Flow generation on agricultural fields, forests, hedge rows and riparian zones is simulated with the HEDGE module, on urban cadastral units and roads with the URBS module and in retention basins and lakes with SISTBA. The landscape is thus divided in a mesh of polygons and lines. Each polygon is attributed to one of the flow generation modules in which the 1D vertical water flux is calculated in meters per second.

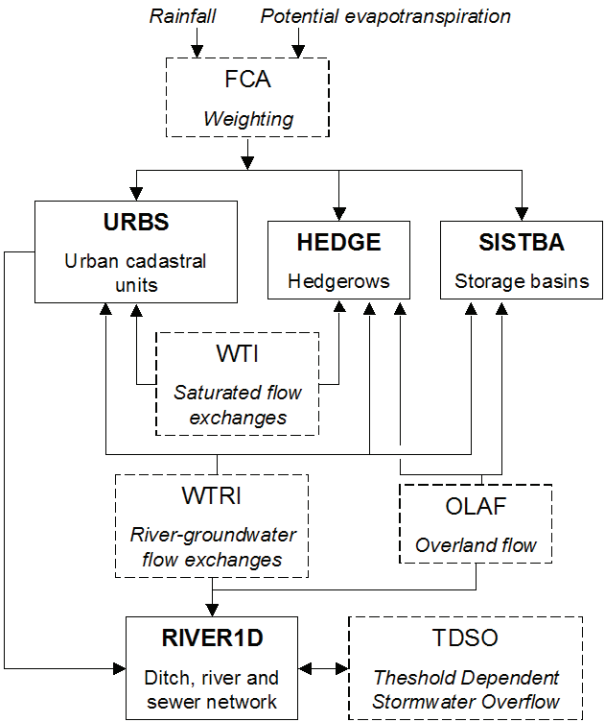

Figure 5.3.1.: Structure of the PUMMA model and couplings between the modules.

The drainage network, consisting of the natural river, artificial ditches and underground sewer pipes is simulated with the RIVER1D module. In the model mesh the drainage

network consists of lines, which should correspond to the polygon borders if lateral flow exchange want to be modeled. Lateral sub-/surface flow between model units and flow exchange with the drainage network is modeled with the interface modules WTI, WTRI and OLAF, which allows the flow transfer from the model units to the drainage network. The flow exchange between the interfaces and the runoff generation modules is in cubic meters per second. The TDSO module, simulating storm water overflow devices, is coupled between two river instances of the RIVER1D module.

5.3.2. Connections to represent transfer processes

The LIQUID framework allows to use the same module several times in the same model using different connections. They are then called module instances. For the lateral subsurface flow three WTI instances were necessary: *hedge2hedge, hedge2urbs* and *urbs2urbs* and for the lateral subsurface flow exchange with the river network four WTRI instances: *hedge2river, hedge2sistba, urbs2river* and *urbs2sistba*. Each WTI/WTRI instance has four connections: They receive the water level from the adjacent model units or river reaches and send in return the discharge as positive value to the downstream model unit and as negative value to the upstream model unit. As one model unit can receive discharge from several WTI/WTRI or OLAF interfaces, the signaled discharge is connected to PLUS module instances, whereas the water level connection is directly between the WTI/WTRI interface and the main module.

The overland flow from HEDGE model units is modeled with four OLAF instances: *olaf_hedge2hedge, olaf_hedge2urbs, olaf_hedge2river* and *olaf_hedge2sistba*. Each of these interfaces has three connections, one for the upstream water level and two for the discharge. As for WTI the signaled discharge is connected to PLUS instances.

The overland flow from URBS is not modeled with OLAF, but it is directly connected to the drainage network or adjacent model unit, as URBS calculates directly a discharge in cubic meters per second. However, a difference was made between surface runoff from impervious and natural areas. As roof runoff and road runoff is mostly intercepted by sewer pipes, it was directly connected to the overland flow slot of RIVER1D via a PLUS module. However, the natural surface runoff was connected to the overland flow slots of URBS, HEDGE, RIVER1D and SISTBA. Overland flow created on natural urban areas can thus follow the topography towards the lowest neighbor. The module implementation (filling of the input tables) decides then, which of the four connections is activated for which URBS model unit.

The network infiltration signal was only connected to RIVER1D, same as the surface runoff from impervious areas.

5.3.3. Specific connections

Furthermore, the connections described in the following paragraph allowed to represent specific hydrological processes. Infiltrating ditches are simulated by connecting RIVER1D to the overland flow slot of HEDGE or URBS. The water can then infiltrate or create ponding depending on the saturation of the model units.

One catchment can have several rivers, represented by implementations of RIVER1D. This allows to model different or even parallel drainage systems as can be necessary to simulate the natural river network and the sewer system. It is possible for parallel networks to have inverse flow directions, which can be the case if parts of the sewer network are pumped.

If a lateral storm water overflow device spills towards another sewer system a new RIVER1D implementation will be needed. The addition of a new RIVER1D implementation permits also to simulate loops in the drainage system. In this case the outlet of one river is connected to the source of a second river.

Different RIVER1D implementations are necessary if the drainage network is interrupted by lakes or retention basins, too. The outflow of the inflowing river must then be connected to the inflow slot of SISTBA and the SISTBA outflow has to be connected to the source slot of the outflowing river. Two retention basins or lakes can also be connected in a row. In this case the outflow of the upper basin enters directly as inflow to the lower basin.

5.3.4. Technical realization of the PUMMA model

The PUMMA_SFRER1D model was constructed by writing the xml file *Pumma_sfrer1d.model*. The *Pumma_sfrer1d.model* file, which contains more than 1700 lines, was structured as shown in Figure 5.3.2 for better visibility and error prevention. All module instances are specified in the first part and the connections in the second part.

Modules
- Principal modules
- Interfaces
- Plus
- Input
- Fca
- Output

Connections
- **Input Connections**
  - Input to fca
  - Fca to modules
  - Input to modules
- **Connections between modules**
  - Plus to module
  - Interfaces
  - Direct connections
- **Output connections**

Figure 5.3.2.: Structure of the Pumma.model file.

The module instances are further divided in principal modules, interfaces, plus, input, fca and output instances. PUMMA_SFRER1D contains the four principal modules HEDGE, SISTBA, URBS and RIVER1D, one instance of the interface TDSO, four instances of the interface OLAF, three instances of WTI and four instances of WTRI. Eight instances of the plus module, each time coupled to a different slot, were necessary for the construction of PUMMA_SFRER1D. Five INPUT modules assure the time series information for the model such as rainfall, potential evaporation, irrigation, inflow and the crop coefficient for the HEDGE module. Six instances of the FCA module attend to

the weighting of the evapotranspiration and precipitation over the HEDGE, URBS and SISTBA model area. 28 output modules allow to observe the calculated time series of the different state variables.

The connections are sub-divided in input connections, connections between modules and output connections.

In order to know during the model application, which slot A to J of the PLUS module was connected to which signal, the connections were documented in tables such as the Table 5.3.1 which defines e.g. the connections to SISTBA. Each PLUS instance has its own table and the tables are listed in Appendix C. This table tells that in the PostgreSQL table "plus_plussistba_table" the field id takes the value of the concerned lake or retention basin and for example the slot_id would be the id of the corresponding WTRI instance (wtri_hedge2sistba_main) for slot A.

Table 5.3.1.: Documentation for the PlusSistba instance of PUMMA. The PLUS module instance is connected to the m_slotGroundwater. The id field of the PLUS table corresponds to the id of SISTBA.

Slot	Instance	Signal	Slot_id
A	Hedge2Sistba	m_sigRiverWTLateralFlow	Id wtri
B	Urbs2Sistba	m_sigRiverWTLateralFlow	Id wtri
C	River	m_sigOutletDischarge	Id river
D	Olaf_hedge	m_sigOverlandFlow	Id olaf
E	Sistba	m_sigOutflow	Id sistba
F	City	m_sigPummaToOverlandFlow	Id urbs

5.3.5. Verification of the model building and connections

The PUMMA model was assembled gradually by adding new modules and connections. Each new connection was tested by means of a prototype containing model units of each kind. Furthermore, the urban part of the PUMMA model, more precisely a combination of the URBS, RIVER1D and SISTBA modules, was applied to the Rezé research catchment (Berthier, 1999; Morena, 2004; Rodriguez et al., 2008) in the suburbs of Nantes, in order to compare the first model results to measured data and verify the model coding (Jankowfsky et al., 2010). Both test cases are described in the following sections.

5.3.5.1. Prototype

The prototype, shown in Figure 5.3.3, served to build progressively the PUMMA model. It arises from the test case of the SISTBA module to which new modules and connections were gradually added. The final version consists of 14 URBS model units, 7 HEDGE model units, one SISTBA model unit, one storm water overflow device (TDSO) and three rivers containing 14 river reaches. Three different OLAF and WTI connections were tested, respectively, as well as four different WTRI connections. The robustness and physical coherence of each new connection was checked. Therefore, extreme and sometimes unrealistic parameter values were chosen in order to visualize the impact of the interfaces.

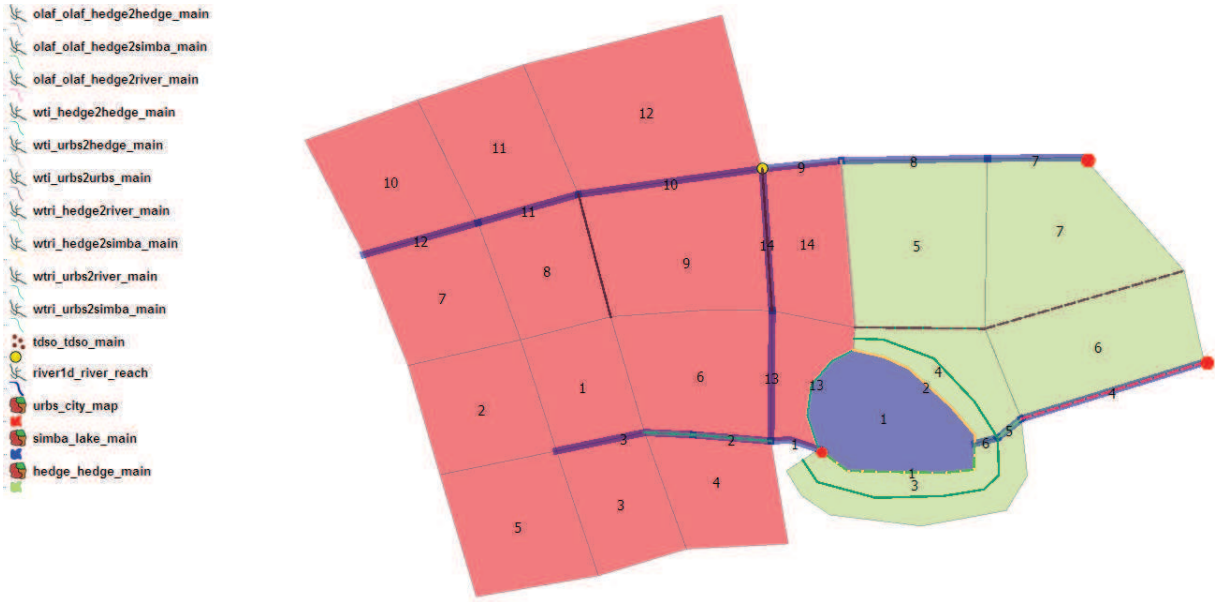

Figure 5.3.3.: The prototype for PUMMA having all possible modules and module connections for testing. The module instances are indicated. The red points are the outlets.

A simulation period of three days at the start of January 1991 was chosen with the rainfall and potential evapotranspiration data of the Rezé catchment as model input (upper panel in Figure 5.2.11). All URBS model units were parameterized equally, except the proportion of built, natural and road area. The default parameters of Morena (2004) were taken and only the saturated zone depth was changed in order to intensify the effect of the interfaces. The HEDGE model units were also parameterized equally, having a soil depth of 3 m, a drainable porosity and retention porosity of 0.1, three soil layers and 20 cells. The initial retention porosity was saturated. The initial water table level varied for each hedge depending on the topography and the test case. The retention time of the lake was one hour and eight-teen minutes and its outflow at 1.8 meters from the lake bottom. The initial water level was 1.5m and the maximal level at 2m. The threshold for the storm water overflow device was 15 cm. The OLAF interfaces had the same parameters as the OLAF test case. The tests showed that the WTI and WTRI interfaces are very sensitive to changes in the permeability. Figure 5.3.4 shows some of the results of the prototype in form of the discharge at the three river outlets. In these graphics we tried to visualize also the effect of some of the interfaces, consequently the permeability of WTRI between the URBS model unit 4 and the river reach 2 was set to 0.00005 which is relatively high. The hydraulic charge between the model units was 0.5m, which caused a high flux from the URBS model unit towards the river in the beginning (second graph of Figure 5.3.4). The third graphic shows the discharge in the sewer system, where the water comes from the adjacent URBS model units. We can see the base flow caused by the network infiltration and the reaction to the surface runoff. The first graphic shows the discharge of the last river, which is basically the lake outflow with the impact of surface runoff from the hedge 6. The OLAF interface was parameterized in this case to extract nearly all the ponding at one time (which is not the case in the current default version of the module). We can also see that the lake has a retentive effect on the discharge.

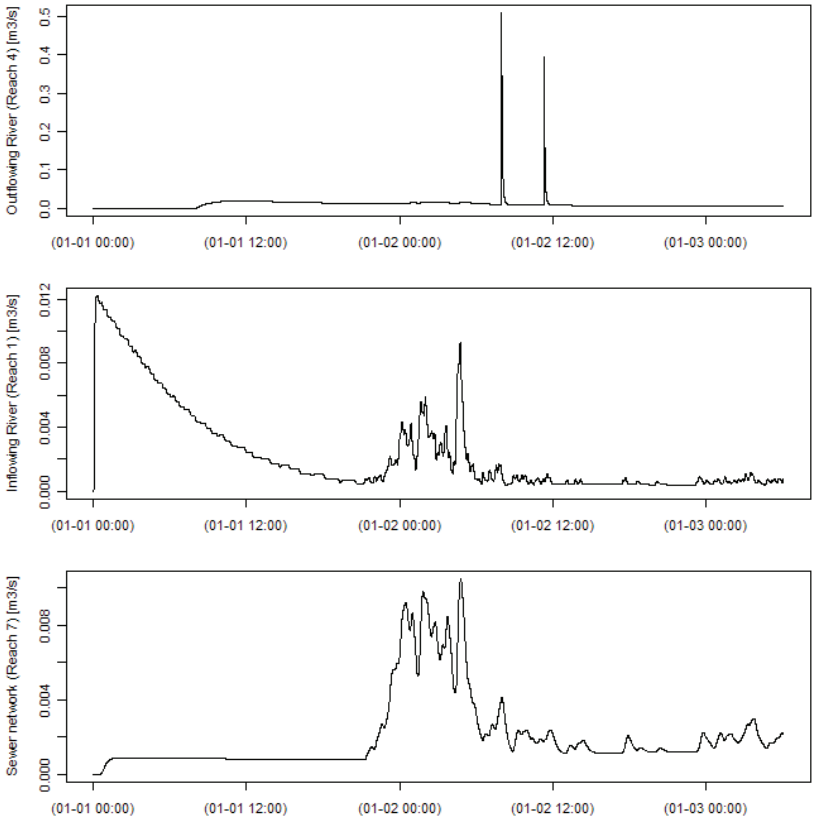

Figure 5.3.4.: Discharge at the catchment outlet (top), in the river entering the lake (middle) and at the sewer outlet (bottom).

5.3.5.2. Rezé

The Rezé catchment (Berthier et al., 1999), which has a size of 4.7 ha, is located in the suburbs of Nantes, France. It contains 67 cadastral units, which were transformed into UHEs, see Figure 5.3.5. The sewer network was extended with the street network to obtain the final drainage network. All UHEs were parameterized equally, except for the percentage of built, road and natural area. The parameters of the URBS module correspond to the retained parameters in Morena (2004). The depth of the drainage pipe was set to 1.2m and the saturated zone depth was 0.7m. The drainage network was represented by a rectangular cross section of 50cm width with a slope of 0.5% and a Manning value of 0.035. The precipitation is the average of three rain gauges (Berthier et al., 1999) and has a time step of 5 minutes. The evapotranspiration data were provided by Météo France. All state variables were initialized to zero. The results were compared to measured flow data of the station shown in Figure 5.3.5.

An hypothetical planning scenario has been tested, by introducing a retention basin downstream of the last drainage reach in order to highlight the simulation results of the SISTBA module. No measured data were available for comparison. The retention basin of 2m depth had a bottom outflow. Two simulations were run with retention parameters of 500 and 1000 s for a rain event on the 3rd of January 1991 including a three day warm-up period to eliminate the effect of the parameter initialisation. No lateral subsurface exchange was modelled, except the infiltration into the sewer pipes.

This first test allows the assessment of the correct functioning and interaction of the

Figure 5.3.5.: The Rezé catchment with its cadastral units, buildings and flow measurement station.

modules. Each implementation of URBS (UHE) signals the sum of the surface runoff from the built, road and natural part and the network infiltration towards the closest drainage reach. RIVER1D routes the received water from one reach to the next and transmits then the discharge to the hypothetical retention basin. Figure 5.3.6 shows the rain event and the simulated discharge at the outlet of the Rezé catchment versus the measured discharge. The total amount of precipitation during the simulation period was 21.3 mm. The modeled discharge corresponds well to the main peaks of the observed discharge. The fluctuation could be caused by the variable time step of the model. Here, we plotted the instantaneous values. Using averaged values for 5 minutes intervals should smooth the flow curve. The flow volume during the simulated period could be reproduced to 98.8% for this specific rain event.

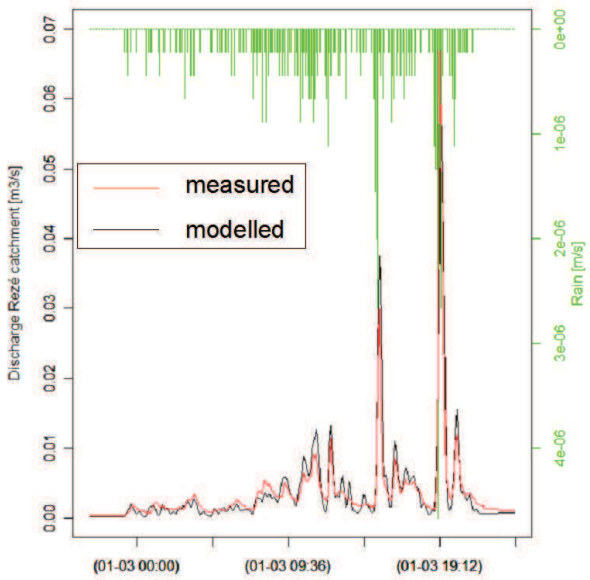

Figure 5.3.6.: Simulated (black) versus measured (red) flow data and the precipitation (green) during the simulation run (3/1/1991). The simulated discharge corresponds to the RIVER1D output at the catchment outlet.

Figure 5.3.7 presents the different flow components of one example UHE. A short re-

sponse of surface runoff to the incoming precipitation can be observed for the UHE, which is typical for urban areas. The built surface contributes to 40.6% to the runoff, the road area contributes to 29.1% and the network infiltration contributes to 30.3%. The response of the road surface is delayed in comparison to the built area, which is due to the parameterization of the UHEs (maximum size of surface reservoirs). The natural area does not contribute to the surface runoff because the soil is not yet saturated. However, the rising water content in the natural soil reservoir provokes an increasing infiltration into the sewer pipes. This response is much slower than the surface response. The discharge of each UHE is added as source term to the closest drainage reach and routed downstream.

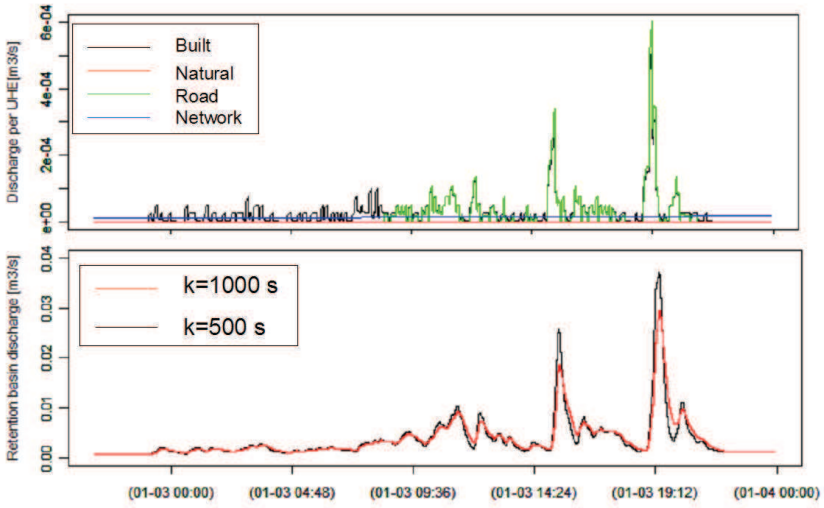

Figure 5.3.7.: The discharge of one UHE divided in network infiltration (blue) and surface runoff from built areas (black), the road (green) and natural areas (red). Discharge from the hypothetical retention basin with 500s (black) and 1000s (red) as retention parameter.

Considering the hypothetical planning scenario using the SISTBA module, a retention effect can be simulated. Depending on the retention parameter chosen for the module, the retention effect of the hypothetical basin is more or less strong. A retention parameter of 500s results in a peak reduction of 36% and a retention parameter of 1000s in a reduction of 49% combined with retardation and dispersion effects.

5.4. Discussion and perspectives

In chapter 3.5 we have seen that Horton overland flow and saturation excess overland flow caused by saturation of the first soil layer are important processes in the modeled catchments. However, by using the HEDGE module for the natural areas, these processes are not represented in the model. Overland flow is thus only possible when the whole soil profile is saturated. The addition of FRER1D would add the possibility to simulate Horton overland flow.

We also have to ask the question whether we can simulate representative groundwater levels without a numerical simulation of the groundwater table over the whole model mesh as for example done in Dehotin (2007). In PUMMA, the groundwater table between model units is equilibrated by means of source and sink terms. This representation allows to

transfer water between model units. However, the quality of the model mesh and the representativity of their average altitudes get thus a large influence on the simulation quality of the groundwater table. Furthermore, the groundwater boundary conditions are neglected in the model simulations. For the Chaudanne catchment, the disregard of the boundary conditions and a complete solution of the groundwater table was justified as no real continuous groundwater table is present in the catchment. In other catchments with an important groundwater table, the BOUSS2D module (Dehotin, 2007) could be added to the model. Due to the modelling framework, boundary conditions could easily be added by means of input models sending constant or variable fluxes.

In the OLAF module, the overland flow between model units is calculated with the Manning equation (5.2.6) which takes as input parameter inter alia the slope. For the moment, the slope is calculated as quotient of the differences in altitude and the distances between model units (equation 5.2.7). However, DeLavenne (2010) showed the differences of overland flow between production, transfer and accumulation sites, which are mainly determined by the morphology. Given that the slope of model units is relatively homogeneous, it would be better to take the slope per model unit for the calculation of the overland flow instead of the slope between model units.

In the current version of SISTBA the geometry of the reservoir has always vertical side walls. This corresponds especially for lakes not to the real geometry and thus storage volume. In a further version of SISTBA a volume-depth relation could be integrated into the model, similar as done in CANOE (Sogreah and Insavalor, 2005). Furthermore, in order to simulate retention basins correctly, it would be appropriate to represent the reservoir rather as river at low flow conditions than as reservoir. For this, the Manning equation (5.1.3) could be used.

Zoppou (2001) concludes in his review, that kinematic wave equations are not suitable for modelling storm water flows as they do not simulate backwater effects, pressurized flows or loops. The objective of this thesis was more on the influence of the spatial organization on the runoff generation, than on the correct simulation of the sewer system. Therefore, we chose the simplified representation of the drainage network with the RIVER1D module based on the kinematic wave equation. However, a possibility would be to add the ELIXIR (Henine, 2010) module simulating pressurized pipe flow, which is already part of the LIQUID framework, or to couple PUMMA to another more sophisticated sewer model. Another perspective would be the simulation of flooding due to sewer surcharge but for this a 2D surface hydraulic model would have to be coupled as well.

5.5. Conclusions

The Peri-Urban Model for landscape MAnagement (PUMMA) was specifically designed for peri-urban areas. It is constructed inside the LIQUID modelling framework, in which models are developed by connecting several process modules. The process modules are applied to an object-oriented, vector based model mesh. PUMMA is thus composed of two runoff generation modules (URBS and HEDGE) which describe urban and rural areas, three interfaces simulating transfer processes (WTI, WTRI, OLAF) and three process

modules describing the routing in artificial and natural channels (RIVER1D), storm water overflow devices (TDSO) and storage basins (SISTBA). Both, HEDGE and URBS represent the runoff generation using a conceptual approach. In HEDGE the soil column is divided in retention and drainage porosity, whereas in URBS the soil is divided in vadose zone and saturated zone. Each URBS model unit is further divided in natural, built and road area. Both modules can create overland flow and subsurface flow, which they exchange via interfaces with the neighboring model units. The OLAF interface simulates hereby the overland flow using the discharge-depth equation, whereas the WTI and WTRI interfaces represent the subsurface flow. Each module has its own independent parameter set, which is read from a PostgreSQL database. The modules can communicate via slots and signals, which allows them to receive and to send information, respectively. The model is constructed by defining the module instances and connections of signals and slots in a XML file. Separate INPUT and OUTPUT modules assure the reading of input data and writing of output data to text files. Rainfall and evapotranspiration are weighted over the model mesh with the FCA module. Finally, the PLUS module allows to connect several signals to the same slot.

Four of the process modules (URBS, SISTBA, OLAF and TDSO) were developed in the framework of this PhD thesis. In order to assure their correctness, simple test cases were designed for each module. The final model was then developed progressively by adding the process modules and testing the new connections on a prototype. The urban part of the model was further tested on the Rezé catchment, which is a small urban research catchment in the suburbs of Nantes.

The version of the PUMMA model presented in this chapter is a first step in the building of a detailed hydrological model adapted to periurban catchments. The discussion shows that other choices could have been done for the formulation of some of the processes/modules. The current structure of the PUMMA model is a compromise taking into account the main objects/processes identified in periurban catchments. Furthermore, we had first to demonstrate the proof of concept and that the model was adequate and useful for the understanding and hierachization of hydrological processes, and it was useless to complexify the model too much. In addition, given the modular structure of the model and the possibility to activate/deactivate processes and connect/disconnect some spatial units, it already offers the possibility to test various functioning hypotheses and scenarios.

6. Creation of model mesh and hydrological routing

This chapter describes the method developed for the creation of the object oriented and vector based model mesh and the geographical input parameters of the PUMMA model. This whole method is based on geographical information systems (GISs). Therefore, the first section gives a review about the use and link of GIS for hydrological modelling. Then, several GIS were tested for its applicability for the PUMMA preprocessing. The second section describes the method developed for the determination of the drainage network and catchment delineation in peri-urban areas. The application of this method to the Chaudanne catchment was subject to a submitted article, which is presented in section 6.2.1. The method was also applied to the Mercier catchment. The resulting sub-basin and drainage network maps were then input to the automatic preprocessing, presented in the subsequent section. Being the main part of this chapter, this section presents the complete developed preprocessing methodology including automatic solutions (in form of scripts) and other parts in which only manual solutions could be found. Beside the developed scripts, which can partly be used for other models, the results of the preprocessing are the model mesh, the geographical parameters and the connections necessary for the hydrological routing for the Chaudanne and Mercier catchment. In section 6.4 the developed preprocessing methodology is discussed and propositions for improvements and further research perspectives are made. The final section summarizes the chapter and gives a list of all developed scripts.

6.1. GIS and hydrological modelling

Distributed hydrological modelling needs many input data, which are in general prepared using a Geographical Information System (GIS) (Smith (1993); Greene and Cruise (1995); Goodchild et al. (1996); Chen et al. (2009); etc.). Furthermore, a GIS allows the visualization and analysis of distributed output in form of maps. The preparation of the input data is commonly called preprocessing, and the analysis of the output postprocessing. The following sections review why GISs are needed for hydrological modelling, how GISs and hydrological models can be linked and give a short review of different GIS softwares.

6.1.1. Why do we need GISs for hydrological modelling?

The use of GISs for the preprocessing of hydrological models can be divided in three stages: the mesh creation or domain decomposition (Bhatt et al., 2008), the attribution of parameters to the model units or data model loader (Bhatt et al., 2008) and the hydrological routing from each model unit towards the catchment outlet. Depending on the type of the model mesh, raster or vector, different GIS functions are necessary to accomplish the three stages.

The delineation of watershed boundaries and sub-basins and the calculation of the river network, necessary for hydrological modelling, is usually done by processing of digital elevation models (DEMs) using a GIS software.

If the model mesh consists of sub-basins, as is the case for most semi-distributed models, the sub-basins extracted from the DEM can be directly used as model mesh. A transformation into vector data might be necessary if the model uses vector data. Lines obtained from raster maps contain still the raster structure. GIS functions, such as the Douglas and Peucker (1973) algorithm are often applied in order to reduce the number of vertexes and smooth the lines. The model mesh of raster based models as SHE (Abbott et al., 1986a) or GSSHA (Downer et al., 2006) consists in general of all grid cells falling inside the watershed boundary. The model mesh grid size should not be less than the DEM grid size in order to assure the correct flow routing. The stream tube mesh consisting out of isocontours of elevation and stream-lines proposed by O'Loughlin (1986) and Grayson et al. (1992a) is also directly derived from DEMs using GIS functions. As mentioned in section 2.2.1, HRUs are derived by intersection of different GIS layers such as sub-basins, land use, soil or geology maps. Therefore, intersecting, simplifying and reclassifying GIS functions are needed. Finally, meshes consisting of TINs can be created using the Delaunay triangulation implemented in most GIS software. Algorithms which allow the integration of constraints, such as anthropogenic features (ditches, agricultural field borders, hedges, etc.) into triangular model meshes (Bocher and Martin (2009); Bhatt et al. (2008)) are under development .

In distributed hydrological models, each model unit contains a certain set of parameters necessary for the execution of the model. This are land use characteristics for evapotranspiration, infiltration rates depending on soil properties, slope, altitudes, etc. which can be assigned to the model units due to GISs.

If the model mesh corresponds to the DEM, which can be raster or TIN based, the hydrological routing from each grid cell towards the catchment outlet is already done during the DEM processing. Stream tubes and subwatersheds integrate hydrological routing in their mesh construction. However, the flow routing from the HRUs towards the river network has to be determined after the creation of the model mesh. Similar algorithms are used than for rectangular grids, in which the water follows the steepest slope (Lagacherie et al., 2010), or the maximum difference in altitude between neighbors. However, in order to correctly identify the right neighbor, a clean topology of the vector data is necessary. A clean vector topology means that adjacent polygons or lines have to share the same boundaries, nodes and vertexes. This makes it possible to extract neighborhood relationships. Furthermore, the data structure is optimized as each boundary and node is only stored once, which avoids thus redundant data.

6.1.2. How do we link GISs and hydrological models?

Sui and Maggio (1999) classify the link between hydrological models and GIS in four categories: (i) Embedding GISs in hydrological modelling, (ii) embedding hydrological modelling in GISs, (iii) tight coupling and (iv) loose coupling. Daniel et al. (2010) classifies it in linking, combining and integration. Examples for (i) are CANOE (Sogreah and Insavalor, 2005), MODFLOW[1] or HEC-RAS[2]. Only a few GIS functions are integrated into the hydrological model, but the development of GIS and model happen simultaneously and no data transfer problems occur. In the (ii) case, the hydrological model can be started from the GIS user interface, and often some specific functions for the data preprocessing

[1]http://www.modflow.com/modflow/modflow.html (2011-10-25)
[2]http://www.hec.usace.army.mil/software/hec-ras/ (2011-10-25

are developed. TOPMODEL (Beven and Kirkby, 1979), SWAT (Srinivasan and Arnold, 1994), ANSWERS (Beasley et al., 1980), AGNPS (Young et al., 1989) and KINEROS (Woolisher et al., 1990) are for example integrated into GRASS GIS[3]. SWAT was also integrated into the commercial ArcGIS software. Bhatt et al. (2008) chose a tight coupling for their Penn State Integrated Hydrological Model (PIHM). They integrated PIHM into QuantumGIS[4] and created thus the open source GIS interface PIHMgis. Contrary to this tight coupling, a loose coupling approach has the advantage of being more flexible, in case the user wants to work with another GIS software and it is less programming effort. However, sometimes several GIS softwares might be necessary, and data conversion between different formats can be tedious (Sui and Maggio, 1999). Examples of loose coupling are the GRASS preprocessing of MHYDAS (Lagacherie et al., 2010) and J2000 (Schwarze, 2008). The GIS functionalities developed for the loose coupling are thus easily available for other models.

6.1.3. Short review of GIS softwares

Like hydrological models, many different GIS softwares exist or are under development. The most common used GIS is probably the commercial ESRI ArcGIS/ArcInfo software, which has the greatest set of available functions. However, it is quite expensive and many functions have to be bought separately. Furthermore, as no source code is available, the functions are like black boxes.

There are two kinds of GIS data formats used in hydrological models, raster data (for example ASCII file format) and vector files (for example shape file format). Most DEMs are raster based and often land use or soil data are available as vector data. Therefore, a precondition for a GIS used for modelling is the capability to scope with both data formats. Furthermore, in order to use vector data as model mesh, topological functions for the extraction of topological relations or the correction of errors are necessary. The tests carried out during this PhD thesis were based on the reviews of Steiniger and Bocher (2009) and Jolma et al. (2008) and are described in more detail in Branger et al. (2011). However, many people are contributing continuously to the development of open source GIS softwares, so that the open source GIS world changes quickly. We mainly tested the following open-source GIS: OpenJump[5], SAGA[6], GRASS (Geographic Resources Analysis Support System)[7], QuantumGIS, OrbisGIS[8], MapWindow[9] and PostgreSQL/PostGIS[10]. Most of the available GISs work with raster and vector data sets, but some are more efficient for one particular data type as for example SAGA, which is more powerful with raster data than with shape files. In contrast, OpenJump and PostGIS contain mainly vector processing functions. GRASS is the only open-source GIS, for which the data structure is topological. It also provides a large set of functions for the topological error correction. Among the other GISs only OpenJump and OrbisGIS provide a small set of topological functions. PostgreSQL is a relational database management system, to which

[3]http://grass.fbk.eu/intro/modelintegration.html
[4]http://www.qgis.org/
[5]http://www.openjump.org/
[6]http://www.saga-gis.org/en/index.html
[7]http://grass.fbk.eu/
[8]http://www.orbisgis.org/
[9]http://www.mapwindow.org/
[10]http://www.postgis.fr/

PostGIS adds a spatial extension. Due to its data base structure mainly vector format is supported. However, the combination of the complete functionalities of a database, including a large set of SQL functions (spatial query language) with many GIS functions, creates a powerful tool to handle vector geometries. The other tested GISs propose only limited SQL support except OrbisGIS, in which raster data can be manipulated via SQL queries, too. OrbisGIS is a new GIS application developed at the IRSTV in Nantes. It has some functions integrated in the graphical user interface, but most operations are directly initiated from the SQL window.

Most of the GISs are based on the same geographical libraries JTS[11] (Java Topological Suite) and GEOS, its C++ counterpart, as well as other libraries such as GDAL for the import of raster data. Instead of developing always new GIS, the tendency is now going to GIS platforms, which can be extended by plugins. Hence, nearly all GRASS functions were integrated as plugin into QuantumGIS in order to benefit from the advantages of both, a nice graphical user interface of QuantumGIS and the powerful GRASS functions. The SEXTANTE[12] plugin provides a large set of functions including all SAGA functions. Furthermore, SEXTANTE is compatible with several Java-based GISs such as OpenJump, gvSIG and uDig and can thus add raster support to originally vector based GIS. This approach avoids repetitive programming effort and it allows at the same time that everybody can choose his favorite GIS.

6.1.4. Conclusion

We have seen that GISs are necessary for hydrological modelling, as they are used e.g. for the preparation of the model mesh, the calculation of parameters such as slopes or altitudes, the watershed delineation and the extraction of flow routing. GISs and models can be integrated into each other using a single graphical user interface, or they can be used separately. There are many existing GISs which are often based on the same libraries. However, not all of them propose the same set of functions. Concerning open-source GISs only GRASS is based on a topological vector structure. OrbisGIS is the only one which permits to query raster data with SQL queries. Futhermore, there are databases such as PostgreSQL/PostGIS which provide a large set of GIS functions. A further evaluation of the presented GISs as use for the preprocessing is given in section 6.3. But before that, we present a method for the sub-basin delineation, which is also based on GIS functions.

6.2. Determination of drainage network and delineation of catchment border and sub-basins

As we have seen in chapter 3 no information was available about the rainwater pipes and artificial ditches of the Chaudanne and Mercier catchments. However, in distributed hydrological modelling, the water flow paths and contributing areas have to be known with as much precision as possible, as they are necessary for the construction of the model mesh, the flow routing and the simulation of the correct water balance. Consequently, a field campaign and visits to the town hall of Grézieu and to the managers of the sewer system (SIAHVY) aimed at mapping the ditches and gathering data about the rainwater pipes.

[11] http://www.vividsolutions.com/jts/jtshome.htm
[12] http://sextante.forge.osor.eu/index.html

The field campaign showed quickly that the catchment borders used by Gnouma (2006) (Figure 6.2.1) did not represent adequately the real contributing areas of both streams. Part of this PhD aimed thus at answering the questions: "Which water contributes to the study catchments?" and "Which flow paths does the water take?". For the more urbanized Chaudanne catchment, this lead to the development of a peri-urban specific method of sub-basin delineation, which was object of an article submitted to Hydrological Processes. The following section consists of this article. The same method was applied to the Mercier catchment and the results are presented subsequently.

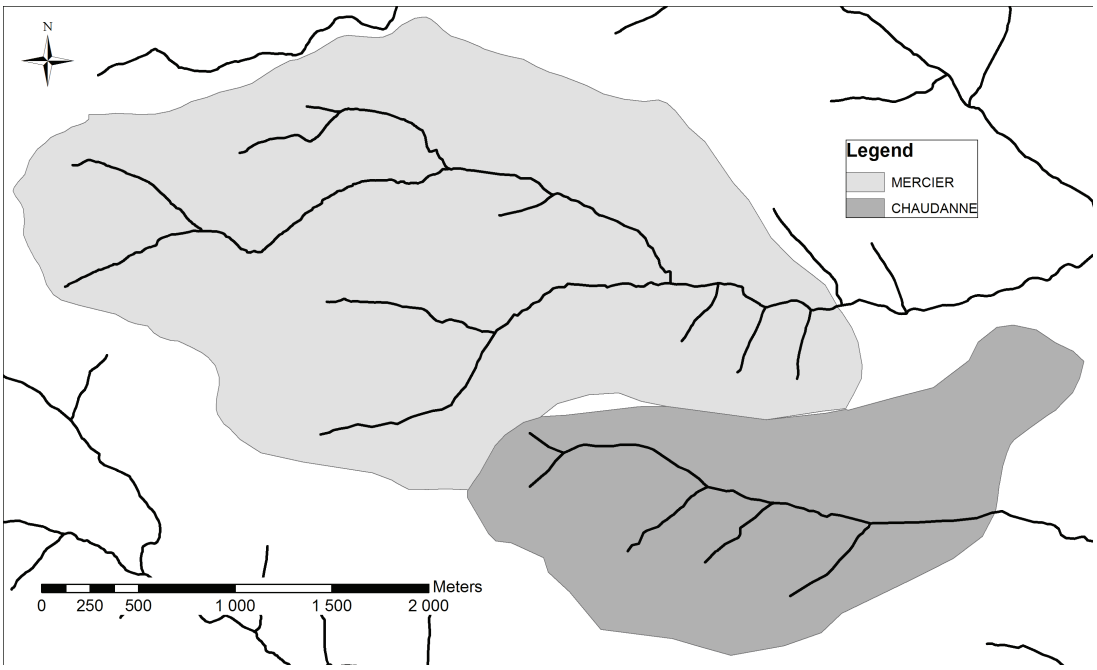

Figure 6.2.1.: Catchment borders of Chaudanne and Mercier used by Gnouma (2006).

6.2.1. Chaudanne catchment

Integration of sewer system maps and field observations in topographically based sub-basin delineation in suburban areas. Application to the Chaudanne catchment.

Sonja Jankowfsky[a], Flora Branger[a], Isabelle Braud[a], Jorge Gironás[b] and Fabrice Rodriguez[c]

a) Cemagref, Hydrology-Hydraulics Research Unit (HHLY), Lyon, France
b) Departamento de Ingeniería Hidráulica y Ambiental, Pontificia Universidad Católica de Chile, Santiago, Chile
c) IFSTTAR, Géotechnique Eau et Risques / Hydrologie et Assainissement, Bouguenais, France

Abstract

Suburban areas are subject to strong anthropogenic modifications, which can influence hydrological processes. Sewer systems, ditches, sewer overflow devices and retention basins are introduced and soils are impermeabilized. The exact knowledge of flow paths and watershed boundaries in these suburban areas is important for storm water management, hydrological modelling and hydrological data analysis. This study proposes a new method for the determination of the drainage network based on time efficient field investigations and integration of sewer system maps into the drainage network for small catchments of up to 10 km2. A new method is also proposed for the delineation of subcatchments and thus the catchment area. The subcatchments are delineated using a combination of an object-oriented approach in the urban zone and GIS based terrain analysis with flow direction forcing in the rural zone. The method is applied to the Chaudanne catchment, which belongs to the Yzeron river network, and is located in the suburban area of Lyon, France. The resulting subcatchment map gives information about subcatchment response and contribution. The method is compared to six other automatic catchment delineation methods based on stream burning, flow direction forcing and calculation of subcatchments for inlet points. None of the automatic methods could correctly represent the catchment area and flow paths observed in the field. The watershed area calculated with these methods differs by as much as 25% from the area computed with the new method.

KEY WORDS suburban, watershed delineation, sewer network, artificial ditches, storm water management

INTRODUCTION

Growing urbanisation mainly concerns suburban areas, which are subject to fast changes due to human activity (Douglas, 2006). Anthropogenic alterations affecting the hydrological processes in these areas include land-use changes, increase of impervious areas and artificial channels (Graf, 1977), and alterations to the natural drainage regime. These modifications increase the peak discharge and accelerate the catchment response (Zheng and Baetz, 1999). They also raise overland flow causing erosion problems (Jones et al., 2000), and reduce infiltration, groundwater recharge and river base flow. Water quality is equally affected by sewer overflows and urban pollutants being washed from the surface (Niemczynowicz, 1999). A good understanding of the hydrological functioning of suburban areas can contribute to reducing the mentioned risks and improving the overall water

management as natural land is urbanized. In particular, in depth knowledge about the drainage system and contributing areas is relevant for several applications in drainage and storm water management (e.g. sizing and location of sewer pipes and retention basins, and construction of hydrological models). Moreover, information about catchment response and pollution risks can be deduced from the land-use properties of contributing areas. However, despite increasing data availability, the determination of drainage networks and catchment borders remains a difficult task in suburban areas, due to their heterogeneity. These areas consist of a mix of purely natural areas without anthropogenic influence, rural areas with dispersed settlements and urban areas, where most of the ground is occupied by built-up cadastral units and natural surfaces are reduced to spots in urban terrain. In natural areas, digital elevation models (DEMs) and geographical information systems (GIS) have allowed the implementation of algorithms for automatic watershed delineation (e.g. O'Callaghan and Mark, 1984; Jenson and Domingue, 1988; Lea, 1992; Costa-Cabral and Burges, 1994, Tarboton, 1997). The most commonly used is the d8 flow direction algorithm (O'Callaghan and Mark, 1984), in which the flow direction follows the steepest gradient towards one of eight neighbours. These algorithms are combined with routines to remove sinks, accumulate the flow, extract the stream network and delineate the watershed and subcatchments. Many studies have improved erroneous watershed delineations in flat areas with missing topographic details (e.g. Garbrecht and Martz, 1997; Augusto et al., 2009). Other aspects to be carefully addressed when computing watershed delineation include the precision and minimum resolution of DEMs (Quinn et al., 1991; Nie et al., 2002; Hammond and Han, 2006), and the threshold value of upstream contributing area to determine the stream network. If river network maps are available, this problem can be overcome by using stream burning methods (Maidment, 1996; Saunders, 1999), surface reconditioning (Hutchinson, 1989; Hellweger, 1997) or flow direction forcing methods (Kenny and Matthews, 2005). All of these three methods improve catchment delineation (Callow et al. 2007; Kenny and Matthews, 2005). Stream burning considers decreases in the elevation of known stream grid cells prior to computing flow directions. Surface reconditioning reduces the elevation of known stream grid cells and cells within a buffer zone around the river network to obtain a smooth slope towards the streams. For the flow direction forcing, the stream network is integrated into the DEM derived flow direction matrix instead of directly altering the DEM (Kenny and Matthews, 2005). Stream burning can lead to watershed distortions (Saunders, 1999) and the creation of parallel streams (Hellweger, 1997). Furthermore, the calculated catchment area depends on the burn depth (Callow et al., 2007). Kenny and Matthews (2005) and Callow et al. (2007) showed that flow direction forcing and surface reconditioning perform better than stream burning. Overall, automatic methods usually result in satisfactory watershed delineation and drainage networks in natural areas when carefully applied (Fried, et al. 2000). In areas under urban influence flow does not always follow topography (Djokic and Maidment, 1991; Smith and Vidmar, 1994) due to the presence of streets, buildings and underground sewer pipes (Denver, 1969; Djordjevic et al., 1999; Smith M.B., 2006). Thus, in most cases drainage patterns and catchment areas cannot be deduced from pure terrain analysis (Djokic and Maidment, 1991; Smith 1993; Doan 2000), even so a number of studies continue to do so (Choi et al., 2003 and 2005; Zheng and Baetz, 1999; Runman et al., 2005). Different methods have been proposed to account for the impact of anthropogenic flow paths on the catchment hydrology. In rural areas, a Light Detection And Ranging (LiDAR) derived raster representation of the DEM with a fine resolution (e.g. 1m) can

already reveal most of the anthropogenic objects like streets and ditches (Murphy et al., 2008). However underground pipes and culvert crossings cannot be detected. Murphy et al. (2008) proposed to integrate culvert crossings manually into the LiDAR derived DEM. Even with integrating field mapped culvert crossings into a 1m-resolution LiDAR DEM Sarrazin et al. (2011) only detected up to 66% of the connected drainage network in a rural setting. The integration of artificial objects as hydrological correction can also be seen in several other studies based on DEMs with a coarser resolution. Streams, streets and sewers are burned in urban areas (e.g. Lhomme et al., 2004, Gironás et al., 2010), or elevation of cells corresponding to buildings are raised (Elgy, 1993; Zech et al., 1994; Nie et al., 2002). The burn depth is usually constant and varies for each study. For urban areas, Gironás et al. (2010) developed a method in which the elevation of streets and pipes is used for determining variable burn depths. They compared this method to a representation where only streets are burned using variable depth while the complete drainage network (natural channels and sewer pipes) is represented in a separate vector layer connected to the surface through defined inlets. They concluded that variable burn depths result in more realistic catchment borders than using a constant burn depth or the raw DEM. Instead of modifying the DEM, Smith and Vidmar (1994) and Kenny and Matthews (2005) forced the flow direction grid to follow the street network. In rural areas, Duke et al. (2003, 2006) integrated ancillary data of artificial drainage elements into DEMs. They classified roads as flat, raised and with ditches, and included information from road cross-sections into the DEM. Road data and location of irrigation channels were used to create forced flow direction grids, in which cross-flow patterns due to siphons, flumes, culverts and split flow elements were also included. They defined dead ends in flow paths and disconnected the corresponding contributing areas from the watershed. Resulting watershed limits were more realistic than those obtained using the d8 algorithm. Djokic and Maidment (1991) manually incorporated anthropogenic objects into a Triangular Irregular Network (TIN) representation. Bocher and Martin (2009) are developing an application for the TANATO2 model (Bocher, 2005) to automatically integrate artificial objects in the TIN representation. Carluer and Marsily (2004) integrated man-made networks into a model mesh consisting of contours and streamlines (Moore and Grayson, 1991; Vertessy et al., 1993) in a rural setting. However, the integration did not change the catchment borders. Hammond and Han (2006) and MacNutt et al. (2004) combined automatic catchment delineation with manual delineation based on maps including artificial features. For urban areas, an object-oriented approach, where single cadastral units are connected to the closest and lowest sewer pipe was adapted in storm water modelling (Greene and Cruise, 1995; Mitchell and Diaper, 2005; Rodriguez et al. 2003, 2005, 2008). None of the previous studies and methods were specifically developed for suburban areas, where slow-growing sewer networks of different types (i.e. urban and rural) coexist. Such mixture of elements does not facilitate the precise identification of the integrated drainage system in suburban catchments. Narrow ditches in rural areas are not easily captured from aerial photographs or DEMs, and underground sewer pipes cannot be detected by DEMs. Detailed sewer data are necessary for the object oriented approach and stream burning. However, these data, which are mostly gathered during the installation of the pipes, are often out of date or consider the wastewater system only. Moreover, the effect of flow conditions typical of urban systems, on catchment delineation is not taken into account by the traditional methods previously discussed. This includes sewer overflow and pumped networks. The approach of Duke et al. (2003, 2006) seems

to be a good solution for rural areas, but it does not include underground sewer pipes either. Furthermore, detailed field campaigns are necessary to derive the road cross sections. Finally, a manual integration of a significant number of anthropogenic objects into the watershed delineation can be quite tedious, especially in strongly urbanized locations. Here, we propose and evaluate a method particularly designed for suburban areas which combines the DEM based methods more adapted to natural zones, and object-oriented methods, which are more applicable to urban settings. The new method allows the determination of the rainwater drainage network based on data analysis and time efficient field investigations for small (up to 10 km2) suburban catchments with multiple outlets. The data analysis includes the differentiation between combined, separated and ditch networks and the integration of sewer overflow devices and pumping stations. The outline of the paper is as follows: In the materials and methods section we describe the relevant hydrological objects in suburban areas for network delineation, as well as the necessary data and general hypotheses. We also present the methodology for drainage network determination and subcatchment delineation. Next, the method is applied to a study area, and compared to six other catchment delineation methods. Finally, we discuss the different methods and present our main conclusions.

MATERIALS AND METHODS

The method is structured in three principal parts (see Figure 1). In the first step, a preliminary catchment border has to be defined in order to better target the field work. For this, three sub-steps, referred to as A to C in Figure 1, are necessary. They are further explained in the following text. The second step consists of the drainage network determination and results in the final drainage network. This is taken as input for step three in which the urban and rural subcatchments are delineated. The method results in the final subcatchment map. For a better understanding the different steps will be referenced as 1A to 3B in the following text.

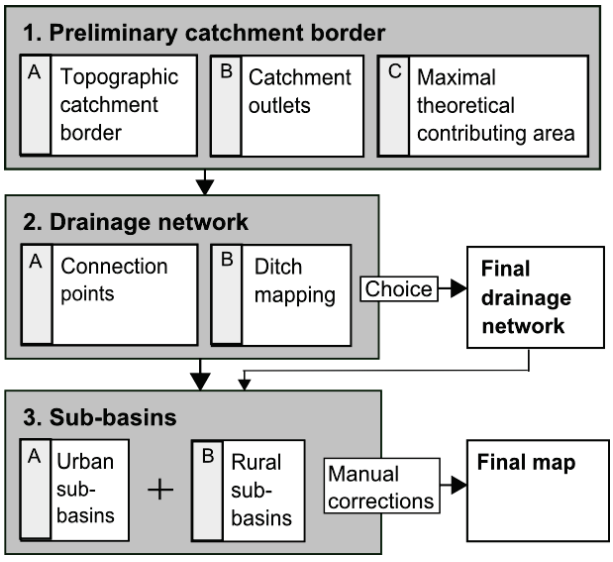

Figure 1: Scheme of the proposed method. The final drainage network and the final map represent the results of the method. The final drainage network is necessary as input for step 3.

General hypotheses
This method builds on the assumption that subsurface flow follows topography. This means that there are no underground source or sink terms. In case of a known discrepancy with this assumption, the resulting catchment boundary should be adapted manually. Only rain water is considered for the catchment delineation; waste water and drinking water are not considered. The method applies to small multi- or single outlet catchments (1-10 km2).

Description of hydrological objects relevant to network delineation in suburban areas
The drainage network in suburban areas can consist of the following network types:

- The combined sewer system evacuates waste and rainwater in the same pipe system towards a waste water treatment plant (WWTP). Some parts of the network can be connected to a pumping station in order to direct all water, even against topography, towards the WWTP. In case of surcharge the network can be connected via storm water overflow devices to the natural river. If no storm water overflow device is installed for extreme rainfall events, the water will flow out of the manholes onto the street. In this study only sewer overflow devices are considered.

- The separated sewer system consists of two unconnected rain and waste water networks. The rainwater network is often directly connected to the natural river, whereas the waste water flows to the WWTP. Retention or infiltration basins and oil water solid separators are sometimes located upstream of rain water injection points to the natural river.

- Roads in rural areas can function as corridors, barriers, sinks or sources (Jones et al., 2000). They are often sided by ditches which intercept surface runoff. The ditches can be connected to the natural river network or end in a dead end (Duke et al., 2006). In this study we only consider the corridor effect of connected ditches.

- Road independent artificial ditches in rural areas might be used for irrigation or drainage purpose.

- The natural river and lake network.

Necessary data
The following section presents the required input data for the determination of the drainage network and subcatchment delineation. First of all, a DEM with a preferably fine resolution is needed. Either aerial photographs, cadastre or detailed land use maps are required; they must correspond to the time period of interest, as suburban areas can change quickly. A map of the river network, preferably one which includes temporary reaches, and a topographic map can be helpful for the field work. All the maps must be digitized and georeferenced. Furthermore, all possible information about the drainage network is useful. This means maps of the sewer network, including flow directions, depth and slope of the pipes and information about the kind of network, the location of sewer overflow devices, pumping stations and retention basins. Information about ditches and rainwater drainage networks is gathered by means of field work here. The amount of field work is reduced if a large number of digital information is available. The contact with local authorities can provide further data and information about intended building

projects and modifications of the sewer system.

Determination of preliminary catchment border and catchment outlets
A preliminary topographic catchment border (1A in Figure 1) for the river of concern has to be determined in order to better target the area for field investigations. This limit determines the area in which all water converge naturally towards the same river (Figure 2). The topographic catchment border can be calculated using standard terrain analysis methods based on DEMs, which are implemented in most GIS softwares. At this step, a drainage network based on the topography of the catchment is also calculated. Suburban catchments equipped with a sewer system connected to a WWTP outside the topographic catchment border have at least two catchment outlets (1B): the natural river and the pipe towards the WWTP (Figure 2). In some cases, additional overflow devices towards other sewer systems can be installed. These outlets have to be determined in order to get a downstream catchment limit. In most cases, a measurement station at the natural river or a confluence will define the river outlet. The sewer system outlets are then determined in reference to this natural outlet. All sewer pipes leading outside the catchment, which are located downstream of the last connection to the natural river are regarded as outlets, refer to Figure 2. After determining the catchment outlets, a first approximate catchment border including the urban zones can be determined. This area should encompass the whole connected sewer system (combined and separated) upstream of the catchment outlets, see Figure 2. Thus, it represents the maximal theoretical contributing area (1C) and limits the area of interest for the next steps.

Determination of the drainage network
A further analysis of the sewer network data and the distinction between combined and separated sewer systems can give information about sewer overflow devices and possible connection points between sewer system and river network (2A), see Figure 2. The rainwater part of separated systems is often directly connected to the natural river. Therefore, special interest should be taken in areas with separated systems close to the river. All the connection points should be mapped in the field after walking along the natural river. Not many data bases provide sufficient information about ditch and rainwater networks. The collection of this information often requires a considerable mapping effort. In order to limit the extent of the field work we propose a systematic approach for ditch mapping (2B). The ditches are only mapped in the subsequent areas of interest:

- Areas with separated systems, where only the location of the waste water pipes is known. This is due to the fact that the rain water will have to flow somewhere and will probably be drained by ditches.

- Along the road network inside the topographic catchment area, as the cumulated water on the impervious surfaces is often collected by ditches. Gravel roads and foot paths can also function as flow paths without a ditch.

- Intersections between the road network and the topographic catchment border. Often the catchment border is influenced by roads, as surface runoff tends to follow the road-ditch network.

- Areas outside the topographic catchment border, connected to pumping stations

or close to the neighbouring river network may contain ditches with inverse flow direction, following topography.

- In the case of an available high resolution DEM (e.g. LiDAR data), the calculated drainage network indicates gullies where channel flow is probable (Sarrazin et al., 2011).

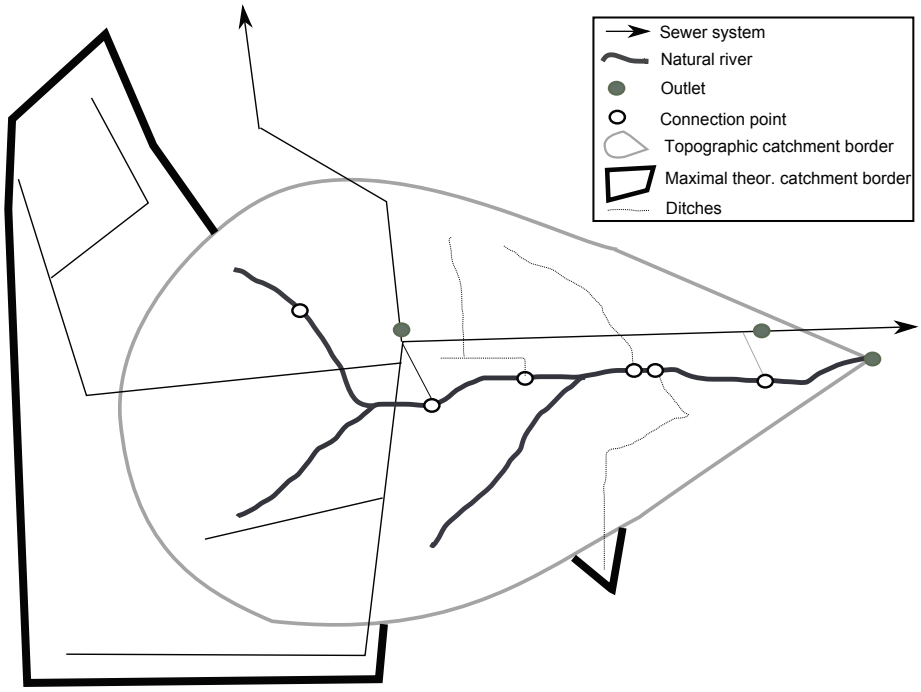

Figure 2: A virtual catchment showing the natural and the artificial drainage network composed of combined sewer system and ditches. The topographical and the maximal theoretical catchment border are indicated, as well as the measurement station at the river and two outlets of the sewer system located after connection points to the river.

The calculated river reaches, which extend the normal river network can give information about possible stream locations. As the ditches follow mostly artificial objects, such as roads which are visible on aerial photographs or topographical maps, they can be noted on these maps during the field work. If a higher accuracy is desired the start and end point of the ditches can be measured with a GPS. Next, retention basins have to be mapped, if they are not known from the available data. The final step is the construction of the drainage network out of the collected data. The drainage network will be the basis for the delineation of the subcatchments and consequently the total catchment area. Thus, the choice of the network parts, which will be connected to the natural river, should be done carefully. As we have seen in the description of drainage networks, rainwater systems are often directly connected to the natural river following topography instead of being pumped to another catchment. Therefore, we propose not to connect the rainwater part of separated sewer systems located outside the topographic catchment boundary to the studied network. Combined sewer network parts located in natural areas outside the topographic catchment are excluded from the final drainage network, because inflow to the sewer system usually happens by means of connected houses, which are non-present

in natural parts. Each connection point and all retention basin should be connected to part of the artificial drainage network.

Delineation of subcatchments
The method of subcatchment and hence watershed delineation proposed here combines different approaches for urban and rural areas. The delineation of the urban subcatchments (3A in Figure 1) follows the object oriented approach mentioned before. Depending on the data availability (vector data like cadastre or land use maps or aerial photographs) the delineation can be done automatically (case of vector data) using GIS functions and scripts (Rodriguez et al., 2003) or manually based on aerial photographs and topographic maps. The principle is the same for both techniques: each cadastral unit with a building is connected to the closest drainage pipe or ditch of the derived drainage network following the principle of proximity (Rodriguez et al., 2003), illustrated in Figure 3.

Figure 3: Aerial photograph (BD ORTHO IGN) showing the urban subcatchment delineation following the principle of proximity. This subcatchment is connected to a retention basin.

In case a cadastral unit is located at equal distance to two sewer pipes, the cadastral unit will be connected to the lowest sewer pipe following the principle of gravity. This results in the delineation of the urban subcatchments due to the structure of the drainage network. Each set of retention basins or sewer overflow devices is regarded as a local outlet, and the upstream area is delineated as separate subcatchment to get an estimation of the contributing area. The subcatchments in the rural area (3B) are delineated automatically using standard terrain analysis methods based on the d8 flow direction algorithm and flow direction forcing (Kenny and Matthews, 2005), as explained in the introduction, with the extended river network including the ditches. The free software Taudem (Tarboton, 2008), which is based on the algorithms developed by O'Callaghan and Mark (1984) and Garbrecht and Martz (1997) can be used for this task. One subcatchment is calculated for each network reach. The rural and urban maps are merged by replacing the urban part on the rural subcatchments map with the urban subcatchments. The question arises of

how to treat dispersed settlements and small villages in the rural part. To account for the fact that buildings are mostly connected to the closest drainage network part, we propose to correct the outside catchment boundary in these dispersed settlements manually following the principle of proximity. This means that, in rural areas outside the topographic catchment boundary, only cadastral units next to a ditch leading inside the catchment are included in the catchment area. In contrast, built-up areas inside the topographic catchment area connected to an outside leading drainage network are excluded from the catchment area.

APPLICATION TO THE CHAUDANNE CATCHMENT

Catchment description

The Chaudanne catchment, part of the Yzeron catchment, is an experimental catchment operated by Cemagref Lyon since 1997. Located in the suburban area south-west of Lyon, France, it was chosen to study the urban influence on hydrology and water quality (Figure 4).

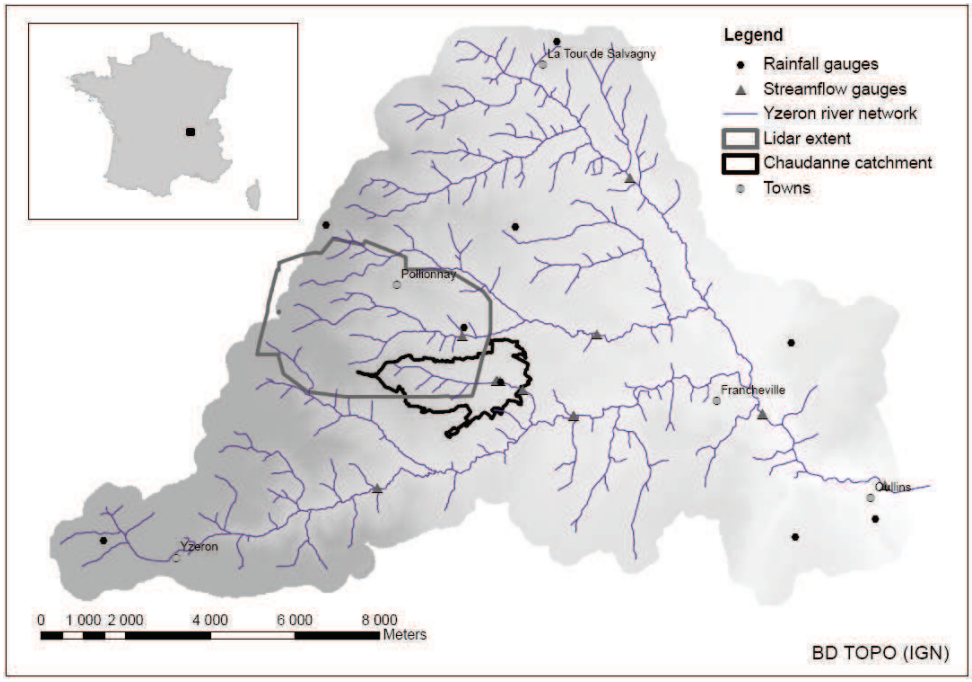

Figure 4: Location and topography of the Yzeron and Chaudanne catchment. The streamflow and rainfall gauges are indicated. The extent of the LiDAR survey is also shown. The Yzeron river network was provided by IGN.

It is one of the study sites of the Field Observatory for Urban Water Management (OTHU, 2010), which gathers eight research institutes and thirteen laboratories. It was equally chosen as a study site for the AVuPUR (Assessing the Vulnerability of Peri-Urban Rivers, Braud et al., 2010) project, to which this study contributes. The project aims at enhancing the understanding and modelling capacity of water fluxes within suburban areas. The watershed covers a surface of about 3.5 km2. Its headwater is located in a rural area and the lower part of the catchment in an urban area. The catchment geology consists

of metamorphic rock of the Monts du Lyonnais series except one alluvial fan in the headwaters (BRGM, 2010) producing soils of silty and argillaceous sand (SIRA, 2010). The climate is temperate with alternating Mediterranean, Continental and Oceanic influences (Gnouma, 2006). The average annual precipitation between 1997 and 2008 was 747.9 mm with a standard deviation of 168.4 mm (Michel, 2009). The Chaudanne is an intermittent stream with a moderate discharge in winter, due to saturated zones and typically a dry period in summer, when the river can become completely dry. A sewer network, consisting of combined and separated rain water and sewer pipes, covers the lower urban part of the catchment. It is connected to a WWTP outside the catchment area. During heavy rain events, the capacity of the sewer system is exceeded, which leads to storm water overflows of mixed water towards the natural river (Lafont et al., 2006). The sewer water has to be pumped at several places. The catchment also contains several retention basins.

Available data
A DEM (BDTopo IGN, Institut Geographic National) with a resolution of 25 m is available for the whole catchment area, as well as a 2 m resolution DEM from LiDAR data, acquired in the framework of the AVuPUR project (Braud et al., 2010, Sarrazin et al., 2011) for the north-western part (Figure 4). The cadastre of the area is provided by CCVL (Communauté de Communes des Vallons du Lyonnais) and Grand Lyon (urban communities). A map of the Chaudanne stream and four temporary tributaries is available (BD Topoâ IGN). The location of four storm water overflow outlets, the pumping station, the combined sewer system and the waste water pipes of the separated sewer system was provided by the SIAHVY (Syndicat Intercommunal d'Assainissement de la Haute Vallée de l'Yzeron, local authority in charge of sewer systems), shown in Figure 5. No digital data of the rainwater network were available in zones with separated sewer systems.

Determination of drainage network
The topographic catchment border (Figure 5) was calculated by means of the 25 m DEM in the eastern part of the catchment and the 2 m LiDAR DEM in the western part. In addition to the natural catchment outlet, two sewer system outlets were defined: the main pipe towards the WWTP and an overflow towards another sewer system in the north-east of the catchment. For the maximal theoretical catchment border the whole sewer system is included, which leads to a 55% bigger catchment area than the topographic catchment. Eleven connection points could be mapped on the natural river from which three are combined sewer overflow devices. The other connection points are linked to rainwater pipes or ditches. It was possible to map the missing rainwater network in zones with separated sewer systems with the help of field investigations and interviews with the sewer system operator. All roads and major foot paths inside the maximal contributing area were investigated and all connected ditches were mapped graphically on a topographical map. A close examination of the intersections between roads and the topographical catchment border led to the extension of the catchment area in four locations, marked as "a" in Figure 5. In the area outside the topographic catchment several ditches with flow directions inverse to the sewer network were found (black arrows in Figure 5). Separated sewer network pipes (marked as b in Figure 5) and combined sewer network pipes in natural areas (marked as c) which were located outside the topographic catchment were excluded from the final network which is shown in Figure 7. The field work took about one to two days.

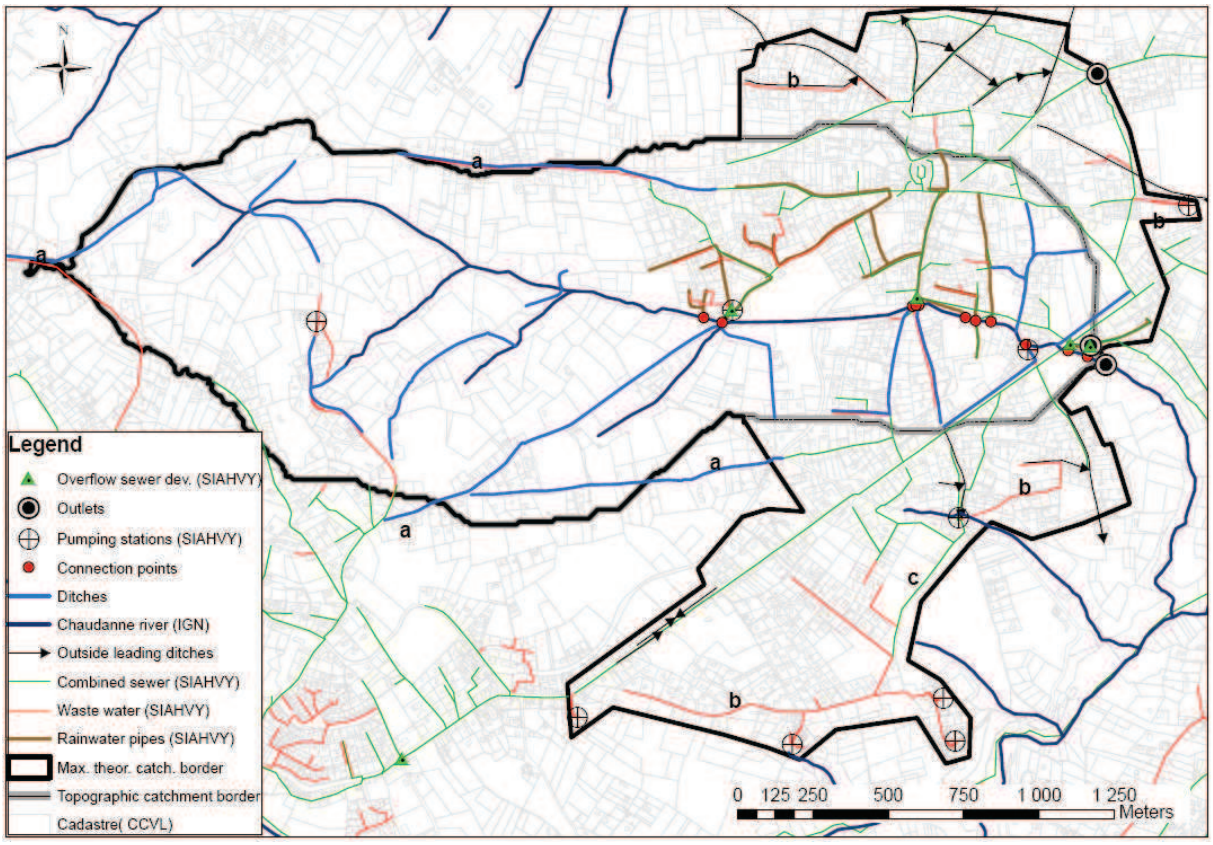

Figure 5: Topographical and maximal contributing catchment area for the Chaudanne river. The drainage network composed of the natural river (BD TOPO, IGN), the rainwater ditches and pipes, the combined sewer system (SIAHVY), waste water pipes (SIAHVY) and ditches flowing in the opposite direction of the sewer system are shown. Most of the ditches follow roads, as can be seen from the cadastre, provided by CCVL. The connection points with the natural river, catchment outlets, pumping stations (SIAHVY) and sewer overflow devices (SIAHVY) are indicated. a, b and c indicate areas of special interest.

Subcatchment delineation

The rural subcatchments were calculated with the Taudem software (Tarboton, 2008). The delineation was conducted using flow direction forcing (Kenny and Matthews, 2005) of the extended river network, including natural, rainwater and ditches networks. Due to the integration of this network into the flow direction matrix one subcatchment is calculated for each river branch (Figure 6a), even if the river network is not in the valley floor, what is often the case for artificial ditches. The urban subcatchments were delineated manually with the help of the aerial photograph by connecting the cadastral units to the closest and lowest sewer pipe (Figure 6b).

Rural and urban maps were merged by replacing the urban part of the rural map with the urban subcatchments, see Figure 7. Manual corrections were necessary in built-up zones located in rural areas outside the topographical catchment. Here, instead of the calculated area, only the cadastral units close to the ditches were connected (see "a" in Figure 7). Cadastral units inside the topographical catchment, but connected to other sewer systems were excluded (b in Figure 7).

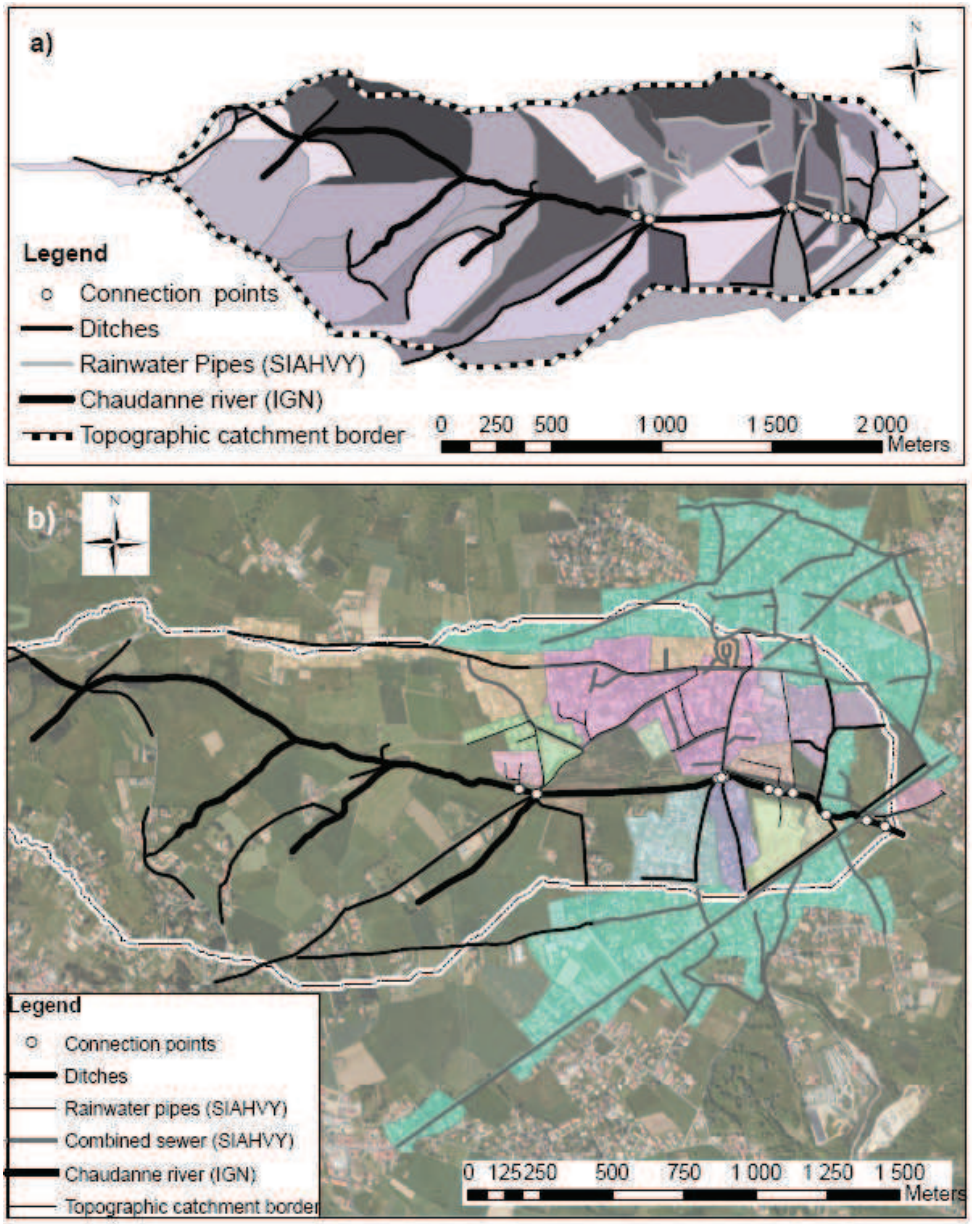

Figure 6: a) The rural subcatchments, calculated with the d8 algorithm and flow direction forcing and b) the urban subcatchments following the borders of cadastral units. The aerial photograph (BD Ortho) was provided by IGN.

The final map of subcatchments (Figure 7) provides information on the contribution of the subcatchments to the discharge at the river outlet. The subcatchments connected via a storm water overflow device (dotted) contribute only if a certain threshold discharge is exceeded. Only the overflowing part enters the natural river, the remaining part of the water flows towards the WWTP. Consequently, the watershed area varies with the discharge. The dry period watershed has a surface of 2.9 km2 and the wet period watershed (when all the sewer overflow devices are activated) has a surface of 4.1 km2. The wet period watershed is 30% bigger than the topographical catchment area. Contrarily to its design, the sewer overflow devices in the Chaudanne catchment are activated nearly at each big rain event. For example, in 2007 a sewer discharge exceeding 5 l/s was measured about 25 times at one of the sewer overflow devices. In addition, the map of subcatchments was

classified depending on the drainage type: natural, ditch drained or urban.

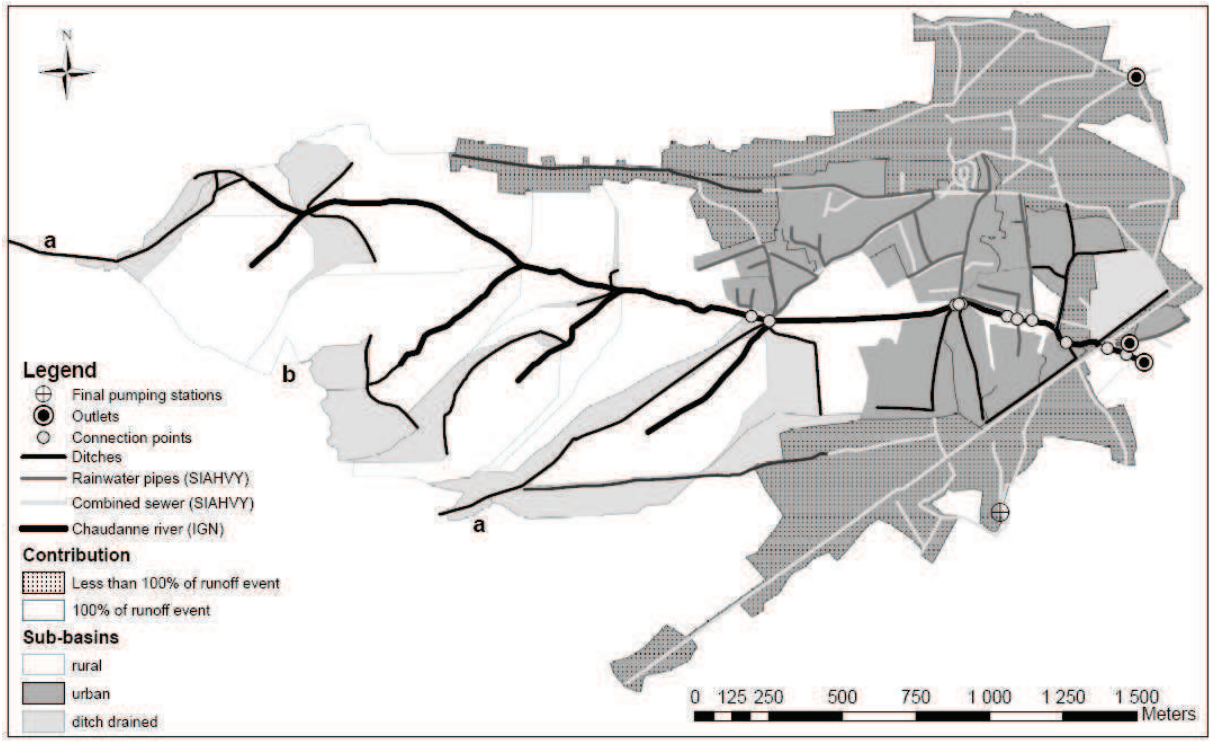

Figure 7: Final map of subcatchments. Urban subcatchments are in black, rural subcatchments in light grey and subcatchments drained by ditches in dark grey. The dotted subcatchments are only connected via storm water overflow devices to the river. a and b indicate areas of special interest.

COMPARISON OF DIFFERENT CATCHMENT DELINEATION METHODS

Description of methods

In order to evaluate the added value of the field work, the presented method for subcatchment delineation and network determination, here referred to as method 1, was compared to six other methods, which were only based on digital data. As input for these methods we used the combined sewer system, the natural river network, the road network and the digital elevation model with 25m resolution and a grid size of 5m. Method 2 consists of flow direction forcing with the combined sewer network and the natural river network using the Taudem software (Tarboton, 2008) as explained for method 1. Hence, with the original DEM calculated flow direction matrix is modified in order to integrate the flow directions of the drainage network. Then, the subcatchments are determined based on this flow direction matrix. In method 3 contributing areas were calculated for each sewer inlet point by means of the ArcGIS SpatialAnalyst/Hydrology/Watershed tool. The distinctive feature of method 3 is the calculation of subcatchments for points instead of lines. As the calculated subcatchments of method 3 correspond only to the catchment area of the sewer system, the surface was merged with the topographical catchment boundary of method 1. Like in method 2, in method 3 the network length corresponds to the length of the natural river and the combined sewer system. Several variants of stream burning were

tested in method 4. Burned objects were the natural river network, streets, the combined sewer system and buildings. As the addition of buildings (5m was tested) was found to have only a minor influence on the flow paths and catchment area, the results are not shown here. An attempt was made to apply the variable road and sewer system burning proposed by Gironas et al. (2010). However, only the variable road burning could be applied successfully because of missing sewer pipe depth data. The BD TOPO (IGN) provided the altitude data for the roads. This method will be referred to as method 4a. Constant burning of roads with different depths (0.5m, 1m, 5m, 10m, 20m) was equally tested, but will not be shown here, as the variable burning gave more realistic results. In order to compensate for the altitude data of the sewer pipes different burn depths (1m for method 4b, 5m for method 4c and 10m for method 4d) of the combined sewer system and natural river network were tested based on the DEM resulting from the variable road burning (4a). The subcatchments and river networks were calculated for the modified DEMs (4a-d) using the Taudem software without the flow direction forcing option. As the drainage networks of methods 4a to 4d arise from raster maps, the Douglas and Peucker (1973) algorithm for line simplification with 5m threshold was applied. Without this correction, the network length is not representative because the raster based network would be longer than the normal, rather straight, network.

Description of validation criteria
Several criteria were chosen in order to compare the different methods. The criteria evaluate the resulting watershed areas and the drainage network. Method 1 is regarded as the reference, as it is based on additional field information. The criteria are presented in the following list:

1. Watershed area: total calculated watershed area.

2. Overlapping surface: results from intersection of the concerned watershed area with the area of method 1. This criterion shows the capability of the methods to represent the same watershed area.

3. Excessive surface: arises from subtraction of the overlapping surface from the watershed area of method 1. It shows the overestimated surface.

4. Surface drained by sewer system: sum of all subcatchments drained by the combined sewer network. Often this surface is the basis for the sizing of sewer pipes.

5. Subcatchment number: a measure of the discretization of the catchment.

6. Average size of subcatchments

7. Network length: The length of the calculated network.

8. Total network agreement: The length of the calculated network of a given method that lies within a zone defined by a buffer of 10 meters around the total network consisting of combined sewer system, rainwater network and the natural river is compared to the length of this total network (Figure 10).

9. Combined and natural agreement: the length of the calculated network of a given method that lies within a zone defined by a buffer of 10 meters around the network

consisting of combined sewer system and the natural river is compared to the length of this network.

10. Excessive network: consists of the difference of the total network length and the total network agreement of a given method in km, compared to its total network length. It defines erroneously detected network parts.

11. Detected ditches: The network length detected in a buffer of 10 meters around the ditches is compared to the total ditch length. It shows the capability of representing the artificial ditches without field work.

Results of comparison
Table 1 shows the calculated criteria for all of the methods. The maps of the subcatchments and drainage networks are presented in Figure 8.

Table 1: The results for the different criteria and methods. Method 1 is the proposed method, method 2 uses flow direction forcing, method 3 contains subcatchments for inlet points and methods 4a -d use different kind of stream burning: (a) uses just variable road burning; (b), (c) and (d) use variable road burning and the burning of the drainage network of 1, 5 and 10m, respectively.

Criteria/Method	Unit	1	2	3	4a	4b	4c	4d
Watershed area	km^2	4.10	4.55	3.516	3.095	3.10	4.28	4.28
Overlapping surface	%	100	97.88	89.91	85.35	85.43	96.21	96.20
Excessive surface	%	0.0	15.10	04.02	0.99	0.99	11.58	11.58
Surface drained by sewer system	km^2	1.219	2.196	0.656	0.0	0.68	1.97	2.0
Subcatchment number	-	44	134	230	126	39	29	324
Average sub-catchment size	km^2	0.091	0.034	0.003	0.025	0.0795	0.147	0.013
Network length	km	32.19	22.38	22.38	21.23	9.65	11.03	37.85
Total network agreement	%	100	68.52	68.52	30.41	24.15	33.64	70.95
Combined and natural agreement	%	100	100	100	31.32	33.59	48.95	89.82
Excessive network	%	0	0.38	0.38	53.38	18.58	0.76	39.01
Detected ditches	%	100	0	0	28.98	3.44	0	29.98

Regarding Figure 8, we can remark that the calculation of contributing areas for inlet points in method 3 results in a discontinuous catchment area with many small subcatchments. All the other watersheds have continuous surfaces. Method 2, 4c and 4d have the largest watershed areas and represent 96 and 98% of the reference watershed, respectively. However, they overestimate the catchment by 12 to 15%.

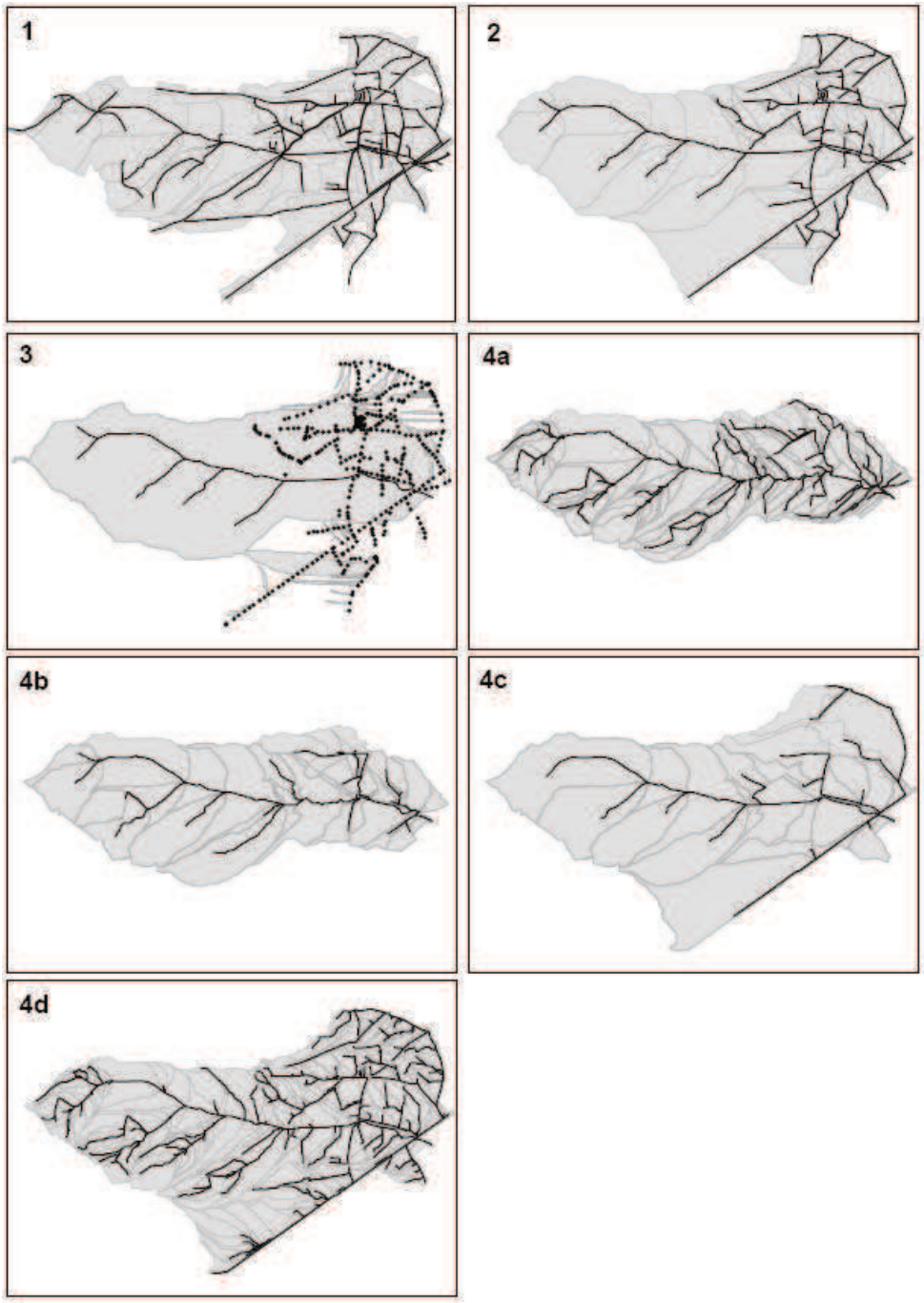

Figure 8: Subcatchment maps and calculated drainage networks for methods 1, 2, 3, 4 a-d.

This occurs mainly in the southern part outside the topographical catchment border; a zoom of this region is shown in Figure 9. In this location, field observations showed that a small stream crosses the road and its parallel sewer pipe via a culvert. The ditches beside the road are connected to this stream. Hence, the natural area upstream of the road, which is drained by this stream and the ditches, was excluded from the watershed in method 1. Only method 1 and 2 are capable of connecting the pumped area (Figure 9 right of centre) to the watershed. Nevertheless, method 2 also connects the natural part in the south, see c in Figure 5. Method 4a and 4b, which have the smallest watershed

area and the smallest overlapping surface could not capture the combined sewer system part outside the topographical catchment border. A stream burning depth of at least five meters was required in order to do so.

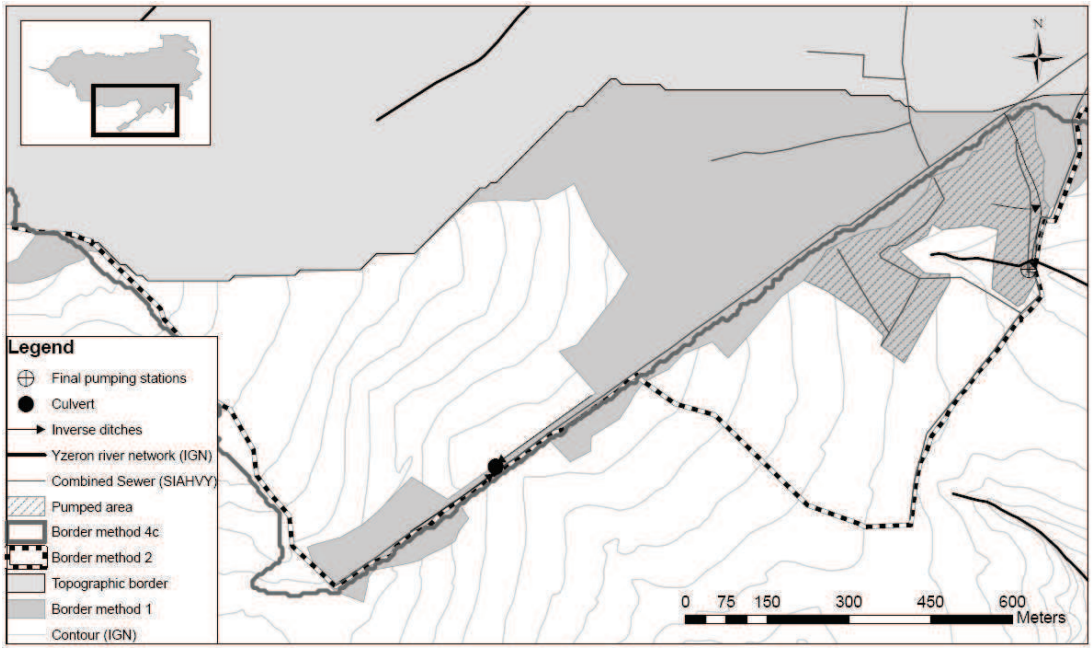

Figure 9: Zoom of the southern part of the catchment showing a comparison of the watershed limits using methods 1, 2 , 4c and the topographical catchment border. The contour lines (IGN) indicate a natural thalweg, which is perpendicular to the sewer system and crosses via the culvert. Artificial ditches are connected to the natural flow path, not the sewer system. In the eastern part of this region a pumped area is visible.

None of the methods correctly represent the surface drained by the sewer system. Methods 3, 4a and b underestimate the surface by at least 44%, whereas methods 2, 4c and d overestimate it by 60 %. The number of calculated subcatchments varies between 29 and 324 and their average size between 0.003 and 0.147 km2. It is interesting to note that the increase of the burn depth to 10m only has an influence on the number of subcatchments and the network density and not on the general shape of the watershed. As can be seen in Figure 8, the longest network length can be found with method 4d, caused by the stream burning depth of 10 m. The complete network is best represented by methods 2, 3 and 4d, which is shown by the total network agreement. However, looking at the excessive network criterion, we can see that nearly 40% of method 4d's network does not correspond to any network observed in the field. Consequently, methods 2 and 3, which are also the only methods capable of reproducing 100% of their input network, lead to a more realistic result. Nevertheless, these two methods cannot detect artificial ditches. These could only be detected with methods 4a and 4d. Figure 10 shows an extract of the urban part of the watershed. The drainage networks of method 4a and 4b are compared to the road network and the buffer around the drainage network of method 1. We can see that the introduction of the sewer system stream burning reduces the network density, but enhances the agreement with the real network represented by the buffer. Nonetheless, the agreement with the road network decreases.

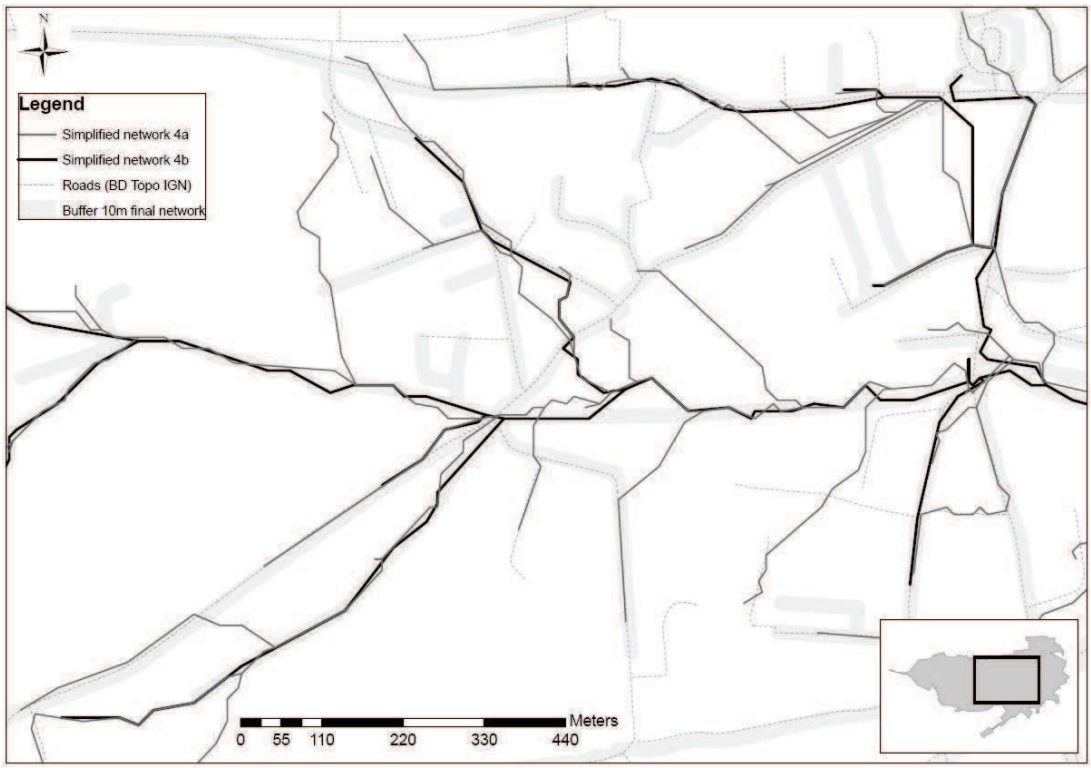

Figure 10: Drainage network of methods 4a and b compared to the buffer around the total network and the roads.

DISCUSSION

Each suburban catchment is different. It depends on the country, city size, population growth, climate and last but not least drainage habits. Here, we developed a method based on a French suburban area. The method is as general as possible. However, because the available data for each catchment are different, the method might have to be slightly adapted when applied to another catchment. As we have seen, drainage patterns in suburban areas can be quite complex. In case sewer systems and connections of houses were not mapped during installation, the detection of their location and connections during field surveys can be difficult. Many ditches are also piped in some parts and the determination of flow directions and links to other pipes, especially on road cross-sections or roundabouts, can require tracer investigations. This involves time consuming field experiments. The calculation of the rural subcatchments is based on the DEM and thus its resolution plays an important role. In our case, we had the LiDAR DEM with 2m resolution only for part of the rural catchment area and a DEM with a resolution of 25m for the rest of the catchment. It would be interesting to see the results based on a LiDAR DEM for the whole catchment area, especially for the urban part. Concerning the delineation of the urban subcatchments only the manual method based on aerial pictures was shown. This method allows the determination of subcatchments in a more general manner. The automatic method will strictly connect only plots of land classified as urban cadastral units leading to a spotted subcatchment map. Hence, the automatic method depends even more on the input data, such as classification of land use units. No parallel sewer systems are permitted in the automatic method. This means that the results of the

automatic and manual methods will not necessarily be the same. The automatic method will give a result which is easily exploitable by a hydrological model, whereas the result of the manual method is, amongst other things, useful for the calculation of runoff coefficients. Concerning the object oriented approach, the question arises as to whether or not it is correct to consider an administrational cadastral unit as hydrological unit. Does the water in the yard really flow to the same place as the building, which is connected via underground pipes (Rodriguez et al. 2008)? The answer might lie between the object oriented and the topographical approach. And there is also uncertainty in the drainage network to which a building is actually connected when there are several close by. The comparison with the digital data based methods showed that none of them were capable of capturing all the field observations. Either the catchment area was too small, as for methods 3, 4a and 4b, or too big as for methods 2, 4c, and 4d. Due to the continuous development of suburban areas, a wide variety of drainage networks can be found in these areas. It is difficult to reproduce these drainage networks, as they consist of different sources, such as the sewer system, the natural river and ditches. By means of the variable road burning, part of the ditches can be detected, but without verification in the field, they cannot be distinguished from the erroneous detected flow paths. The methods of comparison are mainly based on topography, except method 3, which makes it complicated to represent cross-flow patterns, different flow directions of the drainage network and parallel networks. By calculating subcatchments for each inlet point, as used in most storm water models, the drainage network is independent of the topography and cross-flow patterns can be reproduced. However, this results in many miniscule subcatchments, and the continuity of the flow along ditches is no longer represented. Only with method 2 and 3 it was possible to obtain the complete input network, and thus include the pumped area. The process times of the individual methods vary significantly. The flow direction forcing and constant stream burning is relatively straightforward, whereas the preparation of the data for the variable stream burning is quite tedious. In addition, elevation data for sewer pipes are typically not available. The time spent in the field for method 1 was only one to two days. The treatment of the field data and calculation of subcatchments took about one week. However, cost of fieldtrips might be relevant, particularly when the basin is in a location not easy to access. These results show the importance of field investigations and the difficulty to capture all observed suburban drainage characteristics with one method. Thus, a combination of different approaches as in method 1 provides better representation of the urban and natural features of suburban areas. It enables the capturing of all of the networks with cross-flow patterns, sewer overflow devices with split flow patterns, parallel drainage networks and pumped areas.

CONCLUSIONS

Slowly growing suburban areas often have complex drainage systems, consisting of a combination of ditches, sewer systems, sewer overflow devices, pumping stations and retention basins. The accurate knowledge and representation of this drainage system and the contributing watershed area are important for storm water management, water quality questions, calculation of hydrological criteria as runoff coefficients and hydrological modelling. This study points out that purely automatic methods for catchment delineation and calculation of drainage systems based on DEMs are not able to correctly represent the suburban terrain. Unfortunately the relevance of field observations is many times disregarded when

automatic methods and digital information are available. Detailed information and terrain investigations are necessary in order to fully understand the hydrological processes in suburban areas. Contact with local authorities is strongly recommended as they can provide further data and information about intended building projects and modifications of the sewer system. Due to the combination of the object oriented approach and the flow direction forcing in the proposed method, both the urban and the rural zones could be well represented. Time efficient field work added valuable information about flow paths and improved the watershed delineation. This study shows the significance of dry and wet period watershed variability, which is often not considered. Taking a constant watershed area instead of a variable one can introduce errors, e.g. when calculating runoff coefficients. The distinction in urban, natural and ditch-drained subcatchments can give information about the response time, as urban subcatchments with a higher impermeable fraction will respond faster than natural subcatchments. Because of the road runoff, ditch drained subcatchments have a quicker response time than natural subcatchments. The resulting subcatchment map is also interesting for water quality issues. The contamination risk in urban and ditch drained subcatchments is higher than in natural subcatchments. If a natural subcatchment is located downstream of an urban subcatchment the water quality might improve due to dilution. The resulting subcatchment map can be directly used for storm water management questions and hydrological modelling. A hydrological model is under construction based on the drainage network and subcatchments determined in this article (Jankowfsky et al., 2010). To further reduce the uncertainties still incorporated in the map, it would be interesting to perform some tracer experiments at points of interest. Also, the gathering of data about road cross-sections would permit the application of the approach described by Duke et al. (2003, 2006) and thus allow the determination of hydrologically unconnected areas. It would be interesting to validate the subcatchment map by means of detailed discharge data from subcatchment outlets. This would also allow the estimation of flow threshold values for the sewer overflow devices, and it would permit the determination of the flow threshold which defines the limit between dry and wet period catchment area.

ACKNOWLEDGEMENTS

The study was funded by the by the French Agence Nationale de la Recherche (ANR) under contract nř ANR-07-VULN-01. CCVL, IGN, Grand Lyon, SAGYRC, SIAVHY, Sol-Info Rhône-Alpes provided data used in the study. Finally, the Chilean FONDECYT program provided partial support through Grant No. 11060312.

REFERENCES

Augusto CVG, Bonnet MP, Filho OCR, Mansur WJ. 2009. Improving hydrological information acquisition from DEM processing in floodplains. Hydrological Processes 23: 502-514.

BRGM, 2010. Bureau de recherches géologiques et minières. http://infoterre.brgm.fr/viewer/MainTileForward.do;jsessionid=C6247604415C79ABC47269563FD5969E. Consulted on 2010/09/21.

Bocher E. 2005. Impacts des activités humaines sur le parcours des écoulements de surface dans un bassin versant bocager : essai de modélisation spatiale. Application au Bassin versant du Jaudy-Guindy-Bizien (22). Thèse de l'Université de Rennes, 337 p.

Bocher E, Martin JY. 2009. TANATO2: TIN-based approach to evaluate impact of natural and anthropogenic artefacts. Abstracts Proceedings of the International Opensource Geospatial Research Symposium OGRS 2009, Nantes, France, 8-10 July 2009: 56-59.

Braud I, Chancibault K, Debionne S, Lipeme Kouyi G, Sarrazin B, Jacqueminet C, Andrieu H, Béal D, Bocher E, Boutaghane H, Branger F, Breil P, Chocat B, Comby J, Dehotin J, Dramais G, Furusho C, Gagnage M, Gonzalez-Sosa E, Grosprêtre L, Honegger A, Jankowfsky S, Joliveau T, Kermadi S, Lagouy M, Leblois E, Martin JY, Mazagol PO, Michell K, Molines N, Mosini ML, Puech C, Renard F, Rodriguez F, Schmitt L, Thollet F, Viallet P. 2010. The AVuPUR project (Assessing the Vulnerabiliy of Peri-Urban Rivers) : experimental set up, modelling strategy and first results. Proceedings of the 7th Novatech 2010 Conference, June 28-July 1 2010, Lyon, France, 10pp.

Callow JN, Niel KPV, Boggs GS. 2007. How does modifying a DEM to reflect known hydrology affect subsequent terrain analysis? Journal of Hydrology 332: 30-39. DOI: 10.1016/j.jhydrol.2006.06.020.

Carluer N, Marsily GD. 2004. Assessment and modelling of the influence of man-made networks on the hydrology of a small watershed: implications for fast flow components, water quality and landscape management. Journal of Hydrology 285: 76-95.

Choi JY, Engel BA. 2003. Real-Time Watershed Delineation System Using Web-GIS. Journal of computing in civil engineering 17(3): 189-196. DOI:10.1061/(ASCE)0887-3801(2003)17:3(189).

Choi JY, Engel BA, Theller L, Harbor J. 2005. Utilizing web-based GIS and SDSS for hydrological land use change impact assessment. Transactions of the ASAE 48(2): 815-822.

Costa-Cabral MC, Burges SJ. 1994. Digital elevation model networks (DEMON): a model of flow over hillslopes for computation of contributing and dispersal areas. Water Resources Research 30: 1681-1692.

Denver Council of Governments. 1969. Anon., 1969. Urban Storm Drainage Criteria Manual, Wright-McLaughlin Engineers 1969.

Djokic D, Maidment DR. 1991. Terrain analysis for urban stormwater modelling. Hydrological Processes 5(1): 115-124.

Djordjevic S, Prodanovic D, Maksimiovic C. 1999. An approach to simulation of dual drainage. Water Science and Technology 39 (9): 95-103.

Doan JH. 2000. Hydrologic model of the Buffalo Bayou using GIS. Hydrologic and hy-

draulic modelling support with geographic information systems, DR Maidment and D Djokic (eds). ESRI, Redlands, Calif., 113-143.

Douglas I. 2006. Peri-urban ecosystems and societies transitional zones and contrasting values. In Peri-Urban Interface: Approaches to Sustainable Natural and Human Resource Use, edited by D. McGregor, D. Simon, D. Thompson, pp. 18-29. London, UK: Earthscan Publications Ltd.

Douglas DH, Peucker TK. 1973. Algorithms for the Reduction of the Number of Points Required to Represent a Digitized Line or Its Caricature. Canadian Cartographer 10(2):112-122. DOI: 10.3138/FM57-6770-U75U-7727.

Duke GD, Kienzle SW, Johnson DL, Byrne JM. 2003. Improving overland flow routing by incorporating ancillary road data into Digital Elevation Models. Journal of Spatial Hydrology 3(2): 1-27.

Duke GD, Kienzle SW, Johnson DL, Byrne JM. 2006. Incorporating ancillary data to refine anthropogenically modified overland flow paths. Hydrological Processes 20: 1827-1843.

Elgy J, Maksimovic C, Prodanovic D. 1993. Matching standard GIS packages with urban storm drainage simulation software. Proceedings of Vienna Conference-HydroGIS 93: Applications of Geographic Information Systems in Hydrology and Water Resources, Vol. 211, IAHS, Wallingford, UK, 151-160.

Fried JS, Brown DG, Zweifler MO, Gold MA. 2000. Mapping Contributing Areas for Stormwater Discharge to Streams Using Terrain Analysis. In: Terrain Analysis: Principles and Applications. Wilson JP, Gallant JC (eds). John Wiley & Sons, ISBN 0-471-32188-5, 183-203.

Garbrecht J, Martz LW. 1997. The assignment of drainage direction over flat surfaces in raster digital elevation models. Journal of Hydrology 193: 204-213.

Gironas J, Niemann JD, Roesner LA, Rodriguez F, Andrieu H. 2010. Evaluation of methods for representing urban terrain in storm-water modelling. Journal of hydrologic engineering 15(1): 1-14.

Gnouma R. 2006. Aide à la calibration d'un modèle hydrologique distribué au moyen d'une analyse des processus hydrologiques : application au bassin versant de l'Yzeron. Thèse de l'institut national des sciences appliquées de Lyon. 263 pp.

Graf WL. 1977. Network characteristics in suburbanizing streams. Water Resources Research 13(2): 459-463.

Greene RG, Cruise JF. 1995. Urban watershed modelling using geographic information system. Journal of Water Resources Planning and Management 121(4): 318-325.

Hammond M, Han D. 2006. Issues of digital maps for catchment delineation. Proceedings of the Institution of Civil Engineers. Water Management 159. 45-51.

Hellweger FL. 1997. AGREE - DEM Surface Reconditioning System, http://www.ce.utexas .edu/prof/maidment/gishydro/ferdi/research/agree/agree.html consulted on 15/10/2010.

Hutchinson MF. 1989. A new procedure for gridding elevation and stream line data with automatic removal of spurious pits. Journal of Hydrology 106: 211-232.

Jankowsky S, Branger F, Braud I, Debionne S, Viallet P, Rodriguez F. 2010. Development of a suburban catchment model within the LIQUIDő framework. Proceedings of the International congress on Environmental Modelling and Software, iEMSs 2010, 5-8 July 2010, Ontario, Ottawa.

Jenson S, K Domingue JO. 1988. Extracting topographic structure from digital elevation data for geographic information system analysis. Photogrammetric engineering and remote sensing 54(11): 1593-1600.

Jones JA, Swanson FJ, Wemple BC, Snyder KU. 2000. Effects of roads on hydrology, geomorphology and disturbance patches in stream networks. Conservation Biology 14(1): 76-85.

Kenny, F Matthews B. 2005. A methodology for aligning raster flow direction data with photogrammetrically mapped hydrology. Computers and Geosciences 31: 768-779.

Lafont M, Vivier A, Nogueira S, Namour P, Breil P. 2006. Surface and hyporheic oligochaete assemblages in a French suburban stream. Hydrobiologia 564: 183-193. DOI 10.1007/s10750-005-1718-8.

Lea NL. 1992. An aspect driven kinematic routing algorithm. In: Overland Flow: Hydraulics and Erosion Mechanics, Parsons AJ, Abrahams AD (eds). Chapman & Hall: New York, BY; 393-407.

Lhomme J, Bouvier C, Perrin JL. 2004. Applying a GIS-based geomorphological routing model in urban catchments. Journal of Hydrology 299(3-4): 203-216.

MacNutt W, Dare P, Dalton S. 2004. Use of digital terrain model as a means of urban watershed delineation in Fredericton, New Brunswick. Geomatica 58(2): 107-119.

Maidment D. 1996. GIS and hydrological modelling: an assessment of progress. In: Third International Conference on GIS and Environmental Modelling, Santa Fe, NM, 20-25 January 1996.

Michel C. 2009. Exploitation des données de deux sous-bassins versants de l'Yzeron : la Chaudanne et le Mercier. Rapport de Stage de Master 1 Sciences de l'Eau dans l'Environnement Continental effectué au Cemagref Lyon. Université des Sciences et Techniques du Languedoc Montpellier II, pp. 32.

Mitchell VG, Diaper C. 2005. Simulating the urban water and contaminant cycle. Environmental Modelling and Software 21: 129-134.

Moore ID, Grayson RB. 1991. Terrain-based catchment partitioning and runoff prediction using vector elevation data. Water Resources Research 27 (6): 1177-1191.

Murphy PNC, Ogilvie J, Meng FR, Arp P. 2008. Stream network modelling using LiDAR and photogrammetric digital elevation models: a comparison and field verification. Hydrological Processes 22: 1747-1754.

Nie L, Schilling W, Killingtveit A, Saegrov S, Selseth I. 2002. GIS based urban drainage analyses and their preliminary applications in urban stormwater management. Proceedings of 9th International Conference On Urban Drainage (CD-ROM). Strecker EW, Huber WC (eds). ASCE, Reston, Va. 1-13.

Niemczynowicz J. 1999. Urban hydrology and water management - present and future challenges. Urban Water 1: 1-14.

O'Callaghan JF, Mark DM. 1984. The Extraction of Drainage Networks From Digital Elevation Data. Computer Vision, Graphics and Image Processing 28: 328-344.

OTHU, 2010. http://www.graie.org/othu/. Consulted on 2010/9/16.

Quinn P, Beven K, Chevallier P, Planchon O. 1991. The prediction of hillslope flow paths for distributed hydrological modelling using digital terrain models. Hydrological Processes 5: 59-79.

Rodriguez F, Andrieu H, Creutin JD. 2003. Surface runoff in urban catchments: Morphological identification of unit hydrographs from urban databanks. Journal of Hydrology 283(1-4): 146-168.

Rodriguez F, Cudennec C, Andrieu H. 2005. Application of morphological approaches to determine unit hydrographs of urban catchments. Hydrological Processes 19(5): 1021-1035.

Rodriguez F, Andrieu H, Morena F. 2008. A distributed hydrological model for urbanized areas - Model development and application to case studies. Journal of Hydrology 351: 268-287.

Runman N, Lin G, Li J. 2005. Investigation of GIS-based Surface Hydrological Modelling for Identifying Infiltration Zones in an Urban Watershed. Environmental Informatics Archives 3: 315-322.

Sarrazin B, Braud I, Puech C. 2011. A functional typology of headwater channels extracted from high resolution LiDAR DEM, to be submitted to Hydrological Processes.

Saunders W. 1999. Preparation of DEMs for use in environmental modelling analysis. ESRI User Conference, July 24-30, 1999, San Diego, California.

SIRA, 2010. Sol Info Rhône-Alpes, sira@rhone-alpes.chambagri.fr - http://www.rhone-alpes.chambagri.fr/sira/. Consulted on 2010/09/14.

Smith MB. 1993. A GIS-based distributed parameter hydrologic model for urban areas. Hydrological Processes 7: 45-61.

Smith MB, Vidmar A. 1994. Data Set Derivation for GIS-based Urban Hydrological Modeling. Photogrammetric Engineering and Remote Sensing 60(1): 67-76.

Smith MB. 2006. Comment on 'Analysis and modelling of flooding in urban drainage systems'. Journal of Hydrology 317: 355-363.

Tarboton GD. 1997. A new method for the determination of flow directions and upslope areas in grid digital elevation models. Water Resources Research 33(2): 309-319.

Tarboton G.D. 2008. TAUDEM Terrain Analysis Using Digital Elevation Model. Software description. User Guide. Utah State University. http://hydrology.neng.usu.edu/taudem/taudem3.1/index.html.

Vertessy RA, Hatton TJ, O'shaughnessy PJ, Jayasuriya MDA. 1993. Predicting water yield from a mountain ash forest catchment using a terrain analysis based catchment model. Journal of Hydrology 150: 665-700.

Zech Y, Sillen X, Debources C, Van Hauwaert A. 1994. Rainfall-runoff modelling of partly urbanized watersheds: Comparison between a distributed model using GIS and other models sensitivity analysis. Water Sciences Technology 29(1-2): 163-170.

Zheng PQ, Baetz BW. 1999. GIS-based analysis of development options from a hydrology perspective. Journal of urban planning and development 125(4): 164-180. DOI: 10.1061/(ASCE)0733-9488(1999)125:4(164).

6.2.2. Mercier catchment

The drainage network and sub-basins of the Mercier catchment were determined with the method developed for the Chaudanne catchment. However, as the Mercier catchment consists mainly of rural areas, only the method for the rural part was applied. First of all, the drainage network and topographic catchment border were calculated based on the Lidar DEM with 2m resolution using the d8 algorithm and the default parameters of Taudem for the contributing area threshold. Then, this Lidar based drainage network was taken as orientation for the mapping of the artificial ditches on the field. The final drainage network and the Lidar based drainage network are shown in Figure 6.2.2. The final drainage network differs slightly from the drainage network defined by Sarrazin (2012) as his objective was not the determination of the drainage network for hydrological modelling.

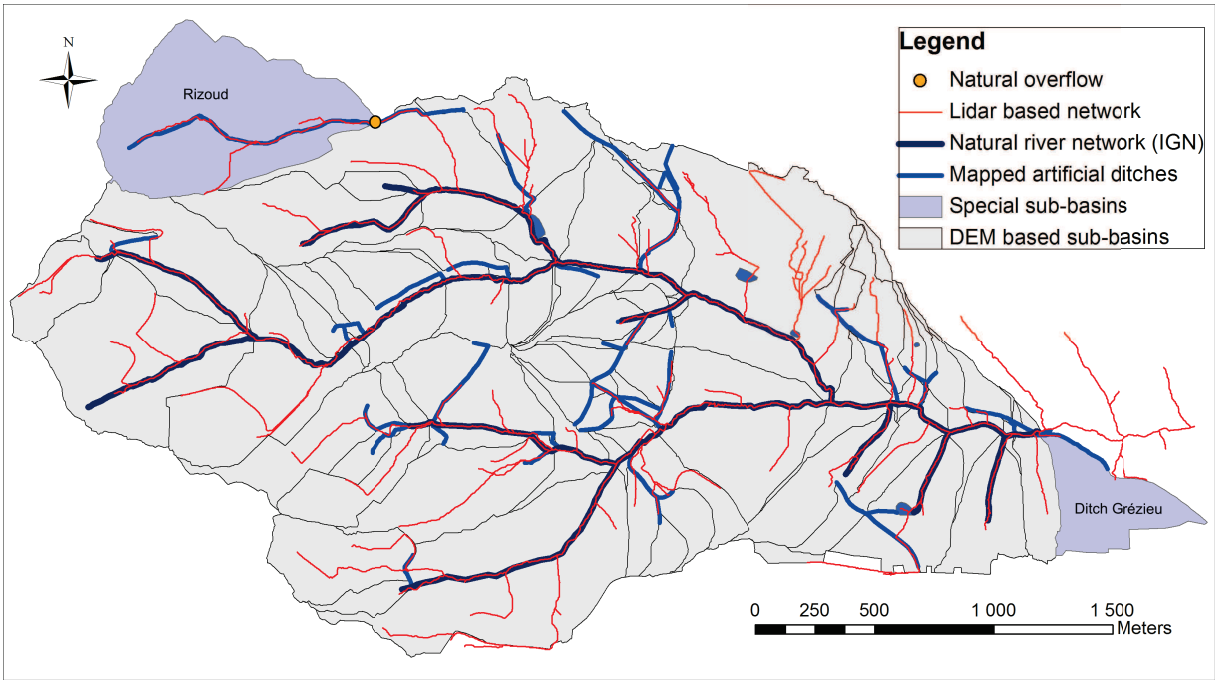

Figure 6.2.2.: Natural stream network (BD Topo IGN) and the on the field mapped artificial ditches for the Mercier catchment. The sub-basins were calculated with stream-burning of the natural stream network and the mapped ditches. The with the default parameters of Taudem extracted drainage network based on the Lidar DEM is also shown in red. It was used as orientation for the field survey. The Rizoud sub-basin depends on a natural overflow and the Grézieu sub-basin consists of an urban residential development of Grézieu, which is drained by a concreted ditch. The Grézieu sub-basin was added manually.

Compared to the original catchment border used by Gnouma (2006) (Figure 6.2.1), which is based on the DEM with 25m resolution, the Lidar data revealed a connection of the Rizoud stream to the Mercier catchment (Sarrazin, 2012). At the connection point, the Rizoud stream crosses a forest track located on a ridge. When the water level passes a certain threshold, water overflows towards a ditch beside the track leading into the Mercier catchment. The comportment is thus similar to a storm water overflow device. Furthermore, field investigations showed that just upstream of the Mercier measurement

station an artificial concreted ditch flows into the Mercier. This roadside ditch is actually draining a residential development of Grézieu with separated sewer system.

The sub-basins were then calculated using the terrain analysis algorithms of the TAUDEM software, which includes flow direction forcing with the complete drainage network of the Mercier. The urban sub-basin draining the residential area of Grézieu was adapted manually including all cadastral parcels located in proximity and above the ditch. The final sub-basin map is shown in Figure 6.2.2.

6.3. Geographical Pre-processing

6.3.1. Choice of GISs and technical realization of the preprocessing of the PUMMA model

The input data format for models built within the LIQUID framework is the PostgreSQL/PostGIS data base format. This would suggest to use the PostGIS functionalities for the development of the data preprocessing. However, the experience of Branger et al. (2011) showed that PostGIS has problems to handle correctly the topology of vector layers. For this reason different GISs were tested (see section 6.1.3) for their topological functions. Concerning open-source GISs, only GRASS GIS provides the necessary functionalities. GRASS has a topological data structure, which is different from other GIS data structures, such as ESRI shape files. The following 2D vector objects are supported (Neteler and Mitasova, 2008):

- point
- line: a directed sequence of connected vertices with two endpoints called nodes
- boundary: the border line of an area, which can be composed of several lines
- centroid: a point inside the closed boundary, but not necessarily the center of gravity
- area: composition of boundary and centroid

These data are structured topologically, enabling the extraction of neighbor relationships. The topology is thus automatically built during the import of the vector layer. For erroneous vector layers containing isles or holes between polygons and overlapping areas several GRASS layers are created: a layer with the original data, a layer with the overlapping areas and a layer with the isles or holes in form of polygons. The detected errors can then easily be corrected. GRASS has a modular structure: each functionality consists of one compiled C program, shell or python script, which can be run individually. The functions are differentiated into raster functions, called r.*, vector functions (v.*), data base (db.*/pg.*), general (g.*) functions and some other functions, which are less relevant for our purposes. The modular structure facilitates the scripting and automation of program sequences. As script languages Shell, Perl or Python are compatible with GRASS. Shell was the traditional script language used with GRASS, as GRASS runs originally only on Linux platforms. However, for the new version of GRASS (7) all scripts were translated into Python. Furthermore, Python is compatible with most GIS softwares and seems to be the new standard for scripting. Python is the fastest interpreted language using object oriented concepts, and it is portable to other platforms

(http://www.python.org/). For this reason we chose to develop the preprocessing for the PUMMA model with Python scripts calling GRASS functions. However, GRASS has only limited SQL support (SQLlite) and some preprocessing tasks can be easily solved using SQL queries. Therefore, we decided to integrate SQL functions into the Python scripts using PyGreSQL (http://www.pygresql.org/), which is a Python interface to a PostgreSQL data base. At the beginning, we developed the scripts on a Windows platform, but due to some incompatibilities, we finally changed to a Linux platform. Nevertheless, most of the scripts should run on both platforms.

6.3.2. Methodology of geographical preprocessing

The preprocessing of the geographical data can be divided in four subsequent tasks, as shown in Figure 6.3.1: the preparation of the input data, the creation of the model mesh, the calculation of the geometrical parameters of the model and finally the extraction of the hydrological routing. The preparation or cleaning of the input data is necessary before

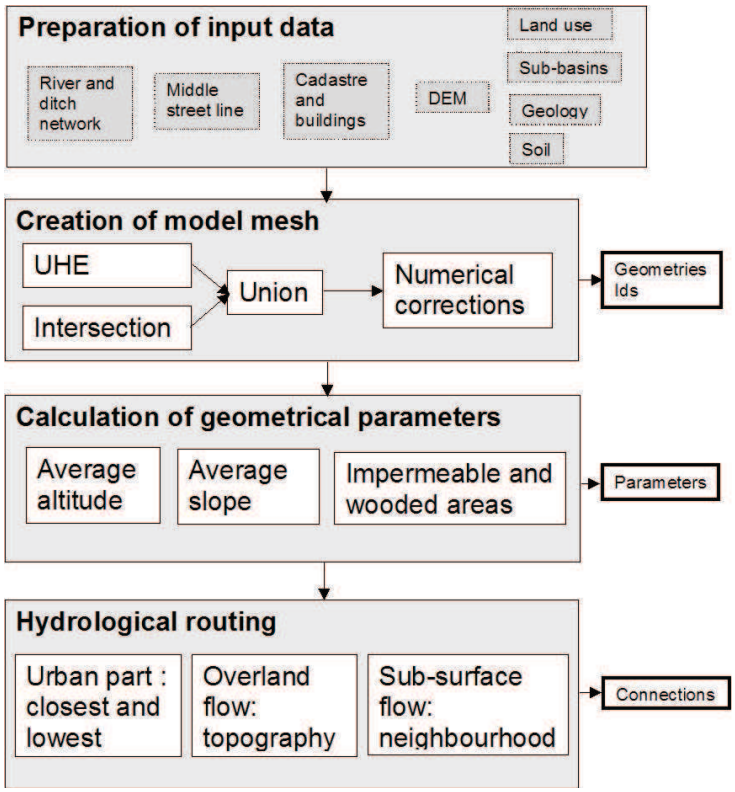

Figure 6.3.1.: Workflow of geographical pre-processing. Input data are in dark grey and processes in white. On the right side are the outputs of the data processing and thus inputs to the model.

the other tasks can be performed. During the creation of the model mesh, the geometries of the HRUs and UHEs as well as of the drainage network are produced and attributed to the different LIQUID modules. The calculation of the geometrical parameters treats the calculation of average altitudes and slopes as well as the percentages of built, road and natural areas for the URBS module. The hydrological routing extracts the flow transfer in the catchment, which means the connections between the model units and the river network.

The realization of this preprocessing was an important part of this PhD thesis. Three master students that I supervised helped me in this task. The work was subdivided into three parts, the preparation of the UHEs and calculation of urban parameters; the creation of the HRUs and the specification of their parameters; and the hydrological routing. These topics were addressed by Paillé (2010), Sanzana (2011) and Brossard (2011), respectively. For each master student a detailed description of the necessary tasks was prepared, which are shown in Appendix D.

The objective was to develop a methodology and scripts which are applicable to other case studies and which can serve in general for the preparation of the input data of PUMMA and similar models. For this reason, we tried to develop as much scripts and reapplicable solutions as possible. However, not everything could be solved by an automatic solution. Therefore, some manual processing of the data was necessary. Lagacherie et al. (2010) developed a similar preprocessing for the MHYDAS model called GEOMHYDAS. The Perl and Shell scripts were published in autumn 2010 with an open-source license and were thus available for us. We tried to use the scripts as far as compatible with the LIQUID framework. The next paragraph summarizes shortly the GEOMHYDAS (Lagacherie et al., 2010) functions (all called *m.*), which we applied.

Table 6.3.1.: Summary of the principal GEOMHYDAS (Lagacherie et al., 2010), GRASS and PostgreSQL/PostGIS functions used for the automatic preprocessing.

Name	Source	Description
m.seg	GEOMHYDAS	Segmentation procedure allowing to set priorities
m.dispolyg	GEOMHYDAS	Dissolving of small polygons under consideration of constraints
m.disline	GEOMHYDAS	Unifying small lines to adjacent lines depending on threshold
m.snaplp	GEOMHYDAS	Moving a line towards a polygon boundary
m.douglas	GEOMHYDAS	Smoothing of lines by removing of vertexes
v.generalize	GRASS	Proposes different smoothing functions such as Douglas (deletion of vertexes) or Snakes (no deletion of vertexes) algorithm
v.clean	GRASS	Topological cleaning with many options, such as rmarea with which small areas can be unified with adjacent polygons
v.edit flip	GRASS	Changes vector line direction
Touches	PostGIS	Tests if two geometries have a common point
Group by	PostgreSQL	Calculation of aggregation function (e.g. mean, sum) based on one attribute

GEOMHYDAS (Lagacherie et al., 2010) integrates man-made features such as ditches, roads and agricultural fields. They developed a simplification methodology in order to reduce the total number of model units, which keeps all hydrologically relevant model units (*m.dispolyg*). For this, a priority can be set on the different factors such as land use, soil, geology, sub-basins, etc. during the intersection with the *m.seg* algorithm. If the priority is set to the land use map, all land use features, e.g. roads, ditches, hedgerows, etc. are conserved. We applied furthermore the m.disline script, which unifies all lines of a drainage network, which are smaller than a certain threshold value to adjacent lines,

except at intersections. The m.snaplp algorithm moves line vertexes to close by polygon boundaries, or replaces the lines by the polygon boundaries. Finally, the m.douglas script allows to smooth lines using the Douglas and Peucker (1973) algorithm. The applied GEOMHYDAS scripts as well as other used GRASS or PostgreSQL functions are summarized in Table 6.3.1.

Other GRASS scripts were developed by Schwarze (2008) for the J2000 model. However, these scripts are mainly raster based and were not applicable to our set of problems. The next sections describe all steps, automatic and manual, which are necessary for the data preprocessing and propose thus a complete methodology.

6.3.2.1. Preparation of input data

The upper box of Figure 6.3.1 shows all GIS layers which are necessary for the preprocessing and thus the model. The land use, sub-basin, geology and soil maps, as well as the river and ditch network are necessary for the creation of the HRU maps. The processing for the urban part needs a land register map (cadastre), which was in our case already integrated into the land use map, maps of buildings and impervious areas inside the cadastral parcels and a vector line file indicating the middle of the street. The DEM serves the calculation of some of the parameters and the hydrological routing. The input vector files have to fulfill certain constraints in order to be used for the creation of the model mesh, which are explained in the following sections.

Creation of hydrologically oriented vector land use map
The land use maps for the Mercier and Chaudanne catchments, which were presented in chapter 3.1.4, were digitized by the Geography laboratory "Environment Ville Société" UMR5600 (Béal et al., 2009; Jacqueminet et al., 2011). The Mercier map was digitized manually and consisted of one GIS layer. In contrast, the land use map of the Chaudanne basin was digitized by a different person who created one layer for each land use class: urban cadastral parcels, agricultural fields, roads, lakes and wooded areas. A semi-automatic method was used, in which the vegetation layer was generated automatically from raster maps. This lead to overlapping of the vegetation layer with the other layers (left panel in Figure 6.3.2). However, a unique land use map containing representative, simplified land use objects, is necessary for modelling. Thus, the layers had to be intersected and then a choice was necessary, as only one land use type per polygon was allowed. For this choice, the hydrological processes happening on the different land use types had to be considered. A vegetated area consists of the tree crown, which is important for interception and the root zone, from which water is extracted due to transpiration. If the vegetated area overlaps a road, mainly the interception process plays a role. Furthermore, if we would choose the vegetation before the road, the originally impermeable surface, which is subject to evaporation would then be considered permeable and it would be subject to evapotranspiration. Therefore, the vegetated areas were reduced by the road and lake surfaces. This allowed also to keep the connectivity of the roads.

Further reflections were made about the correction of topological problems, such as holes inside a polygon. The middle panel in Figure 6.3.2 shows the attempt to create topological vegetated areas while keeping their original surface. Hence, the holes and the overlapping forest on the other side of the road were unified manually in the attempt to keep the vegetated surface constant. However, this processing is too time consuming.

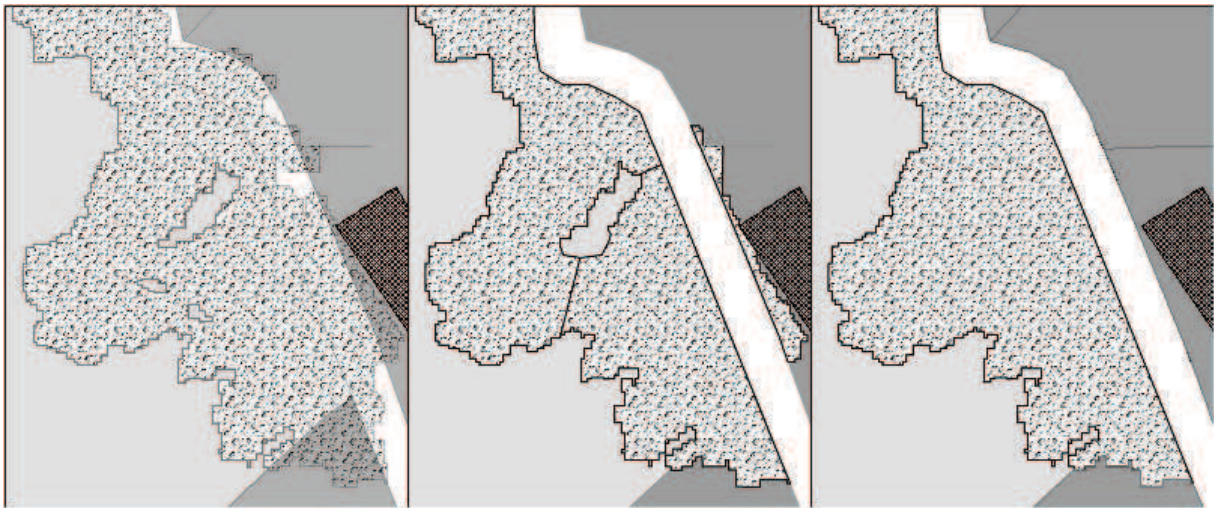

Figure 6.3.2.: Extract of detailed land use map with choice of overlaps (Béal et al., 2009). The original data layers are on the left and the corrected in the middle and on the right. In both cases the connectivity of the road is kept, but in the middle the holes in the wooded area are corrected by creating one hole with the representative surface of all holes and intersection of the polygon with hole. The wooded surface on the other side of the road was unified to create only one polygon. In the right panel, the forest on the other side of the road and the holes were erased, which is less time consuming.

Therefore, automatic methods, such as the suppression of the small polygons (as shown in the right panel of Figure 6.3.2) were chosen (Béal et al. (2009), Branger et al. (2011)).

Catchment borders
First of all, all of the layers used for the HRUs need to have the same catchment borders. If all original layers are larger than the catchment border the unnecessary part is just removed. However, the data have to be extrapolated if the layers are too small, which was the case for the geology and soil maps in our case. The missing geometries can be obtained by intersection and union commands (Sanzana, 2011).

Topological cleaning
The topology of each input vector layer has to be cleaned before it can be used for the rest of the preprocessing, as most GIS functions refuse the execution on topologically incorrect layers. Errors like overlapping of polygons, gaps between polygons, dangles (self intersecting lines) or areas without or with duplicate centroids, have to be corrected. Paillé (2010) wrote the Python scripts *clean_ogr.py* and *clean_ogr2.py* based on GRASS functions which clean vector files without and with attribute table. The first script is useful after geometrical operations, which can introduce new errors and the second script for the correction of imported shape files.

Smoothing of raster derived boundaries
Information derived from raster data, as for example the vegetation polygons in the land use map of the Chaudanne basin, have to be smoothed. Lines derived from raster maps have usually a zigzag structure. The WTI and WTRI interfaces use the length of the interface (polygon boundary) for the calculation of the wetted section. A zigzag line is longer

than a straight line which corrupts the calculation. Sanzana (2011) tested the *m.douglas* script for the smoothing, which was developed by Lagacherie et al. (2010) based on the Douglas and Peucker (1973) algorithm but did not obtain satisfying results. The snakes algorithm (Kass et al., 1987) which minimizes the internal energy of polygons and which is implemented in the GRASS *v.generalize* function solved the problem. However, this algorithm does not reduce the number of vertexes, which caused problems at a later task of the preprocessing.

Manual correction of middle street line
An UHE consists of a cadastral parcel plus half of the adjoining street (Rodriguez et al., 2003). In order to create this geometry, the streets have to be cut in halves. Paillé (2010) searched for algorithms dividing the street, but did not find a simple solution feasible in the time of his internship. Finally, he chose to use the BD TOPO road data, which is a line file located approximately in the middle of the road. However, the end points did not correspond to the polygon borders and at some places the lines intersected the road polygon. Hence, the file had to be adapted manually. This file served later also to extend the sewer system in the urban part.

Processing of river sources
The intersection of lines (e.g. the drainage network) and polygon maps (e.g. the HRU map) is problematic when the line ends inside a polygon. This can be the case at the sources or end points of the drainage network. Sanzana (2011) proposed three solutions to extend such lines to the polygon boundaries: the calculation of the minimum distance from the line node to the polygon boundary, the calculation of a line which follows the deepest depression from the river source or the calculation of the contributive area for the river source, see Figure 6.3.3. He developed a script which identifies the river end points located inside a polygon and two other scripts for the calculation of the contributive areas and the intersection of the line and polygon map. However, the contributive areas were most of the time inside other polygons, which created concave polygons. Furthermore, the raster based script introduced topological errors depending on the raster resolution. Therefore, the drainage network was finally adapted manually in order to fit to the last polygon border. An automatic solution of this last approach may be possible, but was not developed due to time limits.

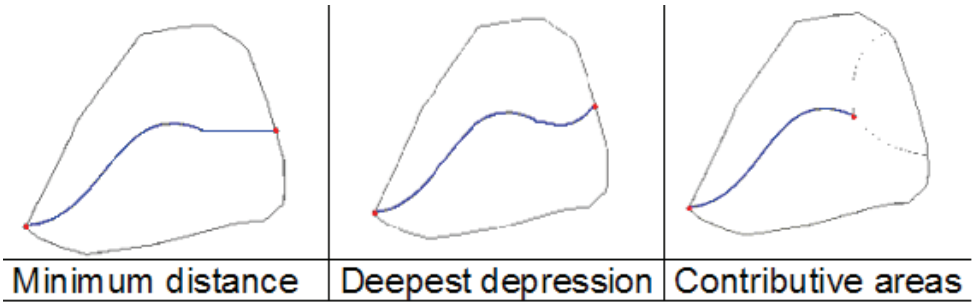

Figure 6.3.3.: Different possibilities to process the river sources falling inside a polygon (Sanzana, 2011).

Correction of ditch network
In order to extract the WTRI interfaces, the HRU polygon map has to be intersected

with the drainage network. Due to incorrect digitalization or different data sources, the ditches along the sides of roads may cross polygon boundaries. An intersection of such a ditch layer with the HRU map would create small insignificant polygons, which can easily induce numerical problems caused by their great (boundary length)/area ratio. A possible solution would be to unify these small polygons with adjacent polygons with which they share the longest boundary by means of the GRASS command *v.clean (rmarea)*, or to polygons with the same land use by means of the *m.dispolyg* script developed by Lagacherie et al. (2010). However, this would not necessarily keep the intersection along the ditch line, which is required for the extraction of the WTRI interfaces.

For this reason, the ditches have to be snapped to the closest polygon boundaries (mostly roads) before the intersection. Sanzana (2011) applied the m.snalp algorithm developed by Lagacherie et al. (2010). This algorithm has two options, either the vertexes of the lines can be snapped towards the polygon border, or the complete line can be replaced by polygon borders. Unfortunately, this algorithm did not work well for thin polygons such as roads (Sanzana, 2011). Therefore, we had to find another solution. We finally developed a semi-automatic method which allowed us to get a drainage network completely composed of polygon boundaries. This means, instead of moving the lines towards the polygon boundaries, we replace them with the polygon boundaries. For this, the drainage network was separated into the reaches for which an intersection was intended (mostly the natural) and reaches (principally the ditches) for which an intersection was not intended. The intersection was thus just performed with a part of the drainage network.

The other part of the drainage network was modified after obtention of the final model mesh as follows: The polygon boundaries of the final model mesh were first extracted (with the function Planar Graph of OpenJump, as we had some problems with the corresponding GRASS functions). Then, we had to assign the right line attributes to the right polygon boundaries. SQL queries using a simple intersection of both lines or of a buffer around one line and the other line did not give satisfying results, as often wrong lines were selected. In order to avoid this problem, we calculated the centroid of the boundaries with GRASS and created a buffer of 0.05m around them. The ditch lines were then corrected manually until all of the boundaries close to a ditch could be selected by intersection of the buffer with the ditch, see Figure 6.3.4. For this technique, the buffer size has to be smaller

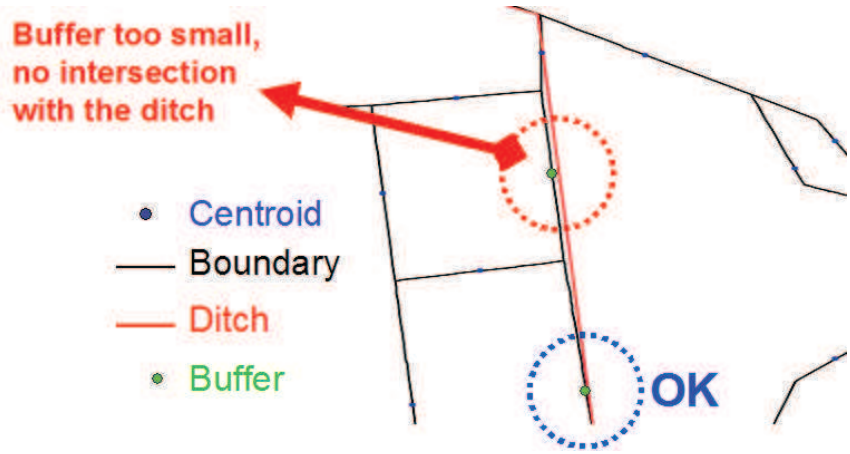

Figure 6.3.4.: Schema indicating the topological corrections of the drainage network. In the upper example the ditch does not intersect with the buffer and has to be adapted manually and in the lower example no manual corrections are necessary.

than the smallest boundary in order not to select wrong boundaries. This allowed us to obtain a perfect geometry of the drainage network without moving each vertex manually. However, the manual part was still time consuming. Discussions with the developer of the GEOMHYDAS scripts, did not lead to further ideas to reduce the manual part.

6.3.2.2. Creation of model mesh

The creation of the model mesh consists of different sub-tasks. First of all the UHEs have to be created using the urban cadastral parcels, the roads and the middle line of the roads. Then the land use, soil, geology and sub-basin maps have to be intersected with the natural drainage network to obtain the HRU map. After that the UHEs are integrated into the HRU map. They are not intersected with the HRU map, but replace the HRUs at the overlapping places in order to keep the object oriented approach based on the cadastral parcels. Small polygons have then to be unified and the map has to be adapted to numerical needs. The single tasks are described in more detail in the following paragraphs.

UHE creation
For the original version of the URBS model, Rodriguez (1999) developed a preprocessing method based on the GIS MapInfo. However, this method does not create the UHEs as polygons which are needed for the lateral flow exchange in LIQUID (WTI/WTRI). Therefore, Paillé (2010) worked on the automatic extraction of these polygons. He wrote the Python script *trottoir.py*, which cuts the road in halves and the script *uhe.py*, which unifies the halves with the adjacent polygons. For the partitioning of the road he extracted the nodes of the cadastral parcels which are adjacent to the road and projected an orthogonal on the middle line of the road, see Figure 6.3.5. He composed then the

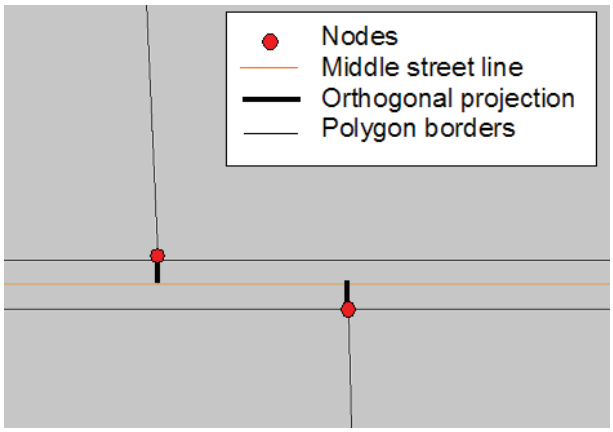

Figure 6.3.5.: Illustration of method for the cutting of the road. Orthogonal projection from polygon nodes to middle street line (Paillé, 2010).

new road polygons out of lines and extracted the identifier of the neighboring cadastral parcel for the union. Figure 6.3.6 shows the original data and the final UHEs for the Rezé catchment, which was taken as first simple test case.

HRU creation and union with UHEs
Sanzana (2011) applied the script *m.seg* developed by Lagacherie et al. (2010) for the intersection of the land use, geology, soil and sub-basin maps with the drainage network.

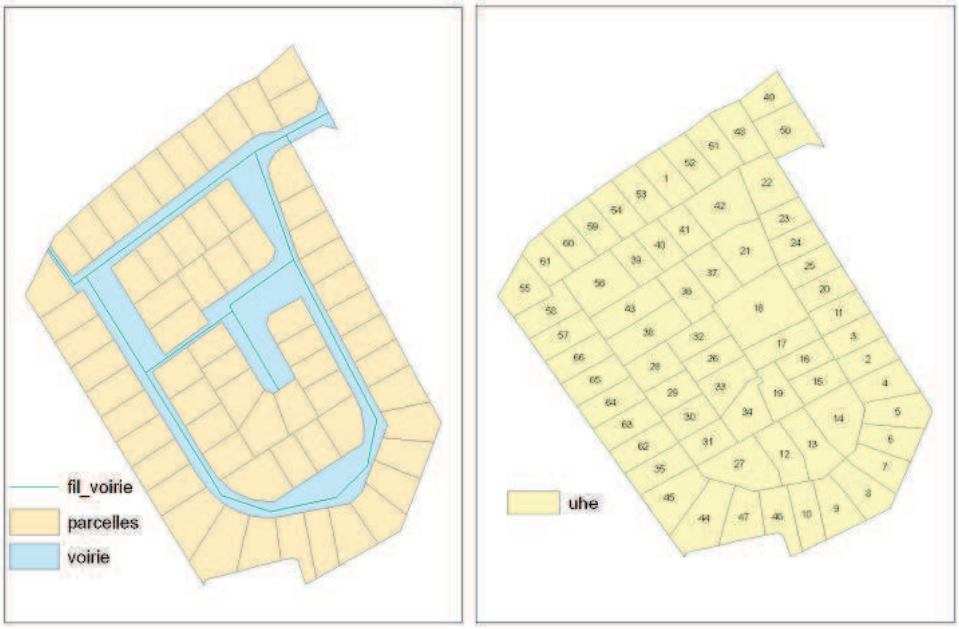

Figure 6.3.6.: The Rezé catchment before and after UHE creation (Paillé, 2010).

Compared to classical overlay functions available in most GISs, the script overlays all polygon and line files at once. Furthermore, the user can indicate a hierarchical order according to the hydrological importance, which will then orientate the further cleaning procedures (Lagacherie et al., 2010). The script *m.dispolyg* also from Lagacherie et al. (2010) was then used to merge the small polygons. *M.dispolyg* takes into account the hierarchical structure set during the segmentation process. The priorities were set to land use, sub-basins, soil and at last geology. It was necessary to choose an area threshold up to which the polygons were merged. This threshold depends on the smallest features we want to keep. In the Chaudanne catchment we had a retention basin with an area of 2 m^2. However, this threshold seemed us too small, so we decided to set it to 10 m^2 in order to keep thin features as hedgerows. Sanzana (2011) unified then the corrected HRU map with the UHE map by means of standard GIS overlay functions.

Slope segmentation

Instead of transforming the raster based slope map into a vector map and integrating it during the intersection for the HRU creation, which would lead to a great number of polygons and thus long computation times, we decided to integrate the slope information only in the polygons where the standard deviation was too large. This allowed to keep the object oriented character of the HRU map.

Sanzana (2011) wrote thus the script *slope_ segmentation.py* which segments those polygons for which the standard deviation is larger than a threshold value. The input data for the script are the HRU map, the DEM and the threshold value. The script uses the inter quartile Range ($= thirdquartile - firstquartile$) in order to define the morphological boundaries for the segmentation. The boundaries divide the slope in three rather homogeneous classes, see Figure 6.3.7. As the boundaries are extracted from the slope raster, a simplification of the zigzag lines is necessary. Figure 6.3.7 shows the lines simplified only with the Snakes algorithm and with a combination of Snakes and Douglas Peucker algorithms. As we want to avoid the creation of concave polygons, the second solution was

selected. The algorithm was only applied to the Mercier catchment, as the slope is more uniform and the polygons are already smaller in the Chaudanne catchment. Furthermore, the DEM of the Mercier catchment had a finer resolution (2m against 25m). A threshold value of 6.0 was determined visually for the standard deviation of the Mercier slope.

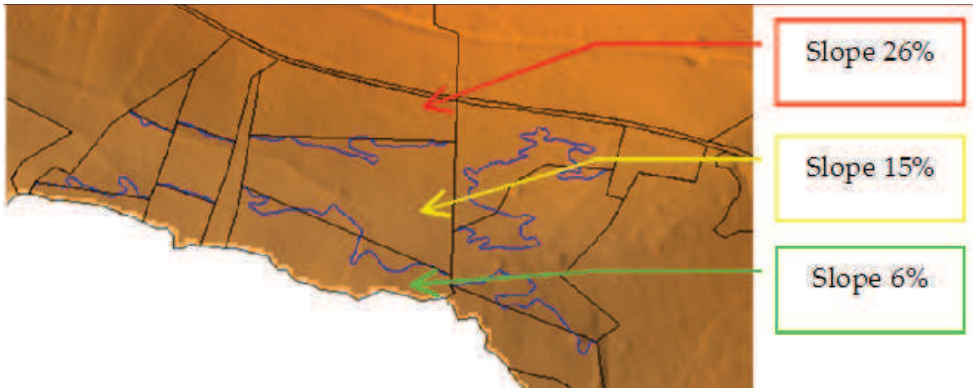

Figure 6.3.7.: Slope segmentation in the Mercier catchment. The blue lines are obtained with the Snakes algorithm and the black lines with the Douglas Peucker and Snakes algorithms (Sanzana, 2011).

Numerical corrections

In order to run PUMMA on the model mesh a couple of numerical corrections are still necessary. First of all, polygons, located inside other polygons (so called islands) have to be corrected. In PUMMA, one implementation of a module is applied to each polygon. Hence, we would have a module implementation which is inside another module implementation, which is not possible. Therefore, Sanzana (2011) wrote the script *polygons_holes.py*, which divides polygons with holes. The script calculates the nearest distance from all vertexes of the island polygon to the boundary of the surrounding polygon. Then, the largest and smallest distance are chosen for the division of the surrounding polygon, see Figure 6.3.8.

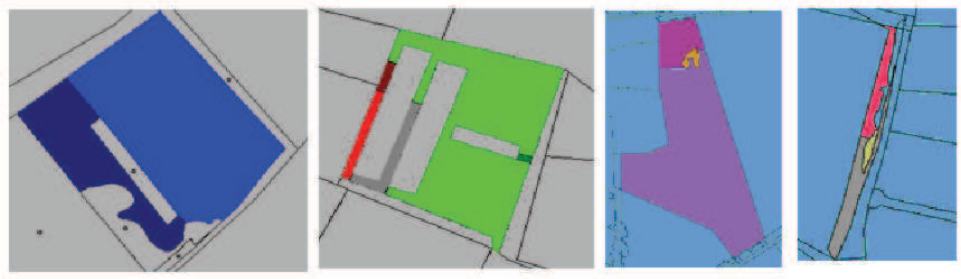

Figure 6.3.8.: Intersection of polygons with holes with the largest and smallest distance to the outside polygon boundary (Sanzana, 2011). These are example polygons of the Chaudanne catchment.

The distance between the centroids of the polygons is used for the calculation of the subsurface and overland flow. This distance should thus be representative of the average distance between the polygons, which is the case for convex polygons. However, for concave or weird-shaped polygons the centroid can be located outside of the polygon or

close to the boundary, which corrupts the use of the distance as parameter, see Figure 6.3.9.

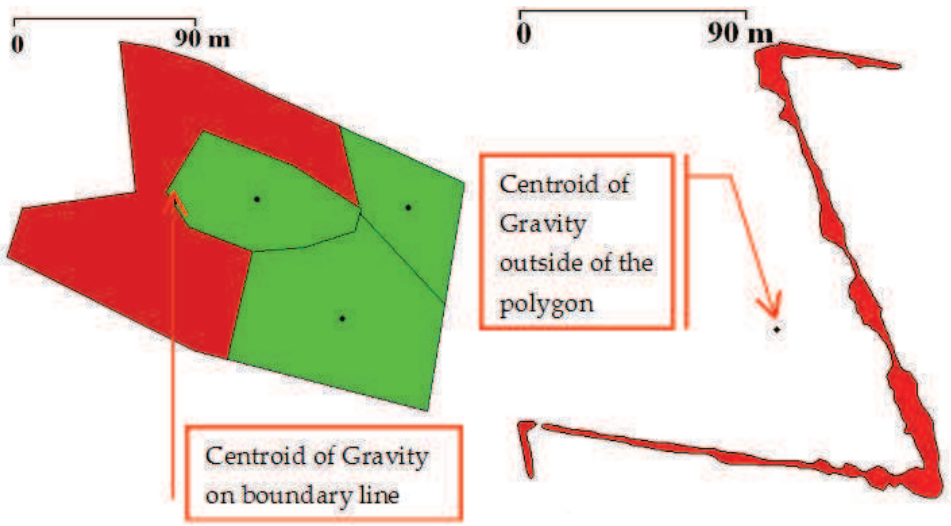

Figure 6.3.9.: Concave, weird-shaped polygons having their centroid outside of the polygon boundary (Sanzana, 2011).

For this reason, we decided to correct concave polygons. An easy way to create convex polygons is a triangulation between all vertexes of the polygon boundaries. However, this would create a high number of long-drawn polygons with relatively small size and we would loose the object oriented character of the model mesh. Sanzana (2011) created thus an automatic solution to subdivide those polygons into irregular convex polygons. For this, it is at first necessary to determine a criterion for the selection of the polygons, which we want to correct. The script *shape_factors.py* (Sanzana, 2011) calculates the following criteria:

- Solidity ($Area/ConvexArea$)
- Convexity ($ConvexPerim/Perim$)
- Compactness ($Perim/(2 * (\pi * Area)^{0.5}$)
- Form Factor($4 * \pi * Area/Perim^{0.5}$)

where ConvexArea or ConvexPerim are the area or perimeter of a convex polygon with the same size as the concave polygon. Based on visual analysis of these form factors, we decided to use the convexity index as criterion. A threshold value of 0.75 was chosen visually, which resulted in a total number of 22 polygons to correct in the Mercier and 47 in the Chaudanne catchment. These polygons are then extracted and exported with a R script to the poly format needed for the application of a C++ triangle algorithm (Shewchuck, 1996). Sanzana (2011) chose this algorithm in favor of e.g. a delaunay triangulation available in GRASS, as it creates larger and less long-drawn polygons. The triangulated polygons are then reimported to GRASS using another R script. In the next step, the triangles are dissolved with the script *convextiy_segmentation.py* (Sanzana, 2011) starting from the biggest polygon, see Figure 6.3.10. The polygons are only dissolved if the convexity index stays below a certain threshold value. Depending on the threshold value

the result can be different. In some cases, it can be useful to apply the dissolving script twice, first with a smaller threshold (e.g. 0.88) and then with a higher threshold (e.g. 0.95). The segmented polygons have then to be intersected with the HRU map. It is possible that this step introduces topological problems. So it might be necessary to rerun the *clean_ ogr script*. Depending on the number of vertexes on the polygon boundaries,

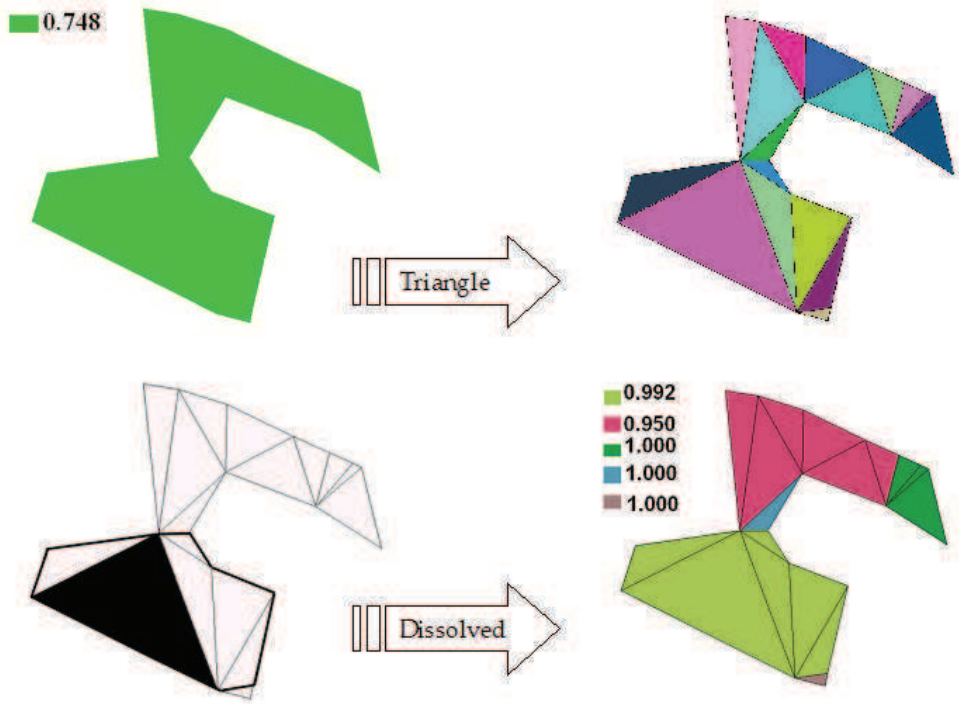

Figure 6.3.10.: The convexity segmentation process for a polygon of the Mercier catchment using a convexity index of 0.95 (Sanzana, 2011).

this algorithm can take quite some time to run. During the triangulation, triangles are built starting from all vertexes. The correction of the Mercier polygons needed thus only a couple of hours, whereas the correction of the Chaudanne polygons required several days even with parallel processing. This was caused by the high number of vertexes of the vegetation layer, which was obtained from raster data. Consequently, it would be better to reduce the number of the vertexes prior to running this algorithm.

In the PUMMA model, lateral flows (subsurface and overland flow) are transferred from one polygon to the next by means of sink and sources terms. The discharge entering a model unit in m^3s^{-1}, is divided by the polygon surface, as the module internal calculations are made in ms^{-1}. If water flows from a large polygon to a small polygon the impact on the water level will be higher. In order to prevent unnatural high water levels (ponding or groundwater table) caused by these numerical issues, the polygons should have a relatively comparable size. Therefore, we decided to reduce the difference in polygon size by dividing the polygons which area exceeds a certain threshold value. Sanzana (2011) developed thus the script *area_ segmentation.py*, which uses the same principle as the convexity segmentation script, except that the area is taken as criteria for the polygon selection and merging. The maximal size of the polygons in the Mercier catchment was thus reduced from 192 144 m^2 to 46 055 m^2. However, as the smallest polygons are about 10 m^2, the difference in polygon size is still large.

Attribution of HRUs and UHEs to modules
A SQL query assigns the module type to each model unit. The land use classes of UMR 5600 (Chapter 3.1.4, Jacqueminet et al. (2011)) are taken as criteria. Water bodies having the code 403 are modeled with SISTBA and urban objects with a code greater than 600 with URBS. It was intended to model roads (502, 513) with FRER1D, but for the moment they are modeled with URBS. FRER1D was also supposed to model agricultural objects (values starting from 200) and forests (values starting from 100) and HEDGE only hedgerows (151). However, as FRER1D is not yet integrated into the model, it was replaced by HEDGE.

Preparation of drainage network
The drainage network of the Chaudanne catchment consists of the combined sewer system, the rainwater pipes, the ditches and the natural stream network. Like Rodriguez (1999) we consider that the water follows the street network until the water is intercepted in the sewer system. Therefore, in urban areas far from sewer pipes, the drainage network was extended with the middle street line. The union of all different networks was done with SQL queries. However, some manual corrections were necessary to obtain a topologically clean network.

There are two options for the discretization of the drainage network. Either the drainage network is divided at each polygon intersection creating a large number of river reaches, or the river reaches are only separated for reaches with different attributes and at network intersections. During the topological correction of the ditch network, the complete drainage network was composed of polygon boundaries, providing a GIS layer for the first solution. This resulted in 1777 drainage reaches with lengths varying between 0.11 m and 478 m for the Chaudanne catchment. The script *m.disline* of Lagacherie et al. (2010) can be used to unify short reaches depending on a minimal length, while keeping the reaches separated at intersections.

For the calculation of the flow routing, the topology of the river network has to be cleaned, which means that each node has to correspond to the node of the adjacent river reach. Even if attention was paid to the topology, errors are always possible, which have to be located and corrected manually. Due to the reduced number of river reaches and thus less manual correction, we chose to apply the second option. For this, Sanzana (2011) developed the script *re_build_ditch_segments.py*, which unifies all reaches with the same attribute value. We obtained thus 521 drainage reaches for the Chaudanne catchment with lengths between 1.8 and 550 m.

6.3.2.3. Calculation of geometrical parameters

The PUMMA model requires several geometrical input parameters, such as average altitudes for each polygon and drainage reach as well as the slope for each drainage reach. Furthermore, special parameters are necessary for the URBS module.

Mean altitude and slope
GRASS provides the v.rast.stats function which enables the calculation of average altitudes for each polygon based on a DEM. However, the function works only for polygons which are greater than the raster resolution. To calculate the missing altitudes, Sanzana

(2011) developed the script *fill_polygons_nulls.py*, which extracts the altitudes for each polygon centroid from the DEM. Both functions can also be applied to other rasters, such as a slope grid. Sanzana (2011)'s script *river_h_s.py* calculates the mean altitude and slope for each river reach. The script extracts the altitude information at the nodes of the drainage reaches from a DEM. The altitude is calculated as a mean of both values. For the calculation of the slope, the difference in altitude is divided by the length of the river reach.

URBS parameters
As input parameters the URBS model needs the area of the built, road and natural part as well as the percentage of each part covered by trees. Furthermore, a representative length of the cadastral parcel is used for the calculation of the infiltration into the sewer pipes. The built surface of a cadastral parcel can be composed of several polygons (buildings). In order to calculate the surface per UHE, the buildings have to be associated to the correct UHEs, which can be done with the script *bati.py* (Paillé, 2010). The sum of the areas is then calculated in PostgreSQL with a SQL query using the "group by" function. The road area is calculated based on the *trottoir* layer created by means of the trottoir script (refer to the paragraph "UHE creation" in section 6.3.2.2) . The natural area results from the UHE surface minus the built and road surface.

Instead of calculating the length parameter as distance from the farthest point to the road like Rodriguez (1999), the *length.py* script of Paillé (2010) calculates the length as distance from the GRASS UHE centroid to the middle line of the street and doubles it. The length for UHEs which are not road sided is the doubled distance from the centroid to the closest polygon boundary.

The tree covered percentages per land use type (either built, road or natural area) can be calculated with the script *surfaces_boisees.py* developed by Paillé (2010). The script takes a raster with the tree cover as input as well as the vector file of the extracted land use type. The natural area has thus to be created beforehand by geometrical subtraction of built and road area from the UHEs.

6.3.2.4. Hydrological routing

Drainage network
The RIVER1D module requires a certain structure for the drainage network, in order to be able to find the upstream river reaches and ensure thus the flow routing. The line direction of the drainage network reaches has to be from downstream to upstream, and the outlet reach needs to have the lowest identifier. The river reach identifiers have to increase from downstream to upstream, see Figure 5.1.2. Sanzana (2011) developed the script *river_direction.py* which flips all lines with wrong direction. The script calculates the distance from each node to the outlet and evaluates the difference between the start and end node distances for each drainage segment. All segments with a positive difference are flipped. Brossard (2011) developed the script *numRiver.py*, which assigns the correct numbering to the drainage reaches. The program uses a recursive function, which scans through the drainage network and determines connected reaches by means of the *touches* PostGIS function. The script works only properly if the topology of the river network is as clean as possible. However, even if there are errors in the topology, the script can be used to locate the errors, as the correct numbering stops when it encounters an error.

Overland flow (OLAF)

For the OLAF module the overland flow paths have to be determined. The objective is to obtain a routing of runoff from model unit (HRU or UHE) to model unit following the topography until the drainage network is reached. We chose to work per sub-basin for the determination of the overland flow paths. In each sub-basin, the overland flow path from each polygon towards the drainage network is determined based on topography using the script *interfOlaf.py* developed by Brossard (2011). The script uses a recursive function and PostgreSQL queries. We decided to develop a simple and robust algorithm. Therefore, a single flow direction algorithm was chosen, where each parcel is connected to its lowest neighbor. At first, the algorithm connects all parcels adjacent to the river network to the river network and it connects isolated parcels having only one neighbor to this, see Figure 6.3.11. Then, each remaining parcel is temporarily connected to its lowest neighbor until an outlet towards the river is found for the drainage branch. If no outlet is found, the algorithm tries to find another flow path until all parcels are connected. The approach per sub-basins integrates already some topographical information, which excludes the possibility that the downhill parcels of hill parallel ditches can be connected to this against topography. Therefore, the hypothesis that all parcels adjacent to a drainage reach are directly connected to this seems physically correct.

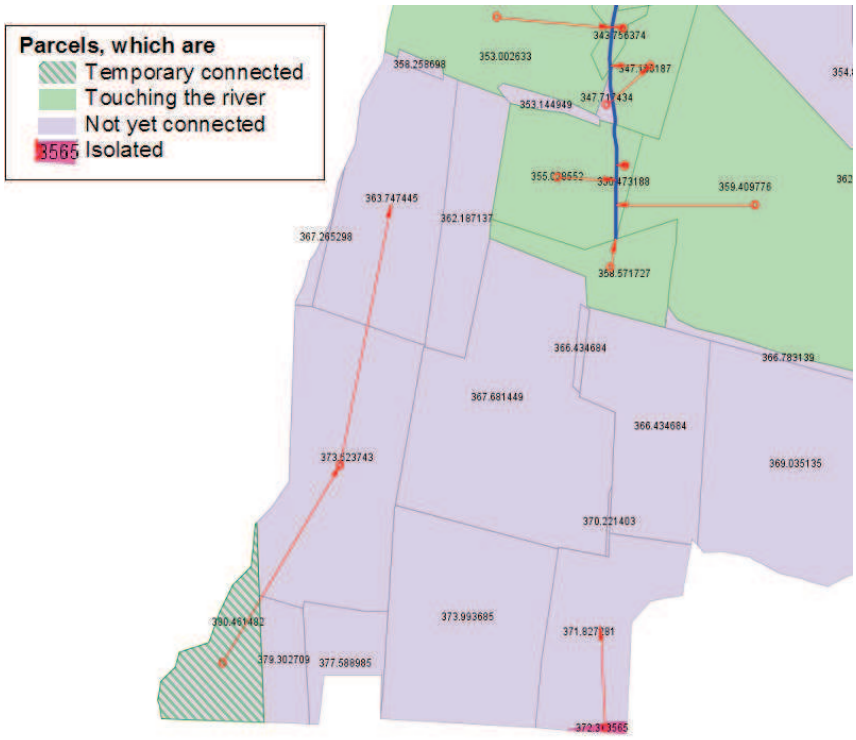

Figure 6.3.11.: Determination of overland flow paths. First, the isolated parcels and those touching the river are connected, then the others are temporary connected until an outlet is found (Brossard, 2011).

In the Chaudanne Léchère catchment, overland flow paths were only determined inside the topographic catchment border. This was justified by the fact, that outside the topographic catchment border the overland flow follows the topography towards another drainage system.

Concerning the UHEs of the URBS module, we assumed that only the natural surface

runoff follows the overland flow paths determined with the interfOlaf script. The built and road surface runoff, as well as the network infiltration were connected with the conUhe script, explained in the subsequent section.

Routing of UHEs
In urban areas, the water is drained by pipe systems for which topography plays a minor role. However, pumping water against topography is also expensive. Therefore, we decided to connect UHEs to the closest or lowest drainage network reach in our model (as Rodriguez (1999)), independently from the sub-basins. The script *conUhe.py* (Brossard, 2011) determines the connections of the UHEs to the drainage network. Like the interfOlaf script, this script is based on a recursive function and PostgreSQL queries. All UHEs adjacent to a drainage network reach are directly connected to this one. Isolated UHEs are connected to the closest natural or artificial drainage reach and for all other UHEs a similar algorithm as for OLAF searches for the lowest neighbor UHE until the drainage network is reached. The connection is then directly made between the UHE and the river reach, without taking into account intermediate UHEs. This could be improved in a further version of the preprocessing by connecting rural UHEs with the OLAF algorithm to either HRUs, UHEs or drainage reaches.

The script works only for drainage networks without parallel network parts. Therefore, a manual choice of the appropriate drainage network was made based on the information gathered during the determination of the urban sub-basins.

Subsurface flow (WTI/WTRI)
For the exchange between parcels the WTI interface is applied, whereas the WTRI interfaces calculate the exchange with the river network and water bodies (lakes or retention basins), refer to Chapter 5. The subsurface flow exchange can be multi-directional. Each model unit can exchange water with all of its neighbors. The topography is of minor influence, as the flow direction depends on the difference in hydraulic head. The calculated flow depends on the wetted section, for which the length of the interface is necessary. Consequently, we have to create the geometries for the interfaces, defined as the intersection (line) between two polygons or one polygon and the river network (see Figure 5.1.3 in Chapter 5). Furthermore, we need to extract the ids of the neighboring polygons or river reach.

Brossard (2011) developed the script *all_wti.py* for the extraction of the WTI interfaces and the WTRI interfaces between parcel and lake or retention basins. These interfaces are polygon intersections, which can be extracted thanks to polygon topology in GRASS. The script *all_wti* extracts thus all polygon boundaries and neighborhood relations based on GRASS functions. It deletes also the exterior boundaries having only one neighbor.

The obtaining of WTRI boundaries, for which line - polygon relations are necessary, is more complicated. They are extracted with SQL queries using the same principle as the reconstruction of the river network out of boundaries (see Figure 6.3.4). The buffer around the centroids of the boundaries is intersected with the polygon and the river map in order to obtain the neighborhood relations between river and parcel. The WTRI interfaces with lakes and retention basins are then added to the WTRI interface table.

One WTI or WTRI interface can be composed of several boundaries, as not all polygons are convex. Therefore, the boundaries with the same neighbors are unified to a multi-line.

Then, a set of filters is applied to all WTI and WTRI interfaces. The interfaces which

are smaller than a threshold length, here 5 m, are deleted in order to save computing time. Additionally, we chose to delete the WTRI interfaces where the bottom of the river reaches is made of concrete as groundwater exchange with the river network can only happen, if the river bottom is permeable. WTRIs are replaced by WTIs at these places to account for groundwater exchange between parcels. This allows to have exchange of subsurface flow between two parcels below a concreted ditch. Similarly, for the permeable drainage reaches the WTI are deleted and the WTRI kept. As the URBS module already calculates the network infiltration, we decided to delete all WTRI interfaces with URBS model units.

The WTRI and WTI interfaces are then assigned to the right module instance, e.g. hedge2hedge, urbs2urbs, hedge2river, hedge2sistba, etc (refer to Chapter 4).

6.3.3. Results for the Chaudanne and Mercier catchments

The described preprocessing method allowed us to obtain the model mesh, the geographic parameters and the different connections necessary for the hydrological routing for the Mercier and Chaudanne catchments.

Figures 6.3.12 and 6.3.13 show the final model meshes obtained for the Mercier and Chaudanne catchments. Due to a larger urban area, the Chaudanne catchment has much more URBS implementations than the Mercier catchment. Both catchments have five lakes, however the Chaudanne catchment has additionally six retention basins. There are six TDSO in the Chaudanne catchment and only one TDSO in the Mercier basin, which represents a natural divergence. Despite the numerical corrections, the model unit areas vary still between 2 and nearly 50 000 m^2 for the Chaudanne catchment.

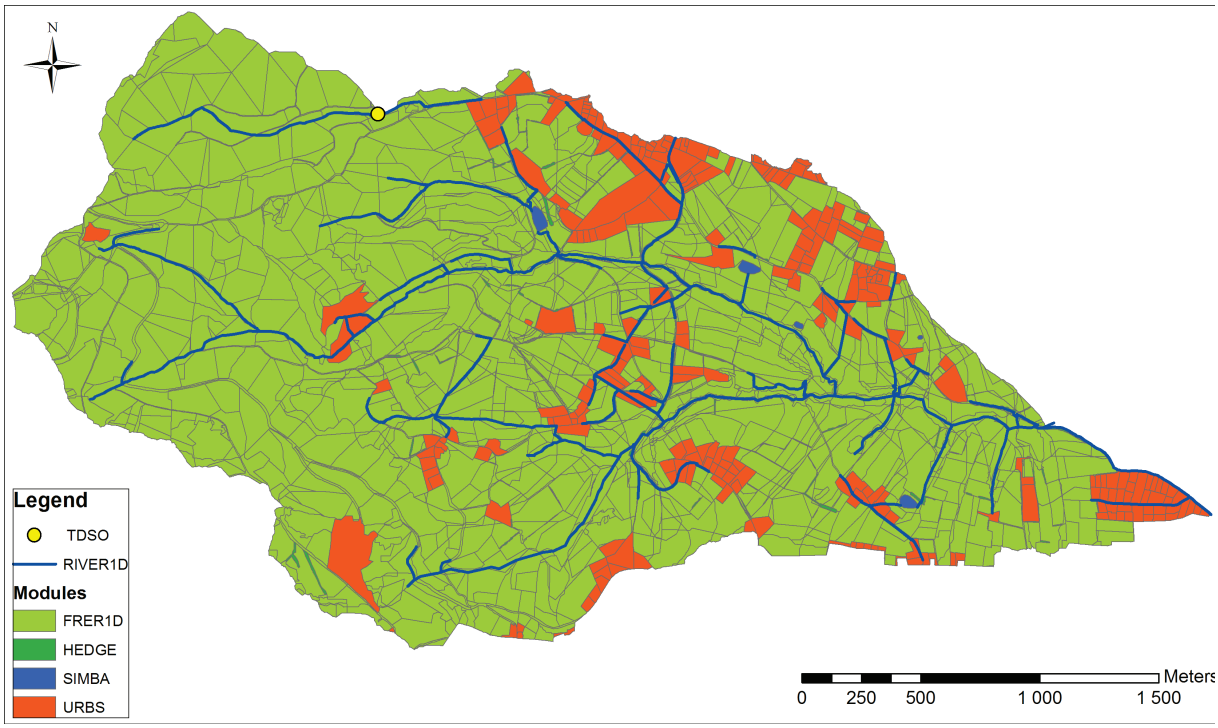

Figure 6.3.12.: Final model mesh of Mercier catchment with module attribution.

Figures 6.3.14 and 6.3.15 show the overland flow paths (OLAF module) obtained for both catchments. It was possible to determine the flow path for each parcel. We can see

Figure 6.3.13.: Final model mesh of Chaudanne catchment with module attribution.

the urban influence in the lower Chaudanne catchment, as the drainage pipes intercept the overland flow. The overland flow paths were only determined for the topographic catchment border. The natural surface runoff from urban parcels outside the topographic catchment border is thus lost to the water balance of the study catchment. This approach tries to take into account the ditches leading outside the study catchment (see article in 6.2.1). Figure 6.3.16 shows the influence of the numerical correction of the model mesh

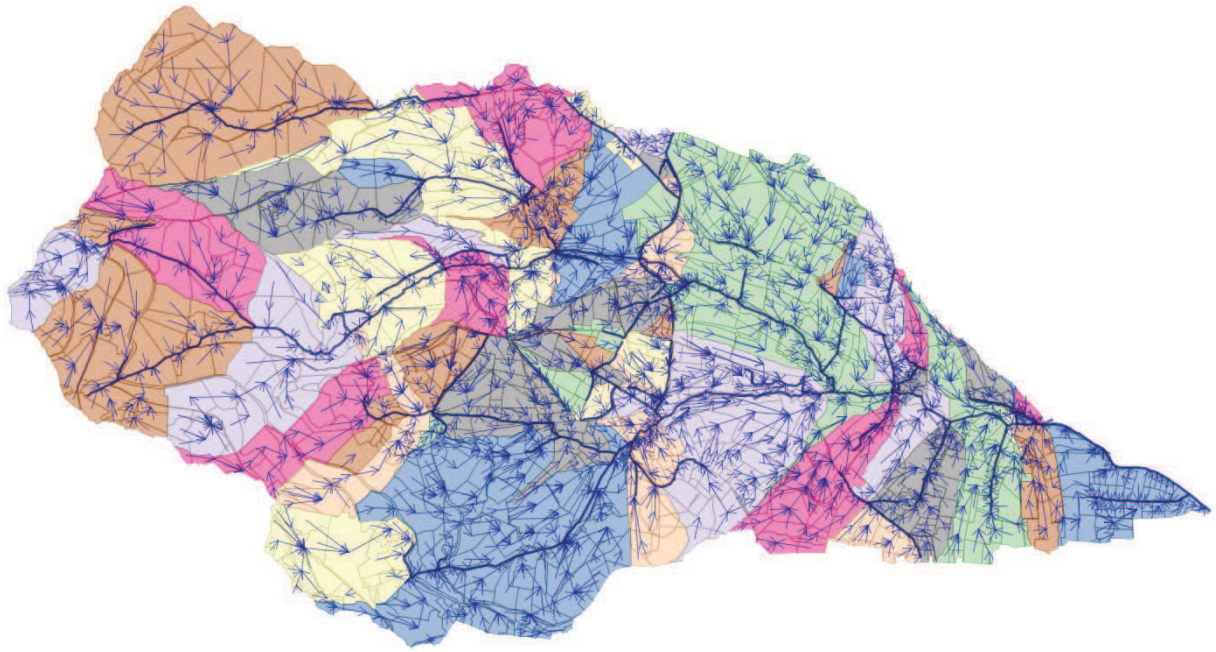

Figure 6.3.14.: Overland flow paths and sub-basins (colored) of Mercier catchment. The arrows indicate the flow direction. Results of script InterfOlaf.

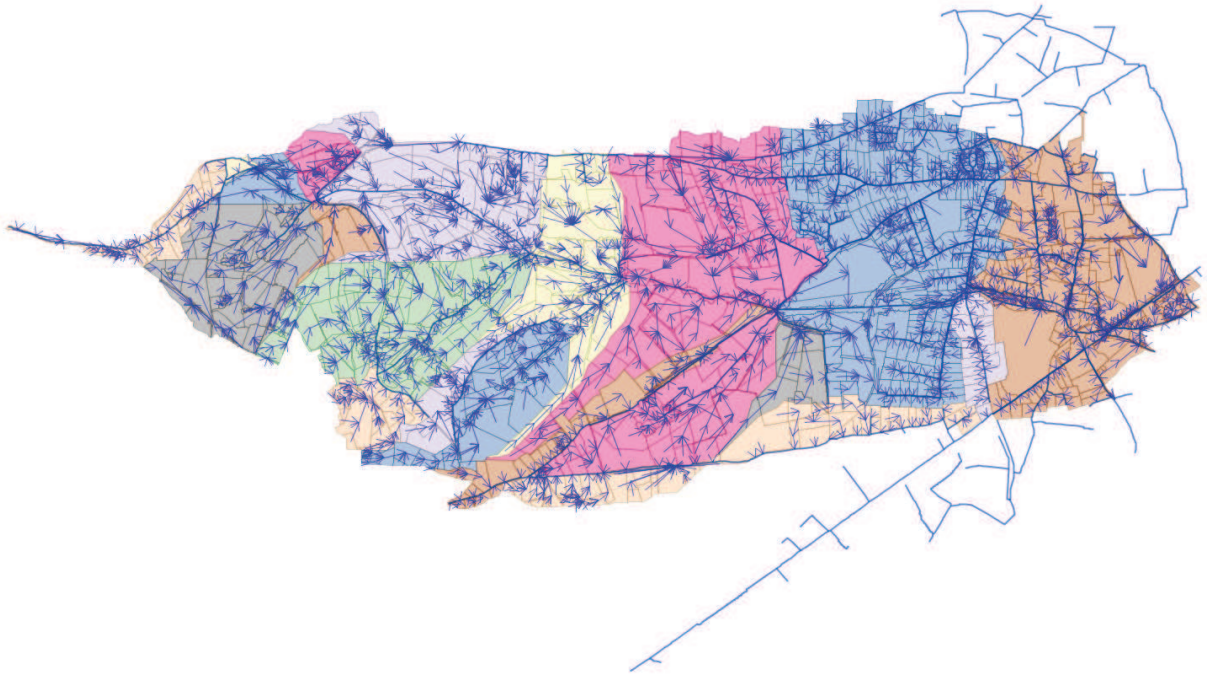

Figure 6.3.15.: Overland flow paths and sub-basins (colored) of Chaudanne catchment. The arrows indicate the flow direction. The overland flow was determined only for the area inside the topographic catchment border. Results of script InterfOlaf.

on the calculated overland flow paths. The extract is from the upper part of the Mercier catchment. The uncorrected map (left) contains a large concave polygon, which centroid lies outside the polygon border. This produces an overland flow path which crosses the river for one polygon. In contrast, the numerical corrections (left) allowed to obtain a dendritic drainage network.

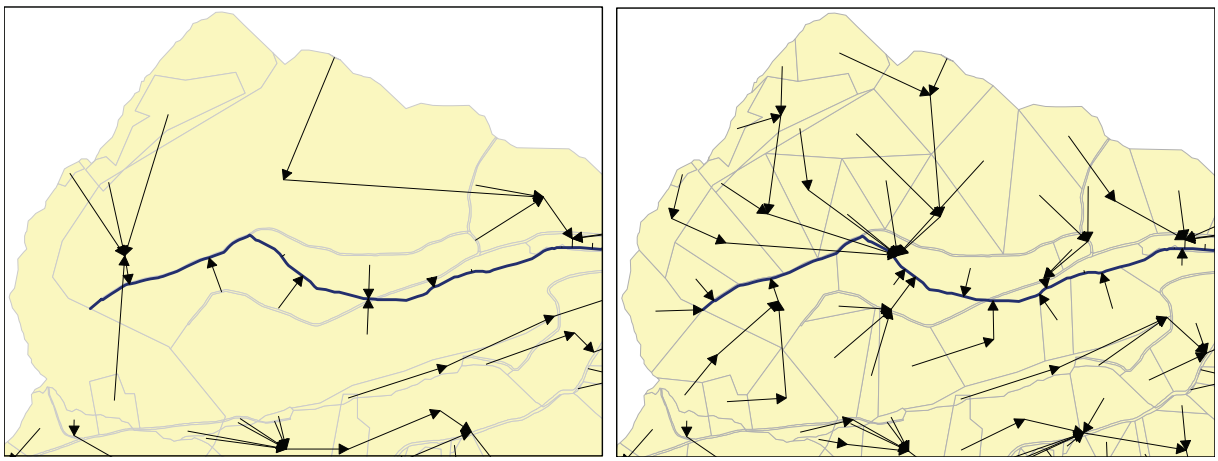

Figure 6.3.16.: Comparison of overland flow paths for the numerically uncorrected map (left) and the corrected map (right) in the Mercier catchment. The overland flow path is calculated from polygon center to polygon center.

Figures 6.3.17 and 6.3.18 show the connections of the URBS model units to the drainage network. The presented results of the Mercier catchment are per river reach, whereas they are per river id in the Chaudanne catchment. This assures a better visibility for the Chaudanne catchment, as the river reaches in the urban part are relatively short.

The roads are also connected to the closest or lowest drainage network, because they are modeled with URBS here. Figure 6.3.18 also shows the connections to the different

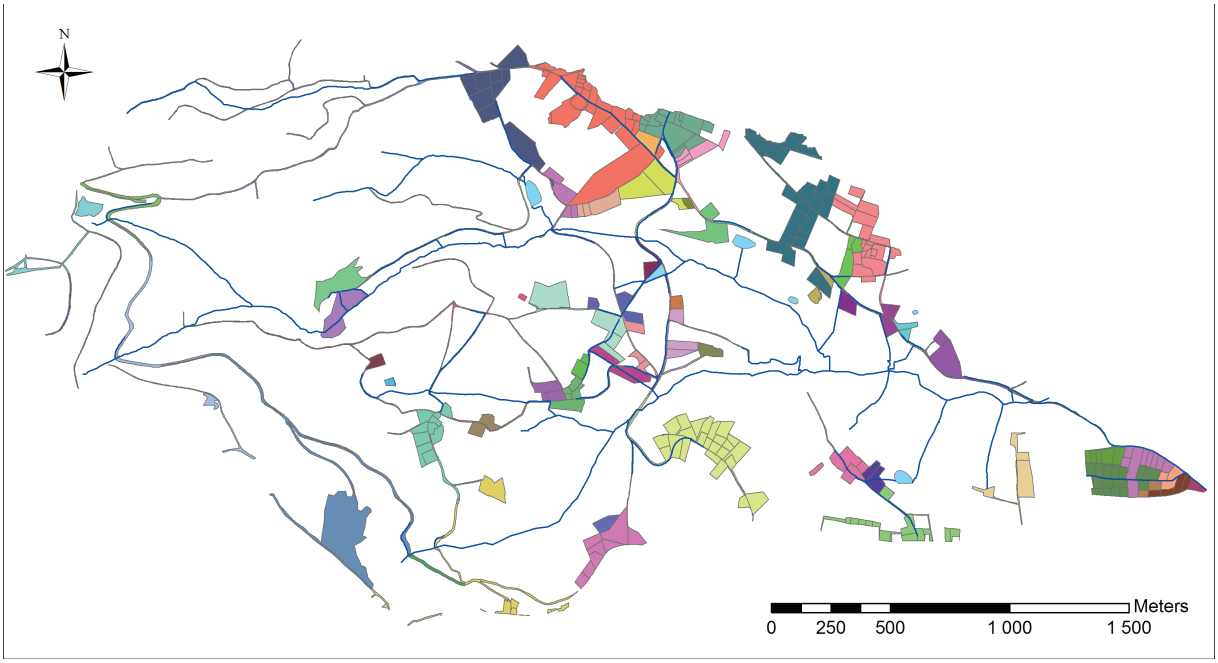

Figure 6.3.17.: UHE connections in Mercier catchment. The different colors indicate different drainage reaches. Results of script conUHE.

drainage networks. The pink sub-basin is the contributive area to the three retention basins at PdB, whereas only the dark blue parcels are connected to the SOD at PdB. The largest sub-basin is the sub-basin connected to the SOD at La Léchère, which intercepts the whole area outside the topographic catchment border. The red parcels are directly connected to the natural river by separated sewer systems. In the upper part of the Chaudanne basin all parcels (green parcels in Figure 6.3.18) are connected to the roadside ditch in the north. However, for the green parcels south this is a wrong representation of the observed flow paths, as the distance to the connected ditch is too far and sometimes against topography. It might thus be better to process the cadastral parcels which are far from a drainage network differently.

The WTI/WTRI interfaces for the Mercier and Chaudanne catchments are presented in Figures 6.3.19 and 6.3.20. For the Mercier catchment only the interfaces for the numerically uncorrected model mesh is shown, as the interfaces for the corrected map have still to be determined. Altogether the Chaudanne catchment has more than 6000 WTI interfaces and about 600 WTRI interfaces.

6.4. Discussion

The discussion in the following section addresses mainly the developed preprocessing method. A detailed discussion of the sub-basin delineation method was done in the article in section 6.2.1. Several subjects are discussed such as the definition of area thresholds, or the choice of criteria for the model adaptation, as well as different points concerning the routing and transfer preprocessing and topological constraints. The last point takes drawbacks from the segmentation process used for the HRU creation and proposes a new

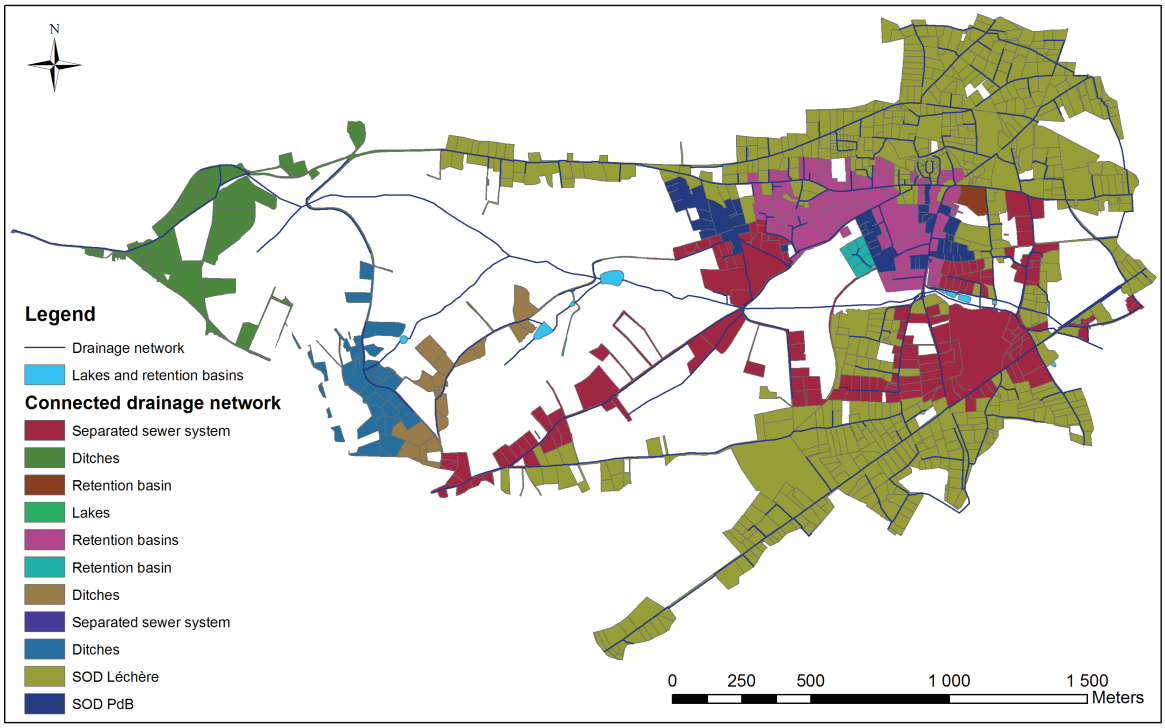

Figure 6.3.18.: UHE connections in the Chaudanne catchment. The different colors indicate different river instances, which can be mainly ditches, separated sewer systems, SODs, lakes or retention basins. Results of script conUHE.

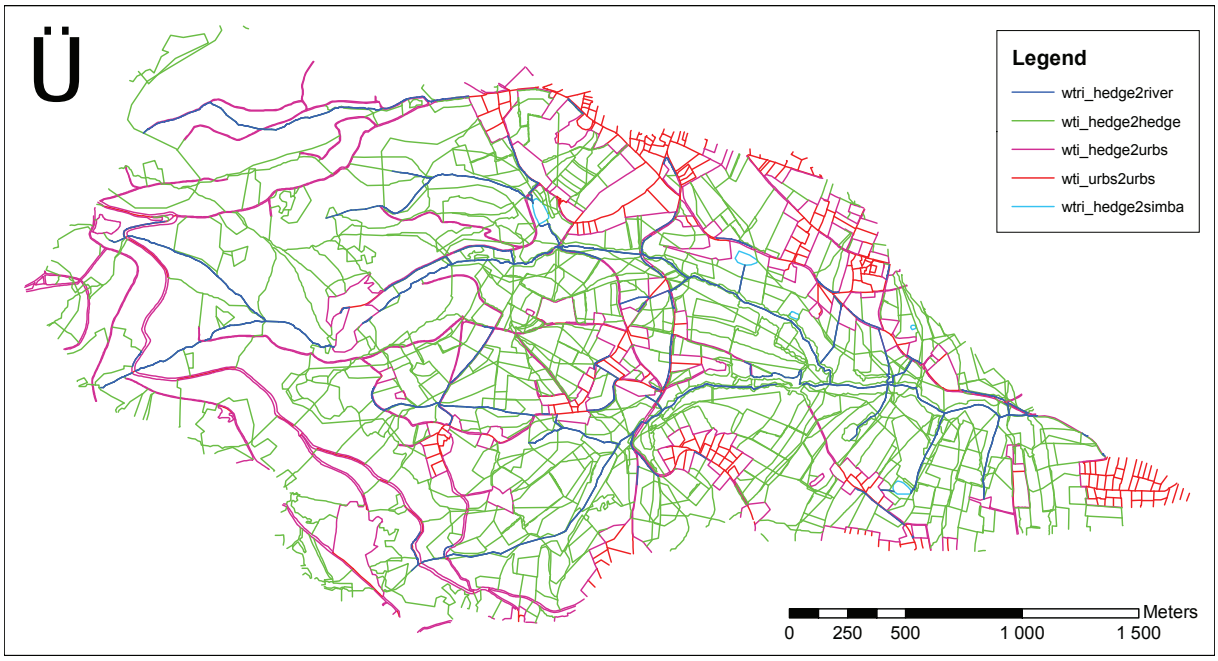

Figure 6.3.19.: WTI and WTRI interfaces of Mercier basin with their assignment to the module type.

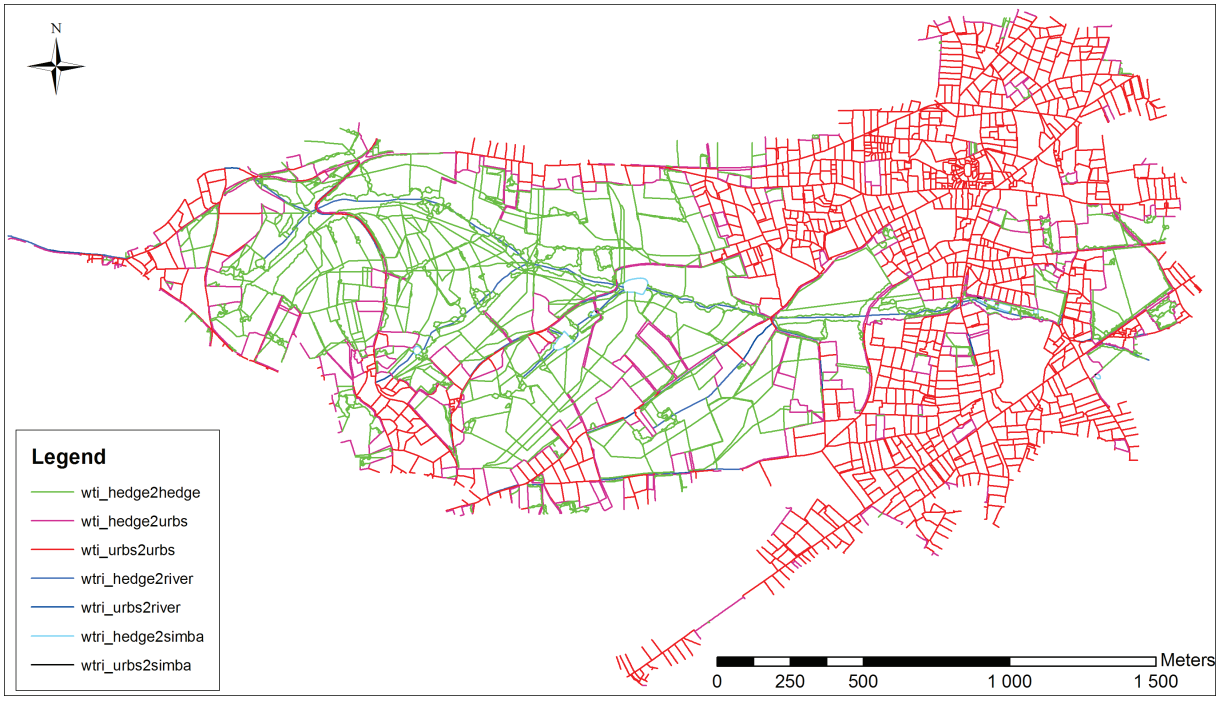

Figure 6.3.20.: WTI and WTRI interfaces of Chaudanne basin with their assignment to the module type.

method based on database concepts.

Definition of area thresholds
For the model mesh of PUMMA, which is specific for peri-urban areas, we decided to take an object oriented approach. The challenge was thus to represent rural and urban objects in the same model mesh. As urban objects we chose to take UHEs, which are based on the land register (Rodriguez et al., 2003). This approach has the advantage that cadastral maps are widely available. Furthermore, it facilitates the simulation of land use change, as urban development is based on the land register. However, the cadastral parcels can have different sizes, as supermarkets including parking places have a larger surface than single family houses with gardens. To this difference in size we have to add the rural objects. We decided to take HRUs, as the hydrological comportment inside the HRUs is supposed to be uniform (Flügel, 1995). It is mainly the land use information which influences the size of the model units. This results in large model units in the forested area, and smaller model units in the agricultural and rural zones. We also decided to keep hedgerows in order to take into account their influence on the hydrology of the agricultural areas. However, their size is much smaller than the size of the agricultural fields. Consequently, we are faced to rather heterogeneous model meshes, where the difference in model unit size can reach up to 2:200 000 m^2. Even, if we tried to adapt the model unit sizes, it would probably be adequate to reconsider the question "what is really the smallest object important for the hydrology of the catchment?". It would for example be possible to summarize small cadastral parcels representing the same type of development into larger areas. We should also assess whether the representation of hedges at the scale of the complete basin is really important.

Criteria for model mesh adaptation
We decided to take the convexity criteria for the correction of the polygons, though the application of the *InterfOlaf* algorithm showed that we should also have corrected the roads. In the original land use map, great parts of the roads were unified into one large polygon. This was cut during the intersection with the soil, sub-basin and geology layers. Despite this intersection many long polygons remained. The criteria for the overland flow routing is the average altitude of the polygons, though, the mean altitude of a long polygon is not very representative of the local altitude. The roads acted thus as barriers for the overland flow, which had to be corrected manually. Of the calculated shape factors the compactness factor is able to distinguish long polygons. The roads and other long polygons, such as the hedges could probably be corrected by taking the compactness factor as criterion in the convexity segmentation script.

We included slope information into the model mesh. However, as the altitudes are the basis for the determination of flow exchange between model units, it would have been good if we had also taken into account the altitude. Instead of defining classes, the polygons in which the difference in altitude is too large, could be intersected with contour lines. This would probably also be another solution for the intersection of the roads.

The topographic index and aspect could be integrated into the model mesh as well, following the same methodology as the slope segmentation. However for the latter, the model should be able to calculate the energy balance and potential evapotranspiration, which is not the case in the current version.

Overland flow routing with sinks in the model mesh
The InterfOlaf algorithm was designed to be able to connect all polygons, even if polygons are sinks, which means that their altitude is lower than the altitude of all surrounding polygons. However, the calculation of overland flow which is done inside the OLAF module is the same for all polygons (sinks or not sinks) and uses the real altitudes for slope calculation (see Chapter 5.2.3). This created problems of overland flow water accumulation in the sink polygons, which had theoretical outlets according to the InterfOlaf algorithm but no real outlets according to the OLAF calculations. This could be solved by adapting manually the altitude of the sink polygons. As a lesson learned from this experience, it would be better to add an algorithm which rises the altitude of sink polygons to the altitude of neighboring parcels, while searching for the overland flow path, similarly to the fill sink procedures used for raster DEMs. It would probably also be physically more consistent with the OLAF calculation to take the steepest slope as criterion instead of the lowest adjacent polygon or river reach in the InterfOlaf algorithm.

Integration of parallel networks to preprocessing
At the moment, the conUHE and interfOlaf algorithms need a unique drainage network, which implies a manual choice of the network to be processed. It would probably be possible to think about an algorithm which allows parallel drainage networks. For this, clear rules would have to be defined, indicating in which cases which drainage network has to be preferred. Perhaps an integration of the urban sub-basins determined in section 6.2.1 could facilitate this task.

Processing of UHEs
In order to keep the object oriented character, we decided not to cut UHEs neither during

the numerical corrections nor by intersection with the sub-basin map or drainage network. This caused several problems in particular for the reconstitution of the drainage network with the polygon boundaries. In some UHEs, no boundaries were close enough to the drainage network to be selected as new drainage reaches. This lead to only partly reconstituted drainage networks. We had thus to add afterwards the lost drainage reaches.

Furthermore, problems occurred for large polygons, which were sometimes located in two sub-basins. For the routing of the surface runoff these UHEs had to be assigned to only one sub-basin. This created hydrological barriers in the other sub-basins, which had to be corrected manually. Consequently, it would probably be better to subdivide larger UHEs, especially in the rural part. This would mean to process UHEs in the rural part differently.

A different processing would also be appropriate for the connection of these rural UHEs to the drainage network, because the connection to the closest drainage network is not always physically representative. The subsurface flow of these rural UHEs should thus only be modeled by WTI and WTRI and the network link coefficient set to zero. In this case, it would be necessary to classify the built-up cadastral parcels in urban cadastral parcels and rural parcels at the beginning of the preprocessing.

Segmentation of river reach
For topological and computation time reasons, we decided to segment the drainage network quite coarsely, only if the attributes of the reach were different and at the intersections. However, same as for long polygons, the mean altitude for a long river reach is not always representative of the local altitude, which can cause problems for the lateral flow routing through WRTI interfaces. In some cases, the river was actually drained by some of the surrounding polygons because of non representative altitudes, creating problems similar as those encountered with the sink polygons. We had to correctthe altitudes of many river reaches manually by lowering them below the height of the lowest neighboring polygon. It would be possible to calculate the real altitudes of the WTRIs but the solution should be robust enough to handle multiline geometries. An automatic solution would be to calculate the altitudes of WTRIs before unifying them to multi-geometries and to calculate then the length weighted average of the altitude for the multi-lines. Another possibility would be to take the segmented river reach for the river geometries.

Topological constraints: vector versus raster model mesh
The strong topological constraints were mainly caused by the WTRI and WTI interfaces. Especially the extraction of the WTRI interfaces and their neighbor identification requires a perfect topology between polygons and lines. However, a perfect topology does not exist, neither technical solutions to solve this problem. Furthermore, most GIS provide only functions for each type (polygon or line) at a time, and there are not many functions were both types can be related. Therefore, another approach should be developed for the representation and delineation of these interfaces to avoid the topological problems that could be solved only partially here.

The question is also whether a vector based model mesh, which brings the topological constraints along, has really an advantage before a raster based model mesh? A vector based model mesh has the advantage of being object oriented, which means that houses, streets, gardens, agricultural fields or sewer pipes are regarded as separate objects

which can communicate with the surrounding objects. The communication can follow topographic rules, but also other rules. In a raster based model mesh, these objects are subject to the raster resolution. Consequently, depending on the resolution, a single object can be represented by several raster pixels, or even one raster pixel can cover several objects. In the second case, a choice of the pixel property gets necessary which changes the original information.

HRU delineation: from experience to a new method?
We started the development of these pre-processing tools inspired by the methodology of Lagacherie et al. (2010), in which HRUs are created by intersecting all layers at once at the beginning of the preprocessing. This leads to many small polygons, which have to be merged to neighboring polygons in an intelligent manner. For this, their object type (mostly land use type) has to be determined, and then the right neighboring polygon has to be selected for the union. In order to keep the object oriented character of the model mesh better and to circumvent these problems, a new methodology for HRU delineation (compared to the method presented in section 6.3.2.2) based on the acquired experience can be proposed. It takes advantage of the database concept and the SQL language, which allows to query and process each polygon differently. This methodology consists of four steps:

- Definition of one object layer and several property layers. A difference should be made between vector and raster based property layers. In our case the object layer corresponds to the land use map and the vector based property layers to the subbasin, soil and geology maps. The raster based properties are slope and altitude, but could also be aspect or the topographic index.

- Intersection of the object map with the vector based property maps, one by one. After each intersection, the resulting polygons are tested for their size using SQL queries. If they are smaller than the threshold size, the original polygon of the object map is kept and the attribute from the property layer with the higher surface percentage is assigned to it. No real intersection is made in this case.

- Integration of raster property layers. Once all vector based intersections are completed, the raster based informations are integrated into the map for the polygons for which the standard deviation of each property exceeds a certain threshold, as described for the slope segmentation in section 6.3.2.2.

- The final step is the correction of polygons to fulfill numeric constraints. Concave, long-drawn and too large polygons are corrected using the convexity segmentation script (section 6.3.2.2) based on the convexity and compactness index and the area correction script, always this respect of the size constraint. If the final size would be too small, no intersection is made.

The implementation of this method would be a valuable improvement for the preprocessing tools and could be used profitably for other models than PUMMA.

6.5. Conclusions

The PUMMA model mesh follows an object oriented, vector based approach consisting of HRUs in the rural part and UHEs in the urban part. For the preparation of this model mesh several preprocessing tasks were necessary, which were realized by means of GIS functionalities. A loose coupling was chosen for the link between PUMMA and GIS, which allows the use of the developed scripts for other models and which minimizes the programming effort. For the realization of the preprocessing, GRASS GIS was chosen for its topological functions and PostgreSQL because of its data base approach. A set of Python scripts was written for the preparation of the input data, the creation of the model mesh, the calculation of the geometrical parameters and the hydrological routing. The scripts are summarized in Tables 6.5.1 and tab:scripts2. The preprocessing method has the land use, land register, sub-basins, geology and soil vector polygon maps, the drainage network and street vector line maps and the raster DEM as input data. The drainage network and sub-basin map was obtained based on a method developed especially for peri-urban areas, which integrates field investigations. Different functions, as e.g. for the topological cleaning of these maps, were developed in order to adapt the data to the constraints necessary for the subsequent preprocessing tasks summarized in the following paragraph.

The model mesh creation task consists of the preparation of the UHE geometries and the intersection of different property layers for the HRUs. Additional information such as slope can be integrated. Furthermore, some of the scripts handle the numerical correction of the model mesh, such as the division of concave polygons and the reduction of the difference in polygon size. The geometrical and topographical parameters can be extracted automatically. As the water flow paths in urban areas are often different than in natural areas, different rules were applied for the hydrological routing. The urban parcels are connected to the closest drainage network, whereas the natural overland flow follows the topography. The sub-surface flow is multi-directional and depends thus on the neighborhood. The determination of the overland flow paths showed the importance of the numerical corrections. However, not all tasks could be automatized, leaving a couple of manual tasks to do. The preprocessing provided the model mesh of the Mercier and Chaudanne catchments and its geographical parameters necessary for modelling with PUMMA. The developed method is applicable to further catchments and some of the scripts can be useful for other models. Finally, the gained experience lead to the proposal of a new methodology concerning the HRU creation and perspectives for the further improvement of the method.

Table 6.5.1.: Summary of scripts developed for the preprocessing with indication if GRASS or PostgreSQL functions are used,if another script has to be run before and the reference to the Author.

Script	Description	GRASS	PostgreSQL	after	Author
Data preparation					
clean_ogr	topological cleaning without attributes	yes	no		Paillé (2010)
clean_ogr2	topological cleaning with attributes	yes	no		Paillé (2010)
RiverFrom-Boundary.sql	creates river out of polygon boundaries	no	yes	numRiver	Jankowfsky
Model mesh creation					
trottoir	divides road	yes	no		Paillé (2010)
uhe	creates uhe polygon	yes	no	trottoir	Paillé (2010)
slope_segmentation	divides polygons in slope classes	yes	no		Sanzana (2011)
shape_factors	calculates convexity index, compactness, form factor and solidity	yes	no		Sanzana (2011)
convexity_ segmentation	segments concave polygons	yes	no	shape_factor, R script	Sanzana (2011)
area_segmentation	segments too big polygons	yes	no	convexity segmentation, R script	Sanzana (2011)
polygons_holes	divides polygons with islands	yes	no		Sanzana (2011)
rebuild_ditch_ segments	merges lines with same attribute	yes	no		Sanzana (2011)

Table 6.5.2.: Continuation of summary of scripts developed for the preprocessing.

Script	Description	GRASS	PostgreSQL	after	Author
Geometrical parameters					
river_h_s	calculates mean altitude and slope per river reach	yes	no		Sanzana (2011)
fill_polygons_nulls	addition to v.rast.stats when polygons smaller than raster resolution	yes	no	v.rast.stats	Sanzana (2011)
length	calculates length of UHE	yes	no	uhe	Paillé (2010)
bati	calculates built area per UHE	yes	no		Paillé (2010)
surfaces_boisees	calculates tree covered percentage per land use	yes	no	uhe	Paillé (2010)
Hydrological routing					
river_direction	orientates all river reaches in upstream direction	yes	no		Sanzana (2011)
numRiver	numbering of drainage network	no	yes	river_direction	Brossard (2011)
interfOlaf	determination of overland flow path	no	yes	numRiver	Brossard (2011)
conUhe	connections of UHE to river	no	yes	numRiver	Brossard (2011)
all_wti	extraction of WTI interfaces	yes	yes	numRiver	Brossard (2011)

Part III.

Application

This part describes the application of the PUMMA model to the scale of a small catchment. This test of the model helped to identify some last errors in the modules and the LIQUID framework using a full set of real data. Furthermore, the calculation of the model had to be optimized in order to run several simulations in a reasonable time. The Chaudanne PdB catchment (see Figure 6.5.1) was chosen for this first application of the PUMMA model due to its peri-urban character and the available continuous discharge measurements in the natural river, the sewer system and the sewer overflow device. The model was tested progressively on this test case, as the interfaces were added gradually. The final runtime of the model could be optimized to two and a half hours per year of simulation on a personal computer. The simulations for the Chaudanne Léchère and Mercier catchments were also prepared. However, due to time limits, the model could not be applied to these two catchments. The next chapters describe thus the model setup and application for the Chaudanne Pont de la Barge catchment. The parameters presented in Chapter 7 were based on field data and literature values and were used as the default parameter set. The corresponding simulation results are described in detail in Chapter 8.1. This simulation was then taken as reference simulation for the analysis of several sensitivity and scenarios tests, which are also presented in Chapter 8.2.

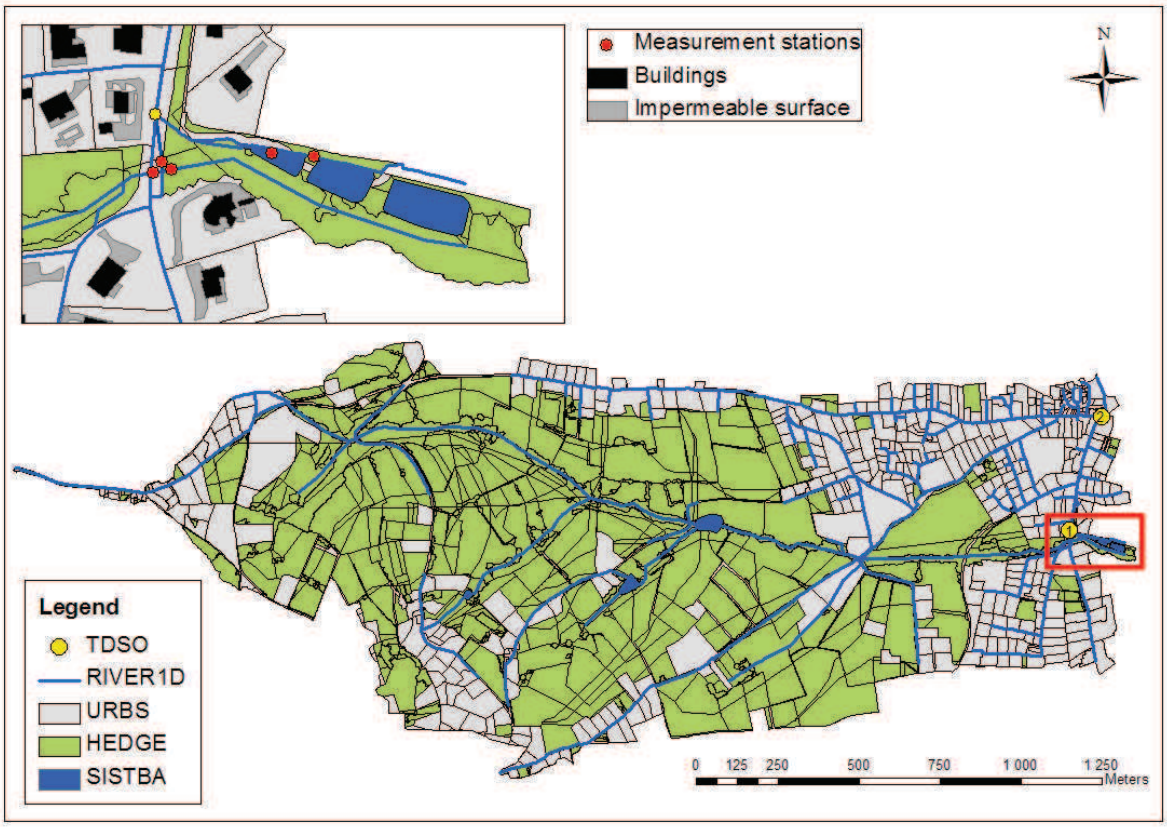

Figure 6.5.1.: The model mesh of the Chaudanne PdB catchment showing a zoom of the catchment outlet at PdB and the measurement stations.

7. Model setup

This chapter presents how the model parameters explained in chapter 5, were specified from the available information. We remind that the model was run a priori with parameters derived from field investigations and literature values and that no specific calibration was carried out. However, some of the parameters, such as the soil depth, the depth of the lakes or the retention parameters of the lakes had to be estimated based on field knowledge. The main parameters are the soil parameters, which are slightly different depending on the module, the URBS parameters specifying the connections to the network and the tree cover, the crop coefficients for HEDGE, the Manning roughness coefficients for RIVER1D and OLAF, the retention parameters for SISTBA and the overflow threshold for TDSO. First, the strategy for the choice of the climatic forcings and the simulation period is presented, then the calculation of the necessary soil parameters is described, which lead to the development of a soil database providing the soil parameters for different modules such as HEDGE, FRER1D or URBS. Subsequently, the parameterization of the reference simulation is presented for each of the PUMMA modules and at last the initial conditions are explained and a short conclusion is given.

7.1. Strategy for climatic forcings and simulation period

Continuous time series of precipitation data are available from 1997 for two measurement stations and from 2005 for three stations. The PET calculated with the SAFRAN data is available from 1970 to mid 2010. In Chapter 3 we have seen that the climatic conditions in the Chaudanne and Mercier catchment are very variable, with some dryer and wetter years. In order to test the model capacity to simulate dry and wet conditions, we chose to simulate two contrasting years. Further criteria for the choice of the simulation period were the data quality and changes in the sewer system of the Chaudanne catchment, which would have caused a change of the RIVER1D network. We selected thus the years 2008 and 2009 as simulation period. 2008 was relatively wet with about 965 mm of rainfall and 2009 was a dry year with 578 mm of rainfall in the Chaudanne catchment (refer to Table 3.2.2 in Chapter 3). As initialization period, it was decided to start the simulation one year prior to the evaluation period. The simulation was thus run continuously for a three year period, including 2007 as initialization period. The rain data were regionalized with Thiessen polygons, as these polygons correspond well to the altitude distribution, they are considered sufficient for the regionalization of the rain data. The PET was taken as homogeneous model input.

7.2. Generation of soil parameters

7.2.1. Soil parameters

The soil parameters are based on the Brooks and Corey (1964) model, which allows to represent the retention curve $h(\theta)$, relating the soil water pressure $h(m)$ to the soil

volumetric water content $\theta(m^3m^{-3})$, and the hydraulic conductivity curve $K(\theta)$, relating the soil hydraulic conductivity $K(ms^{-1})$ to the soil water content. The retention curve is for $\theta_r = 0$ as follows:

$$\begin{cases} for h < h_{BC} : \frac{\theta}{\theta_s} = \left(\frac{h_{BC}}{h}\right)^{\lambda} & : \\ for h_{BC} \leq h : \frac{\theta}{\theta_s} = 1 & : \end{cases} \tag{7.2.1}$$

where θ_r is the residual water content in m^3m^{-3} and θ_s is the saturated water content in m^3m^{-3}, λ is the pore size distribution index , K_s is the saturated conductivity in cm hr^{-1} and h_{BC} the bubbling pressure in cm. The hydraulic conductivity curve can be written as:

$$\frac{K(\theta)}{K_s} = \left(\frac{\theta - \theta_r}{\theta - \theta_s}\right)^{\eta} \tag{7.2.2}$$

where η is the form parameter of the saturated hydraulic conductivity curve.

The soil parameters for the first soil horizon were derived from the particle size distribution measured by Gonzalez-Sosa et al. (2010), whereas the data of the DONESOL database (SIRA, 2011) were taken for the parametrization of the lower soil horizons, see chapter 3.1.3. As no information about urban soils was available in the DONESOL database (SIRA, 2011), the urban soils were replaced with adjacent soil types. The final soil map is shown in Figure 7.2.1.

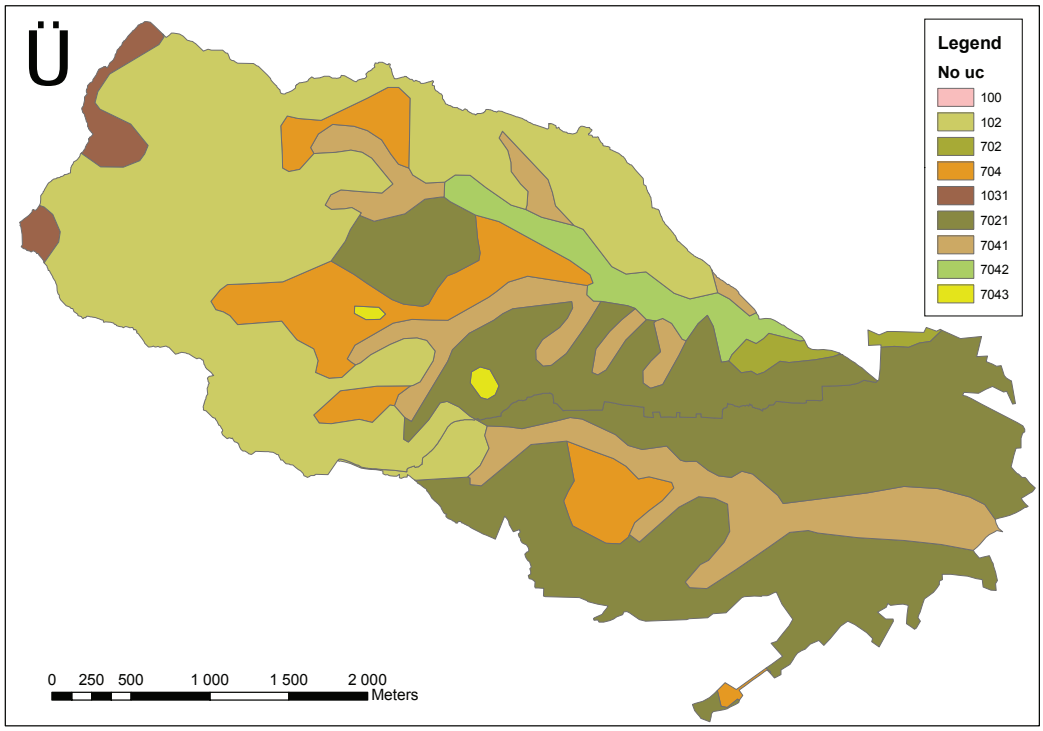

Figure 7.2.1.: Extended soil map for urban areas (SIRA, 2011). The No us code is explained in table 3.1.1 in Chapter 3.1.3

.

The thickness of the first soil horizon was set to 10 cm. Gonzalez-Sosa et al. (2010) analyzed the soil data depending on the in situ land use classes and related it to most

of the UMR 5600 land use classes (Jacqueminet et al., 2011), see map in chapter 3.1.3. However, we needed soil data for all of the land use classes. Therefore, we assigned also the missing land use classes to the situ land use classes.

Another problem arises as the DONESOL database provides a map for the NO_UC classes (chapter 3.1.3), but not for the NO_US classes for which the soil properties are available. One NO_UC class consists of one or a combination of NO_US classes. In this case, the dominant soil type was selected. Only one soil (NO_UC 102) had equal percentages (NO_US 4/5). We chose NO_US class 5, as it already covers large parts of the catchment.

Like Manus et al. (2009), we chose the Rawls and Brakensiek (1985) pedo-transfer function (see Appendix E) to calculate the Brooks and Corey (1964) parameters: the pore size distribution index λ, the saturated conductivity k_s in cm hr^{-1}, the bubbling pressure h_{BC} in cm and the residual water content θ_r. The Rawls and Brakensiek (1985) pedo-transfer function takes as input the percentage of the clay and sand fractions, which have to be between 5 and 60 %, or 70 %, respectively, as well as the total porosity. The total porosity of the topsoil data had been calculated by Gonzalez-Sosa et al. (2010), but the DONESOL database did not provide the porosity values. Like Manus (2007), we derived the porosity from the soil texture triangle, using the relation determined by Brakensiek et al. (1981), see Appendix E. They determined minimal, maximal and average porosity values for given particle size distributions. We set the porosity to the average value.

The Brooks and Corey parameters are necessary for the FRER1D module or the URBS module, however, the HEDGE module needs the retention porosity and the drainage porosity. The retention porosity was obtained with the Brooks and Corey (1964) equation for field capacity (Braud et al., 2005):

$$\theta = \theta_s \left(\frac{3.3}{h_{BC}} \right)^{-\lambda} \tag{7.2.3}$$

where θ_s is equal to the total porosity and θ to the retention porosity. The drainage porosity can then be calculated as

$$por_{dr} = \theta_s - \theta \tag{7.2.4}$$

The final parameters were then stored in the database shown in Figure 7.2.2, which allowed the combination of the topsoil parameters with the parameters of the lower soil horizons. In the database the soil properties were separated from the cartographic properties. This database served then to calculate the final parameters for the HEDGE, WTI and WTRI modules and it could also provide the parameters for the FRER1D module. However, the URBS parameters were calculated with the Cosby et al. (1984) pedo-transfer function (see Appendix E), as was done for the original URBS model (Morena, 2004).

7.2.2. Soil depth

The DONESOL database did not provide the thickness for the lowest soil horizons. The soils in the Chaudanne and Mercier catchments had between 2 and 4 soil horizons. The soil depth up to the last soil horizon was obtained by summing up the horizon depth. This soil depth varied between 55 and 95 cm. In particular in the upper part of the

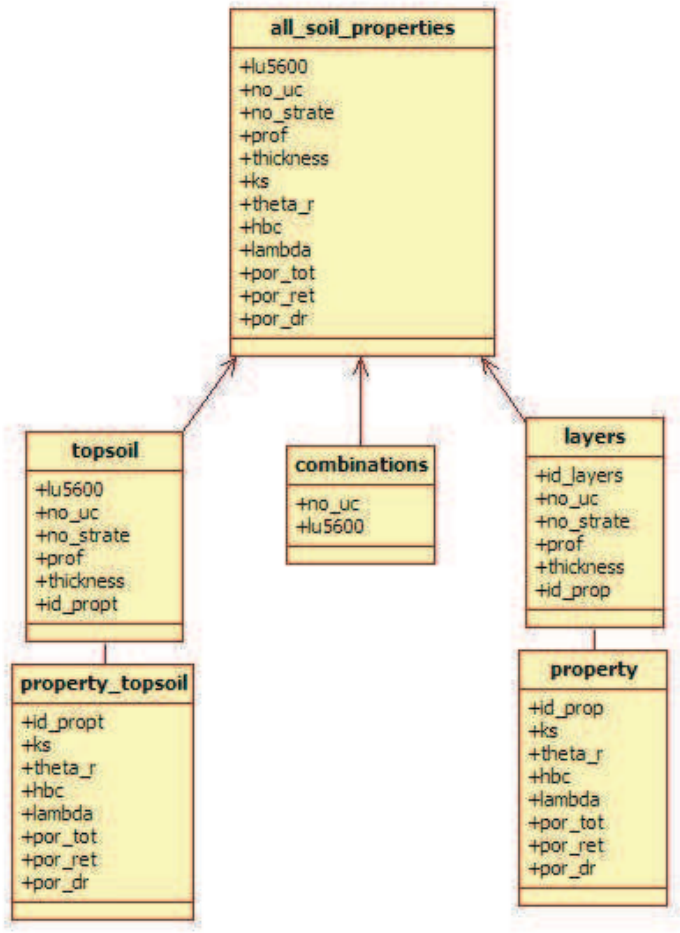

Figure 7.2.2.: Soil database for the Mercier and Chaudanne. The all_soil_properties table combines the parameters of the topsoil with the lower soil horizons. Lu5600 are the land use classes and NO_uc the soil classes.

Mercier catchment the bedrock is occasionally visible at the surface. The geophysical measurements propose a soil depth of 1 to 2m in the valley bottoms with an additional weathered and altered layer of about 5 to 20m. Ruysschaert (2004) determined also a soil depth of about 1 to 2m with his piezometers (Chapter 3). For the reference simulation we chose a homogeneous soil depth of 1 m as first approximation.

7.3. Parameters per module

7.3.1. HEDGE

The soil in the HEDGE module is characterized by an average drainage porosity and a retention porosity per soil horizon (refer to Tables 5.1.1 and 5.1.2 in Chapter 5.1.1). The average drainage porosity was calculated as weighted average over the horizon depth, whereas the retention porosities could be copied directly from the developed soil database. Furthermore, the position and the bottom depth of the soil horizons were derived from the database. The retention porosities in the Chaudanne catchment ranged between 0.07 and 0.23. The range of the drainage porosity was between 0.21 and 0.28. The thickness of

the calculation cells was set to 10 cm. Therefore, the nb_cells parameter was calculated as soil depth*100/10, where the soil depth was 1m.

Besides the constant parameters, the HEDGE module needs time series of the crop coefficient as input data, which govern the evapotranspiration. We took the values proposed by Viaud et al. (2005), as the HEDGE module was derived from their TNT2 model. They modeled an agricultural catchment and used two different time series for crop cells and hedgerows cells, see Figure 7.3.1. Furthermore, Viaud (2004) indicates that the crop

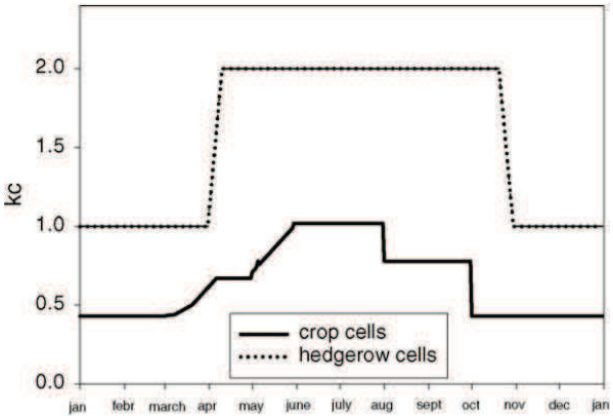

Figure 7.3.1.: The time series for the crop coefficient of crop and hedgerows according to Viaud et al. (2005).

coefficient for grass is constantly 1.0. From this information we derived six crop coefficient classes as shown in table 7.3.1, which we assigned to the UMR 5600 land use classes (Béal et al., 2009). We also explored the data from AUP (Agence Unique de Payement du ministère de l'agriculture) giving information about the cereal type planted on the agricultural parcels. However, we only had the data for 2006 and 2007, whereas we wanted to simulate from 2007 to 2009. Furthermore, the information covered only some selected parcels. Consequently, we could not use these data.

Table 7.3.1.: The crop coefficient classes with their minimum and maximum values according to Viaud et al. (2005) and the UMR 5600 land use class (Jacqueminet et al., 2011) to which they were assigned (refer to Figure 3.1.6 in chapter 3.1.4) .

class	description	min	max	land use class
1	hedge, forest	1.0	2.0	101,111,151,161
2	bare soil	0.35	0.35	301
3	grass	1.0	1.0	211,221
4	scrubland, vegetation in rows	1.0	1.0	171,181,231,241,271,283
5	crop cultivated	0.45	1.0	201
6	pine trees	1.5	1.5	131

7.3.2. URBS

The URBS parameters describe the tree cover and the surface and soil characteristics of an urban cadastral parcel. Furthermore, the connections of the parcels to the sewer system are parameterized (refer to Tables 5.2.1 and 5.2.2 in Chapter 5.2.1). Morena (2004)

(p.33) and Rodriguez et al. (2008) applied the URBS model to the Rezé catchment in the peri-urban area of Nantes, France. It was considered for our study, that the hydrological characteristics of urban cadastral parcels are similar throughout France. For this reason, the same parameters as Rodriguez et al. (2008) were taken for the typical urban parameters of the URBS model units in the Chaudanne PdB catchment. These parameters concern the permeabilities and retention capacities of sealed areas, urban vegetation, as well as some soil and sewer characteristics. Their values are shown in table 7.3.2.

Table 7.3.2.: URBS parameter corresponding to the default values of Rodriguez et al. (2008).

Class	Parameter	Value
trees	interception_level_min	1.0 mm
trees	interception_level_winter_min	0.3 mm
trees	interception_level_discharge_coef	0.04 min^{-1}
trees	root_depth	1.3 m
surface	built_surface_level_max	0.5 mm
surface	road_surface_level_max	3.5 mm
surface	natural_surface_level_max	5.0 mm
surface	built_surface_k_sat	0 m s^{-1}
surface	road_surface_k_sat	7.5 $10^{-}8$ m s^{-1}
soil	m	0.2
soil	α	0.5
sewer system	μ	2

The soil parameters θ_{sat}, ψ_e, b and k_{sat}^{nat} were derived from local soil data. The layer thickness weighted means of the clay, silt and sand contents were calculated for each DONESOL soil type present in the Chaudanne catchment. The values for θ_{sat},ψ_e,b and k_{sat}^{nat} were then derived with the Cosby et al. (1984) pedo-transfer function, see Appendix E. The range of the parameters is given in table 7.3.3.

Table 7.3.3.: Range of soil parameters calculated with Cosby equation.

Parameter	min	max
θ_{sat}	0.40	0.43
ψ_e	0.10 m	0.21 m
b	4.60	6.39
k_{sat}^{nat}	4.58 $10^{-7} ms^{-1}$	1.06 $10^{-6} ms^{-1}$

The radier depth parameter (refer to Table 5.2.2 in Chapter 5.2.1) means the depth of the drainage pipe, which is important for the sewer system infiltration. For the pipes, for which the sewer system data of the SIAHVY provided the relevant information, this parameter was set to the depth of the drainage pipe. The depths vary between 0.8 and 2.65 m. For the other URBS parcels the depth was set to 1m in a first approximation.

Rodriguez et al. (2008) showed that a groundwater coefficient λ of 40 instead of 2 lead to a better representation of the observed discharge. λ varies between 0 and 100 and represents the state of the sewer system. A higher value of λ characterizes a sewer system with many defects, whereas a low value of λ signifies a leak-proofed sewer system. From chapter 3 we know that in the Chaudanne catchment the percentage of parasite water

in the sewer pipes is quite high, which means that there are many defects in the sewer system. For this reason, we chose a value of 40 for λ.

In the reference simulation, the link coefficients connecting the surface runoff of the roofs, road and natural parts to the drainage network were set to 1, which means that all surface runoff created on these areas is directly connected to the drainage network. We also set the network link coefficient to 1, instead of 0.37 like in Rodriguez et al. (2008), in order to account for the bad condition of the sewer system in the Chaudanne catchment. If one of the link coefficients is inferior to 1, the rest of the water is added to the natural part of the UHEs. This implies, that for UHEs having no natural part (as in our case the roads in the rural part), the link coefficients have to be 1 in order to keep the mass balance correct.

7.3.3. SISTBA

In the rural part of the Chaudanne PdB catchment, there are four lakes and in the urban part five retention basins. The retention basins or lakes are characterized by their depths (maxlevel), heights of the outflow (S3) and retention parameters (μ), refer to Table 5.2.10 in Chapter 5.2.4. The maxlevel and S3 level for the retention basins were directly measured on the field during a field campaign. The S3 level corresponded to the height of the outlet pipe for the retention basins and for the lakes it was set to the maxlevel. The maxlevels of the lakes were estimated based on the local topography. The surface levels a.s.l were derived from the DEM during the geographical preprocessing and then, the maxlevel was subtracted in order to get the basin bottom. The size of the basins influenced the choice of the retention parameters. A possibility would also be to determine the retention parameters with tracer experiments (Passeport et al., 2010), although, this are all private lakes, and access is not really possible. The four retention basins at PdB were connected directly to the upstream and downstream basins without RIVER1D instances between the basins. The parameters of the basins are shown in table 7.3.4.

Table 7.3.4.: SISTBA parameters such as the maximal height, the height of the outlet and the retention parameter for Chaudanne PdB.

Id	type	Maxlevel [m]	S3 [m]	μ [s]
222	lake	1.0	1.0	1200
590	ret bas	1.45	0	6500
592	ret bas	1.45	0	4000
595	ret bas	1.42	0	4000
2345	lake	2.0	2.0	4000
2346	lake	1.8	1.8	4000
2347	lake	1.0	1.0	2000
2350	ret bas	1.48	0	1000
2943	ret bas	1.7	0.68	600

7.3.4. TDSO

There are two sewer overflow devices (SODs) in the Chaudanne PdB catchment. The SOD at PdB, for which we have measured discharge data and another SOD, called “T”, which

connects the upper part of the combined sewer system in the PdB catchment, flowing towards la Léchère, to the SOD at PdB. Figure A.0.4 shows a scheme of the storm water overflow chamber at PdB, where the pipe to the river is located in the lower right corner. The crest length of the chamber is 1.54 m and the height of the overfall boundary is 15 cm upstream and 20 cm downstream (Bernoud, 1998). According to INGETUD (1997) the threshold for the storm water overflow is 40 l s^{-1}. The pictures show the storm water overflow chamber with two pipes coming from both sides of the river on the left side and the shutter to the sewage plant as well as the pipe to the SOD on the right side. The

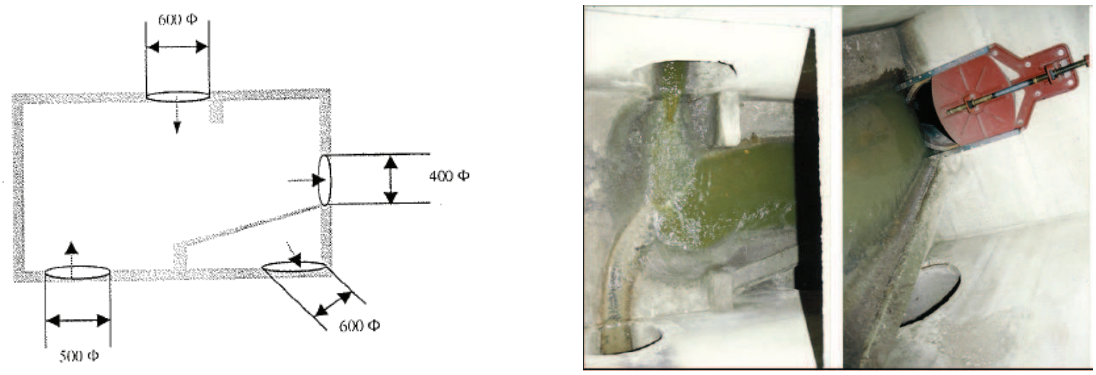

Figure 7.3.2.: Scheme and photos of the storm water overflow at the Pont de la Barge. The pipe in the lower right corner is the storm water overflow towards the Chaudanne (Bernoud, 1998). The pictures are arranged so that the pipe outlets correspond to the scheme with the storm water overflow in the lower right corner. Photos of P. Breil, Cemagref Lyon.

diameter of the outflow pipe and thus the modelled width is 0.6 m (refer to Table 5.2.5 in Chapter 5.2.2). The overflow height was set to the lower measured value of 0.15 m, which resulted in an orifice top of 0.75 m, see table 7.3.5.

Figure A.0.2 shows the scheme and a picture of the SOD T. The shutter closes the part going to the Pont de la Léchère. The overflow pipe has a diameter of 0.4 m (Belhaouane, 1999). Therefore the width of the overflow was set to 0.4 m and the top of the orifice to the overflow height plus the pipe diameter, see table 7.3.5. No measured data of the overflow height were available, and it was set to 0.4 m. The discharge coefficient of both SODs was

Figure 7.3.3.: Schema and picture of the intersection "T" (Belhaouane, 1999). The overflow (400mm) is perpendicular to the sewer pipe. The regular outlet can be regulated with a shutter. Photo of P. Breil, Cemagref Lyon.

set to the default value of 0.82 proposed in Carlier (1972) (p.182). The identifiers of the

in- and outflowing river reaches were determined manually from the RIVER1D drainage network.

Table 7.3.5.: TDSO parameters such as the overflow height, the top and width of the outlet pipe and the discharge coefficient for Chaudanne PdB.

Id	Name	overflow height [m]	orifice top [m]	width [m]	μ [s]
2	T	0.4	0.8	0.4	0.82
3	SOD PdB	0.15	0.75	0.6	0.82

7.3.5. RIVER1D

The drainage network of the Chaudanne catchment consists of the natural stream, the combined sewer system, separated sewer systems and artificial ditches, which were represented with 11 different RIVER1D implementations. Two of them describe the combined sewer system, which is interrupted by the two sewer overflow devices. Two other RIVER1D implementations describe the separated sewer system which leads towards the retention basins. The natural river and the ditches are modelled with 7 RIVER1D implementations, as the network is interrupted by retention basins and lakes, which causes each time a new RIVER1D implementation. The 11 rivers of the Chaudanne PdB catchment are divided in 239 river reaches for which the parameters (refer to Table 5.1.5 in Chapter 5.1.2) were defined.

Trapezoidal and rectangular cross sections were chosen as river geometry. During a field campaign representative bottom widths, top widths and heights of the main channel or pipe diameters were measured for each drainage branch in the Chaudanne and Mercier catchment. These were about 100 measured cross sections per catchment. Descriptions of the bottom characteristics were also noted for each of the cross sections in order to define the Manning roughness values. The batter was derived as $(top\_width - bottom\_width)/height$ from the measured data. For the pipes, representative rectangular cross sections were derived as the square root of the pipe cross sections.

According to the description noted on the field, nine roughness classes were determined. The Manning values were then assigned based on the descriptions given by Chow (1973), see table 7.3.6.

Table 7.3.6.: Manning ids, values and field description.

Id	Manning value	Field description
39	0.013	sewer pipes out of concrete or plastic
40	0.017	sewer pipes out of concrete with gravel
41	0.025	ditches with sand,gravel,earth bottom
42	0.033	ditches with sandy, rocky bottom, sided by dry rubble or riprap
43	0.035	natural channels with bedrock or high grass
44	0.04	minor streams, woody, sandy, rocky bottom
45	0.045	minor streams with big stones and high grass
46	0.08	ditches with high grass
47	0.25	ditches with sandy or gravel bottom

The slopes and mean elevation values were calculated from the DEM during the geographic preprocessing. Only the sewer system slopes and altitudes were derived from the sewer system data, provided by the SIAHVY.

7.3.6. OLAF

For α and β the standard values corresponding to the Manning equation were taken, corresponding to 0.5 and 5/3, respectively (refer to Table 5.2.6 in Chapter 5.2.3). The Manning values were chosen from Chow (1973) and Engman (1986) depending on the land use property, see table 7.3.7. The other parameters such as the altitude and geometries of the adjacent model units were copied from the HEDGE, URBS, SISTBA or RIVER1D tables. The slope is then directly calculated in the OLAF module based on the geometries and altitudes.

Table 7.3.7.: Manning roughness values per land use type chosen from Chow (1973) and Engman (1986).

Manning	Land use class
0.013	283
0.016	723,613,602,502
0.02	513,301
0.035	231,241,271,601,623
0.05	111,141,161
0.08	201,131,171
0.1	151,101,121
0.15	221
0.24	211

7.3.7. WTI

The permeability of the interface was calculated as average of the permeability of the adjacent model units. For URBS model units, this corresponded to the k_s calculated with the Cosby et al. (1984) equation and for HEDGE model units, the permeability was derived from the developed soil data base as thickness weighted average of the Rawls and Brakensiek (1985) permeabilities (refer to Table 5.1.7 in Chapter 5.1.3). The bedrocks in the WTI module were calculated as difference of the surface level of each model unit and its soil depth. The soil depth of the interface was calculated as the distance weighted average of the model unit depths. This worked well for the HEDGE module, however, the soil depth in the URBS module corresponded to the depth of the pipe and can be close to the surface if the parcel is connected to ditches. The soil depth in the URBS module (parameter "radier_depth") had therefore to be greater than zero and to correspond to the depth of the ditch. The center of the model units was extracted automatically from its geometry. The surface level of the interface was also calculated as distance weighted average. A better way would have been to derive it directly during the geographical preprocessing from the DEM. An attempt was undertaken, however, the use of multi-geometries for the interface geometry created problems for the calculation of the average altitude.

7.3.8. WTRI

The permeabilities were set to the permeability of the adjacent model units (refer to Table 5.1.9 in Chapter 5.1.4). The river bottom level in WTRI was copied from the river1d_reach table. The river bottom width was extracted from the trapezoidal and rectangular section tables of the RIVER1D module. For the WTRI instance which is coupled to SISTBA, the river bottom width, or rather lake bottom width, was calculated as the distance between the centers of the lake and the plot. The plot_bedrock was derived from the difference of the soil surface and the depth and the center_plot from the geometry of the plot like for the WTI module.

7.4. Initial conditions

We set the initial groundwater table to half of the soil depth in HEDGE, which means 50 cm below surface level. Furthermore, the initial water content of the HEDGE retention porosity was saturated. In URBS, the saturated zone depth was initialized at the depth of the drainage pipes and the initial levels of the built, road and natural surface reservoirs were set to 0.0. The initial lake levels were set to the maxlevel and to 0.0 for the retention basins. Finally, the RIVER1D drainage network was initialized with dry conditions.

Even if lake water use for irrigation was observed during field visits, no data were available. There are only a few lakes in the Chaudanne PdB catchment and irrigation is mainly important for low water levels. Therefore, irrigation was neglected during the simulations.

7.5. Conclusions

All parameters could be defined for the application of the PUMMA model to the Chaudanne PdB catchment. Most of the parameters were based on measured or literature values. A general classification of the PUMMA input parameters and a description of the SQL queries for the filling of the PLUS and FCA modules is given in Appendix F. The development of the soil database provides also the parameters for a future application of the FRER1D module or an application to the Mercier catchment. Some of the parameters as the soil depth, the depth of the lakes or the retention parameters of the lakes had been estimated based on field knowledge. This parameterization gives a good set of parameters for the reference simulation and it can still be improved based on sensitivity tests or further field investigations.

8. Results

This chapter presents in a detailed manner the results of the reference simulation using the parameters described in chapter 7. For the simulation, we chose the relatively wet 2008 year and dry 2009 year in order to test the capability of the model to simulate these different hydrological situations. 2007 was taken as initialization period and the model was thus run continuously for a three year period. The results were analyzed on an annual and event basis. In Chapter 3.2.3 we have seen that summer and winter events have different characteristics, therefore three summer and three winter events were chosen for the event analysis.

The second section describes the sensitivity of PUMMA to the change of some URBS and soil parameters. Concerning URBS we test the influence of the connectivity of the surface runoff from urban impervious areas to the drainage network and the influence of two URBS network infiltration parameters. Concerning the natural processes in the catchment, we test the influence of the soil depth and the lateral hydraulic conductivity, as these two parameters are prone to high uncertainties.

In the third section the impact of the introduction of the interfaces OLAF and WTRI into the model is shown and the last section demonstrates the model ability to simulate different scenarios, such as catchment processes without urban influence and the disconnection of an urban sub-basin from the natural river.

These different tests allow the use of the model as an hypotheses testing tool.

8.1. Reference simulation

8.1.1. Analysis of longterm simulations

8.1.1.1. Yearly discharge analysis

For the validation of the longterm simulations of the years 2008 and 2009, the measured discharge data at the measurement stations UpstreamSOD in the natural river, the station in the combined sewer system and the station in the storm water overflow device (SOD) were available, refer to Figures 6.5.1 and 3.2.2. As PUMMA only simulates the rainwater component of the sewer system, the measured wastewater component determined using filtering methods ((Braud et al., 2011b), see also Section 3.2.3.3) was subtracted from the measured discharge time series in the combined sewer system. Consequently, the simulated sewer discharge could be compared to the rainwater component of the sewer system.

Figure 8.1.1 shows the simulated versus the measured discharge at UpstreamSOD, Figure 8.1.2 in the sewer system and Figure 8.1.3 in the sewer overflow device for 2008 and 2009.

Concerning the discharge in the natural river, we can see that PUMMA overestimates most peaks and underestimates the large flood event in November 2008. However, the model is able to represent the rise of the base flow in winter and the drying of the river bed in summer. The dry year 2009 is better simulated than the wet year 2008.

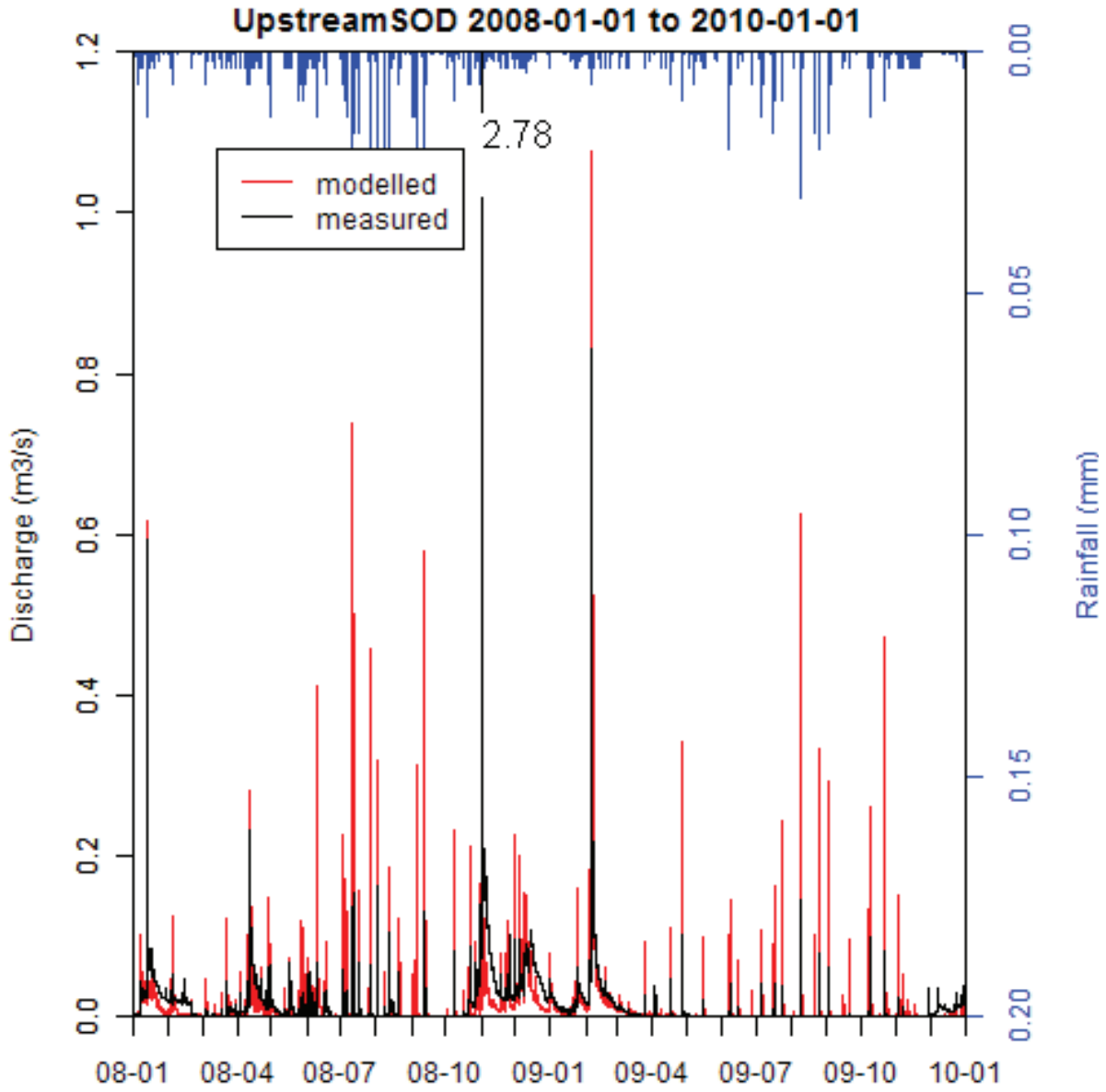

Figure 8.1.1.: Simulated versus measured discharge in the natural river with a 30 min time step.

The model overestimates all peaks in the sewer system, as it simulates peaks of up to 1 m^3s^{-1}, but the measured sewer discharge is limited to a discharge of about 0.05 m^3s^{-1}. The overestimation can have several possible reasons such as an overestimation of fast surface runoff, an overestimation of the contributive areas or a wrong simulation of the overflow thresholds in the two sewer overflow devices which are located upstream of the measurement station. This reveals the uncertainty evoked in chapter 6.2.1 concerning the contributive areas and connections. Furthermore, the non-simulation of pressurized pipe flow by the model could play a role for large flood events. On the other hand, Figure 8.1.2 shows that the model underestimates the observed sewer base flow, which consists mainly of groundwater seepage.

Most of the major storm water overflow events could be simulated with the threshold for the SOD at 15 cm, which corresponds to the threshold measured on the field. However,

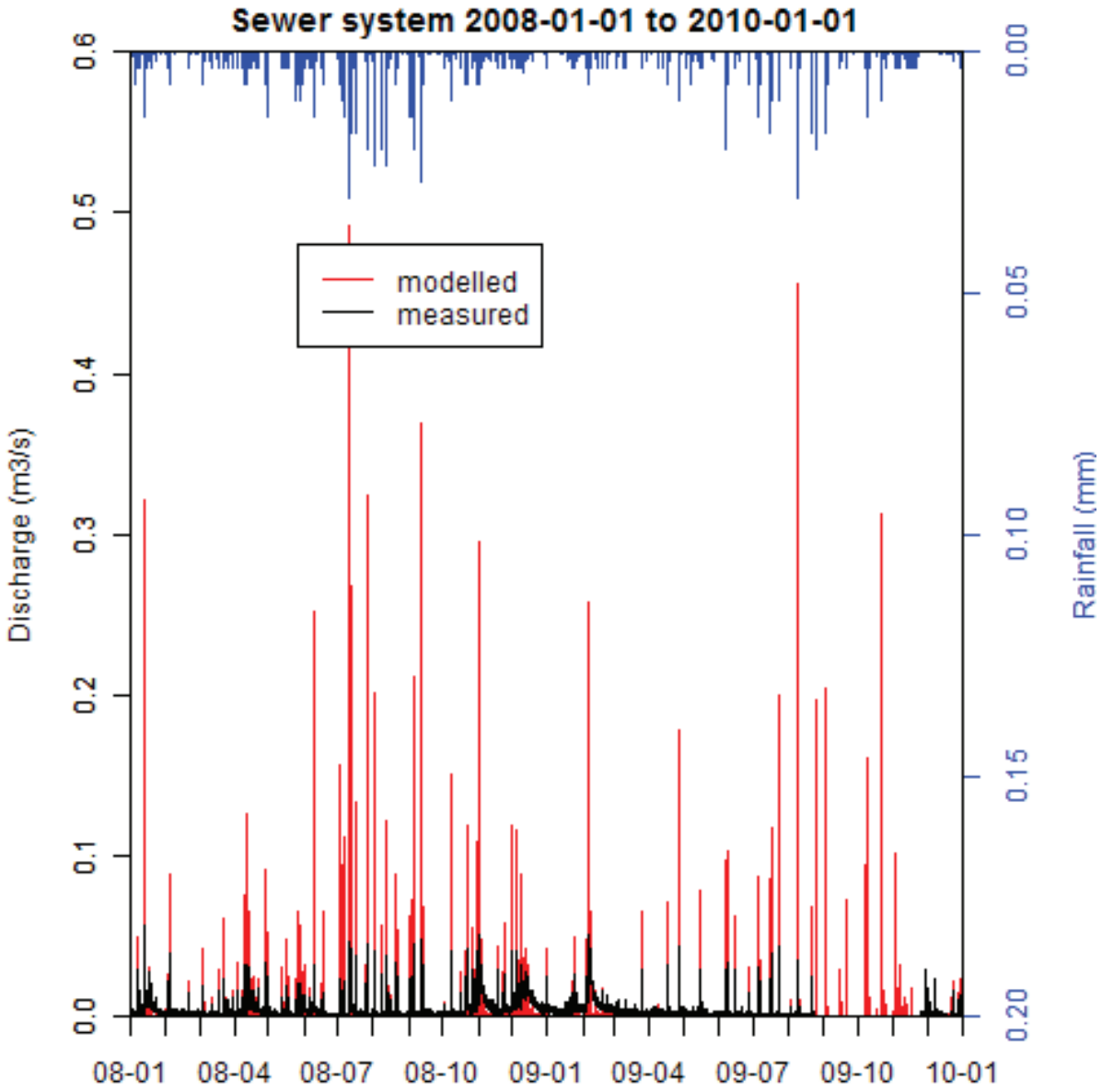

Figure 8.1.2.: Simulated versus measured discharge with a 30 min time step in the sewer system for 2008 and 2009. The red points are missing data.

the small events in the SOD below 0.02 m^3s^{-1} were not detected by the model.

Figure 8.1.4 shows the discharge of the other two catchment outlets, which are the pipe towards the retention basins and the sewer pipe towards La Léchère which is connected via the second SOD, called "T". The simulated discharges in both pipes are similar to the simulated discharge in the sewer system shown in Figure 8.1.2. The pipe discharges fluctuate with only a minor base flow and the amount of discharge in the three pipe systems is of the same order of magnitude. Unfortunately, no measured data was available.

In order to confirm and precise the general trends shown above, all simulated discharge data with a time step of 6 min were plotted against the measured discharge data with the same time step, see Figure 8.1.5. All data above the diagonal overestimate the discharge and all data below underestimate the discharge. The discharge in the natural river were overestimated in 2009. The same pattern is observed for 2008 for the same range of

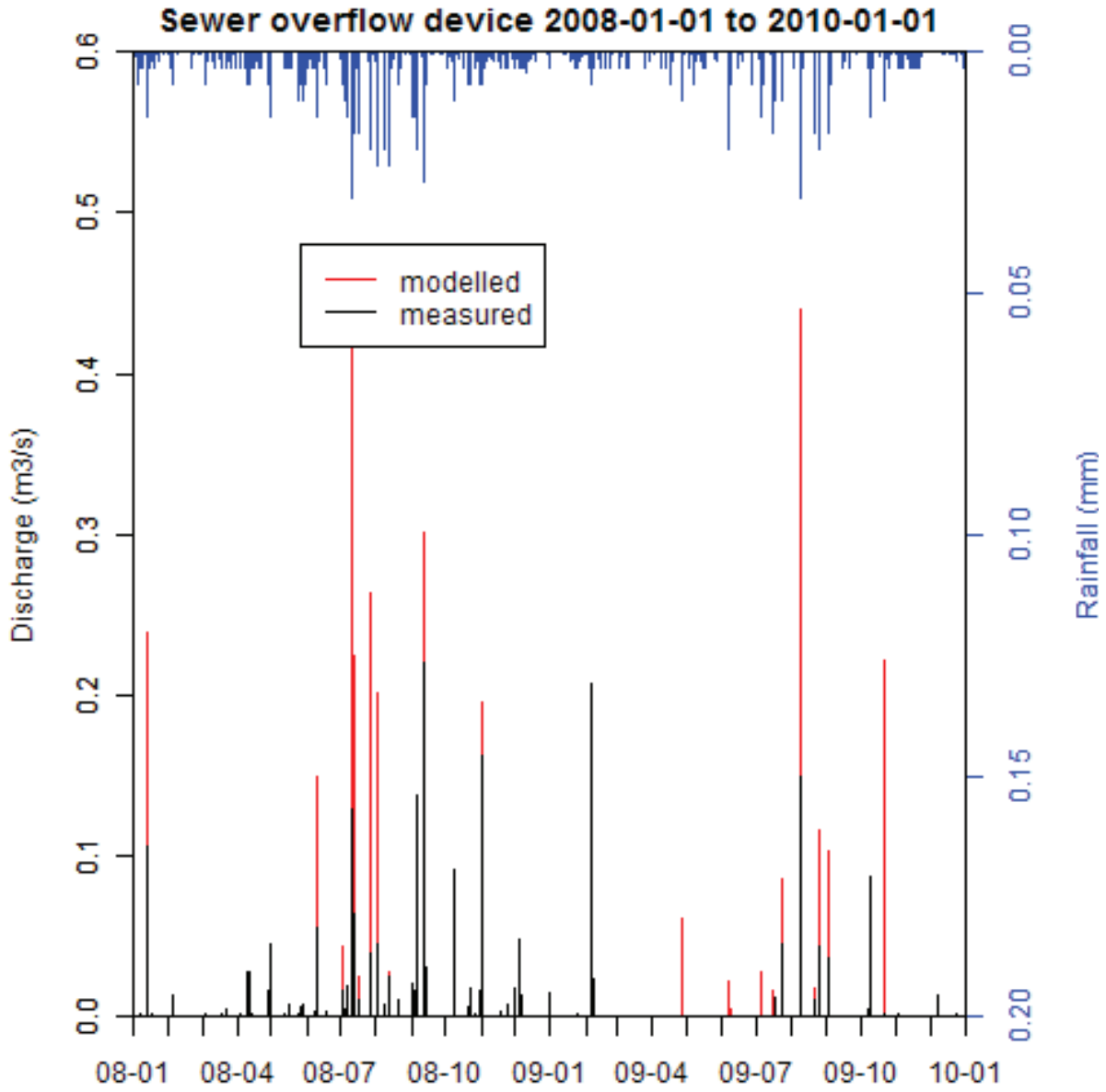

Figure 8.1.3.: Simulated versus measured discharge in the sewer overflow device with a 30 min time step.

discharge (0-1 $m^3 s^{-1}$ on observed data), yet the large events are underestimated (probably only the 1st November event). The comparison of the sewer data shows clearly the overestimation of the sewer discharge for large events. The small sewer discharge values are rather underestimated. This could be due to an underestimation of the drained soil water as explained above.

In the SOD, most sewer events were detected by the model, see Figure 8.1.5. However, the smaller values are rather underestimated and the larger values overestimated, especially in 2008. Furthermore, the model simulates larger peaks with up to 0.7 $m^3 s^{-1}$ against maximal measured values of up to 0.45 $m^3 s^{-1}$.

Table 8.1.1 shows the Nash and Sutcliffe (1970) coefficients and the differences of the simulated and measured discharge volumes for the three flow gauges calculated with the

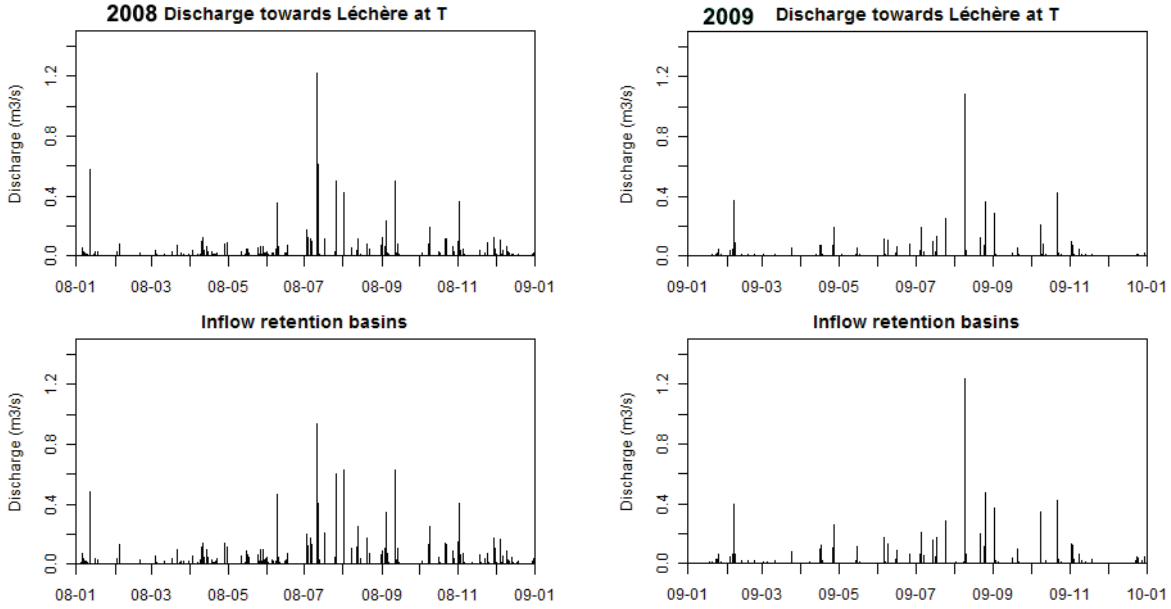

Figure 8.1.4.: Simulated discharge towards La Léchère and the retention basins for 2008 on the left and for 2009 on the right. No measured values were available.

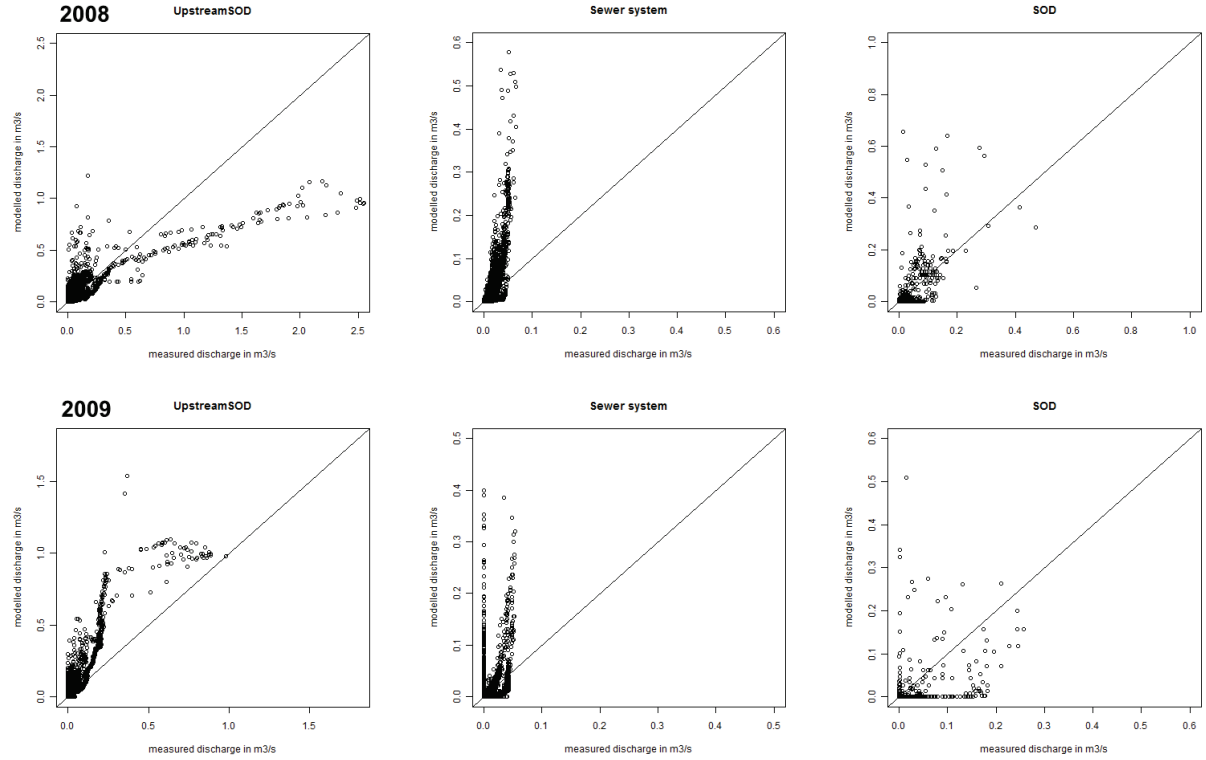

Figure 8.1.5.: Regressions of simulated and measured discharges of the year 2008 in the upper row and 2009 in the lower row. Data are shown with a 6min time step for the measurement stations UpstreamSOD in the natural river(left), the sewer system (middle) and the sewer overflow device (SOD, right). The scales for 2008 and 2009 are not the same.

6 min time step data. The Nash and Sutcliffe (1970) coefficient, which is calculated with equation 8.1.1, can vary between $-\infty$ and 1, where 1 signifies a perfect simulation. If

the Nash-Sutcliffe coefficient is below zero, the simulated discharge is a worser estimation than the average of the observed discharges.

$$N = 1 - \frac{\sum(Q_{obs} - Q_{sim})^2}{\sum(Q_{obs} - \overline{Q_{obs}})^2} \tag{8.1.1}$$

However, the Nash-Sutcliffe coefficient is very sensitive to small time steps, such as our 6min time step. Furthermore, the Chaudanne is an intermittent stream with a very variable regime, which is not favorable for the calculation of the Nash-Sutcliffe coefficient. The Nash-Sutcliffe coefficient has thus to be interpreted carefully.

Table 8.1.1.: Nash-Sutcliffe criteria (N) and difference of simulated and measured runoff volumes ($Diff_{Vol}$) in the natural river, the sewer system and the SOD for the simulation periods 2008 and 2009.

Year	N UpstreamSOD	N Sewer	N SOD	$Diff_{Vol}$ [%] UpstreamSOD	$Diff_{Vol}$ [%] Sewer	$Diff_{Vol}$ [%] SOD
2008	-2.14	0.27	0.42	-29.94	77.34	7.08
2009	0.68	0.23	0.28	30.96	27.08	-24.15

The Nash-Sutcliffe coefficient confirms our conclusion, that the dry year 2009 is rather well simulated, having a value of 0.68, whereas the simulation of 2008 is even below 0, concerning the discharge in the natural river. This is mainly the influence of the 1st November event, as the Nash-Sutcliffe coefficient gives considerable weight to high flow values.

The Nash-Sutcliffe coefficients for the sewer data are similar for 2008 and 2009 with about 0.25, whereas the sewer overflow was better simulated in 2008.

The difference of the volumes in the natural river, which was obtained by equation 8.1.2, shows an overestimation in 2009 and an underestimation in 2008, which confirms the interpretations of the regression graphs and is consistent with the Nash-Sutcliffe coefficient. The discharge volume in the sewer system was overestimated by 30 to 77 %. In 2008 the sewer overflow volume was relatively well simulated, whereas the volume in 2009 was underestimated by about 25 %.

$$Diff_{Vol} = \frac{Vol_{sim}^{year} - Vol_{obs}^{year}}{Vol_{obs}^{year}} \times 100 \tag{8.1.2}$$

8.1.1.2. Monthly regime

Figure 8.1.6 shows a comparison of the average monthly simulated and observed discharges. First of all, the graphs highlight the high annual and seasonal variability of the discharge, which the model is able to represent. The monthly discharge of the natural river is rather well simulated in 2009, whereas in 2008 the underestimation of the flood event in November can be seen. The discharge in the sewer system has a high seasonal variability which depends probably on the higher groundwater seepage in the wetter winter months. The model simulates well the monthly summer discharge in the sewer system, but it underestimates the winter discharge. This suggests that the groundwater seepage simulated by the model is too low. In 2009 there is a long period with missing data for the SOD. The simulation of the monthly SOD discharge in 2008 is rather good, whereas in 2009 the wet period at the start of the year was underestimated.

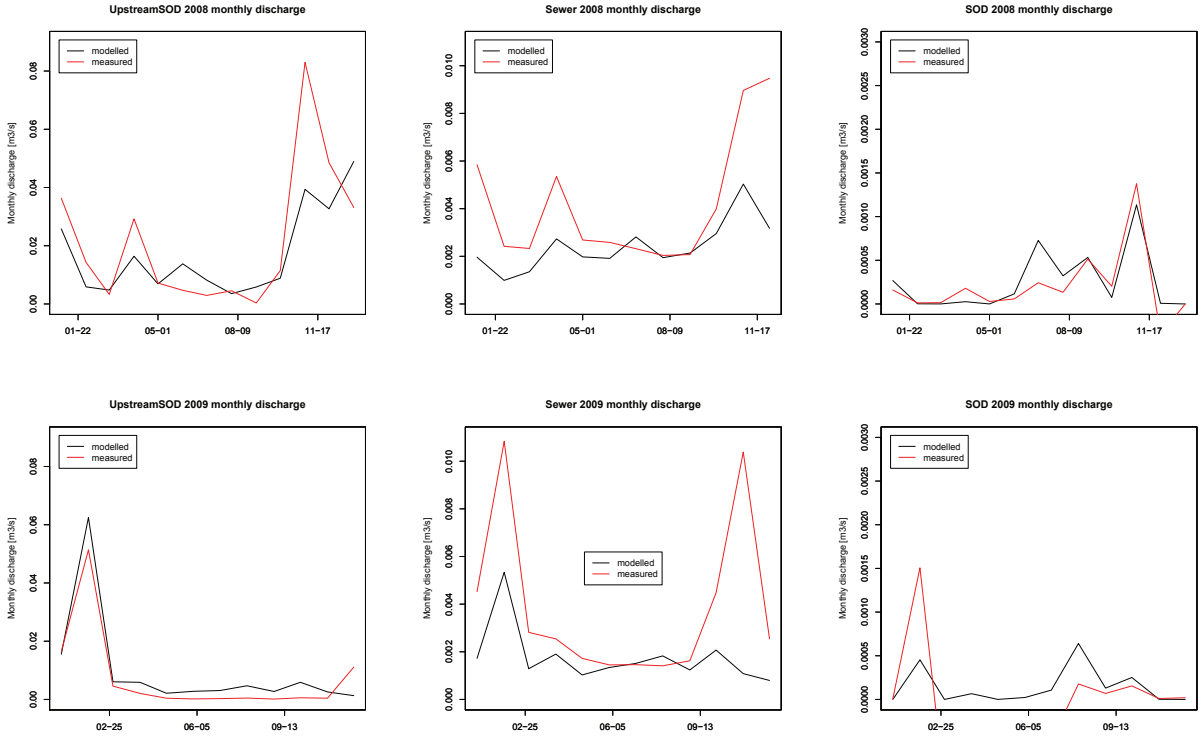

Figure 8.1.6.: Monthly measured and modelled discharge for 2008 in the upper graphics and 2009 in the lower graphics. The monthly discharge values are shown for the measurement stations UpstreamSOD in the natural river (left), the sewer system (middle) and the sewer overflow device (SOD, right). Measured values below zero indicate missing data.

8.1.1.3. Analysis of runoff coefficients and mass balance

Figure 8.1.7 shows the measured and modeled runoff coefficients in 2008 and 2009 for the measurement stations UpstreamSOD, SS and SOD. The runoff coefficients were calculated as: discharge volume/rainfall volume $\times 100$. The total annual rainfall volume in m^3 was calculated for the subbasin of the measurement station upstreamSOD and for the subbasin connected to the sewer system (which is relevant for SS and SOD).

For all stations the runoff coefficients do not exceed 30 % and especially in the natural river and the sewer system they are very variable. In 2008 more than 25 % of the rainfall in the natural part created discharge, whereas in 2009 it was only 15 %. However, the model calculated in both years runoff coefficients of about 20 %. The observed runoff coefficients in the sewer system were also very variable, whereas the simulated runoff coefficients were rather constant. Furthermore, the model overestimated in both years the sewer system runoff coefficient. Around three percent of the rainfall contributed to the sewer overflow events, which was relatively well represented by the model.

The mass balance presented in Figure 8.1.8 shows that the evapotranspiration is the most important process in terms of water volume at the catchment scale. The simulated actual evapotranspiration remains approximately the same for both years, in spite of a smaller rainfall volume in 2009 and a smaller potential evapotranspiration in 2008 (833

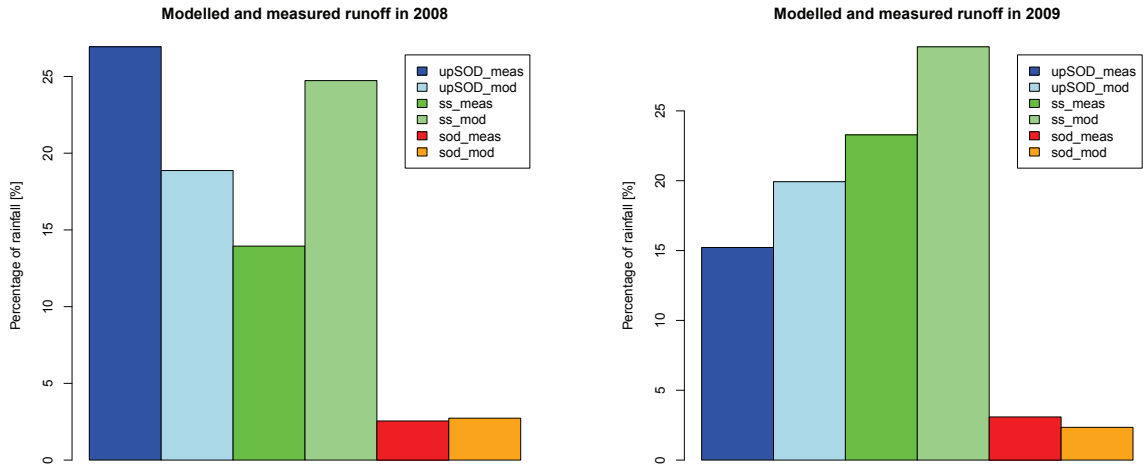

Figure 8.1.7.: Simulated and measured runoff coefficients of the natural river (blue), the sewer system (ss in green) and the sewer overflow device (SOD in orange/red) as percentage of the annual rainfall for 2008 (left) and 2009 (right).

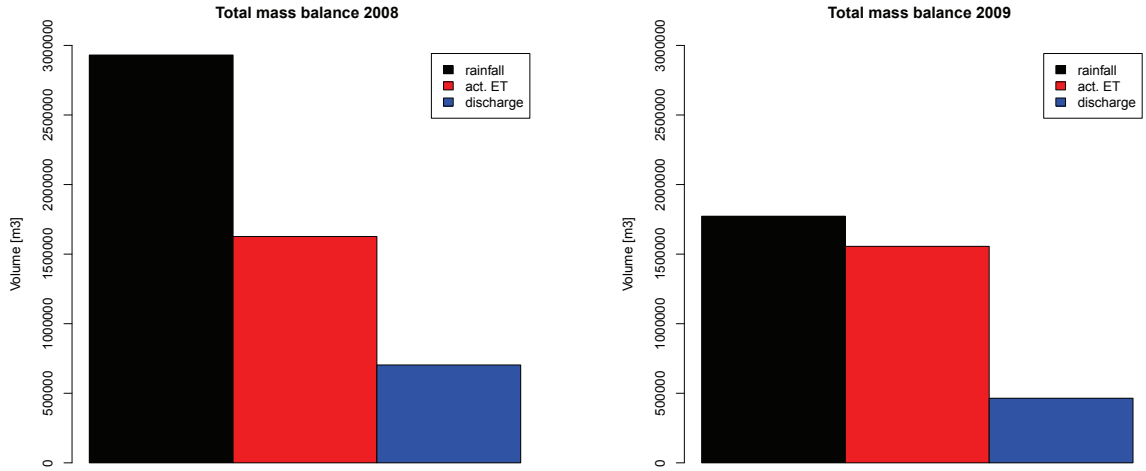

Figure 8.1.8.: Total observed rainfall, simulated actual evapotranspiration (ET) and simulated discharge for 2008 (left) and 2009 (right). The simulated discharge is the sum of all outlets, which are UpstreamSOD, SS, SOD, SOD T and the pipe towards the retention basins.

mm versus 940 mm in 2009). The discharge volume in 2009 was less than in 2008. The sum of discharge plus AET is smaller than the rainfall in 2008, whereas it is larger in 2008. These elements indicate that in 2008 more water was stored in the soil, and that in 2009 this soil storage was emptied.

8.1.1.4. Analysis of runoff components

In order to further enhance the understanding of the model functioning, the different components which compose the discharge in the natural river, the combined sewer system and the separated sewer system leading to the retention basins, were analyzed. For this, the annual discharge volumes of the different LIQUID modules connected to the drainage network were calculated and divided into contributions to the natural river, to the sewer system and to the pipes towards the retention basins. The discharge could thus be divided intoă:

- subsurface contributions from WTRI interfaces connected to HEDGE and URBS
- contributions from network infiltration in URBS
- surface runoff contributions from HEDGE via the OLAF module
- contributions of the different surface runoff components from URBS (built, road, natural)

Percentages were then calculated in reference to the sum of all contributing discharge volumes. These components were further summarized into overland flow components and subsurface flow components, as well as contributions from HEDGE and URBS.

The results for 2008 and 2009 are shown in Figures 8.1.9 and 8.1.10. There is no significant difference between the components in 2008 and 2009, which probably means that the component pattern is caused by the model setup and not by different climatic conditions.

For all of the three drainage networks, even the natural river, the main contribution is overland flow (80%) and subsurface flow (20%) takes only a minor role. Most of the HEDGE model units are connected to the natural river, which explains why the HEDGE contribution to the sewer system and the retention basins is quite small. The annual amount of overland flow from HEDGE model units for upstreamSOD is similar to the runoff from roofs. At the annual scale, the contribution from URBS elements represents about 60% of the total volume and the contribution from the rural part (HEDGE modules) about 40%. The rural contribution is composed of a little bit more surface runoff (from OLAF) than subsurface flow (from WTRI). The surface runoff from the natural part of URBS is rather small for upstreamSOD and more important for the sewer system and the retention basins. It seems that on the long term the WTRI interfaces connected to URBS infiltrate water from the natural river into the soil (the cumulative discharge values are negative), whereas the network flow drains the soil. The WTRI interfaces equilibrate thus the draining effect of the network flow. This behavior of the model is surprising and does not seem to correspond to “real” hydrological processes. It should be further investigated and possibly corrected in future. A possibility would be to create two URBS instances, a “urban” URBS instance drained by network infiltration and a “rural” URBS instance without network infiltration, but with subsurface flow modeled with WTRIs.

Figure 8.1.11 shows the annual evolution of the different components for the natural sub-basin (upstreamSOD). These components were calculated as the sums of all URBS, OLAF and WTRI signals, respectively, connected to the natural stream at each time step (6 minute time step). As the routing of these components in the river channel is not taken

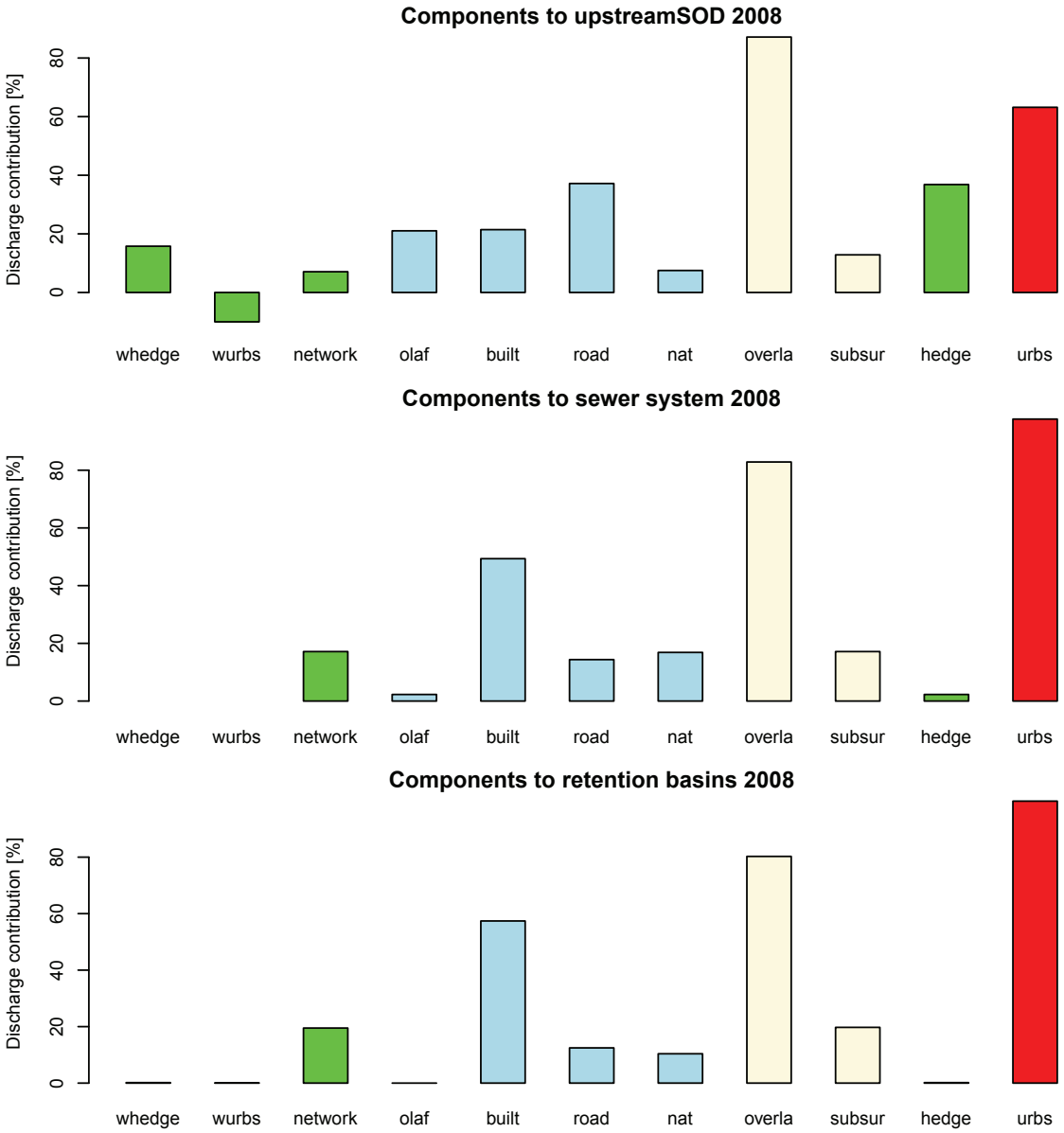

Figure 8.1.9.: Analysis of the different components contributing to the discharge in the natural river (top), the sewer system (middle) and the retention basins (bottom) in 2008. From left to right, the components are subsurface flow components in green (discharge from WTRI interfaces connected to HEDGE (whedge) and URBS (wurbs) and the URBS network infiltration), overland flow components in blue (contribution from OLAF, surface runoff from URBS divided in runoff from built, road and natural areas (nat)). The beige columns summarize the module contributions into overland (overla) and subsurface flow (subsur), and the green and red column into contributions from HEDGE and URBS. The percentages were calculated in reference to the sum of all contributing discharge volumes (sum of green and blue columns in the beginning).

into account[1], this component analysis is more a succession of snapshots of contributions to the river at a given time than a real hydrograph separation for the discharge at the measurement stations. In particular, the sum of discharge components may not correspond

[1]The separate routing of flow components is not implemented in the current version of RIVER1D

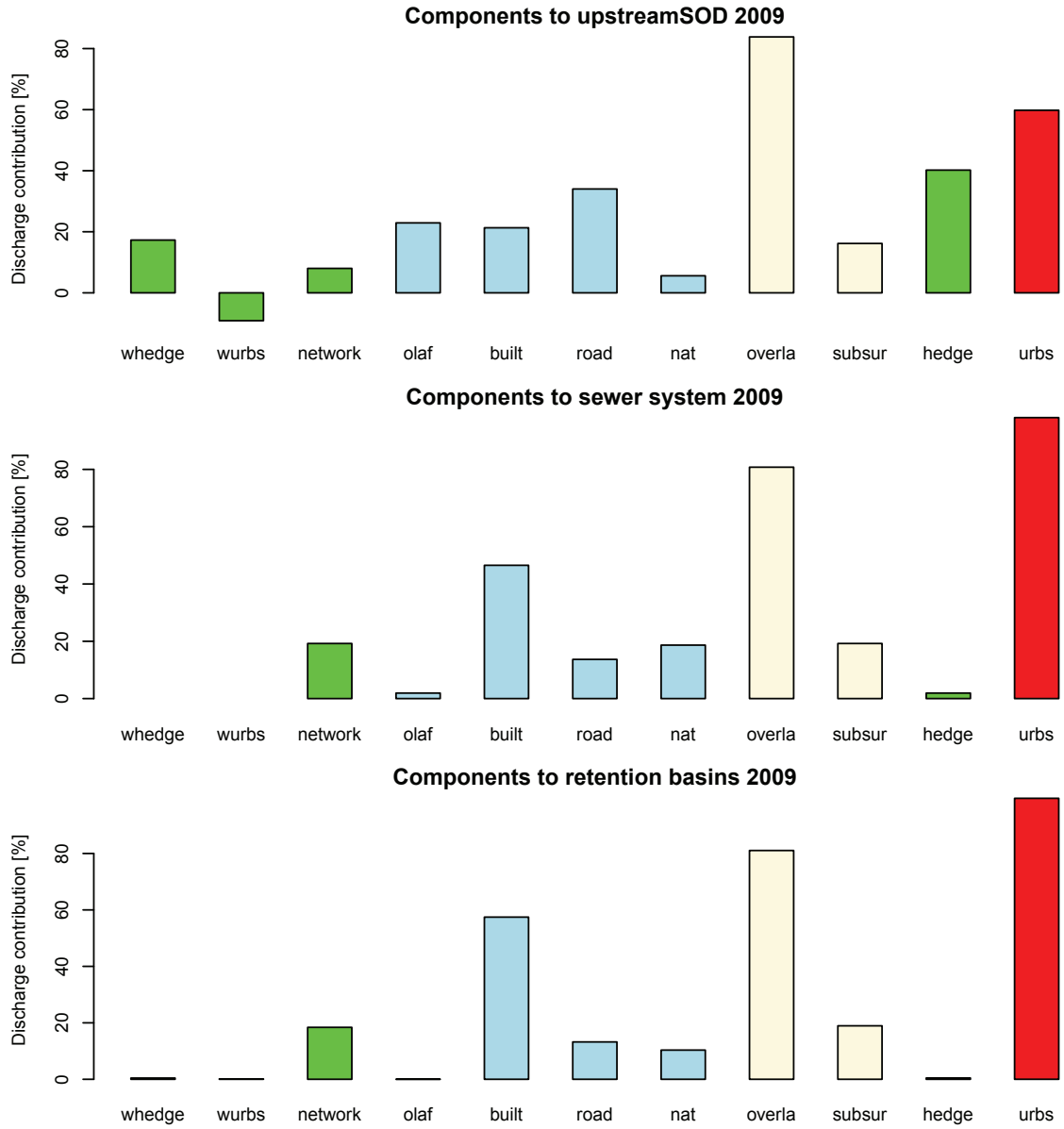

Figure 8.1.10.: Analysis of the different components contributing to the discharge in the natural river (top), the sewer system (middle) and the retention basins (bottom) in 2009. From left to right, the components are subsurface flow components in green (discharge from WTRI interfaces connected to HEDGE (whedge) and URBS (wurbs) and the URBS network infiltration), overland flow components in blue (contribution from OLAF, surface runoff from URBS divided in runoff from built, road and natural areas (nat)). The beige columns summarize the module contributions into overland (overla) and subsurface flow (subsur), and the green and red column into contributions from HEDGE and URBS. The percentages were calculated in reference to the sum of all contributing discharge volumes (sum of green and blue columns in the beginning).

to the total discharge simulated by the model in the natural river at UpstreamSOD station. Nevertheless, this component analysis can give valuable information about the functioning and importance of the different processes and modules.

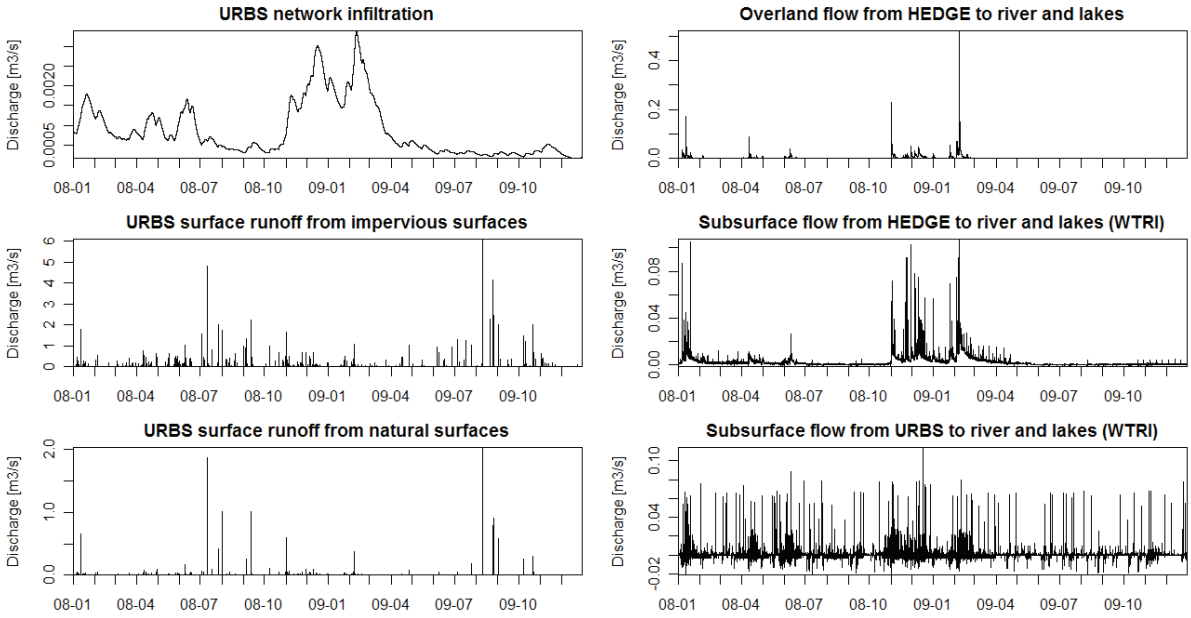

Figure 8.1.11.: The yearly development of the discharge components of the natural stream (upstreamSOD) in 2008 and 2009. On the left are the URBS network infiltration and surface runoff from impervious and natural areas and on the right the overland flow and subsurface flow contribution from HEDGE and URBS.

We can see that the instantaneous contribution of the surface runoff from impervious areas (built and road) can reach values up to 6 m^3s^{-1}, the surface runoff from gardens up to 2 m^3s^{-1} and the surface runoff from HEDGE overland flow only up to 0.5 m^3s^{-1}. Subsurface flow simulated with WTRI has maximal instantaneous values of 0.1 m^3s^{-1}, whereas the URBS network infiltration is one to two orders of magnitude smaller. Only the WTRIs connected to URBS vary between in- and exfiltration (as shown also on Figures 8.1.9 and 8.1.10).

We can observe that the subsurface flow from the WTRI interfaces has sharp fluctuations, whereas the network infiltration curve is smoother. This is a numerical effect, caused by the threshold for WTRI flow calculations which was implemented in the WTRI code in order to improve the calculation time. This fluctuation is not a real process observed on the field, and could probably be reduced by decreasing the threshold value for subsurface flow interactions, which is at the moment at a groundwater level change of 1cm.

The HEDGE subsurface flow shows clearly the wet winter period 2008/2009, which induces also more overland flow from HEDGE model units. In contrast, the surface runoff from the URBS model units has its maximum in the summer months. Yet as the HEDGE module simulates only saturation excess overland flow, this difference cannot be interpreted as a difference of behaviour between the rural and urban areas. It must more likely be attributed to the model structure. This component analysis shows thus that the surface runoff from URBS model units is the main discharge contributor. This could explain the overestimation of small events.

8.1.1.5. Simulated groundwater table

Figure 8.1.12 shows the average groundwater level per date (each day at 5:00 o'clock and at 17:00 o'clock) of all HEDGE and URBS model units. We can see a similar behavior of

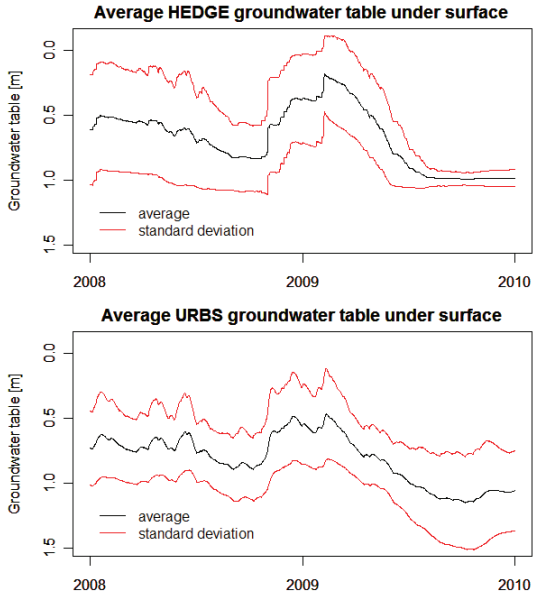

Figure 8.1.12.: Average groundwater depth from surface of the HEDGE (top) and URBS (bottom) model units. 0.0 corresponds to the surface level.

the HEDGE and URBS groundwater table with a maximum in the winter rainy period 2008/2009 and a minimum during the dry summer of 2009. The URBS groundwater level is on average about 20 cm lower than the HEDGE level, probably caused by the draining effect of the network infiltration. As the HEDGE soil was limited to 1m in this simulation, the groundwater disappears in the summer of 2009, whereas the URBS groundwater level, which is not limited, drops even lower than 1 m. In HEDGE, even if the groundwater table drops to the bedrock, there is still water available for the plants which is stored in the retention porosity. The groundwater table standard deviation is larger for HEDGE than for URBS elements except in summer 2009. This can be a consequence of the regulating effect of infiltration within the sewer drainage network. In summer 2009, the standard deviation of the HEDGE modules is smaller than that of UBRS module, because the groundwater table disappeared in most of the HEDGE modules due to the 1m soil depth.

Figure 8.1.13 shows the average groundwater table per model units in 2008 and 2009, respectively. As already shown by Figure 8.1.12, the groundwater table in the URBS model units is in general lower than in the HEDGE model units. Also the groundwater table of some of the URBS model units is more than 1m below surface level. The soil is generally dryer in 2009 than in 2008 due to the different climatic conditions. This confirms our conclusions concerning the water balance, that in 2009 the soil storage was emptied.

The map of 2008 also highlights the importance of the geographical preprocessing, which means that the average altitude of the polygons and river reaches governs the subsurface lateral flow pattern. Therefore, the manner how the polygons are divided and arranged is important. For example, in the south-west corner (black rectangle in Figure 8.1.13) there are two model units with a higher groundwater table, because they border a long road polygon, which average altitude is not really representative. We can also see that

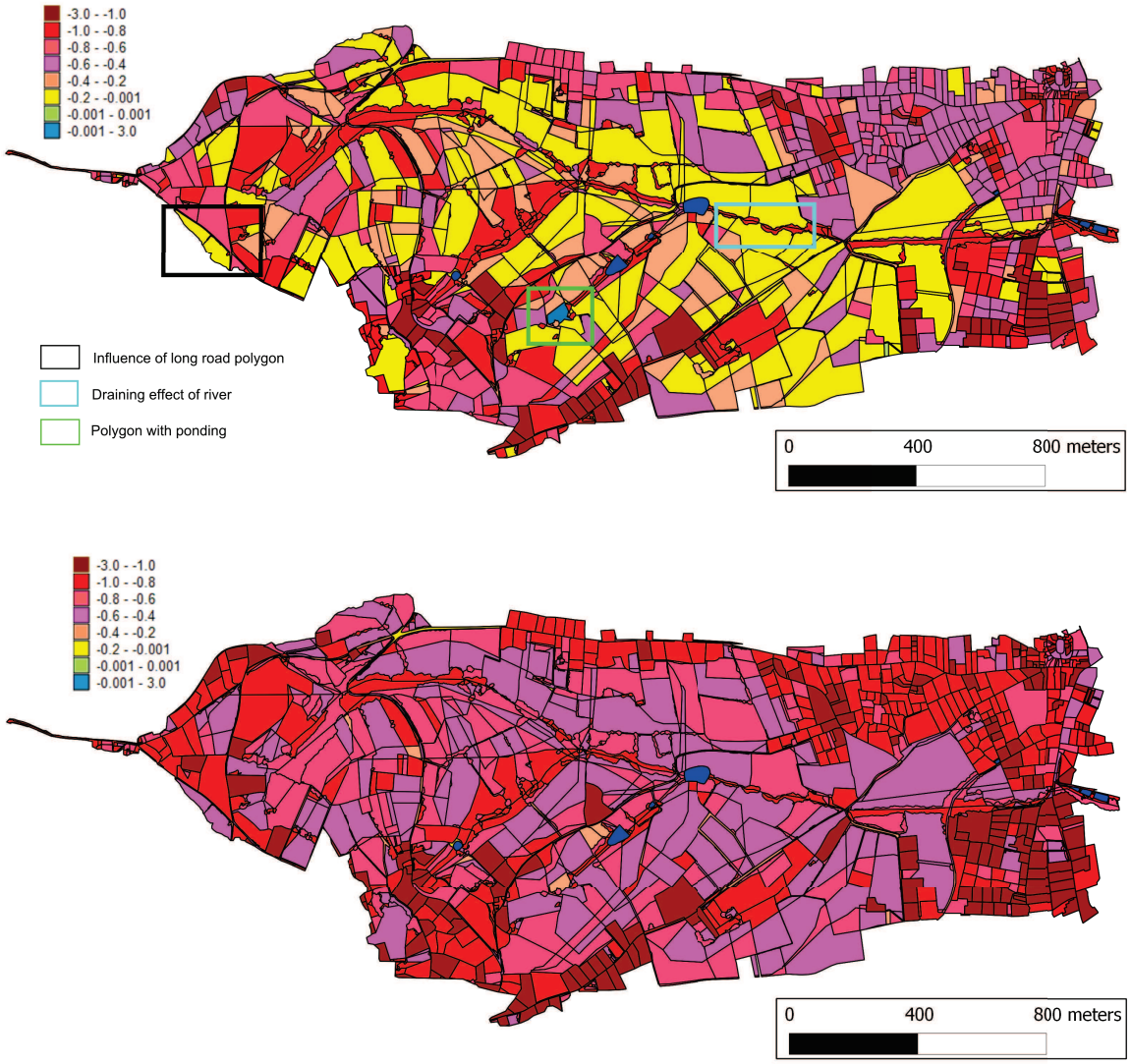

Figure 8.1.13.: Map of average groundwater table (distance from surface level [m]) in 2008(top) and 2009 (bottom). Positive values signify ponding.

the model units adjacent to drainage reaches (blue rectangle) are dryer than the other model units. This could be caused by the altitude of long drainage reaches, which was set below the lowest bordering polygon. There are also a couple of model units with nearly constant ponding (green rectangle), located in depressions.

8.1.1.6. Simulated evapotranspiration

Figure 8.1.14 shows the annual actual evapotranspiration (AET) in 2008 and 2009 for the HEDGE and URBS model units, as well as the annual actual evaporation for the lakes and retention basins. In 2008 the actual evaporation of the lakes was between 800 and 1000 mm, whereas in 2009 it was between 1000 and 1200 mm, which is caused by the higher insolation in 2009.

The URBS model units can be clearly discerned as their AET is up to ten times lower

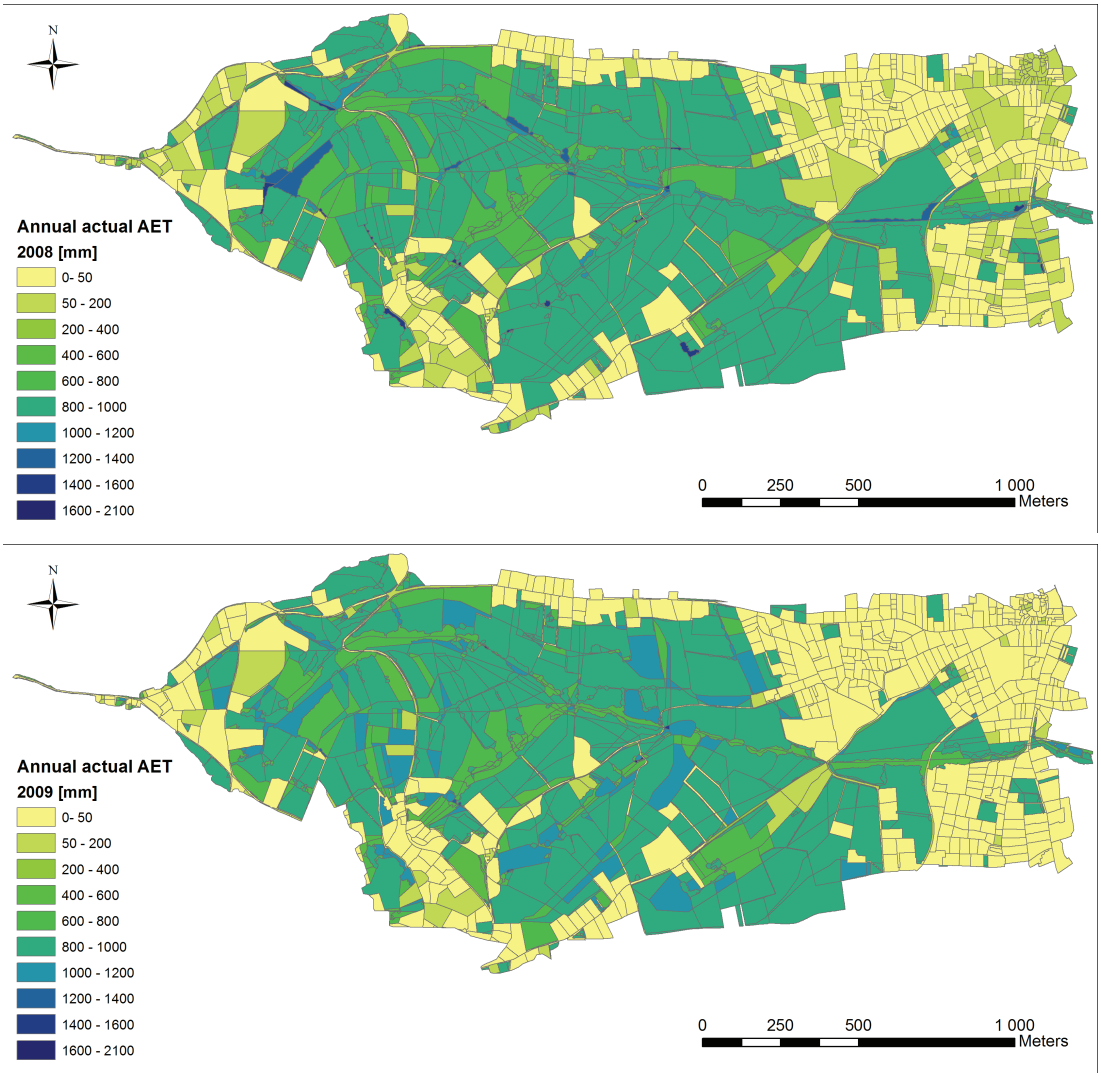

Figure 8.1.14.: Maps of simulated annual actual evapotranspiration (AET) in 2008(top) and 2009 (bottom). The AET is given in mm per year.

than the AET of most of the HEDGE model units. Only some parcels with bare soil (modeled with HEDGE), where the crop coefficient was set to a constant value of 0.35 are in the same order of magnitude than the URBS parcels with 50 to 200 mm of AET. The low AET of the URBS model units can be related to several factors. First of all, the impervious surface creates direct runoff and thus the water is no longer available for evapotranspiration. Furthermore, there is less vegetation in the urbanized area and the soils of HEDGE and URBS model units are represented differently. In HEDGE, the soil is separated in retention and drainage porosity (refer to section 5.1.1), where the retention porosity is drained by evapotranspiration and the drainage porosity serves the lateral subsurface flow. This separation avoids that the soil is completely drained by groundwater interaction and it keeps water available for evapotranspiration until the permanent wilting point is reached, which is in contrast to the simple reservoir representation of the soil in URBS. In 2008 there are some URBS units with a higher AET, which is probably due to the wetter conditions and thus the higher water availability.ă

Concerning the HEDGE model units, in particular in 2008 the AET differences can

be related to the different crop coefficient classes (see Table 7.3.1 in Chapter 7) and thus to the different land use classes. In 2008, the highest AET values with more than 1200 mm were caused by forest, for which the crop coefficient rises up to a value of 2. Furthermore, cultivated crop can be distinguished, having an AET of 600 to 800 mm. In 2009 the forest had lower AET values than in 2008, which indicates that probably in 2009 there was not enough water for trees. However, some of the agricultural parcels have an evapotranspiration reaching more than 1000 mm of AET.

8.1.2. Event based analysis

Three summer and three winter rainfall events were selected for the event analysis. As 2009 was a dry year with a limited number of events, only two events are in 2009 and the other four in 2008. The main characteristics are summarized in Table 8.1.2.

Table 8.1.2.: Selected events with characteristics of the observed discharge, such as the peaks in the natural stream (upstreamSOD), the sewer system (ss) and the sewer overflow device (SOD), as well as the base flow of the natural stream.

Name	Date	Rain mm	Peak upstreamSOD m^3s^{-1}	Peak ss m^3s^{-1}	Peak SOD m^3s^{-1}	Baseflow m^3s^{-1}
Jan2008	2008-01-11	29.5	0.71	0.07	0.20	0.029
Jul2008	2008-07-11	34.9	0.22	0.09	0.40	0.01
Aug2008	2008-08-01	15.9	0.19	0.08	0.16	0.001
Nov2008	2008-11-01	83.3	2.78	0.06	0.20	0.087
Feb2009	2009-02-06	61.6	1.13	0.06	0.27	0.052
Aug2009	2009-08-09	25.1	0.58	0.1	0.49	0.0

The winter storm events had the largest peak values, between 0.71 and 2.78 m^3s^{-1} at upstreamSOD, whereas the peaks of the summer storm events varied between 0.19 and 0.58 m^3s^{-1}, see table 8.1.2. One of the summer storm event happened on a dry stream bed, whereas the base flow of the winter storm events rose up to 87 ls^{-1}. All of the events triggered combined storm water overflow of up to 490 ls^{-1}. A relatively homogeneous rainfall with a total amount of 83.3 mm caused the largest runoff event on the 1st to 2nd of November 2008. The rainfall volume of the other events varied between 15.9 and 61.6 mm, see table 8.1.2. The sewer system reacted only little to most of the rainfall events, with maximal peak values of 100 ls^{-1}. For the winter storm events the rainfall lead to a rise in the base flow of the sewer system, which indicates groundwater infiltration.

Figures 8.1.15 to 8.1.17 show the comparison of the simulated and observed hydrographs for all of the events and the three measurement stations upstreamSOD in the natural river, the sewer system and the SOD.

In order to better compare the observed and simulated values the following criteria were calculated: the difference of the peak values, of the base flows at the begin and at the end of the event, the difference of the discharge volumes and of the peak time. These criteria were calculated as absolute values and as percentage in relation to the measured values, see table 8.1.3.

The discharge volumes are also shown as runoff coefficients (percent of the rainfall) in Figure 8.1.18. Regarding this figure, the winter storm events are clearly distinguishable

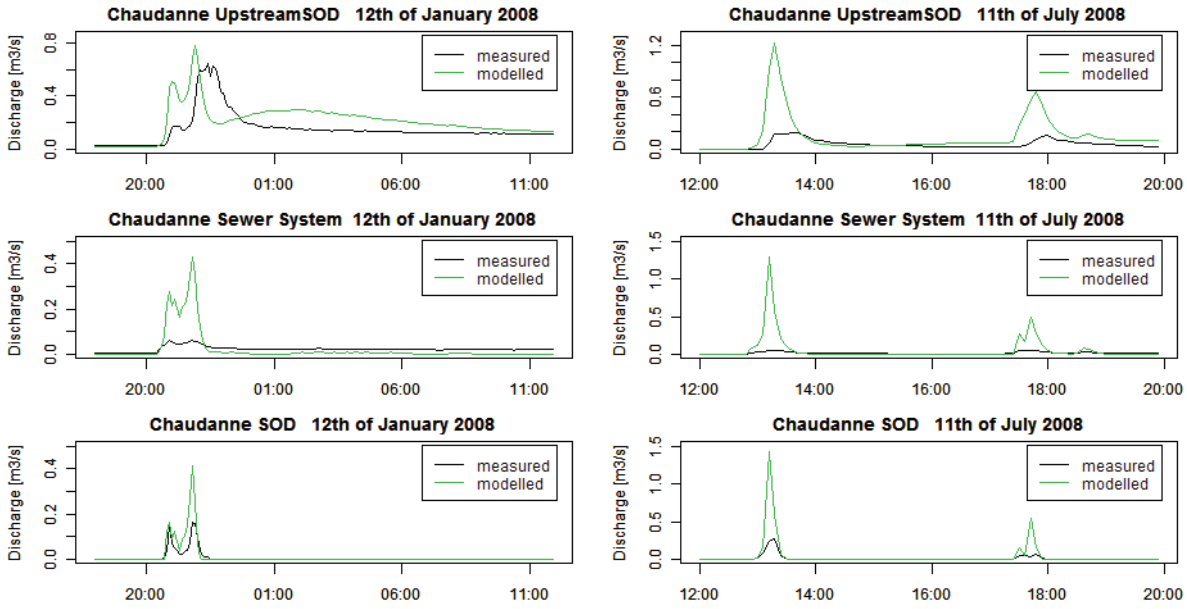

Figure 8.1.15.: Simulated versus observed discharge for the events at the 11th of January 2008 (left) and at the 11th of July 2008 (right). The upper graphics show the discharge at upstreamSOD, the middle graphics the discharge in the sewer system and the lower in the sewer overflow device (SOD). The limits of the y-axis are different.

from the summer events, as their runoff coefficients in the "natural2 catchment (UpstreamSOD) are much larger. The discharge volumes in the natural stream for nearly all of the events, except the events in January and November 2008, were overestimated by the model. Most of the sewer overflow volumes were also overestimated. Concerning the discharge in the natural stream, the peaks of all summer storm events were largely overestimated with peak values exceeding the measured values of up to 1 m^3s^{-1}, see table 8.1.3. However, the winter storm peaks of the events in January 2008 and February 2009 were well simulated and the peak of the event in November 2008 was underestimated.

In the sewer system, the base flows before and after the events were always underestimated. PUMMA simulates high peaks in the sewer system for all of the events (of up to 1.8 m^3s^{-1} more than the observed values), but no significant increase in the base flow after the events, although this is observed in the measured values. This can be seen in table 8.1.3, as the difference in the base flow increased for each event from the start to the end of the event. An increase in the base flow, or tailing, can only be seen in the simulation of the natural stream. Regarding the composition of the model, nearly no HEDGE model units are connected to the sewer system, but only URBS model units. This means, that apparently URBS simulates with the current parameterization too high peaks and a too low groundwater infiltration into the sewer system. However, the difference of the simulated and the observed peak values is much larger than the difference of the base flow values.

The errors in the peak times were just a couple of minutes for the summer events in all of the drainage networks. The winter events, which lasted longer, had differences of 30 to 110 minutes in the natural stream. For four of the six events the times of the sewer overflow events had only 1 to 2 minutes error, see table 8.1.3. The peaks of the winter sewer overflow events were relatively well simulated, whereas the peaks of the summer

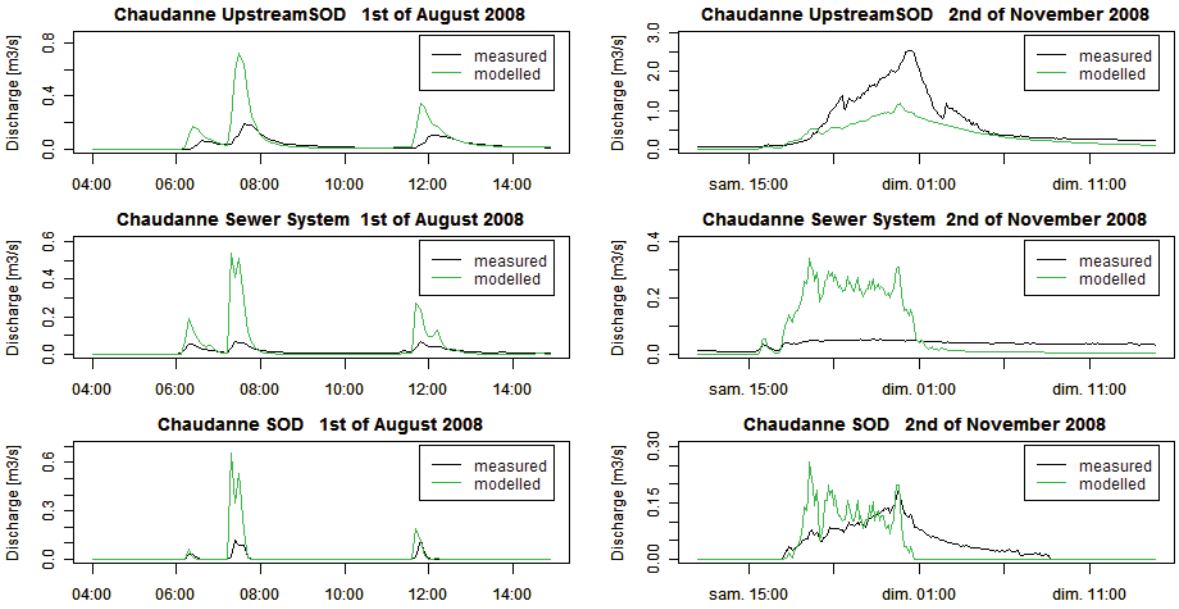

Figure 8.1.16.: Simulated versus observed discharge for the events at the 1st of August 2008 (left) and at the 2nd of November 2008 (right). The upper graphics show the discharge at upstreamSOD, the middle graphics the discharge in the sewer system and the lower in the sewer overflow device (SOD). The limits of the y-axis are different.

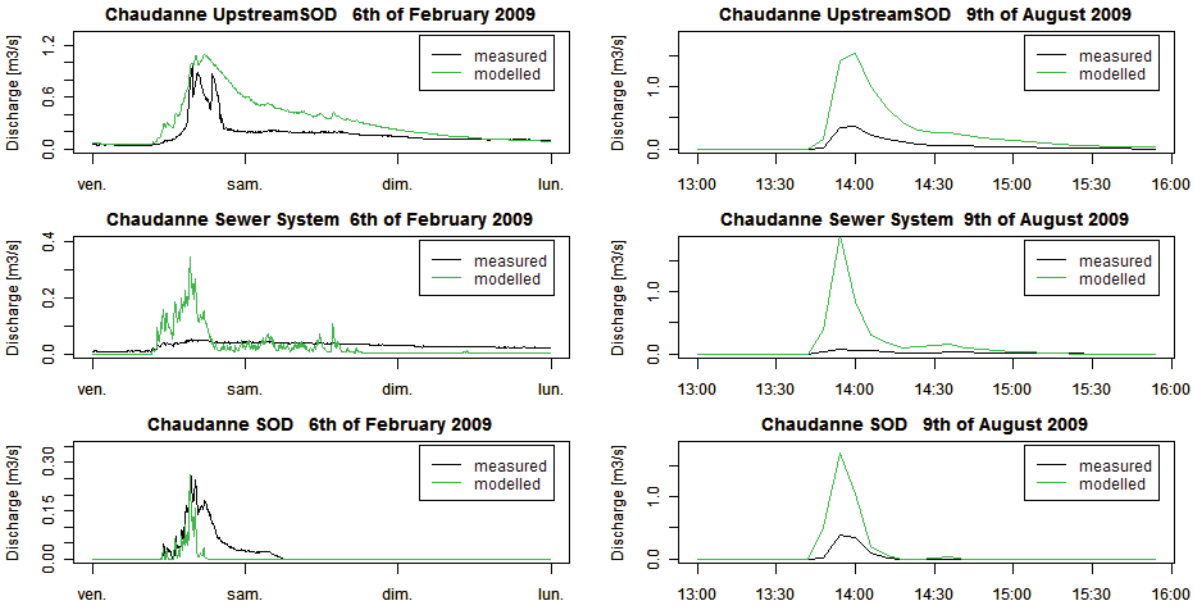

Figure 8.1.17.: Simulated versus observed discharge for the events at the 6th of February 2009 (left) and at the 9th of August 2009 (right). The upper graphics show the discharge at upstreamSOD, the middle graphics the discharge in the sewer system and the lower in the sewer overflow device (SOD). The limits of the y-axis are different.

events were overestimated by 0.5 to 1.2 m^3s^{-1}. The SOD, which is activated only during large storm events, has no base flow, which was correctly simulated by PUMMA.

Figure 8.1.19 shows the groundwater level before and after a summer and winter event. The event in August 2009 was selected as summer event, and the event in November 2008

Table 8.1.3.: Differences (modelled - observed) of the peak values, the base flow at the begin and end of the event, the time to peak and the volumes in absolute values and percent. Negative values signify underestimation of the observed discharge by the model, positive values overestimation. The percent are calculated in comparison to the observed values. The difference in base flow is shown in ls^{-1} as its values are small. The interpretation of the base flows has to be done carefully as the measured discharges at low flow have a high uncertainty.

Event	River	Peak $m^3s^{-1}(\%)$	Base flow begin $ls^{-1}(\%)$	Base flow end $ls^{-1}(\%)$	Time to peak (min)	Volume $m^3(\%)$
Jan2008	upSOD	0.07(10)	-5.2(-18)	-37.9(-57)	-26	-3651(-12.2)
	SS	0.37(594)	-1.9(-64.1)	-7.9(88.1)	54	-2744(-58.7)
	SOD	0.21(107)	0	0	2	309(76.4)
Jul2008	upSOD	1.0(460)	-8.3(-83)	-1.7(-34)	5	3808(109.8)
	SS	1.2(2170)	-0.3(-27.1)	-4.3(-85.9)	0	625(50.9)
	SOD	1.0(261)	0	0	-1	817(256)
Aug2008	upSOD	0.53(274)	-0.07(-6.7)	3.4(114)	-2	1433(91.8)
	SS	0.47(715)	-0.4(-36.5)	-2.4(-79.2)	-6.0	699(63)
	SOD	0.5(323)	0	0	-2	554(263)
Nov2008	upSOD	-1.61(-58)	-56.5(-65)	-120.4(-75)	-38	-42985(-49.5)
	SS	0.29(546)	-10.3(-93.3)	-17(-89.8)	-180	-311(4.4)
	SOD	0.06(31)	0	0	-307	-552(-16)
Feb2009	upSOD	-0.04(-3)	17.5(34)	-13.5(-75)	108	36197(78.1)
	SS	0.29(553)	-8.2(-82.0)	-19.2(-87.3)	-12	-862.7(-10.8)
	SOD	-0.01(-4)	0	0	-11	-3292(-4)
Aug2009	upSOD	0.96(165)	0.8(-)	41.3(-)	6	4022(605.6)
	SS	1.81(2453)	-1.48(-74.1)	-1.45(-73.3)	0	1402(396)
	SOD	1.2(248)	0	0	1	969(304)

as winter event. First of all, we can remark the difference in the groundwater level during the dry and wet periods. The rainfall event leads to an increase of the groundwater level in the case of the winter event, but not for the summer event. This confirms the hypothesis that during summer events, most of the rainfall contributes to surface runoff and not to the subsurface flow. We can also see that for the large event in November 2008 many HEDGE model units had ponding and created thus overland flow.

Figures 8.1.20 and 8.1.21 show the contributions of the discharge components coming from different LIQUID modules to the natural river network at one moment for a summer and a winter event. The graphs are similar to the graphs for the annual analysis in Figure 8.1.9 and 8.1.10. Here, the discharge corresponds to the sum of all contributions of one module signal (e.g. URBS network infiltration) to the concerned drainage network at a given time.

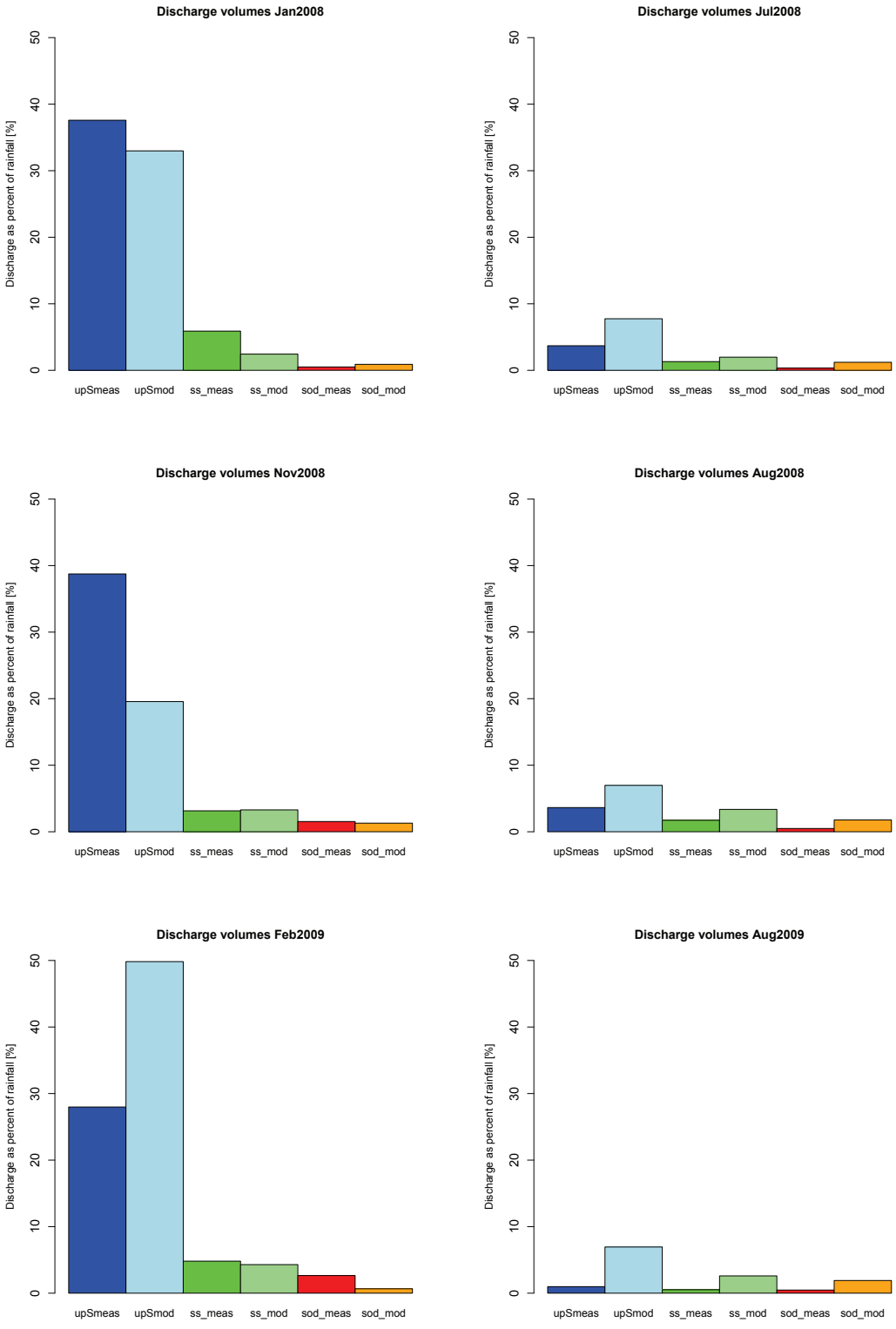

Figure 8.1.18.: Measured (meas) versus modeled (mod) discharge volumes in percent of the rainfall volume for the three measurement stations (upS-upstreamSOD in blue, ss-sewer system in green, SOD-sewer overflow device in red/orange) and for all events.

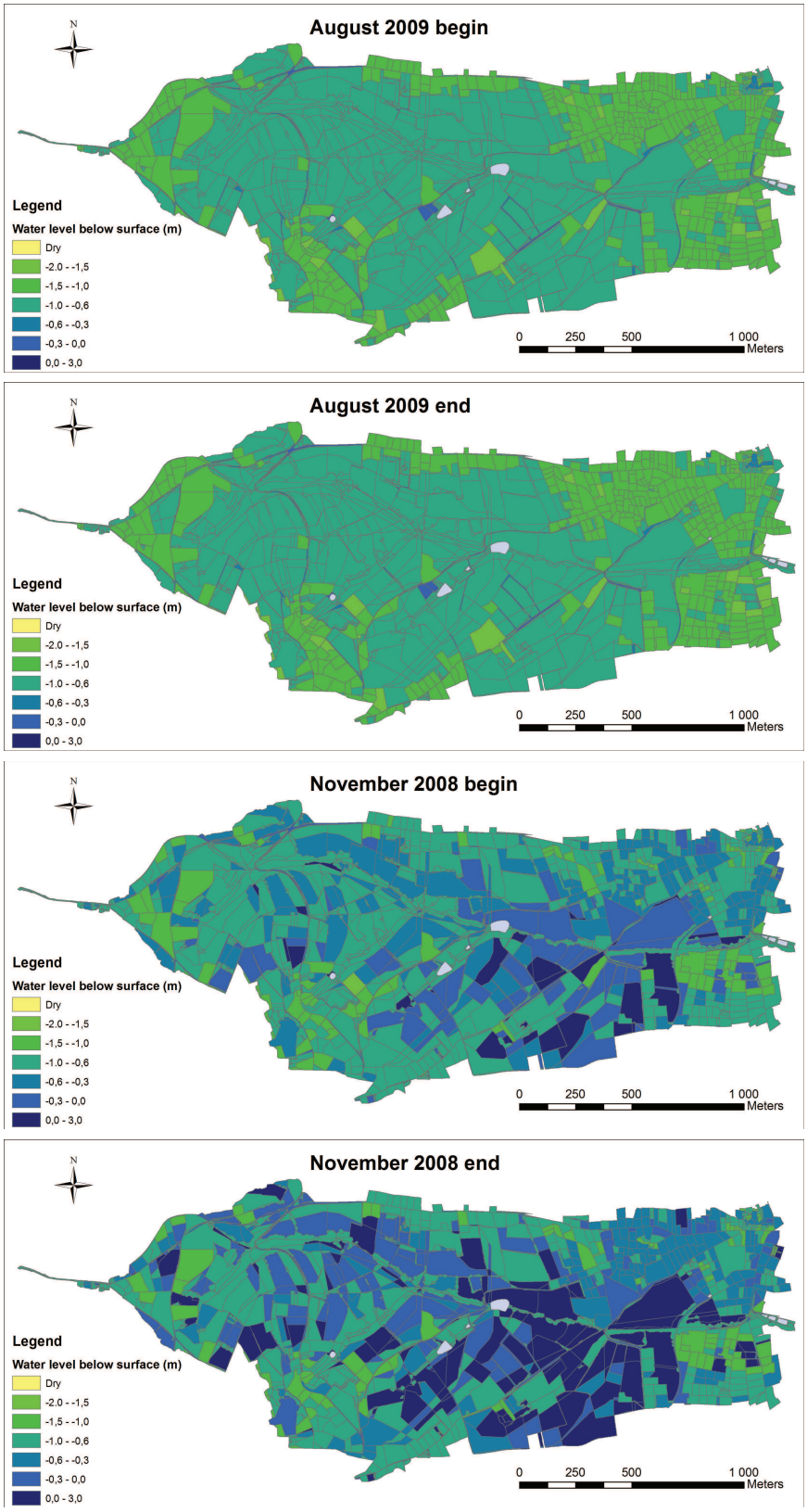

Figure 8.1.19.: Maps of the groundwater depth below surface for a summer (August 2009, upper graphs) and winter event (November 2008, lower graphs). The groundwater depth before the events is shown on the left side and after the events on the right side.

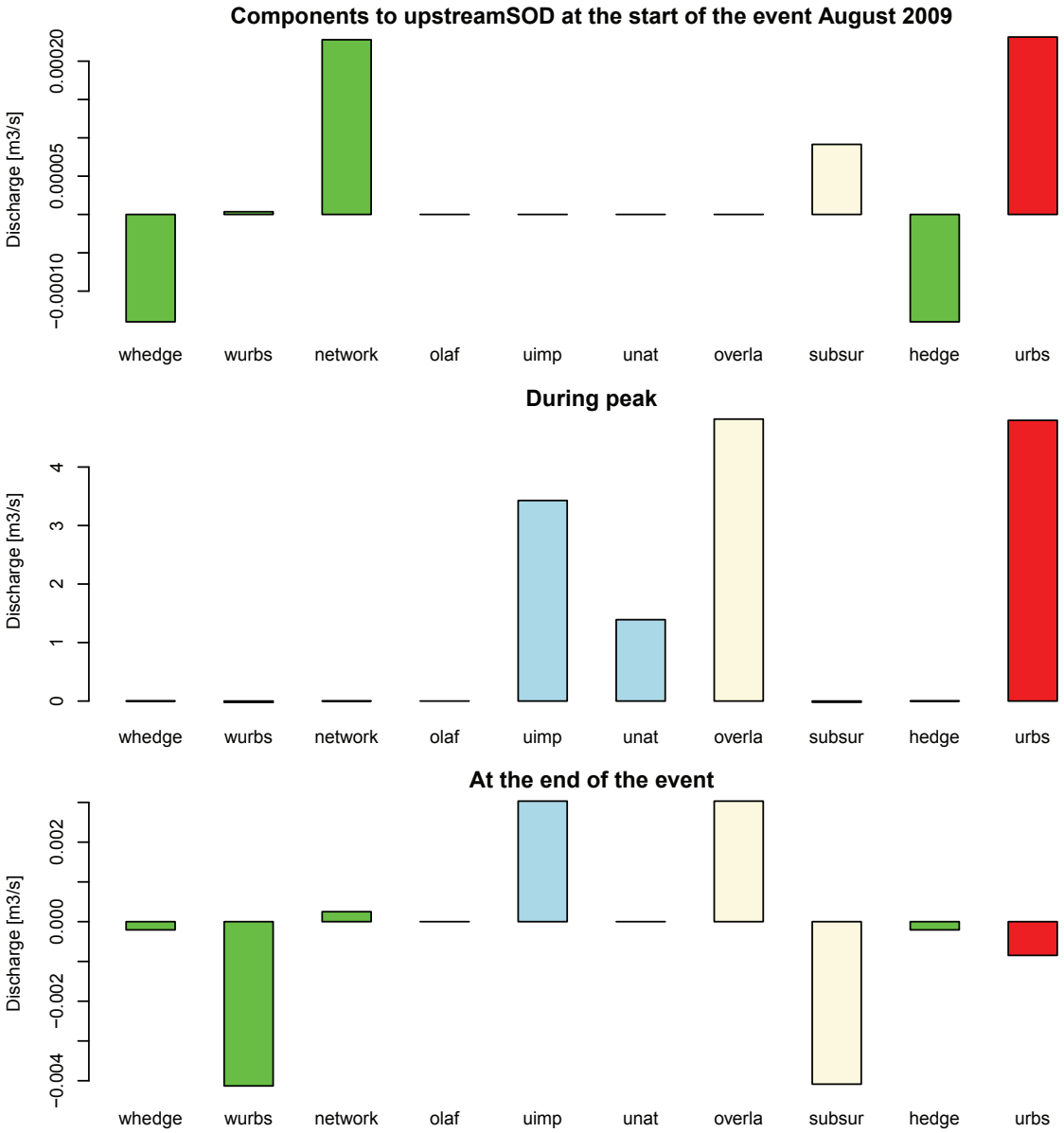

Figure 8.1.20.: Analysis of the different components contributing to the discharge in the natural river for the summer event in August 2009. Each Figure shows the discharge before(top), during(middle) and after(bottom) the events. From left to right, the components are the discharge from WTRI interfaces connected to HEDGE(whedge) and URBS(wurbs), the URBS network infiltration (network), the contribution from OLAF and thus HEDGE modules(olaf), the surface runoff from URBS divided in runoff from the impervious surfaces(uimp) and natural areas(unat). The beige columns summarize the module contributions into overland(overla) and subsurface flow(subsur), and the green and red columns into contributions from HEDGE and URBS.

This means, that we do not show a real hydrograph separation into components of the discharge at the measurement station.[2] However, it still gives important information about the characteristics of the discharge, e.g. if it is rather composed of base flow or

[2]This would require the development of component routing in the RIVER1D module, which does not exist in the current version.

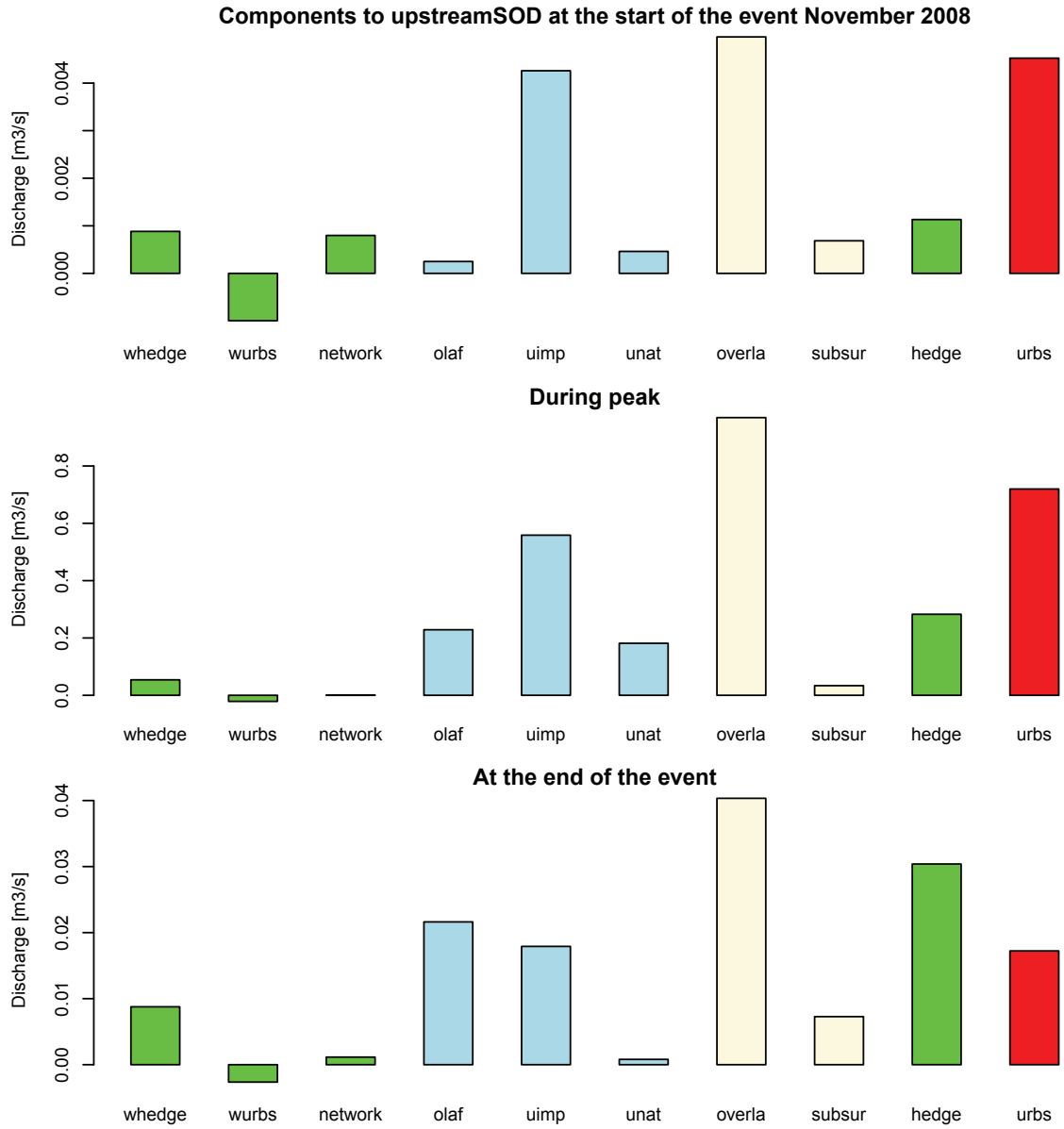

Figure 8.1.21.: Analysis of the different components contributing to the discharge in the natural river for the winter event in November 2008. Each Figure shows the discharge before(top), during(middle) and after(bottom) the events. From left to right, the components are the discharge from WTRI interfaces connected to HEDGE(whedge) and URBS(wurbs), the URBS network infiltration (network), the contribution from OLAF and thus HEDGE modules(olaf), the surface runoff from URBS divided in runoff from the impervious surfaces(uimp) and natural areas(unat). The beige columns summarize the module contributions into overland(overla) and subsurface flow(subsur), and the green and red columns into contributions from HEDGE and URBS.

surface runoff, and which module (URBS or HEDGE) creates more discharge.

The analysis of the components shows that the URBS module with its surface runoff on impervious and pervious surfaces is the main discharge contributor. This is especially the case for the peaks of summer storm events. Before and after the events, the URBS network infiltration is the most important factor. However, the order of magnitude for the network

infiltration is at least three orders of magnitude smaller than the peak surface runoff. Only for the winter rain event in the natural stream (Figure 8.1.21) before and after the flood event, the HEDGE contributions become more important than the URBS contributions. This HEDGE discharge is composed of overland and subsurface flow, whereas during the peak the overland flow takes the major part. A clear difference between summer and winter events is only visible for the natural stream and not for the sewer system or the pipes towards the retention basins (not shown here). After the summer storm event, the WTRI interfaces connected to URBS enable the infiltration of water from the natural stream into the urban soil (Figure 8.1.20 top). Figures G.0.1 to G.0.4 in the appendix show the contributions of the discharge components to the combined sewer network and the rainwater pipes leading to the retention basins for the summer and winter event. As mainly URBS model units are connected to the pipes, it is the main contribution. We can also see that for summer and winter events the main contribution during the peak is overland flow, whereas subsurface flow dominates the start and end of the events.

8.1.3. Conclusions

The analysis of the reference simulation showed that PUMMA is able to simulate the hydrological dynamics of small peri-urban catchments with mixed drainage systems. It simulates well the different dynamic of fast urban response and slower rural response. The timing of summer and winter peaks was well represented, as well as the rise of the base flow during wet winter months and the drying of the stream bed in summer. This can also be seen in the simulated monthly discharge regimes, for which the simulation of the seasonal variability corresponds well to the measured values. However, the peak values of summer storm events in the sewer system and the natural stream were overestimated. The component analysis showed that this high discharge is mainly caused by surface runoff from URBS model units. Furthermore, it was shown that the simulated URBS network infiltration is lower than the raise of the sewer base flow observed in the field.

On the annual basis, the model showed that the actual evapotranspiration on HEDGE model units is higher than on URBS model units. However, it was rather similar for the wet 2008 year and the dry 2009 year, which indicated that there was enough water in the soil to satisfy the plant uptakes in 2009, even if the groundwater table dropped towards value set for the bedrock depth in 2009.

In the following section we will investigate if a change of some URBS parameters can lead to a decrease of the surface runoff peak values and a raise of the sewer base flow. Concerning the natural processes in the catchment, we will test the influence of the soil depth and the lateral hydraulic conductivity.

8.2. Sensitivity tests

8.2.1. Urban parameters

The previous chapter showed that the overestimation of the peak flows for small events is mainly caused by URBS surface runoff. The URBS module provides two parameters, the built and road link coefficients, which define the quantity of created surface runoff, which is directly connected to the drainage system. In the reference simulation, both coefficients

were set to 1, which means that 100% of the surface runoff created on impervious areas was directly connected to the sewer system. By reducing these factors, the surface runoff from impervious areas can be divided into runoff directly entering the drainage system and runoff flowing onto the natural part, which can then infiltrate, evaporate or run off. In order to test the influence of these parameters, we set the built link coefficient to 0.5 and the road link coefficient to 0.6. However, this concerned only about 70 % of the URBS model units, as the link coefficients were kept at 1 for the URBS model units without a natural part, such as the rural roads, as this would have caused a loss of water. Figure 8.2.1 shows a comparison of the discharge at the upstreamSOD station simulated with the modified link coefficients and the reference simulation. We can see that the change of the link coefficients causes a decrease of most peaks in the natural river. In the sewer system (Figure G.0.5 in the appendix) some peaks are lower, others are higher than during the reference simulation and in the SOD (Figure G.0.6 in the appendix) the change of the link coefficients lead rather to higher than to lower peaks.

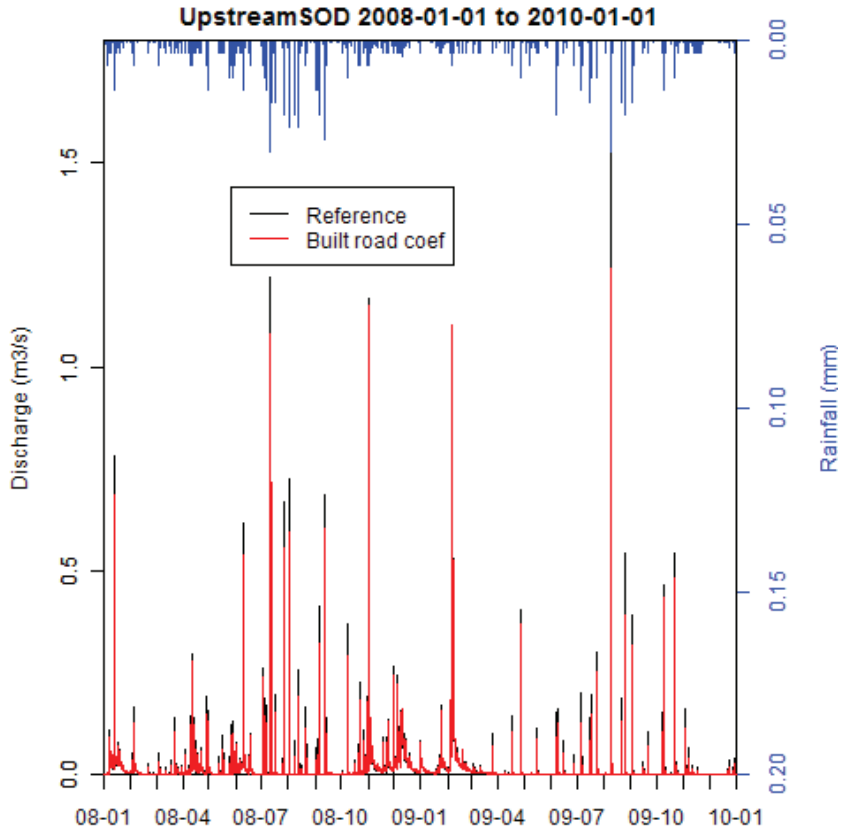

Figure 8.2.1.: Simulation with modified URBS built/road link coefficients compared to the reference simulation in the natural river (UpstreamSOD). The built link coefficient is 0.6 instead of 1, and the road link coefficient 0.5.

In order to better understand the influence of these parameters, Figure 8.2.2 shows a comparison of the URBS surface runoff components to the reference simulation. As we expected, the runoff from impervious surfaces decreased. Probably due to a higher infiltration of water on the natural part, the network infiltration increased (left panel in Figure 8.2.4), as did the natural surface runoff. This is supposably related to a higher ponding on the natural part of URBS, caused by the extra runoff from impervious areas.

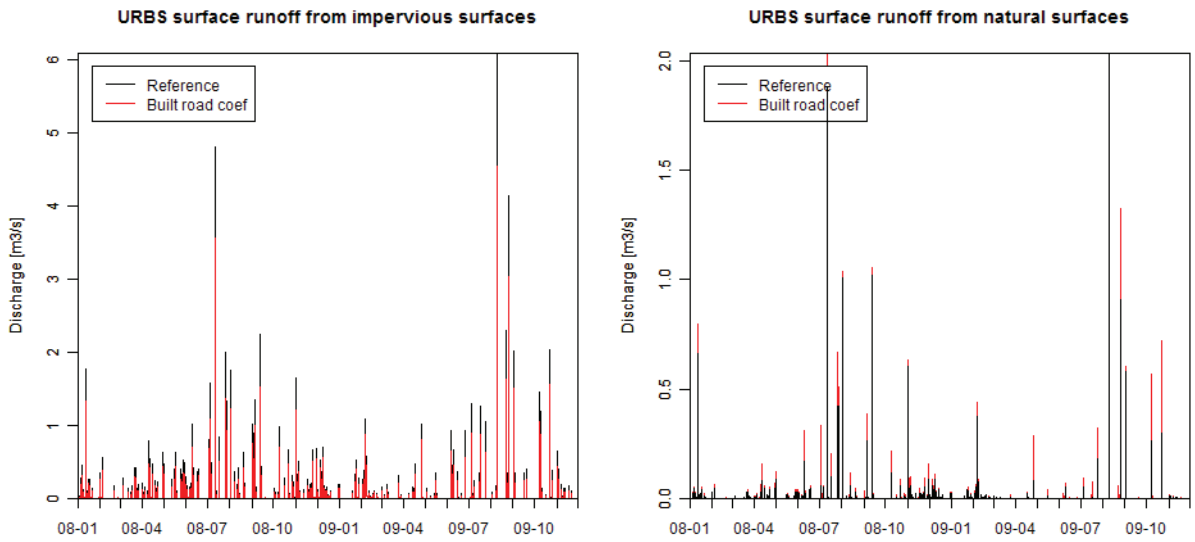

Figure 8.2.2.: URBS surface runoff from impervious (left) and natural areas (right) for modified built/road link coefficients compared to the reference simulation for years 2008 and 2009. The built link coefficient is set to 0.6 and the road link coefficient to 0.5

Figure 8.2.3 shows the average groundwater level of all URBS model units. As we expected, the groundwater level increased as compared to the reference simulation, probably because of the higher infiltration in the natural part of URBS.

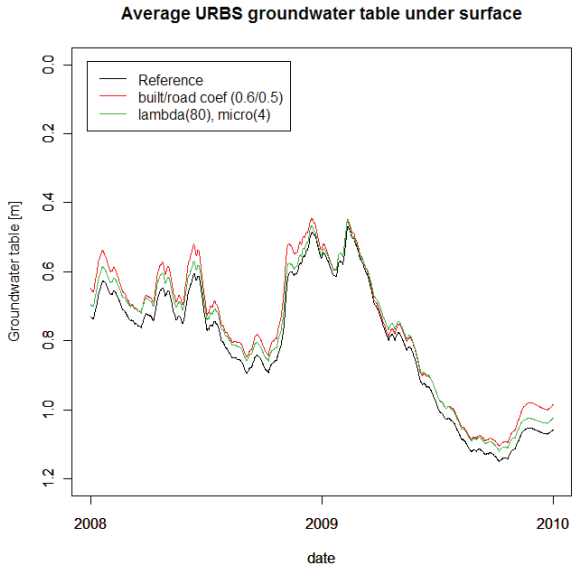

Figure 8.2.3.: Sensitivity of URBS groundwater table evolution to changes in the built and road link coefficients (set to 0.6 and 0.5), and URBS λ and μ network parameters (80/4), refer to Tables 5.2.1 and 5.2.2 in Chapter 5.2.1.

The analysis of the reference simulation (section 8.1) also pointed out the underestimation of the raise in the sewer base flow after events. In URBS the network infiltration is calculated with the ideal drain approach (equation 5.2.1), which is governed by several parameters. We chose to test the influence of λ, which is the groundwater drainage coefficient varying between 0 and 100, and μ, which is the groundwater drainage exponent. In order to increase the network infiltration and thus the base flow, we doubled λ from 40 to 80 and μ from 2 to 4. The sensitivity of these parameters on the discharge was relatively small . The right panel of Figure 8.2.4 shows the URBS network infiltration for this simulation and there, we can see an increase of the network infiltration peaks. However, the network infiltration during dry periods is slightly lower than in the reference simulation. This probably causes the increase of the URBS groundwater table visible in Figure 8.2.3. This raise could also be enhanced by contributions from WTRI interfaces as was shown in Section 8.1.1.4.

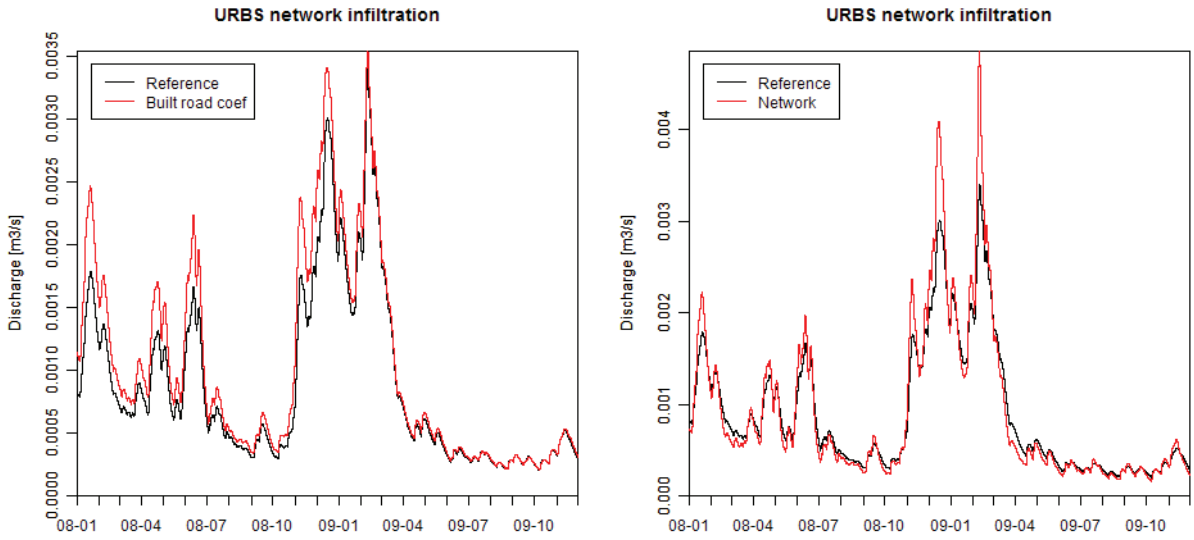

Figure 8.2.4.: URBS network infiltration for modified built/road link coefficients (left) and modified network parameters (right) compared to the reference simulation for years 2008 and 2009. The built link coefficient is set to 0.6, the road link coefficient to 0.5, λ to 80 and μ to 4.

8.2.2. Soil parameters

8.2.2.1. Soil depth

As we have seen in chapter 3 no distributed information of the soil depth was available. The geophysical investigations and installation of the piezometers showed soil depths between 1 and 2m, with a large altered bedrock layer below. We chose a constant soil depth of 1 m for the reference simulation as first approximation. However, Thoré (2008) showed that the soil depth is correlated to the altitude. Therefore, we tested the variation of the soil depth with the altitude, distributing it into three classes: the soil depth of model units with altitudes between 300 to 400 m a.s.l. was set to 3m, between 400 and 500 m to 2m and between 500 and 600 m to 1m. Like for the reference simulation, the

groundwater table was initialized at half of the soil depth at the start of 2007, and at the pipe level for the URBS model units.

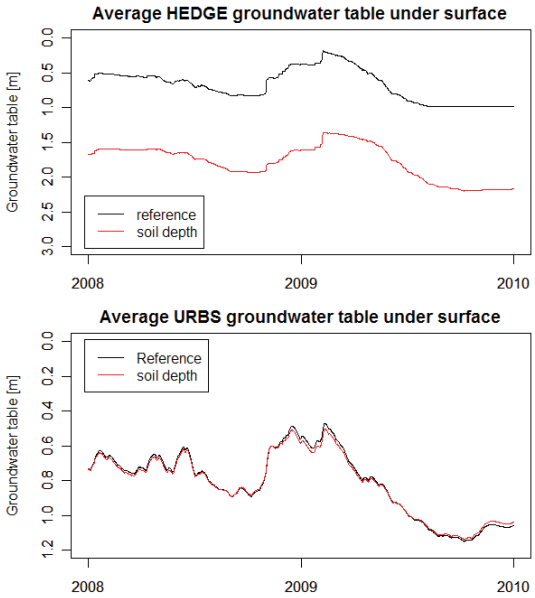

Figure 8.2.5.: Sensitivity of HEDGE and URBS groundwater table evolution to changes in the soil depth from 1m to a between 1 and 3 m varying soil depth.

Figure 8.2.5 shows the average groundwater level of the HEDGE and URBS model units for the simulation with the varying soil depth compared to the reference simulation. The first significant change that we can observe is the decrease of the groundwater table in the HEDGE model units of around 1 m. This is probably caused by the increased soil storage, but also due to the different initial conditions. The dynamic of the HEDGE groundwater table is similar for both simulations. The URBS groundwater table level drops slightly in 2008 and rises at the end of 2009 during the dry season compared to the reference simulation.

Concerning the discharge in the natural stream, the increase of the soil depth induces a decrease of the winter base flow and peak values and an increase of the summer peak values, see Figure 8.2.6. This leads to a less realistic representation of the observed discharge, as we already underestimate the winter base flow and overestimate the summer peaks (see Figure 8.1.1). In contrast, the influence of the soil depth on the discharge of the sewer system and pipes towards the retention basins is only minor, see Figures G.0.7 and G.0.8 in the appendix.

This change of the river discharge is caused by the decrease of the HEDGE surface runoff and subsurface flow, which are important in winter (see Figure 8.2.7 and Figure G.0.10 in the appendix) and the increase of the URBS surface runoff components from natural and impervious areas (see Figure 8.2.7 and Figure G.0.9 in the appendix). The URBS network infiltration decreases also slightly, especially in the wetter periods (Figure G.0.9 in the appendix). The change of the soil depth influences also the WTRI subsurface flow from the URBS model units to the river, however, without a clear tendency.

This simulation shows that the model is quite sensitive to the soil depth. A thinner soil facilitates the simulation of winter base flow in the natural river, as it increases HEDGE subsurface and overland flow. The increase of the overland flow for the 1m soil depth

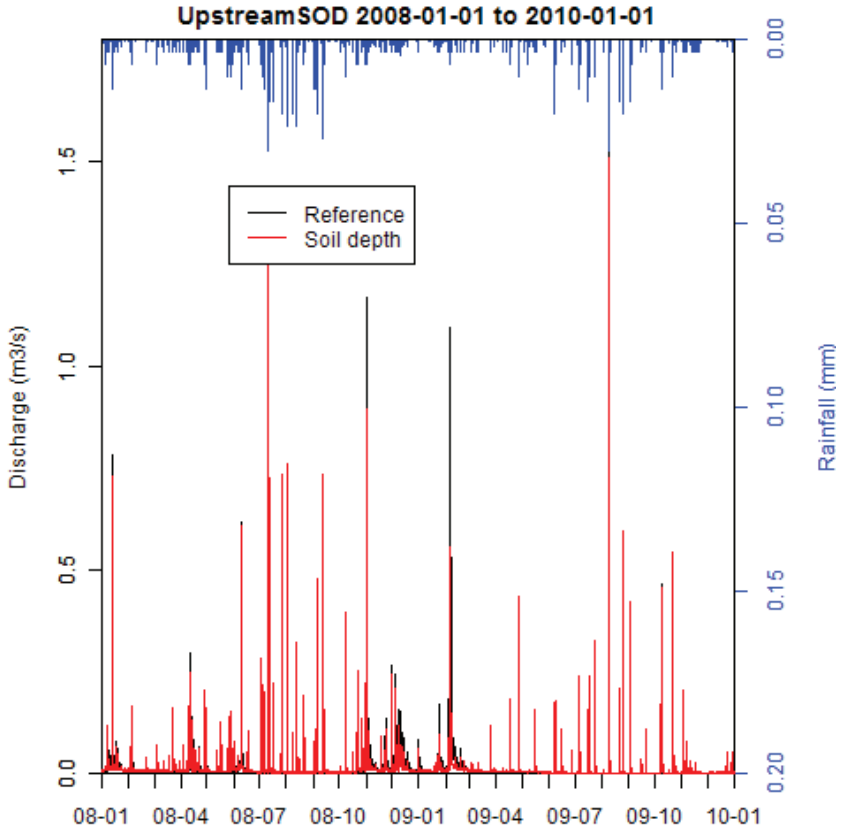

Figure 8.2.6.: Simulation with modified soil depth compared to the reference simulation in the natural river. The soil depths varies between 1 and 3 m instead of the constant 1 m soil depth of the reference simulation.

is probably caused by the structure of the HEDGE module, as it allows overland flow only when the soil profile is completely saturated. A thinner soil enables the creation of saturated zones during wet periods and it increases thus the event discharge. However, we know from field investigations (Ruysschaert, 2004; Goutaland, 2009) that the soil can be deeper than 1 m. Therefore, before concluding from the model results to the real soil depth, it would be interesting to exchange the HEDGE module with the FRER1D module, a physically based soil module, in which the soil is represented by different layers and with which Horton overland flow can be simulated.

8.2.2.2. Permeability

The hydraulic conductivities for the reference simulation were derived from particle size distributions based on pedo-transfer functions, see chapter 7. The particle size distributions determined by Gonzalez-Sosa et al. (2010) and (SIRA, 2011), are based on field samples, which are point measurements. In order to take into account the local variability Gonzalez-Sosa et al. (2010) took three samples per site. However, for lateral flow processes not only the soil texture is important, but also the presence of macropores, preferential flow paths or interflow on locally present layers with low permeabilities. The geology of the Chaudanne catchment with its altered gneiss favors the generation of relatively impervious clay layers on which interflow can happen. Newman et al. (1998) for example made the following conclusions based on environmental tracer investigations for a hill-slope in

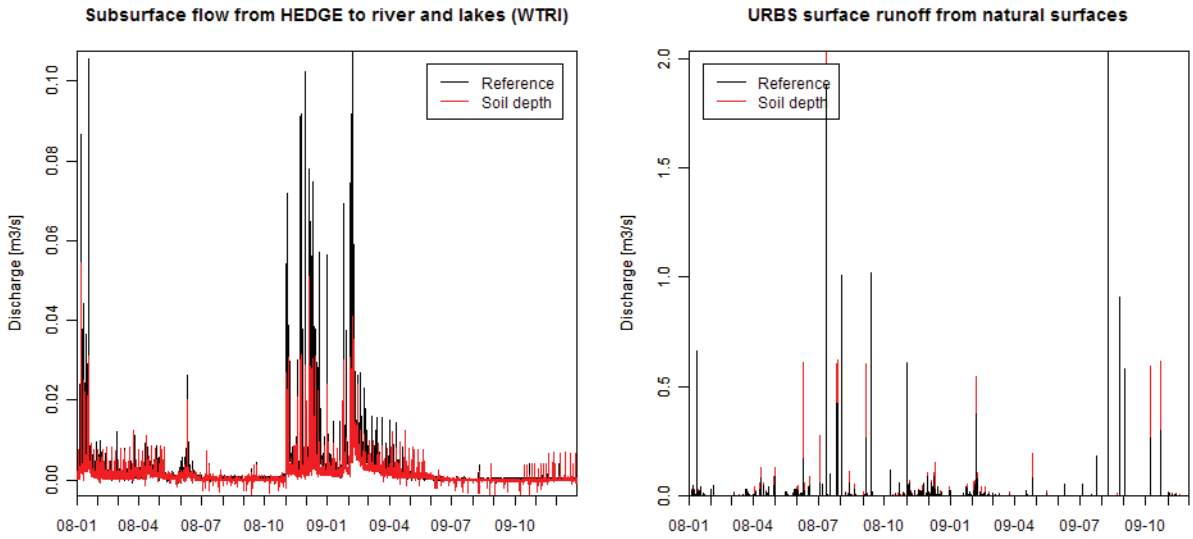

Figure 8.2.7.: Network infiltration, URBS surface runoff from impervious and natural areas, HEDGE overland flow and subsurface flow from HEDGE and URBS with WTRI contributing to the natural river (upstreamSOD). The simulation with the soil depth varying between 1 and 3 m is compared to the reference simulation having a constant soil depth of 1m.

the semi-arid area of New Mexico. They showed thus, that during rain events with high rain intensities, lateral subsurface flow bypasses the soil matrix having low hydraulic conductivities. The change of scale, from point measurements towards regional values, may thus require an adaptation of the hydraulic conductivity. Varado (2004) showed that the optimal hydraulic conductivity value depends on the model mesh resolution. In her case, based also on an irregular polygon model mesh, it depended on the average polygon area. A change of the average polygon size by a factor 5, lead to an increase of the hydraulic conductivity by a factor 10 in order to get the best simulation results.

For these reasons, we chose to test the sensitivity of the saturated hydraulic conductivity and increased the lateral hydraulic conductivity of the WTI and WTRI interfaces by a factor 10. In the same simulation run, we increased the vertical hydraulic conductivity of the natural urban part by the same factor. This is justified by the high uncertainty of the urban soil parameters, which were derived from natural soil data, because no information about urban soil was available. In order to better differentiate the influence of the change in the WTI/WTRI hydraulic conductivities and the URBS permeability, first of all, we will have a look at the different components shown in Figure 8.2.8. The permeability in URBS is a factor of the ideal drain equation (equation 5.2.1), which causes the network infiltration to rise considerably, see the upper left panel in Figure 8.2.8. It also leads to a clear decrease of the natural urban surface runoff. This confirms our expectations, as more water can infiltrate into the sewer system due to the higher conductivity. Surprisingly, it decreases also slightly the surface runoff from impervious urban areas (refer to Figure G.0.13 in the appendix), what we did not expect. This should be explored further in future.

Concerning the change in the lateral hydraulic conductivity (WTI/WTRI), the right

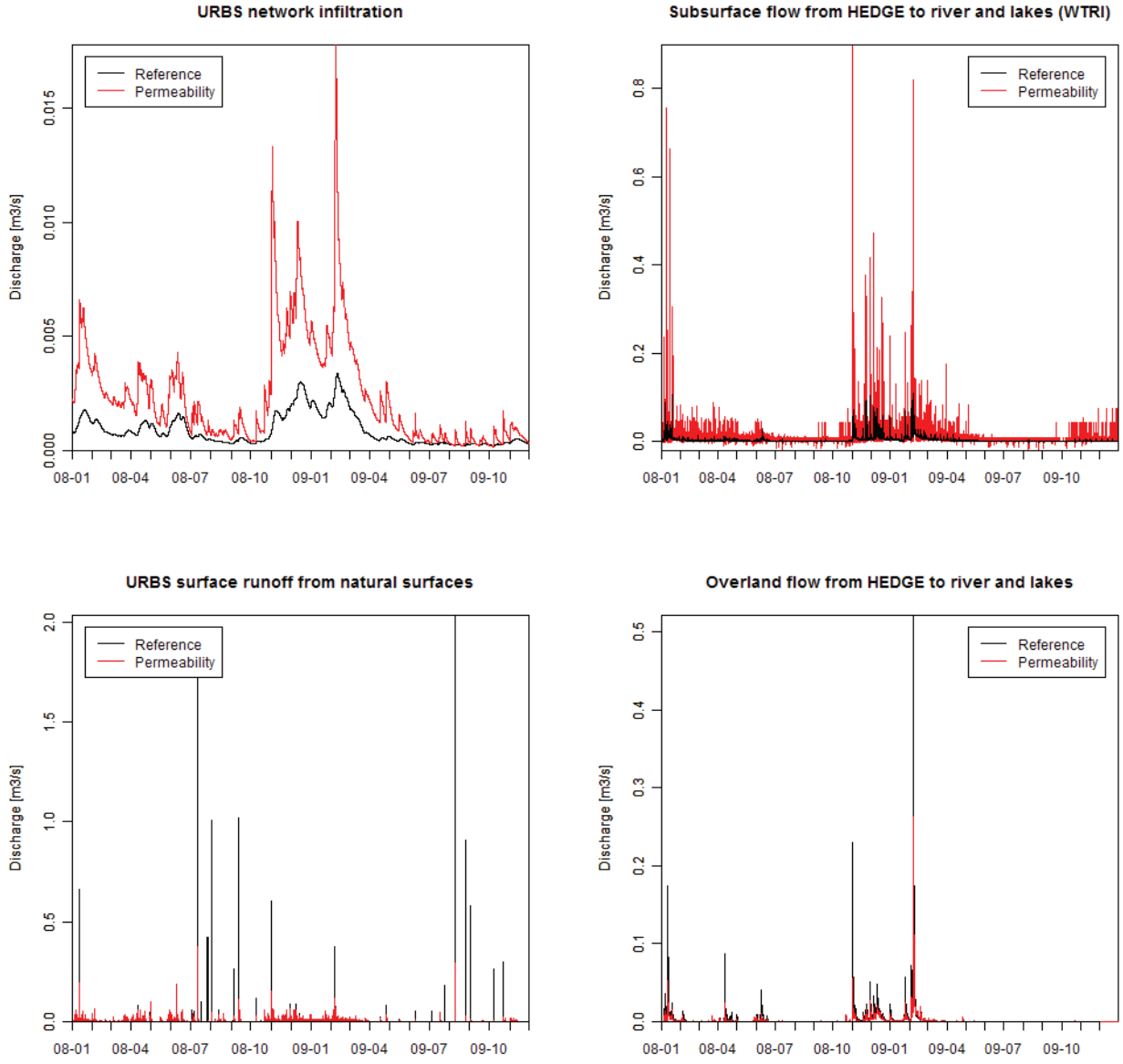

Figure 8.2.8.: Network infiltration, URBS surface runoff from natural areas, HEDGE overland flow and subsurface flow from HEDGE with WTRI contributing to the natural river (upstreamSOD). The reference simulation is compared to the simulation with an about the factor 10 increased permeability.

panel of Figure 8.2.8 shows its influence on the lateral subsurface flow and on the HEDGE overland flow. We can see that the lateral subsurface flow increases about a factor 10, which corresponds to the increase of the hydraulic conductivity. This can be explained by the linear relation in the Darcy equation (5.1.5). This increase of the lateral subsurface flow and network infiltration leads to a better drainage of the HEDGE and URBS model units and thus less ponding and overland flow. Consequently, the average groundwater table of the HEDGE and URBS model units decreases about 20 cm, see Figure 8.2.9.

If we look now at the effect on the discharge in the natural stream (Figure 8.2.10), we can observe a significant decrease of the peak values and an increase of the base flow, which

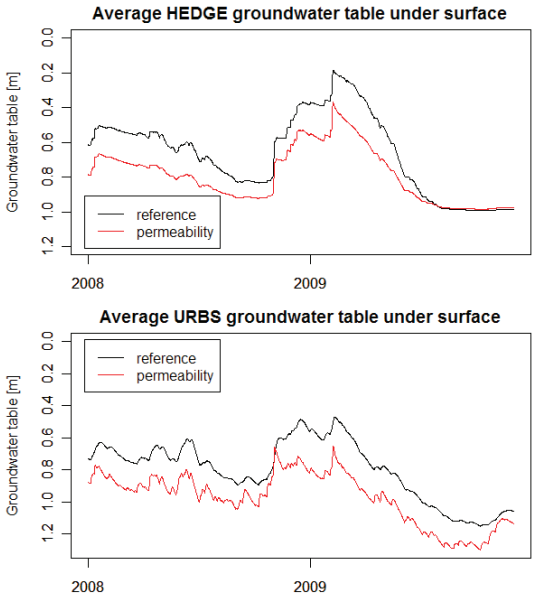

Figure 8.2.9.: Sensitivity of HEDGE and URBS groundwater table evolution to increase of hydraulic conductivity about a factor of 10.

confirms our expectations. Also the peaks in the sewer system and the pipes towards the retention basins are significantly reduced, see Figures G.0.11 and G.0.12 in the appendix. This decline of the peaks is valid for all events, whatever summer or winter events. Figure 8.2.11 shows the summer event on the 9th of August 2009 and the winter event on the 2nd of November 2008 as example. For the summer event the decrease of the discharge peaks leads to a significant improvement of the simulation in all of the networks, whereas the simulation of the already underestimated peak of the November 2008 event in the natural river gets worse.

8.2.3. Conclusions

The analysis of the reference simulation showed that PUMMA overestimates summer flood peaks due to a too high urban surface runoff contribution and underestimates the winter base flow. One objective of the sensitivity analysis of PUMMA was thus to investigate if a change of some of the URBS parameters can lead to a reduction of peak flows and an increase of the sewer base flow. Therefore, the influence of the built and road link coefficients, as well as the λ and μ network parameters was tested. The first hypothesis could be confirmed, as the decrease of the link coefficients lead to a decrease of the summer storm peaks and a slight rise in the base flow. However, the network parameters were not very sensitive and lead only to a small increase of the network infiltration. Furthermore, it was not possible to simulate a significant annual cycle of the base flow in the sewer system. The simulation of the sewer base flow requires thus further investigations.

Concerning the natural parameters, we chose to test the sensitivity of the soil depth and the hydraulic conductivity, as these parameters have a high uncertainty. An increase of the soil depth to up to 3m resulted in higher peak values and lower base flows. Furthermore, the HEDGE groundwater table dropped about 1m. This shows that the model is quite sensitive to soil depth, for both subsurface and overland flow. For overland flow, it is all the more sensitive that HEDGE simulates only saturation excess runoff (no Horton

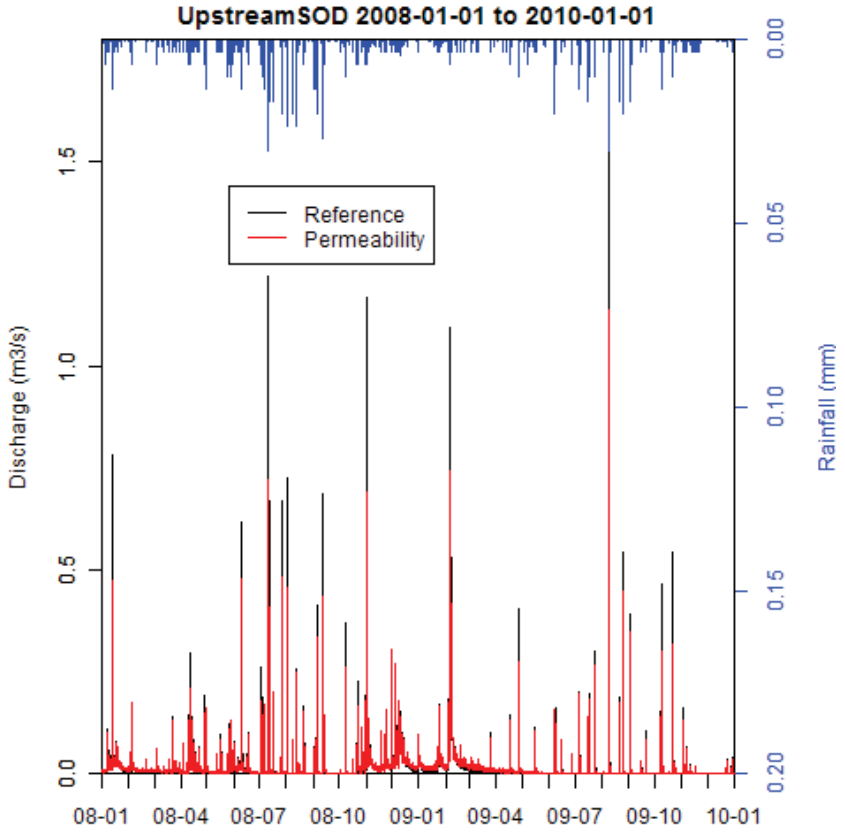

Figure 8.2.10.: Simulation with modified hydraulic conductivity compared to the reference simulation in the natural river. The hydraulic conductivity was increased by the factor 10.

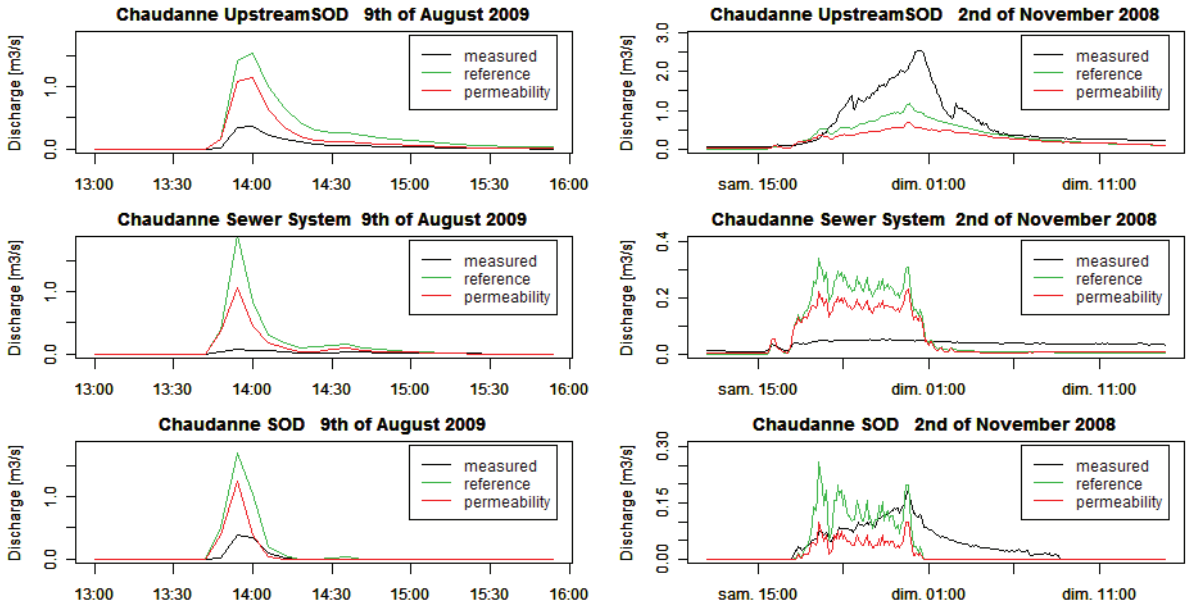

Figure 8.2.11.: The influence of the change in permeability on a summer (August 2009, left) and winter event (November 2008, right).

overland flow). Simulations with FRER1D, which adds this process, would probably lead to complementary results and allow us to complete the interpretation.

The hydraulic conductivity appeared as the most sensitive parameter. The increase by a factor 10 lead to a significant decrease of all peak values and a rise of the base flow. The simulated discharge corresponded thus better to the observed discharge, which confirms the hypothesis of Varado (2004) that hydraulic conductivity values necessary for modelling are often much larger than the values of local field measurements, as other processes such as macropores, interflow or piston flow have to be considered.

8.3. Influence of interfaces

In this section we want to show the interest in some of the new developments we added to LIQUID. The first part investigates thus the influence of the OLAF module and the second part the influence of the lateral subsurface flow which was added to URBS.

8.3.1. Influence of OLAF

For this test we deleted all OLAF module implementations and their connections and compared then the simulation results to the reference simulation.

The OLAF module routes accumulated ponding by means of surface runoff. Without OLAF the water can only be drained by subsurface flow, which is a slower discharge component. The model units are thus less drained, which leads to an increase of the average water table level, see Figure 8.3.1. We can see that the largest impact on the HEDGE groundwater table is during dry periods and the lowest impact during wet periods. A possible explanation can be, that during the wet period, even for the reference simulation the model units with accumulated ponding reach an equilibrium at their maximal ponding level. This can be caused by the altitude relation between neighboring model units, which influences the subsurface flow processes.

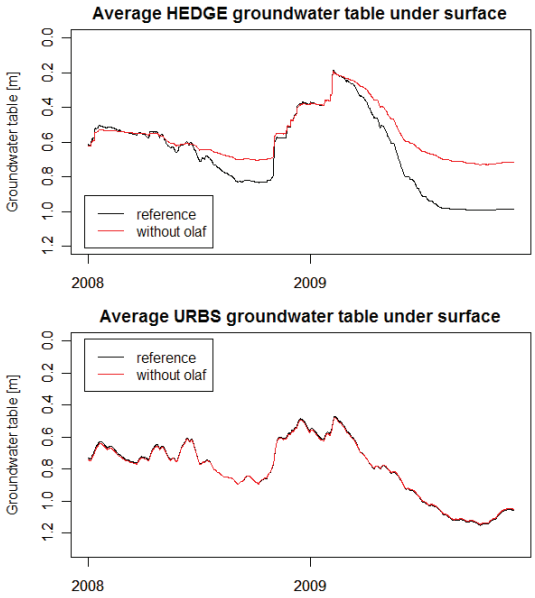

Figure 8.3.1.: Sensitivity of HEDGE and URBS groundwater table evolution to the inclusion of the OLAF module into PUMMA.

Figure 8.3.2 shows the annual average water table level (including ponding) in 2008 of the simulation without OLAF compared to the reference simulation (same map as in

Figure 8.1.13). During the reference simulation, ponding only occurred on three HEDGE model units, whereas without OLAF, about 290 of the HEDGE model units had ponding with a maximal ponding height of up to 2.40m.

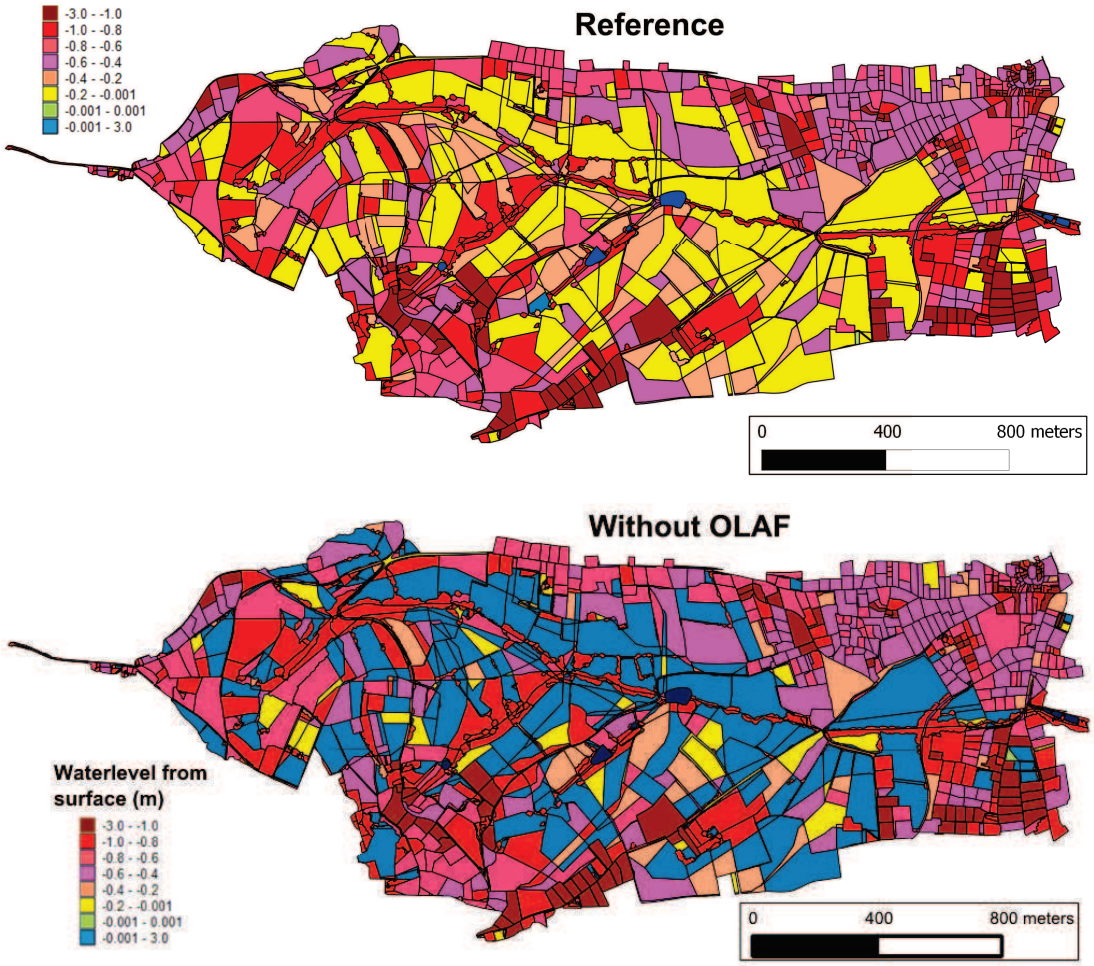

Figure 8.3.2.: The annual average groundwater table (negative values) and ponding (positive values) from surface level [m] for the simulation without OLAF (right) in comparison to the reference simulation (left) for 2008.

The influence on the URBS groundwater table is only minor, see Figures 8.3.1 and 8.3.2, although it leads to a small change in the URBS network infiltration (Figure 8.3.3). The URBS surface runoff is directly connected to the drainage network without using the OLAF module, therefore the URBS surface runoff components remain unchanged. However, we can observe a slight increase of the HEDGE subsurface flow simulated with WTRI, see Figure 8.3.3.

The influence of the missing overland flow on the total flow is then a decrease of the winter base flow and a slight decrease of the peak values in the natural stream, see Figure 8.3.4. Only a minor impact can be observed for the discharge in the sewer system and the sewer overflow device (Figures G.0.14 and G.0.15 in the appendix).

Figure 8.3.5 shows the impact of the OLAF module on the summer event of the 9th of

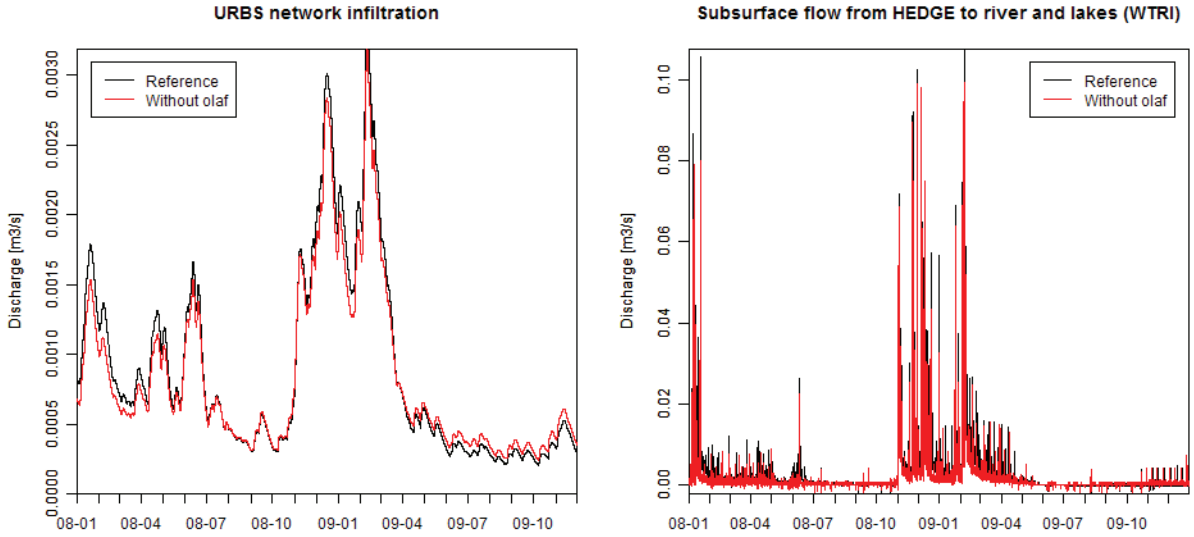

Figure 8.3.3.: Network infiltration and HEDGE subsurface flow contributing to the natural river (upstreamSOD) in 2008 and 2009. The reference simulation is compared to the simulation without OLAF module.

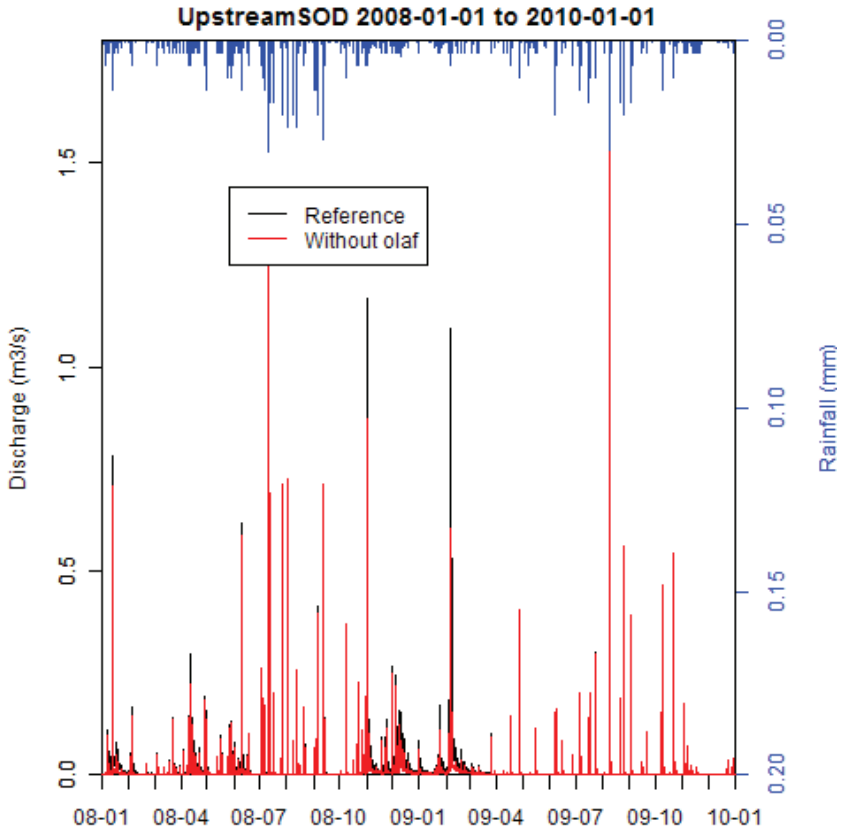

Figure 8.3.4.: Simulation without OLAF module compared to the reference simulation in the natural river.

August 2009 (left) and on the winter event on the 2nd of November 2008 (right). We can see that overland flow is only important for the winter event, for which the underestimation of the peak gets worse without the OLAF module. This difference between summer and winter events is probably induced by the structure of the HEDGE module. As already pointed out, HEDGE creates only ponding caused by saturation excess of the whole soil profile and not by Horton infiltration excess. As in summer, the soil profiles are not saturated, no ponding occurs and the OLAF module, which transfers the ponding, has thus no influence on the simulation results. If we used a module, which is able to simulate Horton infiltration excess, such as FRER1D, we could prossibly see an influence of the OLAF module on the summer events as well.

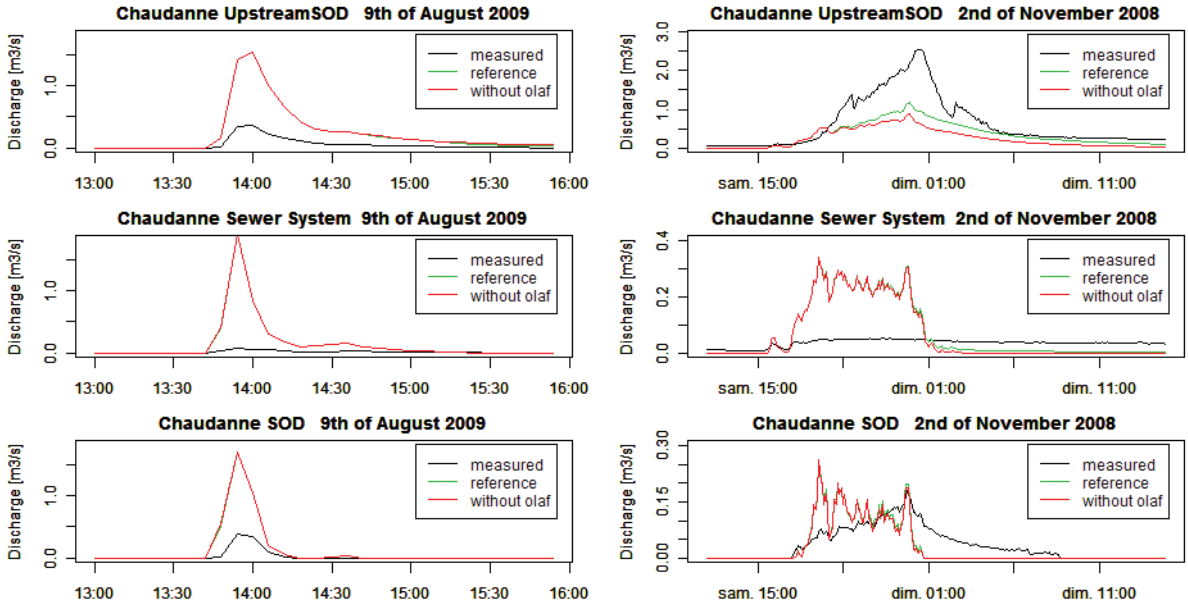

Figure 8.3.5.: The influence of the OLAF module on a summer (August 2009, left) and winter event (November 2008, right).

As conclusion, this section showed the importance of the OLAF module for the winter base flow and discharge volume. Furthermore, OLAF assures a more realistic simulation of the water level in the HEDGE model units, as without OLAF, ponding occurs on many HEDGE model units.

8.3.2. Influence of WTI/WTRI connection to URBS

In order to have a spatially continuous simulation of the groundwater table over the whole catchment, lateral subsurface flow was added to the URBS module using WTI/WTRI interfaces between URBS/HEDGE/RIVER1D/SISTBA modules in addition to the network infiltration (see Chapter 5.3.1). We expected to have less discontinuity between the groundwater table of URBS and HEDGE model units than without lateral subsurface flow. The WTI and WTRI interfaces calculate the water flux depending on the groundwater table level in neighboring model units (refer to chapter 5). In this section, we investigate the influence of this newly added connection by comparison of the reference simulation to a simulation without the WTI/WTRI connection to URBS.

Figure 8.3.6 shows the average annual groundwatertable in the HEDGE and URBS

model units. We can observe an increase of the URBS groundwater table of a few centimeters, whereas the change in the HEDGE groundwater table is only minor. Removing

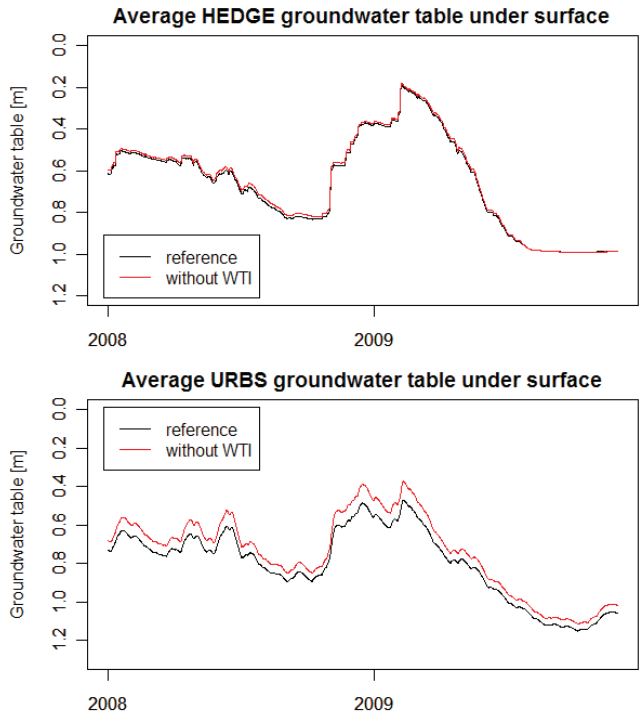

Figure 8.3.6.: Sensitivity of HEDGE and URBS groundwater table evolution to the addition of the URBS subsurface lateral flow with WTI and WTRI.

the WTRI subsurface flow results thus in less drainage of the URBS model units and a rising groundwater table. This induces a higher network infiltration (Figure 8.3.7 left panel).

The increase of the URBS groundwater table results in a better correspondence between the URBS and HEDGE groundwater table (see Figure 8.3.8). This contradicts our assumption, as we had expected that the addition of the URBS subsurface flow, which allows water exchange between the URBS and HEDGE model units, would lead to a better continuity of the URBS and HEDGE groundwater table.

Regarding Figure 8.3.7 the deletion of the URBS subsurface flow leads to a decrease of the HEDGE subsurface flow. Only a minor decrease is visible for the URBS and HEDGE surface runoff components (see Figure G.0.18 in the appendix) and the effect of the addition of WTRI and WTI to URBS on the stream discharge is thus small. Only a slight decrease of the peak values at upstreamSOD is discernible in Figure 8.3.9. The discharge in the sewer system and SOD, which is mainly composed of surface runoff, is nearly identical to the discharge obtained with the reference simulation (Figures G.0.16 and G.0.17 in the appendix). An event analysis of summer and winter events (not shown here) showed also no difference in the discharge between both simulations.

We can conclude, that the WTRI/WTI connection to URBS, which was added in the reference simulation, does not change significantly the simulation results. The addition of the WTI/WTRI to URBS serves mainly the soil drainage, which decreases the URBS groundwater table. However, in our simulation, it does not lead to an equilibration of the water table level between HEDGE and URBS model units.

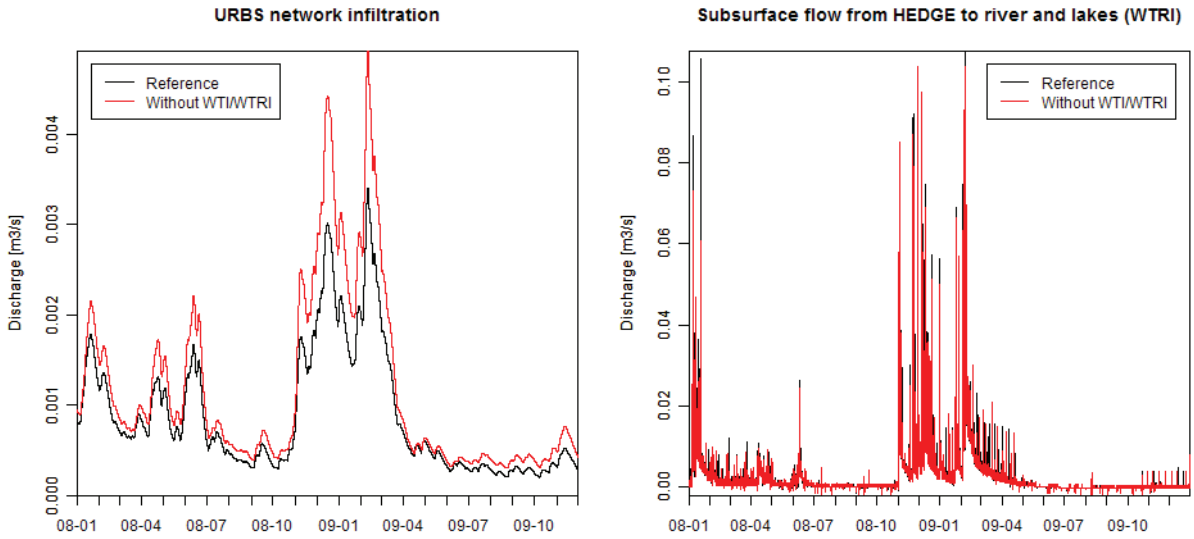

Figure 8.3.7.: URBS network infiltration and HEDGE subsurface flow contributing to the natural river (upstreamSOD). The reference simulation is compared to the simulation without URBS lateral subsurface flow.

8.4. Scenarios

The next section shows the capability of PUMMA to simulate different management scenarios. We chose to develop two scenarios. The first one investigates the catchment behavior in natural conditions by removing the urban influence. The urban influence is considered here as the impact of the impervious area and the impact of the pipe drainage. Therefore, three simulations were run:

- the first simulation assumed that there was no network infiltration ("perfect pipes")
- the second simulation assumed that there were no impervious areas
- the third simulation was the combination of both

In the second scenario an urban sub-basin with separated sewer system was identified and disconnected from the natural stream. This could be the case if for example an infiltration basin would be installed at the outlet of the urban sub-basin. This scenario highlights the influence of connections of flow to artificial drainage networks and is possible thanks to the distributed character of the model.

8.4.1. Natural catchment

8.4.1.1. No network infiltration

In order to have perfect pipes with no network infiltration, the λ parameter of URBS (refer to Table 5.2.1 in Chapter 5.2.1) was set to 0. This lead to an increase of the URBS groundwater table of 20 to 50cm and a slight increase of the HEDGE groundwater table, see Figure 8.4.7. Consequently, there was more ponding on the natural areas of URBS which induced a higher natural surface runoff (Figure 8.4.1). Furthermore, the runoff

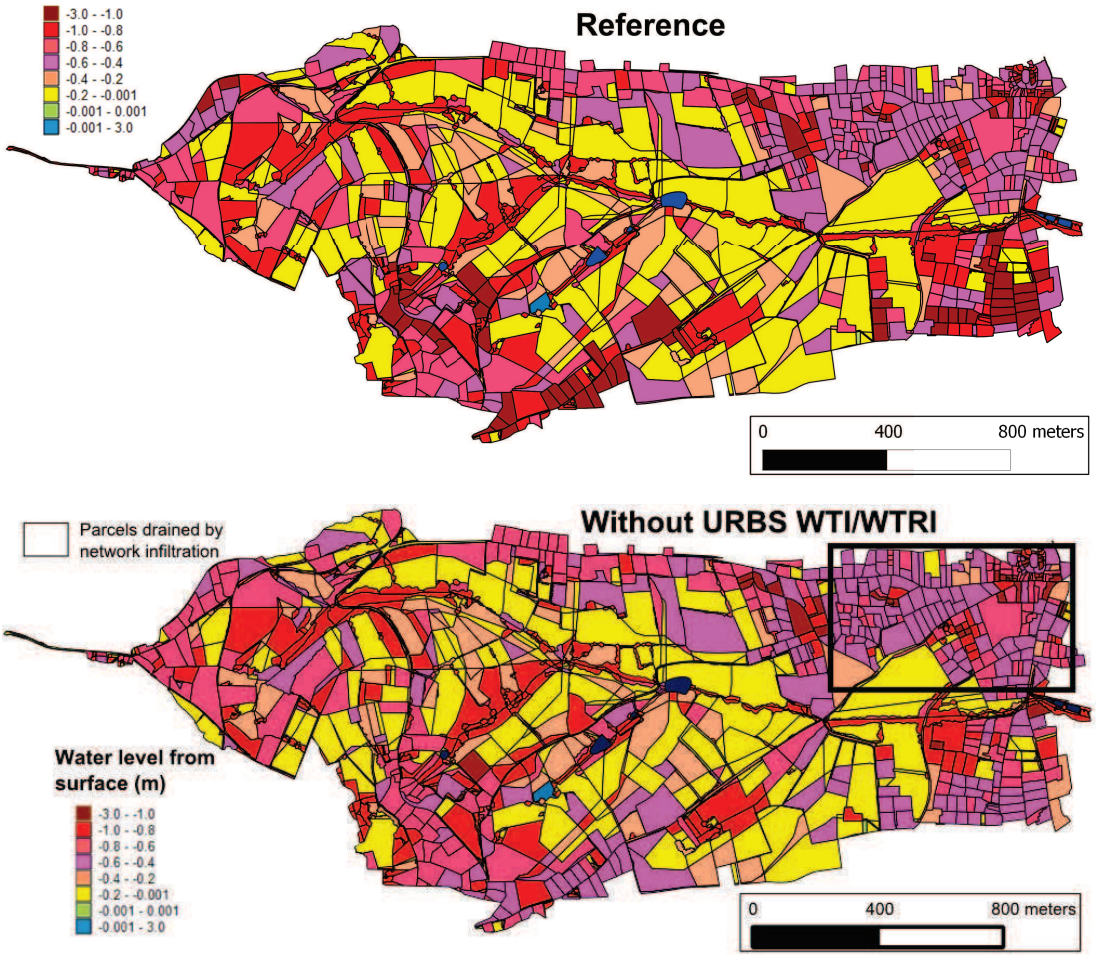

Figure 8.3.8.: The annual average groundwater table (negative values) and ponding (positive values) from surface level [m] for the simulation without URBS subsurface flow (right) in comparison to the reference simulation (left) for 2008.

from impervious areas increased slightly. The missing network infiltration changed the WTRI interactions, but no real tendency is distinguishable (Figure G.0.21).

However, the additional natural surface runoff increases considerably the peak flows in all of the three networks, see Figure 8.4.2 and Figures G.0.19 and G.0.20 in the appendix. Regarding Figure 8.4.2 the scenario "perfect pipes" has a similar influence on summer and winter events, whereas we would have expected a smaller impact for summer events on dry soils.

8.4.1.2. No impervious areas

In this simulation, the built and road areas in URBS were replaced by natural area in order to simulate natural conditions. This modification removed the runoff from impervious surfaces, which was shown to be one of the major runoff components in section 8.1. As compensation, the runoff from natural surfaces doubled its quantity caused by the increased natural area, see Figure 8.4.3. The HEDGE surface runoff increased also slightly,

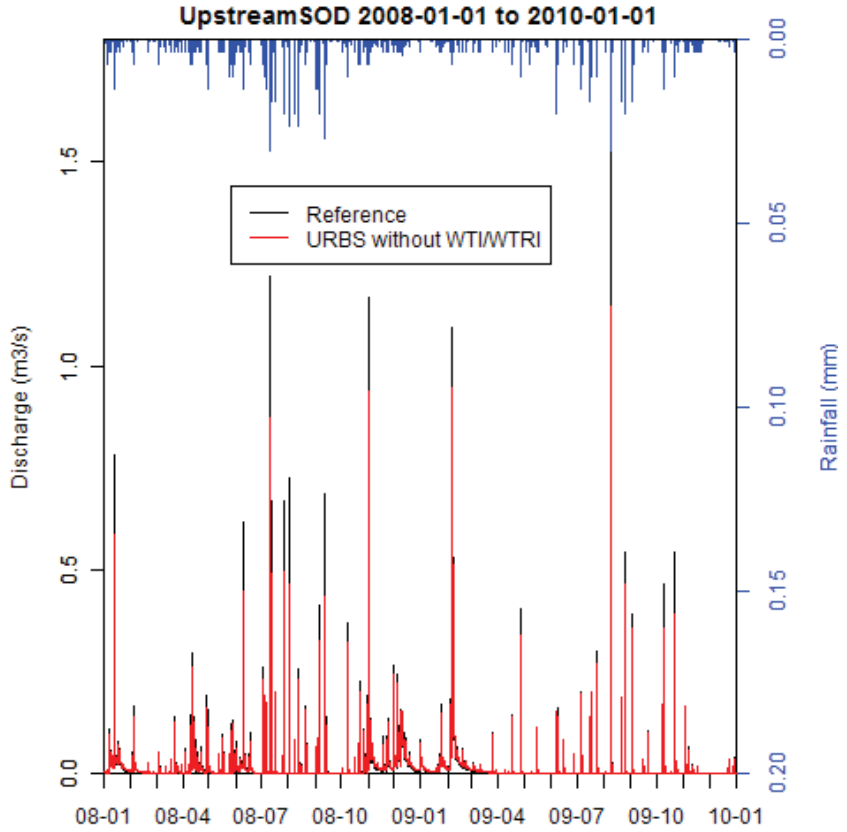

Figure 8.3.9.: Simulation of the discharge in the natural stream (UpstreamSOD) without URBS lateral subsurface flow compared to the reference simulation.

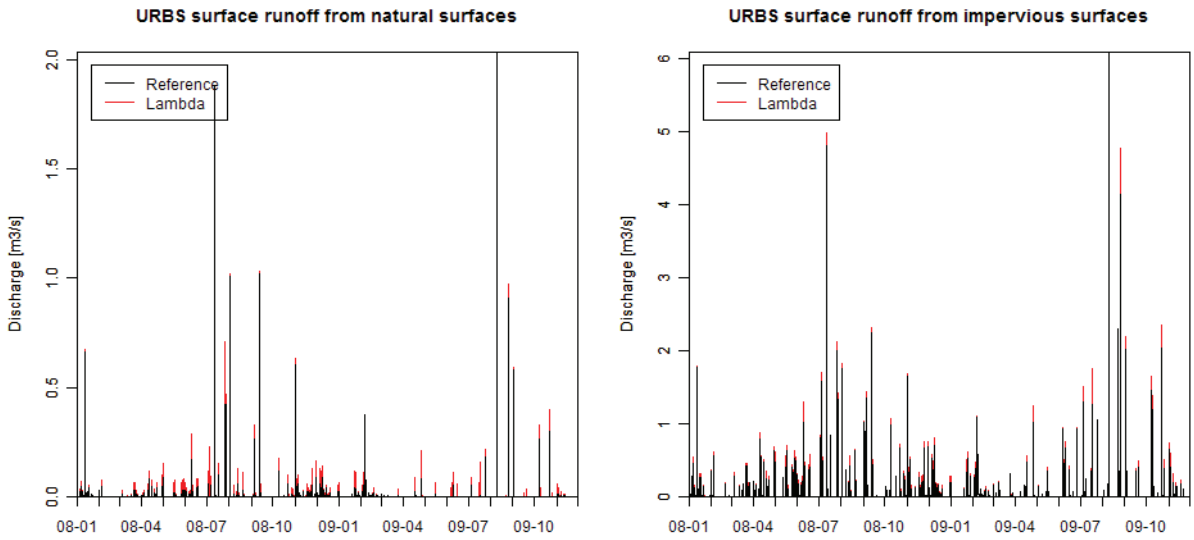

Figure 8.4.1.: The reference simulation is compared to the simulation without network infiltration (λ=0). The URBS surface runoff from impervious (right) and natural areas (left) contributing to the natural river (upstreamSOD) are shown.

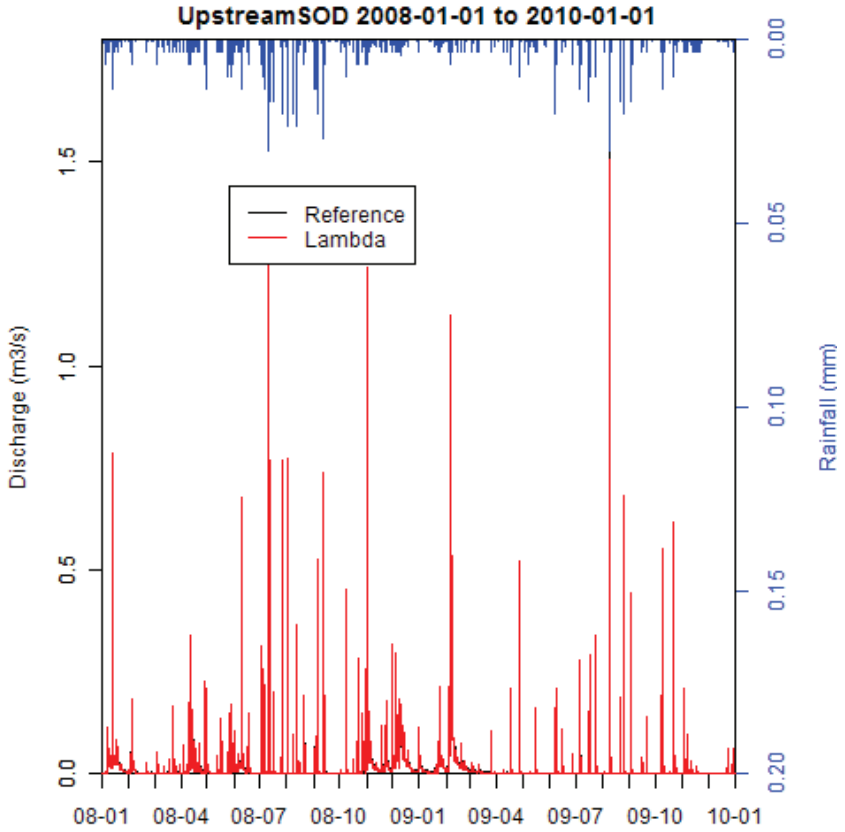

Figure 8.4.2.: Simulation of the discharge in the natural stream (UpstreamSOD) without network infiltration ($\lambda = 0.$).

see Figure G.0.25 in the appendix.

The URBS groundwater table (Figure 8.4.7) dropped considerably during the summer months and increased in the winter months. This is probably due to higher infiltration and higher evapotranspiration possible on natural areas compared to impervious areas. This caused an increase of the network infiltration in winter. In summer, the soil dries completely out, which results in a stop of the network infiltration and the lateral flow from URBS model units, see Figure 8.4.3. The HEDGE subsurface flow remains relatively unchanged (see Figure G.0.24 in the appendix).

Without impervious areas, the discharge peaks decrease considerably in all networks (natural stream, sewer system and SOD), see Figure 8.4.4 and Figures G.0.22 and G.0.23 in the appendix. Some of the summer events on dry river beds disappear nearly completely. However, the winter base flow is not affected by the presence of impervious areas in the catchment, which is coherent with the observations of Sarrazin (2012).

This simulation shows also the differences between HEDGE modules and URBS modules simulating natural areas. We would expect that the order of magnitude of surface runoff from both modules would be similar for natural conditions without impervious areas. However, the surface runoff from URBS is still ten times higher than from HEDGE. This could be related to the different vegetation cover and the different representation of the soil and evapotranspiration processes. Therefore, it would be interesting to investigate this in more detail, e.g. by comparing only one HEDGE unit to one URBS unit with the same tree cover.

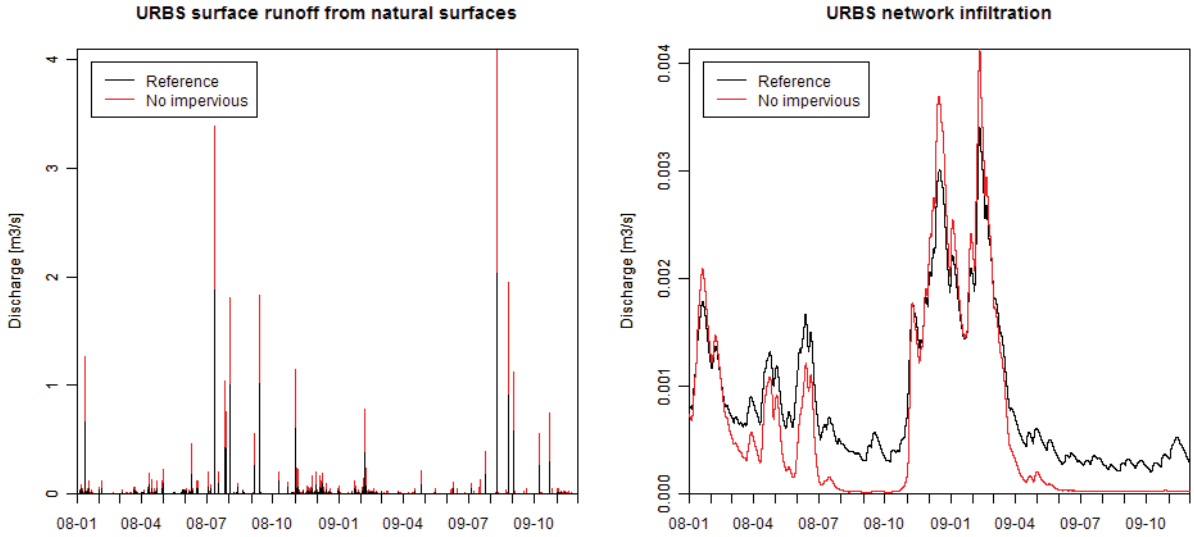

Figure 8.4.3.: Network infiltration, URBS surface runoff from natural areas, HEDGE overland flow and subsurface flow from HEDGE with WTRI contributing to the natural river (upstreamSOD). The reference simulation is compared to a simulation without URBS impervious areas.

8.4.1.3. Simulation of natural catchment

This simulation combines both effects, the removing of the pipe drainage and the replacement of the impervious surfaces with natural surfaces in URBS and is referred to as natural simulation in the following text. The discharge in the river is thus only composed of surface runoff from natural areas and subsurface flow modelled with WTRI. The simulated surface runoff from the natural areas of URBS is even higher than that of the simulation without impervious areas (Section 8.4.1.2), as the impact of the missing pipe drainage is combined with the effect of the missing impervious areas (Figure 8.4.5). This causes also an increase of the HEDGE overland flow and subsurface flow (see Figure G.0.28 in the appendix).

The increased natural surface runoff, leads thus to a discharge in the natural river, sewer system and SOD, which is higher than the discharge simulated with the removed impervious area, but lower than the simulated discharge without pipe drainage, see Figure 8.4.6 and Figures G.0.26 and G.0.27 in the appendix.

Figure 8.4.7 shows the groundwater table of all three simulations in comparison to the reference simulation and Figure 8.4.8 shows the maps corresponding to the average water table in 2008.

The average URBS groundwater table of the natural simulation is above the water level of the simulation without impervious areas, which leads to a similar groundwater table in HEDGE and URBS model units. Regarding the map of the simulation without impervious areas (lower left panel), there is only a slight increase of the water table in some of the URBS model units as compared to the reference simulation (upper left panel), whereas many more model units have a higher water level in the simulation without network infiltration (upper right panel). If we compare now, the effect of the network infiltration

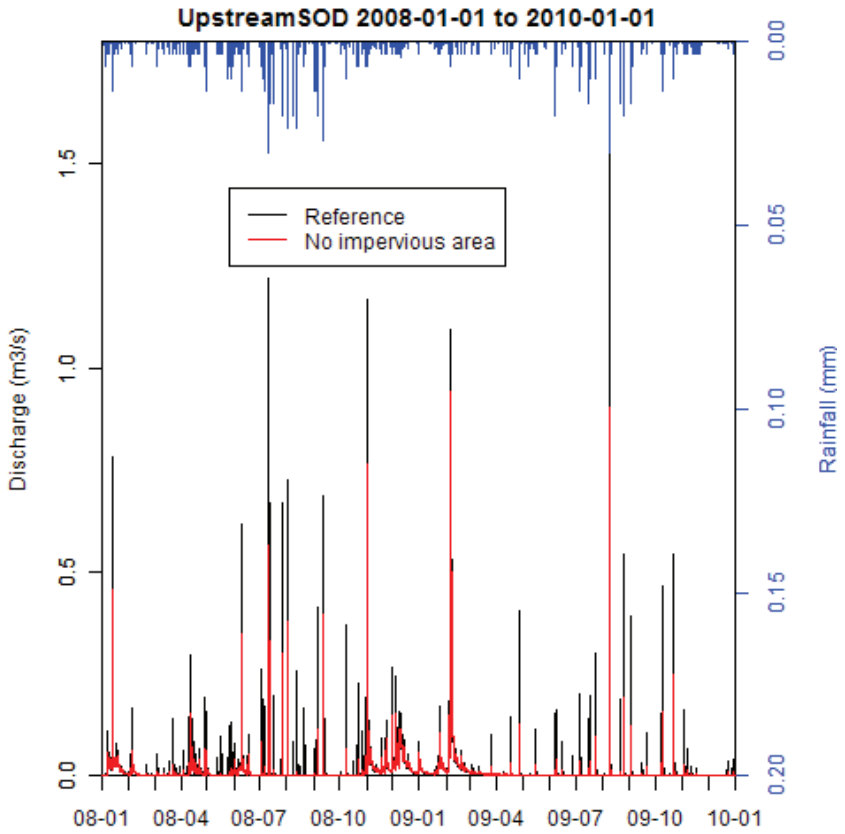

Figure 8.4.4.: Simulation of the discharge in the natural stream (UpstreamSOD) for which all URBS impervious areas was changed to natural area in comparison to the reference simulation.

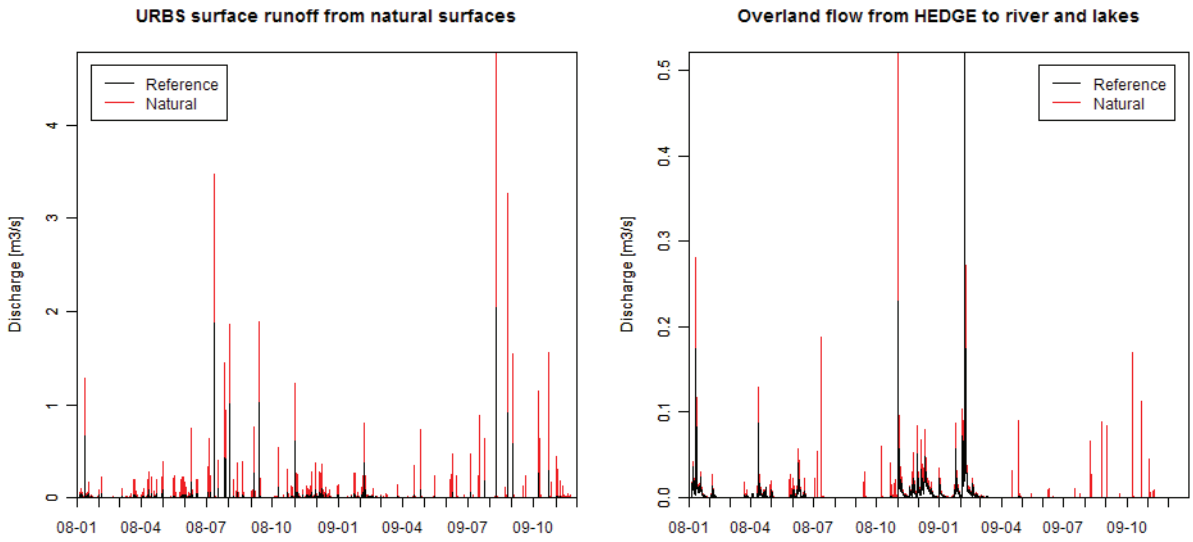

Figure 8.4.5.: URBS surface runoff from natural areas and HEDGE overland flow contributing to the natural river (upstreamSOD). The reference simulation is compared to a simulation without URBS impervious areas and without network infiltration.

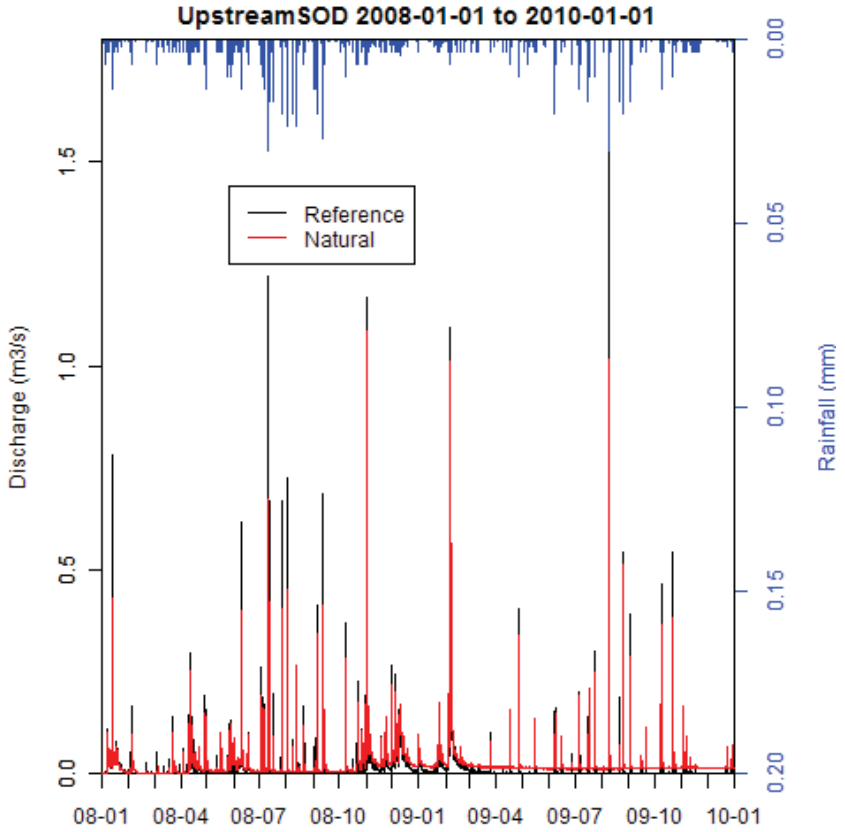

Figure 8.4.6.: Simulation of the discharge in the natural stream (UpstreamSOD) for a natural catchment without pipe drainage for which all URBS impervious areas was changed to natural area in comparison to the reference simulation.

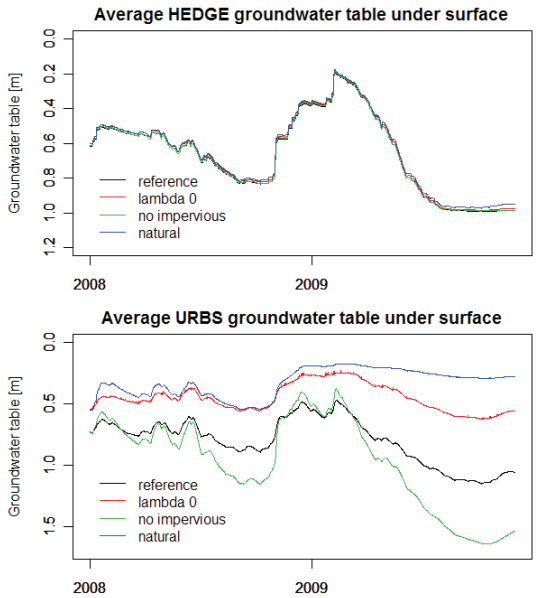

Figure 8.4.7.: Sensitivity of HEDGE and URBS groundwater table evolution to the presence of network flow (lambda = 0) and the presence of impervious areas. Both, the network infiltration and the impervious area are set to 0 in the "natural".

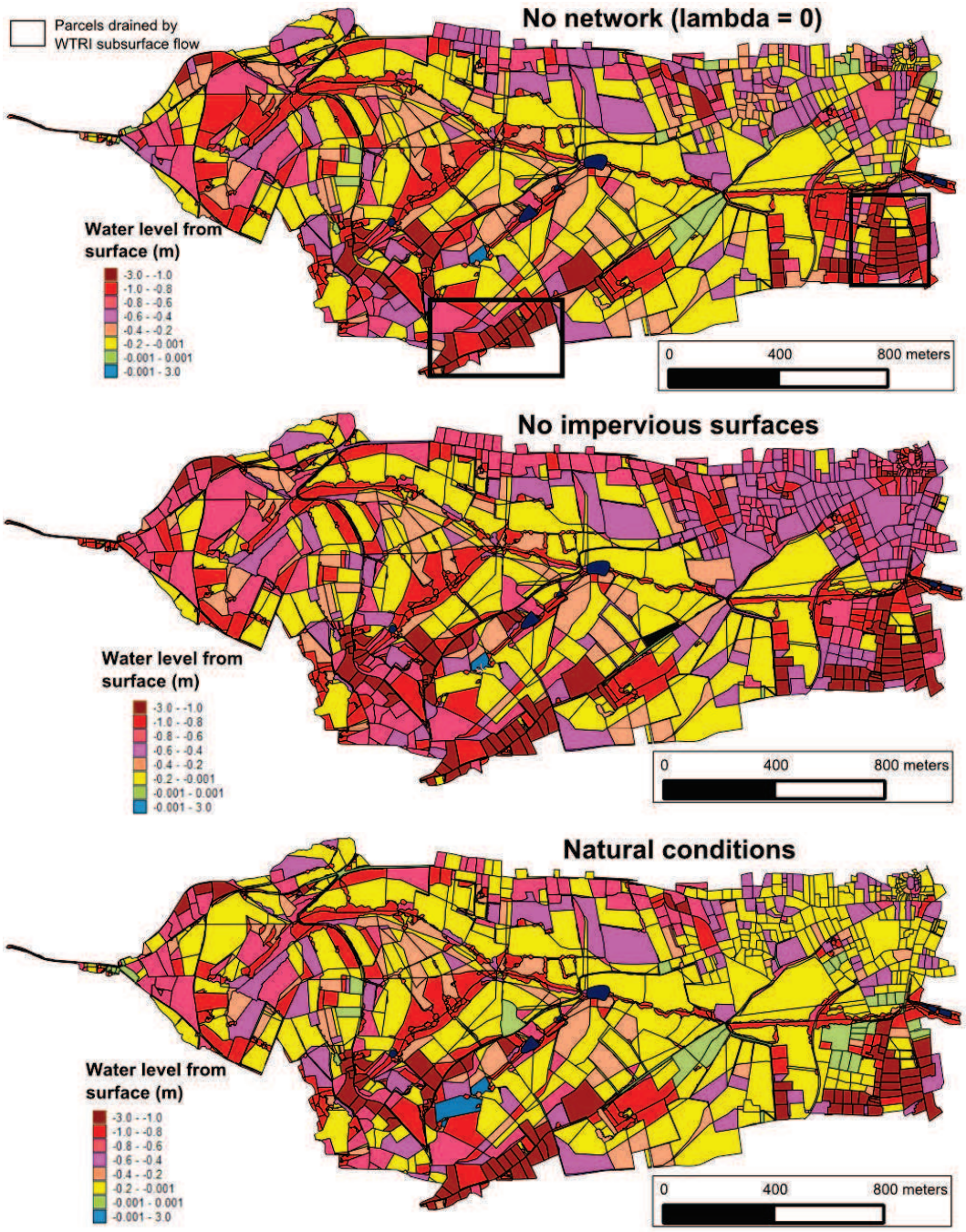

Figure 8.4.8.: Groundwater table maps of the simulation without network infiltration (top), without impervious areas (middle) and the natural simulation (bottom) having neither network infiltration nor impervious areas.

on the water table with the effect of the URBS subsurface flow (Figure 8.3.8), we can observe that some URBS model units are rather drained by the network infiltration (left bank of Chaudanne, see black rectangle in Figure 8.3.8) and others by the WTRI/WTI subsurface flow (right bank of Chaudanne, see black rectangles in Figure 8.4.8). The strong difference in the water table between HEDGE and URBS model units is probably caused by the double drainage (network infiltration plus subsurface flow) of the URBS model units.

8.4.1.4. Conclusions

These scenarios showed that the impervious areas and the pipe drainage have mainly an impact on peak discharge values and not on the winter base flow. The peak discharges increase without network infiltration and decrease considerably without impervious areas. Furthermore, the network infiltration has a significant draining effect on the groundwater table, even if it is only a minor contribution to the stream or sewer discharge. These simulations showed also the different behaviors of the URBS and HEDGE modules under natural conditions.

8.4.2. Disconnection of urban sub-basin

In this last scenario, we identified an urban sub-basin with a separated sewer system, which is connected to the natural stream upstream of the SOD, see Figure 8.4.9. The two sewer pipes or ditches (23 and 26 on Figure 8.4.9) coming from this sub-basin were then disconnected from the natural stream in order to determine their impact on the discharge in the natural stream at the upstreamSOD measurement station. This scenario explores the influence of flow connections to artificial drainage networks. Additionally, in a more applied perspective, this scenario would be interesting to assess whether the installation of a retention basin at the outlet of the sub-basin would be worth an investment.

The sub-basin and the concerned river reaches are shown in Figure 8.4.9. The disconnected river reaches drain an industrial and residential urban area on river left (red urban model units in Figure 8.4.9). Additionally, they intercept the overland flow from the natural area uphill of the residential area (arrows in Figure 8.4.9 show the overland flow paths). The river reaches 23 and 26 enter the natural stream (reach 19) at a confluence with two ditches (33,28) draining roads on the other side of the natural stream and one thalweg (34).

In Figure 8.4.10 (left panel) we show the contribution of the different tributaries for the reference simulation. The contributions from river right tributaries (23 and 26) and river left tributaries (28,33,34) are summarized, respectively, and compared to the discharge in the natural stream upstream of the confluence (19). In order to analyze the different contributions during dry and wet periods, the summer event from the 9th of August 2009 and the winter event from the 2nd of November 2008 are shown. During the summer event, the contribution from the urban sub-basin (red in Figure 8.4.10) appears as sharp, high discharge peaks. The peak values more than double the discharge in the natural stream upstream of the conjunction, whereas the contribution from the other, rural side of the road is inferior to the discharge in the natural stream. For the winter event, we can observe an inverse behavior. The discharge from the left, rural side of the road adds about the double peak discharge and discharge volume than the natural stream, whereas the discharge from the urban sub-basin is much smaller and resembles the simulated discharge in the sewer system or SOD (refer to Figure 8.1.16 in section 8.1). We can thus clearly differentiate the urban contribution from the natural contribution.

The right panel of Figure 8.4.10 shows the discharges at the measurement station upstreamSOD and compares the simulation, in which reaches 23 and 26 were disconnected to the reference simulation. The peak reduction for the summer event is about 40%, whereas the impact for the winter event is rather small, which is consistent with the flow contribution analysis shown in the left panel of Figure 8.4.10 and corresponds to the conclusions of Braud et al. (2011b): large events are mainly controlled by rural zones and the main

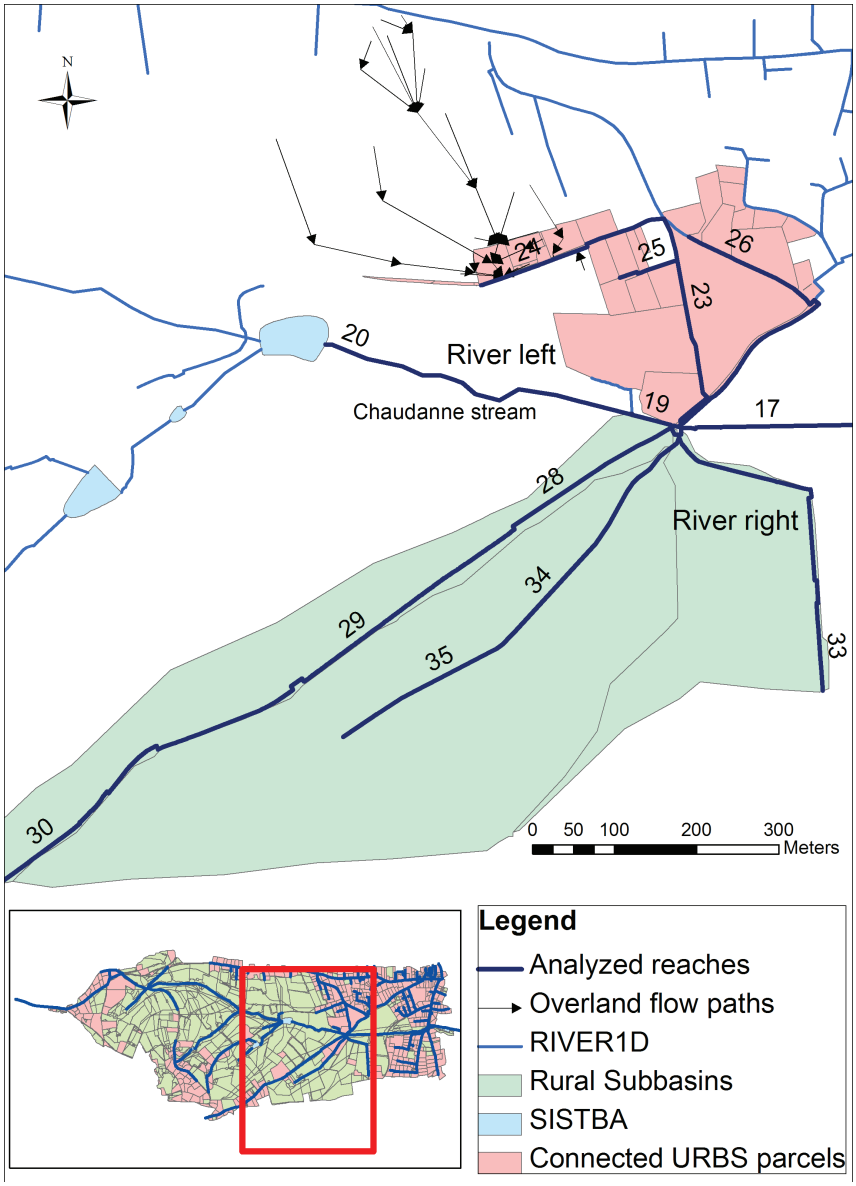

Figure 8.4.9.: Urban sub-basin disconnected for the scenario. River reaches 23 and 26 were disconnected. The red polygons are URBS model units, which are directly connected to the disconnected river reaches. These river reaches drain also via overland flow (arrows) the upper natural part. The rural sub-basins on river right are drained by roadside ditches (28,33) and a thalweg (34).

impact of urban zones is an increase of the flood frequency as small events are enhanced. The operational conclusion of this scenario would be that the introduction of a retention basin at the outlet of this urban sub-basin would be mainly interesting for the decrease of small events, which can be important for water quality and erosion issues but not for flood control.

8.5. Conclusions

The PUMMA model developed in chapter 5 was parameterized with measured or literature values and applied to the Chaudanne PdB catchment. No calibration was undertaken.

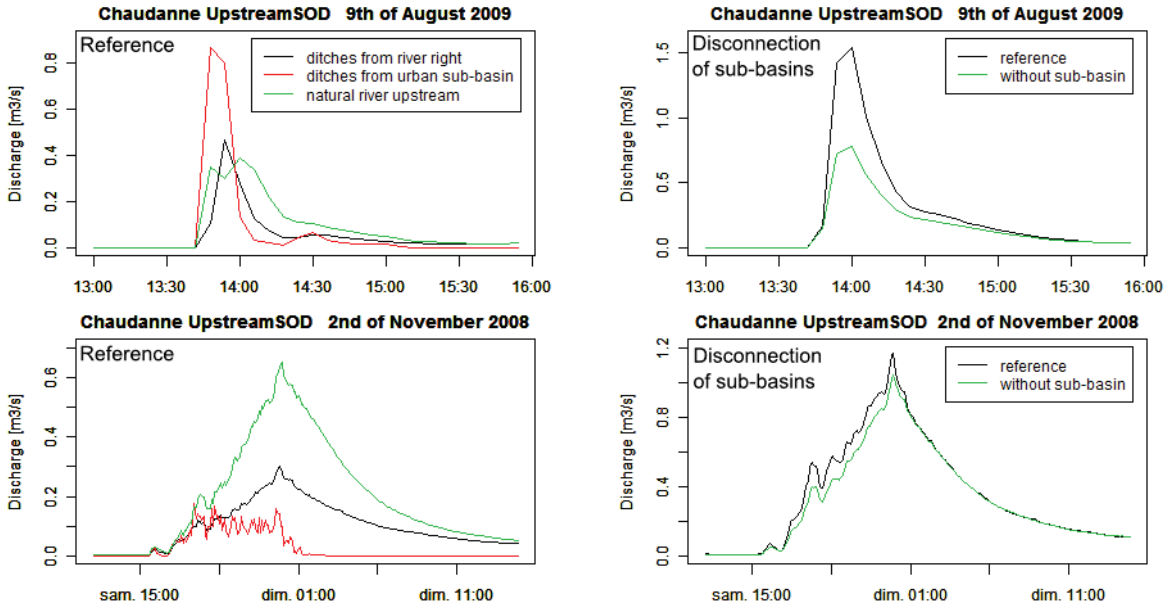

Figure 8.4.10.: On the left: discharges from different river reaches at the confluence with the ditches from the urban sub-basin for the reference simulation. The discharge in the natural stream upstream is shown, the discharge which comes from the ditches on river right and the discharge from the two ditches/pipes on river left. On the right: the discharge in the natural stream (upstreamSOD) for the reference simulation compared to the simulation in which the ditches on river left have been unconnected. A summer and winter event is shown.

The results of this reference simulation showed, that the model is able to represent the hydrological dynamic of small peri-urban catchments with a different behavior between winter and summer. This means, that PUMMA simulates well the drying of the river bed in summer and the rise of the base flow in winter. However, the base flow was generally underestimated in winter in the natural river, and the model was not able to simulate the larger base flow in the sewer system in winter. The simulation of the dry year 2009 revealed to be better than the simulation of the wet year 2008. This is probably due to the overestimation of small summer peaks and underestimation of large winter events, which were present in 2008. However, the timing of the simulated peaks fits well to the observations.

Regarding the water balance for 2008 and 2009, it can be concluded that the wet year 2008 filled up the soil storage, whereas during the drier year 2009, the soil storage was emptied. The spatial pattern of the simulated actual AET showed that in 2009 transpiration was limited by water availability in the soil for the high demanding vegetation (trees).

The sensitivity tests showed that a reduction of the summer peaks is possible by decreasing the URBS built and road link coefficients. However, the increase of sewer base flow observed in the measured data could not be represented by increasing the λ and μ groundwater drainage coefficients. Furthermore, the sensitivity of the soil depth and saturated hydraulic conductivity were tested. An increase of the soil depth from 1 to 3m

resulted in higher peak flows and less base flow. In contrast, the multiplication of the hydraulic conductivity with a factor of 10 had inverse effects, as it decreased the peak flows and increased the base flow. Larger values of the lateral saturated hydraulic conductivity lead to simulated results which are more in agreement with the observations in the natural river. This parameter has a large uncertainty and the method for its specification should be investigated further.

An addition of the FRER1D module to the PUMMA model would allow a better physical representation of the soil processes and would probably lead to other results concerning the soil depth and lateral hydraulic conductivity parameters. This should be investigated in more depth.

The tests of some of the new developments showed that the PUMMA model was very sensitive to the inclusion of overland flow through the OLAF module. The addition of the OLAF module allowed thus the simulation of the raise of the base flow in winter. Furthermore, its function as ponding extractor is primordial for the simulation of the water table.

The addition of the URBS lateral flow through WTI/WTRI interfaces adds considerably to the groundwater drainage in URBS model units, which leads to a large difference of the water table between HEDGE and URBS model units, which seems unrealistic. It would be interesting to gather data of the groundwater table in urban and rural areas to verify this on the field.

Nevertheless, the addition of the URBS lateral flow allows to use the URBS module in a natural context without drainage by pipes. It would thus be more realistic to differentiate between urban URBS parcels with pipe drainage and rural URBS parcels with lateral subsurface flow. Due to the use of the LIQUID modelling framework, a second instance of URBS for rural parcels with different connections could easily be added.

In the last section four different scenarios were simulated in order to investigate the response of the catchment to natural conditions. A sealing of the sewer pipes would thus lead to an increase of the groundwater table of about 20 to 50cm. The impervious area in the catchment is mainly responsible for small summer events and higher peak discharges. Therefore, a natural catchment compared to an urbanized catchment, has reduced peak flows and a higher groundwater table. If we interpret these results in relation to the trend of further urbanization, we can expect an increase of small summer peak flows and a decrease of the groundwater table in the future.

9. General conclusions

The work presented in this PhD addresses peri-urban catchments. Throughout the manuscript, we have illustrated how peri-urban areas have a complex hydrological setting. Located at the urban fringe, peri-urban catchments are neither completely urban, nor natural. They have complex drainage systems and they often have several outlets such as the natural river and a waste water treatment plant. Furthermore, areas outside the topographic catchment boundary can be connected to the catchment via pipe systems. It is often difficult to quantify which part of the water is intercepted by these pipes. It includes roof and street runoff, part of overland flow on natural areas and groundwater drainage. In some catchments with combined sewer systems, the impact of sewer overflow devices must also be considered. It is all the more difficult that the amount of overflowing water depends on threshold values. In peri-urban catchments, it is therefore difficult to close the water balance, because the system is not closed. On the other hand, they are threshold dependent systems with many interactions. Additionally, due to the growing urbanization the water infrastructure is constantly adapted as new impervious areas are added. We are therefore also faced with a changing system with a high degree of uncertainty. When modelling those systems, hypotheses have to be defined, as all the components of the systems cannot be monitored.

This PhD dealt with this problem and aimed at increasing our understanding of the hydrological functioning of peri-urban catchments, by building a detailed modelling approach which allows the test of various functioning hypotheses. Hereby, the main assumption underlying this PhD is that a continuous distributed hydrological model, taking explicitly into account the spatial organization of the landscape (urban, agricultural, forest areas, hedges,..) and the water pathways, as determined by topography but also roads and sewer networks, can help to understand and hierarchize the role of various landscape elements on the hydrological response of small hydrosystems. The objective was thus to develop a distributed hydrological model adapted to small peri-urban catchments (of about 1-10 km^2), which benefits from field observations and collection of GIS data layers. In order to use the model as hypothesis tester and for process understanding, the model was parameterized without calibration by means of existing information taken from field observations or the literature.

The methodology proposed in this PhD thesis to achieve these goals is summarized below.

1. First, a literature review and/or previous field studies allowed the identification of the main hydrological processes encountered in peri-urban catchments which had to be taken into account. Existing modelling approaches addressing both rural and urban areas were also reviewed. Both the process representation and spatial discretization were considered in this analysis. This step allowed the definition of the peri-urban model requirements and provided guidelines about the existing models or pieces of models, representing explicitly urban and rural processes, which were useful for the building of our peri-urban catchment model.

2. We therefore designed the Peri-Urban Model for landscape MAnagement (PUMMA) simulating the rainfall-runoff processes both in urban and in rural areas (chapter 5). For this, the urban model URBS (Rodriguez et al., 2008) was integrated into the LIQUID modelling framework (Branger et al., 2010) already containing modules describing hydrological processes in rural areas. Additionally, three process modules were developed describing sewer overflow devices, overland flow as well as retention basins and lakes. The use of the LIQUID modelling framework ensures the reusability of the developed model pieces and allows the coupling to other process modules.

   PUMMA follows an object-oriented approach. The landscape is discretized into cadastral parcels in urban areas and irregular hydrological response units in rural areas. In order to apply PUMMA to the catchment scale, automatic methods were developed for the pre-processing of the geographical data (chapter 6). First a method for the delineation of suburban catchments including the separation into dry and wet weather contributing areas was developed (article in section 6.2.1), as the exact knowledge of the drainage system and contributing areas are crucial for hydrological modelling. Then, vector based object oriented model meshes with more than 2000 model units were created using the newly developed preprocessing tools. These model meshes integrate the main factors relevant for the modelled processes, such as anthropogenic flow paths, soil characteristics, land use and land register, slope, etc., and respond at the same time to several numerical constraints such as size and convexity constraints. The preprocessing functions also allow the determination of the overland and subsurface flow paths as well as artificial flow paths (such as sewer pipe connections) necessary for distributed hydrological modelling in peri-urban areas.

3. Finally, the PUMMA model was applied to a real test case in the Yzeron catchment, the Chaudanne sub-basin ($2.2 km^2$), which is located in the peri-urban area of Lyon, France. The sub-basin is monitored since 1997 by the Cemagref in the framework of the OTHU observatory. The upper part of the catchment has mainly agricultural land use, whereas a large urban area covers the lower part. The rural part is drained by the natural river and ditches and the urban part by a mix of combined and separated sewer systems. In order to understand the impact of the various process modules and parameters, the model was run continuously using parameter values taken from observations and the literature, without calibration. Two contrasting years (rather dry for 2008 and humid for 2009) were chosen. A sensitivity analysis to various parameters and model configurations was also performed, before analysing the impact of various water management scenarios on the hydrological response.

9.1. Main results

This section highlights the main results obtained from the model development process and the model application to the Chaudanne sub-basin.

In terms of hydrological processes, the application of the catchment delineation method to the Chaudanne catchment (Chapter 6.2.1) showed that the wet period watershed area is about 30% larger than the topographical catchment area, which would be used for

"traditional" hydrological modelling. The resulting sub-basin map of the Chaudanne, which was classified in urban, natural and ditch drained sub-basins, is also interesting for water quality and water management questions.

The Chaudanne is an intermittent stream with dry periods in summer interrupted by thunderstorms and continuous discharge in winter. Summer and winter flood events are thus clearly different. In summer, the main contribution is overland flow from impervious areas, and in winter the whole catchment gets saturated and contributes to the stream discharge. Therefore, most winter events have higher peak values and more water volume, whereas the smaller summer flood peaks are subject to the urban influence due to the runoff from impervious areas, which causes a higher flood frequency.

The comparison of the model results with observed discharges in the natural stream, the sewer system and a sewer overflow device at the annual and event temporal scales (Chapter 8) showed that the model is able to simulate realistically the observed discharges and in particular different responses under dry and wet conditions, controlled by the soil saturation, although summer peak discharge is often overestimated. An analysis of the different model components showed that the summer peak discharges came mostly from surface runoff from impervious areas. This suggested that either the model overestimates surface runoff generation on impervious surfaces, or that this runoff is stored or reinfiltrated before it reaches the stream. In that case, the retention capacity of the catchment during dry periods would be larger than simulated by the model.

Furthermore, sensitivity tests to various processes/parameters showed the importance of the urban influenced processes on the hydrological response, in particular surface runoff generation on impervious and natural urban surfaces, infiltration into the sewer system and the connexion of urban areas to the natural hydrographic network. Soil depth and lateral saturated hydraulic conductivity were also found influential on the base flow dynamics. We finally showed the model potential for the evaluation of various rain water management scenarios.

The work also demonstrated the interest of a modular modelling approach for the modelling of this complex system with PUMMA. As each landscape object is represented by a separate module and that the outputs of each module can be controlled and examined, it is easier to identify the impact of specific parameters on the hydrological response. For example it was possible to show that the overestimation of the summer peaks came mainly from surface runoff on impervious areas, as mentioned before. This reduced the number of parameters influencing the summer peak discharge to the URBS parameters. A change of these URBS specific parameters does not influence the processes on e.g. HEDGE model units, representing the natural areas. The equifinality problem is thus confined to the processes representation and parameters values in one type of module. This shows one of the advantages of a distributed model based on a modelling framework like PUMMA. Furthermore, verifications and comparisons to field data are possible at different scales such as a model unit, a hillslope, a sub-basin or the whole catchment.

Additionally, the model simulation gave us feedback about the quality of the irregular model mesh and thus the preprocessing tools developed in chapter 6.3. It was shown that average altitudes of model units are crucial for the routing of the overland flow and groundwater. The shape of the model units should thus allow a correct routing, which means e.g. that long shaped model units such as roads or hedgerows should be avoided as they can easily act as barriers.

9.2. Conclusions and Perspectives

This thesis has contributed to the convergence of urban and rural hydrology by creating a common tool benefiting of the research progress from both directions. The urban URBS model (Rodriguez et al., 2008) was enriched by the addition of subsurface flow and overland flow, which allows the integration of urban areas, or dispersed settlements in natural areas to a peri-urban model. Rural models, where urban areas where described mostly by percentages of impervious areas beforehand, gained a detailed description of urban areas and thus the possibility to take into account the effect of the spatial organization of rural and urban areas on runoff generation. It is thus now possible to model the runoff generation in peri-urban areas in an integrated manner.

However, it was not possible to address all the points in the framework of this PhD thesis and several research perspectives can be defined, concerning the model improvement and its validation, as well as further use of the developed model.

Modelling toolset development The research perspectives in terms of model improvements are presented below:

- In order to better represent the natural soil in the model, including the simulation of Horton overland flow, the FRER1D module, simulating vertical infiltration based on the Richards equation (Ross, 2003) complemented with the development of Varado et al. (2006a) for the inclusion of vegetation processes, could be added to PUMMA. It could be used to simulate agricultural fields and roads instead of the HEDGE module which was used in this work. Another possibility would be the addition of Horton overland flow to the HEDGE module.

- Instead of simulating the sewer system with the kinematic wave approach, the ELIXIR (Henine, 2010) module simulating pressurized pipe flow, which is already part of the LIQUID framework (Branger et al., 2010), could be coupled to PUMMA, or even another more sophisticated sewer model, such as CANOE (Sogreah and Insavalor, 2005) or SWMM (Rossman, 2010).

- For the application to catchments with an important groundwater aquifer, the BOUSS2D module (Dehotin, 2007), which solves the Boussinesq equation, could be added to the model. Due to the modelling framework, groundwater boundary conditions could easily be added by means of input models sending constant or variable fluxes.

- The developed modules SISTBA and OLAF, simulating storage basins and overland flow, respectively, could be further improved. SISTBA could be improved by including a volume-depth relation such as e.g. done in CANOE (Sogreah and Insavalor, 2005), into the calculation, instead of the simple linear reservoir approach which is currently used. In OLAF, which solves the Manning equation, the slope of the model unit could replace the slope calculated between the centroids of two model units. This could improve the representation of accumulation and transfer sites in the model.

- Concerning the geographical preprocessing, further research could treat the optimization of the WTRI/WTI (subsurface flow) and OLAF (overland flow) prepro-

cessing with the objective of reducing the topological constraints. Furthermore, altitude information could be integrated into the model mesh, by intersecting model units with a great range of altitude with iso-contours. This would improve the transfer of water between model units, as it is governed by the average altitudes of the model units.

In the long term, the addition of water quality modelling to the LIQUID framework as well as the simulation of tracer transport would be a valuable perspective for peri-urban areas. Couplings with geomorphology and biological species population models could also be considered for a complete assessment of stream quality.

From modelling to field observation In this work, we relied on previous field studies for the design of the PUMMA model. However, the modelling experience can also provide feedback for future field studies, in order to document more closely some particular hydrological processes or to improve model validation. We have seen that due to the use of the modelling framework, verifications and comparisons to field data are possible at different scales such as a model unit, a hillslope, a sub-basin or the whole catchment. The following paragraph presents different perspectives for model validation at different scales:

- At the model unit scale, it would be interesting to measure the runoff components from one urban cadastral unit including the roof runoff, the runoff from roads and natural areas and the infiltration into sewer pipes and to compare it to the model results.

- Concerning the natural area, it would be interesting to concentrate on the correct simulation of one hillslope with production, transfer and accumulation sites. One of the Dehotin and Breil (2011) sites could for example be used, as soil moisture data are available for validation. This could also give feedback about the spatial discretization which is necessary to represent hillslope processes correctly.

- At the catchment scale, a further step would be to apply the model on the whole Chaudanne catchment and on the Mercier catchment, where additional validation data are available and could not be used in this work. In particular the comparison of the simulation results to the water height series of Sarrazin (2012) in the Mercier catchment would be really interesting, as it could give feedback if the model simulates correctly intermittent thalwegs and ditches and thus the sub-basin and catchment dynamics.

- In order to validate the model capacity to simulate the right separation in urban and rural surface runoff and subsurface flow, further hydrograph separations as in Gnouma (2006) could be done using environmental tracers.

- The addition of some new measurement stations could help to close the water balance over the catchment, as for example a measurement station at the sewer intersection (T) in the Chaudanne Pont de la Barge catchment. Concerning the Chaudanne catchment up to La Léchère, two measurements would be necessary in the sewer system, one in the pipe towards the waste water treatment plant and one in the overflow towards another sewer system (see sub-basin 13 in Appendix A). In the Mercier catchment it would also be interesting to investigate the draining effect

of the waste water pipe which is located below the stream bed. This could give valuable information for water managers, as it could demonstrate the importance of the sewer pipe locations for the efficiency of the sewer system.

Future potential use of the model The last point treats the possible use of the model.

- PUMMA is based on land register maps (cadaster), available in most European countries, which are the basis for land use planning and urban development. Most communities and engineering companies work already with these land register maps. It is thus interesting for them to have a model based on these land registers, as it facilitates the investigations of the influence of the development of new built-up areas on the catchment hydrology.

- The integration of the URBS module (Rodriguez et al., 2008; Morena, 2004), in which the natural, road and built area of each cadastral unit is modelled separately, allows the evaluation of the impact of rain water management scenarios, such as grassed roofs or infiltration trenches on the catchment hydrology as was explored in Morena (2004). As new policies towards local water retention are promoted and experimented, the PUMMA model can provide interesting feedback about the impact of the these new practices at the catchment scale, which is still poorly documented (Walsh et al., 2005).

- The detailed model can give feedback for simpler modelling approaches. The most important hydrological processes determined in the Chaudanne catchment, which should be represented in a simpler modelling approach were: the different behaviour in summer and winter with surface runoff on impervious areas in summer as main discharge contributor and subsurface flow as well as saturation excess overland flow in winter. In large catchments, in which the outlet of the waste water treatment plant is located inside the catchment, the deviation of water in sewer pipes can be neglected.

Part IV.

Appendices

A. Technical report: Delineation of sub-basins in the Chaudanne catchment

Introduction

A peri-urban area can be defined as a transition or interaction zone, where urban and rural activities are juxtaposed, and landscape features are subject to rapid modifications, induced by human activity Douglas (2006). Due to the anthropogenic influence, the risk of floods, droughts and pollution can increase. As areas under development, a detailed understanding of the hydrological functioning of these zones can contribute to a better water management, reducing the mentioned risks. While analysing hydrological processes in peri-urban areas, both urban and rural aspects have to be considered. In the framework of the AvuPUR project the peri-urban watershed of the Chaudanne river, situated in the south-west of Lyon, was analysed in detail in order to construct a hydrographical network with corresponding sub-basins for modelling reasons. The following report gives a description of each urban sub-basin. The hydrographical network, including the connections points to the river will be explained while describing the sub-basins. Each sub-basin belongs to one of the three flow measurement stations, which determines the structure of the report. However, not all questions could be answered satisfactorily. For further investigations the remaining questions will be mentioned in this report.

Detailed description of hydrological processes in each sub-basin

The numbered sub-basins with their drainage network and outlet are shown in Figure A.0.11 in the Appendix. The urban catchments are presented in red, the natural in green and the rural with influence of an anthropogenic ditch in violet. The catchment areas of the old and new pont de la Barge are separated by thick black lines. In the following text only the urban catchments will be explained in detail.

Measurement station at New Pont de la Barge

The contributory area to the measurement station at the New Pont de la Barge is about 2.19 km^2, whereas most of the surface consists of rural area. Though, an area of 0.146 km^2 is covered by three urban sub-basins. The measurement station was installed in 1997 and continuous flow data are available since then.

Sub-basin 1

Industrial area at Ferrières with a separated sewer system. The rain water is directly injected into the Chaudanne before the bridge. The plan of the separated system can be seen in Figure A.0.12 in the Appendix. The corresponding digital data for the pluvial system were not provided, only for the sewage network.

Sub-basin 2

This sub-basin represents the larger part of Ferriere with a separated network. The pluvial outlet joins the Chaudanne river under the bridge, see Figure A.0.1. It is not sure if the ditch following the "Voie Nouvelle des Ferrieres" in basin 4 is connected to the pluvial

network.

Figure A.0.1.: The river at the bridge is canalised with two parallel pipes. The outlet of the pluvial network is visible inside the right pipe.

Sub-basin 3
During the storm event on the 21st of August a considerable discharge was observed at a ditch coming from a residential area. Therefore, this area was aggregated to a sub-basin even if there is equally an unitary network. The ditch follows the main street, as well as the unitary network. There is also a residential development with separated sewer system, where the rainwater is probably connected to the ditch. However, the exact flow processes in this area are not verified, and probably part of the water is in reality connected to the unitary network.

Measurement station at the Old Pont de la Barge
Between the flow measurement stations at the new and the old Pont de la Barge three pipe outlets join the river. These come from ditches of both sides of the main road and the storm water overflow of the unitary network. The ditch coming from rivers left is part of sub-basin 7, which is actually not included in the contributory area of the Old Pont de la Barge. This is due to the construction of a separate pluvial network, which was connected to the three retention basins at the Pont de la Barge. However, the outlet of the retention basins is after the measurement station, counting therefore only for the water budget at the Pont de la Lechere. Though, it may be that part of the water entering sub-basin 7 is drained by the ditch beside Rue Lucien Blanc and by the old unitary network. These additional terms should be taken into account while considering the water balance. Continuous flow data exist since 1997.

Sub-basin 4
This sub-basin belongs to the unitary network and is connected via the storm water overflow device under the Pont de la Barge to the river. It is divided into two parts due to the disconnection of sub-basin 7 from the unitary network. The unitary network connected to the storm water overflow is in reality further outspread than this sub-basin, but the other parts were regarded disconnected due to existing parallel rain water pipes and ditches. The sewage water of all the other urban sub-basins upstream of the storm water outlet, which means sub-basins 1,2,3,5,6 and 7, has to be added as source term to the water balance of this catchment. Furthermore, some water might come from sub-basins 3 and 7, as they have a parallel pluvial and unitary network. In the left part of the sub-basin it is not sure, whether the two ditches following L'Arabie and Voie Nouvelle des Ferrieres are connected to the pluvial network of sub-basins 7 and 2. Further investigations, and

tracer experiments could help to get a better comprehension of the flow processes.

Besides the storm water outlet at the Pont de la Barge, there is also an overflow towards the unitary network in sub-basin 13 at the intersection Grand Rue and Rue Lucien Blanc. This point of divergence is called T and its functioning is shown in Figure A.0.2. The shutter closes the part going to the Pont de la Lechere (Belhaouane, 1999). The horizontal direction is located under the road D24. The threshold value of the pipe to the Pont de la Barge has still to be determined.

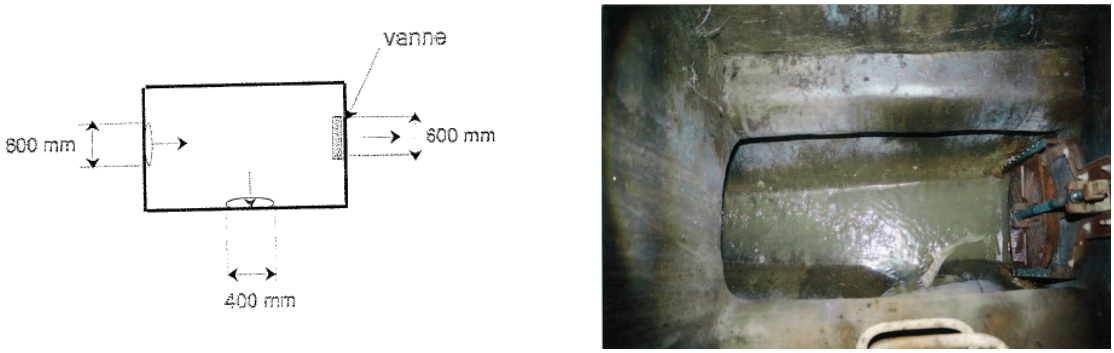

Figure A.0.2.: Schema and picture of the intersection "T" (Belhaouane, 1999). Photo of P. Breil, Cemagref Lyon.

The third outlet of this sub-basin, and the only one in low flow, is the pipe to the sewage plant. A measurement station is installed since 1997, called "Collecteur d'assainissement".

The flowmeter inside the storm water outlet itself was installed in 2001. Fig. A.0.3 shows the outlet of the storm water overflow in action. The flexible shutter was installed to cause the water to enter the open pipe in order to take water samples.

Figure A.0.3.: Picture of the storm water outlet under the Pont de la Barge in action (photo from équipe métrologie Cemagref Lyon).

Fig. A.0.4 shows a schema of the storm water overflow chamber, where the conduit to the river is located in the lower right corner. The crest length of the chamber is 1.54 m and the height of the overfall boundary is 15 cm upstream and 20 cm downstream (Bernoud, 1998). According to INGETUD (1997) the threshold for the storm water overflow is 40 l/s.

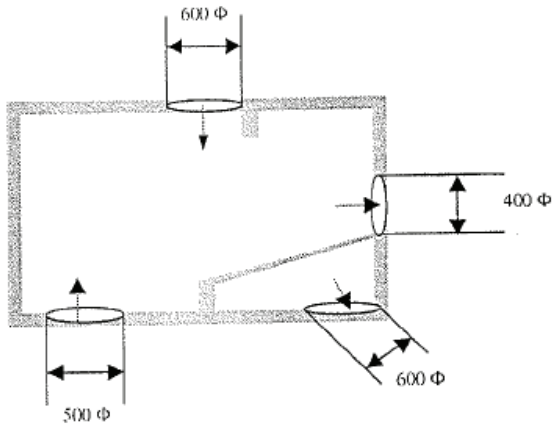

Figure A.0.4.: Schema of the storm water overflow at the Pont de la Barge. The pipe in the lower right corner is the storm water overflow towards the Chaudanne (Bernoud, 1998).

In Fig. A.0.5 we can see the storm water overflow chamber with two pipes coming from both sides of the river on the left side and the shutter to the sewage plant as well as the pipe to the river on the right side.

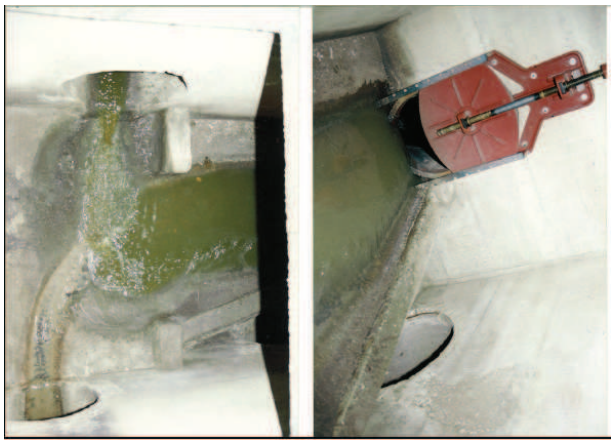

Figure A.0.5.: Pictures of the storm water overflow chamber at the Pont de la Barge. The outlet is in the lower left corner and has a diameter of 600 $\Phi[mm]$ (Photos of P. Breil, Cemagref Lyon).

Sub-basin 5
This sub-basin contains the "Avenue Benoit Launay" and the bordering houses. Along the street is a separated sewer network, where the rainwater is collected in a ditch. The outlet is a pipe just after the new Pont de la Barge, at the right side of the Chaudanne.

Measurement station at the Pont de la Lechere
The measurement station at the Léchère was installed in 1999. The contributory area for this measurement station is about 4.089 km^2, with 47.52 % of urban area.

Sub-basin 6
Residential development with small retention basin at outlet, which is probably connected to the pluvial network of basin 7. For the model the dimensions of the retention basin

will have to be determined.

Sub-basin 7
This area was disconnected from the unitary network early in 2003 (Faure, 2002) and a separate pluvial network was installed. The rain water pipes are connected to three storm water retention basins in series at the pont de la barge. The outlet of the retention basins is after the two measurement stations with a discharge of 216 l/s at the bottom outlet. The altitude of the overflow in the first basin is 305.95 m, in the second basin it is 305.12 m and the surface inlet of the third basin is at 304.89 m. The surface of the basins is 251.37 m^2, 547.40 m^2 and 914.63 m^2. A detailed plan from the SIAHVY is available. Concerning the water balance of this basin, some rain water might still infiltrate in the old unitary pipes. Furthermore, there is a ditch following the road L. Blanc, which is directly connected to the Chaudanne in between the measurement stations. In the actual subdivision in sub-basins, this ditch is not considered. The inflow to the retention basins was measured during two short periods from 09/09/08 to 18/09/08 and 21/01/09 to 03/04/09, with a gap of 10 days. The water level is constantly measured in each basin. During the storm event on the 21st of august 2009 the first basin was filled.

Sub-basin 8
In the old plans, which are available at the town hall of Grézieu, there are two sewer systems with direct rainwater outlet at the Chaudanne indicated in this area. The outlet could not yet be verified on the field, and may be connected to the retention basin of the school complex.

Sub-basin 9
According to Mr. Ruffin of the SIAHVY the new part of the school in the "Rue des Nouvelles Ecoles" and the rest of the street is connected to the retention basin 4 at the Pont de la barge. However, the question remains if the ditch following the "Rue de l'Ancienne Gare" is connected to the retention basin. In this case the sub-basin would have to be extended to the south. The exact volume of the retention basin is unknown at the moment.

Sub-basin 10
This sub-basin contains the Leclerc supermarket. Three underground cisterns were built in order to minimise the impact to the river. The total volume is 700 m^3 with an outflow of up to 65 l/s. The overflow pipe has a diameter of 600 mm, whereas the diameter of the outflow pipe is only 160 mm. A diagram of the cisterns is shown in Figure A.0.6. The information was provided during an interview by Mr. Ruffin from the SIAHVY, who has the original plans of the retention basins. He indicated that probably only 500 m^3 are used as retention basin and 200 m^3 of water are conserved for fire protection. During the storm event on the 21st of august 2009 only a very small discharge was observed. This can be explained by the retention effect of the cisterns after dry weather conditions.

Sub-basin 11
This area has a principal ditch parallel to the unitary network. Field investigations showed that part of the houses are connected to the main ditch, as well as some surface runoff along a track to the east. However, some part of the water might go to the unitary network. Due to the slope, the ditch following the rue de l'ancienne gare was connected to

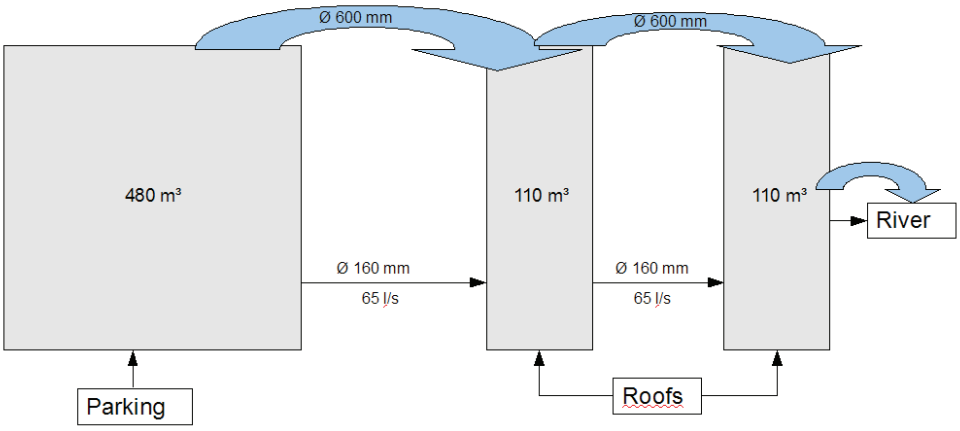

Figure A.0.6.: Schema of the retention basins of the Leclerc supermarket. Information delivered by the SIAHVY.

this basin, instead of basin 4, which is drained by the unitary network. The rain water pipe from the school complex (basin 9) crosses this basin, and it is not sure whether the western part of the catchment is connected to the pipe from the school complex. The main ditch following the rue de la Morellière might be connected to the ditch of the rue du Crest.

Sub-basin 12
The area close to the river has a separated sewer system, where the waste water is pumped towards the sewage plant. The rain water is directly connected to the river via two pipe outlets, see Figure A.0.7. Apparently the ditch following the main road is also connected to this outlet, but it is not sure to which extent. Especially, the connection under the roundabout at the Leclerc supermarket could not be verified. Furthermore the ditch beside the road le Matoret might be connected to this outlet. During the storm event a lot of water came from these outlets.

Sub-basin 13
This area is connected to the storm water overflow at the Lechere. The ditches in the striped parts are leading outside of the catchment and are in areas with unitary network. The crossed part with unitary sewer system is connected via the pumping station Drut. Not only the discharge created in this sub-basin, but also the discharge in the sewer network created upstream has to be considered in the water balance. The discharge in the sewer network coming from the pont de la barge is continuously measured at the "Collecteur d'assainissement" and can consequently be quantified. Though, at high flow rates some more sewer water can come from the overflow ("T") of catchment 4. Some areas with only a waste water network are not included into the surface of this area. However, an estimated source term (constant inflow) has to be added to the discharge in the pipes. There are 4 source terms:

1. Waste water coming from the "impasse de Varenne". The rain water ditch was connected to the Mercier catchment due to field investigations.

Figure A.0.7.: Pictures of the two outlets of basin 12.

2. Waste water coming around the "Rue du Crest" close to the roundabout towards Vaugneray.

3. Waste water from "Maison Blanche" in Vaugneray.

4. The whole part below the pumping station Drut. There are also some unitary pipes. As they are in rural area, they were excluded from the watershed.

In the "route des pierres blanches", there is a storm water overflow towards the sewer system of the Courly. This has to be considered like a loss term. The diameter of the incoming pipe is 30 cm and the overflow is 30 cm above, compare Figure A.0.8. A second overflow is planned towards the Ratier (north), and the works will be finished during 2010 (Information from SIAHVY).

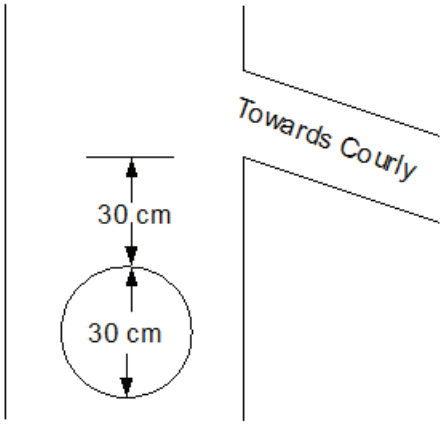

Figure A.0.8.: Schema of the overflow towards Courly. [Information from SIAHVY].

Some water in the pipes may come from the unitary network in sub-basins 8, 11 and 12. The parasite water in the pipe at the pont de la Léchère is about 12 m^3/h, which was measured during the night, where a low water consumption is assumed. 67 % of this water

is coming from the route de Bordeaux and route du Col de la Luère (Communication of the SIAHVY).

Some modifications of the unitary network at the Pont de la Lechere started not long ago. When the constructions are finished, the northern part of this sub-basin will no longer flow past the storm water overflow outlet, as a direct connection with bigger pipes will be built towards the sewage plant, compare the map A.0.13 in the appendix. Probably, the connection will not be cut completely, leaving an overflow possibility towards the DO7.

Fig. A.0.9 shows the storm water overflow chamber at the Pont de la Léchère with the storm water outflow pipe in the lower left corner, marked "Déversoir". The horizontal pipes are under the road D489, the vertical pipe is coming from the measurement station at the Pont de la Barge and the exit towards the sewage plant is in the lower right corner. It is remarkable that the inlet pipes having a summarized diameter of 1800 mm are much bigger than the summarized outlet pipes, which have a diameter of 1000 mm. The threshold of the storm water pipe inlet is 0.28 m in the chamber (Bernoud, 1998) and corresponds to a flow of 70 l/s according to INGETUD (1997). In the schema directive of the SIAHVY the height of the overflow is indicated with 200 mm. During the storm

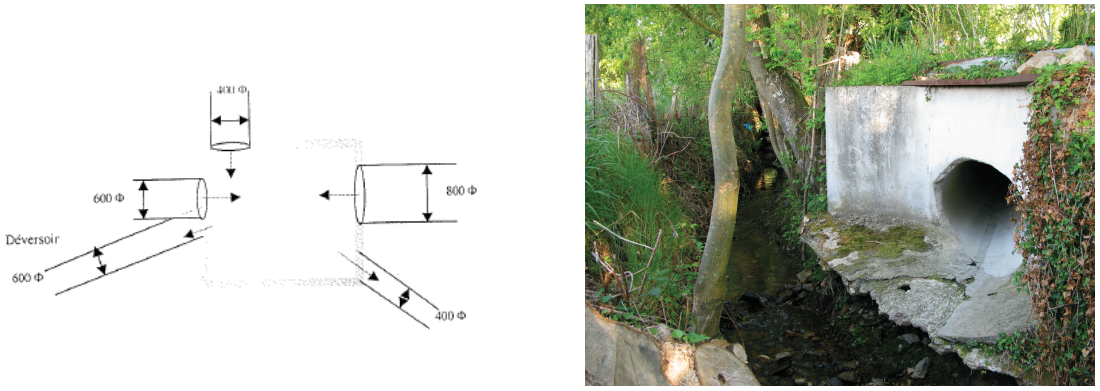

Figure A.0.9.: Schema of the storm water overflow chamber (DO7) at the Pont de la Léchère at left. The outlet is in the lower left corner and has a diameter of 600 $\Phi[mm]$ (Bernoud, 1998). On the right hand side is a picture of the storm water outlet.

event the 21 august 2009 a great discharge could be observed at the storm water overflow outlet.

In the western part the route du Col de Luere and some natural area north of it were excluded from the Chaudanne catchment, as the ditches beside this road are leading westwards towards a series of retention basins at the roundabout towards Vaugneray. According to Mr. Ruffin these retention basins are connected to the neighbouring sewer network southwards. It is not sure whether the ditch beside the route neuve du col de la luère is also connected to these retention basins. Some further investigations, as for example a tracer experiment at the roundabout would be necessary.

Sub-basins 14

Pluvial network with some bad sewage connections, which flows directly towards the Chaudanne at DO8 (storm water overflow). Figure A.0.10 shows the schema of this storm water overflow outlet. The diameter of all the pipes is 400 mm. This storm water overflow outlet was eliminated in autumn 2009.

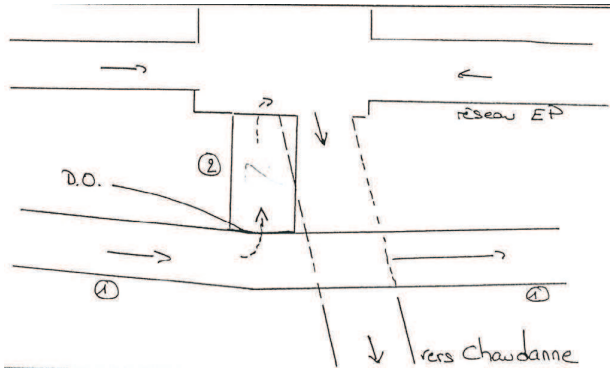

Figure A.0.10.: Schema of the rain water overflow (DO8) of basin 14 [SIAHVY].

Sub-basin 15
Ditch beside the road, which is probably connected to the unitary network. Due to this ditch the catchment boundary was extended to the south.

Appendix

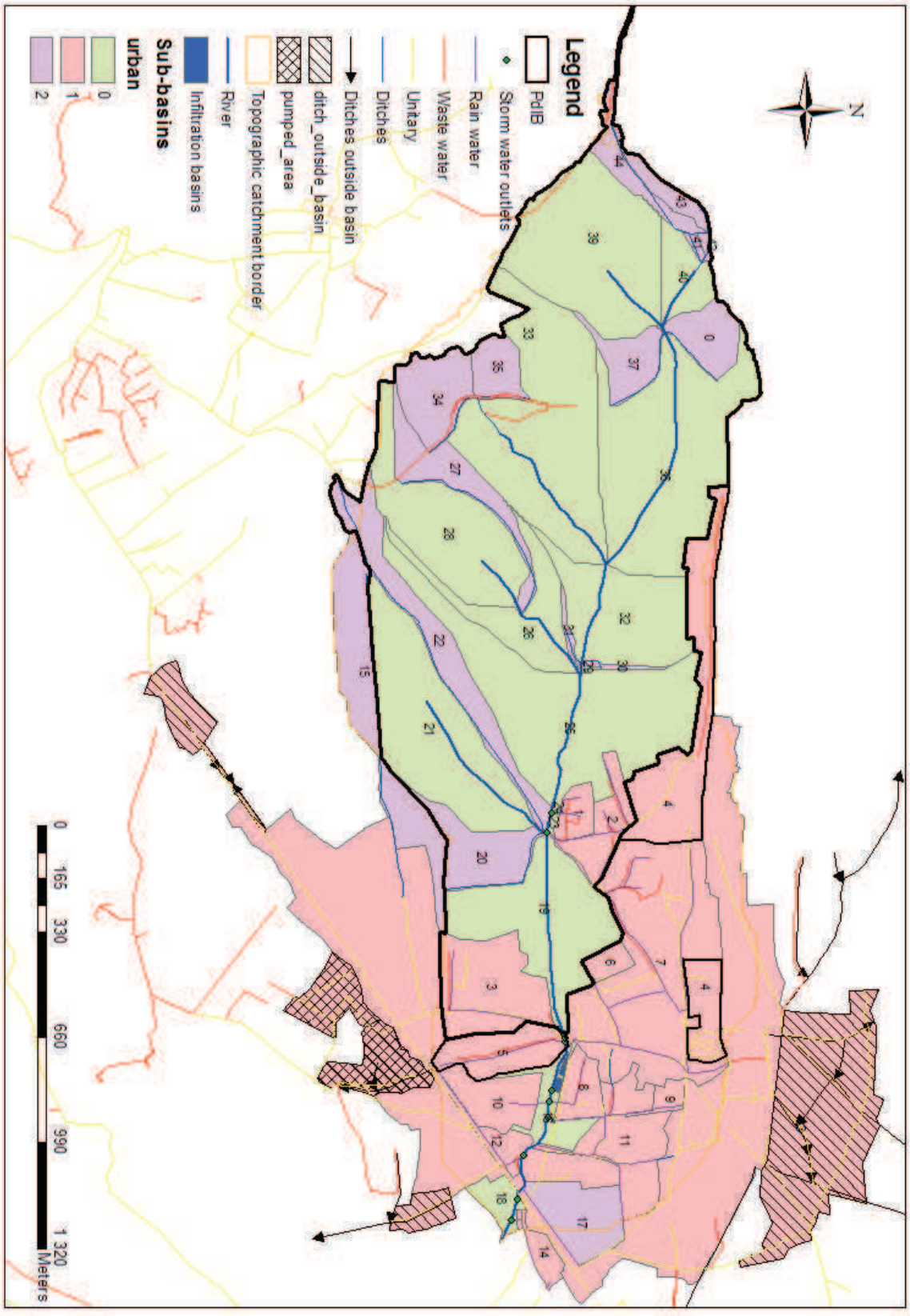

Figure A.0.11.: Sub-basins of the Chaudanne catchment. Urban sub-basins are in red, natural in green and rural under influence of a ditch in violet. The catchments of the Old and New Pont de la Barge are separated by a thick black line. The ditches with arrows are leading to another stream than the Chaudanne.

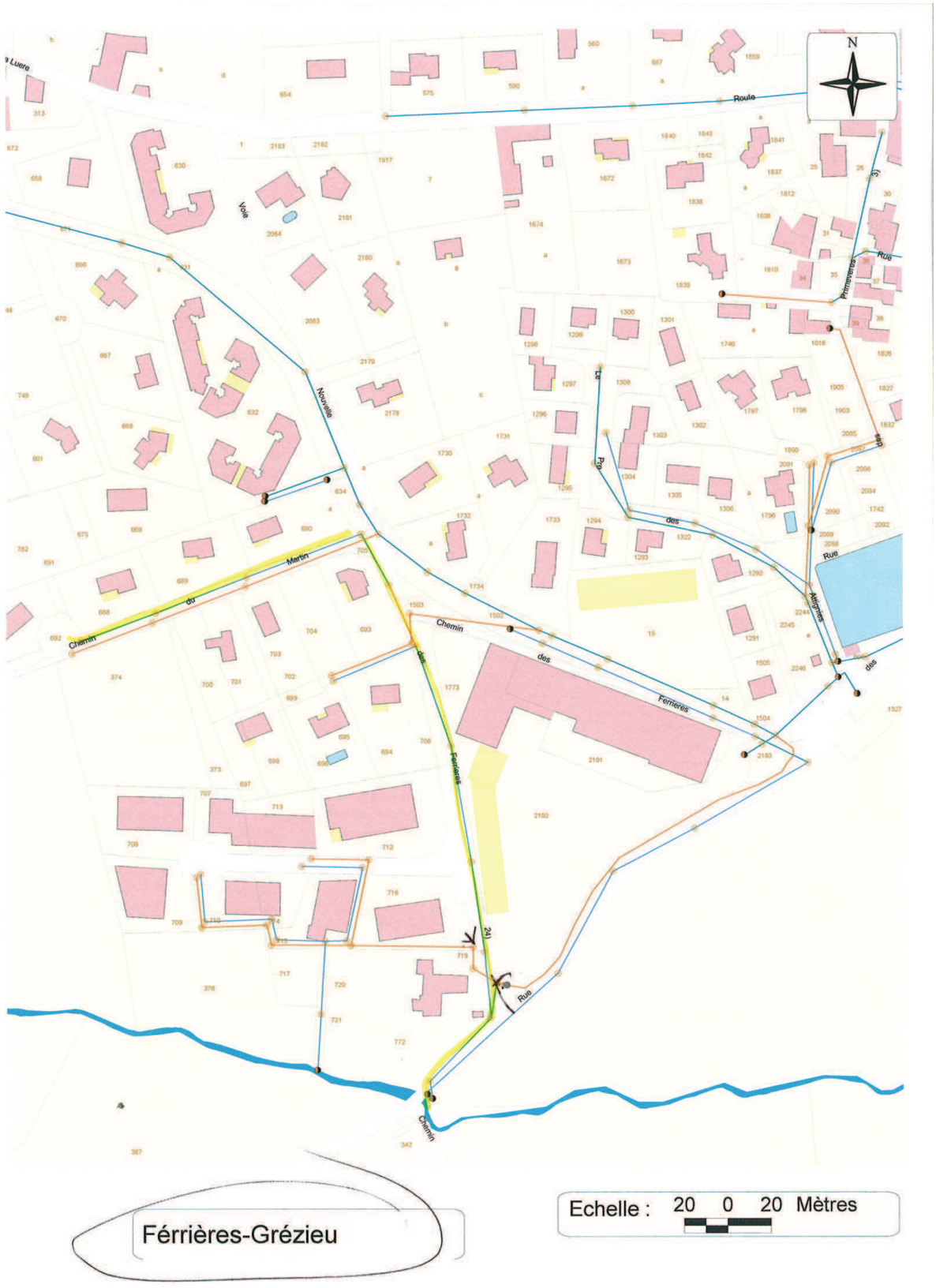

Figure A.0.12.: Plans of the sewer system at Ferriere from the SIAHVY. The digital data of the sewer system do not have the rainwater pipe system included.

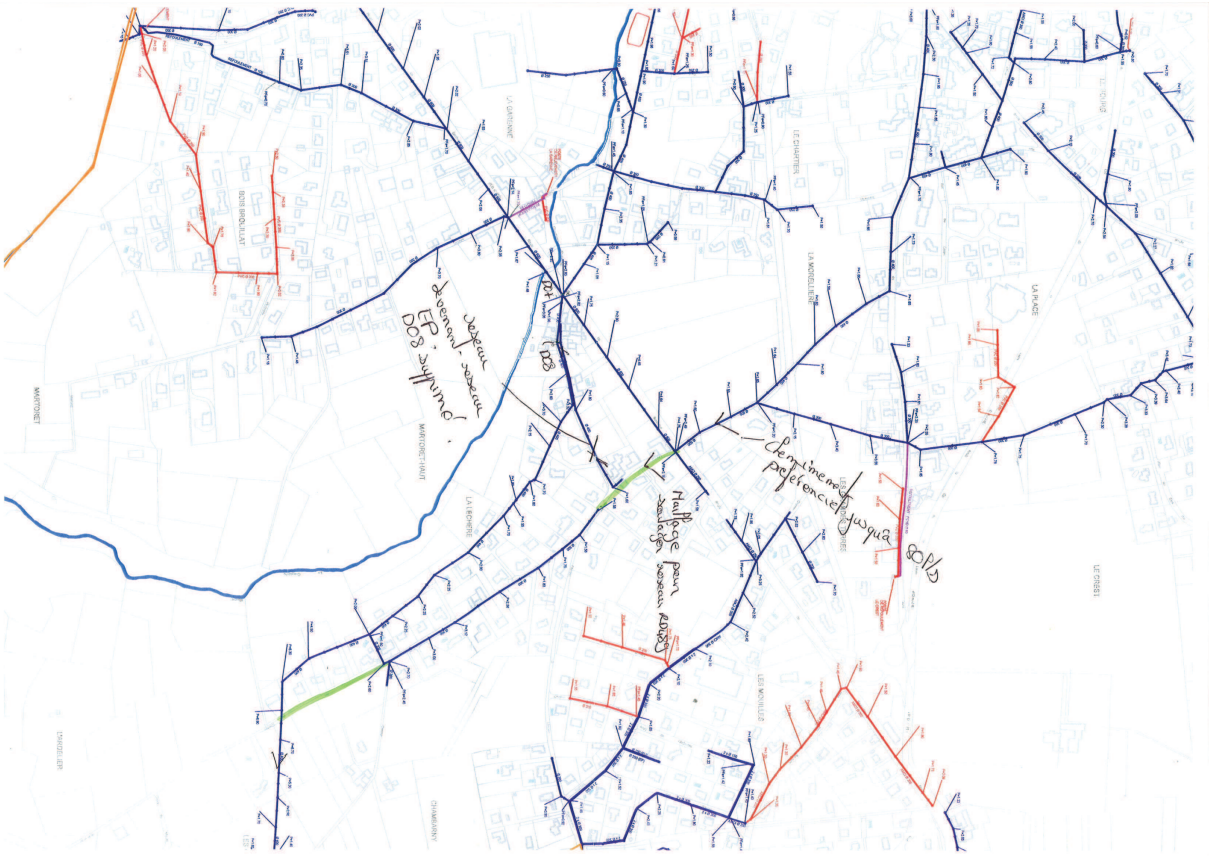

Figure A.0.13.: Map of the new connections under construction in sub-basin 13 [SIAHVY].

B. Sub-basins delineated by SED

The SED (2011), an engineering company, developed a rainwater management plan for the community of Grézieu-la-Varenne and modeled for this reason the rainwater drainage system with the model CANOE (Sogreah and Insavalor, 2005). Figure B.0.1 shows their sub-basins, modelled drainage sections and retention basins, which represented their model mesh.

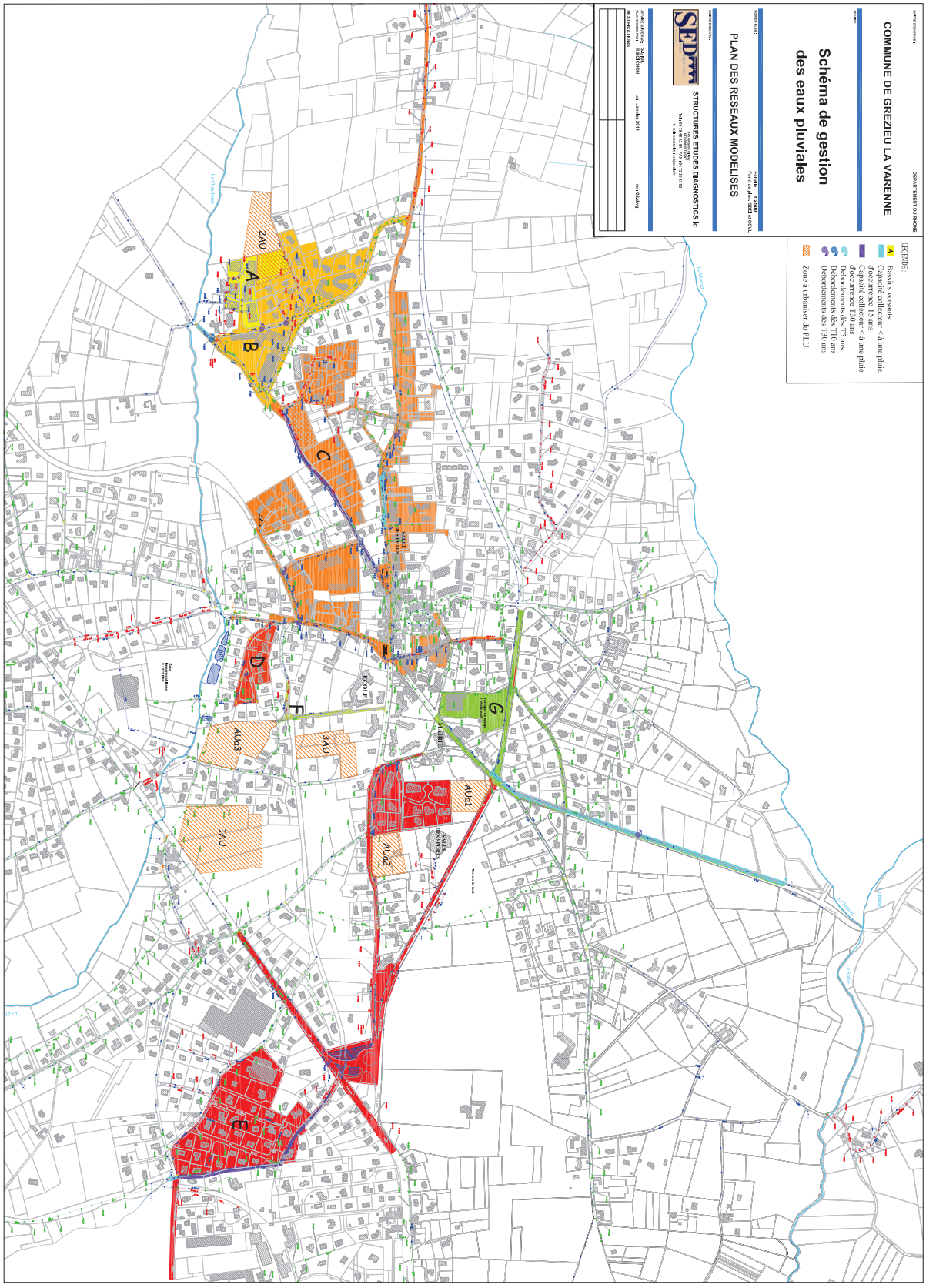

Figure B.0.1.: Sub-basins of the Chaudanne Sewer system used for CANOE modelling, which were determined by the SED (2011).

C. Documentation for PLUS module

Table C.0.1.: Documentation for the PlusHedge instance of PUMMA. The PLUS module instance is connected to the m_slotLateralFlow. The id field of the PLUS table corresponds to the id of HEDGE.

Slot	Instance	Signal	Slot_id
A	Hedge2Simba	m_sigRiverWTLateralFlow	Id_wtri
B	Hedge2Hedge	m_sigLateralFluxA	Id_wti
C	Hedge2Hedge	m_sigLateralFluxB	Id_wti
D	Hedge2River	m_sigRiverWTLateralFlow	Id_wtri
E	Urbs2Hedge	m_sigLateralFluxB	Id_wti

Table C.0.2.: Documentation for the PlusHedgeOverland instance of PUMMA. The PLUS module instance is connected to the m_slotOverlandFlow. The id field of the PLUS table corresponds to the id of HEDGE.

Slot	Instance	Signal	Slot_id
A	Olaf_Hedge2hedge	m_sigPondingExtractionFlow	Id_olaf
B	Olaf_Hedge2hedge	m_sigOverlandFlow	Id_olaf
C	Olaf_hedge2river	m_sigPondingExtractionFlow	Id_olaf
D	Olaf_hedge2simba	m_sigPondingExtractionFlow	Id_olaf
E	River	m_sigOutletDischarge	Id_river
F	city	m_sigPummaToOverlandFlow	Id_urbs
G	Olaf_hedge2urbs	m_sigPondingExtractionFlow	Id_olaf

Table C.0.3.: Documentation for the PlusRiverSurface instance of PUMMA. The PLUS module instance is connected to the m_slotLateralSurface. The id field of the PLUS table corresponds to the reach id of RIVER1D.

Slot	Instance	Signal	Slot_id
A	city	m_sigPummaToRiver	Id_urbs
B	Tdso	m_sigInDischarge	Id_tdso
C	Olaf_hedge2river	m_sigOverlandFlow	Id_olaf
D	city	m_sigPummaToOverlandFlow	Id_urbs
E	lake	m_sigOutflow	Id_simba

Table C.0.4.: Documentation for the PlusRiverSubsurface instance of PUMMA. The PLUS module instance is connected to the m_slotLateralSubsurface. The id field of the PLUS table corresponds to the reach id of RIVER1D.

Slot	Instance	Signal	Slot_id
A	Hedge2River	m_sigWTRiverLateralFlow	Id_wtri
B	Urbs2River	m_sigWTRiverLateralFlow	Id_wtri

Table C.0.5.: Documentation for the PlusRiverSource instance of PUMMA. The PLUS module instance is connected to the m_slotSource. The id field of the PLUS table corresponds to the reach id of RIVER1D.

Slot	Instance	Signal	Slot_id
A	Inflow	m_sigData	Id_input = Id_RiverReach
B	Simba	m_sigOutflow	Id_simba
C	Tdso	m_sigOutDischarge	Id_tdso
D	River	m_sigOutletDischarge	Id_river

Table C.0.6.: Documentation for the PlusSistba instance of PUMMA. The PLUS module instance is connected to the m_slotGroundwater. The id field of the PLUS table corresponds to the id of SISTBA.

Slot	Instance	Signal	Slot_id
A	Hedge2Sistba	m_sigRiverWTLateralFlow	Id_wtri
B	Urbs2Sistba	m_sigRiverWTLateralFlow	Id_wtri
C	River	m_sigOutletDischarge	Id_river
D	Olaf_hedge	m_sigOverlandFlow	Id_olaf
E	Sistba	m_sigOutflow	Id_Sistba
F	city	m_sigPummaToOverlandFlow	Id_urbs

Table C.0.7.: Documentation for the PlusUrbs instance of PUMMA. The PLUS module instance is connected to the m_slotSZSinkSource. The id field of the PLUS table corresponds to the id of URBS.

Slot	Instance	Signal	Slot_id
A	Urbs2Urbs	m_sigLateralFluxA	Id_wti
B	Urbs2Urbs	m_sigLateralFluxB	Id_wti
C	Urbs2River	m_sigRiverWTLateralFlow	Id_wtri
D	Urbs2Hedge	m_sigLateralFluxA	Id_wti
E	Urbs2Sistba	m_sigRiverWTLateralFlow	Id_wtri

Table C.0.8.: Documentation for the PlusUrbsOverland instance of PUMMA. The PLUS module instance is connected to the m_slotOverlandFlow. The id field of the PLUS table corresponds to the id of URBS.

Slot	Instance	Signal	Slot_id
A	City/urbs2urbs	m_sigPummaToRiver	Id_urbs
B	Olaf_hedge2urbs	m_sigOverlandFlow	Id_olaf

D. Geographical pre-processing: work plan of the Master students

Detailed list of tasks and plannings (in French or English):

Planning Yvan Paillé: Stage du février 2010 au juillet 2010

Sujet: Préparation des zones urbaines pour la modélisation avec PUMMA

Objectif : Remplir la table Postgresql avec les paramètres/géométries nécessaires :

1. UHE (géométrie, the_geom)
2. built area
3. road area
4. natural area
5. wooded percentage
6. longueur de l'UHE (hee_deep)
7. Altitude moyenne par parcelle
8. Distance to center of building

Différentes Tâches :

1. Créer l'UHE (Urban Hydrological Element) : il faut ajouter un bout de la route à la parcelle cadastrale.

a) Cas simple :1 parcelle + bout d'une route (route pas découper au milieu)
   - extraire ligne qui touche route
   - tampon autour de cette ligne
   - découper route (v.overlay)
   - fusionner avec parcelle à côté

b) Une route avec 5 parcelles (d'une côté de la route)
   Ecrire script en phyton

c) Une route avec 3 parcelles de chaque côté (script python)
   - Essayer algorithme v.centerline
   - Si cela ne marche pas : Prendre route déjà découpée

d) Toute la Chaudanne
   - Corrections manuelles des places (couches voierie)
   - Eventuellement corrections manuelles de la couche réseau linéaire si v.centerline ne marche pas
   - Appliquer l'algorithme développé dans b)

2. Calculer les surfaces et paramètres (entrée dans table Postgresql)
   - bâti (allées+bâti)
   - route
   - naturelle = surface(UHE) – bâti – route - piscine
   - piscine
   - (pourcentage boisée par parcelle) il faut attendre les données de Kristell
   - longueur de l'UHE (hee_deep)
   - altitude moyenne par parcelle (MNT + area(MASK), boucle sur les polygones)

Planning Pedro Sanzana: Master thesis September 2010-February 2011

A) Creation of intermediary HRU maps

1) Cut all input polygon layers according to the latest catchment borders
Already done for land use maps.

2) Automatic topological corrections for each layer
The topology of each input layer (land-use, sub-basins, geology and soil) should be cleaned. See if *clean_ogr* of Yvan is enough. Apply it to soil, geology map and sub-basins.
Land use maps are already treated (see new data I sent you)

Try to apply a smoothing algorithm (*m.Douglas* or other grass functions) to the land-use map in order smooth the hedgerows, see Figure 1.

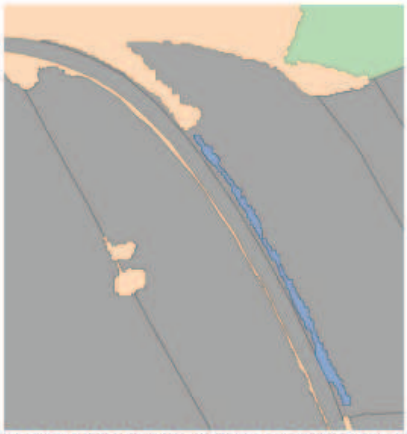

Figure 1: An extract showing polygons with big dangles and the too detailed structure of the hedgerows.

If Yvan's algorithm isn't enough, a description of problems which have to be faced is given in the first description of the master thesis.

3) Union of urban map (UHEs created by Yvan) with landuse map
We want to keep the UHEs as they are (no intersection with sub-basin, land-use, soil and geology layer). For this, the part of the HRU map which is covered by the UHE map has to be replaced by the UHEs. This will need two v.overlays (first "not" and then "or"; substraction and addition).

4) Fitting of the ditch network towards the landuse map (roads/UHE borders).
The land-use map should not change hereby. The ditch will be corrected with the street or UHE borders. This will need a snap function, where the land-use map can be given as reference. Try a threshold of 5 in the beginning and see what you get. Then try a threshold of 10 and see if the result is still realistic. Maybe at some places we have to correct it manually.
→ script *m.snaplp* of Geomhydas
input: ditch network(lines) + land use map (polygons) united with UHEs.
The river network consists of two files (natural network-ditches and the combined sewer system)

Figure 2: An extract showing the unclean topology of a ditch beside the road. The ditch should follow the road boarder.

To clean and check the river geometry apply also the *m.network* algorithm.

5) Intersection of the topological clean maps and the river network
Same as for the landuse map: Replace the part covered by the UHEs with them for the geology, soil and sub-basin map. This will need two v.overlays (first "not" and then "or"; substraction and addition). Manual correction might be necessary for the sub-basin map close to the border of the UHEs.
Try then to apply the m.seg algorithm with the landuse-UHE, sub-basinUHE, soilUHE and geologyUHE maps and the natural river network. You might have to treat the river sources manually, and see if m.seg works with a non-connected river network file (caused by the lakes).

6) Automatic topological corrections of the intersected map without changing the land-use map. The land-use map represents the criteria for the choice of the module. It contains small features like hedges which have a great influence on the hydrology compared to their size. In order to keep these important features, the borders of the land-use units should not be changed during the topological corrections, but only the borders of geological, soil and sub-basin units. The algorithm *m.dispolygseg* and *m.sliverpolygseg* should be able to treat this task. In detail the corrections should concern:

- Removing of duplicate features
- Snapping of close lines and vertexes
- Fusion of small areas to reduce the number of HRUs and accelerate the calculation process of the model.

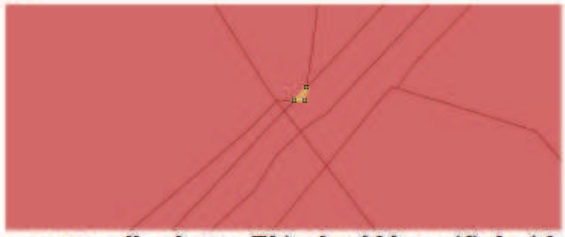

Figure 3: An extract showing a too small polygon. This should be unified with the road (long polygon).

- Check if vertexes between polygons are corresponding, see Figure 4:
- Cut polygons with holes

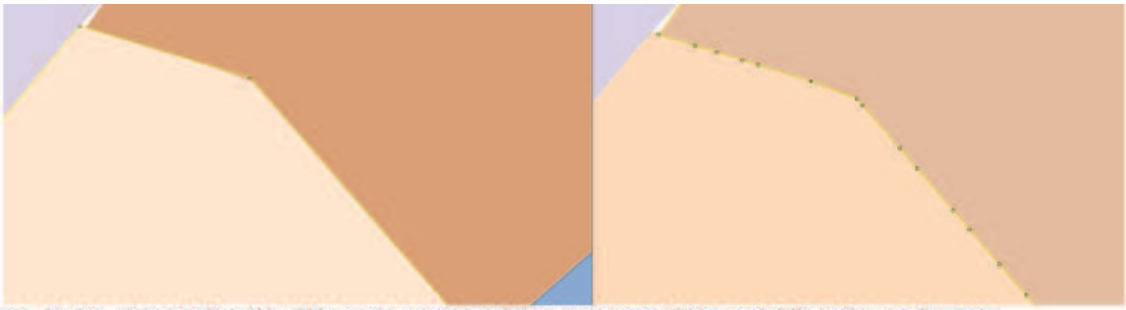

Figure 4: An extract showing the not corresponding vertexes of two neighbouring polygons.

7) Preparation of real river network

a) **Segmentation of river network.** Instead of re-creating the correct geometry of the ditch reaches, we will take the boundaries of the polygons as ditch.
   a. For this, create a small buffer around the layer "filvoirie" for the urban part.
   b. Intersect the buffer with the boundaries of the polygons (apply v.type and probably v.category before) with v.overlay.
   c. Select then all lines longer than the buffer distance. Verify that you didn't loose any river lines (parts of filvoirie).
   d. Once you have the segmented river, Sonja will compare this road network to the real sewer network and adapt it in some parts.
   e. We will have to think how to get the attributes of the ditch/sewer network file in a later step (*v.distance?)*
   f. Also, the algorithm for the rural ditches will be a little bit different.

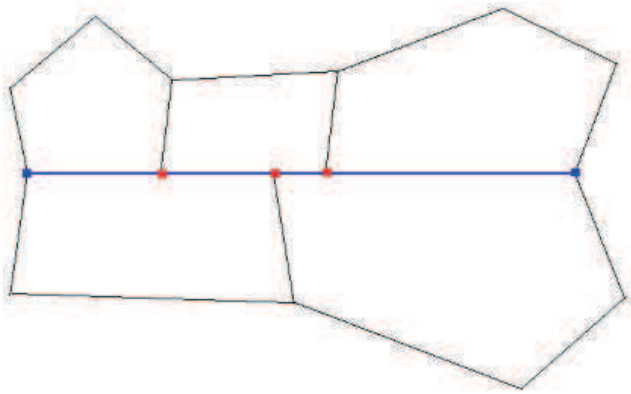

Figure 5: Polygon mesh with river network (blue). The river network has to be intersected at the red points.

b) Fusion of too small lines depending on a threshold value, *m.disline*

c) Verify the line direction, *v.edit/flip.* If a script seems too complicated, we will do this manually. A script could be based on *v.to.points* and a comparison of the coordinates. *v.edit/flip can be used for the correction.*

Develop an algorithm for the right numbering of the river network (similar to *m.toporeach*). The source has the lowest reach number. In case of several rivers the reach numbering has to be continuous. For example: the first river has reach numbers from 1 to 10, then the second river will start from 11. A new river has to start in case of interruption with a lake. Use as input the segmented river file and a point shape file containing the different outlets, where the total outlet has the identifier 1. The idea is to run through a loop for the outlets and

a) then for each reach. The question will be to keep the reach numbers in memory. Use also the postgresql function touch. And correct the geometry of the lines before (export to text format and reimport to postgresql format of the geometries.).

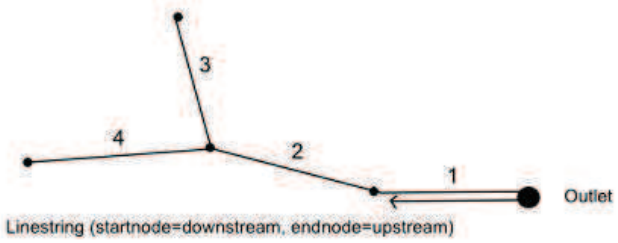

Figure 6: Scheme of a river, where the numbering starts with 1 at the outlet. The line direction of the river reaches is from downstream to upstream.

8) Calculation of mean slope and altitude for each river reach and HRU segment with the help of the digital elevation model and storage in the attributes file.
→ Yvan's script *hauteur_moyenne* for polygons, rest to develop.

B) Improvement of the HRU map and adaptation to numerical needs (Pedro)

The model will run with any input geometry. However, the results might not be very realistic. For example, the interfaces use the distance between the centroids for the Darcy equation. If the centroid is outside the polygon, this distance does not have a real physical sense. Also, the polygons and river reaches should be of comparable size. So, the idea is to develop algorithms to adapt the geometries depending on certain criteria and threshold values.
The result map of task 6 (after the correction of the polygons with holes) will be the reference map. Simulations will be executed based on this map, and in comparison on maps including the following corrections.

1. Calculate mean slope and standard deviation (std) for each polygon. Create an algorithm: If the std is too big (depending on a threshold value) cut the polygon in two depending on the slope.

2. Convexity
   - if centroid outside of polygon → cut the polygon. The question is following what kind of rule?

3. Maximal size of polygons
   - if the polygon is bigger than a certain size → cut the polygon. Rule?

4. Maximal length of river reaches
   if reach length > threshold cut in the middle

Figure 7: An extract showing a polygon in an another polygon, which creates a hole. A solution of cutting is proposed in black lines.

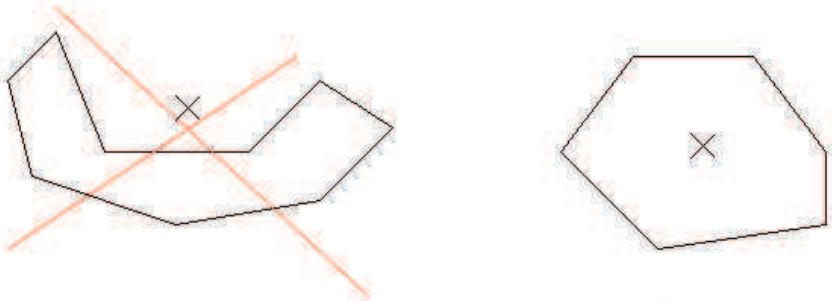

Figure 8: A scheme showing a concave polygon with its centre outside of the polygon on the left side and a convex polygon, with its centre inside the polygon on the right side.

Planning Florent Brossard: "Stage" from November 2010 to February 2011

Objective: Hydrologic routing of the model: Connexion of HRUs/UHEs to the river network

1) Connection between URBS and RIVER1D

Develop algorithm of F. Rodriguez (thesis page 65 top) for the connection of the urban part. This algorithm connects the cadastral parcels to the closest and lowest drainage reach. The correspondences have to be defined in the plus_plusriversurface_table:

Table 1 : Input parameter table of the module PLUS.

Id (Slot)	Slot_name	Slot_id
Id river reach	A	Id UHE

2) WTI/WTRI interfaces

The model differentiate two interfaces which allow the exchange of a subsurface flow via the Darcy law: Water Table Interface (WTI) between two agricultural fields or hedgerows and Water Table River Interface (WTRI) between the river and the adjoining field. The flow direction depends only on the hydraulic pressure in the adjacent fields and can therefore be in all directions. Figure 1 shows two agricultural fields (polygons) which are separated by a Water Table Interface (line). Table 2 represents the input table (in a Postgresql/Postgis database) of the module WTI and Table 3 the input table for WTRI. This task of the pre-processing aims at writing the right GIS data, like here id_a, id_b, surface_level of the line, the coordinates of the line (the_geom) and of the centroids of field a and field b. The other parameters are not geometric and will not be considered in this master thesis. The corresponding tables are automatically created by the model PUMMA.

A different input table exist for each kind of connection:

- wti_hedge2hedge, wti_hedge2frer1d, wti_hedge2urbs, wti_urbs2urbs, wti_urbs2frer1d, wti_frer1d_frer1d
- wtri_hedge2river, wtri_hedge2simba, wtri_urbs2river, wtri_urbs2simba, wtri_frer1d2river, wtri_frer1d2simba

The first task will therefore be to identify all equal neighbours and to extract the lines in between. Then the necessary variables can be assembled in one table. The surface_level of the interface will have to be calculated due to a linear interpolation between the altitudes and the distance between the centroids.

The correct filling of the tables will assure a correct flow routing during the model run.

Table 2 : Input parameter table of the interface module WTI.

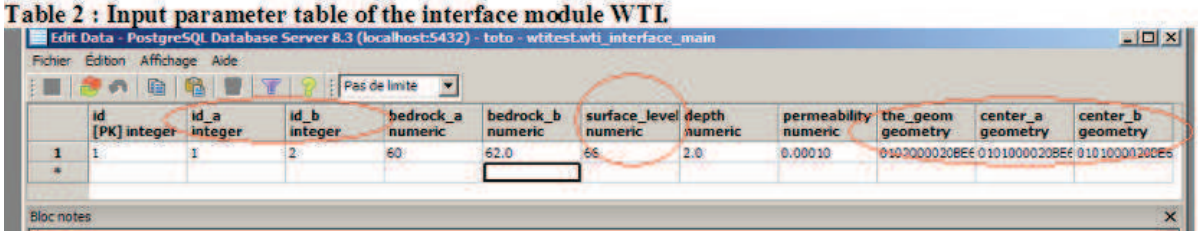

Table 3 : Input parameter table of the interface module WTRI.

Edit Data - PostgreSQL Database Server 8.3 (localhost:5432) - toto - pummasfo3.wtri_hedge2river_main

Fichier Édition Affichage Aide

Pas de limite

	id [PK] integer	id_plot integer	id_riv integer	riv_bottomwidth numeric	riv_bottomlevel numeric	riv_bedrock numeric	plot_bedrock numeric	permeability numeric	the_geom geometry	center_plot geometry
1	1	4	5	0.3	199.5	199	199.2	0.000005	0102000020BE6	0101000020BE6
2	2	3	5	0.3	199.5	199	199.2	0.000005	0102000020BE6	0101000020BE6
*										

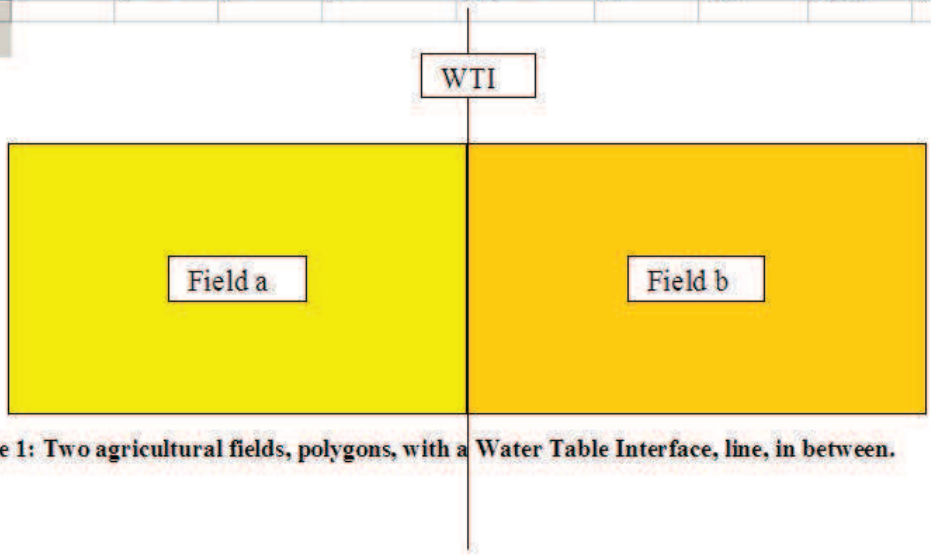

Figure 1: Two agricultural fields, polygons, with a Water Table Interface, line, in between.

3) OLAF

OLAF (Over Land Flow) is a module which calculates, similar to the WTI/WTRIs, the overland flow with a Manning equation. The overland flow is based on topography and for the moment, the flow direction between polygons has to be unique. For this reason, only the interfaces (intersecting lines) between the polygons with the steepest slope have to be selected. The algorithm *m.toposu* or parts of it might be useful for this task. A different input table exist for each kind of connection:

- olaf_hedge2hedge, olaf_hedge2frer1d, olaf_frer1d_frer1d, olaf_hedge2river, olaf_hedge2simba, olaf_frer1d2river, olaf_frer1d2simba
- olaf_urbs2urbs, olaf_hedge2urbs, olaf_urbs2frer1d, olaf_urbs2river, olaf_urbs2simba

Table 4 : Input parameter table of the module OLAF.

Fichier Édition Affichage Aide

Pas de limite

	id [PK] integer	id_in integer	id_out integer	n numeric	alpha numeric	beta numeric	ngf_in numeric	ngf_out numeric	the_geom geometry	geom_in geometry	geom_out geometry
1	1	1	1	0.08	0.5	1.666667	201	200	0102000020BE6	0103000020BE6	0103000020BE6
*											

E. Cosby and Rawls and Brakensiek pedo-transfer functions

The Cosby et al. (1984) pedo-transfer function, which permits the calculation of the Brooks and Corey (1964) parameters θ_s (%), h_{BC} (cm), K_s (inch/h) and λ, is based on the percentages of sand, silt and clay.

table	Paramètres □= c1+c2Cl+c3Sa+c4Si			
Coefficients	log(Hbc)	1/λ	θs	log(Ks)
c1	1,54	3,1	50,5	-0,6
c2	0	0,157	-0,037	-0,0064
c3	-0,0095	-0,003	-0,142	0,0126
c4	0,0063	0	0	0

Figure E.0.1.: Cosby et al. (1984) pedo-transfer function.

The Rawls and Brakensiek (1985) pedo-transfer function, can also be used to calculate the Brooks and Corey (1964) parameters (θ_r (m^3m^{-3}), h_{BC} (cm), K_s (cm/h) and λ). It includes the porosity Φ (m^3m^{-3}) additionally to the percentages of sand and clay into the calculation. The equation is valid for soil texture with $5\% \leq sand \leq 70\%$ and $5\% \leq clay \leq 60\%$.

Function type f=c1 + c2.[argile] + c3.[sable] + c4.f + c5.[argile]² + c6.[argile].Φ+ c7.[sable]² + c8.[sable]. Φ+ c9. Φ² + c10.[argile]. Φ²+ c11.[argile]².[sable] + c12[argile]². Φ+ c13.[argile].[sable]² + c14.[argile]². Φ² + c15.[sable]². Φ+ c16.[sable]². Φ²
avec [argile]=taux d'argile(%), [sable]=taux de sable(%) et Φ=porosité(m^3/m^3)

Coefficients	exp(f) Hbc	exp (f) λ	(f) θr	exp (f) Ks
c1	5.3396738	- 0.7842831	-0.01824820	-8.968470
c2	0.1845038	0	0.00513488	-0.028212
c3	0	0.0177544	0.00087269	0
c4	- 2.48394546	-1.0624980	0.02939286	19.53480
c5	0.00213853	- 0.00273493	-0.00015395	-0.0094125
c6	- 0.61745089	0	0	0
c7	0	-0.00005304	0	0.00018107
c8	- 0.04356349	-0.03088295	-0.00108270	0.077718
c9	0	1.11134946	0	-8.395215
c10	0.50028060	-0.00674491	-0.00235940	0
c11	0.00000540	0	0	-0.0000035
c12	0.00895359	0.00798746	0.00030703	0.0273300
c13	- 0.00001282	-0.00000235	0	0.0000173
c14	- 0.00855375	-0.00610522	-0.00018233	-0.0194920
c15	- 0.00072472	0	0	0.0014340
c16	0	0	0	0
c17	0.00143598	0.00026587	0	-0.00298

Figure E.0.2.: Rawls and Brakensiek (1985) pedo-transfer function.

The porosity can be estimated based on the FAO soil texture triangle (Figure E.0.3), as Brakensiek et al. (1981) derived a correlation between the soil texture and the porosity based on 1000 samples.

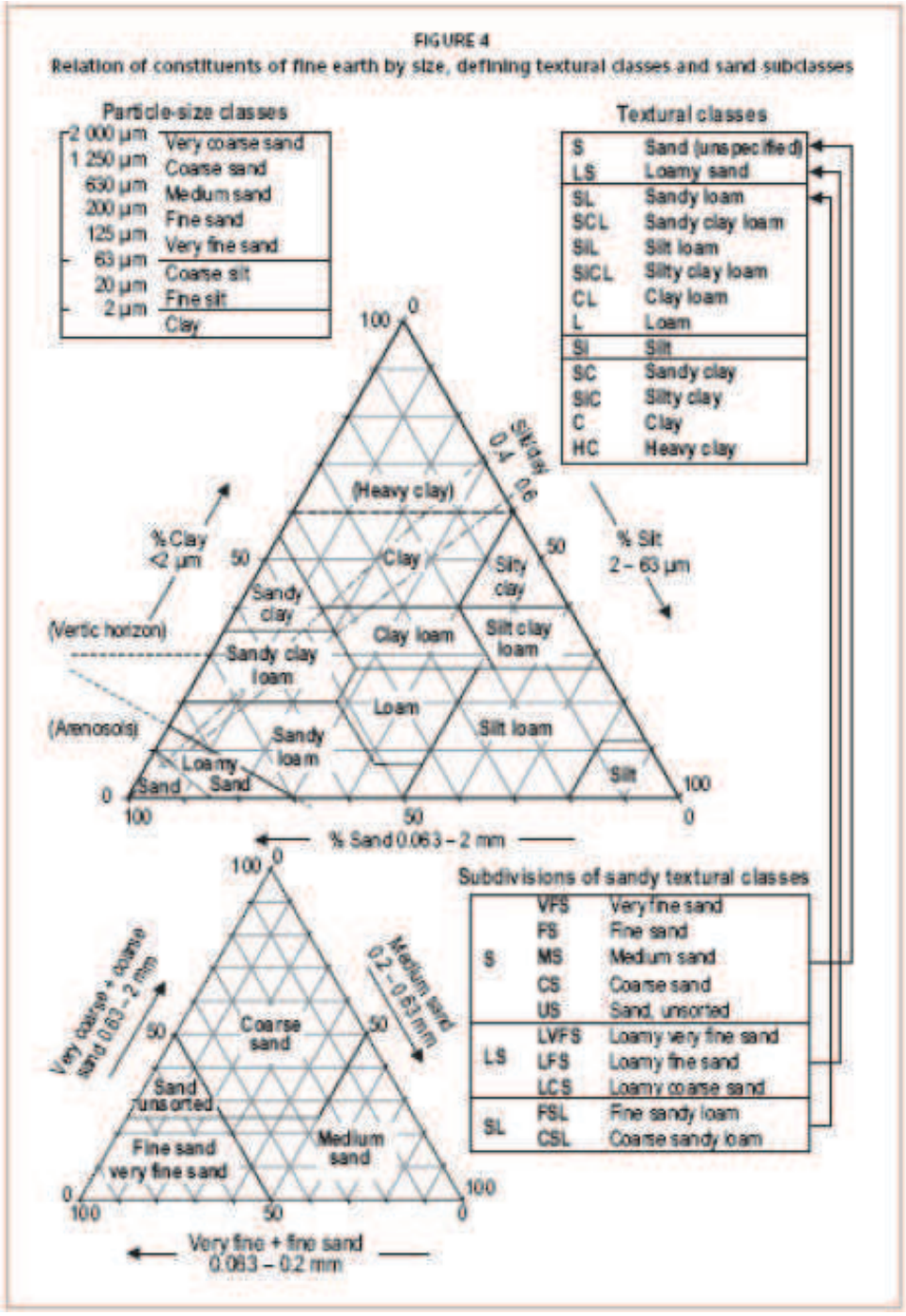

Figure E.0.3.: Soil texture triangle of FAO, 1990.

They calculated the mean and standard deviations, which they added to the mean in order to obtain minimal and maximal values, see Figure E.0.4.

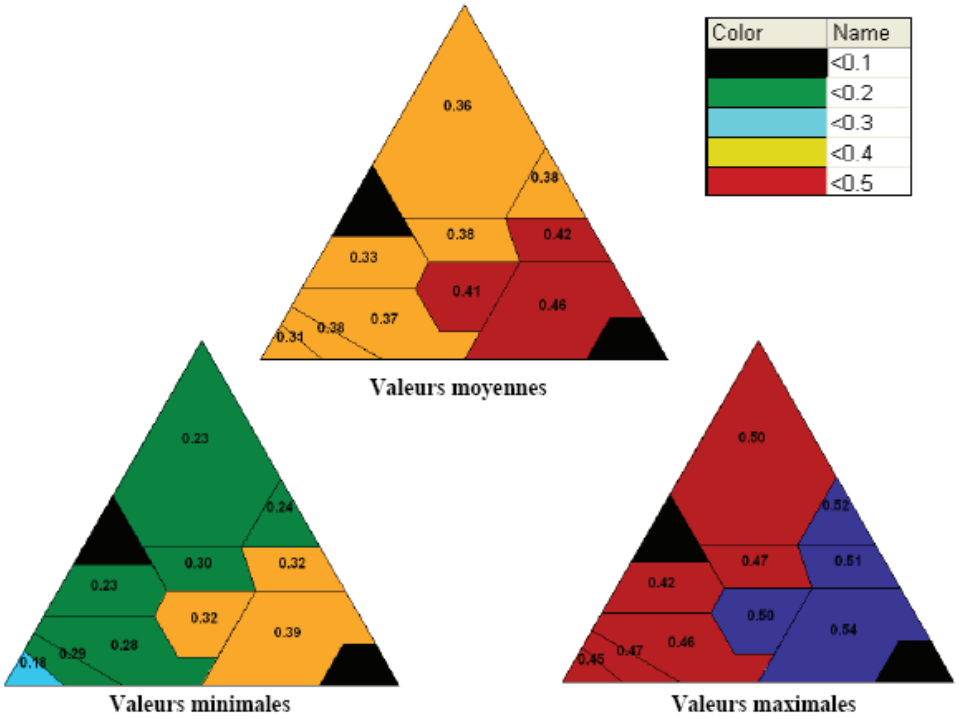

Figure E.0.4.: Porosities derived from soil texture (Brakensiek et al., 1981).

F. Steps and SQL queries for specification of parameters in PUMMA input tables

Each LIQUID module has its own input data tables in order to assure the independence of the modules. This has the disadvantage of creating a database with redundant data. In order to structure the preparation of the input parameters most efficiently, the parameters were classified into three groups:

- Original parameters
- Geographical parameters
- Redundant parameters

The original parameters have to be determined using external sources and data bases. Their determination was explained in section 7. The geographical parameters arise from GIS data layers and they are obtained by the geographical preprocessing explained in section 6.3. A set of SQL queries was developed in order to derive the redundant parameters automatically from the original data. Redundant or derived data can be found in the interfaces WTI, WTRI and OLAF, as well as in most of the PLUS instances and the FCA instances.

The FCA module has two tables per instance, the input and output table. The geometries and ids of the spatial rain and evaporation input tables are copied to the FCA input tables, and the geometries and ids of the HEDGE, URBS and SISTBA modules are copied to the output tables. The geometries of the rain correspond to the Thiessen polygons and for the evapotranspiration to a large rectangle covering everything. The flux type of the FCA input table is set to "unitary". The geometries of the crop coefficient table are also automatically copied from the HEDGE input table.

The bedrocks in the WTI module are calculated as difference of the surface level of each model unit and its soil depth. The soil depth in the interface is calculated as distance weighted middle of the model unit depths. This works well for the HEDGE module, however, the soil depth in the URBS module corresponds to the depth of the pipe and can be close to the surface if the parcel is connected to ditches. The soil depth in the URBS module (parameter "radier_depth") should therefore be greater than zero and correspond to the depth of the ditch. The center of the model units is extracted automatically from its geometry. The surface level of the interface is also calculated as distance weighted middle. A better way would be to derive it directly during the geographical preprocessing from the DEM. An attempt was undertaken, however, the use of multi-geometries for the interface geometry created problems for the calculation of the average altitude. The permeability of the interface is calculated as average of the permeability of the adjacent model units. A weighted middle might be more appropriate.

The river bottom level in WTRI is copied from the river1d_reach table. The river bottom width is extracted from the trapezoidal and rectangular section table of the RIVER1D module. For the WTRI instance which is coupled to SISTBA, the river bottom width,

or rather lake bottom width, is calculated as the distance between the centers of the lake and the plot. The plot_bedrock is derived from the difference of the soil surface and the depth like for the WTI module and the center_plot from the geometry of the plot. The geometry of the interface is determined during the geographical preprocessing and can be part of the line geometry of the river reach. The permeability is set to the permeability of the plot. For the OLAF module, the altitude of the adjacent model units, as well as their geometries are copied from the corresponding tables.

The connections (id_in, id_out) of the WTI, WTRI, OLAF, TDSO or SISTBA modules are determined during the geographical preprocessing. These connections are then copied as redundant data to the corresponding PLUS tables, where the id of PLUS corresponds to id_out and the slot_id to id_in. During this SQL query, the correct slot_name (A to J), is equally filled into the PLUS table. However, not all of the PLUS tables contain redundant data. The following tables had to be filled in directly from external data sources: the connections for the URBS overland and network flow, the river to hedge connection (PlusHedgeOverland, E) representing infiltrating ditches, the connection from URBS and SISTBA to the river (PlusRiverSurface, A and E), the connection between two retention basins (PlusSISTBA, E) and the connection between two rivers (PlusRiverSource, D).

G. Complementary figures to Chapter 8

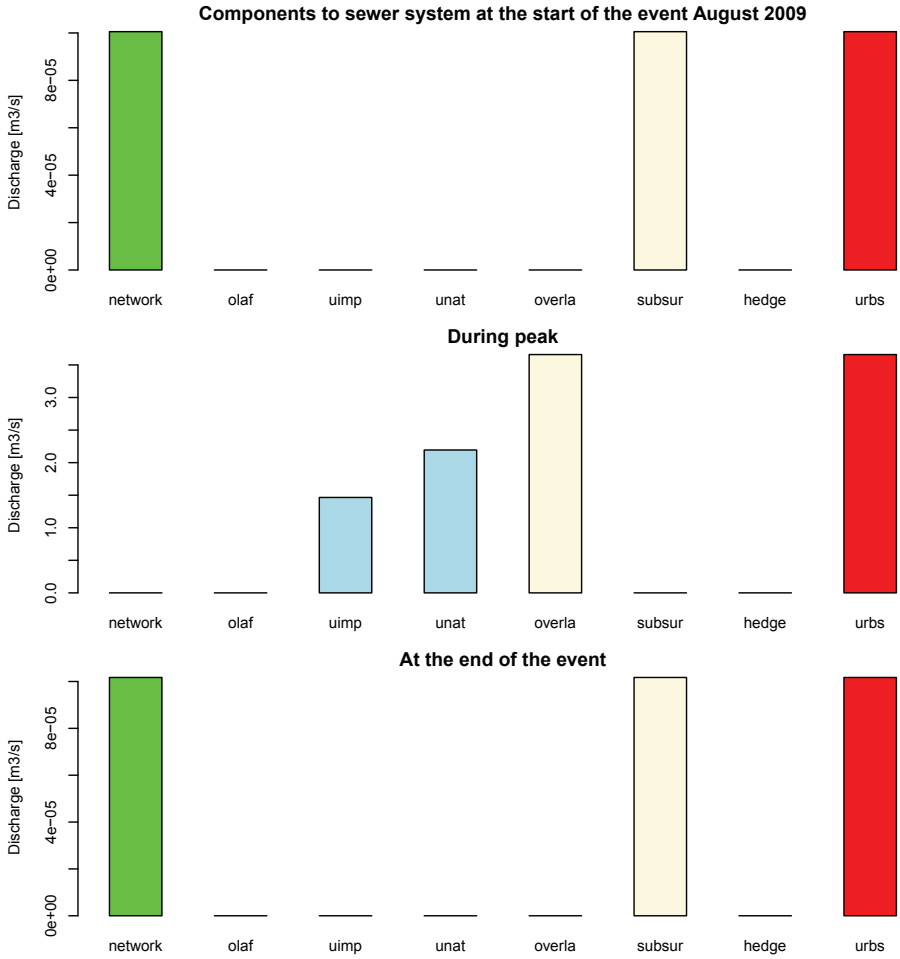

Figure G.0.1.: Analysis of the different components contributing to the discharge in the sewer system for the summer event in August 2009. The discharge before(top), during(middle) and after(bottom) the events is shown. From left to right, the components are the URBS network infiltration (network), the contribution from OLAF and thus HEDGE modules(olaf), the surface runoff from URBS divided in runoff from the impervious surfaces(uimp) and natural areas(unat). The beige columns summarize the module contributions into overland(overla) and subsurface flow(subsur), and the green and red columns into contributions from HEDGE and URBS. The scales of the axis are different.

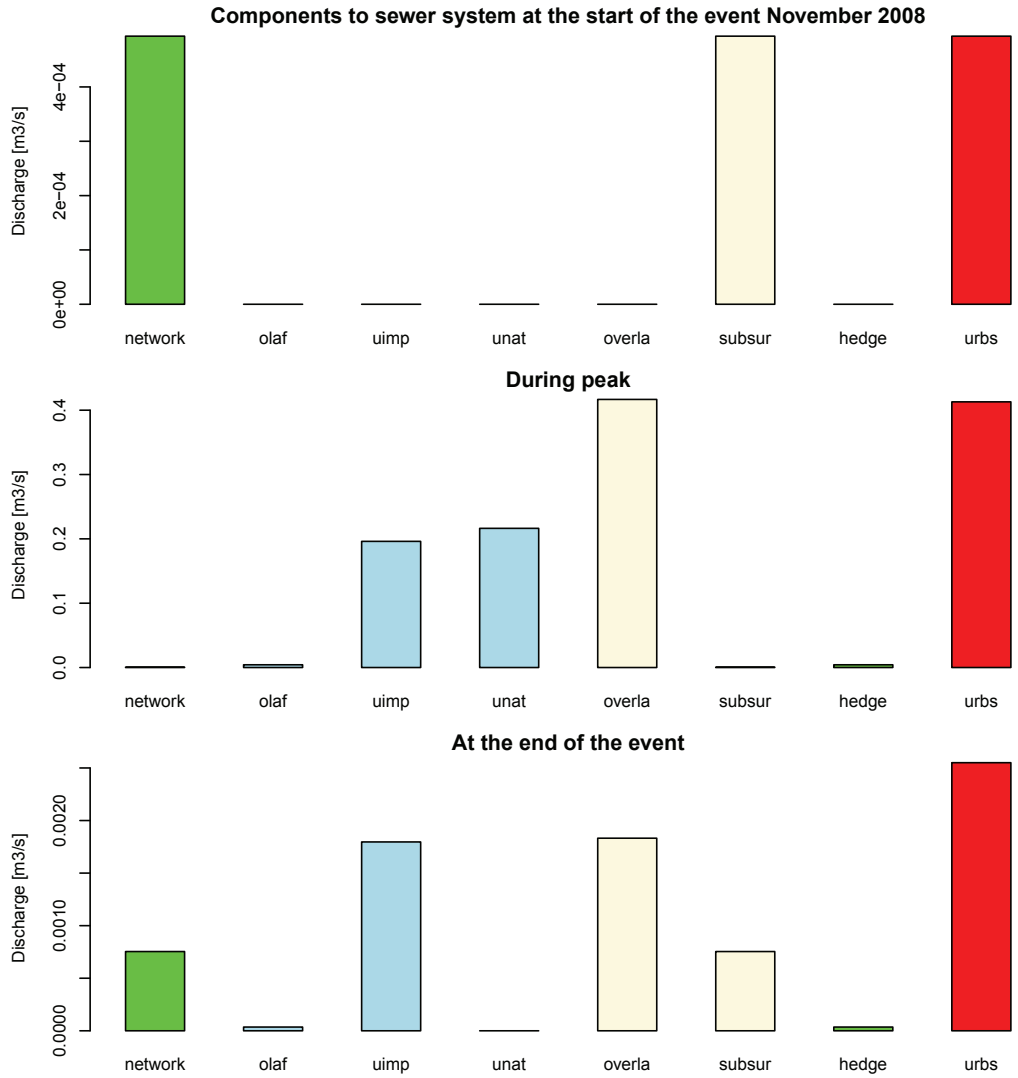

Figure G.0.2.: Analysis of the different components contributing to the discharge in the sewer system for the winter event in November 2008. The discharge before(top), during(middle) and after(bottom) the events is shown. From left to right, the components are the URBS network infiltration (network), the contribution from OLAF and thus HEDGE modules(olaf), the surface runoff from URBS divided in runoff from the impervious surfaces(uimp) and natural areas(unat). The beige columns summarize the module contributions into overland(overla) and subsurface flow(subsur), and the green and red columns into contributions from HEDGE and URBS. The scales of the axis are different.

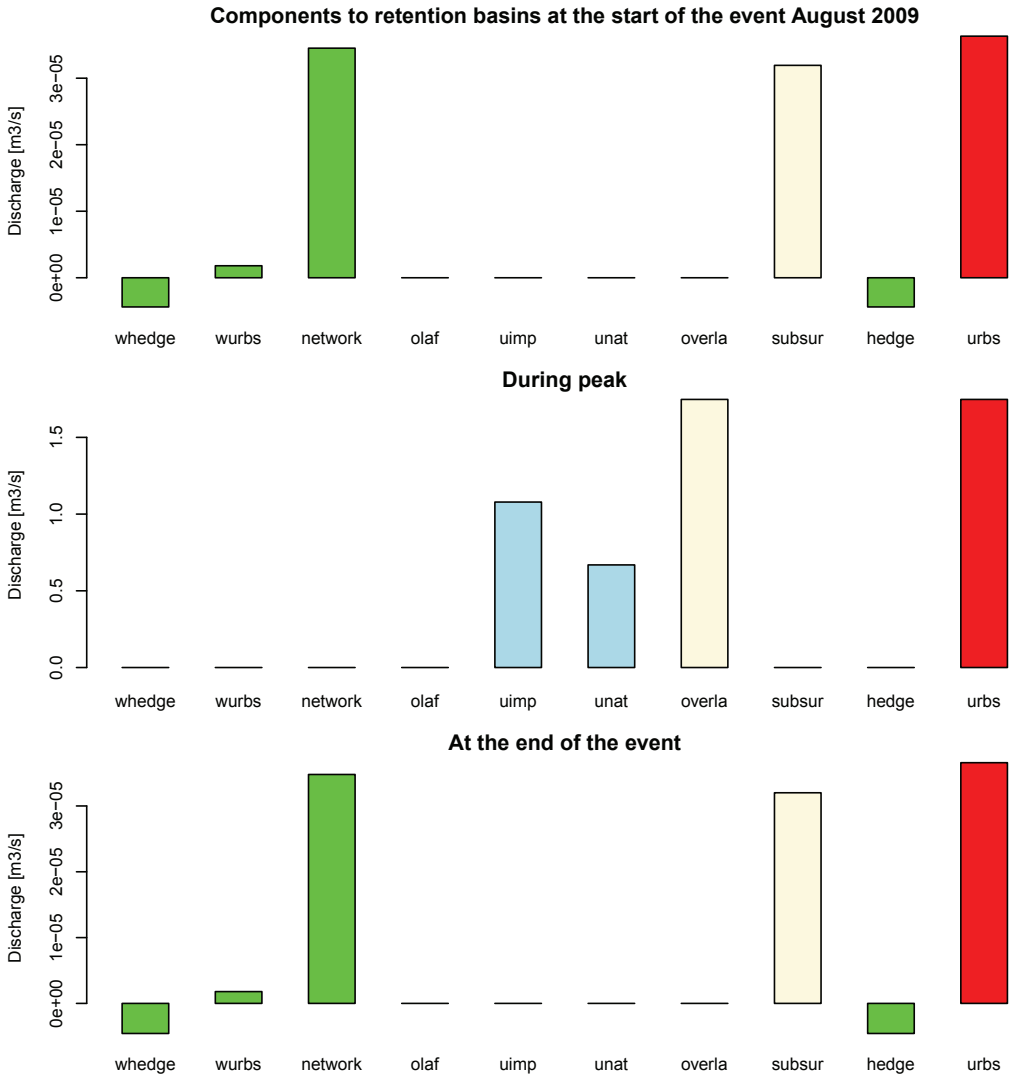

Figure G.0.3.: Analysis of the different components contributing to the discharge in the pipes towards the retention basins for the summer event in August 2009. The discharge before(top), during(middle) and after(bottom) the events is shown. From left to right, the components are the URBS network infiltration (network), the contribution from OLAF and thus HEDGE modules(olaf), the surface runoff from URBS divided in runoff from the impervious surfaces(uimp) and natural areas(unat). The beige columns summarize the module contributions into overland(overla) and subsurface flow(subsur), and the green and red columns into contributions from HEDGE and URBS. The scales of the axis are different.

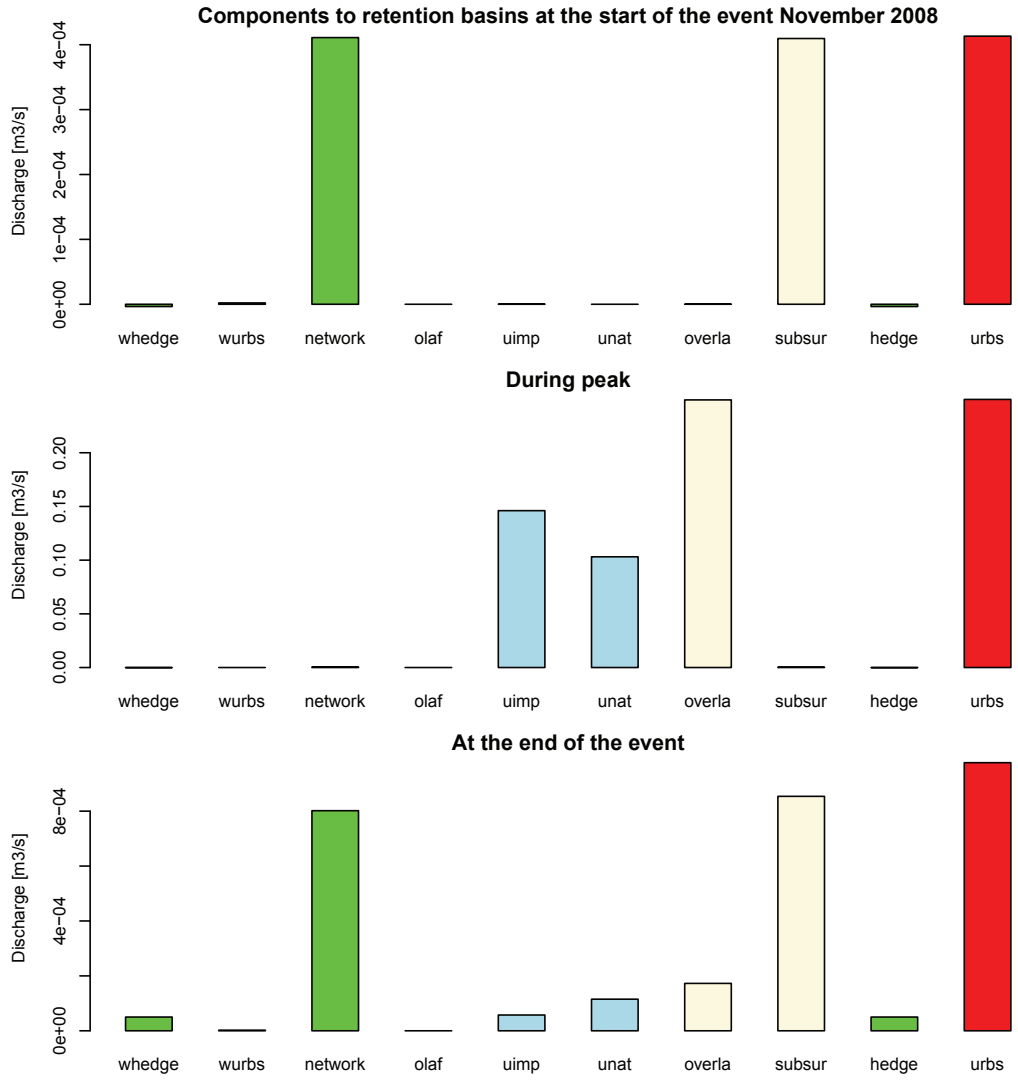

Figure G.0.4.: Analysis of the different components contributing to the discharge in the pipes towards the retention basins for the winter event in November 2008. The discharge before(top), during(middle) and after(bottom) the events is shown. From left to right, the components are the URBS network infiltration (network), the contribution from OLAF and thus HEDGE modules(olaf), the surface runoff from URBS divided in runoff from the impervious surfaces(uimp) and natural areas(unat). The beige columns summarize the module contributions into overland(overla) and subsurface flow(subsur), and the green and red columns into contributions from HEDGE and URBS. The scales of the axis are different.

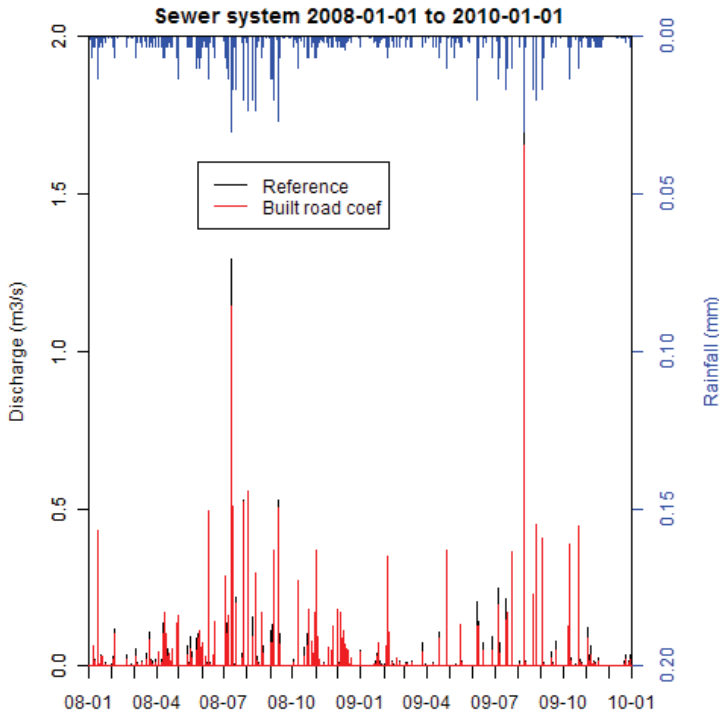

Figure G.0.5.: Simulation with modified URBS built/road link coefficients compared to the reference simulation in the sewer system. The built link coefficient is 0.6 instead of 1, and the road link coefficient 0.5.

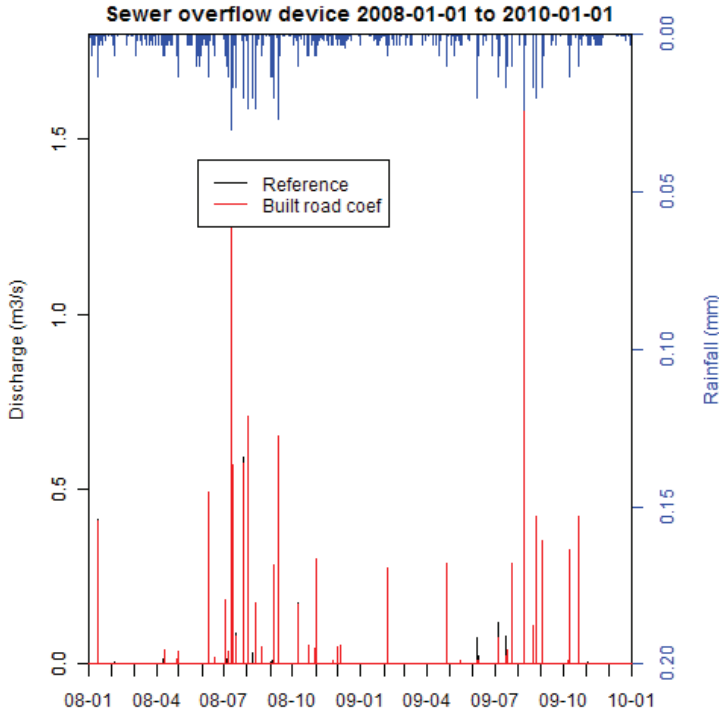

Figure G.0.6.: Simulation with modified URBS built/road link coefficients compared to the reference simulation in the sewer overflow device. The built link coefficient is 0.6 instead of 1, and the road link coefficient 0.5.

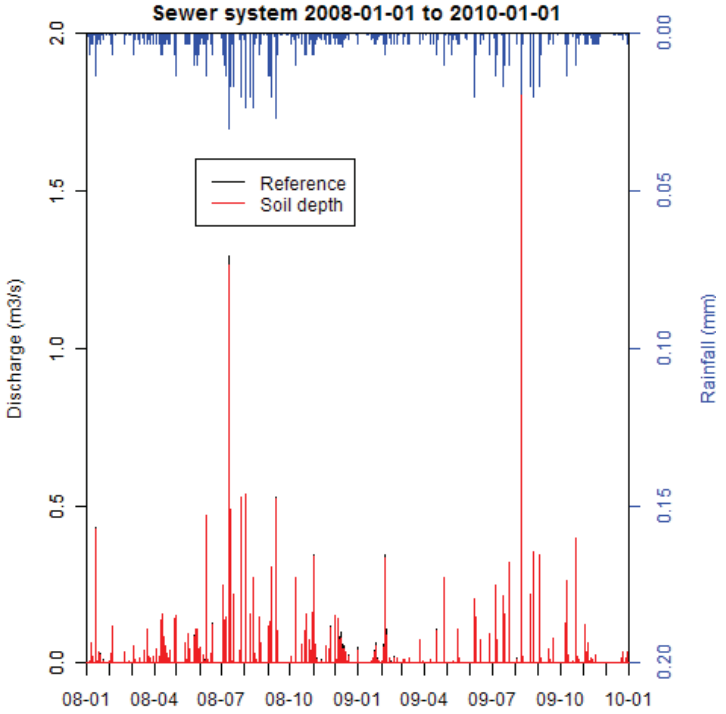

Figure G.0.7.: Simulation with modified soil depth compared to the reference simulation in the sewer system. The soil depths varies between 1 and 3 m instead of the constant 1 m soil depth of the reference simulation.

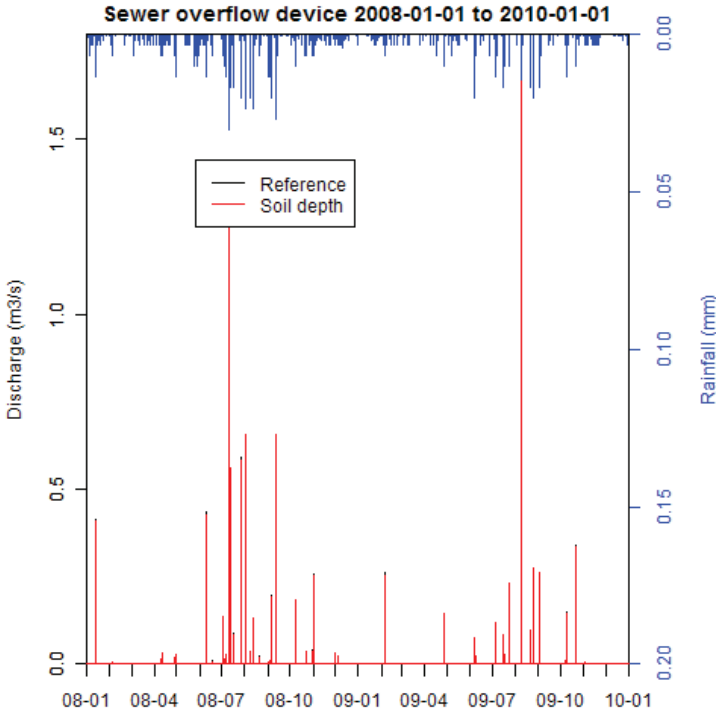

Figure G.0.8.: Simulation with modified soil depth compared to the reference simulation in the sewer overflow device. The soil depths varies between 1 and 3 m instead of the constant 1 m soil depth of the reference simulation.

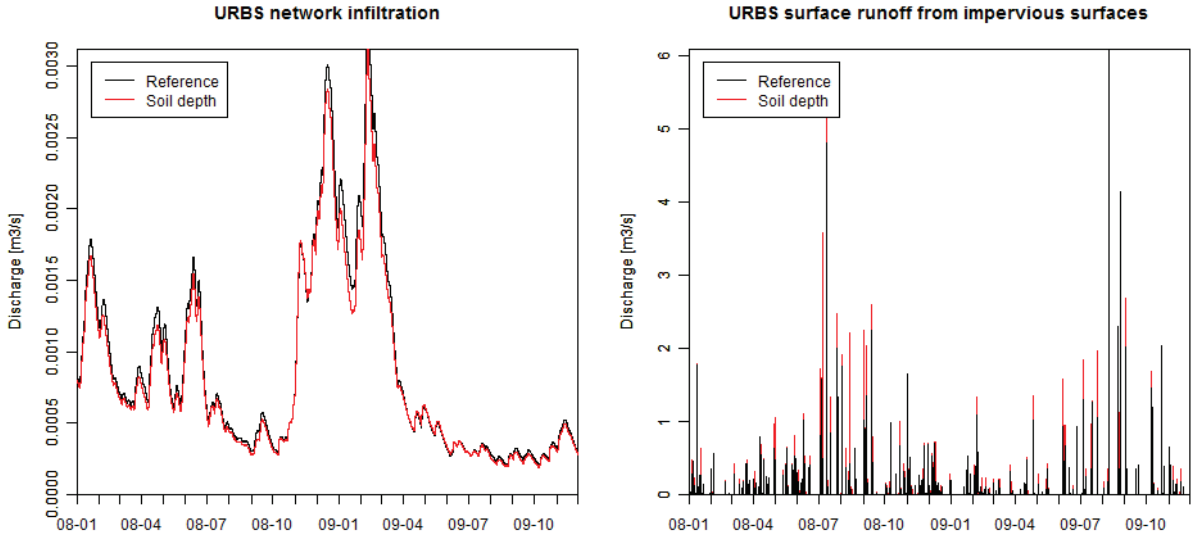

Figure G.0.9.: URBS network infiltration (left) and URBS surface runoff from impervious areas (right) contributing to the natural river (upstreamSOD) in 2008 and 2009. The simulation with the soil depth varying between 1 and 3 m is compared to the reference simulation having a constant soil depth of 1m.

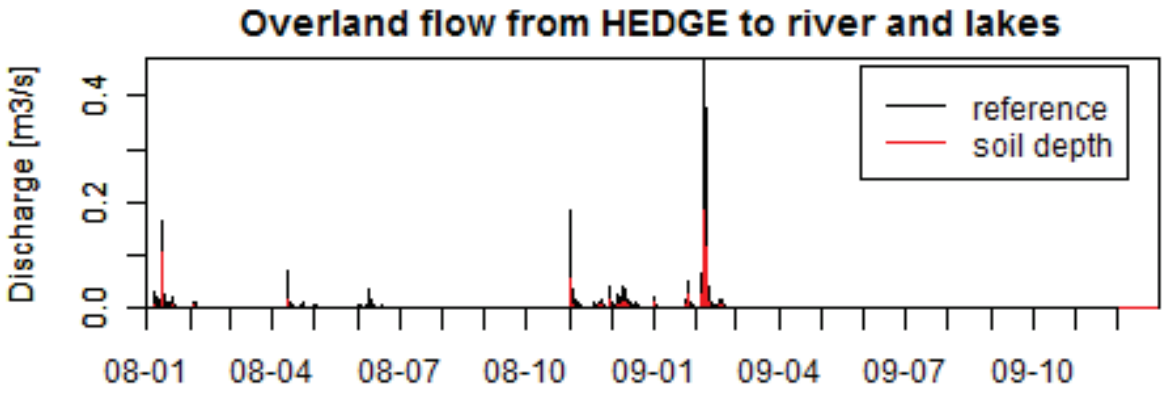

Figure G.0.10.: HEDGE overland flow contributing to the natural river (upstreamSOD). The simulation with the soil depth varying between 1 and 3 m is compared to the reference simulation having a constant soil depth of 1m.

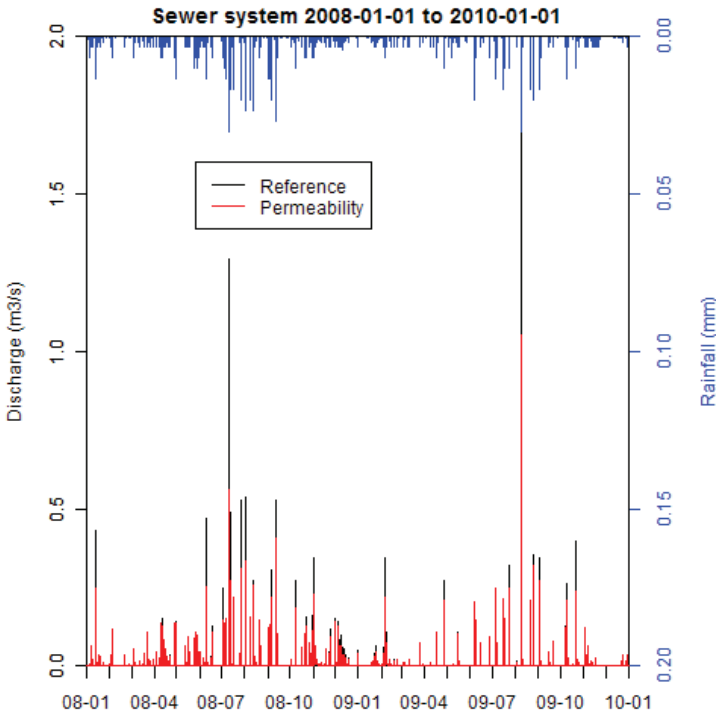

Figure G.0.11.: Simulation with modified hydraulic conductivity compared to the reference simulation in the sewer system. The hydraulic conductivity was increased by the factor 10.

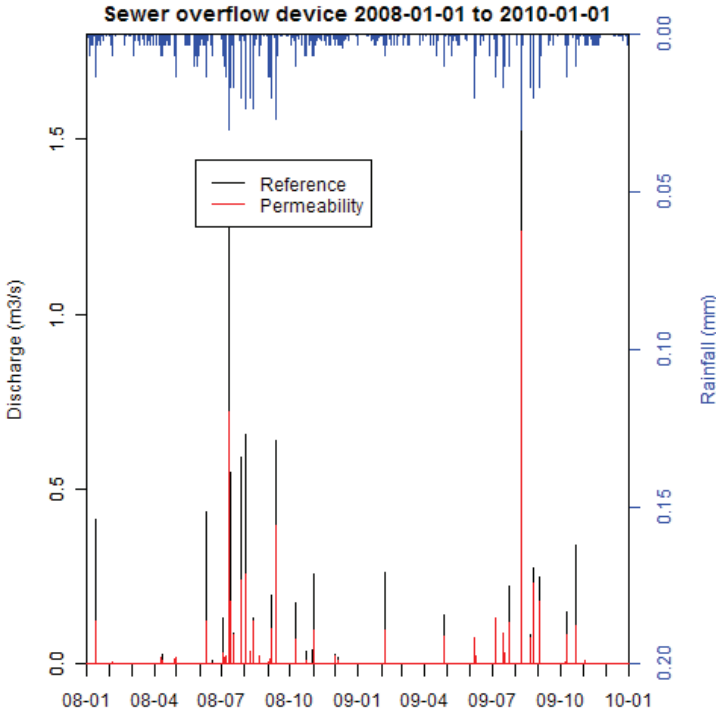

Figure G.0.12.: Simulation with modified hydraulic conductivity compared to the reference simulation in the sewer overflow device. The hydraulic conductivity was increased by the factor 10.

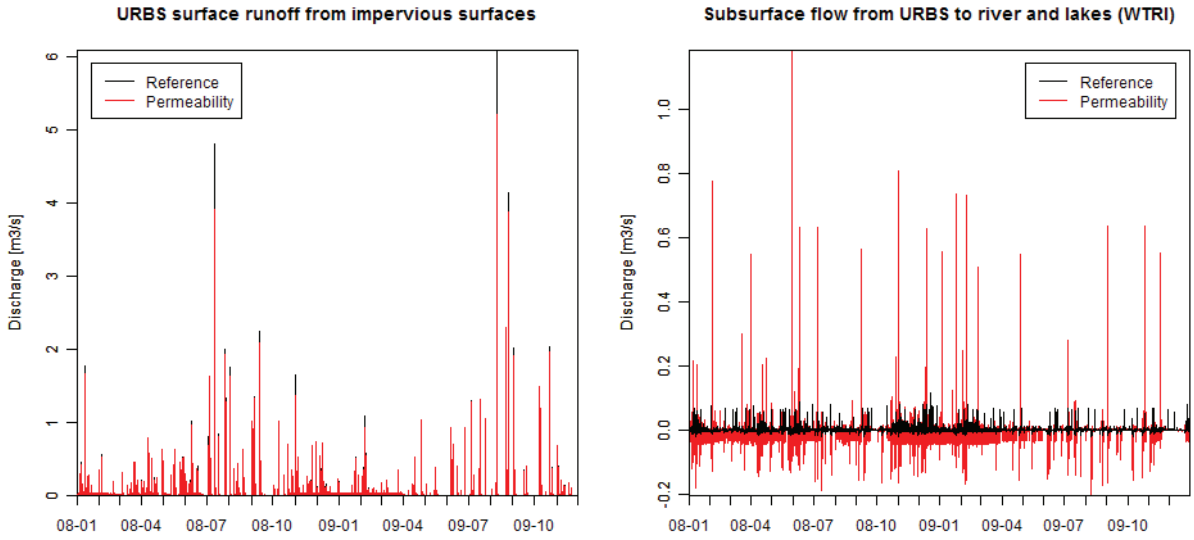

Figure G.0.13.: URBS surface runoff from impervious areas (left) and URBS lateral flow (right) contributing to the natural river (upstreamSOD) in 2008 and 2009. The reference simulation is compared to the simulation with an about the factor 10 increased permeability.

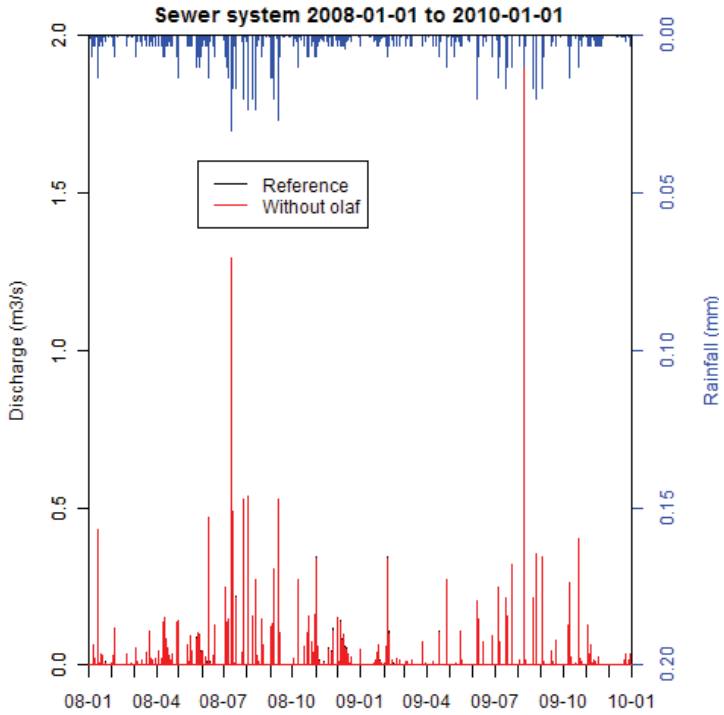

Figure G.0.14.: Simulation without OLAF module compared to the reference simulation in the sewer system.

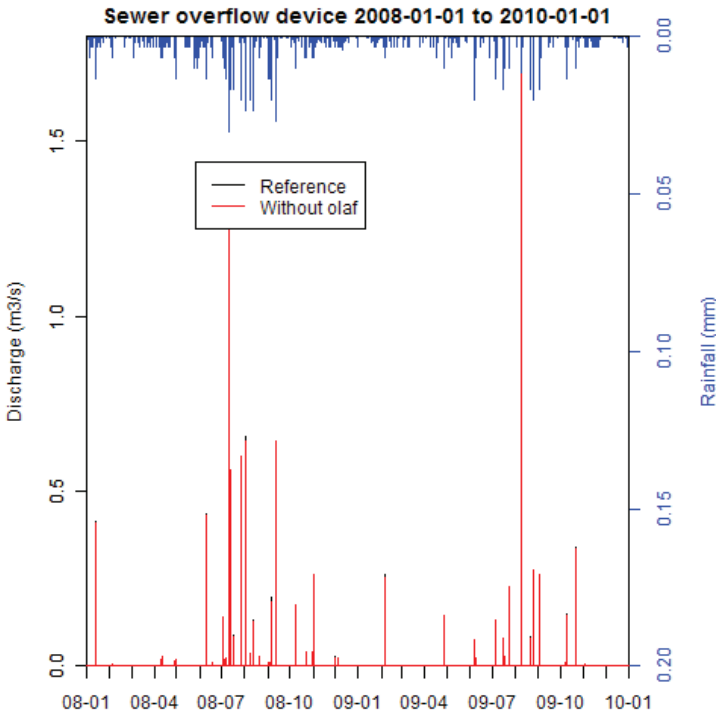

Figure G.0.15.: Simulation without OLAF module compared to the reference simulation in the sewer overflow device.

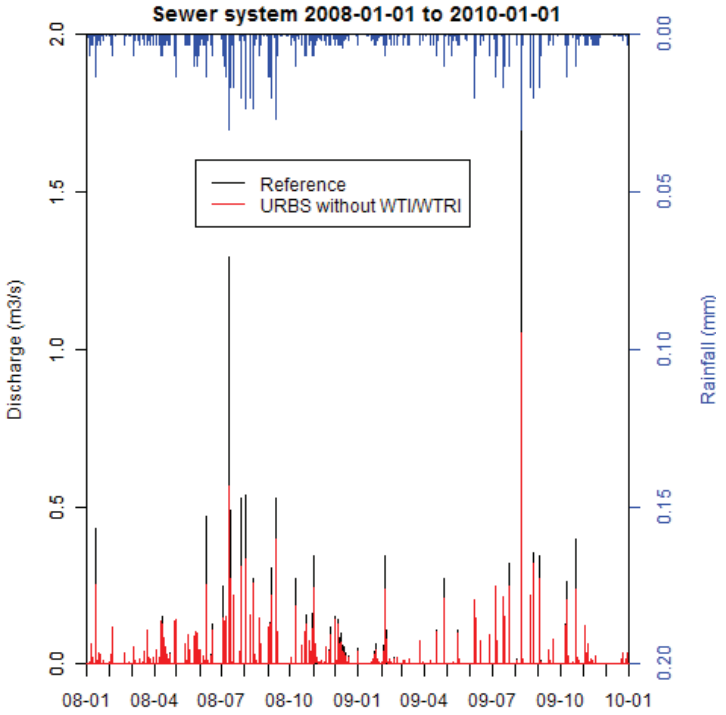

Figure G.0.16.: Simulation of the discharge in the sewer system (SS) without URBS lateral subsurface flow compared to the reference simulation.

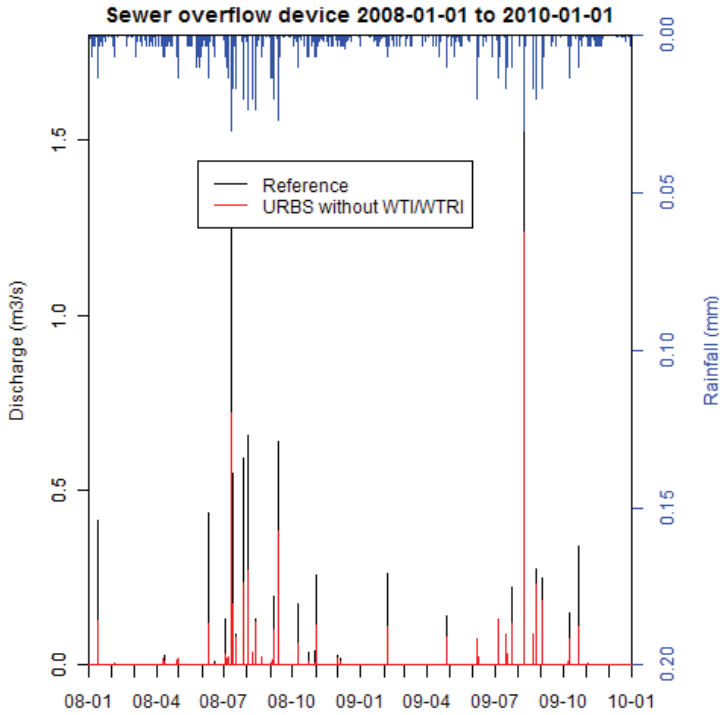

Figure G.0.17.: Simulation of the discharge in the sewer overflow device (SOD) without URBS lateral subsurface flow compared to the reference simulation.

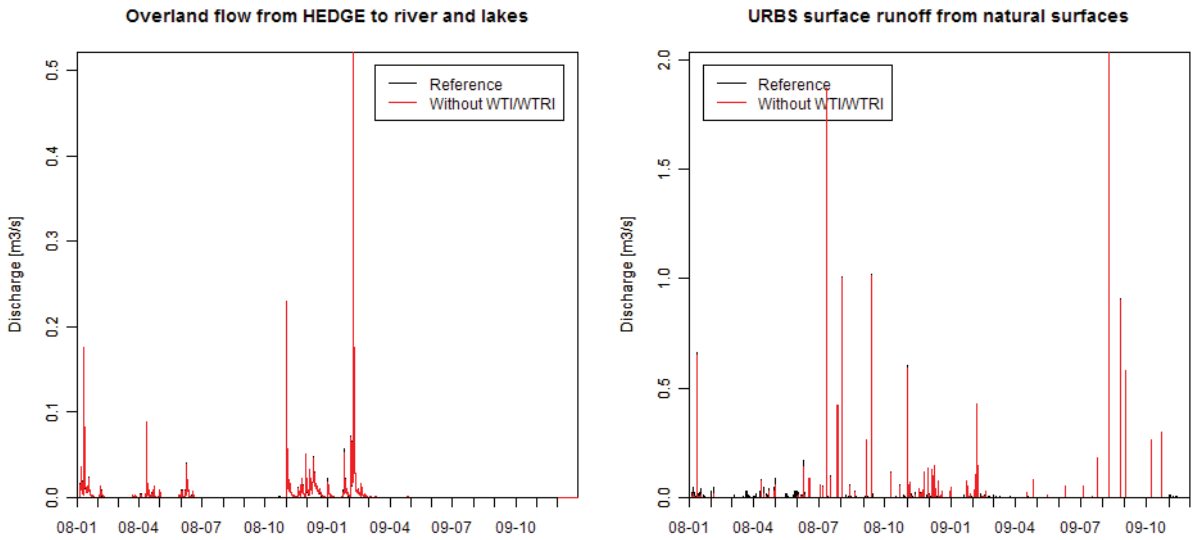

Figure G.0.18.: HEDGE and URBS overland flow contributing to the natural river (upstreamSOD). The reference simulation is compared to the simulation without URBS lateral subsurface flow.

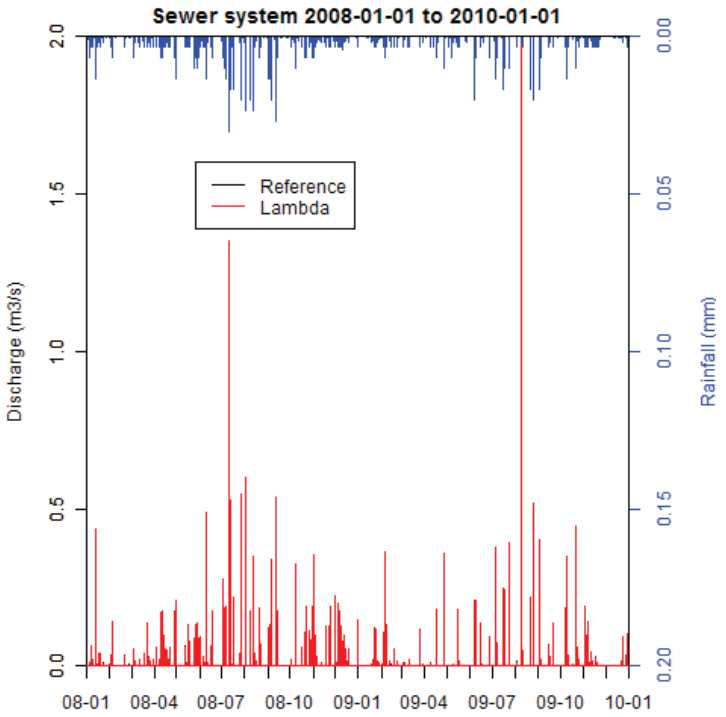

Figure G.0.19.: Simulation of the discharge in the sewer system (SS) without network infiltration ($\lambda = 0.$).

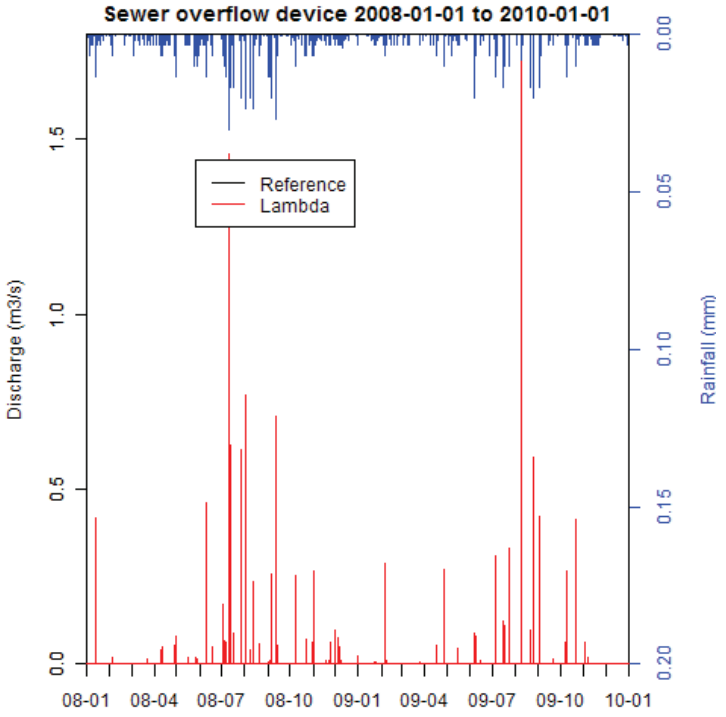

Figure G.0.20.: Simulation of the discharge in the sewer overflow device (SOD) without network infiltration ($\lambda = 0.$).

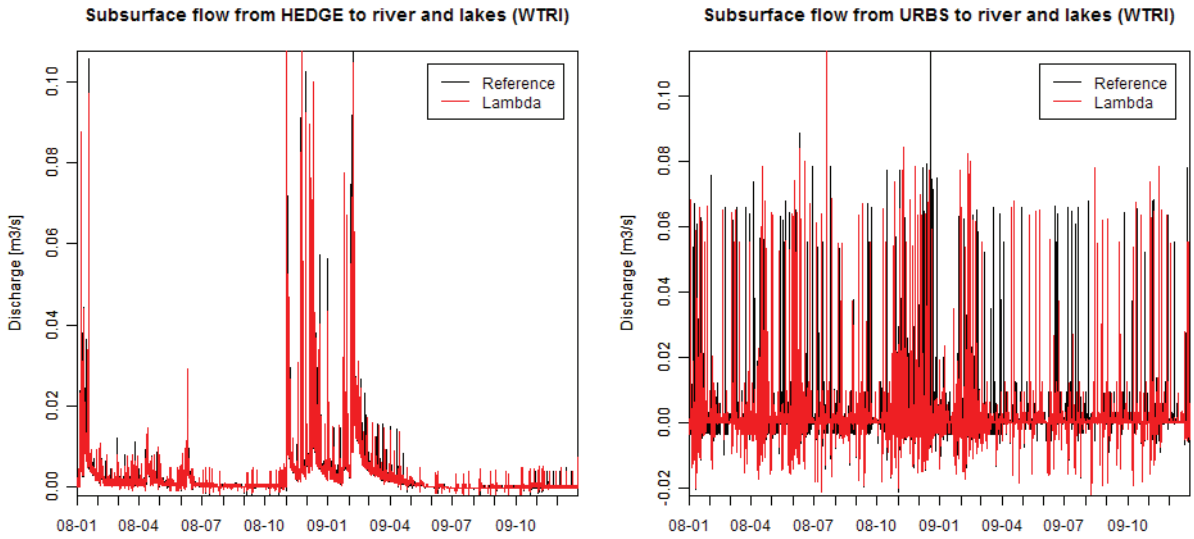

Figure G.0.21.: The reference simulation is compared to the simulation without network infiltration (λ=0). The HEDGE (left) and URBS (right) subsurface flows contributing to the natural river (upstreamSOD) are shown.

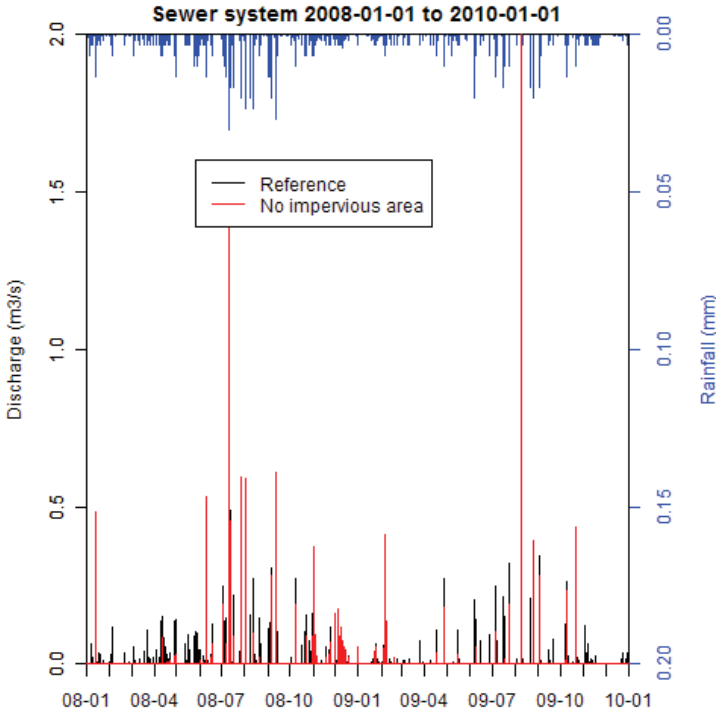

Figure G.0.22.: Simulation of the discharge in the sewer system (SS) for which all URBS impervious areas was changed to natural area in comparison to the reference simulation.

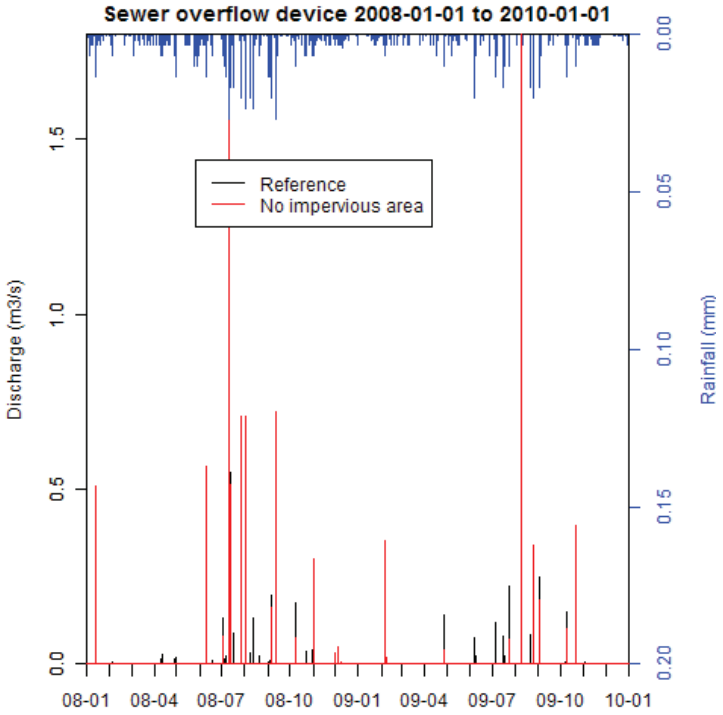

Figure G.0.23.: Simulation of the discharge in the sewer overflow device (SOD) for which all URBS impervious areas was changed to natural area in comparison to the reference simulation.

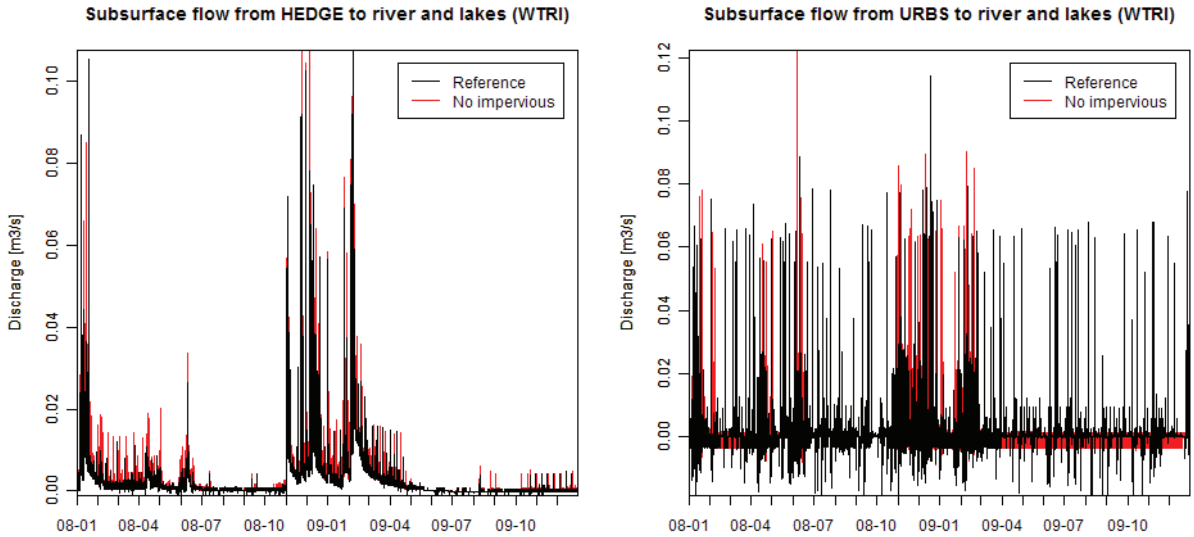

Figure G.0.24.: HEDGE and URBS subsurface flow simulated with WTRI contributing to the natural river (upstreamSOD). The reference simulation is compared to a simulation without URBS impervious areas.

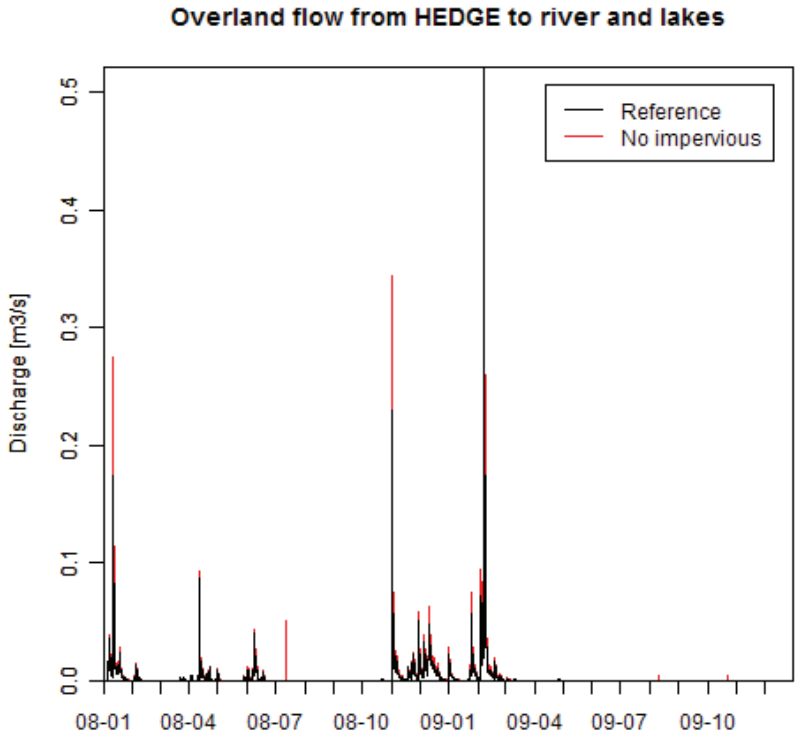

Figure G.0.25.: HEDGE overland flow contributing to the natural river (upstreamSOD). The reference simulation is compared to a simulation without URBS impervious areas.

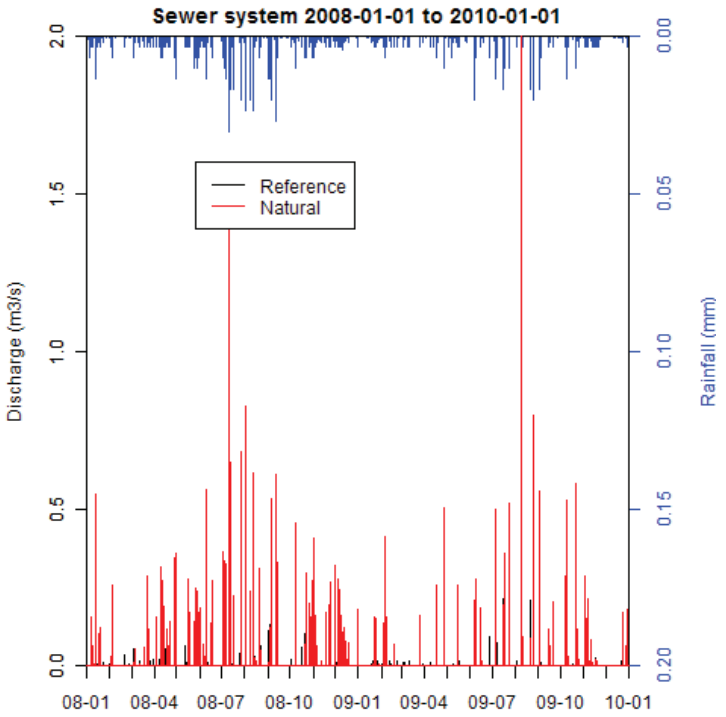

Figure G.0.26.: Simulation of the discharge in the sewer system (SS) for a natural catchment without pipe drainage for which all URBS impervious areas was changed to natural area in comparison to the reference simulation.

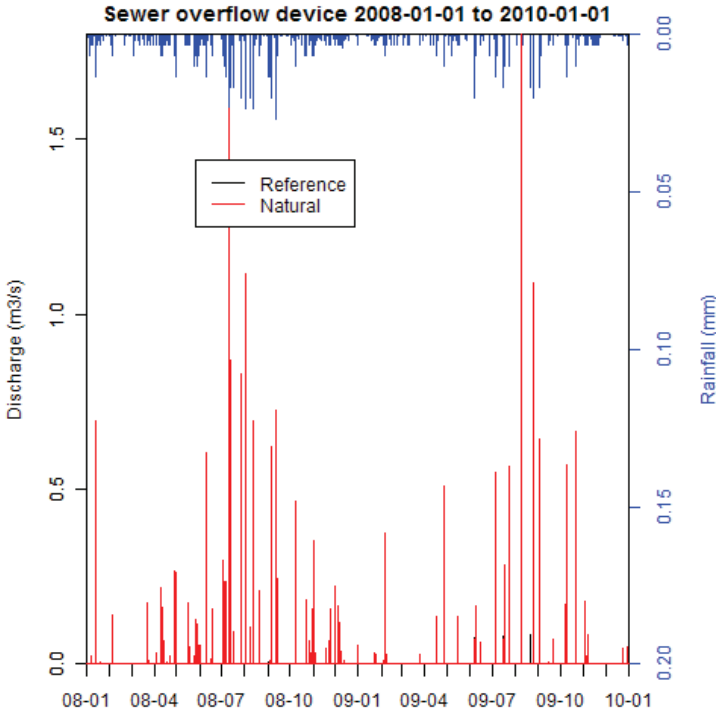

Figure G.0.27.: Simulation of the discharge in the sewer overflow device (SOD) for a natural catchment without pipe drainage for which all URBS impervious areas was changed to natural area in comparison to the reference simulation.

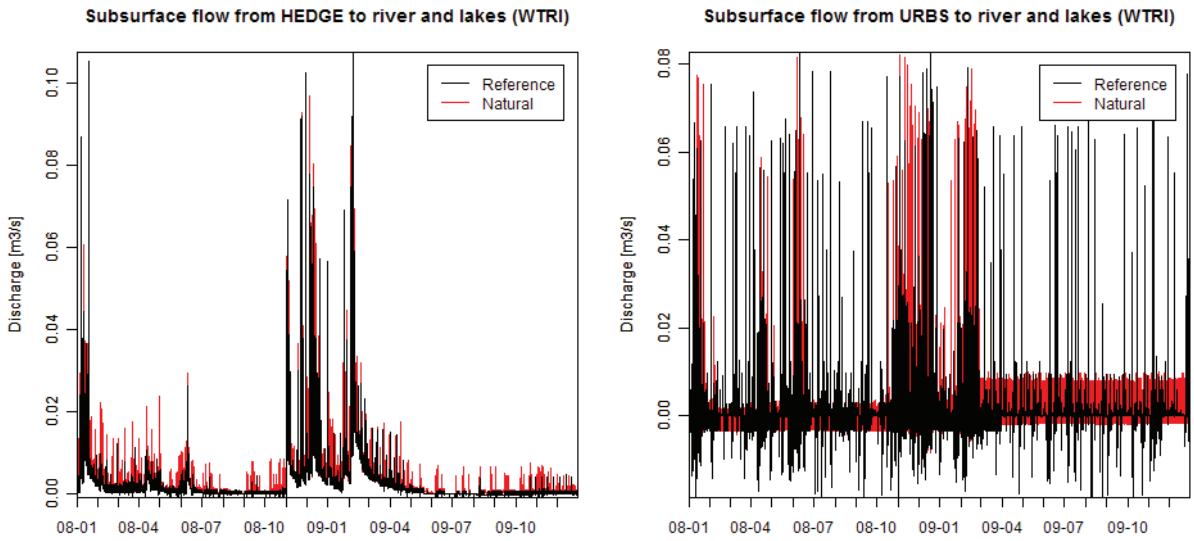

Figure G.0.28.: HEDGE and URBS subsurface flow contributing to the natural river (upstreamSOD). The reference simulation is compared to a simulation without URBS impervious areas and without network infiltration.

Bibliography

Abbott, M., Bathurst, J., Cunge, J., O'Connell, and P.E., Rasmussen, J. (1986a). An introduction to the european hydrological system - systeme hydrologique europeen, "she", 1: History and philosophy of a physically-based, distributed modelling system. *Journal of Hydrology*, 87(1-2):45–59.

Abbott, M., Bathurst, J., Cunge, J., O'Connell, and P.E., Rasmussen, J. (1986b). An introduction to the european hydrological system - systeme hydrologique europeen, "she", 2: Structure of a physically-based, distributed modelling system. *Journal of Hydrology*, 87(1-2):61–77.

Allen, R., Periera, L., Raes, D., and Smith, M. (1998). Crop evapotranspiration - guidelines for computing crop water requirements. *FAO Irrigation and drainage. FAO - Food and Agriculture Organization of the United Nations, Rome*, 56. http://www.fao.org/docrep/X0490E/x0490e00.htm, consulted on 07/11/2011.

Alley, W. and Smith, P. (1982). Distributed routing rainfall-runoff model: version ii. multi-event urban runoff quality model. open file report 82-344/764. Technical report, U.S. Geological Survey, Washington, D.C.

Andrieu, H. and Chocat, B. (2004). Introduction to the special issue on urban hydrology. *Journal of Hydrology*, 299:163–165.

Anquetin, S., Braud, I., O.Vannier, Viallet, P., B., B., Creutin, J., and Manus, C. (2010). Sensitivity of the hydrological response to rainfall fields estimation and soil variabilities in the context of flash floods. *Journal of Hydrology*, 394:134–147.

Argent, R. (2004). An overview of model integration for environmental applications - components, frameworks and semantics. *Environmental Modelling & Software*, 19:219–234.

Argent, R., Voinov, A., Maxwell, T., Cuddy, S., Rahman, J., Seaton, S., Vertessy, R., and Braddock, R. (2006). Comparing modelling frameworks - a workshop approach. *Environmental Modelling & Software*, 21:895–910.

Arnold, J., Srinivasan, R., Muttiah, R., and Williams, J. (1998). Large area hydrologic modeling and assessment. part i: Model development. *J. Am. Water Resour. Assoc.*, 34(1):73–89.

Aronica, G. and Lanza, L. (2005). Drainage efficiency in urban areas: a case study. *Hydrological Processes*, 19(5):1105–1119.

Ashley, R. M., Newman, R., Walker, L., and Nowell, R. (2010). Changing a culture: Managing stormwater sustainably in the uk city of the future - learning from the usa and australia. In *Low Impact Development 2010: Redefining Water in the City - Proceedings of the 2010 International Low Impact Development Conference*, pages 1571–1584.

Bach, M. (2010). *Integrierte Modellierung für Einzugsgebiete mit komplexer Nutzung*. PhD thesis, Technische Universität Darmstadt.

Bach, M., Muschalla, D., Schröter, K., and Ostrowski, M. (2007). Integrated model approaches for urban waste water systems and diffuse sources. In *Novatech 2007, Lyon*, pages 515–522.

Béal, D., Gagnage, M., Jacqueminet, C., Kermadi, S., Michel, C., Jankowfsky, S., Branger, F., and Braud, I. (2009). Cartographie de l'occupation du sol pour la modélisation hydrologique spatialisée du cycle de l'eau en zone péri-urbaine. In Biramonte, S., Miralles, A., and Pinet, F., editors, *Proc. 2ème atelier SIDE2009, Toulouse/France, 26 May*, pages 23–32. http://eric.univ-lyon2.fr/ sbimonte/side2009.html, consulted on 29/3/2011.

Beasley, D., Huggins, L., and Monke, E. (1980). Answers: a model for watershed planning. *Trans. ASAE*, 23:938–944.

Beighley, R., Dunne, T., and Melack, J. (2005). Understanding and modeling basin hydrology: interpreting the hydrogeological signature. *Hydrological Processes*, 19:1333–1353.

Belhaouane, M. (1999). Modélisation d'un réseau d'assainissement. etude des fréquences de déversement d'un déversoir d'orage. Master's thesis, Ecole National de l'eau et de l'Environnement de Strasbourg.

Bernholdt, D., Allan, B., Armstrong, R., Bertrand, F., Chiu, K., Dahlgren, T., Damevski, K., Elwasif, W., Epperly, T., Govindaraju, M., Katz, D., Kohl, J., Krishnan, M., Kumfert, G., Larson, J., Lefantzi, S., Lewis, M., Malony, A., McInnes, L., Nieplocha, J., Norris, B., Parker, S., Ray, J., Shende, S., Windus, T., and Zhou, S. (2006). A component architecture for high-performance scientific coumputing. *International Journal of High Performance Computing Applications*, 20:163–202.

Bernoud, S. (1998). Réponse écologique d'un reseau périurbain aux rejets de temps de pluie. Master's thesis, Ecole Nationale du Génie de l'Eau et de l'Environnement de Strasbourg.

Berthier, E. (1999). *Contribution à une modélisation hydrologique à base physique en milieu urbain. Elaboration du modèle et première évaluation.* PhD thesis, Institut national polytechnique de Grenoble. 196p.

Berthier, E., Andrieu, H., and Creutin, J. (2004). The role of soil in the generation of urban runoff: development and evaluation of a 2d model. *Journal of Hydrology*, 299:252–266.

Berthier, E., Andrieu, H., and Rodriguez, F. (1999). The rezé urban catchments database. *Water Resources Research*, 35(6):1915–1919.

Beven, K. and Kirkby, M. (1979). A physically based, variable contributing area model of basin hydrology. *Hydrological Sciences Bulletin*, 24(1):43–69.

Bhatt, G., Kumar, M., and Duffy, C. (2008). Bridging the gap between geohydrologic data and distributed hydrologic modeling. In Sànchez-Marrè, M., Béjar, J., Comas, J., Rizzoli, A., and Guariso, G., editors, *Proceedings of the iEMSs Fourth Biennial Meeting: International Congress on Environmental Modelling and Software (iEMSs 2008)*, volume 2 of *ISBN: 978-84-7653-074-0*, pages 743–750, Barcelona. http://www.iemss.org/iemss2008/index.php?n=Main.Proceedings, consulted on 07/11/2011.

Bicknell, B., Imhoff, J., Kittle, J., Jobes, T., and Donigian, A. (2005). Hydrological simulation program - fortran: Hspf version 12.2 user's manual. Technical report, U.S. Environmental Protection Agency: Athens, GA. http://water.epa.gov/scitech/datait/models/basins/bsnsdocs.cfm consulted on 08/06/2011.

Biegel, M., Schanze, J., and Krebs, P. (2005). Arcegmo-urban - hydrological model for point sources in river basins. *Water Science & Technology*, 52(5):249–256.

Bocher, E. and Martin, J. (2009). Tanato2: Tin-based approach to evaluate impact of natural and anthropogenic artefacts. In *Abstracts Proceedings of the International Opensource Geospatial Research Symposium OGRS 2009, Nantes, France, 8-10 July*, pages 56–59.

Bongartz, K. (2003). Applying different spatial distribution and modelling concepts in three nested mesoscale catchments of germany. *Physics and Chemistry of the Earth*, 28:1343–1349.

Borah, D. (2011). Hydrologic procedures of storm event watershed models: a comprehensive review and comparison. *Hydrological Processes*. in press.

Borah, D. and Bera, M. (2003). Watershed-scale hydrologic and nonpoint-source pollution models: Review of mathematical bases. *Transactions of the ASABE*, 46(6):1553–1566.

Brakensiek, D., R.L., E., and Rawls, W. (1981). Variation within texture classes of soil water parameters. *Transactions of the ASAE*, 24(2):335–339.

Branger, F. (2007a). River1d: module simplifié d' écoulement en rivière. documentation du module.

Branger, F. (2007b). *Utilisation d'une plate-forme de modélisation environnementale pour représenter le rôle d'amenagements hydro-agricoles sur les flux d'eau et de pesticides. Application au bassin versant de la Fontaine du Theil (Ille-et-Vilaine)*. PhD thesis, INP - Grenoble.

Branger, F. (2008a). Réseau de mesures hydrométriques et pluviométriques sur le bassin versant de l'yzeron. courbes de tarrage des stations de débit existantes. Technical report, Cemagref Lyon, HHLY.

Branger, F. (2008b). Wtri: module d'interface nappe-rivière pour les modules frer1d et hedge. documentation du module.

Branger, F., Braud, I., Debionne, S., Viallet, P., Dehotin, J., Henine, H., Nedelec, Y., and Anquetin, S. (2010). Towards multi-scale integrated hydrological models using the liquid framework. overview of the concepts and first application examples. *Environmental Modelling & Software*, 25(12):1672 – 1681.

Branger, F., I.Braud, P.Viallet, and S.Debionne (2008). Modelling the influence of landscape management practices on the hydrology of a small agricultural catchment. In Wang, S., Kawahara, M., Holtz, K., T.Tsujimoto, and Toda, Y., editors, *Proceedings of the 8th International Conference on HydroScience and Engineering, Nagoya, Japan*, pages 586–594.

Branger, F., Jankowfsky, S., Vannier, O., Viallet, P., Debionne, S., and Braud, I. (2011). *Geospatial free and open source software in the 21st century. Lecture notes in Geoinformation and Cartography.*, chapter Use of open-source GIS and data base software for the pre-processing of distributed hydrological models, page 12. Springer.

Branger, F., Tournebize, J., Carluer, N., Kao, C., Braud, I., and Vauclin, M. (2009). A simplified modelling approach for pesticide transport in a tile-drained field: The pestdrain model. *Agricultural Water Management*, 96(3):415–428.

Braud, I. (2007). Avupur project description. Technical report, Cemagref Lyon.

Braud, I. (2008a). Analyse des données pluie-débit sur les sous-bassins du mercier et de la chaudanne. periode 1997-2007. données de base, critique de données pluies, programmes fortran et utilisation de r pour cette analyse, résultats. Technical report, Cemagref Lyon, projet AVuPUR. pp. 84.

Braud, I. (2008b). Description form of the frer1d, roli, etpart, vegint, crlinpg modules and wbmls model. Technical report, Cemagref Lyon.

Braud, I. (2009). Analyse géostatistique des mesures de la teneur en eau collectées sur le sous-bassin du mercier (bassin versant de l'yzeron) lors de la campagne des 12-13 mars. contribution au wp1: Hydrological and gis data collection du projet anr avupur. Technical report, Cemagref Lyon HHly.

Braud, I., Branger, F., Chancibault, K., Jacqueminet, C., Breil, P., Chocat, B., Debionne, S., Dodane, C., Honegger, A., Joliveau, T., Kermadi, S., Leblois, E., Lipeme Kouyi, G., Michel, K., Mosini, M., Renard, F., Rodriguez, F., Sarrazin, B., Schmitt, L., Andrieu, H., Bocher, E., Comby, J., and Viallet, P. (2011a). Assessing the vulnerability of peri-urban rivers. rapport scientifique final du projet avupur, 87 pp. Technical report, (ANR-07-VULN-01).

Braud, I., Breil, P., Thollet, F., and Lagouy, M. (2011b). Impact of urbanization on the hydrological regime of periurban rivers. what can we learn from data analysis? *Journal of Hydrology*. submitted.

Braud, I., Chancibault, K., Debionne, S., Kouyi, G. L., Sarrazin, B., Jacqueminet, C., Andrieu, H., Béal, D., Bocher, E., Boutaghane, H., Branger, F., Breil, P., Chocat, B., Comby, J., Dehotin, J., Dramais, G., Furusho, C., Gagnage, M., Gonzalez-Sosa, E., Grosprétre, L., Honegger, A., Jankowfsky, S., Joliveau, T., Kermadi, S., Lagouy, M.,

Leblois, E., Martin, J., Mazagol, P., Michell, K., Molines, N., Mosini, M., Puech, C., Renard, F., Rodriguez, F., Schmitt, L., Thollet, F., and Viallet, P. (2010a). The avupur project (assessing the vulnerabiliy of peri-urban rivers) : experimental set up, modelling strategy and first results. In *Proceedings of the 7th Novatech 2010 Conference, June 28-July 1 2010, Lyon, France*, page 10.

Braud, I., Dantas-Antonino, A. C., Vauclin, M., Thony, J. L., and Ruelle, P. (1995). A simple soil-plant-atmosphere transfer model (sispat) development and field verification. *Journal of Hydrology*, 166(3-4):213 – 250.

Braud, I., DeCondappa, D., Soria, J., Haverkamp, R., Angulo-Jaramillo, R., Galle, S., and Vauclin, M. (2005). Use of scaled form of the infiltration equation for the estimation of unsaturated soil hydraulic properties (the beerkan method). *European Journal of Soil Science*, 56:361–374.

Braud, I., Gonzalez-Sosa, E., Mastachi-Loza, C., Aubert, M., Leblois, E., Jankowfsky, S., and Baghdadi, N. (2009). Variabilité spatiale de la teneur en eau de surface des sols nus par mesures in situ et imagerie radar. In *Actes des 34ème journées du GFHN, 25-26 Novembre 2009, Aix en Provence, France*, page 6.

Braud, I., Roux, H., Anquetin, S., Maubourguet, M.-M., Manus, C., Viallet, P., and Dartus, D. (2010b). The use of distributed hydrological models for the gard 2002 flash flood event: Analysis of associated hydrological processes. *Journal of Hydrology*, 394(1-2):162 – 181. Flash Floods: Observations and Analysis of Hydrometeorological Controls.

Breil, P. (2010). Principe de séparation des écoulements dans un collecteur d'eau unitaire (eaux de pluie + eaux usées + eaux claires parasites). Technical report, Cemagref Lyon HHly.

Breil, P., Grimm, N., and Vervier, P. (2007). *Hydroecology and ecohydrology: past, present and future*, chapter Surface water groundwater exchanges processes and fluvial ecosystem function: an analysis of temporal and spatial scale dependency, pages 93–108. Wiley & sons.

Breil, P. and Jouan, H. (2001). Simulation d'un réseau pluvial: étude d'un bassin d'orage pour la réduction des rejets de temps de pluie. Technical report, Cemagref Lyon, Département Gestion des Milieux Aquatiques.

Bremicker, M. (2000). Das wasserhaushaltsmodell larsim - modellgrundlagen und anwendungsbeispiele. In *Freiburger Schriften zur Hydrologie, Band 11*. Institut für Hydrologie der Universität Freiburg.

BRGM (2011). Bureau de recherches géologiques et minières. http://infoterre.brgm.fr/viewer/MainTileForward.do;jsessionid=C6247604415C79ABC47269563FD5969E. Consulted on 03/07/2011.

Brooks, R. and Corey, A. (1964). Hydraulic properties of porous media. Hydrology papers, Colorado State University. 24 pp.

Brossard, F. (2011). Automatisation du prétraitement des données spatiale pour la modélisation hydrologique distribuée en zone périurbaine. Master's thesis, EPMI Cergy.

Burton, A. and Pitt, R. (2001). *Stormwater Effects Handbook: A Toolbox for Watershed Managers, Scientists, and Engineers*, chapter Appendix H: Watershed and Receiving Water Modeling, pages 843–866. CRC Press.

Calder, I. (1977). A model of transpiration and interception losses from a spruce forest in plynlimon central wales. *Journal of Hydrology*, 33:247–275.

Carlier, M. (1972). *Hydraulique générale et appliquée*, volume 14 of *Collection de la Direction des études et Recherches d'électricité de France*. Editions Eyrolles, 61, Bd Saint-Germain Paris 5ème.

Carluer, N. and Marsily, G. D. (2004). Assessment and modelling of the influence of man-made networks on the hydrology of a small watershed: implications for fast flow components, water quality and landscape management. *Journal of Hydrology*, 285:76–95.

Cassan, M. (1986). Aide-mémoire d'hydraulique souterraine. presses de l'école nationale des ponts et chaussées.

Castaings, W., Dartus, D., Le Dimet, F., and Saulnier, G.-M. (2009). Sensitivity analysis and parameter estimation for the distributed modeling of infiltration excess overland flow. *Hydrology and Earth System Sciences*, 13:503–517.

Chapuis, G. (2010). Analyses de données hydrologiques pluie-débit sur le bassint versant de l'yzeron. Master's thesis, INP Toulouse ENSEEIHT. pp. 49.

Charef, A. (1996). Etude de l'écoulement en vue d'une modélisation pluie-débit sur un bassin versant périurbain. etat de l'art, et essai d'un modèle en utilisant l'information topographique sur le bassin de grézieu-la-varenne, dans l'ouest lyonnais. Master's thesis, Ecole Nationale du Génie de l'Eau et de l'Environnement, ENGEES.

Chen, J., Hill, A., and Urbano, L. (2009). A gis-based model for urban flood inundation. *Journal of Hydrology*, 373:184–192.

Chennu, S. (2008). *Flood mitigation at watershed scale through dispersed dry dams: Analysis of the impact on discharge-frequency regimes*. PhD thesis, INP - Grenoble.

Cho, J., Barone, V., and Mostaghimi, S. (2009). Simulation of land use impacts on groundwater levels and streamflow in a virginia watershed. *Agricultural Water Management*, 96:1–11.

Chocat, B., Lipeme-Kouyi, G., and Boutaghane, H. (2010). Modélisation intégrée du bassin de l'yzeron. Présentation lors de la réunion du projet AVuPUR, 16 novembre 2007.

Chow, V. (1973). *Open Channel Hydraulics. International students edition.* McGrawHill Civil Engineering Series, London,.

Ciarapica, L. and Todini, E. (2002). Topkapi: a model for the representation of the rainfall-runoff process at different scales. *Hydrological Processes*, 16(2):207–229.

Cook, F., Jordan, P., Waters, D., and Rahman, J. (2009). Watercast - whole of catchment hydrology model: An overview. In Anderssen, R., Braddock, R., and Newham, L., editors, *Proc. of the 18th World IMACS Congress and MODSIM09 International Congress on Modelling and Simulation, Cairns, Australia*, pages 3492–3498.

Cosby, B., Hornberger, G., Clapp, R., and Ginn, T. (1984). A statistical exploration of the relationships of soil moisture characteristics to the physical properties of soils. *Water Resources Research*, 20(6):682–690.

Coulais, C. (2011). Modélisation du bassin versant de grézieu-la-varenne. etude du comportement du bassin d'orage. Master's thesis, ENTPE.

Daniel, E., Camp, J., LeBoeuf, E., Penrod, J., Abkowitz, M., and Dobbins, J. (2010). Watershed modeling using gis technology: A critical review. *Journal of Spatial Hydrology*, 10(2):13–28.

David, O., Schneider, I., and Leavesley, G. (2004). Metadata and modelling frameworks: the object modelling system example. In *Proc. of the iEMSs 2d Biennial Meeting: International Congress on Envrionmental Modelling and Software (iEMSs2004), Osnabrück, Germany*.

de la Varde, G. P. (2010). Modélisation comparée du ruissellement des petits bassins versants urbains en vue d'estimer les rejets de temps de pluie vers le milieu naturel. Master's thesis, ENSGTI Pau.

Dehchali, J. S. (1997). *La modélisation de la transformation pluie-débit sur les bassins versants periurbains*. PhD thesis, Institut National des Sciences Appliquées de Lyon, INSA.

Dehotin, J. (2007). *Prise en compte de l'héterogéneité des surfaces continentales dans la modélisation hydrologique spatialisée. Application sur le haut-bassin de la Saône*. PhD thesis, INP Grenoble.

Dehotin, J. (2009a). Découpage spatial et caractérisation des unités de modélisation de l'yzeron. wp3 - simplified representation at the catchments scale. Technical report, Cemagref Lyon HHly. AvuPur project.

Dehotin, J. (2009b). Wp1: Hydrological and gis data collection. Technical report, Cemagref Lyon HHly. AvuPur project.

Dehotin, J. and Braud, I. (2008). Which spatial discretization for distributed hydrological models? proposition of a methodology and illustration for medium to large-scale catchments. *Hydrology and Earth System Sciences*, 12(3):769–796.

Dehotin, J. and Breil, P. (2011). Rapport technique du projet irip: Cartographie de l'aléa inondation par ruissellement. Technical report, Cemagref Lyon, HHly, Juillet 2011.

Dehotin, J., Breil, P., and DeLavenne, A. (2010). Cartographie du risque de ruissellement intense pluvial. rappot d'avancement du projet irip, juin 2010. Technical report, Cemagref Lyon, UR HHLY.

Dehotin, J., deLavenne, A., Breil, P., Braud, I., and Lagouy, M. (2011a). Runoff detection on a small french catchment: Deverse observation system, in preparation.

Dehotin, J., Vazquez, R., Braud, I., Debionne, S., and Viallet, P. (2011b). Modeling of hydrological processes using unstructured and irregular grids: 2d groundwater application. *Journal of Hydrologic Engineering*, 16(2):108–125.

DeLavenne, A. (2010). Risque d'inondation par ruissellement. instrumentation terrain et analyse géomatique. Master's thesis, Ecole Supérieure d'Agriculture d'Angers.

Devito, K., Creed, I., Gan, T., Mendoza, C., Petrone, R., Silins, U., and Smerdon, B. (2005). A framework for broad-scale classification of hydrologic response units on the boreal plain: Is topography the last thing to consider? *Hydrological Processes*, 19(8):1705–1714.

(DHI), D. H. I. (2009). Mike urban cs - building a simple mouse model in mike urban - step-by-step training guide. Technical report, DHI Water and Environment, Horsholm, Denmark. http://www.chemeng.lth.se/vva030/Arkiv/01_Building_a_simple_MOUSE_model_in_MIKE_URBAN.pdf accessed 8 June 2011.

Dingman, S. (2002). *Physical Hydrology*. Prentice-Hall, Upper Saddle River, New Jersey, USA, 2nd edition.

Dols, A. (2010). Yzeron calibration report. Technical report, Civil Engineering Department, Monash University.

Domingo, N., Refsgaard, A., Mark, O., and Paludan, B. (2010). Flood analysis in mixed-urban areas reflecting interactions with the complete water cycle through coupled hydrologic-hydraulic modelling. *Water Science and Technology*, 62(6):1386–1392.

Dorval, F., Chocat, B., Emmanuel, E., and Lipeme-Kouyi, G. (2010). Une nouvelle approche de représentation des processus hydrologiques sur des bassins-versants: le modèle multi exutoire. In *4ème Journées doctorales en hydrologie urbaine*, pages 39–46.

Douglas, D. and Peucker, T. (1973). Algorithms for the reduction of the number of points required to represent a digitized line or its caricature. *Cartographica*, 10(2):112–122.

Douglas, I. (2006). *Peri-Urban Interface: Approaches to Sustainable Natural and Human Resource Use*, chapter Peri-urban ecosystems and societies transitional zones and contrasting values, pages 18–29. Earthscan Publications Ltd., London, UK.

Downer, C., Ogden, F., Neidzialek, J., and Liu, S. (2006). *Watershed Models*, chapter Chapter 6: Gridded surface/subsurface hydrologic analysis (GSSHA) model: a model for simulating diverse streamflow-producing process, pages 131–157. CRC Taylor and Francis: Boca Raton, Fl.

Duke, G., Kienzle, S., Johnson, D., and Byrne, J. (2006). Incorporating ancillary data to refine anthropogenically modified overland flow paths. *Hydrological Processes*, 20:1827–1843.

Dunne, T. and Black, R. (1970). An experimental investigation of runoff production in permeable soils. *Water Resources Research*, 6(2):478–490.

Elliot, A. and Trowsdale, S. (2007). A review of models for low impact urban stormwater drainage. *Environmental Modelling & Software*, 22:394–405.

Engman, E. (1986). Roughness coefficients for routing surface runoff. *Journal of Irrigation and Drainage Engineering*, 112(1):39–53.

Erbe, V., Frehmann, T., Geiger, W., Krebs, P., Londong, J., Rosenwinkel, K., and Seggelke, K. (2002). Integrated modelling as an analytical and optimisation tool for urban watershed management. *Water Sciences and Technology*, 46(6-7):141–150.

Etchevers, P. (2000). *Modélisation de la phase continentale de l'eau à l'échelle régionale. Impact de la modélisation de la neige sur l'hydrologie du Rhône.* PhD thesis, Université Paul Sabatier. Toulouse III.

EuropeanEnvironmentAgency (1994). Corine land cover - part 2: Nomenclature. http://www.eea.europa.eu/publications/cor0-part2/land_coverpart2.1.pdf, consulted on 19/09/2011.

Fabre, J., Louchart, X., Moussa, R., Dagés, C., Colin, F., Rabotin, M., Raclot, D., Lagacherie, P., and Voltz, M. (2010). Openfluid: a software environment for modelling fluxes in landscapes. In *LANDMOD2010*, Montpellier, France. Symposcience.

Faure, J. (2007). Documentation théorique du code mage. Technical report, Cemagref Lyon.

Faure, Y. (2002). Letter of the siahvy to the cemagref on the 03/10/2002.

FitzHugh, T. and Mackay, D. (2000). Impacts of input parameter spatial aggregation on an agricultural nonpoint source pollution model. *Journal of Hydrology*, 236(1-2):35–53.

Fletcher, T. (2010). Oral communication on 13/10/2010.

Flügel, W. . (1995). Delineating hydrological response units by geographical information system analyses for regional hydrological modelling using prms/mms in the drainage basin of the river brol, germany. *Hydrological Processes*, 9(3-4):423–436.

Frames (2011). http://www.epa.gov/athens/research/modeling/3mra.html as seen on 15/06/2011.

Franczyk, J. and Chang, H. (2009). The effects of climate change and urbanization on the runoff of the rock creek basin in the portland metropolitan area, oregon, usa. *Hydrological Processes*, 23:805–815.

Furusho, C. (2011). *Modélisation hydrologique des bassins versants périurbains.* PhD thesis, Ecole Centrale de Nantes. p.210.

Galéa, G. and Prudhomme, C. F. (1997). Notions de base et concepts utiles pour la compréhension de la modélisation synthétique des régimes de crue des bassins versants au sens des modèles qdf. *Revue des Sciences de l'Eau*, 1:83–101.

Gnouma, R. (2006). *Aide à la calibration d'un modéle hydrologique distribué au moyen d'une analyse des processus hydrologiques: application au bassin versant de l'Yzeron.* PhD thesis, L'institut national des sciences appliquées de Lyon.

Gonzalez-Sosa, E. and Braud, I. (2009a). Measure and spatialization of topsoil hydraulic properties on the mercier catchment. Technical report, Cemagref Lyon, AVuPUR project.

Gonzalez-Sosa, E. and Braud, I. (2009b). Mesures de la teneur en eau pour l'utilisation de l'imagerie satellitaire (radar) pour l'étude du bassin de l'yzeron. campagne des 12-13 mars 2009. contribution au wp1: Hydrological and gis data collection, anr avupur project. Technical report, Cemagref de Lyon HHly.

Gonzalez-Sosa, E., Braud, I., Dehotin, J., Lassabatère, L., Angulo-Jaramillo, R., Lagouy, M., Branger, F., Jacqueminet, C., Kermadi, S., and Michell, K. (2010). Impact of land use on the hydraulic properties of the topsoil in a small french catchment. *Hydrological Processes*, 24(17):2382–2399.

Goodchild, M., Steyaert, L., Parks, B., Johnston, C., Maidment, D., Crane, M., and Glendinning, S. (1996). *GIS and Environmental Modeling: Progress and Research Issues.* Number ISBN 1-882610-11-3. GIS World Books.

Gourdol, F. (2000). Identification des critères pluies/débits de déclenchement d'une chaîne d'acquisition d'indicateurs de la qualité de l'eau d'une rivière. Master's thesis, Ecole Centrale de Lyon.

Goutaland, D. (2009). Programme anr avupur: Prospection géophysique par panneau électrique de trois parcelles d'un sous-bassin versant de l'yseron. Technical report, CETE de Lyon.

Grayson, R. B., Moore, I. D., and McMahon, T. A. (1992a). Physically based hydrologic modeling 1. a terrain-based model for investigative purposes. *Water Resources Research*, 28(10):2639–2658.

Grayson, R. B., Moore, I. D., and McMahon, T. A. (1992b). Physically based hydrologic modeling 2. is the concept realistic? *Water Resources Research*, 28(10):2659–2666.

Greene, R. and Cruise, J. (1995). Urban watershed modeling using geographic information system. *Journal of Water Resources Planning and Management*, 121(4):318–325.

Gregersen, J., Gijsbers, P., and Westen, S. (2007). Openmi: Open modelling interface. *Journal of Hydroinformatics*, 9:175–191.

Gustafsson, L. (2000). Alternative drainage schemes for reduction of inflow/infiltration - prediction and follow-up of effects with the aid of an integrated sewer/aquifer model. In *1st International Conference on Urban Drainage via Internet*, pages 21–37.

Gustafsson, L., Winberg, S., and Refsgaard, A. (1996). Towards a physically based model description of the urban aquatic environment. In Verworn, F.-R., editor, *7th ICUDSD*, pages 1467–1472, Hannover.

Henine, H. (2010). *Couplage des processus hydrologiques reliant parcelles agricoles drainées, collecteurs enterrés et émissaire à surface libre: intégration à l'échelle du bassin versant*. PhD thesis, Université Pierre et Marie Curie, Paris.

Henine, H., Nédélec, Y., Augeard, B., Birgand, F., Chaumont, C., Ribstein, P., and Kao, C. (2010). Effect of pipe pressurization on the discharge of a tile drainage system. *Vadose Zone Journal*, 9:36–42.

Hernebring, C., Jönsson, L., Thorén, U., and Moeller, A. (2002). Dynamic online sewer modelling in helsingborg. *Water Sciences and Technoloy*, 45(4-5):429–436.

Horton, R. (1939). Analysis of runoff-plot experiments with varying infiltration capacity. *Transactions of the American Geophysical Union*, pages 693–711.

Houdré, G. (2002). Modélisation du réseau d'assainissement d'oullins (69) et création du modèle hydraulique de surface en vue de leur couplage. Master's thesis, Institut des sciences de l'ingénieur de Montpellier, Université de Montpellier.

Hulin, S. (1995). L'yzeron: du rural au périurbain en passant par topsimpl 1.0, modèle hydrologique semi-distribué. Master's thesis, Ecole Nationale Supérieure Agronomique de Rennes.

Im, S., Kim, H., Kim, C., and Jang, C. (2009). Assessing the impacts of land use changes on watershed hydrology using mike she. *Environmental Geology*, 57:231–239.

INGETUD (1997). Raccordement de grézieu la varenne sur le réseau de la courly, etude du fonctionnement du réseau par temps de pluie, modélisation du réseau, 1- memoire. Technical report, Département du Rhône, SIAHVY.

Jacobson, C. (2011). Identification and quantification of the hydrological impacts of imperviousness in urban catchments: A review. *Journal of Environmental Management*, 92:1438–1448.

Jacqueminet, C., Kermadi, S., Michel, K., Béal, D., Branger, F., Jankowsky, S., and Braud, I. (2011). Land cover mapping using aerial and vhr satellite images for distributed hydrological modelling of periurban catchments: application to the yzeron catchment (lyon, france), submitted to the journal of hydrology special issue on "hydrology of periurban catchments: processes and modelling".

Jagers, H. (2010). Linking data, models and tools: An overview. In Swayne, D., Yang, A. W., Voinov, A., Rizzoli, A., and Filatova, T., editors, *iEMSs 2010 International Congress on Environmental Modelling and Software. Modelling for Environment's Sake., Fifth Biennial Meeting, Ottawa, Canada*.

Jandot, A. (2010). Développement et évaluation d'une modélisation hydrologique simplifiée sur le bassin versant de l'yzeron dans le cadre du projet avupur. Master's thesis, Ecole Nationale Supérieure des Ingénieurs en Art Chimiques et Technologiques, Toulouse.

Jankowfsky, S. (2007). Modélisation des échanges entre les écoulements en surface et le réseau d'assainissement lors des inondations en ville. Master's thesis, Albert-Ludwigs-Universität Freiburg.

Jankowfsky, S., Branger, F., Braud, I., Debionne, S., Viallet, P., and Rodriguez, F. (2010). Development of a suburban catchment model within the liquid framework. In *Proceedings of the International congress on Environmental Modelling and Software, iEMSs, 5-8 July 2010, Ontario, Ottawa, Canada*, page 8.

Jolma, A., Ames, D., Horning, N., Mitasova, H., Neteler, M., Racicot, A., and Sutton, T. (2008). Chapter ten: Free and open source geospatial tools for environmental modelling and management. *Developments in Integrated Environmental Assessment*, 3:163–180.

Jones, J., Swanson, F., Wemple, B., and Snyder, K. (2000). Effects of roads on hydrology, geomorphology and disturbance patches in stream networks. *Conservation Biology*, 14(1):76–85.

Jouan, H. (2001). Faisabilité hydraulique de déversements volontaires pour gérer un grand réseau d'assainissement unitaire. Master's thesis, Ecole Nationale du Génie de l'Eau et de l'Environnement de Strasbourg, ENGEES.

Jürgens, C. (2001). Application of a hydrological model with integration of remote sensing and gis techniques for the analysis of land-use change effects upon river discharge. In *Remote Sensing and Hydrology 2000 (Proceedings of a symposium held at Santa Fe, New Mexico, USA, April 2000)*, volume 267 of *IAHS Publ.*

Kampf, S. and Burges, S. (2007). A framework for classifying and comparing distributed hillslope and catchment hydrologic models. *Water Resources Research*, 43(W05423):1–24.

Kaniewski, L. (2005). Couplage des modèles rubar20 et canoe, définition de la méthode, application à la ville d'oullins (69). Master's thesis, ENTPE Vaulx en Velin.

Karpf, C. and Krebs, P. (2011). Quantification of groundwater infiltration and surface water inflows in urban sewer networks based on a multiple model approach. *Water Research*, 45:3129–3136.

Kass, M., Witkin, A., and Terzopoulos, D. (1987). Snakes: Active contour models. In *International Conference on Computer Vision (ICCV), IEEE*, pages 259–268.

Klawitter, A. (2006). *Ein Modellkonzept zur integrativen Betrachtung von Urban- und Ruralhydrologie auf Einzugsgebietsebene.* PhD thesis, TU Darmstadt.

Klawitter, A. and Ostrowski, M. (2005). A 2-layer approach to simultaneously model rainfall runoff events in urban catchments and in their rural surroundings. In *10th International Conference on Urban Drainage, Copenhagen/Denmark, 21-26 August 2005.*

Kouwen, N., Soulis, E., Pietroniro, A., Donald, J., and Harrington, R. (1990). Grouped response unit for distributed hydrologic modeling. In *Proc. of International Symposium on Remote Sensing and Water Resources, Enschede, Netherlands, 20-24 August*, pages 289–305.

Kralisch, S. and Krause, P. (2006). Jams - a framework for natural resource model development and application. In Gourbesville, P., Cunge, J., Guinot, V., and Liong, S., editors, *Proc. of the 7th International Conference on Hydroinformatics, Nice, France*, volume 3, pages 2356–2363.

Krause, P. (2002). Quantifying the impact of land use changes on the water balance of large catchments using the j2000 model. *Physics and Chemistry of the Earth*, 27:663–673.

Kuhn, Y. (2010). Water-sensitive urban design: An integral piece of ecological sustainable development. In *Watershed Management Conference 2010: Innovations in Watershed Management under Land Use and Climate Change - Proceedings of the 2010 Watershed Management Conference*, volume 394, pages 838–849.

Labbas, M. (2011). Impacts de la charactérisation de l'occupation des sols par différentes sources sur la simulation des processus hydrologiques. application au bassin versant de l'yzeron. Master's thesis, ENGREF.

Lafont, M., Vivier, A., Nogueira, S., Namour, P., and Breil, P. (2006). Surface and hyporheic oligochaete assemblages in a french suburban stream. *Hydrobiologia*, 564:183–193.

Lagacherie, P., Rabotin, M., Colin, F., Moussa, R., and Voltz, M. (2010). Geo-mhydas: A landscape discretization tool for distributed hydrological modeling of cultivated areas. *Computers & Geosciences*, 36(8):1021 – 1032.

Lagouy, M. (2009). Recueil de données métrologiques sur le bassin versant de l'yzeron. ur hhly. année 2009. Technical report, Cemagref Lyon.

Lassabatère, L., Angulo-Jaramillo, R., Soria Ugalde, J., Cuenca, R., Braud, I., and Haverkamp, R. (2006). Beerkan estimation of soil transfer parameters through infiltration experiments. *Soil Science Society of America Journal*, 70:521–532.

Le-Barbu, M. (2007). Modélisation hydraulique des faibles tirants d'eau dans un tronçon de rivière. Master's thesis, Centrale Lyon, Cemagref.

Leavesley, G., Markstrom, S., Restrepo, P., and Viger, R. (2002). A modular approach to addressing model design, scale, and parameter estimation issues in distributed hydrological modelling. *Hydrological Processes*, 16:173–187.

Leavesley, G. and Stannard, L. (1995). *Computer Models of Watershed Hydrology*, chapter The precipitation-runoff modeling system - PRMS, pages 281–310. Water Resources Publications: Highlands Ranch, CO.

Lepioufle, J.-M. (2009). *Modélisation spatio-temporelle d'un champ de pluie. Application aux pluies journalières du bassin versant de la Loire.* PhD thesis, Institut National Polytechnique de Grenoble, Grenoble, France.

Lhomme, J., Bouvier, C., and Perrin, J. (2004). Applying a gis-based geomorphological routing model in urban catchments. *Journal of Hydrology*, 299:203–216.

Lijklema, L., Tyson, J., and Souef, A. L. (1993). Interurba - interactions between sewers, treatment plants and receiving waters in urban areas. *Water Sciences and Technoloy*, 27(12):1–244.

Maheshwari, B. (1992). Suitability of different flow equations and hydraulic resistance parameters for flows in surface irrigation: A review. *Water Resources Research*, 28(8):2059–2066.

Maniak, U. (1997). *Hydrologie und Wasserwirtschaft, Eine Einführung für Ingenieure*. Springer Verlag, 4. edition.

Manus, C. (2007). Analyse de la variabilité de la réponse hydrologique à la variabilité des caractéristiques des sols en région cévennes-vivarais. Master's thesis, INP Grenoble, ENSHMG.

Manus, C. (2008). Hydrate project - contribution to wp6 "analyse of major flash flood events". Technical report, LTHE, Cemagref.

Manus, C., Anquetin, S., Braud, I., Vandervaere, J., Creutin, J. ., Viallet, P., and Gaume, E. (2009). A modeling approach to assess the hydrological response of small mediterranean catchments to the variability of soil characteristics in a context of extreme events. *Hydrology and Earth System Sciences*, 13(2):79–97.

Marce, R., Ruiz, C., and Armengol, J. (2008). Using spatially distributed parameters and multi-response objective functions to solve parameterization of complex applications of semi-distributed hydrological models. *Water Resources Research*, 44(2).

Meirlaen, J., Assel, J. V., and Vanrolleghem, P. (2002). Real time control of the integrated urban wastewater system using simultaneously simulating surrogate models. *Water Sciences and Technology*, 45(3):109–116.

Mercado, R. (2006). Couplage dynamique des modèles rubar20 et canoe avec l'interface openmi. Master's thesis, Université Lyon I.

Michel, C. (2009). Exploitation des données de deux sous-bassins versants de l'yzeron: la chaudanne et le mercier. analyse des données 1997-2008. Master's thesis, Université des Sciences et Techniques du Languedoc. pp. 49.

Mignot, E., Paquier, A., and Haider, S. (2006). Modeling floods in a dense urban area using 2d shallow water equations. *Journal of Hydrology*, 327(1-2):186–199.

Miles, J. (1985). The representation of flows to partially penetrating rivers using groundwater flow models. *Journal of Hydrology*, 82(3-4):341–355.

Mitchell, V. and Diaper, C. (2006). Simulating the urban water and contaminant cycle. *Environmental Modelling & Software*, 21:129–134.

Mitchell, V., Duncan, H., Inman, M., M.Rahilly, Stewart, J., Vieritz, A., Holt, P., Grant, A., Fletcher, T., Coleman, J., Maheepala, S., Sharma, A., Deletic, A., and Breen, P. (2007). State of the art review of integrated urban water models. In *Proceedings of NOVATECH conference, Lyon*, pages 507–514.

Müller, J. (2009). *Multi-agent Based Simulation XI*, chapter Towards a formal semantics of event-based multi-agent simulations, pages 110–126. LNAI 5269, Springer Verlag.

Morena, F. (2004). *Modélisation hydrologique distribuée en milieu urbanisée*. PhD thesis, INP- Grenoble.

Morison, P. J. and Brown, R. R. (2011). Understanding the nature of publics and local policy commitment to water sensitive urban design. *Landscape and Urban Planning*, 99(2):83–92.

Moussa, R. and Bocquillon, C. (1996). Criteria for the choice of flood-routing methods in natural channels. *Journal of Hydrology*, 186:1–30.

Moussa, R., Voltz, M., and Andrieux, P. (2002). Effects of the spatial organization of agricultural management on the hydrological behaviour of a farmed catchment during flood events. *Hydrological Processes*, 16:393–412.

MétéoFrance (2011). Climat. http://climat.meteofrance.com/chgt_climat2/climat_france?73928.path=climatnormales%252FFRANCE. Consulted on 03/06/2011.

Muschalla, D., Ostrowski, M., and Klawitter, A. (2007). Innovative simulation and optimisation tools for basinwide urban stormwater management. In *Int. Symposium on New Directions in Urban Water Management. UNESCO Paris, 12-14 September*, page 8.

Nascimento, N. (1995). *Appréciation à l'aide d'un modèle empirique des effets d'actions anthropiques sur la relation pluie-débit à l'échelle du bassin versant.* PhD thesis, CERGRENE / ENPC, Paris, France. 550 pp.

Nash, J. and Sutcliffe (1970). River flow forecasting through conceptual models - part i - a discussion of principles. *Journal of Hydrology*, 10(3):282–290.

Neteler, M. and Mitasova, H. (2008). *Open Source GIS a GRASS GIS Approach*. Springer, third edition edition. ISBN 978-0-387-35767-6.

Newman, B., Campbell, A., and Wilcox, B. (1998). Lateral subsurface flow pathways in a semiarid ponderosa pine hillslope. *Water Resources Research*, 34(12):3485–3496.

Niemczynowicz, J. (1999). Urban hydrology and water management - present and future challenges. *Urban Water*, 1:1–14.

O'Loughlin, E. M. (1986). Prediction of surface saturation zones in natural catchments by topographic analysis. *Water Resources Research*, 22(5):794–804.

O'Loughlin, G., Huber, W., and Chocat, B. (1996). Rainfall-runoff processes and modelling. *Journal of Hydraulic Research*, 34(6):733–751.

Ostrowski, M. (2000). Modellierung hydrologischer prozesse in urbanen gebieten in unterschiedlichen räumlichen und zeitlichen skalen. In *Workshop on Preventive Flood Protection, new approaches to storm water management*. Saarlouis.

Paillé, Y. (2010). Automatisation du prétraitement des données spatiales pour la modélisation hydrologique distribuée en zone periurbaine. a l'aide du logiciel libre grass. Master's thesis, Université de Nantes.

Palacios-Velez, O. L. and Cuevas-Renaud, B. (1992). Shift: a distributed runoff model using irregular triangular facets. *Journal of Hydrology*, 134(1-4):35–55.

Palmstrom, N. and Walker, W. (1990). The p8 urban catchment model for evaluating nonpoint source controls at the local level, enhancing states' lake management programs, 67-76. Technical report, USEPA.

Paquier, A. (2009). Projet rives "risques d'inondations en ville et etude de scénarios", rapport scientifique final, février 2009. Technical report, Cemagref Lyon.

Passeport, E., Tournebize, J., Jankowfsky, S., B., P., Chaumont, C., Coquet, Y., and Lange, J. (2010). Artificial wetland and forest buffer zone: hydraulic and tracer characterization. *Vadose Zone Journal*, 9(1):73–84.

Pitt, R. (1998). Unique features of the source loading and management model (slamm). In James, W., editor, *Modeling the Management of Stormwater Impacts, vol. 6. Computational Hydraulic International, Guelph, Ontario*, pages 13–35.

Praskievicz, S. and Chang, H. (2009). A review of hydrological modelling of basin-scale climate change and urban development impacts. *Progress in Physical Geography*, 33(5):650–671.

Press, W., Teukolsky, S., Vetterling, W., and Flannery, B. (2002). *Numerical Recipes in C++.* Cambridge University Press.

Quintana-Seguàŋ, P., Moigne, P. L., Durand, Y., Martin, E., Habets, F., Baillon, M., Canellas, C., Franchisteguy, L., and Morel, S. (2008). Analysis of near surface atmospheric variables: Validation of the safran analysis over france. *Journal of Applied Meteorology and Climatology*, 47:92–107.

Radojevic, B. (2002). *Méthode d'évaluation de l'influence urbaine sur le régime des crues d'un bassin versant de 130 km*^{2}. PhD thesis, Institut National des Sciences appliquées de Lyon, INSA.

Radojevic, B., Breil, P., and Chocat, B. (2010). Assessing impact of global change on flood regimes. *International Journal of Climate Change Strategies and Management*, 2(2):167–179.

Rauch, W., Aalderink, H., Krebs, P., Schilling, W., and Vanrolleghem, P. (1998). Requirements for integrated wastewater models - driven by receiving water objectives. *Water Sciences and Technology*, 38(11):97–104.

Rauch, W., Bertrand-Krajewski, J., Krebs, P., Mark, O., Schilling, W., Schütze, M., and Vanrolleghem, P. (2002). Deterministic modelling of integrated urban drainage systems. *Water Sciences and Technology*, 45(3):81–94.

Rawls, W. and Brakensiek, D. (1985). Prediction of soil water properties for hydrologic modelling. In Jones, E. and Ward, T., editors, *Watershed management in the eighties: proceedings of the American Society of Civil Engineers symposium, Denver, April 30-May 1. ASCE, New York*, pages 293–299.

Rebai, A. (2007). Modélisation des échanges entre les écoulements en surface et le réseau d'assainissement. Master's thesis, Université Joseph Fourier, Grenoble I.

Refsgaard, J. (1996). *Spatial Patterns in Catchment Hydrology - Observation and Modelling*, chapter Terminology, Modelling Protocoll and Classification of Hydrological Model Codes, pages 17–39. ISBN 0-7923-4042-6. Kluwer Academic Publishers, water science and technology library 22 edition.

Reggiani, P., Sivapalan, M., and Hassanizadeh, S. (1998). A unifying framework for watershed thermodynamics: balance equations for mass, momentum, energy and entropy, and the second law of thermodynamics. *Advance in Water Resources*, 22(4):367–598.

Renard, B., Kavetski, D., Leblois, E., Thyer, M., and Kuczera, G. (2011). Towards a reliable decomposition of predictive uncertainty in hydrological modelling : characterizing rainfall errors using conditional simulation. *Water Resources Research*. doi:10.1029/2011WR010643, in press.

Renouf, E. (2004). Vers une modélisation couplée de modèles hydrauliques de surface et de réseau d'assainissement dans le cas de la ville d'oullins (69). Master's thesis, ENSHMG Grenoble.

Reussner, F., Alex, J., Bach, M., Schütze, M., and Muschalla, D. (2009). Basin-wide integrated modelling via openmi considering multiple urban catchments. *Water Science and Technology*, 60(5):1241–1248.

Robbez-Masson, J. (1994). *Reconnaissance et délimitation de motifs d'organisation spatiale. Application à la cartographie de pédopaysages.* PhD thesis, Ecole Nationale Supérieure Agronomique de Montpellier.

Rodriguez, F. (1999). *Interêt des banques de données urbaines pour l'hydrologie. Détermination des fonctions de transfert de bassins versants urbains.* PhD thesis, Institut national polytechnique de Grenoble.

Rodriguez, F., Andrieu, H., and Creutin, J. (2003). Surface runoff in urban catchments: morphological identification of unit hydrographs from urban databanks. *Journal of Hydrology*, 283:146–168.

Rodriguez, F., Andrieu, H., and Morena, F. (2008). A distributed hydrological model for urbanized areas - model development and application to case studies. *Journal of Hydrology*, 351:268–287.

Ross, P. (2003). Modelling soil water and solute transport. fast, simplified numerical solution. *Agronomy Journal*, 95(6):1352–1361.

Rossman, L. (2010). Storm water management model user's manual version 5.0, report no. epa/600/r-05/040. Technical report, U.S. EPA National Risk Management Research Laboratory, Cincinnati, OH. http://www.epa.gov/nrmrl/wswrd/wq/models/swmm/epaswmm5_user_manual.pdf accessed 8 June 2011.

Roy, A., Wenger, J., Fletcher, T., Walsh, C., Ladson, A., Shuster, W., Thurston, H., and Brown, R. (2008). Impediments and solutions to sustainable, watershed-scale urban stormwater management: Lessons from australia and the united states. *Environmental Management*, 42:344–359.

Ruysschaert, F. (2004). Autoépuration des petites rivières à faible capacité de dilution. Partie de manuscrit de thèse.

Santra, P., Das, B., and Chakravarty, D. (2011). Delineation of hydrologically similar unit in a watershed based on fuzzy classification of soil hydraulic properties. *Hydrological Processes*, 25:64–79.

Sanzana, P. (2011). Automatic pre-processing for a distributed hydrological model using the hru (hydrological response units) concept with grass-gis. Master's thesis, University of Chile, Santiago de Chile.

Sarrazin, B. (2012). *Approches spatiales pour décrire le réseau de drainage et suivre sa dynamique de fonctionnement en milieu rural dans une perspective d'aide àă la modélisation hydrologique*. PhD thesis, Ecole doctorale Terre, Univers, Environnement. l'Institut National Polytechnique de Grenoble. Soutenance prévue en Janvier 2012.

Schubert, J., Sanders, B., Smith, M., and Wright, N. (2008). Unstructured mesh generation and landcover-based resistance for hydrodynamic modeling of urban flooding. *Advance in Water Resources*, 31:1603–1621.

Schwarze, C. (2008). Deriving hydrological response units (hrus) using a web processing service implementation based on grass gis. In *Geoinformatics FCE CTU 2008 Workshop, Prague, Czech Republic, 18-19th September*, pages 67–78.

SED (2011). Schéma directeur des eaux pluviales. Technical report, Département du Rhéne, Commune de GREZIEU LA VARENNE (Maître d'Ouvrage).

Semadeni-Davies, A., Hernebring, C., Svensson, G., and Gustafsson, L. (2008). The impacts of climate change and urbanisation on drainage in helsingborg, sweden: Suburban stormwater. *Journal of Hydrology*, 350:114–125.

Shewchuck, J. (1996). *Applied Computational Geometry: Towards Geometric Engineering*, volume 1148, chapter Triangle: Engineering a 2D Quality Mesh Generator and Delaunay Triangulator, pages 203–222.

Singh, V. and Woolisher, D. (2002). Mathematical modeling of watershed hydrology. *Journal of Hydrologic Engineering*, 7(4):270–292.

SIRA (2011). Sol info rhône-alpes, sira@rhone-alpes.chambagri.fr - http://www.rhone-alpes.chambagri.fr/sira/. consulted on 2011/06/05.

Smith, M. (1993). A gis-based distributed parameter hydrologic model for urban areas. *Hydrological Processes*, 7:45–61.

Smith, M. (2006). Comment on 'analysis and modeling of flooding in urban drainage systems'. *Journal of Hydrology*, 317:355–363.

Smith, R. and Parlange, J. (1978). A parameter-efficient hydrologic infiltration model. *Water Resources Research*, 14(3):533–538.

SOGREAH (2006). Schéma intercommunal d'assainissement, document final. Technical report, S.I.A.H.V.Y.

Sogreah and Insavalor (2005). Manuel d'utilisation de canoe. Technical report.

Speisser, V. (2008). Modélisation hydraulique des transferts verticaux entre la colonne d'eau et le substrat. Master's thesis, ENTPE, Cemagref Lyon.

Srinivasan, R. and Arnold, J. (1994). Integration of a basin-scale water quality model with gis. *Water Resources Bulletin*, 30(3):453–462.

Steiniger, S. and Bocher, E. (2009). An overview on current free and open source desktop gis developments. *Journal of Geographical Information Science*, 23:1345–1370.

Sui, D. Z. and Maggio, R. C. (1999). Integrating gis with hydrological modeling: Practices, problems, and prospects. *Computers, Environment and Urban Systems*, 23(1):33–51.

Thollet, F. (2007). Recueil de données du bassin versant de l'yzeron. ur hhly. année 2007. Technical report, Cemagref Lyon.

Thollet, F. and Branger, F. (2008). Recueil de données du bassin versant de l'yzeron. ur hhly. année 2008. Technical report, Cemagref Lyon.

Thoré, M. (2008). Etablissement d'une carte numérique des profondeurs de sol sur le bassin versant de la bléone. Master's thesis, Agrocampus Rennes, LTHE.

Tiemeyer, B., Moussa, R., Lennartz, B., and Voltz, M. (2007). Mhydas-drain: A spatially distributed model for small artificially drained lowland catchments. *Ecological Modelling*, 209:2–20.

Turner, A. and Chanmeesri, N. (1984). Shallow flow of water through non-submerged vegetation. *Agricultural Water Management*, 8:375–385.

Turpin, N., Bontems, P., Rotillon, G., Bérlund, I., Kaljonen, M., Tattari, S., Feichtinger, F., Strauss, P., Haverkamp, R., Garnier, M., Porto, A. L., Benigni, G., Leone, A., Ripa, M. N., Eklo, O.-M., Romstad, E., Bioteau, T., Birgand, F., Bordenave, P., Laplana, R., Lescot, J.-M., Piet, L., and Zahm, F. (2005). Agribmpwater: systems approach to environmentally acceptable farming. *Environmental Modelling & Software*, 20(2):187 – 196.

Valcke, S. and Morel, T. (2006). Oasis and palm, the cerfacs couplers.technical report tr/cmgc/06/38. Technical report, Centre Européen de Recherche et Formation Avancées en Calcul Scientifique.

Valeo, C. and Moin, M. (2000). Grid-resolution effects on a model for integrating urban and rural areas. *Hydrological Processes*, 14:2505–2525.

Vannier, O. and Braud, I. (2010). Calcul d'une évapotranspiration potentielle (etp) spatialisée pour la modélisation hydrologique àă partir des données de la réanalyse safran de météo-france. note de travail du plateau somme (synenergie observation modélisation en modélisation de l'environnement) d'envirhônalp. Technical report, Cemagref, LTHE, Envirhonalp.

Varado, N. (2004). *Contribution au dévéloppement d'une modélisation hydrologique distribuée. Application au bassin versant de la Donga, au Benin.* PhD thesis, Institut national polytechnique de Grenoble. p. 157.

Varado, N., Braud, I., and Ross, P. (2006a). Development and assessment of an efficient numerical solution of the richards' equation including root extraction by plants. *Journal of Hydrology*, 323:258–275.

Varado, N., Ross, P., Braud, I., and Haverkamp, R. (2006b). Assessment of an efficient numerical solution of the richards' equation for bare soil. *Journal of Hydrology*, 323:244–257.

Vertessy, R., Hatton, T., O'shaughnessy, P., and Jayasuriya, M. (1993). Predicting water yield from a mountain ash forest catchment using a terrain analysis based catchment model. *Journal of Hydrology*, 150:665–700.

Viallet, P., Debionne, S., Braud, I., Dehotin, J., Haverkamp, R., Saâdi, Z., Anquetin, S., Branger, F., and Varado, N. (2006). Towards multi-scale integrated hydrological models using the liquid framework. In Gourbesville, P., Cunge, J., Guinot, V., and Liong, S., editors, *Proceedings of the 7th International Conference on Hydroinformatics, Nice, France*, volume 1, pages 542–549.

Viaud, V. (2004). *Organisation spatiale des paysages bocagers et flux d'eau et de nutriments. Approche empirique et modélisations.* PhD thesis, Ecole nationale supérieure agronomique de Rennes (ENSAR).

Viaud, V., Durand, P., Merot, P., Sauboua, E., and Saâdi, Z. (2005). Modeling the impact of spatial structure of a hedge network on the hydrology of a small catchment in temperate climate. *Agricultural Water Management*, 74(2):135–163.

Vidal, J., Martin, E., Franchisteguy, L., Baillon, M., and Soubeyroux, J. (2010). A 50-year high-resolution atmospheric reanalysis over france with the safran system. *International Journal of Climatology*, 30(11):1627–1644.

Voinov, A. (2010). 'integronsters' and the special role of data. In Swayne, D., Yang, A. W., Voinov, A., Rizzoli, A., and Filatova, T., editors, *iEMSs 2010 International Congress on Environmental Modelling and Software. Modelling for Environment's Sake., Fifth Biennial Meeting, Ottawa, Canada.*

Voinov, A., Fitz, C., Boumans, R., and Costanza, R. (2004). Modular ecosystem modelling. *Environmental Modelling & Software*, 19(3):285–304.

Walsh, C., Fletcher, T., and Ladson, A. (2005). Stream restoration in urban catchments through redesigning stormwater systemes: looking to the catchment to save the stream. *Journal of the North American Benthological Society*, 24(3):690–705.

Walter, H. and Lieth, H. (1967). *Klimadiagramm-Weltatlas*. Gustav Fischer Verlag Jena. http://de.wikipedia.org/wiki/Klimadiagramm, consulted on 07/11/2011.

Winter, T. C. (2001). The concept of hydrologic landscapes. *Journal of the American Water Resources Association*, 37(2):335–349.

WMO (2008). Urban flood risk management - a tool for integrated flood management, associated programme on flood management. Technical report.

Wong, T., Fletcher, T., Duncan, H., Coleman, J., and Jenkins, G. (2002). A model for urban stormwater improvement conceptualisation. In *International Environmental Modelling and Software Society Conference, Lugano, Switzerland*.

Woolisher, D., Smith, R., and Goodrich, D. (1990). Kineros: A kinematic runoff and erosion model: Documentation and user manual, ars-77. Technical report, U.S. Department of Agriculture-Agricultural Research Service: Fort Collins, CO. http://www.tucson.ars.ag.gov/kineros/ consulted 08/06/2011.

Young, R., Onstad, C., and Bosch, D. (1989). Agnps: A nonpoint source pollution model for evaluating agricultural watersheds. *J. Soil Water Conservation*, 44:168–173.

Zoppou, C. (2001). Review of urban storm water models. *Environmental Modelling & Software*, 16:195–231.